

Cope-Type Hydroamination of Alkenes with Hydroxylamines and Hydrazines
- Scope and Mechanism -

Francis Loiseau

Thesis submitted to the
Faculty of Graduate & Postdoctoral Studies
in partial fulfillment of the requirements
For the Ph.D. degree in the

Ottawa-Carleton Chemistry Institute
Faculty of Science
University of Ottawa

Abstract

Hydroamination stands as a desirable approach to nitrogen-containing molecules, which have important applications ranging from pharmaceuticals (fine chemicals) to paints, coatings, insecticides and agrochemicals (bulk chemicals). It features the use of alkene and alkyne starting materials, which are abundant and rarely used in the formation of C-N bonds. This work aims at building on the improved Cope-type reactivity developed in the Beauchemin group by expanding the reach of the reaction and understanding its mechanistic complexities.

The first part of this thesis describes the development of cascade reactions to provide a thermodynamic driving force for the intermolecular Cope-type hydroamination of alkenes. The methodology serves as a proof of concept that the dipolar reaction intermediates can be engineered to further react irreversibly to more stable products, and has shown potential in improving the syntheses of natural alkaloids.

The second part of the thesis describes the expansion of Cope-type hydrazide hydroaminations through a systematic investigation of hydrazine analogs as reactants. Optimized reagents are featured in the first reported intermolecular Cope-type hydrohydrazidation of alkenes. Mechanistic investigations and isolation of ammonium ylide intermediates support a 5-membered concerted and planar mechanistic pathway for hydrazide hydroaminations, similar to that observed with hydroxylamines.

The final section presents mechanistic data disproving a previously assumed difficult proton transfer step in the hydroamination using hydroxylamines. From such findings, early results are presented towards a hydrogen-bond catalyzed hydroamination, which has potential applicability across the field of Cope-type hydroaminations and beyond.

Résumé

L'hydroamination est une approche désirable pour la formation de molécules azotées et elle peut être utilisée tant dans l'industrie des produits chimiques fins que dans celle des produits chimiques de base. Les réactifs de cette réaction sont des alcènes et des alcynes, lesquels sont abondants et peu utilisés dans la formation de liaisons C-N. La présente thèse vise le développement de la réactivité d'hydroamination de type Cope en augmentant la portée de la réaction et la compréhension des complexités de son mécanisme.

La première partie décrit l'élaboration de réactions en cascades capable d'apporter une aide thermodynamique à l'hydroamination intermoléculaire de type Cope sur alcènes. Cette méthodologie sert de preuve de concept démontrant comment des intermédiaires dipolaires modifiés peuvent réagir davantage et de façon irréversible. Elle a également permis d'améliorer la synthèse d'alcaloïdes naturels utilisant l'hydroamination de type Cope.

La deuxième partie décrit l'expansion des hydroaminations de type Cope avec hydrazides par la recherche systématique d'analogues de l'hydrazine comme réactifs. Ces réactifs optimisés figurent dans la première hydrohydrazidation intermoléculaire publiée de type Cope sur alcènes. Des études mécanistiques ainsi que l'isolation d'intermédiaires (ylures d'ammonium) soutiennent un mécanisme réactionnel concerté comprenant un état de transition planaire à 5 membres, semblable à celui observé avec les hydroxylamines.

La dernière section présente des données mécanistiques qui permettent d'infirmer une étape difficile de transfert de proton précédemment supposée pour l'hydroamination avec hydroxylamines. Cette étude est suivie de résultats préliminaires indiquant la possibilité d'une hydroamination catalysée par liaisons hydrogènes, qui pourrait être utilisée dans le domaine de l'hydroamination de type Cope comme dans d'autres réactions semblables.

Acknowledgments

Through years (and years) in school, I wanted for a while to be a medical doctor to show that you could be one and care about your patients; a lawyer or policeman to show you didn't have to be corrupted; a businessman to show you could do business without being greedy. Chemistry, being the first field I was passionate about without wanting to jump in it just to prove something, ended up being the right option for a field to study into.

My meeting with André was the catalyst that started this whole Ph.D. journey. The motivation he showed on the day I met him, the certainty he had that he was onto something great, never wavered in the past 5 years, and have confirmed I made the right choice of supervisor. Many discussions, QOMSBOC memories and countless failed and successful reactions later, I see everyday a remarkable scientist, who I still strongly believe has the best photographic memory ever; lead his lab with an overwhelming and contagious passion for chemistry. André, thank you for making work with you feel like an opportunity much more than a job.

I have been lucky to work with such a large group of remarkable people that thanking them properly would deserve its own chapter. I'll try to be brief, and just remember that if I was less sober and writing this with you at a Christmas party or any QOMSBOC, this would take forever. My first thanks have to go to Joe, who in my opinion is the best first grad student a group can hope for. I told him enough time he was the best, there's not much more I can say :D. To Pamela and Isabelle, your love of Justin may have been questionable, but the description of your honey covered pillow fights will stay in my memory for a long time.

Even good first impressions can be misleading. Joffré, who seemed like a great guy initially, may have helped my decision to join the group (he hiked mountains, in the US!!). He exceeded any expectations I had and turned out to be a great mentor and a fantastic friend, and the last few years will have been as much about completing grad school, as they will have been about the start of a friendship I am most grateful for. Thanks for showing me how to study for a grad class properly, and for never letting me down when I needed a beer.

I joined the lab at the same time as four other Master's students. The support we've shown one another, the unity we've had in preparing for early courses and exams stands out

to me, in a field where teamwork can sometimes be frowned upon. Jean, with whom I've shared the smallest lab on the planet, is a great friend, and a guy you can always count on to get a party going. Jenn, with whom I shared a bay for a fun year of Comp exams and stress, became a close friend, and her advice has been invaluable from both a career and personal perspective. Toni, who discovered at Qomsboc that ice and lemon make for great urinals, and Hao, who showed us many great ways to pronounce Briostatin, your company was always appreciated. Ashley and Pete, who joined soon after, proved a great match for the group, and have both become great companions in both grad school and life.

Just when I thought my people were leaving and I'd feel lost, along came Mel, Matt and Tom, who made 431 the coolest lab on this earth, and made my last years as enjoyable (if not more) as the early ones. Mel, you have indeed learned to accept my constant and annoying advice in some constructive way, and may deserve a medal for putting up with me. Thanks for the swimming lessons and many character building guidelines. Tom and Matt, if it were not for the fact that one of you LOVES radiohead, and that I managed to bring the other along with me in the Rockies, I may still wonder if you are indeed separate beings. You three became a foster family of sorts and I am grateful that life (...André) put you in my path.

Thanks to Derek for proving there could be a taller Beauchemin than me; to Nic for being one of the most avid Quebecers alive; to Christian for teaching me that fibres are somewhat good for the human body; to Bashir for his surprise reactions when we did cross paths; to Amanda for her love of weddings; to Keira for her incredible calmness and enjoyment of climbing; to Jean-François for sharing some of my frustrations against bilingualism issues; to Lyanne for her amazing laugh and Thanks to our post-docs, Wei, Shubin and French Nic for joining the group and bringing a new wealth of knowledge (special thanks to Nic for late-night email entertainment :P).

Undergrads can sure bring a lot of life to a lab. Special thanks to Émilie, Jean-Philippe, Michaël, Alishya, Pierre, Éric who have worked on my projects and made possible the completion of many sections of this thesis, and to all the others (Elena, Anna, Anne-Catherine, Catherine, Marija, Lei, Amy, Mark, Valérie, Charlotte, Patrick, Kashif, Sandrine, Nicholas). It has been amazing seeing them come through the lab and go on to accomplish magnificent things in chemistry and many other fields :).

I'd like to acknowledge the friendship of many Fagnou (Sophie, David, Elisia, Daniel, Marc), Barriault (Francis) and Ben (Chantelle, Anna, Malay, Devon, Jenny, Matt, Matthieu) group members I've had a chance to interact with over the years. The University of Ottawa Organic Chemistry Profs, Drs Ben, Barriault, Fagnou, Ogilvie, Durst, Keillor, Flynn, Chica, Pratt and Boddy, have created a great atmosphere in the department, and have always been approachable to talk about science, which is invaluable and appreciated.

The Chemistry Department Staff, Annette, Josée and Linda at the Department office; Lorraine, Manon, Diane, Elvira at the Faculty of Science; Claude Bison and his team at the Science Store, as well as Julie Lamotte, Alain St-Amant and Glenn Facey are all to be acknowledged for help in Chemistry, NMR, administrative and TA related matters.

I am indebted to a group of wonderful friends, which materialized out of thin air over 12 years ago when I decided to study Science at Champlain College, to be completed slowly over time. The fun we've had together, hiking, skiing, partying, camping and talking till the wee hours of the morning in Tim Horton parking lots have changed me in all the best ways. Although you all know exactly who you are, special thanks are due to Valérie, Daniel, Marianne and Jess, for their constant support through the struggles of the past 5 years, and for knowing how to make me feel better within a minute (or two hour-long) phone call.

C'est ma famille qui est à la base de mes valeurs les plus chères, qui aujourd'hui encore guide mes choix. Merci à une mère et un père extraordinaire, qui ont su se dévouer pour leurs enfants, et m'ont appris à me relever et passer au travers des plus durs défis de la vie. Merci à une grand-mère qui m'a appris l'importance de compter sur soi-même et de savoir garder la tête haute. Merci à Fred et Ben pour avoir été compréhensifs pendant mon exil de Montréal, et pour être les deux frères les plus cool au monde.

Above all else, thanks to my wife Marie for absolutely everything. Falling in love with you remains the most incredible adventure I've lived and am still living, and beats any mountain I could hike, movie I could see or career I could choose. Sarah, thanks for making me the luckiest dad, and for showing me that there will never be a limit to the number of hugs a person can give or receive. It feels right to end these acknowledgements with a quick hello from dad to my kid(s) to come. I may not know your name(s) quite yet, but I sure thought of you a lot while writing this thesis, and I'm looking forward to meeting you in a couple of months! :D

There is no gene for the human spirit

- *Gattaca* -

Table of Contents

Abstract	ii
Résumé	iii
Acknowledgments	iv
Table of Contents	viii
List of Abbreviations	xiii
List of Figures	xvii
List of Schemes	xx
List of Tables	xxii
1 Introduction	1
1.1 <i>Hydroamination – a Desirable and Challenging Transformation</i>	1
Amination Reactions	2
1.2 <i>Background on Intermolecular Hydroamination</i>	3
1.2.1 Hydroamination through Brønsted Acid and Base Catalysis	4
1.2.2 Hydroamination through Metal Catalysis	5
1.3 <i>Cope-type Hydroamination</i>	8
1.3.1 The Origin of the Cope-Type Hydroamination	8
1.3.2 Beauchemin Group Efforts in the Cope-type Hydroamination	11
1.4 <i>Hydroxylamines vs. Hydrazines</i>	12
1.4.1 Structural Characteristics of Hydroxylamines	13
1.4.2 General Uses of Hydroxylamines and Derivatives	14
1.4.3 Structural Characteristics of Hydrazines & Derivatives	14
Hydrazides (N-Acylhydrazines) & Analogs	15
1.4.4 General Uses of Hydrazines and Derivatives	17
Uses of Hydrazines and Alkylhydrazines	17
Uses of Hydrazides and Derivatives	18

1.4.5	Potential Use of Hydroxylamines vs. Hydrazines as End Products.....	20
2	Cope-type Hydroamination with Hydroxylamines – Cascade Reactions.....	22
2.1	<i>Introduction</i>	22
2.1.1	Thermodynamic Neutrality in Hydroaminations of Alkenes	23
2.1.2	Thermoneutrality in the Cope-type Intermolecular Hydroamination	23
	Transition State Structure.....	24
	Potential Energy Surface for Alkenes and Alkynes	26
	Crossover Experiments to Test Thermoneutrality	27
2.1.3	Concept of Cascade Reactions	28
2.1.4	Planned Cascade Reactions	31
2.2	<i>Cope-Type Hydroamination – Meisenheimer Rearrangement Cascade Reaction ..</i>	<i>32</i>
2.2.1	Background on the Meisenheimer Rearrangement.....	32
2.2.2	Initial Approach to Meisenheimer Rearrangement	34
2.2.3	Results and Discussion	35
	Optimization of N-methallylation Procedures	35
	Scope of the reaction	37
2.2.4	Application to Total Syntheses	41
2.3	<i>Sila-Cope Elimination Cascade Reaction</i>	<i>44</i>
2.4	<i>Cope-Type Hydroamination – Cope Elimination Cascade</i>	<i>45</i>
2.4.1	Discovery of the cascade	46
2.4.2	Results and Discussion	46
	Expansion of the reactivity.....	48
2.5	<i>Summary and Outlook</i>	<i>50</i>
3	Scope Expansion of the Cope-type Hydroamination of Hydrazines	51
3.1	<i>Introduction</i>	<i>52</i>
3.1.1	Classical Syntheses of Hydrazines and Hydrazides.	52
3.1.2	Summary of Recent Hydrohydrazination Strategies.....	55
	Titanium Catalyzed Intramolecular Hydrohydrazination of Alkynes.....	55
	Intermolecular Hydrohydrazination of Alkenes using Cobalt and Manganese Catalysis.....	58
	Hydroamination through Lewis Acid Activation of Alkynes.....	60
	Platinum Catalyzed Intramolecular Hydrohydrazination of Alkenes.....	62
3.1.3	Initial Efforts in Thermal Hydroamination using Hydrazines	63
	Early Results for the Hydroamination of Alkenes	64
	Intermolecular Hydroamination of Alkynes with Hydrazines.....	65
3.1.4	Beauchemin Results in the Hydroamination using Hydrazides	66

Early Scan of Hydrazides	67
Aminocarbonylation Side Reactivity	68
Early Solvent Scan for Hydrazide Hydroamination	70
Overview	71
3.2 Computational Analysis of Cope-Type Hydroamination with Hydrazines and Hydrazides	72
3.2.1 DFT Analysis of the Intermolecular Reaction of Hydrazines with Alkynes	72
3.2.2 DFT Analysis of the Intramolecular Reaction of Hydrazides with Alkenes	74
Description of Charges during the Intermolecular hydroamination.....	76
3.3 Scope Expansion of Intramolecular Hydroamination of Alkenes with Hydrazides: Results and Discussion	77
3.3.1 Intramolecular Reactivity with Standard Hydrazides	77
Cyclization of 5-Membered Substrates.....	77
Cyclization of Larger (6- and 7-Membered) Rings	78
Competing Elimination Side Reactivity Observed.....	80
3.3.2 Expansion of Intramolecular Reactivity with Hydrazide Analogs	82
Synthesis of Substrates for Cyclization	83
Scan of Hydrazide Analogues and Derivatives.....	84
Scope of Optimized Cyclization against Benzoic Hydrazide Substrates.	87
3.4 Intermolecular Cope-type Hydroamination of Hydrazides	89
3.4.1 High Throughput Screening For Reactivity	89
3.4.2 Reaction Optimization for <i>N'</i> -Benzyl-3,5-bis(trifluoromethyl) benzoic Hydrazide	92
Identification of the Side Product.....	93
Mechanism for the 1,2-Rearrangement.....	94
Solvent Scope for <i>N'</i> -Benzyl-3,5-bis(trifluoromethyl)-benzoic Hydrazide	94
3.4.3 Hydrazide Alkyl Scope for Intermolecular Reactivity	96
Proof of Structure for the [1,2]-Migration Side Product.....	97
3.4.4 Extension of Intermolecular Hydroamination Beyond Norbornene.....	98
3.5 Other Developments in Cope-type Hydroamination of Hydrazines	99
3.5.1 Confirmation of Scope for the Reactivity of Hydrazines	100
3.5.2 Concurrent Development of Intermolecular Hydroamination of Alkynes with hydrazides	101
3.6 Mechanistic Investigation: Results and Discussion	104
3.6.1 Kinetic Isotope Effects	104
Singleton's Method for Natural Abundance KIE Determination	105
Attempts at Using Singleton's Method for Hydrazide Hydroamination	106
3.6.2 Standard KIE Measurements for The Hydrazide Hydroamination.....	108
Deuteration at the Hydrazide Nitrogens.	108
Deuteration on the Alkene.....	110

3.6.3	Isolation of the Ammonium Ylide Intermediate	111
	Proof of Structure for the Ammonium Ylide Intermediates.....	114
3.7	<i>Summary and Outlook</i>	117
4	Hydrogen Bonding Catalyzed Cope-type Hydroamination.....	119
4.1	<i>Introduction</i>	119
4.1.1	Enzymes Mimics & Oxyanion Holes.....	119
4.1.2	Hydrogen-bond Catalysis	120
4.1.3	Group Efforts for Catalytic Hydroamination	122
4.2	<i>Results and Discussion</i>	123
4.2.1	The Proton Transfer Step & Kinetic Data	124
4.2.2	Determination of the Reaction Order in Both Reactants	126
4.2.3	Development of the Hydrogen Bonding Catalyzed Hydroamination	130
	Selection of Catalysts / Additives	131
4.3	<i>Outlook and Perspectives</i>	135
	Overview of Methodology Developed.....	135
	Catalyst Source and Design.....	136
	Wider Application of the Methodology	137
	Appendix I. Collaboration with the Murugesu Group.....	138
	Appendix II. Claims to Original Research	146
	<i>Claims to Original Research</i>	146
	<i>Publications from This Work</i>	146
	<i>Presentations from This Work</i>	147
	Appendix III. Experimental Section.....	149
	<i>General Experimental</i>	149
	<i>Materials</i>	150
	<i>Procedures and Characterization for Chapter 2</i>	150
	◆ General Comments	150
	◆ Characterization of the Oligomer Obtained from the Side Reactions	150
	◆ Synthesis of <i>N</i> -Methallyl Hydroxylamine Precursors.....	153
	General Procedure A for <i>N</i> -methallylation of hydroxylamines.....	153

◆ Scope Expansion of Intramolecular Hydroamination.....	157
General Procedure B for the reaction of alkenes with <i>N</i> -Alkyl- <i>N</i> -(2-methylallyl)-hydroxylamines.....	157
◆ Typical Procedure for the Hydroamination/Cope Elimination Cascade.....	161
<i>Procedures and Characterization for Chapter 3</i>	162
◆ General Comments	162
◆ Synthesis of Cyclization Precursors	162
General Procedure C for reparation of the Alkylhydrazides.....	162
◆ Synthesis of Precursors to 3.31f and 3.33.....	174
◆ Scope Expansion of Intramolecular Hydroamination – Key Steps	178
General Procedure D for Intramolecular Hydrohydrazidation.....	178
◆ Lead Result in Intermolecular Reactivity of Hydrazides	188
◆ Synthesis of Intermolecular Substrates	189
◆ Intermolecular Cope-Type Hydroamination - Key Steps	194
General Procedure E for Intermolecular Hydrohydrazidation.....	194
◆ Cleavage of the <i>N-N</i> bond for proof of structure:.....	201
◆ Primary KIE by Deuteration at Nitrogens.....	202
◆ Secondary KIE by Deuteration on Alkene	205
◆ Synthesis of Tri-substituted Hydrazine Substrates	207
◆ Isolation of Dipolar Amine Imide Intermediates	210
General Procedure F for synthesis of dipolar amine imide intermediates (Table 3.14)	210
◆ Structural Assignment of Dipolar Amine Imide Intermediates	213
◆ [1,2] & [1,3]-Shift of trisubstituted hydrazine substrates	219
<i>Procedures and Characterization for Chapter 4</i>	221
◆ Kinetic Experiments for Chapter 4.....	221
Appendix IV. NMR Spectra.....	224

List of Abbreviations

Å	angstrom (10 ⁻¹⁰ meters)
Ac	acetyl
AcOH	acetic acid
AM	anti-Markovnikov
<i>anti</i>	against, opposite
aq	aqueous
Ar	aryl
B3LYP	Becke-3-Lee-Yang-Parr
BG	blocking group
Bn	benzyl
Boc	<i>tert</i> -butoxycarbonyl
Bu	butyl
Bz	benzoyl
cat.	catalytic
°C	degree Celsius
cal	calorie
<i>cis</i>	<i>L.</i> , on the same side
Cy	cyclohexyl
δ	chemical shift in parts per million
d	deuterium (in NMR solvents); doublet
Δ <i>G</i>	change in Gibbs-free energy
Δ <i>H</i>	change in enthalpy
Δ <i>S</i>	change in entropy

DBU	1,8-diazabicyclo[5.4.0]undec-7-ene
DFT	density functional theory
DMF	dimethylformamide
DMSO	dimethyl sulfoxide
dr	diastereomeric ratio
E	<i>Ger.</i> , entgegen
ee	enantiomeric excess
EI	electron impact
Eq.	equation
equiv.	equivalent
Et	ethyl
EWG	electron-withdrawing group
g	gram
h	hour
H-bond(ing)	hydrogen bond(ing)
HOMO	highest occupied molecular orbital
HRMS	high-resolution mass spectroscopy
Hz	Hertz
<i>i</i>	iso
IR	infrared
<i>J</i>	coupling constant
k	rate constant
K	equilibrium constant
KIE	kinetic isotope effect
L	liter; ligand

LA	Lewis Acid
LUMO	lowest unoccupied molecular orbital
<i>m</i>	meta
M	molar; metal; Markovnikov
<i>m</i> -CPBA	meta-chloroperbenzoic acid
Me	methyl
mg	milligram
min	minute
mL	milliliter
mmol	millimol
MS	molecular sieves
Na	amide-like nitrogen in a hydrazide
N β	distal nitrogen in a hydrazide
Nu	nucleophile
NMR	nuclear magnetic resonance
<i>o</i>	ortho
<i>p</i>	para
p	-log()
Ph	phenyl
PMB	<i>para</i> -methoxybenzyl
Pr	propyl
Q	charge transfer
R (R [#])	carbon-based substituent
RT	room temperature
s	second

sat.	saturated
SM	starting material
S _N 1 or S _N 2	nucleophilic substitution first order; or second order
S _N Ar	nucleophilic aromatic substitution
<i>syn</i>	together, same side
<i>t</i>	tertiary, <i>tert</i> -
temp.	temperature
THF	tetrahydrofuran
TLC	thin layer chromatography
TS (‡)	transition state
UV	ultra-violet
X	heteroatom or pseudohalide
Z	<i>Ger.</i> , zusammen

List of Figures

- Figure 1.1** Survey of bulk reactions performed in research facilities between 1985-2002. Left: Subdivision of all reaction (15% involving a C-N bond formation). Right: C-N bond forming reactions (amination of alkenes/ynes qualify for the 5% of **other** reactions). 2
- Figure 1.2** Similar mechanism of alkyl sulfoxides thermolysis and Cope elimination 10
- Figure 1.3** Comparison of the pK_a of hydroxylamines to the different forms of hydrazines to be used in the Cope-type hydroamination 13
- Figure 1.4** Hydrazide analogs as potential reagents for Cope-type hydroamination 17
- Figure 1.5** Selected examples of the hydrazine motif for general and medical applications 18
- Figure 1.6** Selected examples of the hydrazide motif for general and medical applications 19
- Figure 2.1** Transition state structures for the Cope-type hydroamination of NH_2OH with norbornene and styrene at the B3LYP/TZVP level of theory; M= Markovnikov, AM=anti- Markovnikov product. The internuclear distances (\AA) are shown only for relevant chemical bonds. 24
- Figure 2.2** Transition state structures for the Cope-type hydroamination of NH_2OH with phenylacetylene at the B3LYP/TZVP level of theory; M= Markovnikov, AM=anti- Markovnikov product. The internuclear distances (\AA) are shown only for relevant chemical bonds. 25
- Figure 2.3** (Top) The transition states for hydroamination of ethylene and acetylene showing the internuclear distances and bond orders (*Italics*) and NPA charges (blue). (Bottom) Major donor-acceptor interactions that contribute to bond formation between the unsaturation and the hydroxylamine. The charge transfer Q for each interaction is shown in green and orange. 26
- Figure 2.4** Schematic representation of the overall thermodynamic effects of concerted or catalyzed reaction on the reaction, vs. the use of cascade reactions. 29
- Figure 2.5** Example of a degradation product isolated from the original Meisenheimer cascade reaction. 34

Figure 2.6 Other attempts at the Cope hydroamination / Cope elimination cascade reactions. Tested in standard conditions, 100 °C for 42 h, with excess alkene (2-5).	49
Figure 3.1 Hydroxylamines versus hydrazines as bifunctional reagents	51
Figure 3.2 Hydrazine sources in recent approaches to hydroamination for the synthesis of hydrazines and hydrazones.	55
Figure 3.3 Odom's titanium catalyzed hydrohydrazination of alkynes	57
Figure 3.4 Carreira's cobalt and manganese catalyzed hydrohydrazination of alkenes. Bottom: proposed mechanism	59
Figure 3.5 Comparison of basic reactivity of hydrazine in hydroamination, in neutral vs. acidic conditions.	65
Figure 3.6 Hydroamination vs. aminocarbonylation in semicarbazides and carbazates.	69
Figure 3.7 Transition state structures and free energies (gas phase and in MeOH) for the reaction between methyl hydrazine (MeNHNH ₂) and phenylacetylene. Internuclear distances (Å) are shown only for relevant chemical bonds. Calculated dipole moments (Debye) are shown in red.	73
Figure 3.8 Gibbs free energy (in kcal/mol, 298K, 1 atm.) profile for the Cope-type hydroamination.	75
Figure 3.9 Transition state structures for the intramolecular hydroamination of N-pent-4-enylbenzohydrazide (A), and for the subsequent proton transfer step of the dipolar intermediate (B). The internuclear distances (Å) are shown only for relevant chemical bonds.	76
Figure 3.10 Different approaches to help better stabilize the build up of negative charge in the hydroamination transition state	83
Figure 3.11 Hydrazides and unsaturated bonds used in SYMYX scan, with conditions.	91
Figure 3.12 Identification of the slow step of the hydroamination of hydrazides based on DTF calculations ($\Delta G^\ddagger = 28.7$ kcal/mol)	104
Figure 3.13 Attempted experiments using Singleton's method for KIE determination at natural abundance.	107
Figure 3.14 Tentative spatial arrangements of amine imide intermediates 3.56a-c based on NOESY and COSY assignments.	115

Figure 3.15 2D NOESY spectrum of isolated amine imide intermediate 3.56c	116
Figure 3.16 Summary of NOE interactions observed in intermediate 3.56c (right), and probable special orientation of functional groups explaining the observed NOEs (left)	116
Figure 4.1 Standard oxyanion hole showing transition state stabilization for a tetrahedral intermediate through multiple H-bond donors. Hydrolysis of acetylcholine with acetylcholinesterase	120
Figure 4.2 Free energies of reaction species and transition states for hydroamination of ethylene, C ₂ H ₄ and norbornene at the B3LYP/TZVP level of theory.	126
Figure 4.3 Reaction order in norbornene (top) and hydroxylamine, determined by following the reaction by NMR using trimethoxybenzene as an internal standard. ^a TMB = 1,3,5-trimethoxybenzene	128
Figure 4.4 List of potential candidates to catalyze or promote the Cope-type hydroaminations in aprotic solvents	131

List of Schemes

Scheme 1.1	Potential amination pathways shown for alkenes.	3
Scheme 1.2	General schemes for the Brønsted acid and base catalyzed intermolecular hydroaminations.	5
Scheme 1.3	Different modes of activation across metal-catalysis for hydroamination. Key points relating to intermolecular reactivity on alkenes are highlighted.	6
Scheme 1.4	The Cope-type hydroamination	8
Scheme 1.5	Originally proposed concerted vs. radical pathway for the reaction	9
Scheme 1.6	Proof of the reaction mechanism by Oppolzer	10
Scheme 1.7	Reasoning for the increased reactivity observed in alcoholic solvents.	11
Scheme 1.8	Summary of reactivity for the Cope-type hydroamination of hydroxylamines	12
Scheme 2.1	Crossover experiment to test that the Cope-type hydroamination of alkenes is under thermodynamic control.	28
Scheme 2.2	Concept of the cascade reaction to address thermodynamic neutrality.	29
Scheme 2.3	Example of a cascade reaction, the last step showing the favorable formation of a 6-membered cyclic amina.	30
Scheme 2.4	Proposed cascade reactions involving an initial Cope-type hydroamination followed by a Meisenheimer [2,3] rearrangement (A), sila-cope elimination (B) or Cope elimination (C).	31
Scheme 2.5	Summary of failed attempts to synthesize the sila-Cope cascade precursor.	44
Scheme 2.6	First attempt at hydroamination / sila-Cope cascade reaction from crude precursor synthesized from the aldonitrone.	45
Scheme 2.7	Proposed pathway for the Cope Elimination / Cope-type Hydroamination concept, generating ethylene gas to drive the equilibrium.	46
Scheme 2.8	1,3-Dipolar addition of norbornene with nitron formed in situ.	48
Scheme 3.1	Standard syntheses of hydrazides through reduction of hydrazones.	53

Scheme 3.2 Hydrazines through N-amination of amines.	54
Scheme 3.3 <u>Top</u> : Beller's zinc catalyzed and zinc promoted hydrohydrazination cascades and syntheses of dihydropyridazinones, indoles and pyrazoles, through hydrazone intermediate. <u>Bottom</u> : Patil's gold-promoted formal hydrohydrazination cascade	61
Scheme 3.4 Steric considerations in the anti-Markovnikov Cope-type hydroamination	65
Scheme 3.5 Optimal conditions favoring hydroamination (Top) and elimination (Bottom) for substrate 3.1c	81
Scheme 3.6 General retrosynthetic approach to the synthesis of cyclization precursors	84
Scheme 3.7 Hydrazone analogues not suitable for precursor synthesis	87
Scheme 3.8 Proton transfer and norbornyl transfer in intermolecular hydroamination of alkenes with hydrazides, shown to stem from the same amine imide intermediate.	94
Scheme 3.9 Reactivity of norbornene analog with hydrazine and methylhydrazine	100
Scheme 3.10 Primary KIE on substrate 3.1a and 3.31a , observed following deuterium substitution on both hydrazone protons.	109
Scheme 3.11 Secondary normal KIE on substrate 3.1a , observed following deuterium substitution at the internal alkene position.	110
Scheme 3.12 Potential for isolation of the tetrahedral ammonium dipolar intermediate to help determine if the mechanism is concerted	111
Scheme 4.1 Standard Lewis acid activation compared with mono and dual hydrogen bonding activation.	121
Scheme 4.2 Recent strategies to catalyze and promote the difficult intermolecular Cope-type hydroamination of alkenes.	123
Scheme 4.3 Proton transfer step, mediated by the solvent or existing hydroxylamines (starting material or product)	125
Scheme 4.4 Concept and desired interaction for the dipolar N-oxide intermediate.	130

List of Tables

Table 1.1 Number of bioactive structures (NIH Small Molecule Repository) containing the hydrazide subunit, sorted by substitution pattern.	20
Table 2.1 Free energies (kcal/mol) of the reaction species for hydroamination reactions (NH ₂ OH) with alkenes and alkynes. The energies are relative to the free reactants.	27
Table 2.2 Selected N-allylation test reactions for hydroxylamine 2.7 .	36
Table 2.3 Optimization of the methallylation of hydroxylamines.	37
Table 2.4 Solvent Scope for the Cope / Meisenheimer cascade reaction	38
Table 2.5 Alkene scope for the Cope / Meisenheimer rearrangement	39
Table 2.6 Hydroxylamine scope for the Cope / Meisenheimer cascade reaction.	40
Table 2.7 Effect of NaCNBH ₃ concentration on yields.	41
Table 2.8 Key hydroamination step in the synthesis of coniine	43
Table 2.9 Key hydroamination step in the synthesis of norreticuline	43
Table 2.10 Solvent and temperature scan for Cope Elimination cascade reaction.	47
Table 3.1 Variation of the hydrazide substituent and effect on the hydroamination and aminocarbonylation product ratios.	68
Table 3.2 Solvent scan for the hydroamination of N'-pent-4-enylbenzohydrazide	70
Table 3.3 Scope of the intramolecular hydroamination of benzoic hydrazides in 5-membered cyclizations	78
Table 3.4 Scope of the intramolecular hydroamination of benzoic hydrazides in 6- and 7-membered cyclizations ^a	79
Table 3.5 Temperature scan for the hydroamination / redox of substrate 3.1c	80
Table 3.6 Scan of hydrazide derivatives for the intramolecular Cope-type hydroamination ^a	85
Table 3.7 Temperature scans for the cyclization of two hydrazide derivatives. ^a	86
Table 3.8 Scope of 3,5-bis(trifluoromethyl)benzoic hydrazides cyclizations ^a	88
Table 3.9 Scope of intermolecular hydroamination of N'-benzyl-3,5-bis(trifluoromethyl)-benzoic hydrazide with norbornene ^a	95

Table 3.10 Hydrazide alkyl scope of the intermolecular hydrohydrazidation on norbornene	96
Table 3.11 Reactivity of Hydrazides in Intermolecular Hydroamination of Phenylacetylene	99
Table 3.12 Scope of hydroamination route to azomethine imines	103
Table 3.13 Scope of the amine imide isolation and migration side reactivity	113
Table 3.14 Reactivity summary of hydrazines and derivatives with alkenes and alkynes.	118
Table 4.1 Systematic investigation of alcohols and polyols to uncover hydrogen-bond potential.	132
Table 4.2 Solvent scan for the hydrogen bonding promoted/catalyzed hydroamination	134

1

Introduction

This chapter aims to give an overview of the Cope-type hydroamination and its current scope, by first contrasting it to other methods of hydroamination. It will then cover progressively known aspects of the reactivity, including a detailed look at the understood mechanism of the transformation. Organized in this way, we will cover key background necessary to understand the challenges associated with thermoneutral intermolecular hydroaminations of alkenes, presented in Chapter 2. It will serve as a solid base for understanding the Cope-type hydroamination using hydrazine derivatives and its mechanism, presented in Chapter 3. Finally, it will also detail our original understanding for the proton transfer step in the reaction, providing a contrast to our current mechanistic rationale, which brought forth the work presented in Chapter 4, with the proposed hydrogen-bond catalyzed Cope-type hydroamination.

1.1 Hydroamination – a Desirable and Challenging Transformation

Nitrogen-containing molecules have always been privileged, with important functions and applications ranging from pharmaceuticals¹ (fine chemicals) to paints, coatings, insecticides and agrochemicals (bulk chemicals). Strategies that efficiently form C-N bonds have thus traditionally been of paramount importance. A survey of reactions that are run in industrial scale production of drug candidates (between 1985 and 2002) reveals that 15% of

¹ (a) Duggers R. W.; Ragan, J. A.; Brown Ripin, D. H. *Org. Proc. Res. Dev.* **2005**, *9*, 253. (b) Carey, J. S.; Laffan, D.; Thomson, C.; Williams, M. T. *Org. Biomol. Chem.* **2006**, *4*, 2337.

all reactions performed involved the formation of a C-N bond (Figure 1.1). Of those, common strategies amenable to large-scale synthesis include classical reactions such as nucleophilic substitutions, S_NAr, reductive aminations and Schiff base formations. Of all reactions used in large-scale industrial projects, none featured the use of a direct amination of a nitrogen source onto a C-C unsaturation.

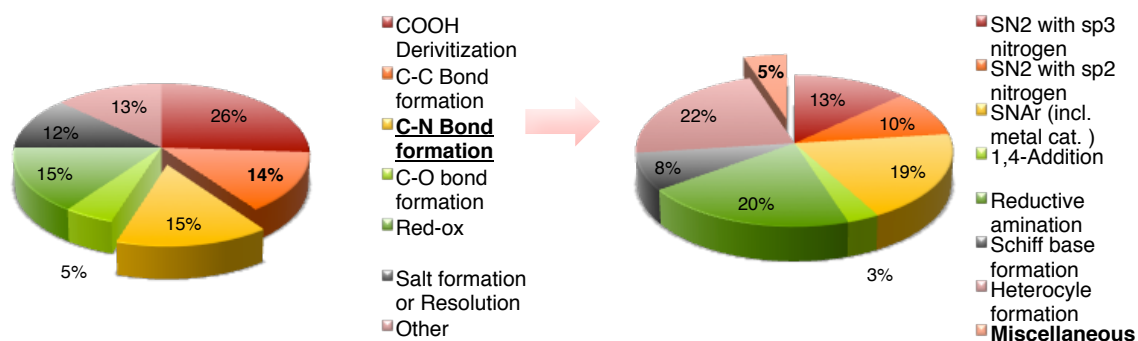


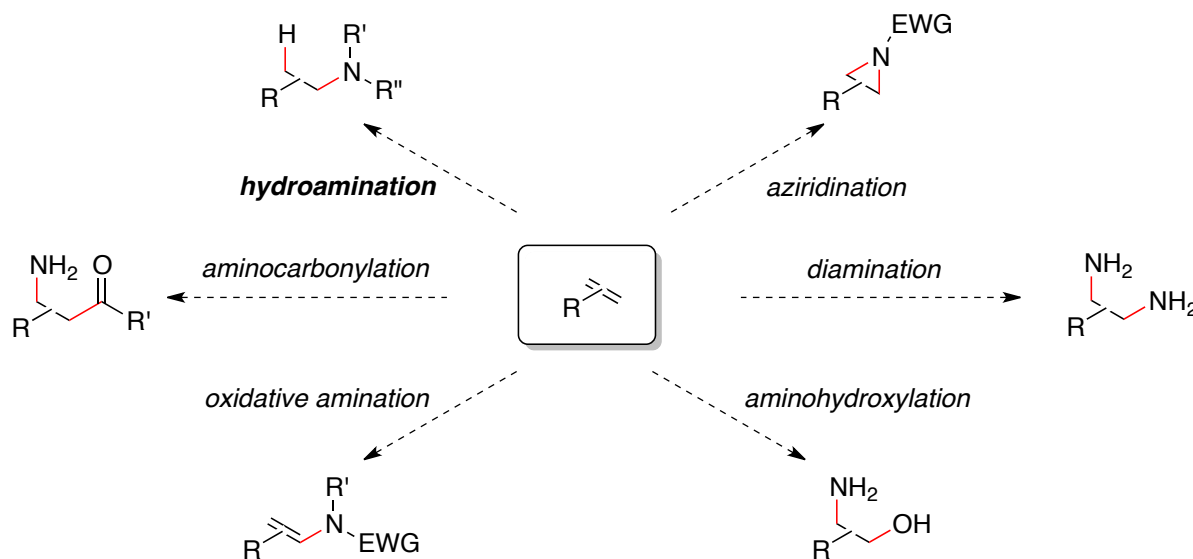
Figure 1.1 Survey of bulk reactions performed in research facilities between 1985-2002. Left: Subdivision of all reaction (15% involving a C-N bond formation). Right: C-N bond forming reactions (amination of alkenes/ynes qualify for the 5% of **other** reactions).

Amination Reactions

The direct amination of unsaturations is highly desirable, integrating amines into organic structures efficiently from a wealth of readily available and often affordable starting materials, including alkenes, alkynes, allenes and arenes, which are traditionally not used in the formation of C-N bonds. Scheme 1.1 illustrates approaches that can be taken to aminate alkenes. Though recognized for its tremendous potential and following decades of continued worldwide research in the area,² particularly in the field of metal catalysis, there remains a

² For selected reviews on the synthesis of nitrogen heterocycles: (a) Nakamura, I.; Yamamoto, Y. *Chem. Rev.* **2004**, *104*, 2127. (b) Álvarez-Corral, M.; Muñoz-Dorado, M.; Rodríguez-García, I. *Chem. Rev.* **2008**, *108*, 3174. (c) Patil, N. T.; Yamamoto, Y. *Chem. Rev.* **2008**, *108*, 3395. (d) Candeias, N. R.; Branco, L. C.; Gois, P. M. P.; Afonso, C. A. M.; Trindade, A. F. *Chem. Rev.* **2009**, *109*, 2703. (e) Majumdar, K. C.; Chattopadhyay, B.; Maji, P. K.; Chattopadhyay, S. K.; Samanta, S. *Heterocycles* **2010**, *81*, 795.

significant interest in methods development to find strategies that are widely applicable in the field.



Scheme 1.1 Potential amination pathways shown for alkenes.

1.2 Background on Intermolecular Hydroamination

Hydroamination, the formal addition of an N-H bond across an unsaturation, remains one of the simplest and most desirable amination methods. It faces several challenges typical of amination methodologies. It typically features a high energy of activation, due to the forced interaction of two electron rich species. The use of catalysis to reverse the natural chemistry of one of the two reaction partners, or to promote a different mechanism globally, is a common approach to solving the problem. Also, with most intermolecular hydroaminations of alkenes being near a thermodynamic equilibrium, they can't be accelerated through the use of high reaction temperatures due to a high entropic cost, and hence typically require highly efficient catalysts. Achieving efficient reactivity at lower temperature (favoring products) in intermolecular alkene hydroaminations is highly desirable

as it could provide a general access to amine derivatives from inexpensive reagents.³ It remains one of the biggest challenges of the field.

To date, many of the achievements in the field have stemmed from the use of metal catalyzed processes, with several noteworthy achievements towards more general reactivity. A non-exhaustive review of standard modes of activation, for both general acid and base catalyzed processes, and their associated reactivity will be covered in the next subsections.

1.2.1 Hydroamination through Brønsted Acid and Base Catalysis

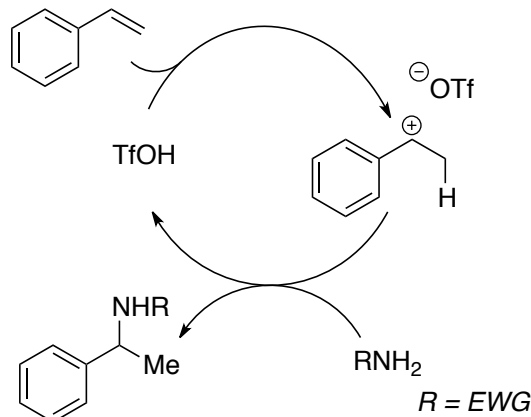
Because of the basic character of the nitrogen atom compared to its unsaturated partner, acid catalysts have been used only sporadically in hydroamination. Brønsted acid-catalyzed reactions rely on activation of the π system through protonation and generation of a carbenium ion (Scheme 1.2). Such a protonation is however always in competition with the concurrent protonation of the nitrogen-containing partner. The approach has resulted in several competent intramolecular systems, including the recent development of stereoselective variants. Intermolecular variants remain fairly unattainable except in biased systems where electron deficient amines (TsNH_2 or CbzNH_2 for example) have a chance at slowly reacting with biased alkenes.^{4,5}

³ For selected reviews: (a) Müller, T. E.; Hultzs, K. C.; Yus, M.; Foubelo, F.; Tada, M. *Chem. Rev.* **2008**, *108*, 3795. (b) Hultzs, K. C. *Adv. Synth. Catal.* **2005**, *347*, 367. (c) Müller, T. E.; Beller, M. *Chem. Rev.* **1998**, *98*, 675

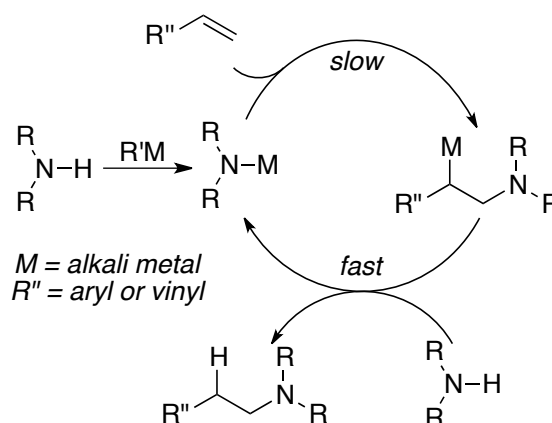
⁴ Rosenfeld, D. C.; Sekhar, S.; Takemiya, A.; Utsunomiya, M.; Hartwig, J. F. *Org. Lett.* **2006**, *8*, 4179.

⁵ Li, Z.; Zhang, J.; Brouwer, C.; Yang, C.-G.; Reich, N. W.; He, C. *Org. Lett.* **2006**, *8*, 4175.

Acid Catalysis



Base Catalysis



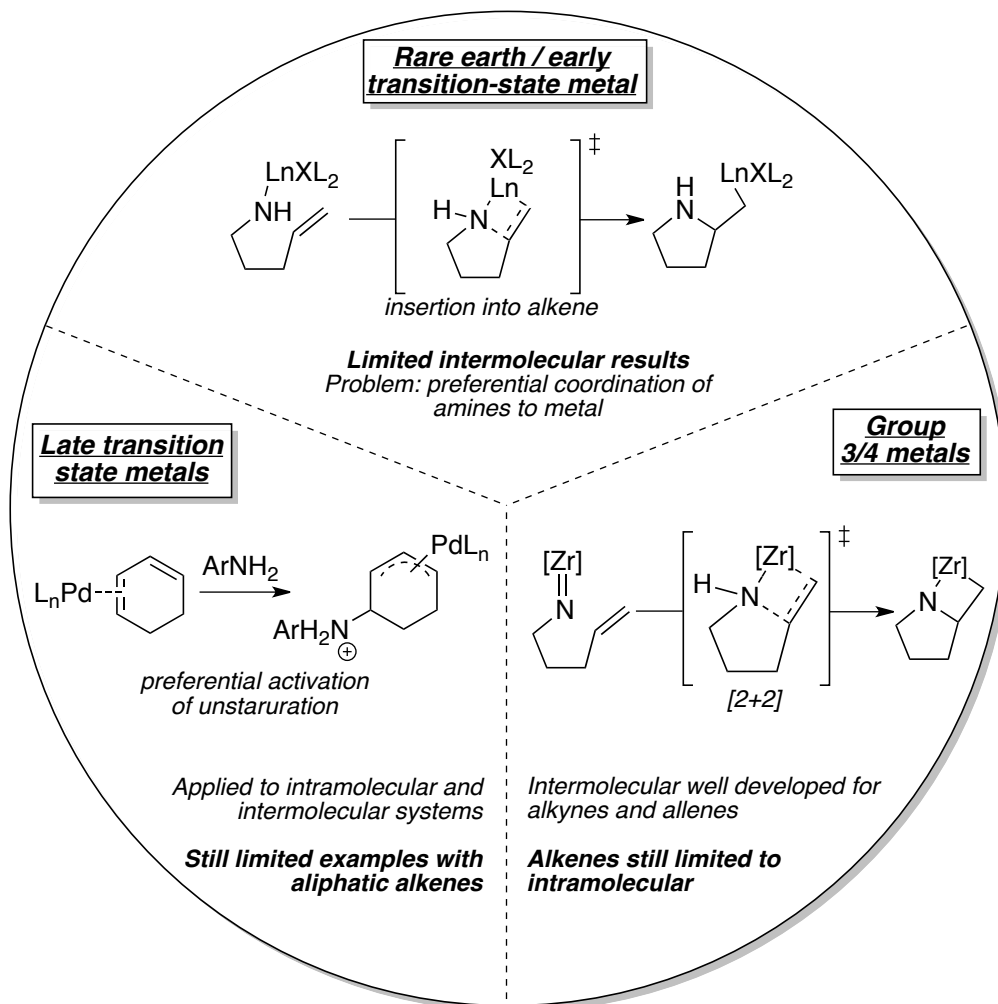
Scheme 1.2 General schemes for the Brønsted acid and base catalyzed intermolecular hydroaminations.

Base catalysis is plagued with parallel concerns. Amine deprotonation by alkali bases easily results in highly nucleophilic alkali amides. These are incompatible with the presence of most other additives, and must still react with electron rich alkenes. Again, intramolecular systems have been more successful, while any attempts towards general intermolecular reactions fails beyond the low reactivity of biased alkenes.

1.2.2 Hydroamination through Metal Catalysis

The field of metal-catalyzed hydroamination has rapidly expanded in the last few decades,³ with a variety of catalyst families operating under diverging mechanistic approaches. They can be summarized in three main categories. The *rare-earth metals* (actinides and lanthanides) primarily form metal amido complexes, which can then add across an unsaturation. *Group 3 and 4 metals* (ex. Ti, Zr) can form a variety of complexes, among which the metal imido complexes can participate in [2+2] cycloadditions with unsaturated partners to yield hydroaminated products. Finally, the use of *late-stage transition metals* has shown capabilities in activating the unsaturation primarily, to be

followed by an attack by the amine partner.⁶ Scheme 1.3 presents these three approaches, along with key information relating to their application to intermolecular systems.

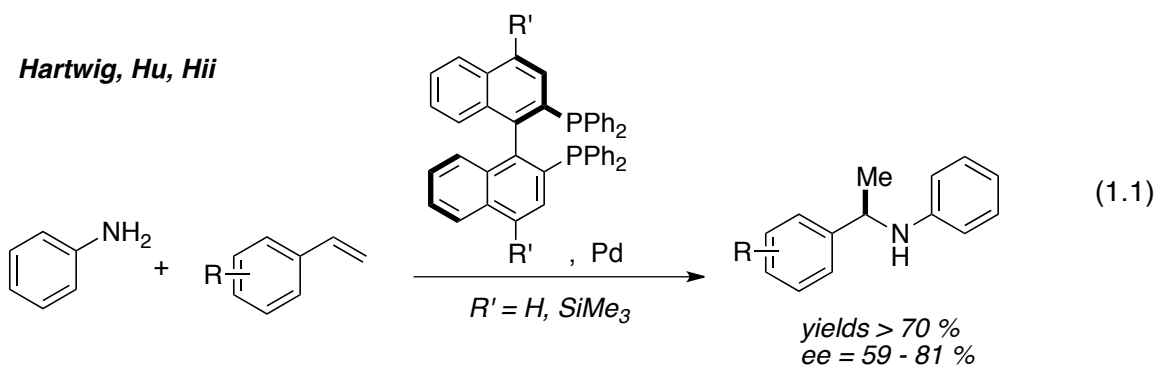


Scheme 1.3 Different modes of activation across metal-catalysis for hydroamination. Key points relating to intermolecular reactivity on alkenes are highlighted.

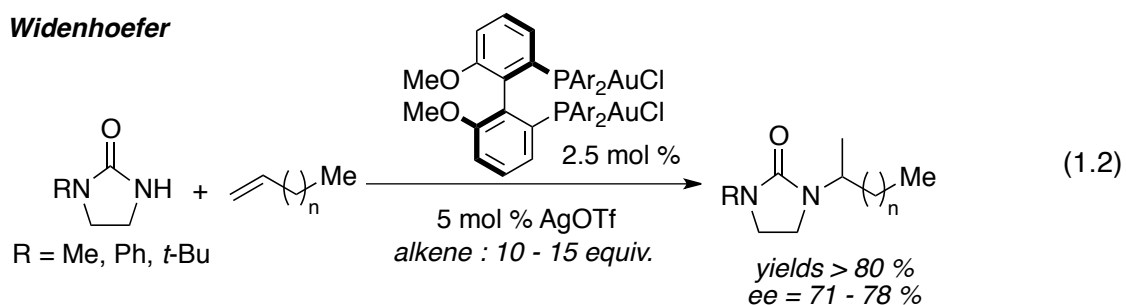
Most systems, even when they can be applied to intermolecular reactions of alkenes, remain limited in scope, most often reacting only with biased substrates (strained alkenes, vinyl arenes, dienes). A specific example of this type of interesting yet limited reactivity can be observed in systems developed for the hydroamination of styrenes using anilines.

⁶ Evidently, metals across these families of catalysts often have their own specific mechanisms, and can also participate in mechanistic pathways associated here to other reagents. These classifications are meant as representative trends of the varying mechanistic approaches to the difficult intermolecular hydroamination of alkenes.

Hartwig, Hu and Hii have all observed great yields and interesting stereoselectivities, in a reaction that remains inherently limited in scope.⁷



Widenhoefer has recently published an intermolecular gold-catalyzed hydroamination of simple alkenes from the use of cyclic ureas as nitrogen source.⁸ While the scope in terms of stereoselectivity is limited, the reaction is a prime example of the selected few systems capable of performing hydroamination on unbiased alkenes.



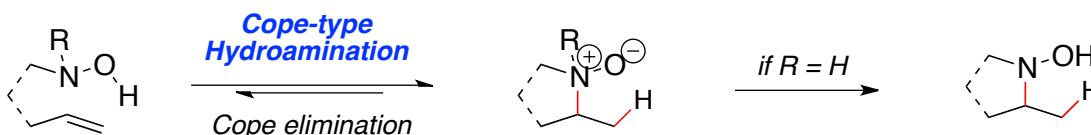
Overall, it remains well agreed that current solutions to intermolecular alkene hydroamination, despite significant progress in recent years, have generally low rates of catalysis and are limited in scope. Powerful catalysts are required to help accomplish olefin hydroamination in a synthetically useful way that could be transferred to industrial processes, and fill the current gap in amination methodologies amongst C-N bond forming techniques.

⁷ (a) Kawatsura, M.; Hartwig, J. F. *J. Am. Chem. Soc.* **2000**, *122*, 9546. (b) Li, K.; Horton, P. N.; Hursthouse, M. B.; Hii, K. K. *J. Organomet. Chem.* **2003**, *665*, 250. (c) Hu, A.; Ogasawara, M.; Sakamoto, T.; Okada, A.; Nakajima, K.; Takahashi, T.; Lin, W. *Adv. Synth. Catal.* **2006**, *348*, 2051.

⁸ (a) Zhang, Z.; Lee, S. D.; Widenhoefer, R. A. *J. Am. Chem. Soc.* **2009**, *131*, 5372. (b) Zhang, Z.; Widenhoefer, R. A. *Angew. Chem. Int. Ed.* **2007**, *46*, 283

1.3 Cope-type Hydroamination

In a conceptually different approach to achieve efficient hydroamination, we became interested in using hydroxylamines as bifunctional reagents in a metal-free process with C-C unsaturations. The reaction, which we refer to as a Cope-type hydroamination,⁹ is presented in Scheme 1.4, and features the intra or intermolecular addition of a hydroxylamine across the unsaturation, yielding initially an *N*-oxide intermediate. From there, if one of the nitrogen substituents is a hydrogen, a proton transfer can yield a formal hydroamination product.



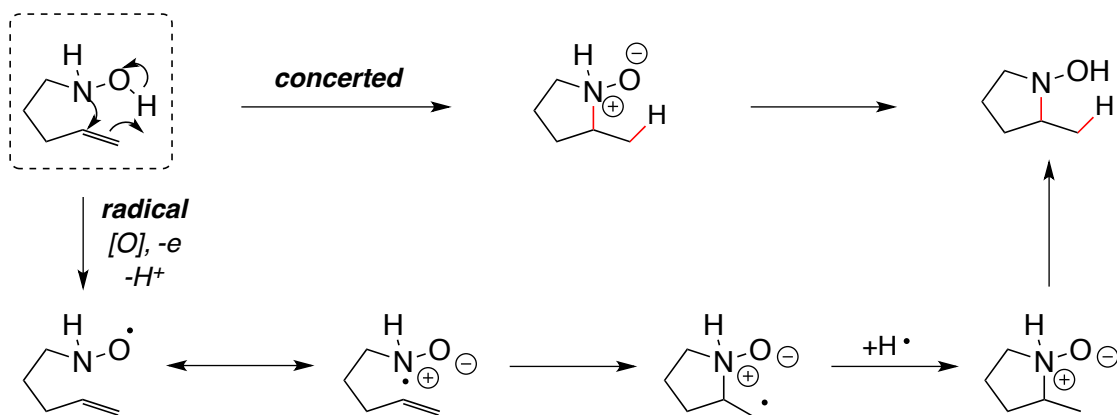
Scheme 1.4 The Cope-type hydroamination

1.3.1 The Origin of the Cope-Type Hydroamination

The reaction has followed a complex road to recognition in the later decades of the 20th century. Reports by Cope, Laughlin, House and Oppolzer first brought it to the attention of the scientific community.¹⁰ Laughlin observed, in the intermolecular thermolysis of 1-dodecene and *N,N*-dimethylhydroxylamine, the formation of isoxazolidine and a tertiary amine, that were later presumed to have originated from an initial hydroamination event. Slow progress on the development of the reaction followed up until the late 80s. Simple 5-membered ring systems were shown to cyclize well at room temperature, in a mechanism presumed concerted or radical-based (Scheme 1.5).

⁹ Alternatively, the reaction has been named the reverse-Cope elimination, the reverse-Cope cyclization, or more simply the Cope cyclization. We are strong advocates of the name Cope-type hydroamination for it inherently describes the process and reaction happening, while keeping its mechanistic origin intact, and is amenable to intermolecular processes as well.

¹⁰ (a) Oppolzer, W; Spivey, A. C.; Bochet, C. G. *J. Am. Chem. Soc.* **1994**, *116*, 3139. (b) Cope, A. C.; LeBel, N. A. *J. Am. Chem. Soc.* **1960**, *82*, 4656. (c) Laughlin, R. G. *J. Am. Chem. Soc.* **1973**, *95*, 3295. (d) House, H. O.; Manning, D. T.; Melillo, D. G.; Lee, L. F.; Haynes, O. R.; Wilkes, B. E. *J. Org. Chem.* **1976**, *41*, 855. (e) House, H. O.; Lee, L. F. *J. Org. Chem.* **1976**, *41*, 863.

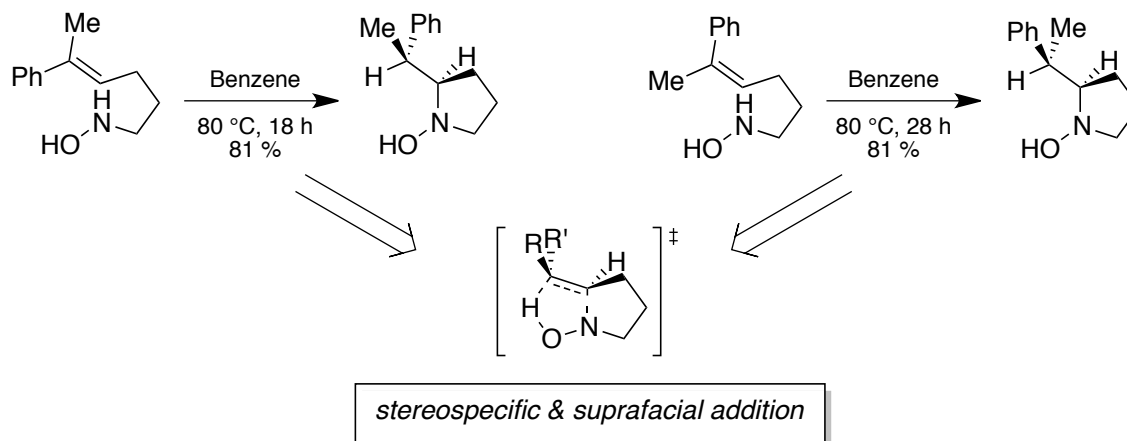


Scheme 1.5 Originally proposed concerted vs. radical pathway for the reaction

Ciganek and Oppolzer were able to strongly support the concerted mechanism of the reaction.¹¹ For example, the cyclization of the Z and E isomer of the otherwise identical alkenylhydroxylamine shown in Scheme 1.6, led to the observation of a single product in each reaction, shown to be diastereoisomers of each other, with a stereochemistry suggesting a syn-addition across the unsaturation. This went against the mechanism being radical based, and instead suggested, along with other observations, the reaction going through a suprafacial, concerted and planar transition state. This effectively presented it as the microscopic reverse of the Cope elimination, an assumption later supported by DFT calculations.¹²

¹¹ (a) Ciganek, E.; Read, J. M., Jr.; Calabrese, J. C. *J. Org. Chem.* **1995**, *60*, 5795. and (b) see ref. 10a

¹² (a) Kwart, H.; Brechbiel, M. *J. Am. Chem. Soc.* **1981**, *103*, 4650, and references cited therein. (b) Komaromi, I.; Tronchet, J. M. J. *J. Phys. Chem.* **1997**, *101*, 3554.



Scheme 1.6 Proof of the reaction mechanism by Oppolzer

In an interesting experimental and theoretical comparison, Jenks analyzed in detail the thermolysis of alkyl sulfoxides, near exclusively present as dipoles, in a process analogous to the Cope elimination, and by association, to the Cope-type hydroamination.¹³ His findings reveal that the single S-O or N-O bond that is not breaking during the process prevents any description of the transition state as pericyclic. Indeed, no evidence of electronic movement between the two heteroatoms, or change in bond length, prevents the formation of a transition state of aromatic character. The process can be described as pseudopericyclic, which merely describes it as a concerted process, in which a cyclic array of reactions occurs, without any intrinsic aromatic character bestowed to the transition state.

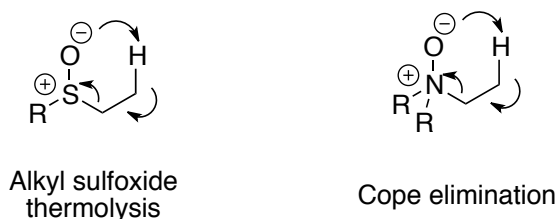
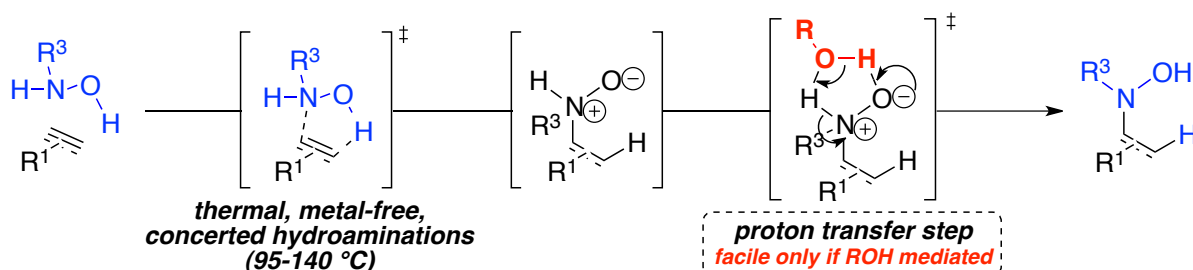


Figure 1.2 Similar mechanism of alkyl sulfoxides thermolysis and Cope elimination

¹³ Cubbage, J. W.; Guo, Y. G.; McCulla, R. D.; Jenks, W. S. *J. Org. Chem.* **2001**, *66*, 8722.

1.3.2 Beauchemin Group Efforts in the Cope-type Hydroamination

The Beauchemin group started further developing the Cope-type hydroamination for optimized intramolecular and intermolecular reactivity. An early observation saw polar protic solvents greatly improving the reactivity of intramolecular substrates and allowing access to interesting intermolecular reactions with a variety of substrates. We suggested that the benefits to the reactions were an indication that the proton transfer step was kinetically relevant to the overall process, and that the protic solvent could help in mediating such a transfer (Scheme 1.7). This was supported by DFT calculations showing that a bimolecular proton transfer would be heavily favored over a unimolecular one (this will be revisited in more details in Chapter 4).

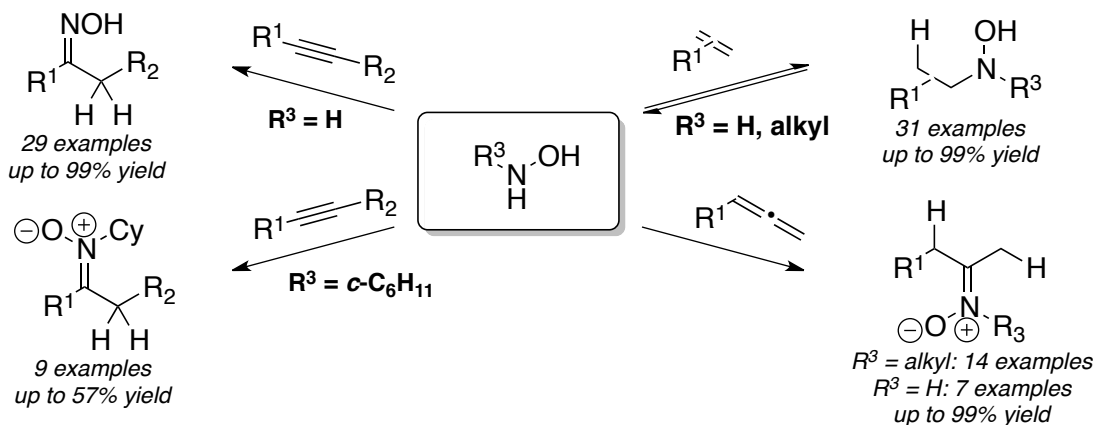


Scheme 1.7 Reasoning for the increased reactivity observed in alcoholic solvents.

This initial discovery of optimal conditions helped the intermolecular reactions of hydroxylamines with a wide variety of alkenes, alkynes and allenes, accessing a variety of oxime, nitron and hydroxylamine products.¹⁴ The reactivity of alkynes and allenes proved general, and gave Markovnikov products efficiently across a variety of substrates, typically

¹⁴ (a) Moran, J.; Pfeiffer, J. Y.; Gorelsky, S. I.; Beauchemin, A. M. *Org. Lett.* **2009**, *11*, 1895. (b) Lebrun, M.-E.; Pfeiffer, J. Y.; Beauchemin, A. M. *Synlett* **2009**, 1087. (c) Bourgeois, J.; Dion, I.; Cebrowski, P. H.; Loiseau, F.; Bédard, A.-C.; Beauchemin, A. M. *J. Am. Chem. Soc.* **2009**, *131*, 874. (d) Moran, J.; Gorelsky, S. I.; Dimitrijevic, E.; Lebrun, M.-E.; Bédard, A.-C.; Séguin, C.; Beauchemin, A. M. *J. Am. Chem. Soc.* **2008**, *130*, 17893. (e) Pathmalingam, T.; Gorelsky, S. I.; Burchell, T. J.; Bédard, A.-C.; Beauchemin, A. M.; Clérac, R.; Murugesu, M. *Chem. Commun.* **2008**, 2782. (f) Cebrowski, P. H.; Roveda, J.-G.; Moran, J.; Gorelsky, S. I.; Beauchemin, A. M. *Chem. Commun.* **2008**, 492. (g) Beauchemin, A. M.; Moran, J.; Lebrun, M.-E.; Séguin, C.; Dimitrijevic, E.; Zhang, L.; Gorelsky, S. I. *Angew. Chem., Int. Ed.* **2008**, *47*, 1410.

requiring heating to temperatures of 95 – 110 °C. However, the reaction of alkenes proved limited to biased substrates, such as norbornene or styrene based alkenes. These last results seemed particularly in line with the known thermoneutrality problems of the intermolecular hydroamination of alkenes, and proposed solutions to the problem will be the main focus of the next section of the thesis (Chapter 2).



Scheme 1.8 Summary of reactivity for the Cope-type hydroamination of hydroxylamines

1.4 Hydroxylamines vs. Hydrazines

Hydrazines and their derivatives serve as a nice contrast to hydroxylamines as starting materials, while still being similar enough to have the potential to participate in the Cope-type hydroamination. A simple look shows different pKas for hydrazines, activated hydrazines (through the presence of EWG or acid activation) compared to hydroxylamines (Figure 3.2). These, combined with varying strength in the nucleophilicity of the main nitrogen (to be involved in the C-N bond formation), are potentially indicative of a wide range of avenues for the activation of the reaction, and its potential catalysis.

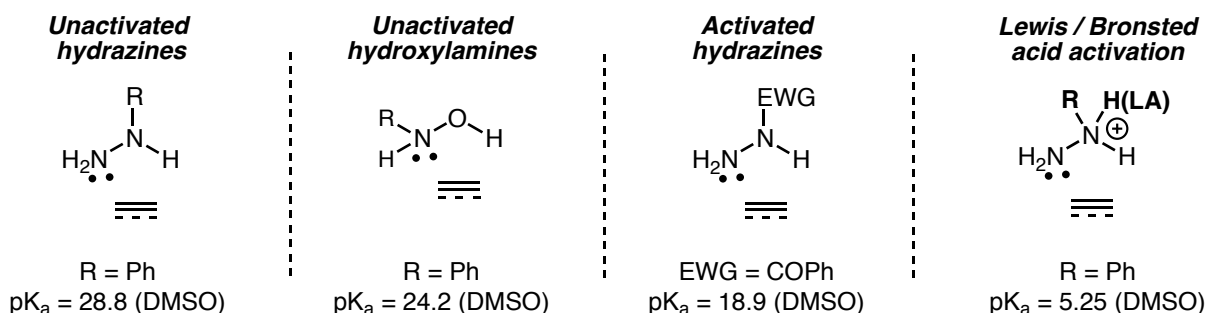


Figure 1.3 Comparison of the pK_a of hydroxylamines to the different forms of hydrazines to be used in the Cope-type hydroamination

Throughout this thesis, we will be discussing hydroamination of alkenes and alkynes, for applications in intramolecular and intermolecular systems. With the Cope-type hydroamination as our preferred strategy to access formally hydroaminated products, hydroxylamine and hydrazine based starting materials will be a constant requirement. These motifs can be conserved or transformed into standard amine products post-reaction. A quick analysis of these functionalities, from reactivity and application standpoints, will offer us perspectives on the implications of using these reagents.

1.4.1 Structural Characteristics of Hydroxylamines

Hydroxylamines (R₂NOH) are characterized by a core made of an oxygen atom bound to a nitrogen atom possessing an unshared pair of electrons. Though less basic than related amines (due to the presence of an electronegative oxygen neighbor), hydroxylamines' nitrogen centers are better nucleophiles, as they can benefit from a significant α-effect from the same neighboring oxygen. With two adjacent groups of some basicity, they also complex well to a variety of metals; a fact responsible for many of the traditional failures in catalyzing the Cope-type hydroamination.

Hydroxylamines are known to be fairly reactive compounds, particularly capable of easily forming radicals and undergoing red-ox processes. This relative reactivity creates

stability issues in many hydroxylamines to be used in processes as reagents. Notoriously, primary hydroxylamines have a strong tendency to oxidize to their oxime counterparts, and this side reaction is favorable in alcoholic solvents.¹⁵

1.4.2 General Uses of Hydroxylamines and Derivatives

Due to the known toxicity of the simple hydroxylamines, due in great part to the aforementioned high chemical reactivity of the compounds, hydroxylamines are seldom used in medicinal and industrial processes. Though not always inherently toxic, the biodegradation of hydroxylamines is in itself cause for concern, since many their known metabolites are themselves considered toxic.

Nevertheless, isolation of hydroxylamine intermediates in several biological systems has opened slight prospects for the potential therapeutic uses of hydroxylamines.¹⁶ An increasing number of N-OH containing compounds, notably *N*-hydroxy- α -amino acids, are found to be bioactive against several diseases, on top of recognized potential as an anti-oxidant. With a better understanding of the N-OH bond within biological system, there remains a potential for hydroxylamine-based therapeutic targets.

1.4.3 Structural Characteristics of Hydrazines & Derivatives

Hydrazine (NH₂NH₂), the simplest diamine compound, has physical properties that are reminiscent of the isoelectronic hydroxylamine. Like the latter, it is hygroscopic and highly energetic. In its anhydrous form can undergo explosive thermal decomposition, and as such

¹⁵ For more the instability of primary hydroxylamines: (a) Ghosh, A. K.; Gong, G. *Org. Lett.* **2007**, *9*, 1437. (b) Horiyama, S.; Suwa, K.; Yamaki, M.; Kataoka, H.; Katagi, T.; Takayama, M.; Takeuchi, T. *Chem. Pharm. Bull.* **2002**, *50*, 996.

¹⁶ Ashani, Y. and Silman, I. "Hydroxylamines and oximes: Biological properties and potential uses as therapeutic agents", in *The chemistry of Hydroxylamines, Oximes and Hydroxamic Acids*, 4th edn, vol 13, John Wiley & Sons, New York, 1995.

has found limited commercial applications outside of its use as a rocket propellant. It is commercially available as its hydrate form, in aqueous solution varying from 35 to 64 wt.%.¹⁷

Hydrazines and alkyl hydrazines are slightly weaker bases than their ammonia and amine counterparts, but have two nucleophilic nitrogens and up to four replaceable hydrogens, paving the way to a variety of different potential substituted derivatives. Several methods for the synthesis of alkyl-substituted hydrazines have difficulty in producing a single product, with mixtures of mono and poly-substitution usually occurring. This makes the range of commercially available alkylhydrazines rather anemic, and fairly expensive.

Hydrazides (N-Acylhydrazines) & Analogs

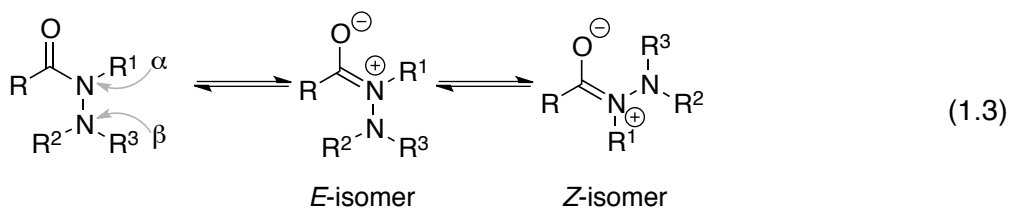
The most frequently encountered derivatives of hydrazine are hydrazides (*N*-acyl hydrazines). With the first members of the family mentioned as far back as 1850,¹⁸ hydrazides have developed into a large family of versatile reagents and end products, with an increasing number commercially available. They offer a wide array of directions that can be taken for their selective functionalization, making them more prominent than simple alkylhydrazine as source material for chemical synthesis. They are of an impressive stability to air and thermal decomposition.

Hydrazides, like their amide counterparts, possess a N–CO bond that has partial double bond character, making the amide-like nitrogen (N^{α}) essentially sp^2 , causing a hindered rotation around that bond, and resulting in two possible conformers possible for all hydrazides (eq. 3.2). In most cases when the hydrazide is poly-substituted, the *E*-isomer is

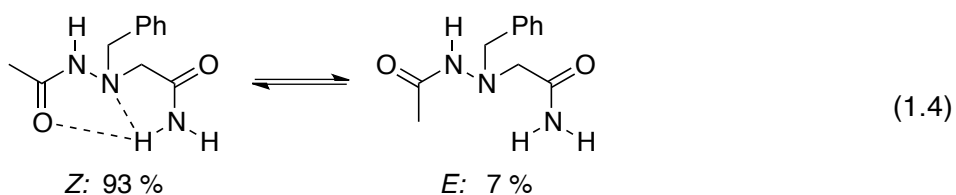
¹⁷ Hydrazine and its Derivatives, in *Kirk-Othmer Encyclopedia Chemical Technology*, 4th edn, vol 13, John Wiley & Sons, New York, 1995.

¹⁸ K. Schöfer, S. Schwan, *J. Prak. Chem.* **1850**, 51, 185.

avored, for both steric and electronic reasons that were first suggested by Knapp, and later evidenced in several studies by Licandro and Perdicchia, as well as Parsons.¹⁹



Electronic repulsion of the distal nitrogen (N^β) and the carbonyl respective lone pairs, along with minimization of 1,3-allylic strain from substituents on N^β , destabilize the *Z*-isomer and hence favor the presence of the *E*-isomer. Increased substituent size on N^β can overcome the electronic effect and force a large portion of the compound to adopt the *Z* conformation. Hydrogen bonding between the carbonyl and some close or distal H-bonding moiety, for example with mono-substituted hydrazides or with modification further on the substituents, can affect these ratios, and also favor the *Z*-isomer. That is notably the case in hydrazide-based peptide analogs described by Roisnel & Potel,²⁰ in which NMR and X-ray data showed that substitution by a free amide on N^β allowed for hydrogen bonds to form with both N^β and the hydrazide carbonyl.



Several compounds have a structure similar to hydrazides and serve as analogs in a variety of applications. Notably, phosphohydrazides, thiohydrazides, semicarbazides,

¹⁹ (a) Knapp, S.; Toby, B. H.; Sebastian, M.; Krogh-Jespersen, K.; Potenza, J. A. *J. Org. Chem.* **1981**, *46*, 2490. (b) F. Ghelfi, A. F. Parsons *J. Org. Chem.* **2000**, *65*, 6249. (c) Licandro, E.; Perdicchia, D. *Eur. J. Org. Chem.* **2004**, 665.

²⁰ Le Grel, P.; Salaün, A.; Mocquet, C.; Le Grel, B.; Roisnel, T.; Potel, M. *J. Org. Chem.* **2011**, *76*, 8756.

thiosemicarbazides and sulfonyl hydrazides (Figure 3.3) all possess a carbonyl equivalent and could serve as bifunctional reagents in hydroamination using hydrazine-based reagents.

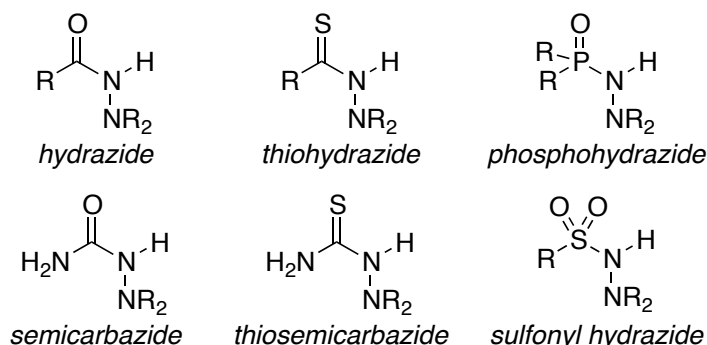


Figure 1.4 Hydrazide analogs as potential reagents for Cope-type hydroamination

1.4.4 General Uses of Hydrazines and Derivatives

Uses of Hydrazines and Alkylhydrazines

The availability of simple monosubstituted hydrazine derivatives has stimulated intense research and led to applications in agriculture (pesticides), polymer chemistry, photographic products and pharmaceuticals (Figure 1.5).²¹ The rich chemical reactivity known from hydrazines originates from the relative instability of the starting materials. The ease of cleavage of the weak N-N bond and the ability to eject nitrogen gas (N₂) from substrates containing hydrazines are responsible for many synthetic applications. These include the Fischer indole synthesis (N-N bond cleavage),²² along with the Wolff-Kishner reduction, Bamford-Stevens reaction and Shapiro reaction (decomposition releasing N₂).²³ While some alkylhydrazines or phenylhydrazines used commercially over the last century

²¹ Ragnarsson, U. *Chem. Soc. Rev.* **2001**, 30, 205.

²² For recent applications of the Fischer indole synthesis: (a) Maruoka, K.; Oishi, M.; Yamamoto, H. *J. Org. Chem.* **1993**, 58, 7638. (b) Cao, C.; Shi, Y.; Odom, A. L. *Org. Lett.* **2002**, 4, 2853. (c) Wagaw, S.; Yang, B. H.; Buchwald, S. L. *J. Am. Chem. Soc.* **1999**, 121, 10251.

²³ (a) Hutchins, R. O.; Hutchins, M. K. *Comp. Org. Syn.* **1991**, 8, 327. (b) Adlington, R. M.; Barrett, A. G. M. *Acc. Chem. Res.* **1983**, 16, 55.

are still in use today, a vast number of compounds have either been banned or removed from the market due to toxicity concerns.

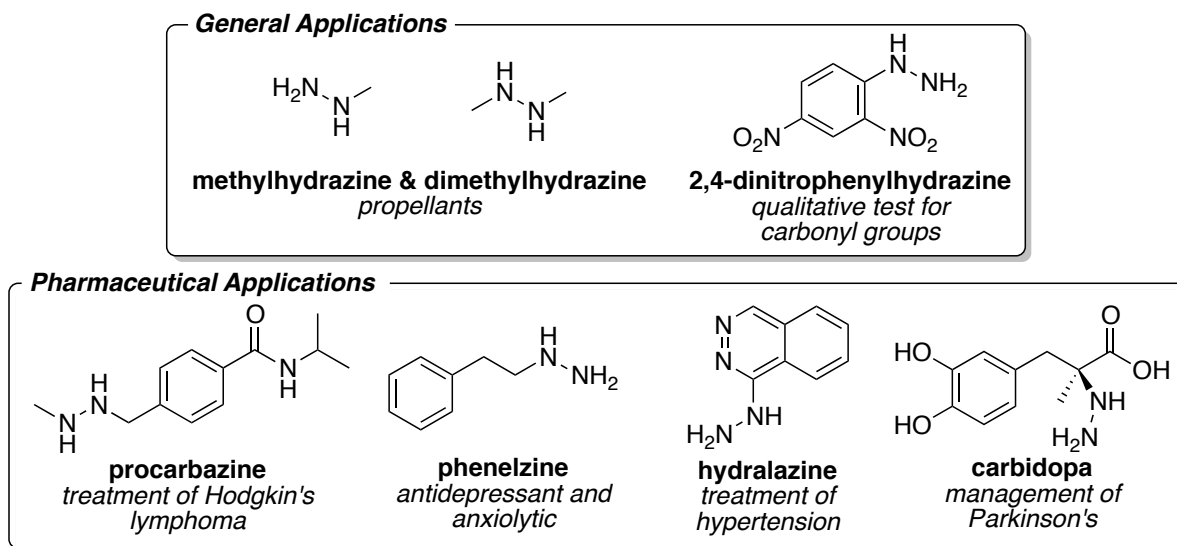


Figure 1.5 Selected examples of the hydrazine motif for general and medical applications

Uses of Hydrazides and Derivatives

Amongst a large variety of uses, hydrazides are notably involved in the synthesis of heterocycles, dyestuffs, photographic products (e.g. phenidone, a developer, Figure 1.6) and polymers, as well as in the fields of agriculture (e.g. daminozide, a plant growth regulator) and forensics (luminol, a chemiluminescent material upon oxidation).

Hydrazides are also embedded within a large number of pharmaceutical targets, and in several marketed products. They can be considered aza-amino acids, and hence have notable use in peptidomimetics (azapeptides).²⁴ Other pharmaceutical applications (shown in Figure 1.6) most often include mono-substituted or less often di-substituted hydrazides (e.g. clopamide, indapamide).

²⁴ For a review, see: Gante, J. *Synthesis* **1989**, 405.

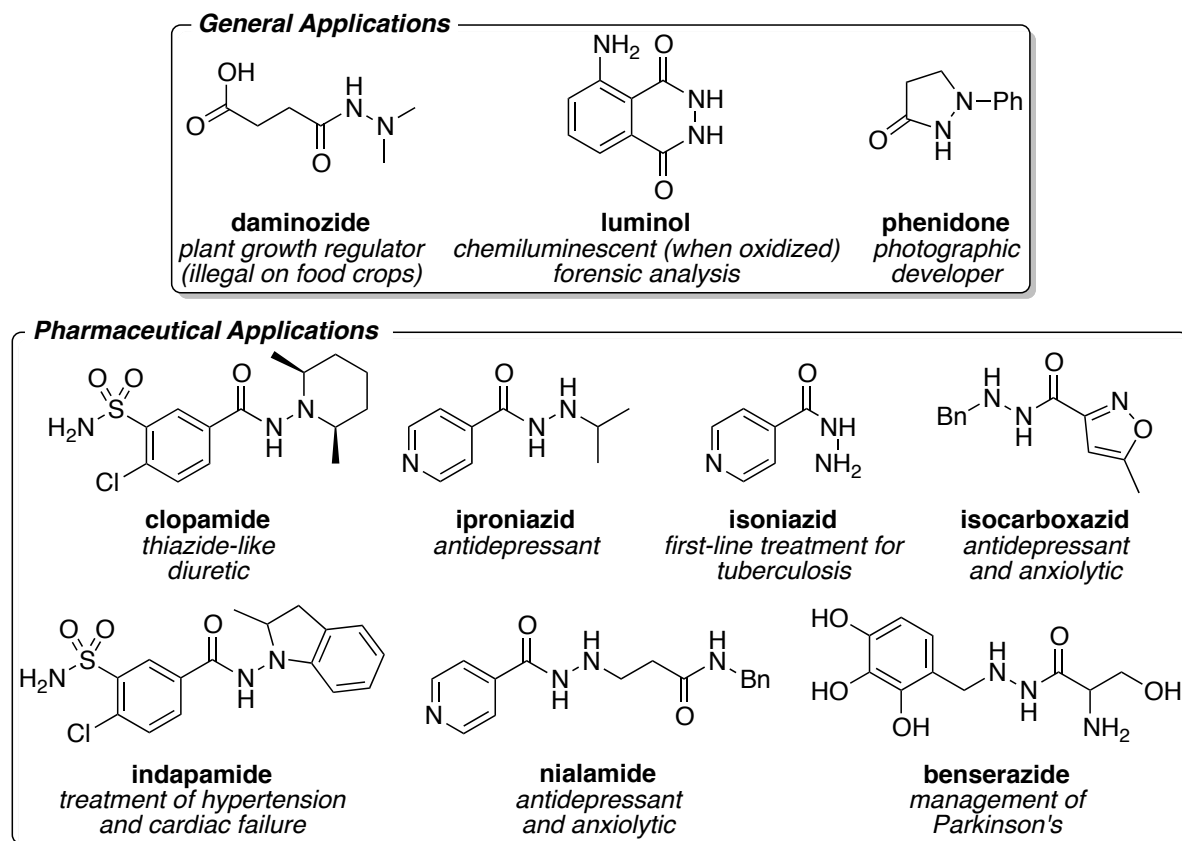


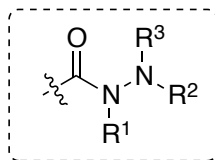
Figure 1.6 Selected examples of the hydrazide motif for general and medical applications

A careful look at the National Institutes of Health Small Molecules Repository (NIH – SMR), which contains a wealth of small molecules available for high throughput screening, reveals that the hydrazides are privileged compounds. Close to ten thousand members with the hydrazide core embedded that have yielded positive bioassays (Table 1.1).²⁵ Separating into the various substitution patterns that are available to hydrazides (non-, mono-, di- and tri-substituted) reveals that all members of the family can be of significance, with thousands of bioactivity screening hits surfacing for di- & tri-substituted hydrazides. This is especially

²⁵ Data was compiled from the NIH pubchem compound database on June 12th, 2012 (<http://www.ncbi.nlm.nih.gov/pccompound>). Search parameters included the desired hydrazide subcategory and required hits being present in the SMR database and having at least one active bioassay report. Numbers shown for each subcategory include described hydrazides, and variations in substitution (when not a hydrogen) require only a carbon as the first atom. Hydrazones are excluded from all results, while several standard structures that include hydrazide cores (ex: N,N'-diacylhydrazines – 2680 hits; pyrazolin-3-one – 1246 hits for all substitutions combined) are included.

noteworthy when one considers the relative difficulty in synthesizing poly-substituted hydrazides and their relatively low commercial availability.²⁶

Table 1.1 Number of bioactive structures (NIH Small Molecule Repository) containing the hydrazide subunit, sorted by substitution pattern.



Substitution	R ¹	R ² & R ³	Number of Active Hits (NIH SMR)
non-substituted	H	H & H	445
mono-substituted	{ subst. H	{ H & H H & subst.	{ 215 5181
di-substituted	{ subst. H	{ H & subst. 2 x subst.	{ 1597 1223
tri-substituted	subst.	2 x subst.	1166
any substitution	---	---	9708¹

¹ NIH SMR: National Institutes of Health, Small molecule repository. ² This number includes compounds containing more than one type of hydrazide.

1.4.5 Potential Use of Hydroxylamines vs. Hydrazines as End Products

Though both of their specific chemical reactivity will be compared at several points in this thesis, it is worth noting the difference in actual applicability of the direct products obtained from the Cope-type hydroaminations of hydroxylamines and hydrazine derivatives.

With their limited uses as pharmaceutical targets, it is understood that Cope-type hydroaminations performed with hydroxylamines would generally be followed for most practical purposes by a cleavage of the N-O bond, to generate the free amine. Thankfully, breaking the N-O bond²⁷ is generally easy and high yielding, and can be performed using a

²⁶ For example, while over two thousand compounds containing the hydrazide core are available from commercial sources, only fifteen are trisubstituted. Data obtained from searches of the emolecules database on June 12th, 2012.

²⁷ Two preferred methods used by our group are Pd catalyzed hydrogenation of the N-O bond, as seen in: ElAmin, B.; Anantharamaiah, G. M.; Royer, G. P.; Means, G. E. *J. Org. Chem.* **1979**, *44*,

variety of conditions. The most common cleavage is a simple zinc / HCl reduction that is amenable to most syntheses bearing previous protection of acid labile groups.

On the other hand, hydrazines and hydrazides are more stable and have found applications in a variety of chemical industries. N-N bond cleavage can also be performed, albeit not as easily as with N-O bonds, and Chapter 3 will go into the more difficult aspects of such a transformation. The Cope-type hydroamination using hydrazine derivatives will be seen shortly to be more difficult to achieve than that of hydroxylamines. It will be important, when assessing the potential of the technique, to consider the process as providing hydrazines of increasing substitution and complexity.

3442; and Zn/AcOH based cleavage: Le Bourdonnec, B.; Goodman, A. J.; Michaut, M.; Ye, H-F.; Graczyk, T. M.; Belanger, S.; Herbertz, T.; Yap, G. P. A.; DeHaven, R. N.; Dolle, R. E. *J. Med. Chem.* **2006**, *49*, 7278.

2

Cope-type Hydroamination with Hydroxylamines – Cascade Reactions

This chapter will present in more detail the thermodynamic problems associated with the intermolecular hydroaminations of alkenes, before displaying different cascade reactions developed to overcome the thermoneutrality of the reaction, and favor the higher yielding and cleaner hydroaminations.²⁸ The application of the developed methodologies to the total synthesis of alkaloids in key hydroamination steps will be highlighted.

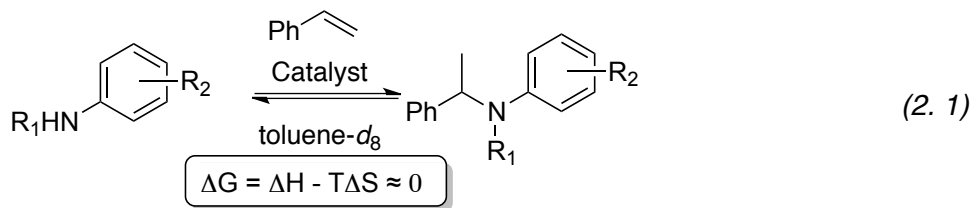
2.1 Introduction

Throughout the development of any synthetic methodology, one always aims for efficient transformations, accompanied by a wide scope of applicability, and mild reaction conditions. The Cope-type hydroamination was shown in Chapter 1 to be applicable to amination of alkynes and allenes in both intra and intermolecular systems, and to alkenes in intramolecular systems. Simple alkenes are some of the most available and affordable starting materials, and the lack of reactivity towards them with intermolecular hydroamination remains problematic, for this Cope-type approach as well as other hydroaminations methodologies.

²⁸ The term cascade reaction will be used to describe multiple-step reactions occurring one-pot, without the need for addition of extra reagents as the reaction proceeds. The same processes could also be classified as “domino”, “tandem” or “sequential” reactions. For a discussion of the nomenclature of cascade reactions, see: Nicolaou, K. C., Edmonds, D. J. and Bulger, P. G. *Angew. Chem. Int. Ed.* **2006**, *45*, 7134. *Note*: Our original publication described the overall process as a tandem sequence.

2.1.1 Thermodynamic Neutrality in Hydroaminations of Alkenes

The thermodynamic problem of hydroamination of alkenes was not always common knowledge. Many reviews over the past few decades have mentioned the simple hydroamination of alkenes to be favored, although such assumptions were not backed by any quantitative thermodynamic results.²⁹ Ultimately Hartwig reported in 2006 experimental values for the hydroamination of styrene with aniline, from measured equilibrium constant for the reaction performed at 80 °C (Eq. 2.1).³⁰ The results showed that the reaction was favored in terms of enthalpy, but rendered thermoneutral due to a large negative entropic term. His measured values showed that steric hindrance and substituents could heavily influence those numbers. Still, it was apparent that the reactivity could be problematic for standard hydroaminations of simple, unbiased alkenes, potentially explaining in part our limited scope with the intermolecular Cope-type hydroamination.



2.1.2 Thermoneutrality in the Cope-type Intermolecular Hydroamination

Though this arguably distant system showed the potential thermoneutrality for the reaction, we became interested in having insight of our own, to see if they could add support to our experimental observations that hydroxylamines are difficult reagents for intermolecular reactions with alkenes, and confirm that those difficulties arise from the same problem as

²⁹ (a) Beller, M.; Breindl, C.; Eichberger, M.; Hartung, C. G.; Seayad, J.; Thiel, O. R.; Tillack, A.; Trauthwein, H. *Synlett* **2002**, 1579. (b) Müller, T. E.; Beller, M. *Chem. Rev.* **1998**, *98*, 675.

³⁰ Johns, A. M.; Sakai, N.; Ridder, A.; Hartwig, J. F. *J. Am. Chem. Soc.* **2006**, *128*, 9306.

those in other systems.³¹ Density functional theory (DFT) calculations were performed in collaboration with Dr. Serge I. Gorelsky to map the potential energy surface of the reaction and to study more specifically the nature of both the hydroamination and proton transfer transition state structures.³²

Transition State Structure

Transition states for both alkenes and alkynes reacting with hydroxylamine have been computed. Shown in Figure 2.1 and Figure 2.2 are the expected transition state structures for norbornene, styrene and phenylacetylene. Calculations are consistent with both alkenes and alkynes going through a standard Cope-type 5-membered, planar transition state when reacting with hydroxylamine. In all cases, the formation of the new C-H bonds precedes formation of new C-N bond, consistent with the observed Markovnikov selectivity of the reaction. Reaction on norbornene is also shown to favor primarily the exo product.

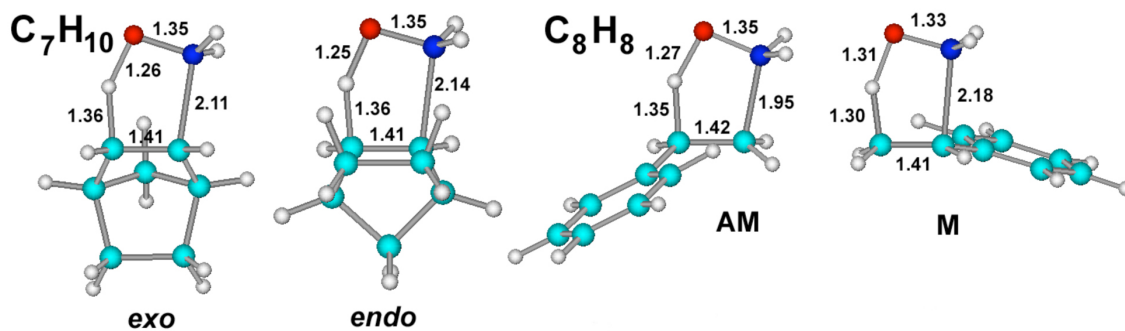


Figure 2.1 Transition state structures for the Cope-type hydroamination of NH_2OH with norbornene and styrene at the B3LYP/TZVP level of theory; M= Markovnikov, AM=anti-Markovnikov product. The internuclear distances (Å) are shown only for relevant chemical bonds.

³¹ Full details can be found in the supporting information of: Moran, J.; Gorelsky, S. I.; Dimitrijevic, E.; Lebrun, M.-E.; Bédard, A.-C.; Séguin, C.; Beauchemin, A. M. *J. Am. Chem. Soc.* **2008**, *130*, 17893-17906.

³² Although DFT calculations were made for all aspects of Cope-type reactivity, this section will focus primarily on those related to alkene hydroaminations.

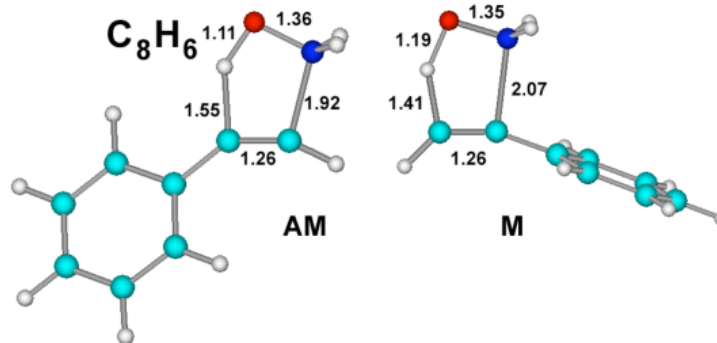


Figure 2.2 Transition state structures for the Cope-type hydroamination of NH_2OH with phenylacetylene at the B3LYP/TZVP level of theory; M= Markovnikov, AM=anti-Markovnikov product. The internuclear distances (\AA) are shown only for relevant chemical bonds.

Both the reactions of ethylene and acetylene, when analyzed in terms of Frontier Molecular Orbital Interactions in the hydroamination transition state, show similar dominant interactions, with the $\text{HOMO}_{\text{NH}_2\text{OH}}$ donating into the LUMO_{CC} and the HOMO_{CC} donating into the $\text{LUMO}_{\text{NH}_2\text{OH}}$ (Figure 2.3). These dominant interactions have two simultaneous charge transfers (Q) between the species at the transition state.³³ These offer an electronic-based support for why the use of more nucleophilic unsaturations and more substituted hydroxylamine can be beneficial to the reaction.

³³ For ethylene and hydroxylamine, $Q = 0.45 e^-$ mainly for the donation of nitrogen non-bonding electrons into the π^* orbital of the alkene, while $Q = 0.30e^-$ mainly for the donation of the electron density of the alkene into the $\text{OH } \sigma^*$ orbital. For acetylene and hydroxylamine, $Q = 0.40 e^-$ mainly from the donation of nitrogen non-bonding electrons into the π^* orbital of the alkyne, while $Q = 0.17e^-$ mainly from the donation of the electron density of the alkyne into the $\text{OH } \sigma^*$ orbital.

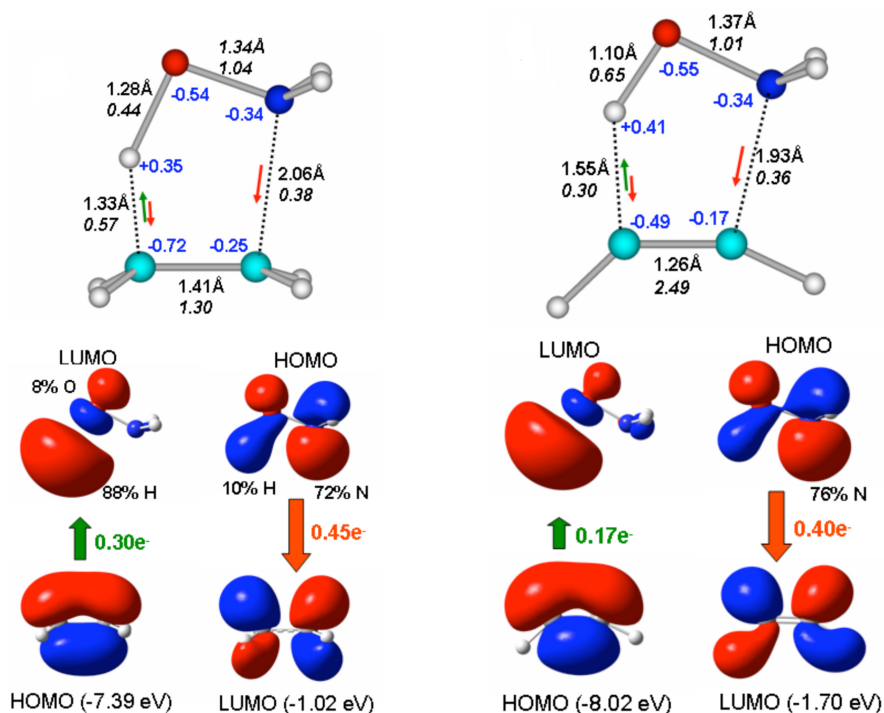


Figure 2.3 (Top) The transition states for hydroamination of ethylene and acetylene showing the internuclear distances and bond orders (*Italics*) and NPA charges (blue). (Bottom) Major donor-acceptor interactions that contribute to bond formation between the unsaturation and the hydroxylamine. The charge transfer Q for each interaction is shown in green and orange.

Potential Energy Surface for Alkenes and Alkynes

We have seen from the previous sets of calculations that the mechanism and dominant interactions for both alkene and alkyne hydroaminations are similar. Allenes show similar results in DFT calculations. A look at the potential energy surfaces for the reactions, which compute the estimated free energy associated with each species along reaction coordinates, is key to identifying why alkenes are not the ideal reaction partners for the intermolecular Cope-type hydroamination.

Summarized in Table 2.1 are the free energies in the reactions of ethylene, styrene, acetylene and phenylacetylene with hydroxylamine (evaluated at 298 K and 1 atm).³⁴ Similar

³⁴ Though calculated, the free energies of the AM pathways, which are unfavorable both with alkyne and alkenes, are not shown for styrene and phenylacetylene.

computed values the reactants complex and hydroamination transition state energy for alkynes and alkenes show that the concerted mechanism is indeed similar between the two reactions, and can occur in at similar temperatures (~ 100 °C). However, the large difference between that stability of the products formed and their relative starting materials reveals in the case of alkynes (-33.4 to -39.4 kcal/mol) a thermodynamically favored process. Alkene hydroamination products are shown to have about the same energy as the free reactants. This is in support of Hartwig's claim that intermolecular alkene hydroaminations, which we can now reasonably extend to include our Cope-type process, are nearly thermoneutral.

Table 2.1 Free energies (kcal/mol) of the reaction species for hydroamination reactions (NH₂OH) with alkenes and alkynes. The energies are relative to the free reactants.

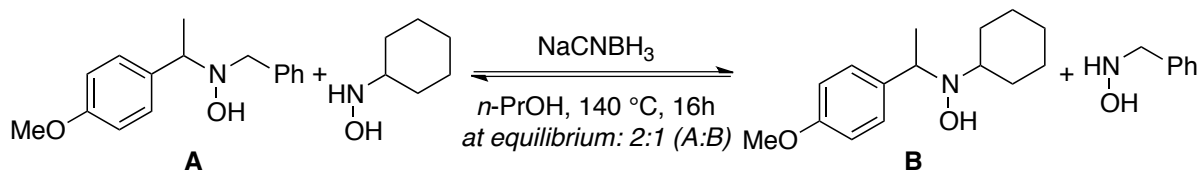
Species	Alkenes		Alkynes	
	CH ₂ CH ₂	PhCHCH ₂ M	HCCH	PhCCH _M
RC ^a	5.1	5.9	4.5	5.6
Hydroamination TS	33.2	33.4	28.5	30.1
N-oxide	13.9	18.7	2.9	8.7
Intramolecular H ⁺ tr. TS	38.3	44.2	23.6	30.1
Bimolecular H ⁺ tr. TS ^b	20.9	25.7 ^c	7.9	13.7 ^c
R-NHOH	-6.4	-0.5	-24.2	-17.2
C=N-OH	---	---	-39.2	-33.4

^a Reactants complex. ^b the transition state for proton transfer between R-NH + O⁻ and i-PrOH. ^c The energy of the transition state was evaluated using the calculated activation free energy for the proton transfer for the C₂H₅-NH₂O...i-PrOH complex (to form C₂H₅-NHOH...i-PrOH) for alkenes and the C₂H₃-NH₂O...i-PrOH complex (to form C₂H₃-NHOH...i-PrOH) for alkynes (7.0 kcal/mol and 5.0 kcal/mol in vacuum, respectively and 9.7 kcal/mol and 7.5 kcal/mol in methanol).

Crossover Experiments to Test Thermoneutrality

Crossover experiments were also designed, to accompany DFT calculations and confirm that the Cope-Type hydroamination of vinyl arenes is indeed under thermodynamic control. In Scheme 2.1, we can see the reaction of a hydroamination product (**A**) at 140 °C in a sealed tube in the presence of one equivalent of *N*-cyclohexylhydroxylamine and

NaCNBH₃. After 16 h, 37% of a crossover product (**B**) was detected in the unpurified reaction mixture by ¹H NMR spectroscopy.



Scheme 2.1 Crossover experiment to test that the Cope-type hydroamination of alkenes is under thermodynamic control.

2.1.3 Concept of Cascade Reactions

Overcoming the challenges associated with the thermoneutrality the Cope-type hydroaminations of alkenes became central to our research early in the investigation of intermolecular reactivity. In line with the observed thermoneutrality, the reaction is fundamentally bimolecular in the forward direction, yet forms a sole product, effectively giving the reaction a negative entropy term. From the Gibbs free energy (Eq. 2.2), we see that this also translates into an impossibility to favor the desired reaction through an increase in temperature, which would effectively worsen the impact of the entropy term on the system.

$$\Delta G = \Delta H - T\Delta S \quad (2.2)$$

Catalysis, often thought of as a solution for difficult reactions, can ultimately be of little help to processes where the starting materials and products have the same energies. As the thermodynamics of the system dominate, an equilibrium will eventually be attained in that the catalyst will favor both processes equally (Figure 2.4). We were drawn to cascade reactions to address thermodynamic neutrality of the reaction. They involve adding an extra exergonic step to convert the initial product into a more stable one.

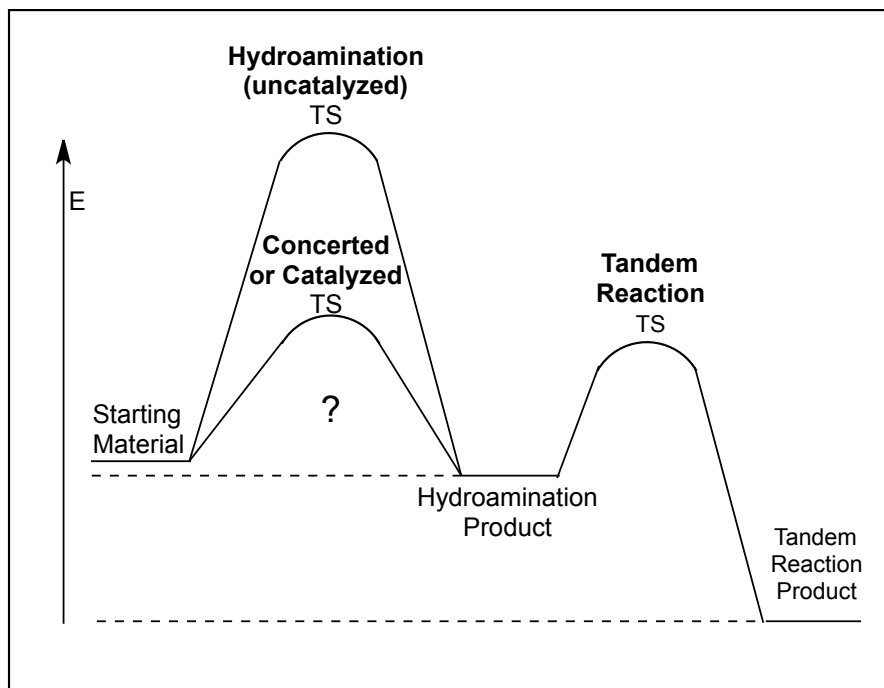
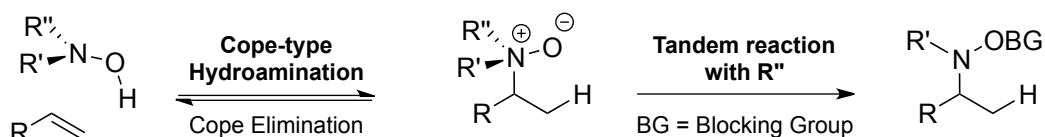


Figure 2.4 Schematic representation of the overall thermodynamic effects of concerted or catalyzed reaction on the reaction, vs. the use of cascade reactions.

Applied to intermolecular hydroaminations, this concept translates into a need for a second step in which the newly formed *N*-oxide intermediate can further be transformed. In a reaction different from a simple proton transfer, it can be made to form a stable formal hydroamination product (Scheme 2.2), “blocked” into a thermodynamic sink and prevented from reverting back to the dipolar intermediate.

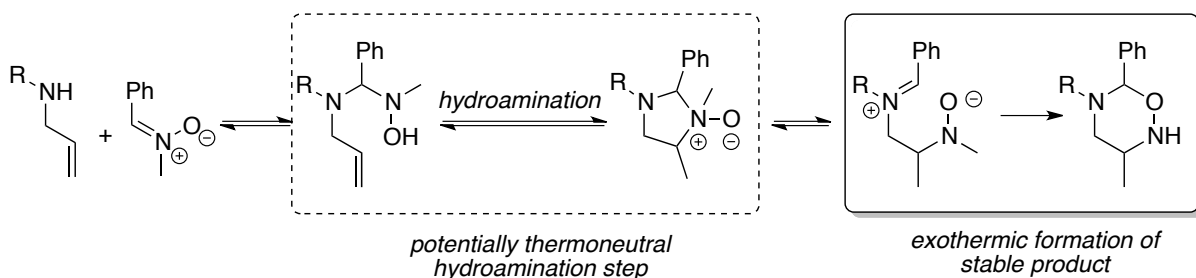


Scheme 2.2 Concept of the cascade reaction to address thermodynamic neutrality.

An illustrative example of how such a cascade could work comes from the work of Knight.³⁵ They presented an intramolecular hydroamination where the intermediate dipole

³⁵ (a) Gravestock, M. B.; Knight, D. W.; Thornton, S. R. *J. Chem. Soc., Chem. Commun.* **1993**, 169.
 (b) Gravestock, M. B.; Knight, D. W.; Abdul Malik, K. M.; Thornton, S. R. *J. Chem. Soc., Perkin*

can be forced, through reaction design, to undergo a second process, in which aminal opening and subsequent closure allows the formation of more stable oxadiazine.³⁶



Scheme 2.3 Example of a cascade reaction, the last step showing the favorable formation of a 6-membered cyclic aminal.

An ideal cascade reaction would meet multiple primary requirements. It would effectively, as mentioned, provide a driving force to irreversibly transform the initial hydroamination adduct into a more stable product, solving the thermodynamic problem of the Cope-type hydroamination. It should have a wide scope of reactivity, being able on one side to undergo the hydroamination cascade reaction with various initial hydroxylamines, themselves reacting on a wide variety of alkenes, especially non-strained or potentially non-terminal ones, while being tolerant of a maximum of other functional groups in the substrate. Finally, the cascade reaction products should be easily converted to free hydroxylamines or amines through easy, reliable transformations.

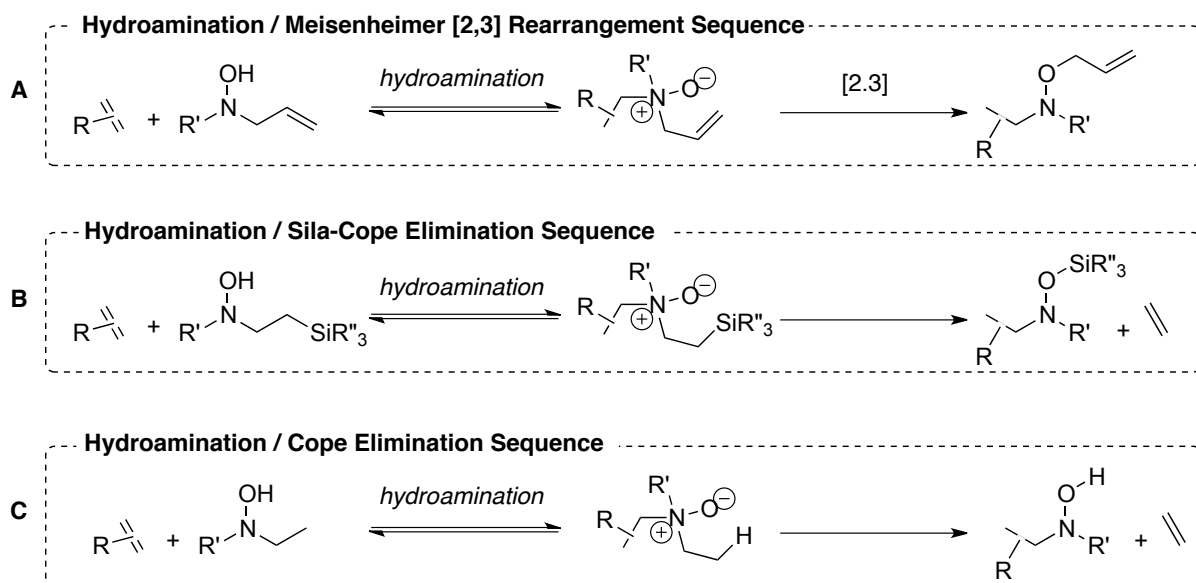
The use of the cascade reactions also has a few other potential advantages. The starting materials would now be di-substituted amines that have an initial nucleophilicity and stability greater than that of mono-substituted hydroxylamines. With primary hydroxylamines having substantial degradation potential in the polar protic solvents used in Cope-type hydroaminations, the extra substitution can be of help in obtaining more efficient reactions.

Trans. 1 **2000**, 3292. (c) Bainbridge, N. P.; Currie, A. C., Cooper, N. J.; Muir, J. C.; Knight, D. W.; Walton, J. M. *Tetrahedron Lett.* **2007**, 48, 7782.

³⁶ Because the reaction is intramolecular and forming a 5-membered ring, it is important to note that it would have been favored thermodynamically regardless of a second step.

2.1.4 Planned Cascade Reactions

The use of various groups added onto a hydroxylamine starting material could promote desired cascade reactions. Among them, the use of the Meisenheimer rearrangement, the sila-Cope eliminations or even the Cope elimination could benefit the reaction (Scheme 2.4). In **(A)**, the [2,3]-rearrangement cascade could neutralize the charges in an effectively irreversible step. In **(B)**, the sila-Cope elimination could be driven by the hydroxylamine's oxygen affinity for the silicon atom and in this case also release a small alkene, effectively rendering the reaction entropically neutral, in contrast to the Meisenheimer cascade. This is also the case for **(C)**, in which the use of a Cope Elimination cascade would also solve the entropic aspects of the thermoneutral reaction.



Scheme 2.4 Proposed cascade reactions involving an initial Cope-type hydroamination followed by a Meisenheimer [2,3] rearrangement **(A)**, sila-cope elimination **(B)** or Cope elimination **(C)**.

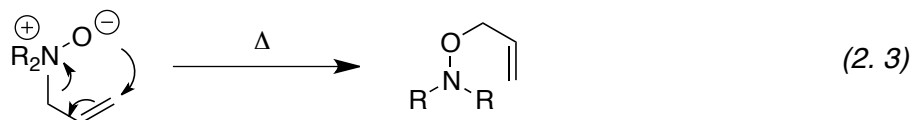
2.2 Cope-Type Hydroamination – Meisenheimer Rearrangement

Cascade Reaction

While looking specifically for reactions an *N*-oxide intermediate could take part in as the second step of the cascade, it is worthwhile looking into the intrinsic nature of the functional group, with a positive tetrahedral nitrogen connected to an oxyanion. We became interested in finding a mechanism by which one group can effectively switch from one end of the dipole to the other. [1,2] and [2,3]-Meisenheimer rearrangements thus became potential candidates to explore this reactivity.

2.2.1 Background on the Meisenheimer Rearrangement

Meisenheimer reported in 1919 the rearrangement of allyldialkylamine oxides and allylalkylaniline oxides to the corresponding *O*-allyl substituted hydroxylamines (Eq. 2.3) upon heating in aqueous sodium hydroxide.³⁷ Cope analysed the mechanism in 1949 and determined it featured a simultaneous formation of the C-O bond and breakage of the N-O bond, essentially going through an envelope-like cyclic five-membered transition state.³⁸ This [2,3] sigmatropic rearrangement was found to be favoured over a [1,2]-allyl shift.³⁹



Other mechanisms similar to the Meisenheimer rearrangements can also occur, with different groups shifting. Particularly, benzylic groups are well known for their [1,2]-

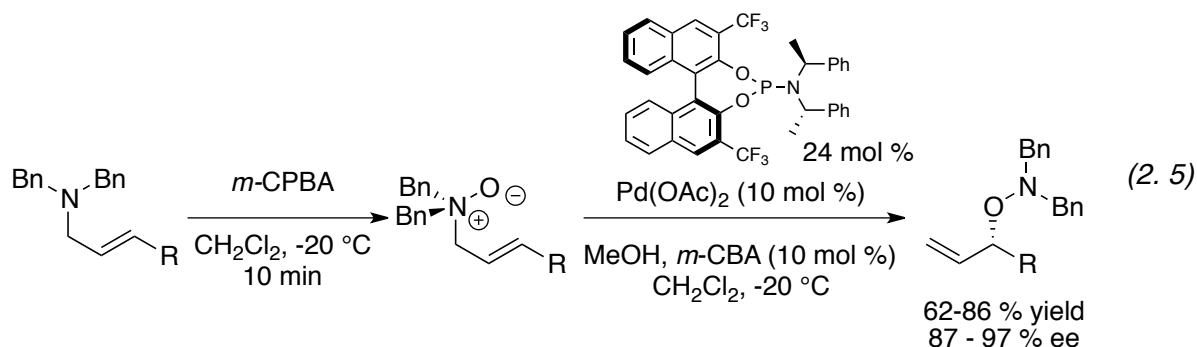
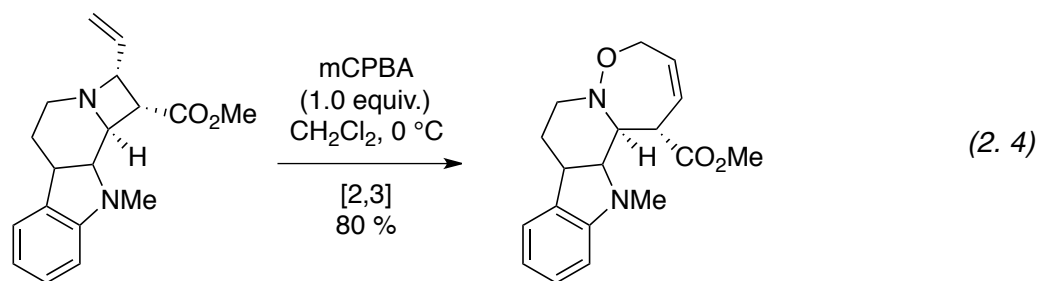
³⁷ Meisenheimer *Ber.* **1919**, 52, 1667.

³⁸ (a) Kleinschmidt, R.F.; Cope, A. C. *J. Am. Chem. Soc.* **1944**, 66, 1929. (b) Cope, A. C.; Towle, P. H. *J. Am. Chem. Soc.* **1949**, 71, 3423 and references therein.

³⁹ *Organic Synthesis*, Vol. 3; Trost, B. M.; Fleming, I., Eds.; Pergamon Press: New York, **1991**, 913–974. (c) Hoffman, R. W. *Angew. Chem., Int. Ed. Engl.* **1979**, 18, 563. (d) In *Organic Reactions*, Vol. 18; Pine, S. H., Ed.; Wiley: Hoboken, **1970**, 403. (e) Sweeney, J. B. *Chem. Soc. Rev.* **2009**, 38, 1027.

Meisenheimer rearrangements, and like their [2,3] counterparts, are known to necessitate no additives or special activation other than a thermal one. Many examples have shown how these rearrangements can be performed in cyclic and acyclic systems.⁴⁰

The [2,3]-Meisenheimer rearrangement can also be used in the context of total synthesis, even as a functionality-building tool. A representative example is that of the rearrangement of the azetidine (Eq. 2.4) that can, following the formation of an *N*-oxide with *m*-CPBA, rearrange to a 7-membered cycle with a hydroxylamine embedded in the structure. Of note is also the recent emergence of enantioselective variants of the reaction.⁴¹ An example is shown (Eq. 2.5), in which Tambar has demonstrated that an *N*-oxide can undergo the [2,3]-rearrangement enantioselectively, in the presence of a catalytic amount of palladium acetate and a chiral phosphine ligand.

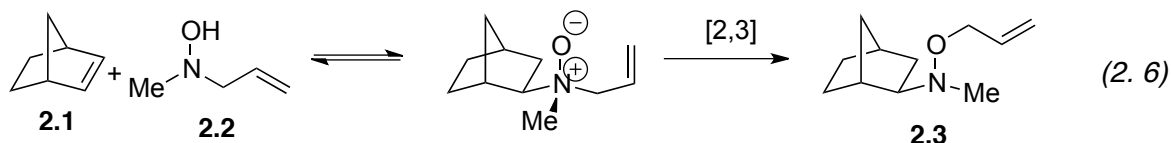


⁴⁰ (a) Johnstone, R. A. W. *Mechanisms of Molecular Migrations* **1969**, 2, 249. (b) Oae, S.; Ogino, K. *Heterocycles* **1977**, 6, 583. (c) Albin, A. *Synthesis* **1993**, 263.

⁴¹ For recent examples of catalytic enantioselective [2,3]-rearrangements, see: (a) Bao, H.; Qi, X.; Tambar, U. K. *J. Am. Chem. Soc.* **2011**, 133, 1206. (b) Bao, H.; Qi, X.; Tambar, U. K.; *Synlett* **2011**, 1789. (c) Murakami, M.; Katsuki, T. *Tetrahedron Lett.* **2002**, 43, 3947. (d) McNally, A.; Evans, B.; Gaunt, M. J. *Angew. Chem. Int. Ed.* **2006**, 45, 2116.

2.2.2 Initial Approach to Meisenheimer Rearrangement

Mr. Joffré Bourgeois worked at the early efforts towards the development of the cascade reaction.⁴² Intermolecular cascades were envisioned between norbornene and *N*-allyl-*N*-methylhydroxylamine (Eq. 2.5). Initially, encouraging conversions were obtained (~20-70%), at high concentration (1M), upon heating at high temperatures (110 – 130 °C, slightly higher than for regular intermolecular hydroamination) and over long time periods (1-3 days). Solvents of choice were observed to be PhCF₃ and THF.



However, it became quickly apparent that the cascade had several issues. Considerable decomposition could be observed at the reaction temperature used, increasing the complexity in purification of the products and affecting the overall yields. Such decomposition is partially attributed to the lability of the allyl group. Following careful isolation of some intermediates in the reaction, compound 2.4 was found in the reaction mixture, resulting from the hydroamination of the allylic portion of the product. Arguably many similar decomposition products could be formed with the forcing conditions used.

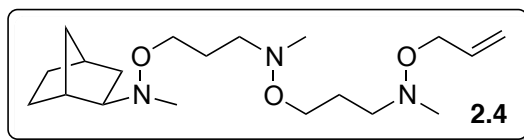
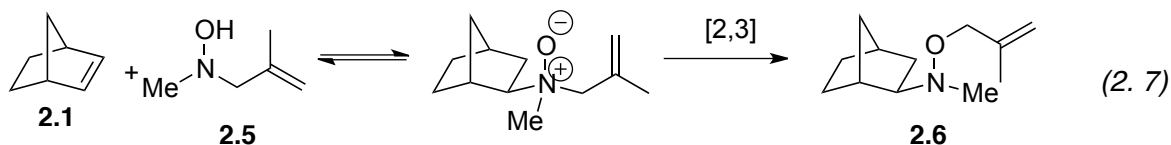


Figure 2.5 Example of a degradation product isolated from the original Meisenheimer cascade reaction.

⁴² Mr. Bourgeois worked with cascade reactions as part of his M.Sc. He established the early work with the allyl-substituted hydroxylamines, and later developed the major part of the scope for methallyl-substituted hydroxylamines. More details on the reactions discussed can be found in his thesis: Bourgeois, J. "Étude et développement de stratégies d'hydroaminations intramoléculaires et développement de la séquence tandem hydroamination de type Cope et réarrangement de Meisenheimer comme nouvelle stratégie pour les hydroaminations." M.Sc. Thesis, University of Ottawa, ON, 2009.

2.2.3 Results and Discussion

While these trials were performed, it was determined in the Beauchemin group that the use of a methallyl (2-methylallyl) substitution was more desirable than the allyl substitution on the nitrogen of the hydroxylamine. The hydroamination product can still undergo the Meisenheimer rearrangement (Eq. 2.7), but solves some of the aforementioned stability issues of products. The focus therefore had to shift to the synthesis of the methallylated hydroxylamines, which were not as easily synthesized as their allyl counterparts.

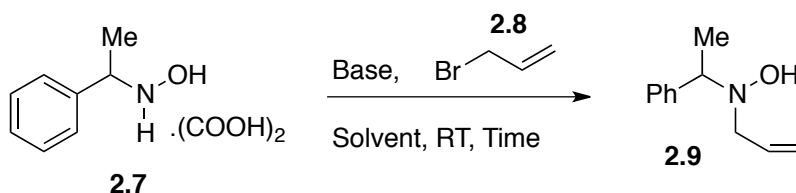


Optimization of N-methallylation Procedures

The use of 3-bromo-2-methylpropene was proposed for the *N*-methallylation, however, due to its quite expensive cost, the less reactive but more affordable 3-chloro-2-methylpropene was a desired precursor. However, it meant the synthetic methods previously used to synthesis the *N*-allylhydroxylamines could not be employed. While the formation of hydroxylamine precursor **2.5** was easy with methyl hydroxylamine, methallylation of any hydroxylamine containing larger alkyl group was challenging, giving initial yields below 10%.⁴³ It is worth noting that some standard *N*-allylation were also found to be quite difficult for more sterically hindered substrates such as hydroxylamine **2.7**, as shown in Table 2.2, and could benefit from improved synthetic methodologies.

⁴³ Dion, I.; Loiseau, F. *unpublished results*.

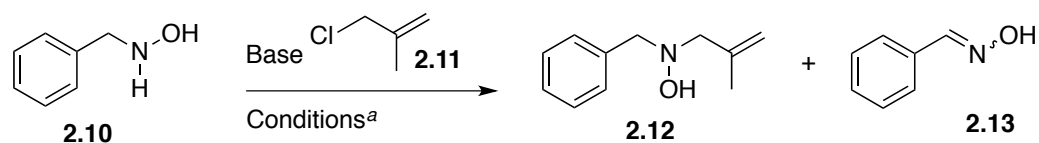
Table 2.2 Selected *N*-allylation test reactions for hydroxylamine **2.7**.



Entry	Allyl (equiv.)	Base (equiv.)	Solvent	Time (h)	Result
1	(5)	K ₂ CO ₃ (2)	THF	4	0%
2	(5)	K ₂ CO ₃ (2)	THF:DMF 5:1	4	~ 10% nmr yield
3	(1.2)	Et ₃ N (1.5)	THF	16	45% nmr yield
4	(1.2)	K ₂ CO ₃ (1)	THF	16	~ 40% nmr yield

Optimization of the and *N*-allylation and *N*-methallylation technique was therefore undertaken, for the benefit not only of the discussed project in intermolecular hydroaminations, but also of multiple ongoing projects in the lab (Cebrowski, Dion, Risk). *N*-Benzylhydroxylamine (**2.10**) was used as a substrate for the development of the reaction. Results in Table 2.3 show that the initial conditions using excess in various bases failed in providing precursors in sufficient quantities.

Table 2.3 Optimization of the methallylation of hydroxylamines.



Entry	2.11 (equiv.)	Base (equiv.)	Solvent	Temp (°C)	Time (h)	NMR Yield 2.12 (%) ^b	NMR Yield 2.13 (%) ^b
1	(1.2)	Et ₃ N (2.5) then K ₂ CO ₃ (3)	THF	reflux	24 then 5	traces	< 5 %
2	(5)	Et ₃ N (3)	THF	RT	24	0	major
3	(5)	DBU (3)	THF	RT	24	47	18
4	(5)	DBU (3)	THF:DMF 5:1	RT	24	45	20
5	(1.1)	DBU (3)	THF	RT	24	0	80
6	(3)	DBU (1.05)	THF	RT	24	traces	major
7	(3)	DBU (1.05)	THF	reflux	2.5	75	traces
8	(3)	DBU (1.05)	THF:DMF 5:1	reflux	2.5	> 95	traces

^a conditions: A: heated norbornene and hydroxylamine **2.10** (1 equiv.) in a sealed tube or stirred in r.b.f. at RT for desired reaction time. ^b ¹H NMR Yield, calculated based on styrene IS.

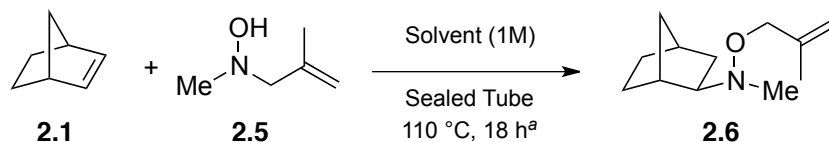
Oxidation of starting material is a significant secondary pathway for the reaction when performed at room temperature, or using large excesses of base. *N*-Methallylation was optimal with the use of DBU as base and heating at reflux for short reaction times. The conditions used to achieve a 95% NMR yield (entry 8) were found to be applicable to the synthesis of all *N*-methallyl hydroxylamines, and could be also used for effective *N*-allylation.

Scope of the reaction

Use of *N*-methallyl hydroxylamines in the cascade reaction proved rapidly to provide better yields and cleaner reactions than the previous *N*-allyl variants. In a quick confirmation of the solvent scan for the reactivity (Table 2.4), Mr. Joffré Bourgeois observed that solvents of varying polarities provided similar NMR yields for the reactivity, all between 65% and 75%,

when reacted at 1M with excess norbornene.⁴⁴ Importantly, the formation of side products such **2.4** was suppressed.

Table 2.4 Solvent Scope for the Cope / Meisenheimer cascade reaction



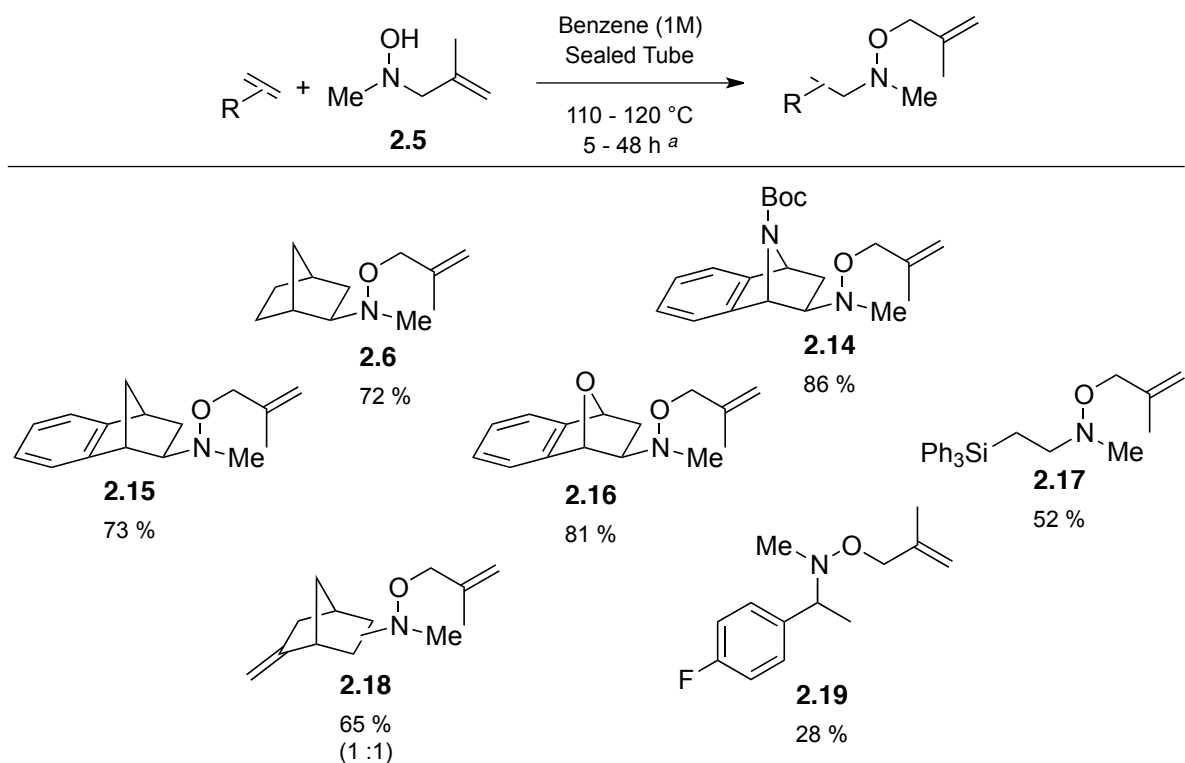
Entry	Solvent	NMR Yield (%)
1	Benzene	75 %
2	PhCF ₃	74 %
3	<i>n</i> -PrOH	69 %
4	Dioxane	66 %
5	THF	65 %

^a conditions: A: heated norbornene (5 equiv.) and hydroxylamine (1 equiv.) in a sealed tube at 110 °C, for 18 h. ^b ¹H NMR Yield, calculated based on the use of styrene as an internal standard.

From these optimized conditions, Table 2.5 presents the alkene scope for the reaction. Strained alkenes mostly derived from norbornene were shown to react efficiently upon heating at 110 – 120 °C. The reactivity could not be fully transferred to unbiased alkenes, yet we were pleased with the moderate reactivities observed for 4-fluorostyrene and vinyltriphenylsilane (to form **2.19** and **2.17**) under similar reaction conditions.

⁴⁴ Results published in the following article: "The Tandem Cope-Type Hydroamination / [2,3]-Rearrangement Sequence: A Strategy to Favor the Formation of Intermolecular Hydroamination Products and Enable Difficult Cyclizations" Bourgeois, J.; Dion, I.; Cebrowski, P. H.; Loiseau, F.; Bédard, A.-C.; Beauchemin, A. M. *J. Am. Chem. Soc.* **2009**, *131*, 874.

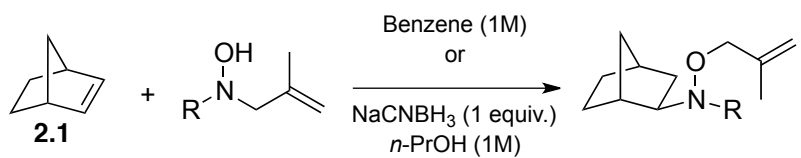
Table 2.5 Alkene scope for the Cope / Meisenheimer rearrangement



^a conditions: heated norbornene (5 equiv.) and hydroxylamine (1 equiv.) in a sealed tube at 110-120 °C, for 5-48 h. Isolated yields are shown.

The scope in hydroxylamine for the cascade is summarized in Table 2.6. The cascade reaction allowed the synthesis of various *N*-alkyl-*N*-methylallyl hydroxylamines (entries 1 to 6), under the usual conditions in benzene or in alternate ones using *n*-propanol as a solvent, with sodium cyanoborohydride as additive. Overall reasonable yields are obtained for small R groups and linear substrates, but the presence of steric hindrance severely limits reactivity (entry 2).

Table 2.6 Hydroxylamine scope for the Cope / Meisenheimer cascade reaction.



Entry	R	Conditions ^a	Temperature	Product	Yield ^b (%)
			(°C)		
1	Me (2.5)	A	110	2.6	72
2	<i>i</i> -Pr (2.20)	A	130	2.21	21
3	<i>n</i> -Pr (2.22)	A	120	2.23	48
4	<i>n</i> -Pr (2.22)	B	130	2.23	57 ^c
5	Bn (2.10)	B	120	2.12	44
6	BnO(CH ₂) ₃ (2.24)	B	130	2.25	52

^a conditions: A: heated norbornene (5-10 equiv.) and hydroxylamine (1 equiv.) in a sealed tube in C₆H₆, for 38 - 45 h. B: heated norbornene (5-10 equiv.) and hydroxylamine (1 equiv.) in a sealed tube in *n*-PrOH, with 1 equiv. of NaCNBH₃, for 48 h. ^b Isolated yield. ^c ¹H NMR Yield, calculated based on styrene IS.

The method is also shown to yield reasonable amounts of hydroamination products for primary linear hydroxylamines (entries 3,4 & 6). This is a vast improvement over the regular intermolecular hydroamination (followed by proton transfer), which saw similar amines have a complete absence of reactivity. The reaction was shown to have very high dependence on the sterics involved, more so than the standard hydroamination of mono-substituted hydroxylamines. Neopentyl and cyclohexyl hydroxylamine failed to provide even small yields in the standard or optimized conditions.

Entries 4-6 feature the use of sodium cyanoborohydride as an additive, first described by Mr. Joseph Moran and Ms. Elena Dimitrijevic.^{31,45} Primary hydroxylamines, having a strong tendency to oxidize in the reaction conditions, especially in alcoholic solvents, seemed to benefit from the presence of sodium cyanoborohydride. Moran and Dimitrijevic observed higher yields and cleaner intermolecular reactions with norbornene, with the most

⁴⁵ Moran, J. "Intermolecular Hydroamination of Alkenes. Strain-Release Hydroamination & Cope-Type Hydroamination." Ph.D. Thesis, University of Ottawa, ON, 2009.

positive effects for substrates with a higher potential for decomposition. Control tests revealed the additive was not reducing directly the related oxime in solution (which would require acidic conditions), but rather the additive seems to stabilize the hydroxylamine starting materials and products, preventing them from decomposing or oxidizing.

In cascade reactions, the same trend was observed, with sodium cyanoborohydride improving the yields and making the reaction noticeably cleaner. Table 2.7 reveals that there is no set amount of sodium cyanoborohydride that is particularly beneficial, with the reactions of hydroxylamines **2.22** and **2.24** responding equally well to 0.5 or 1 equivalents of the additive.

Table 2.7 Effect of NaCNBH₃ concentration on yields.

Entry	Substrate	Solvent	NaCNBH ₃ (equiv.)	Product	NMR Yield ^c (%)
1	 2.24	<i>n</i> -PrOH ^a	0.5	 2.25	59
2		<i>n</i> -PrOH ^a	1		59
3	 2.26	benzene ^b	none	 2.27	26
4		<i>n</i> -PrOH ^a	0.5		44
5		<i>n</i> -PrOH ^a	1		45

^a conditions: heated norbornene (8 equiv.), hydroxylamine (1 equiv.) and NaCNBH₃ in a sealed tube in *n*-PrOH (1M), at 120 °C for 96 h. ^b conditions: heated norbornene (8 equiv.) and hydroxylamine (1 equiv.) in a sealed tube in benzene (1M), at 120 °C for 96 h. ^c ¹H NMR Yield, calculated based on styrene IS.

2.2.4 Application to Total Syntheses

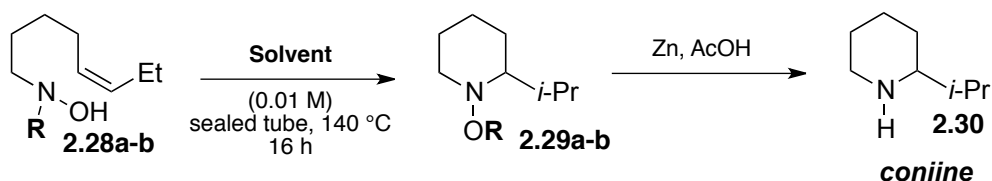
The increased stability of the *N*-methallyl derivatives of primary hydroxylamines suggested that the use of the Meisenheimer rearrangement could be used outside of

intermolecular hydroaminations. In intramolecular Cope-type hydroaminations, the formation of 6-membered rings through reactions with di-substituted alkenes is notoriously difficult, with most methodologies either limited to 5-membered rings or terminal alkenes. The reaction is also slowed by the lack of secondary substitution on the hydroxylamine. The Meisenheimer rearrangement cascade reaction hence became a potential solution to the activation of the reaction, the stability of the starting materials, as to provide a thermodynamic driving force towards the products.

The cascade was first tested by Mrs. Isabelle Dion as part of her Ph.D. work, in the final key steps of her synthesis of coniine. Coniine was selected as a test substrate for hydroamination, for it contained all attributes known to make a Cope-type hydroamination difficult.⁴⁶ The *N*-allyl and *N*-methallyl hydroamination substrates were readily prepared from the primary hydroxylamine precursors already synthesized for the standard cyclizations. After extensive optimization of the key hydroamination cascade, *N*-allyl derivative **2.28b** emerged as a slightly superior cyclization precursor for coniine, likely due to a more facile Meisenheimer rearrangement step (Table 2.8) as well as stabilization of the starting material. The use of rigorously deoxygenated, dilute solutions (0.01 M) drastically minimized side reactions. To put the 47% isolated yield (55% based on recovered starting materials) in context, all attempts to cyclize the simpler primary hydroxylamine precursor failed to provide more than 23% of the desired hydroamination product.

⁴⁶ Formation of 6-membered piperidine rings via hydroamination onto an *internal* alkene are rare. For a summary of reactivity trends: (a) Cooper, N. J.; Knight, D. W. *Tetrahedron* **2004**, *60*, 243. For examples, see: (b) Stubbert, B. D.; Marks, T. J. *J. Am. Chem. Soc.* **2007**, *129*, 4253. (c) Komeyama, K.; Morimoto, T.; Takaki, K. *Angew. Chem., Int. Ed.* **2006**, *45*, 2938. (d) Schlummer, B.; Hartwig, J. F. *Org. Lett.* **2002**, *4*, 1471.

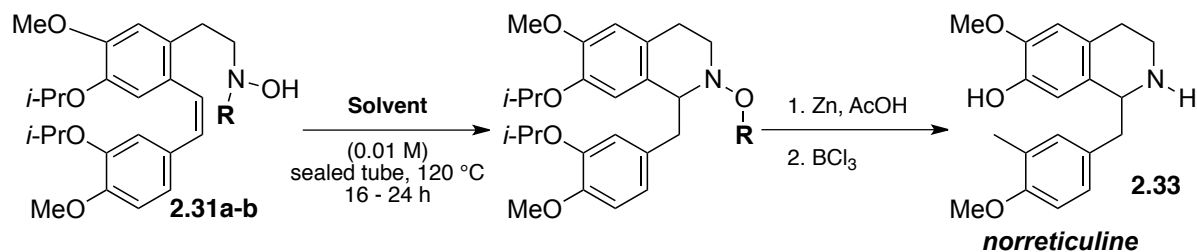
Table 2.8 Key hydroamination step in the synthesis of coniine



Substitution	Solvent	Product	Isolated Yield (%)
R = H	<i>i</i> -PrOH, NaCNBH ₃ (1 equiv.)	2.29a	23 % Yield
R =	Benzene, H ₂ O (10 equiv.)	2.29b	47 % Yield, 15 % SM

The cascade was then successfully applied to the synthesis of a second alkaloid, norreticuline, through a late stage hydroamination methodology employed here as well. Mrs. Dion and Mrs. Pamela Cebrowsky both worked towards this total synthesis. Once again, the *N*-allyl and *N*-methallyl hydroamination substrates were readily synthesized from the standard primary hydroxylamine precursor. In this system, methallyl derivative **2.31b** proved a superior cyclization precursor, affording the desired product **2.32b** in 54% yield (32% of the trans isomer derived from **2.31b** was also isolated). Here as well, the use of the primary hydroxylamine precursor failed to provide more than 27% of the desired hydroamination product (51% with the use of NaCNBH₃ as additive).

Table 2.9 Key hydroamination step in the synthesis of norreticuline

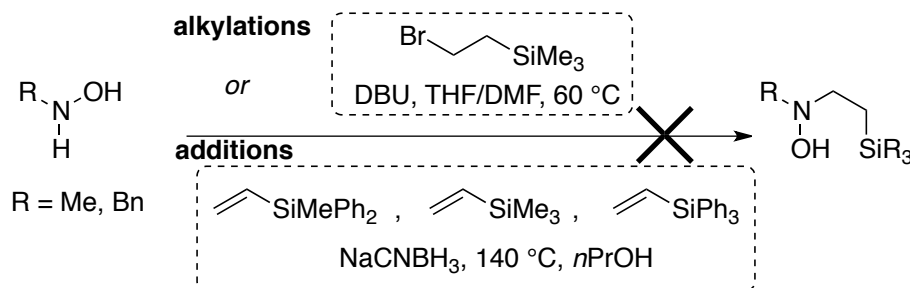


Substitution	Solvent	Product	Isolated Yield (%)
R = H	<i>i</i> -PrOH, NaCNBH ₃ (1 equiv.)	2.32a	51 % Yield
R =	Benzene, H ₂ O (10 equiv.)	2.32b	47 % Yield, 32 % (<i>E</i>)-SM

2.3 Sila-Cope Elimination Cascade Reaction

One of the first cascades we became interested in was one using the sila-Cope elimination (Scheme 2.4). In the second step of such a cascade, the *N*-oxide would react with the adjacent silane, forming a new strong O-Si bond (110 kcal/mol vs. 76 kcal/mol for C-Si),⁴⁷ and eliminating an alkene. This potentially serves well the reaction both in terms of enthalpy, for the newly formed bonds would be stronger, and the now neutral reaction entropy, arising from the formation of two products. The sila-Cope elimination itself, discovered in 1986 by Langlois, has had limited use in the field of organic synthesis.⁴⁸

Early attempts to synthesize the required precursor to the intermolecular cascade were met with repeated failures. Alkylation methods and additions methods from hydroxylamines were tried in a variety of conditions (some summarized in Scheme 2.5) all leading to no reaction or decomposition.



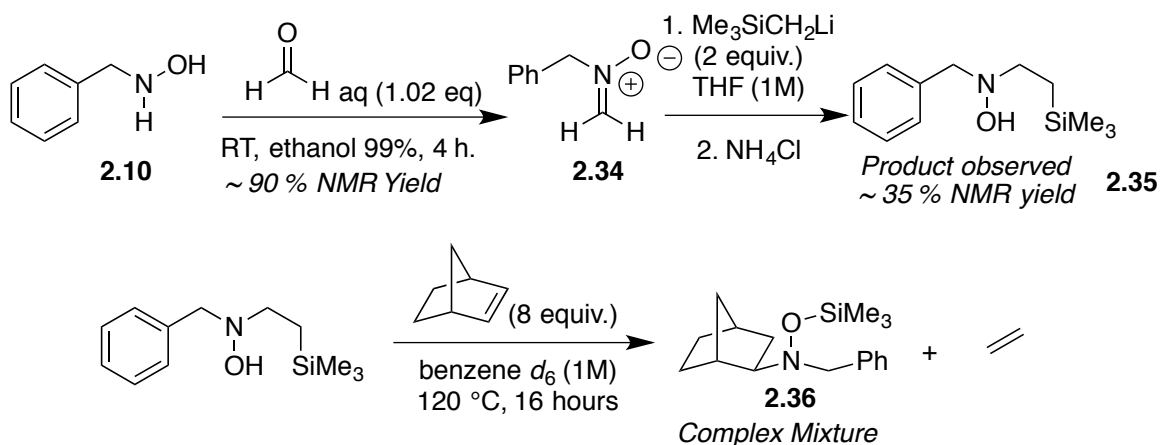
Scheme 2.5 Summary of failed attempts to synthesize the sila-Cope cascade precursor.

As an alternative strategy to synthesize the precursor, a more stepwise approach, in which benzyloxyamine was reacted with formaldehyde to form an initial aldonitrone

⁴⁷ Values taken from R. T. Sanderson: *Chemical Bonds and Bond Energy* (Academic Press, New York, 1976) 2nd ed., p. 77.

⁴⁸ For the original report on the Sila-Cope Elimination: (a) Fall, Y.; Nguyen, V. B.; Langlois, Y. *Tetrahedron Lett.* **1986**, 27, 3611. For uses of the reaction: (b) Horino, Y.; Luzung, M. R.; Toste, F. D. *J. Am. Chem. Soc.* **2006**, 128, 11364. (c) Vidal, T.; Magnier, E.; Langlois, Y. *Tetrahedron* **1998**, 54, 5959. (d) Langlois, Y.; Konopski, L.; Bac, N. V.; Chiaroni, A.; Riche, C. *Tetrahedron Lett.* **1990**, 31, 1865.

(Scheme 2.6). After failing to purify the nitron, it was instead used crude (>90% pure) to undergo a 1,2-addition of $\text{Me}_3\text{SiCH}_2\text{Li}$ and generate our cascade reaction precursor (in ~35% NMR yield). However, problems of stability and purification once again forced us to attempt the cascade reaction directly on the crude precursor. The reaction generated a vast mixture of compounds, many of them containing silyl substituents, demonstrating the little amount of control we had on the reactivity. It was therefore decided not to pursue this specific venue in cascade reactions.

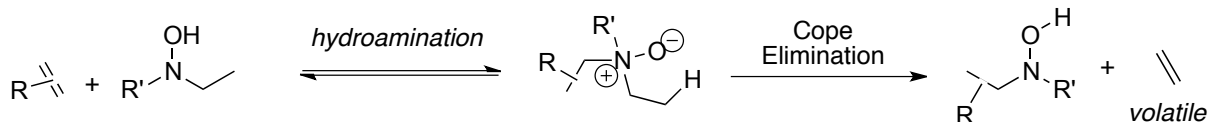


Scheme 2.6 First attempt at hydroamination / sila-Cope cascade reaction from crude precursor synthesized from the aldonitrone.

2.4 Cope-Type Hydroamination – Cope Elimination Cascade

We sought to investigate cascades that would inherently offset the negative entropy associated with the intermolecular hydroamination. We thus proposed a cascade hydroamination / Cope-elimination cascade, that would see *N*-oxide intermediate further reacting with an alkyl side-chain to release an alkene and hence overall generate two neutral compounds.⁴⁹

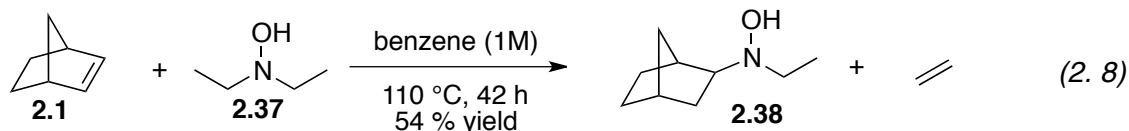
⁴⁹ Mr. Joseph Moran uncovered the lead result for this reactivity, while Ms. Emily Manthorp and Mr Pierre Mouawad, as undergraduate students working under my guidance, expanded on the reactivity.



Scheme 2.7 Proposed pathway for the Cope Elimination / Cope-type Hydroamination concept, generating ethylene gas to drive the equilibrium.

2.4.1 Discovery of the cascade

The reaction of norbornene with commercially available *N,N*-diethylhydroxylamine was selected, for the release of ring strain and formation of volatile ethylene would provide a proof of concept for the potential of the reaction. Thankfully, initial reactions performed in sealed tubes and heated at 110 °C for 11 hours resulted in a 54% isolated yield of the mono-hydroamination product, *N*-ethyl-*N*-norbornylhydroxylamine (**2.38**) (Eq. 2.8). The release of pressure upon opening the cooled sealed tube indicated that ethylene had been released during the reaction.



2.4.2 Results and Discussion

The reactivity was scanned, varying solvents and reaction conditions for the reaction. Table 2.10 represents the extent of optimization performed on the test system (Eq. 2.8). The reaction was found to be compatible with a variety of protic and aprotic solvents, with the reactions achieving better yields in non-polar benzene and alcohols (entries 9-13, up to 80%; 16-19, up to 69%). This observation parallels that made in a variety of systems, with benzene or toluene being notoriously the only solvents other than alcohols capable of achieving the highest reaction yields. Chapter 4 will comment on these issues, and try to address the specific reasons explaining such a phenomenon.

Solvents of intermediate polarities (entries 1-6) were nonetheless successful in achieving modest reactivity (23% – 58%). Comparable efficiency was observed with the cascade hydroamination/[2,3]-Meisenheimer cascade for the substrates of similar sizes (ex. *N*-methallyl-*N*-methylhydroxylamine). The increased steric bulk surrounding the nitrogen atom of the product compared to the starting material attenuates its reactivity, and no bis-hydroamination product was detected in all cases.

Table 2.10 Solvent and temperature scan for Cope Elimination cascade reaction.



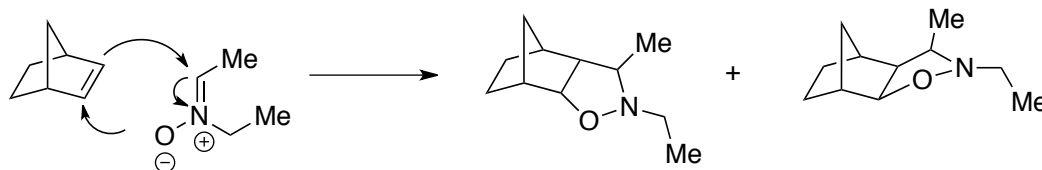
Entry	Solvent	Conc	Conditions ^a	Yield (%) ^b
1	CDCl ₃	1 M	100 °C, 42 h	27
2	EtOAc	1 M	100 °C, 42 h	23
3	MeCN	1 M	100 °C, 42 h	26
4	PhCF ₃	1 M	100 °C, 42 h	49
5	THF	1 M	100 °C, 42 h	54
6	PhCl	1 M	120 °C, 10 h, μw	58
7	Benzene	1 M	90 °C, 42 h	50
8	Benzene	1 M	100 °C, 24 h	55
9	Benzene	1 M	100 °C, 42 h ^c	62
10	Benzene	2 M	100 °C, 42 h	80
11	Benzene	1 M	110 °C, 11 h	54
12	Benzene	1 M	110 °C, 42 h	71
13	Benzene	1 M	110 °C, 5 h, μw	32
14	Benzene	1 M	130 °C, 16 h	61
15	<i>n</i> -PrOH	1 M	100 °C, 42 h	- ^d
16	<i>n</i> -PrOH + NaCNBH ₃ (1 equiv.)	1 M	125 °C, 16 h	66
17	<i>n</i> -PrOH + NaCNBH ₃ (1 equiv.)	1 M	100 °C, 42 h	66
18	<i>t</i> -BuOH	1 M	100 °C, 42 h	64
19	<i>t</i> -BuOH + NaCNBH ₃ (1 equiv.)	1 M	100 °C, 42 h	69

^a conditions: heated 5 equiv. of norbornene and 1 equiv. of **2.44** in a sealed tube in the appropriate solvent, at the set temperature, for 5-42 h. μw: the microwave reactor was used for heating instead.

^b Isolated Yield. ^c 2.5 equiv. of **2.1** were used in this reaction. ^d The cycloadduct from 1,3-dipolar cycloaddition was present in significant quantities.

A temperature and concentration scope performed in benzene (Entries 7-14) shows consistent moderate yields across temperatures (90 – 130 °C), with longer reaction times and higher concentration beneficial to the reaction. Heating the reactions in the microwave did not seem to help this chemistry, and the reactions were therefore run mainly in sealed tubes using conventional heating. The best yield came from the original benzene solvent at 2M, with 5 equivalents of norbornene, in a reaction heated for 42 h at 100 °C (entry 10).

The second best set of solvents, alcohols, offered trends the Beauchemin group has become accustomed to. Using a reagent like a di-alkylhydroxylamine, with linear substitution, is known to cause stability issues in protic solvents. The reactivity was found to shut down in *n*-PrOH, and hinted at the preferential formation of cycloadducts most likely found from initial decomposition of the hydroxylamine to its parent nitrene.



Scheme 2.8 1,3-Dipolar addition of norbornene with nitrene formed in situ.

Expansion of the reactivity.

Later attempts at improving on the initial reactivity of *N,N*-diethylhydroxylamine has been unsatisfactory so far (Figure 2.6). Extending the reactivity to *N,N*-di-*n*-propylhydroxylamine or *N,N*-diisopropylhydroxylamine, which we assumed would make the cascade even more favorable by generating a more stable alkene, in reality shut down the expected reactivity. The mechanistic reasoning behind such a change is presumed to involve the three-dimensional structure of the intermediate *N*-oxide, and the ease in which orbitals can be aligned to favor the elimination. The *N*-oxide must have difficulty in accessing

the protons to be removed on the β carbon, essential forcing a reaction back towards the starting materials instead.

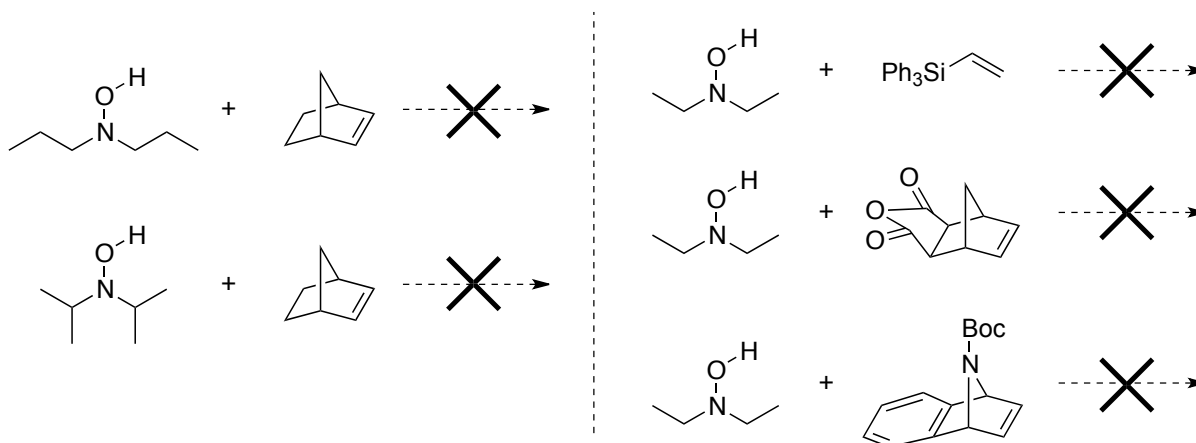


Figure 2.6 Other attempts at the Cope hydroamination / Cope elimination cascade reactions. Tested in standard conditions, 100 °C for 42 h, with excess alkene (2-5).

Reactivity with more sterically hindered biased alkenes also proved difficult for the process, with sterics potentially playing an important role in the orientation of bonds, which here again may cause a difficult proton abstraction event from the *N*-oxide. The observed difficulties required to be surpassed a good knowledge and understanding for the Cope elimination and the factors influencing its speed and efficacy are surely the starting point for the design of optimal reagents.⁵⁰ Rather than using commercially available hydroxylamines, or hydroxylamines easily synthesized, one most think of involving substitution known to facilitate the elimination. For instance, the use of an alkyl chain with β -substitution in the form of aryl groups are known to accelerate the Cope elimination by factors up to 100. Further modifications along those ideas are likely to result in improved applicability for this reaction cascade.

⁵⁰ See Chapter 1, section 1.3.1.

2.5 Summary and Outlook

The Cope-type hydroaminations / Meisenheimer rearrangement cascade was successfully applied to the intermolecular hydroaminations of biased alkenes, and showed 11 examples and yield up to 87%. Though the overall efficacy of cascade reactions in favoring hydroamination is still limited, the methodology did provide us with an additional tool to tackle difficult hydroaminations. The Meisenheimer cascade was applied to the intramolecular cyclizations of coniine and norreticuline, in which one could see the advantages of the method. It allowed for the use of more stable and more reactive di-substituted hydroxylamine; consequently producing better yields than primary hydroxylamines would.

The Cope hydroamination / sila-Cope elimination cascade and the Cope hydroamination / Cope elimination cascade were both presented as new concepts, in an approach that aims at making the overall hydroamination process entropy neutral by regenerating two molecules in the last step of the cascade. The latter was shown to have potential in the intermolecular hydroamination of biased alkenes, through the use of diethyl hydroxylamine as a reagent. Work remains in order to establish efficient reagents that possess intrinsic good reactivity towards hydroamination, yet possess a side chain for which the Cope elimination would be favored and fast.

Overall these approaches have served as proof of concept that cascade reactions could be used alongside the Cope-type hydroamination, and several challenges remain in order to apply these methods to the hydroamination of unbiased alkenes. The design of substrates that combine key elements heavily favoring the second reaction in the cascade will likely be the cornerstone of subsequent developments.

Scope Expansion of the Cope-type Hydroamination of Hydrazines

The Cope-type hydroamination described in Chapters 1 and 2 uses hydroxylamines as bifunctional reagents, and has shown to be an effective reaction with a wide-ranging scope, providing access to formally hydroaminated products upon intra- and intermolecular reactions on alkynes, allenes, and alkenes. While most of the Beauchemin group's initial work in hydroamination focused on the reactivity of hydroxylamines, early goals included the extension of the reactivity to their all-nitrogen analogs, namely hydrazines and their large family of derivatives (Figure 3.1).

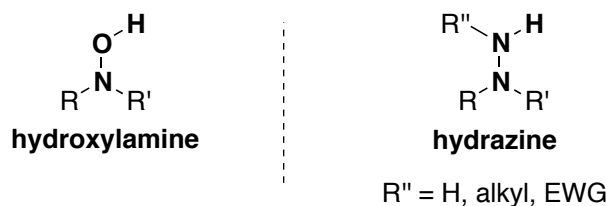


Figure 3.1 Hydroxylamines versus hydrazines as bifunctional reagents

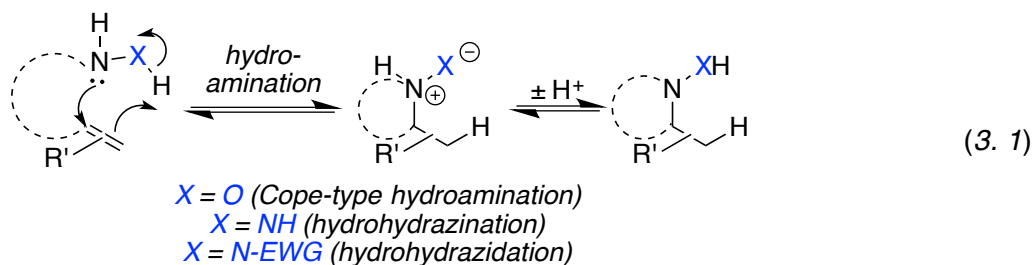
The current chapter will provide a review of classical methods used for the synthesis of hydrazines and hydrazides, along with recent developments in metal catalyzed aminations forming hydrazines.⁵¹ An expansion of the scope of the intramolecular Cope-type hydroamination of hydrazines will be presented, along with the first reported intermolecular

⁵¹ *Hydroaminations* using hydrazines and hydrazine derivatives can also be described in the literature as *hydrohydrazinations* or *hydrohydrazidations*, which depending on the case at hand can be used interchangeably. The results included in the thesis will describe them mainly as hydroaminations, while literature reviews may use the latter terms as well.

hydroaminations of hydrazides onto alkenes. DFT calculations, kinetic experiments and isolation of reaction intermediates will provide insight into the reaction mechanism.

3.1 Introduction

The Cope-type hydroamination can be thought of as the use of a bifunctional reagent to add an N-H bond across an unsaturation. Hydrazines and their derivatives, possessing the same N-X-H core as hydroxylamines, can in theory serve the same role in a reaction, and would have the potential to yield equivalent dipole intermediates as they add across double or triple C-C bonds (Eq. 3.1). Whether these reactions can go through a mechanism that would warrant them to be classified alongside their hydroxylamine counterparts, namely as Cope-type processes that go through concerted, suprafacial transition states for the hydroamination event, is going to be a main focus of the latter part of this chapter.

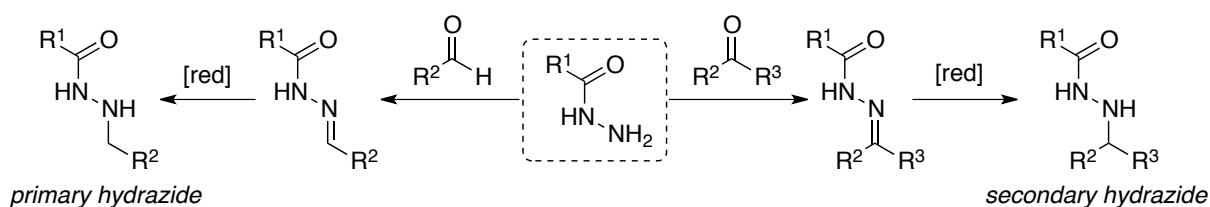


While hydroamination literature is abundant and well reviewed (see Chapter 1), only a selected few reactions stemming from the recent surge of metal catalyzed processes feature the formation of hydrazines or hydrazides as products. They warrant further consideration, to better assess the methodologies developed and discussed later in this chapter.

3.1.1 Classical Syntheses of Hydrazines and Hydrazides.

A first look at classical methods of synthesizing poly-substituted hydrazines or hydrazides is useful before discussing newer strategies. While a plethora of hydrazines are

commercially available, they are usually at most mono or di-substituted. This is expected when we consider the fact that hydrazines and hydrazides possess two adjacent nitrogens that both have the potential to be nucleophilic. This has traditionally created issues with many methodologies in terms of selectivity over the reacting nitrogen, as well as problems of over-alkylation in many classical syntheses. Still, classical methods to access hydrazines can be summarized as (a) *reduction of hydrazones*, (b) *alkylation of hydrazine precursors*, and (c) *amination of amine starting materials*.⁵²



Scheme 3.1 Standard syntheses of hydrazides through reduction of hydrazones.

(a) *The reduction of hydrazones* (themselves easily formed from condensation of hydrazines or hydrazides on carbonyls) remains one of the most reliable and widely applicable ways to add substitution (Scheme 3.1). Hydrazones C=N bonds have been reduced through the use of many reagents, including catecholborane,⁵³ diborane in THF⁵⁴ as well as milder reducing agents like trimethylsilane, NaBH₄ and NaCNBH₃, under mild to fairly acidic conditions.⁵⁵ The applicability of the method remains dependent on the availability of the starting hydrazines and carbonyl compounds.

(b) *The alkylation of hydrazines* is often problematic, forming a variety of side products, yet can be of value for large-scale synthesis of mono- and selected di-substituted derivatives.

All methods become very limited once the syntheses of tri and tetra-substituted hydrazines

⁵² For a comprehensive review see: Ragnasson, U. *Chem. Soc. Rev.* **2001**, 30, 205 and references therein.

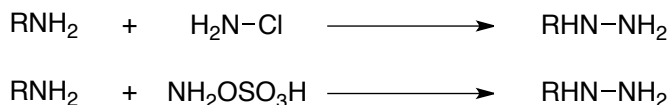
⁵³ Kabalka, G. W.; Baker, J. D.; Neal, G. W. *J. Org. Chem.* **1977**, 42, 512.

⁵⁴ Ghali, N. I.; Venton, D. L. *J. Org. Chem.* **1981**, 46, 5414

⁵⁵ (a) Wu, P.-L.; Peng, S.-U.; Magrath, J. *Synthesis* **1995**, 435. (b) Wu, P.-L.; Peng, S.-U.; Magrath, J. *Synthesis* **1996**, 249. (c) Calabretta, R.; Gallina, C.; Giordano, C. *Synthesis* **1991**, 536.

are attempted. Common strategies to access these involve the use of multiple orthogonal protecting groups on a starting hydrazine, allowing for a sequential addition of the desired substitutions to achieve more complexity.⁵⁶ While effective in providing up to tri-substituted hydrazines, this is a lengthy approach requiring multiple protection/deprotection steps to accomplish the intended synthesis. Also, steric encumbrance prevents the synthesis of a variety of poly-substituted products, if preceding groups are large.

(c) *The electrophilic N-amination of amines* is also present in the literature. Electrophiles such as chloramine and hydroxylamine-*O*-sulfonic acid can react with primary amines in the synthesis of mono-substituted hydrazines (Scheme 3.2), while *N*-protected oxaziridines have been used to generate simple protected mono- and di-substituted hydrazines, in progressively lower yields with increased complexity in substitution.⁵⁷



Scheme 3.2 Hydrazines through *N*-amination of amines.

These few methods, along with a few more specialized ones,⁵⁸ cover the standard techniques to synthesize hydrazines. Starting materials includes amines or hydrazines, as well as carbonyl compounds or alkylating reagents to add substitution. With most of their applications featuring the use of mono-substituted hydrazines and hydrazides, broadly applicable methods to access di-, tri- and tetra-substituted hydrazines are in particular need.

⁵⁶ (a) Mäeorg, U.; Grehn, L.; Ragnarsson, U. *Angew. Chem., Int. Ed. Engl.* **1996**, *35*, 2626. (b) Mäeorg, U.; Ragnarsson, U. *Tetrahedron Lett.* **1998**, *39*, 681. (c) Mäeorg, U.; Pehk, T.; Ragnarsson, U. *Acta Chem. Scand.* **1999**, *53*, 1127-1133. (d) Grehn, L.; Löhn, H.; Ragnarsson, U. *Chem. Commun.* **1997**, *1*. (e) Brosse, N.; Pinto, M.-F.; Jamart-Gregoire, B. *J. Org. Chem.* **2000**, *65*, 4370. (f) Brosse, N.; Pinto, M.-F.; Bodiguel, J.; Jamart-Gregoire, B. *J. Org. Chem.* **2001**, *66*, 2869.

⁵⁷ Vidal, J.; Hannachi, J.-C.; Hourdin, G.; Mulatier, J.-C.; A. Collet, A. *Tetrahedron Lett.* **1998**, *39*, 8845.

⁵⁸ P. R. Huddleston and I. G. C. Coutts, *Comprehensive Organic Functional Group Transformations*, eds. Katritzky, A. R.; Meth-Cohn, O.; Rees, C. W. Pergamon/Elsevier, Oxford, 1995, vol. 2, pp. 371–383.

In this context, uses of hydrazines in the hydroamination of alkenes and alkynes (hydrohydrazination) are only emerging.

3.1.2 Summary of Recent Hydrohydrazination Strategies

Conceptually, hydrohydrazination uses hydrazine-based starting materials and a C-C unsaturation as the reaction partner, which allows the use of readily available and affordable petroleum-based starting materials. Perhaps by virtue of their more widespread occurrence within pharmaceutical targets and their potent intrinsic bioactivities,⁵⁹ several hydroamination methods aimed at the synthesis of substituted hydrazines have been developed over the last decade. Recent and common syntheses of hydrazides through metal catalyzed or promoted hydroamination approaches (Figure 3.2), will put in context the metal-free Cope-type hydroamination (E) reactivity described later in this chapter.

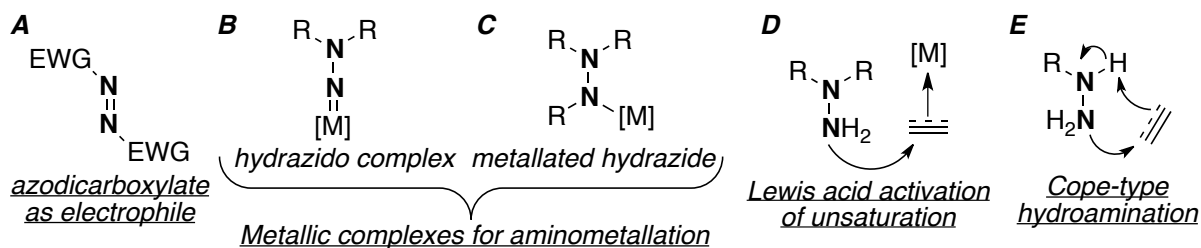


Figure 3.2 Hydrazine sources in recent approaches to hydroamination for the synthesis of hydrazines and hydrazones.

Titanium Catalyzed Intramolecular Hydrohydrazination of Alkynes

Intermolecular hydrohydrazination has been developed by Odom in 2002 that used titanium hydrazido complexes to react with alkynes and form hydrazones.⁶⁰ Beller and Gade

⁵⁹ See Section 1.4.

⁶⁰ Original publication: (a) Cao, C.; Shi, Y.; Odom, A. L. *Org. Lett.* **2002**, *4*, 2853. In depth analysis of hydrazido vs imido complexes: (b) Li, Y.; Odom, A. L. *J. Am. Chem. Soc.* **2004**, *126*, 1794. Follow-up publications: Odom, A. L. *Dalton Transactions* **2005**, 225. (d) Banerjee, S.; Barnea, E.; Odom, A. L. *Organometallics* **2008**, *27*, 1005.

presented similar reactions with variations in the catalyst design.⁶¹ This reactivity is similar in approach to the hydroamination of alkynes with amines covered in Chapter 1. The reaction was demonstrated on a variety of internal and terminal alkynes using simple 1,1-dialkyl hydrazines (Figure 3.3) to yield hydrazones as products in good yields, with a noted preference for Markovnikov products, and moderate preference for the *E*-isomer. Also shown in Figure 3.3 is the main extension for which this reactivity was used when working with phenylhydrazine or 1,1-disubstituted hydrazines, namely the transformation of the initial hydrazone intermediate into NH- or N-substituted indoles in moderate to good yields (42-97%), following a one-pot Fischer indole cyclization.^{60(c,d)}

⁶¹ (a) Tillack, A.; Jiano, H.; Garcia Castro, I.; Hartung, C. G.; Beller, M.; *Chem. Eur. J.* **2004**, *10*, 2409. (b) Schwaz, N.; Alex, K.; Sayyed, I. A.; Khedkar, V.; Tillack, A.; Beller, M.; *Synlett* **2007**, 1091. (c) Weitershaus, K.; Wadepohl, H.; Gade, L. H. *Organometallics*, **2009**, *28*, 3381.

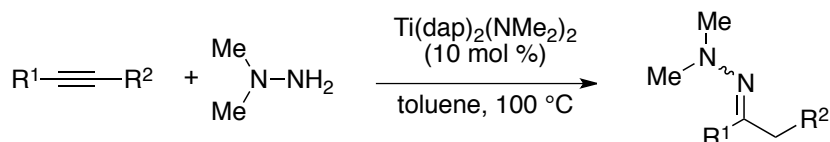
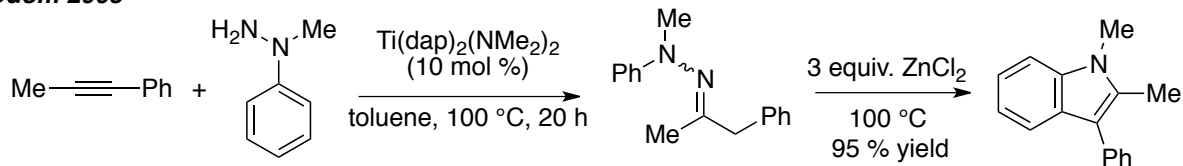
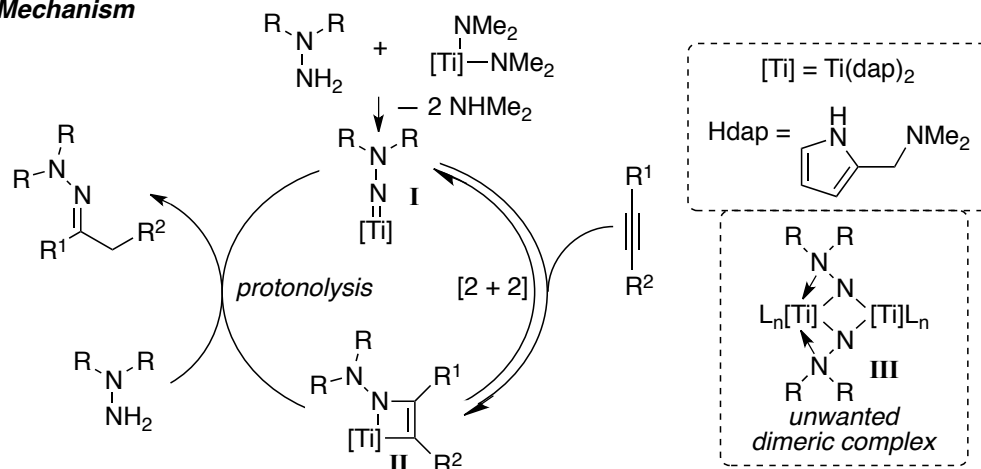
Odom 2002**Odom 2005****Proposed Mechanism**

Figure 3.3 Odom's titanium catalyzed hydrohydrazination of alkynes

The mechanism is expected to stem from the initial formation of a terminal hydrazido titanium complex (Figure 3.3 I), which can undergo a [2+2] cycloaddition with the alkyne and form an azatitanacyclobutene intermediate (**II**).⁶² The metallacycle, following protonolysis with hydrazine, can be converted to the hydrazone and regenerate the catalyst. The reaction is notably more complex than the related metal catalyzed amination of triple bonds, due to the presence of the second nitrogen in the complex, which tends to favor the formation of strong dative bonds with the metal center within non-reactive dimers (**III**). Careful control of

⁶² Similar to the Bergman hydroamination with Zirconocene catalyst: (a) Straub, B. F.; Bergman, R. G. *Angew. Chem., Int. Ed.* **2001**, *40*, 4632. (b) Baranger, A. M.; Walsh, P. J.; Bergman, R. G. *J. Am. Chem. Soc.* **1993**, *115*, 2753. (c) Walsh, P. J.; Baranger, A. M.; Bergman, R. G. *J. Am. Chem. Soc.* **1992**, *114*, 1708.

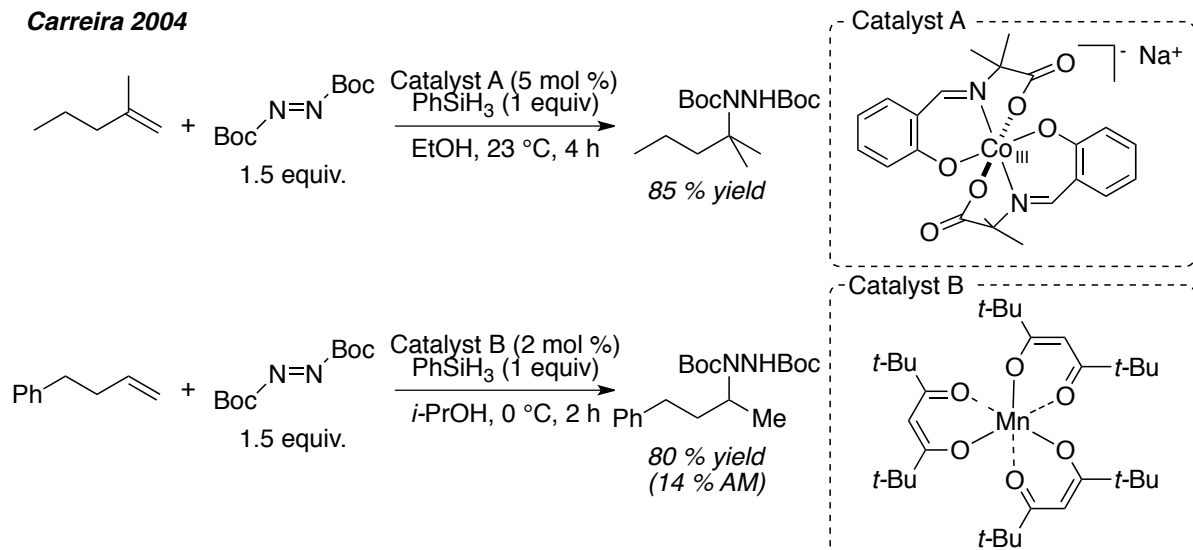
the type and size of ligands is required both to make the metal center more electron rich and to add steric bulk, effectively diminishing the presence of the dative bonds and promoting the formation of the required terminal hydrazido complex.

Intermolecular Hydrohydrazination of Alkenes using Cobalt and Manganese Catalysis

Carreira and co-workers have recently described a hydrohydrazination of olefins that can be performed with azodicarboxylates and silanes, and catalyzed by cobalt and manganese complexes.⁶³ The reaction (Figure 3.4) is equivalent to a direct hydroamination and yields products with a high Markovnikov preference. The reaction works on a remarkably large variety of alkene substrates, from terminal to internal alkenes, α,α -disubstituted and tri-substituted, vinyl styrenes and heterocycles, as well as biased strained alkenes, enynes and dienes. Yields range from the low 10% up to 98% (more typically in between 70 and 90%).

⁶³ Original publications: Waser, J.; Carreira, E. M. *Angew. Chem. Int. Ed.* **2004**, *43*, 4099. (b) Waser, J.; Gasper, B.; Nambu, H.; Carreira, E. M. *J. Am. Chem. Soc.* **2006**, *128*, 11693. (c) Waser, J.; Gonzalez-Gomez, J. C.; Nambu, H.; Huber, P.; Carreira, E. M. *Org. Lett.* **2005**, *7*, 4249. (d) Waser, J.; Nambu, H.; Carreira, E. M. *J. Am. Chem. Soc.* **2005**, *126*, 5676. Use in other systems: (e) Sato, M.; Gunji, Y.; Ikeno, T.; Yamada, T. *Chem. Lett.* **2005**, *34*, 316. (f) Bunker, K. D.; Sach, N. W.; Huang, Q.; Richardson, P. F. *Org. Lett.* **2011**, *13*, 4746.

Carreira 2004



Proposed Mechanism

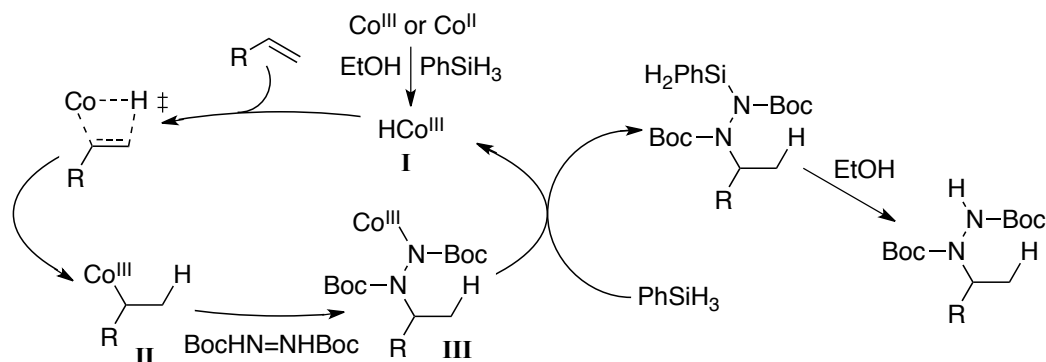


Figure 3.4 Carreira's cobalt and manganese catalyzed hydrohydrazination of alkenes.
Bottom: proposed mechanism

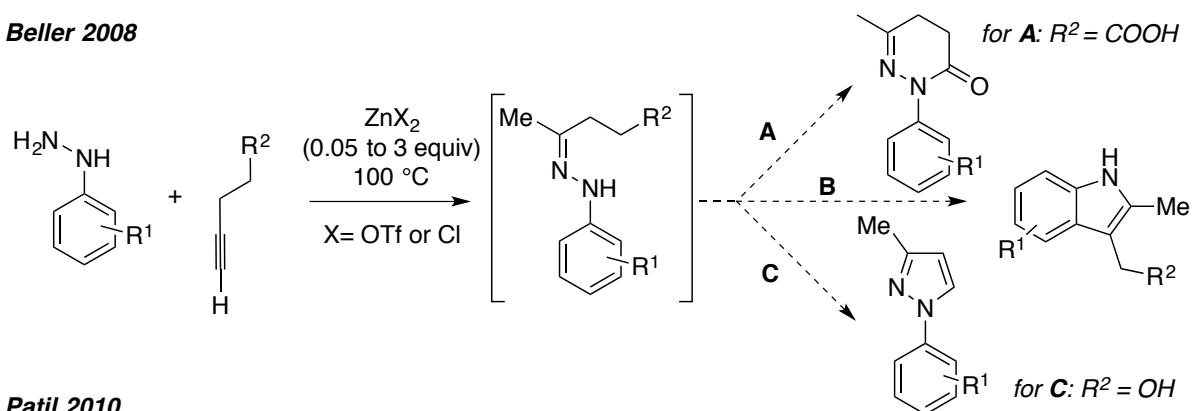
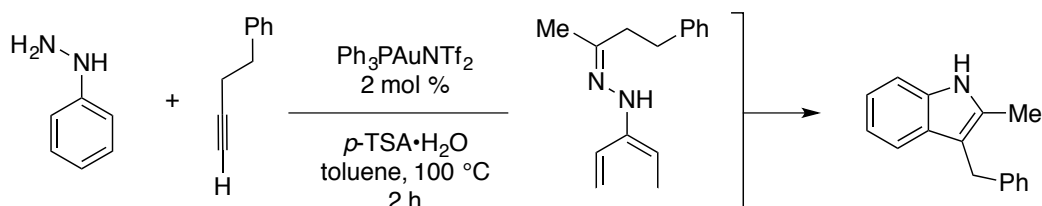
Manganese (III) complexes were found to be potent and complementary catalysts in the same reaction, allowing better reactivity with otherwise problematic α,β -di-substituted olefins, endocyclic alkenes and tetra-substituted alkenes. Both methods are notable on multiple aspects. They use nitrogen and hydrogen sources that are from two distinct reagents. Azodicarboxylates and silanes are used as oxidizing agents and hydride sources respectively, are available commercially, and are relatively inert towards one another, allowing for both species to interact with the alkene substrate. The Co and Mn catalysts are bench stable, and allow for the reaction to occur at room temperature, a noteworthy achievement in intermolecular hydroamination of alkenes. The products can be thought of as

tri-substituted hydrazines, although with two substituents that are protecting groups (Boc, Fmoc), they can more accurately be described as protected mono-substituted hydrazines.

The mechanism for both reactions is thought to be similar, and Carreira further investigated only the cobalt system. The initial formation of a Co-hydride (**I**) is thought to be followed by a Markovnikov hydrocobaltation of the olefin to form a Co-alkyl complex (**II**), which can then react with the electrophilic azodicarboxylate to form complex **III**. The exact nature of the second part of the mechanism is not well understood, because of some background direct reduction of the azodicarboxylate by the silane, and evidence of radical intermediates preventing accurate determination. Complex **III** is thought to finally react with the remaining silane to regenerate the active catalyst, as well as the formally hydroaminated product.

Hydroamination through Lewis Acid Activation of Alkynes

Another approach that has been taken to achieve intermolecular hydrohydrazination, in this case on alkynes, has been through the activation of the unsaturation with a Lewis acidic metal (Figure 3.2D). Beller and Patil have used zinc and gold respectively to achieve Lewis activation of an alkyne, and synthesize intermediate hydrazones (similar to the ones discussed for Odom previously) to be used in a variety of subsequent transformations.

Beller 2008**Patil 2010**

Scheme 3.3 *Top: Beller's zinc catalyzed and zinc promoted hydrohydrazination cascades and syntheses of dihydropyridazinones, indoles and pyrazoles, through hydrazone intermediate. Bottom: Patil's gold-promoted formal hydrohydrazination cascade*

While seeking alternatives to the titanium catalysts, Beller reported that zinc-mediated hydroaminations, performed using stoichiometric quantities of ZnCl_2 were effective in achieving the same one-pot HA-Fischer indole cyclization (Scheme 3.3B). Subsequent publications described other cascades possible, yielding pirdazinones (Scheme 3.3A) and pyrazolines (Scheme 3.3C) from the hydrazone intermediate.⁶⁴ Based on related hydroaminations using amines and zinc catalysis, the reaction is thought to go through a Lewis acid activation of the alkyne, followed by an attack from the neutral hydrazine.⁶⁵ This

⁶⁴ (a) Alex, K.; Tillack, A.; Schwarz, N.; Beller, M. *Tetrahedron Lett.* **2008**, *49*, 4607. (b) Alex, K.; Tillack, A.; Schwarz, N.; Beller, M. *Org. Lett.* **2008**, *10*, 2377. (c) Alex, K.; Tillack, A.; Schwarz, N.; Beller, M. *Angew. Chem., Int. Ed.* **2008**, *47*, 2304.

⁶⁵ For related Zinc-catalyzed hydroaminations: (a) Zulus, A.; Dochnahl, M.; Hollmann, D.; Loehnwitz, K.; Herrmann, J. S.; Roesky, P. W.; Blechert, S. *Angew. Chem. Int. Ed.* **2005**, *44*, 7794. (b) Dochnahl, M.; Pissarek, J. W.; Blechert, S.; Loehnwitz, K.; Roesky, P. W. *Chem. Commun.* **2006**, 3405. (c) Dochnahl, M.; Löhnwitz, K.; Pissarek, J.-W.; Biyikal, M.; Schulz, S. R.; Schön S.; Meyer, N.; Roesky, P. W.; Blechert, S. *Chem. Eur. J.* **2007**, *13*, 6654. Meyer, N.; Roesky, P. W.; Blechert, S. *Chem. Eur. J.* **2007**, *13*, 6654. (d) Meyer, N.; Loehnwitz, K.; Zulus, A.; Roesky, P. W.; Dochnahl, M.; Blechert, S. *Organometallics* **2006**, *25*, 3730.

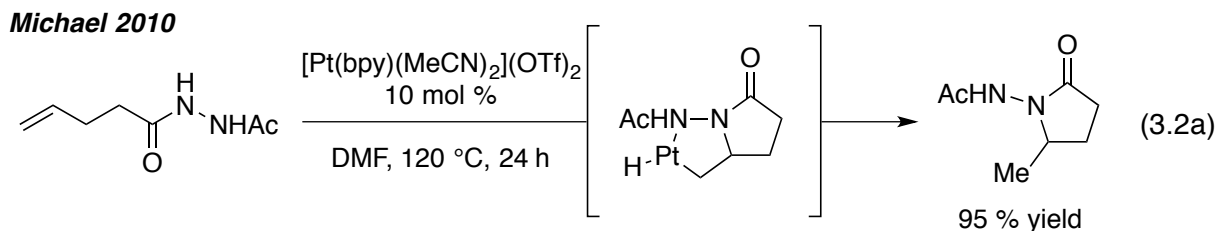
mechanism is thought to be responsible for the good compatibility of this approach with the presence of various functionalities in the substrates, more so than in related titanium-catalyzed reactions.

Patil used a Lewis acid approach, achieving the synthesis of indoles from a gold-promoted reaction of hydrazines with alkynes (Scheme 3.3).⁶⁶ The acidic aqueous conditions used in his system however support a pathway where the alkyne first undergoes hydration to the ketone, and the hydrazine intermediate formation occurs through standard condensation. Formally a hydroamination from a starting material / reagent perspective, the methodology does show how hydrazides and hydrazones could be obtained from alkynes through a conceptually very different approach than those previously discussed.

Platinum Catalyzed Intramolecular Hydrohydrazination of Alkenes

While Carreira's method is unique in using azodicarboxylates as electrophiles, most approaches will instead use the intrinsic nucleophilicity of the hydrazine nitrogen as a starting point for hydrohydrazination on alkenes. In 2010, Michael reported that platinum could catalyze the intramolecular hydroamination of *N*-acylhydrazides possessing an alkenyl moiety, strategically placed for formation of a 5 or 6-membered cycle (Eq. 3.2a). The reaction requires high temperatures and requires further substitution of the hydrazide with an EWG (acetyl, phthalyl or benzoyl groups) at N_β, and gives rise to γ- and δ-*N*-aminolactams. Mechanistic studies support an NH activation of the hydrazide, followed by an insertion of the alkene into the N-Pt bond, over the direct activation of the alkene, followed by attack of a neutral hydrazide. Protonation of the resulting C-Pt bond presumably regenerates the active catalyst, while releasing the hydroamination product.

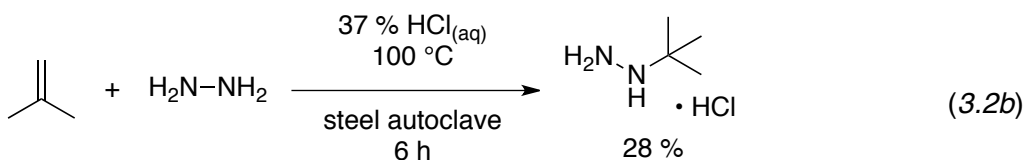
⁶⁶ Patil, N. T.; Konala, A. *Eur. J. Org. Chem.* **2010**, 6831



3.1.3 Initial Efforts in Thermal Hydroamination using Hydrazines

While hydroxylamines have demonstrated good reactivity in a number of intramolecular and intermolecular reactions with a wide variety of carbon-carbon unsaturations, attempts to uncover reactivity for hydrazines involved initial studies of simpler intramolecular processes, or of more reactive alkynes for intermolecular reactivity. Early work by the Beauchemin group proved difficult, with hydrazines proving to be much less reactive than hydroxylamines.

Chemists at Bayer have patented (1990) a procedure for the addition of hydrazine to isobutylene, which formed *tert*-butyl hydrazine upon heating in concentrated hydrochloric acid in a steel autoclave.⁶⁷ Going through a Ritter mechanism and low yielding (28%), the process represents the only example of a basic nitrogen with $pK_{aH} > 5$ reacting in an acid-catalyzed hydroamination prior to the research presented by the Beauchemin group, and clearly demonstrates the absence in the literature of procedures allowing hydrazines or derivatives to interact with unsaturations without the use of a metal catalyst.

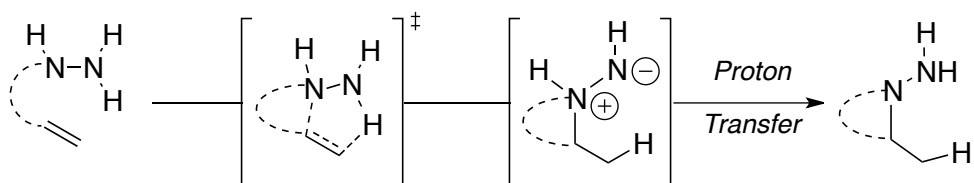


⁶⁷ (a) Kelly, M. J. Preparation of alkylhydrazines. U.S. Patent 4,954,655, September 4, 1990. (b) Eichinger, W.; Fiege, H. Process for the preparation of alkylhydrazine salts. U.S. Patent 5,585,521, December 17, 1996.

With the knowledge gained from the Cope-type hydroamination of hydroxylamines, namely the important solvent effects and necessity for protic solvents to help with the assumed kinetically relevant proton transfer step, the group was optimistic in its capacity to achieve hydroamination using hydrazines or some of its derivatives.

Early Results for the Hydroamination of Alkenes

The choice of hydrazines as reagents comes from the possibility that they could act as bifunctional reagents, providing both the necessary proton and nitrogen sources in a concerted mechanism (Eq. 3.3). However, in contrast with hydroxylamines, which can undergo intramolecular hydroamination of alkenes easily and at room temperature, the related reactivity of hydrazines for the formation of small rings, proved considerably more difficult.



Currently, the best results obtained by Whipp and Chkrebti for the reaction require elevated temperatures (180 °C), low concentrations and have only managed a 50% NMR yield (Figure 3.5). While the mechanism involved may be different, we have shown that acid promoted processes are possible, through the use of excess TFA. This allows for a better conversion to the product (in 98% NMR yield), yet still requires harsh conditions for the formation of a simple pyrrolidine.⁶⁸

⁶⁸ Cebrowski, P. H.; Whipp, C.; Beauchemin, A. M. *unpublished results*.

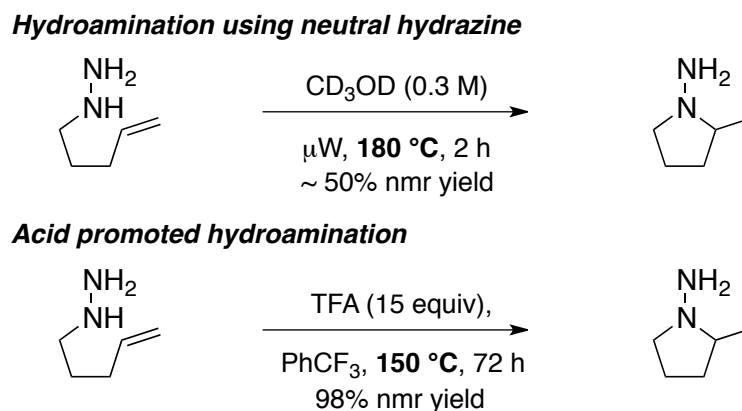
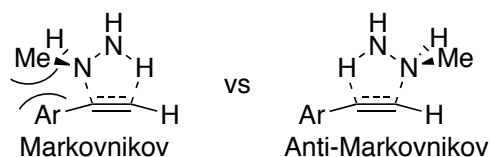


Figure 3.5 Comparison of basic reactivity of hydrazine in hydroamination, in neutral vs. acidic conditions.

Intermolecular Hydroamination of Alkynes with Hydrazines

With the reactivity of alkynes being especially easier for the Cope-type hydroamination, Ms. Cebrowski and Mr. Roveda have investigated the intermolecular hydroamination of alkynes with hydrazines.⁶⁹ Preliminary results saw aqueous hydrazine and phenylacetylene react together to give 53% NMR yield of a 2.5 : 1 mixture of regioisomers favoring the anti-Markovnikov hydrazine product over a Markovnikov side product. The reaction was then optimized using methylhydrazine, to help improve on the observed regioselectivity and favor the formation of the AM product (Scheme 3.4).

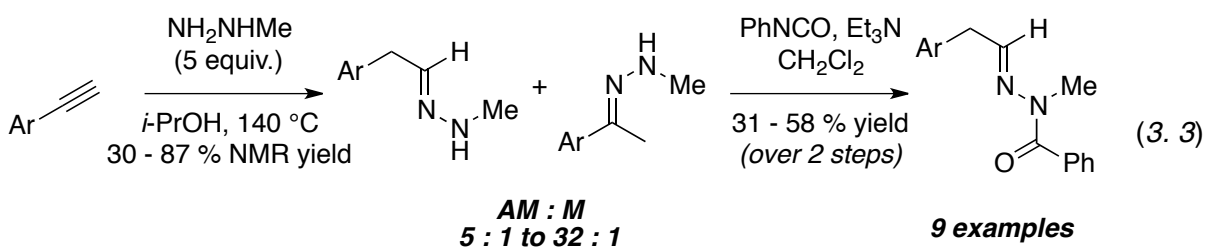


Scheme 3.4 Steric considerations in the anti-Markovnikov Cope-type hydroamination

The result of the change was the development of a reaction that would favor primarily the formation of the anti-Markovnikov hydrazone (Eq. 3.4). A variety of aryl and heterocyclic acetylenes were reacted with methylhydrazine in *i*-PrOH, yielding the two regioisomers in

⁶⁹ Cebrowski, P. H.; Roveda, J.-G.; Moran, J.; Gorelsky, S. I.; Beauchemin, A. M. *Chem. Commun.* **2008**, 492.

ratios ranging from 5 : 1 to 31 : 1 (AM : M) in moderate to good NMR yields. With the purification of such compounds proving arduous, a derivatisation to the *N*-benzoyl hydrazone derivatives was performed on all substrates, to yield these final hydrazones in 31-58% yield.

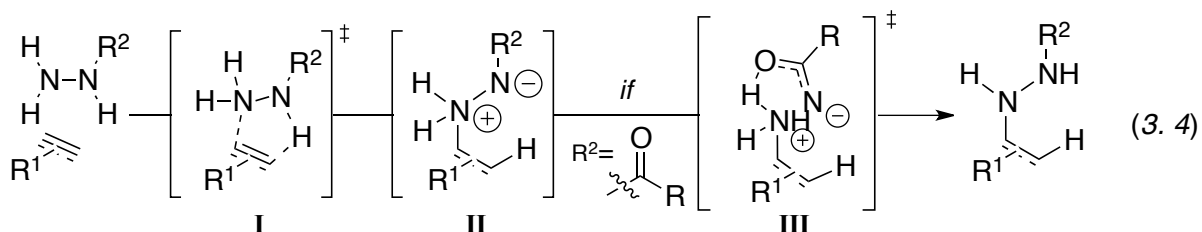


As expected, protic solvents proved key in the development of these reactions to their full potential, with *i*-PrOH providing optimal conversion and regiocontrol for the formation of terminal hydrazone. The reaction was also found to be more efficient at high concentrations (1M), with the use of distilled MeNHNH₂. Ultimately, the use of free hydrazine and alkyl hydrazines directly proved to be challenging for hydroamination, and further developments were geared towards the use of derivatives of hydrazines in the Cope-type hydroamination. Control experiments performed with AcOH or Et₃N added to the reaction did not result in significant changes, suggesting that either acid or base catalysis is not responsible for the observed reaction.

3.1.4 Beauchemin Results in the Hydroamination using Hydrazides

Hydrazides (*N*-acylhydrazines) and their derivatives are the logical extension to hydrazines. Their considerably enhanced stability over both hydrazines and hydroxylamines, both at high temperatures and to ambient air, along with their ease of synthesis and properties (being bench-stable solids), makes them attractive targets as starting materials.

Hydrazides also possess a carbonyl group strategically placed to facilitate the proton transfer step from the expected dipolar intermediate (Eq. 3.5 II \rightarrow III).

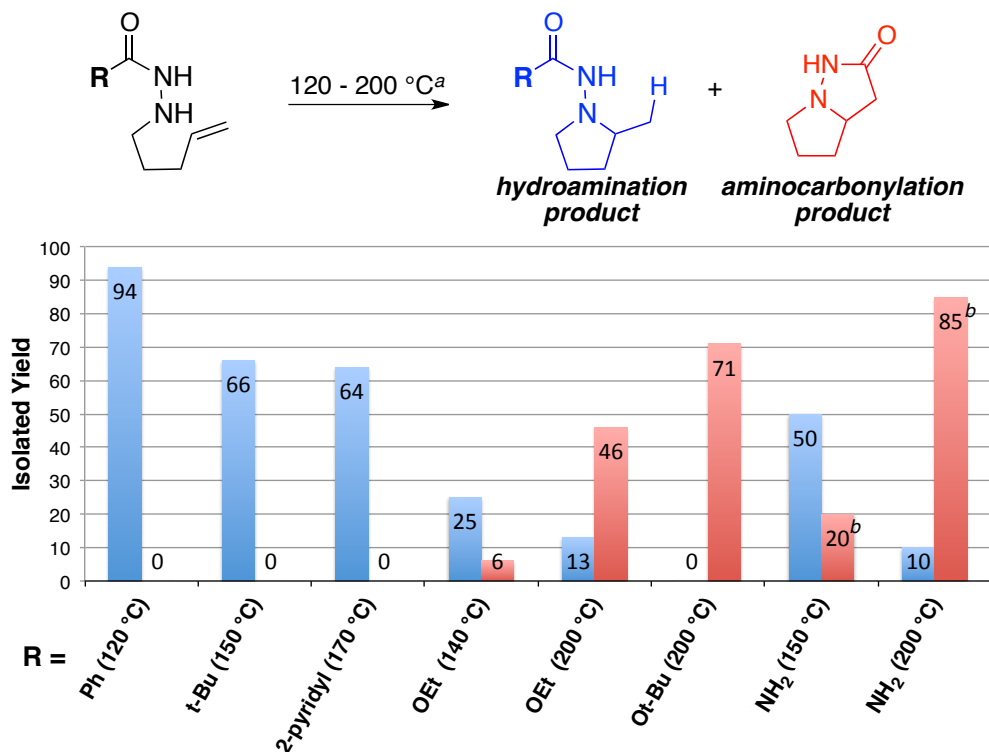


Early Scan of Hydrazides

Following initial leads by Mr. Chris Whipp, Mr. Jean-Grégoire Roveda investigated the intramolecular reactivity of hydrazides with alkenes by first generating a variety of different alkenyl hydrazides from commercially available analogues.⁷⁰ These simple substrates proved effective in generating a simple pyrrolidine ring upon cyclization via a Cope-type process. Table 3.1 presents the results obtained by heating the substrates at elevated temperatures (120 to 200 °C) in trifluorotoluene (PhCF₃) in diluted conditions (0.05M). The reaction formed solely the expected hydroamination product when aryl or alkyl substituted (Ph, t-butyl, 2-pyridyl) hydrazides are used. Arguably the best result came from the use of the alkenyl benzoic hydrazide, which was selected as the best early hydrazide moiety, and will be featured prominently in the developments of the current chapter.

⁷⁰ Original Publication (on Cope-type hydroamination with hydrazides and initial leads in aminocarbonylation): Roveda, J-G.; Clavette, C.; Hunt, A. D.; Gorelsky, S. I.; Whipp, C. J.; Beauchemin, A. M. *J. Am. Chem. Soc.* **2009**, *131*, 8740-8741.

Table 3.1 Variation of the hydrazide substituent and effect on the hydroamination and aminocarbonylation product ratios.



^a conditions: heating performed in PhCF₃ (0.05 M), sealed tube. *left*: hydroamination product isolated yield. *right*: aminocarbonylation product isolated yield. ^b NMR yield using an internal standard.

Aminocarbonylation Side Reactivity

Noticeable in Table 3.1 is the side-product obtained when carbazates (R = OEt, Ot-Bu) or semicarbazides (R = NH₂) are used as starting materials. Obtained in progressively higher yields with increasing temperature, this product was found to be a bicyclic system resulting from an alkene aminocarbonylation reaction, featuring the formation of a new C-N bond and a new C-C bond across the unsaturation. Depicted in Figure 3.6 is a closer look at this reaction, which was found to result from a thermally initiated departure of the **R** leaving group to form an aminoisocyanate, which could then add onto the double bonds.

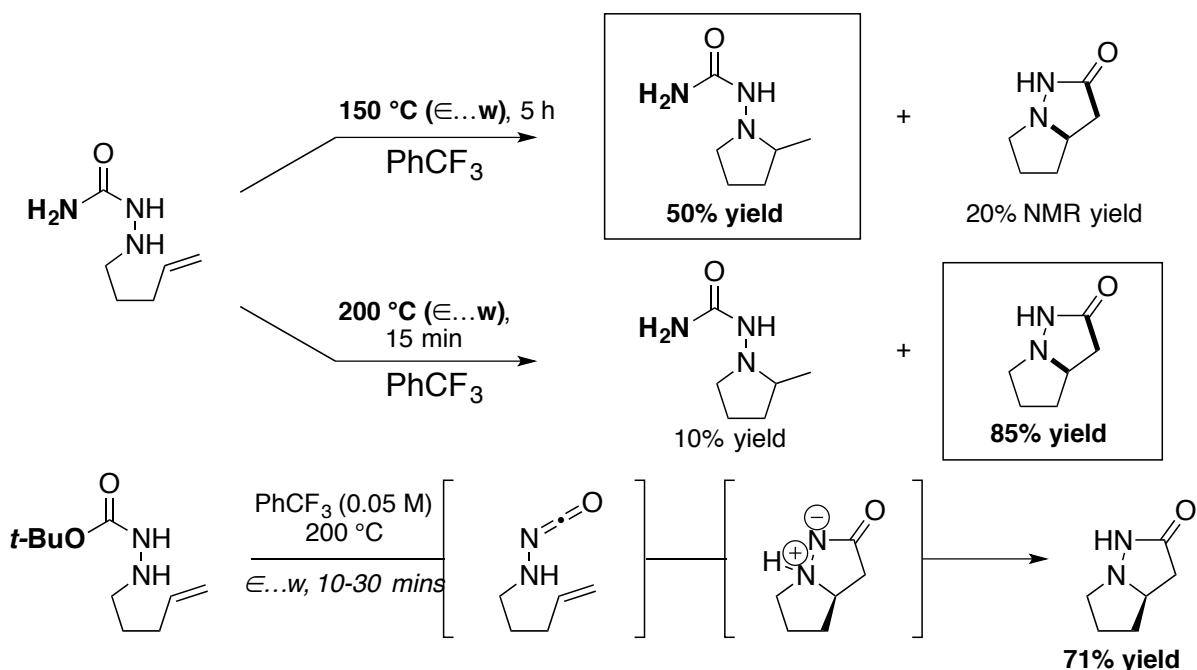
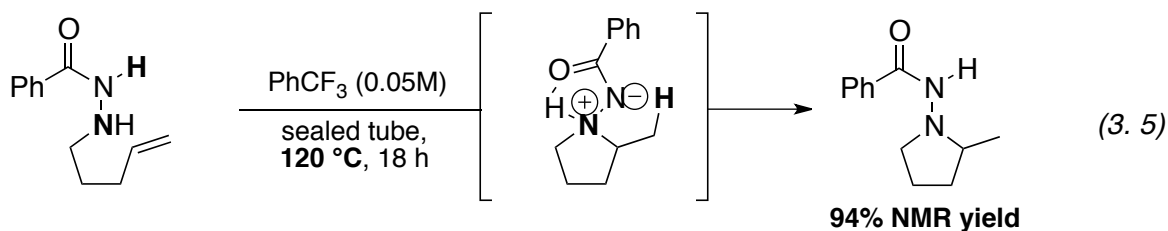


Figure 3.6 Hydroamination vs. aminocarbonylation in semicarbazides and carbazates.

The discovery of this side reaction ruled out the use of hydrazides possessing a potential leaving group for Cope-type hydroamination purposes, but opened a new area of reactivity, which, led by Mr. Christian Clavette, has since evolved and currently receives significant attention from our research group.^{70,71}



The use of benzoic hydrazides for the Cope-type hydroamination was found, as expected, to require higher temperatures when compared to equivalent cyclizations of hydroxylamines. The latter undergo intramolecular cyclization easily at room temperature,

⁷¹ New developments include aminocarbonylation and iminocarbonylation reactivity: Clavette, C.; Gan, W.; Bongers, A.; Markiewicz, T.; Toderian, A. B.; Gorelsky S. I.; Beauchemin A. M. *manuscript submitted for publication*.

while *N'*-pent-4-enylbenzohydrazide cyclizes at 120 °C (Eq. 3.6). The reaction was still the first encouraging achievement in the Cope-type hydroamination using hydrazides.

Early Solvent Scan for Hydrazide Hydroamination

A solvent scan for the reaction hinted at the hydrazide carbonyl group indeed playing its expected role as a proton shuttle, with the reaction providing good yields across a variety of non-polar, polar, protic and aprotic solvents.

Table 3.2 Solvent scan for the hydroamination of *N'*-pent-4-enylbenzohydrazide



At the start of the research presented in this chapter, an initial hydrazide scope had already been performed by Mr. Jean-Grégoire Roveda and published. As this scope was extended as part of the work presented in this thesis, it will be presented at the beginning of the results section along with further investigations.

Overview

The current lack of widespread strategies for synthesizing di- and tri-substituted hydrazides, combined with their aforementioned precarious commercial availability, marks an interesting contrast to the high potential of such targets for a variety of applications (See Section 1.4). This explains the ongoing need for and hence interest in general methods allowing access to poly-substituted hydrazines.

Classical syntheses and modern alkene and alkyne hydroamination methodologies yield varying hydrazines, hydrazides and hydrazones. The latter operate with widely different mechanisms, and include the use of reducing and oxidizing sources of hydrogen and nitrogen, [2 + 2] cycloadditions of metallonitrenes, Lewis acid activation of the unsaturation, and insertion of N-Metal bonds across the unsaturation. Amongst these, intermolecular reactivity on alkynes is often used within cascade reactions to achieve various heterocycles from a hydrazine intermediate. Platinum catalysis is limited to the intramolecular formation of diacylhydrazides. Carreira's methodology using Mn and Co catalysis remains one of the best examples of intermolecular hydroamination of alkenes, featuring good yields on a large scope of alkenes. However, the use of azodicarboxylates as starting material limits the substitution pattern, and if deprotected, yield mono-substituted hydrazines, already available through many standard methodologies alluded to earlier.

There remains a need for methodologies to achieve the synthesis of poly-substituted hydrazines in simple, short steps, both in intramolecular and intermolecular processes. The next sections will cover the investigation of the metal-free Cope-type hydroamination as an alternate strategy towards complex hydrazide synthesis, and its application to intra- and intermolecular reactivity on alkenes and alkynes.

3.2 Computational Analysis of Cope-Type Hydroamination with Hydrazines and Hydrazides

One key question this chapter will address will be whether or not the reaction of hydrazines and hydrazides with unsaturations actually undergoes a Cope-type hydroamination process.⁷² If it were the case, the reaction would proceed through a 5-membered, planar and suprafacial transition state (Eq. 3.5 I), in a process analogous to the reactivity of hydroxylamines. In the early phases of the project, computational calculations were made to support our initial claims and results. These, outlined below, give us a first insight into the mechanism in place, and will serve to fuel the developments in scope expansion and intermolecular variants for the reaction.

3.2.1 DFT Analysis of the Intermolecular Reaction of Hydrazines with Alkynes

Density functional theory (DFT) calculations were performed by Dr. Serge I. Gorelsky at the University of Ottawa on the reaction of MeNHNH₂ with phenylacetylene (Eq. 3.5, Ar = Ph), at the B3LYP/TZVP level (at 298K and 1 atm). The calculations looked specifically at possible concerted 5-membered planar transition states.⁷³ Four transition states depicting anti-Markovnikov and Markovnikov pathway of different regioselectivities are shown in Figure 3.8, along with the activation free energies (ΔG^\ddagger) for both gas phase and taking into account the electrostatic interactions with an alcoholic solvent. Both these approaches support the anti-Markovnikov preference of the reaction (by 1.4 kcal/mol in gas phase and 6.1 kcal/mol in MeOH), with the former closer to explaining the observed reactivity.

⁷² For examples of aza-Cope eliminations, likely occurring through similar TS, see: (a) Morris, D. G.; Smith, B. W.; Wood, R. J. *Chem. Commun.* **1968**, 1134. (b) Posvic, H.; Rogers, D. *J. Org. Chem.* **1974**, 39, 1588.

⁷³ Full details for calculations can be found in the electronic supporting information for the following publication: Cebrowski, P. H.; Roveda, J.-G.; Moran, J.; Gorelsky, S. I.; Beauchemin, A. M. *Chem. Commun.* **2008**, 492.

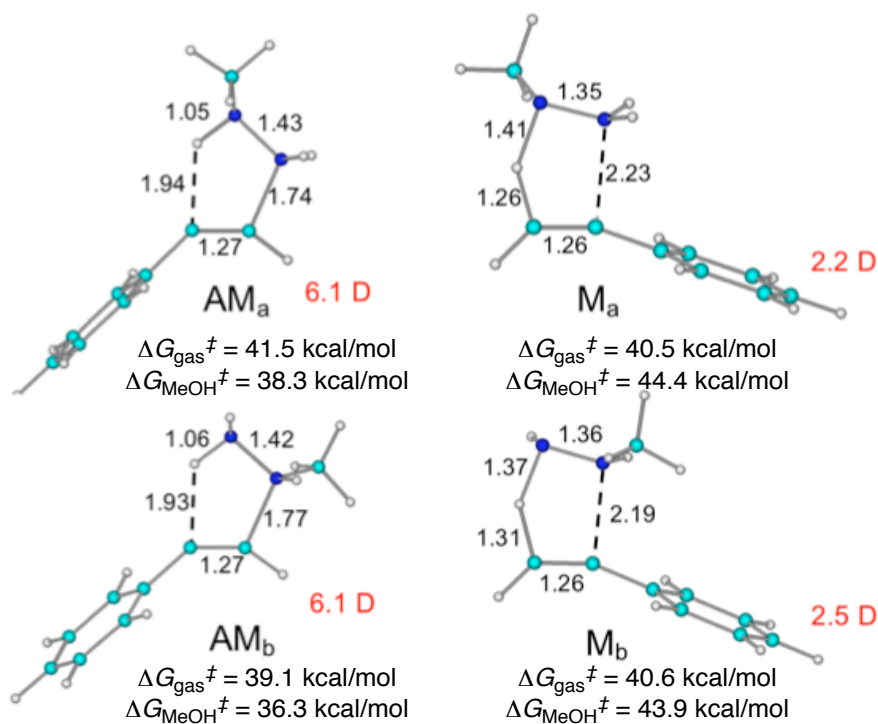


Figure 3.7 Transition state structures and free energies (gas phase and in MeOH) for the reaction between methyl hydrazine (MeNHNH₂) and phenylacetylene. Internuclear distances (Å) are shown only for relevant chemical bonds. Calculated dipole moments (Debye) are shown in red.

A close look at the intermolecular distances reveals a probable planar and concerted process, albeit fairly asynchronous, for the transition state of both the Markovnikov and anti-Markovnikov pathways. They favor an asynchronicity wherein the C-N bond forms faster in the AM pathway, and where the C-H bond forms faster in the less likely M pathway. The Markovnikov transition state is similar, but more asynchronous, to the ones calculated for hydroxylamines reacting with alkynes. These calculations suggest that altering the reagents to make either the hydrazine nitrogen that participates in the C-N bond formation more nucleophilic, or making the hydrogen to be transferred more acidic, could both help reverse the selectivity and favor the Markovnikov process. Overall, these DFT calculations are consistent with the reaction going through a Cope-type concerted process.

3.2.2 DFT Analysis of the Intramolecular Reaction of Hydrazides with Alkenes

Following the successful development of the intramolecular hydroamination of alkenes by hydrazides, DFT calculations were again performed by Dr. Gorelsky to help in the understanding of the reaction and its transition state, and guide further modifications to improve the system.⁷⁴ The cyclization of *N*-pent-4-enylbenzohydrazide was used in those calculations, performed at the B3LYP/TZVP level. A reaction profile depicted in Figure 3.8 depicts both the expected mechanism for the reaction, but also the free energies associated with each optimized intermediates, transition states and products. The activation free energy ($\Delta G_{\text{HA}}^\ddagger$) was calculated to be 28.7 kcal/mol for the cyclization (34.2 kcal/mol for a 6-membered ring). When compared to equivalent Cope-type hydroamination using hydroxylamine, the calculated activation energies of 22.9 kcal/mol (27.2 kcal/mol for 6-membered ring), support the relative ease of hydroxylamines to undergo intramolecular cyclization compared to hydrazides.

⁷⁴ Full details for calculations can be found in the electronic supporting information for the following publication: Roveda, J-G.; Clavette, C.; Hunt, A. D.; Gorelsky, S. I.; Whipp, C. J.; Beauchemin, A. M. *J. Am. Chem. Soc.* **2009**, *131*, 8740-8741.

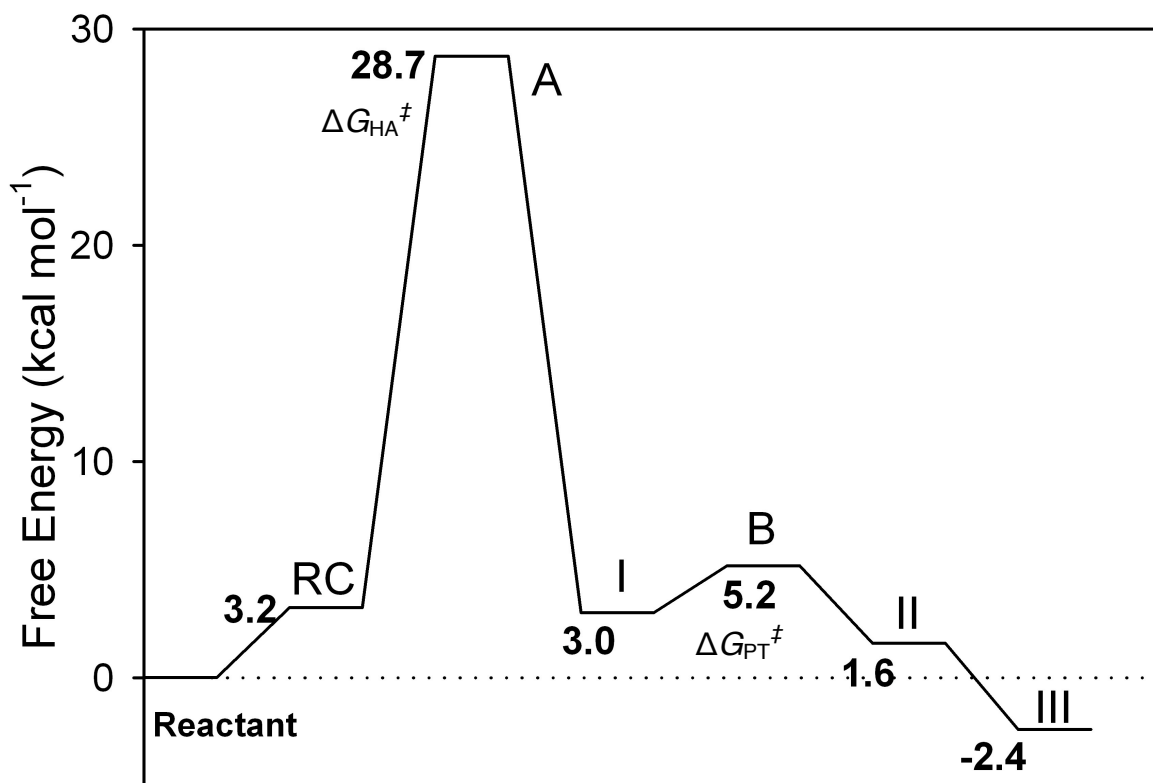
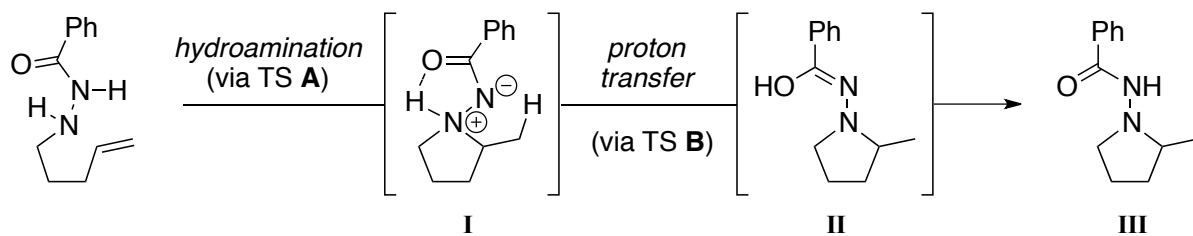


Figure 3.8 Gibbs free energy (in kcal/mol, 298K, 1 atm.) profile for the Cope-type hydroamination.

The free energy profile also supports the participation of the carbonyl group in the proton transfer step, with the proton transfer from the dipolar intermediate (ΔG_{PT}^\ddagger) only requiring 5.2 kcal/mol, explaining the compatibility of the reaction with solvents of varying polarities.

Finally, a look at the optimized transition state structures, depicted in Figure 3.9, supports a concerted asynchronous pathway for the hydroamination (TS A), with earlier formation of the C-H bond. This is in agreement with previous structures obtained for

hydroxylamines, as well as the Markovnikov transition states previously discussed in the reaction of hydrazines with alkynes. The transition state is seen to be planar and suprafacial. The N-H bond on N β is already aligned with the π^* orbital of the carbonyl going through the transition state, well position for a quick proton transfer step in the subsequent step (**TS B**).

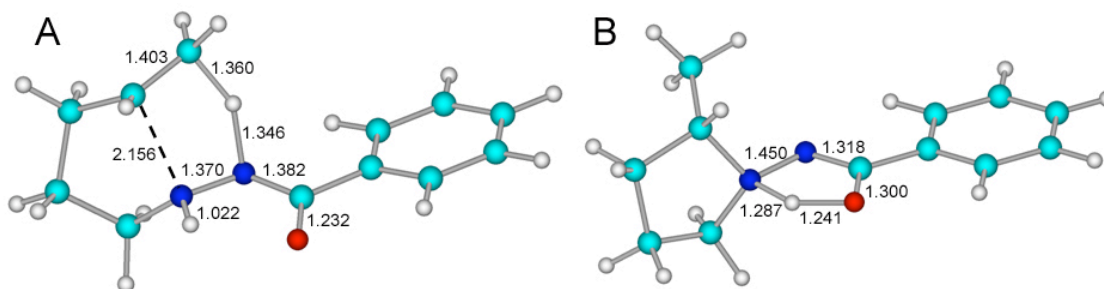


Figure 3.9 Transition state structures for the intramolecular hydroamination of *N*-pent-4-enylbenzohydrazide (**A**), and for the subsequent proton transfer step of the dipolar intermediate (**B**). The internuclear distances (Å) are shown only for relevant chemical bonds.

Description of Charges during the Intermolecular hydroamination

By their nature, hydrazides have their *N*-Acyl substituent attached on the nitrogen that is about to lose its proton while forming the dipolar intermediate. The current transition state analysis hence supports the formation of a partial negative charge on N α , as well as a partial positive charge on the alkene internal carbon. Stabilizing one or both of these partial charges in the transition state, through substrate modification or through the use of additives, has the potential to help in the overall stabilization of the process and improve the Cope-type hydroamination of hydrazides.

3.3 Scope Expansion of Intramolecular Hydroamination of Alkenes with Hydrazides: Results and Discussion

The scope of the intramolecular Cope-type hydroamination will be discussed in this section, starting from an alkenyl substituent scope for the benzoic hydrazides.⁷⁵ An expansion of the reactivity to hydrazide analogues will follow.

3.3.1 Intramolecular Reactivity with Standard Hydrazides

Benzoic hydrazides were selected as the optimal hydrazides for the Cope-type hydroamination, following a preliminary hydrazide analog scope. A solvent optimization resulted in the selection of trifluorotoluene (PhCF₃) as the best solvent. Mr. Jean-Grégoire Roveda then set out to establish the scope of the cyclization, with respect to cycle size and substitution along the alkenyl chain.

Cyclization of 5-Membered Substrates

Table 3.3 shows the results obtained for the cyclization of 5-membered rings, forming simple pyrrolidines. All substrates can cyclize efficiently to form their respective intramolecular cyclization products **3.2**. Primary and secondary hydrazides react under similar conditions (entries 1, 2, 3), cyclizing at 120 °C in good yields. Substitution in the middle of the alkenyl chain, providing significant Thorpe-Ingold effect, can help reduce the temperature required to 85 °C (entry 4). Substitution at the terminal position of the alkene is well tolerated, yet requires more energy to achieve cyclization (175 °C), and results in decreased yields (entries 5, 6). Finally, having the alkenyl chain as part of an aromatic cycle (entry 7), affords the bicyclic compound **3.4**.

⁷⁵ Mr. Michaël Raymond, as part of his summer research and B.Sc. honours thesis work, contributed to many of results of section 3.3. Mr. Jean-Grégoire Roveda presented the early results of this chapter as part of his Master's thesis.

Table 3.3 Scope of the intramolecular hydroamination of benzoic hydrazides in 5-membered cyclizations

Entry	Alkenyl Hydrazide	Temp (°C)	Product	Yield (%) ^b
	 3.1a-f			
1	R ¹ = R ² = R ³ = R ⁴ = H	120	3.2a	93
2	R ¹ = Me, R ² = R ³ = R ⁴ = H	120	3.2b	98 ^c
3	R ¹ = Ph, R ² = R ³ = R ⁴ = H	120	3.2c	40 ^d
4	R ¹ = H, R ² = Me, R ³ = R ⁴ = H	85	3.2d	96
5	R ¹ = R ² = H, R ³ = Me, R ⁴ = H	175	3.2e	61
6	R ¹ = R ² = R ³ = H, R ⁴ = Me	175	3.2f	75
7	 3.3	120	 3.4	68

^a Conditions: ran in sealed tubed or μw in PhCF₃ (0.05M), for 10 - 42 h. ^b Isolated Yield. ^c 2.4 : 1 d.r. ^d 2.9 : 1 d.r.; Yield for one major diastemer

Cyclization of Larger (6- and 7-Membered) Rings

Mr. Roveda also started an investigation into the 6- and 7-membered cyclizations. His results, along with more recent ones, are presented in Table 3.4. The cyclization of larger cycles typically requires higher reaction temperatures (175 – 235 °C), with non-substituted 6-membered rings forming much more efficiently than their 7-membered equivalents (entries 1 and 9).

Table 3.4 Scope of the intramolecular hydroamination of benzoic hydrazides in 6- and 7-membered cyclizations^a

Entry	Alkenyl Hydrazide	Temp (°C)	Product	Yield (%) ^b
	<p>3.5a-d</p>		<p>3.6a-d</p>	
1	X = CH₂	200	3.6a	90
2	X = O	200	3.6b	75
3	X = NC(O)j-Pr	200	3.6c	75
4	X = NTs	200	3.6d	81
	<p>3.7a,b</p>		<p>3.8a,b</p>	
5	R³ = Et, R⁴ = H	220	3.8a	51 ^c
6	R³ = H, R⁴ = Et	220	3.8b	47 ^c
7	<p>3.9</p>	175	<p>3.10</p>	75
8	<p>3.11</p>	200	<p>3.12</p>	84
9	<p>3.13</p>	235	<p>3.14</p>	39 ^c

^a conditions: ran in sealed tubed or μ w in PhCF₃ (0.05M), for 10 - 42 h. ^b Isolated Yield. ^c ¹H NMR yield, calculated from 1,4-dimethoxybenzene internal standard.

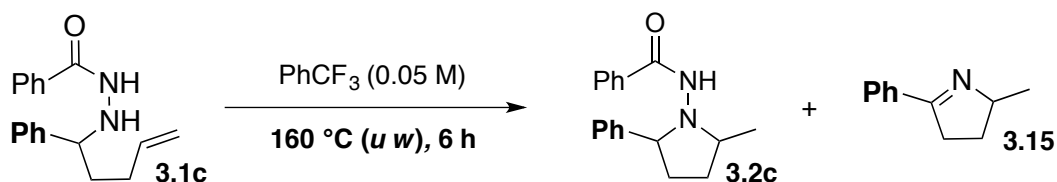
Substitution at the terminal position of the alkene is still tolerated, once again requiring higher reaction temperatures, but producing even lower yields of 51% and 47% for the *trans*

and *cis* alkene respectively (entries 5, 6). Substitution at the internal position of the alkene also gave the expected hydroamination product, this time in a respectable 84% yield (entry 8). Inclusion of heteroatoms within the alkenyl chain proved viable, producing upon cyclization a variety of morpholines and piperazines in good yields (entries 2-4, 8). Embedding an amide within the alkenyl chain allowed for an easier cyclization at 175 °C (entry 7).

Competing Elimination Side Reactivity Observed

In the reaction of compound **3.1c** (Table 3.3, entry 3), a low yield for the expected cyclization product was observed. Instead, traces on the TLCs during the reaction led to the discovery of a side product, identified as the pyrroline **3.15**. A scan of the product distribution across several reaction temperatures revealed that three compounds could result from the cyclization of **3.1c**, namely the *cis* and *trans* hydroamination products, and redox product **3.15**.

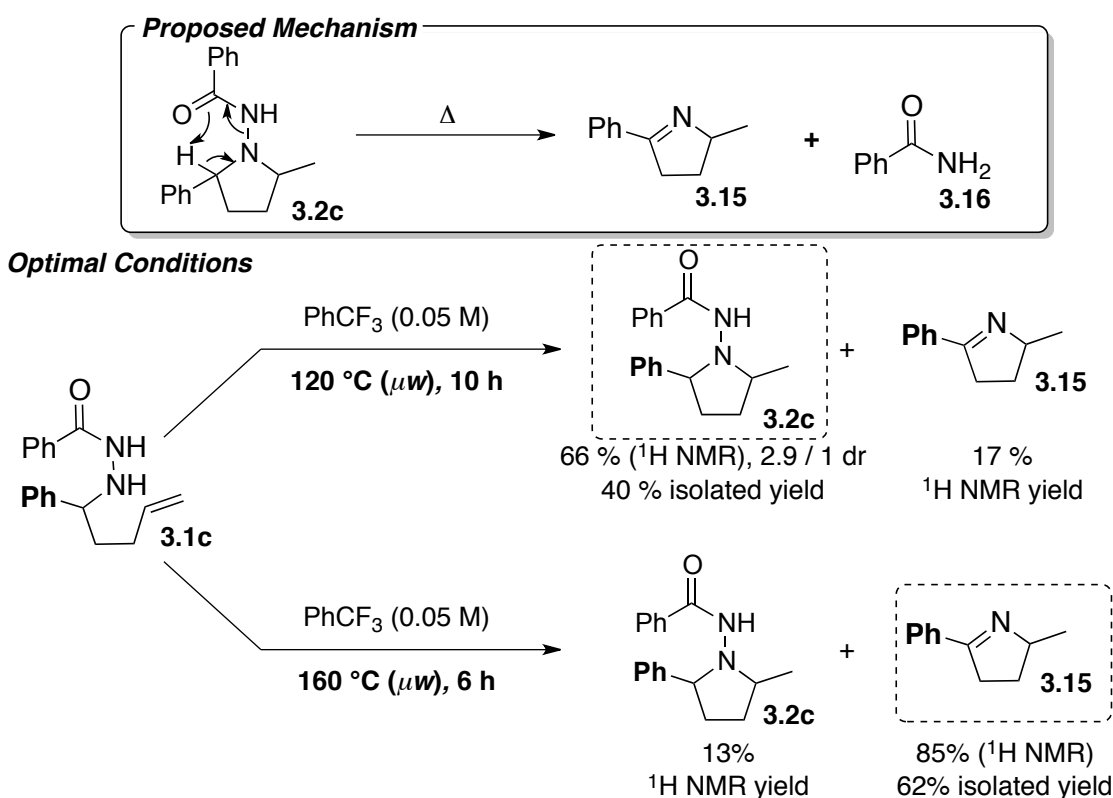
Table 3.5 Temperature scan for the hydroamination / redox of substrate **3.1c**



Entry	Temp (°C), Rxn time	Residual SM (%)	NMR Yield <i>cis</i> - 3.2c (%)	NMR Yield <i>trans</i> - 3.2c (%)	NMR Yield 3.15 (%)
1	100, 16 h	51	9	41	9
2	110, 10 h	32	12	46	12
3	120, 10 h	12	17	48	24
4	120, 16 h	10	22	35	36
5	150, 8 h	0	12	6	54
6	160, 6 h	0	14	0	85

Conditions: heated in PhCF₃ (0.05 M), in a microwave reactor. Assignment of *cis*- and *trans* isomers is arbitrary.

Table 3.5 shows that under the typical cyclization conditions (120 °C, entry 3), a 66% NMR yield for the hydroaminated product (2.9 : 1 d.r.), can be observed, along with 24% of the elimination product. Lowering the reaction temperature prevents formation of the redox product, however also slows the cyclization considerably, resulting in significant residual starting material. Increasing the reaction time mainly results in more conversion to **3.15**. Higher reaction temperatures gradually allow preferential conversion to the redox product (entries 5, 6). Ultimately, the typical conditions for cyclization were still optimal for isolation of a maximal amount of hydroamination product in 40% yield for the major diastereoisomer (see Scheme 3.5).



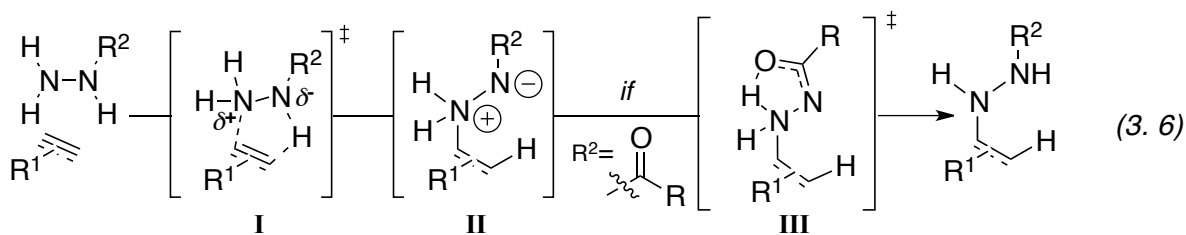
Scheme 3.5 Optimal conditions favoring hydroamination (Top) and elimination (Bottom) for substrate **3.1c**

Product **3.15** is expected to arise from an internal elimination of the hydroamination product **3.2c**, also producing benzamide. A careful look at the ratios hint at one of the

isomers of **3.2c** (presumably the *trans*) converting to **3.15** faster than its diastereoisomer, the latter (*cis*) not being significantly degraded over longer reaction times. The overall process observed, with respect to the original alkene, can be described as a metal-free oxidative amination. This is of particular interest as oxidative aminations are another family of alkene amination reactions, previously introduced in Chapter 1, for which there is a continued interest.⁷⁶

3.3.2 Expansion of Intramolecular Reactivity with Hydrazone Analogs

Based on the mechanism suggested by DFT calculations for the process (see Section 3.2), we believed the Cope-type hydroamination reactivity of hydrazides was indeed going through a concerted, 5-membered transition state to first give rise to an amine imide intermediate, rapidly converted to the hydrazone product due to the presence of the carbonyl moiety facilitating a proton transfer (Eq. 3.7). We speculated that stabilizing the charges being formed in the hydroamination transition state (**I**) could be the key in improving the reactivity of hydrazides.



More specifically, with a transition state in which the C-H bond forms faster than the C-N bond, stabilizing the partial negative charge on N_α was selected as the primary approach. Figure 3.10 depicts the different methods attempted for such stabilization. Analogues such

⁷⁶ For recent examples of oxidative amination, using palladium-catalyzed couplings, see: Lu, Z.; Stahl, S. S. *Org. Lett.* **2012**, *14*, 1234. (b) White, P. B.; Stahl, S. S. *J. Am. Chem. Soc.* **2011**, *133*, 18594. (c) McDonald, R. I.; White, P. B.; Weinstein, A. B.; Tam, C. P.; Stahl, S. S. *Org. Lett.* **2011**, *13*, 2830. (d) Timokhin, V. I.; Stahl, S. S. *J. Am. Chem. Soc.*, **2005**, *127*, 17888.

as phosphohydrazides and thiohydrazides were both thought to possess interesting stabilization potential. Modification of benzoic hydrazides, by inclusion of electron withdrawing groups to stabilize the negative charge through induction, or of hydroxyl groups capable of hydrogen bonding with the carbonyl, were investigated.

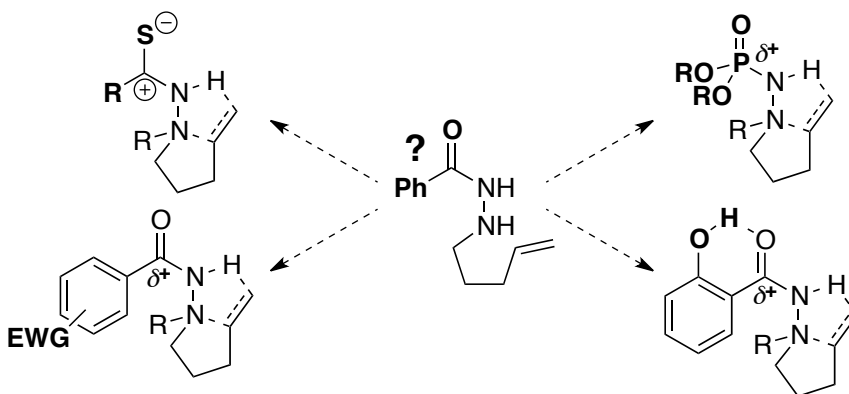
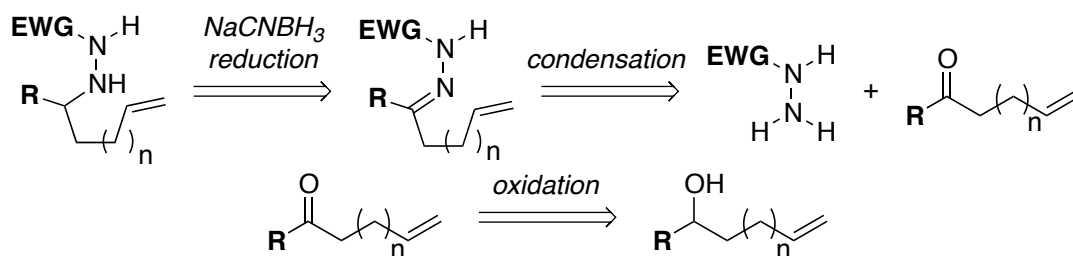


Figure 3.10 Different approaches to help better stabilize the build up of negative charge in the hydroamination transition state

Synthesis of Substrates for Cyclization

The substrates for cyclization all have to contain the alkenyl moiety. Several rounds of optimization by Jean-Grégoire Roveda to synthesize precursors through alkylation methods were mostly unsuccessful. Instead, a standard approach was taken for most substrates, following a condensation/reduction approach, which is depicted in Scheme 3.6.⁷⁷ Starting from either an alcohol or directly from a carbonyl compound containing the alkenyl moiety, condensation gives rise to an intermediate hydrazone, which can then be reduced (typically with NaCNBH_3) to yield the alkenylated hydrazide. Aldehyde intermediates are typically never isolated, and depending on the substrate, the hydrazones obtained post-condensation may also be used crude for the reduction step.

⁷⁷ The same approach is used for nearly all compounds with slight variations. The Experimental section for this Thesis can be consulted for experimental details. Specific substrates that could not be tested, for failure in obtaining the hydrazide precursors from the described methodology, or substrates synthesized through a vastly different approach will however be addressed.



Scheme 3.6 General retrosynthetic approach to the synthesis of cyclization precursors

Scan of Hydrazide Analogues and Derivatives

With a range of primary and secondary alkenylated analogs of hydrazides synthesized, some from the condensation of the free hydrazides on pent-4-enal and others on hex-5-en-2-one, we began a systematic investigation of the Cope-type hydroamination reactivity across the hydrazide family. Table 3.6 shows the generality of the approach and allows a comparison of the relative reactivity of semicarbazides, thiosemicarbazides, phosphohydrazides and hydrazides in the formation of the pyrrolidine ring system (Table 1, entries 1–8). All analogs can form the expected pyrrolidine ring, at temperatures ranging from 100 to 170 °C. Comparison of semicarbazide and thiosemicarbazide (entries 1, 2) show that the thiocarbonyl moiety is effective in lowering the required reaction temperature, and help in preventing the aminocarbonylation side reactivity.⁷⁸ Phosphohydrazides provide extremely clean conversion to cyclized products (entries 3, 4), but have shown to decompose at higher temperatures, potentially limiting their potential as wide-ranging hydrazide substitutes in the reaction.^{79, 80} Mr. Roveda in his initial scope already showed the applicability of carbon-substituted hydrazides, and ultimately benzoic hydrazides, allowing for easy derivatization, were selected to further extend the scope of the reaction.

⁷⁸ Heating semicarbazides at higher temperatures (200 °C) results in the formation of aminoisocyanate intermediates, which can lead to alkene cycloadducts: see Section 3.1 and ref. 70.

⁷⁹ Mr. Christian Clavette performed the cyclizations presented in entries 3 and 4.

⁸⁰ An aza-Cope elimination process of an amine imide formed via proton transfer is suspected at higher temperatures. For related reactivity, see: Morris, D. G.; Smith, B. W.; Wood, R. J. *J. Chem. Soc., Chem. Commun.* **1968**, 1134.

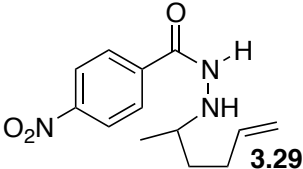
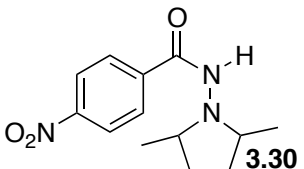
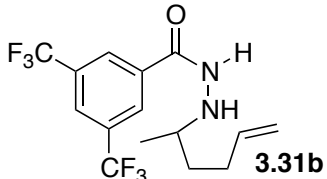
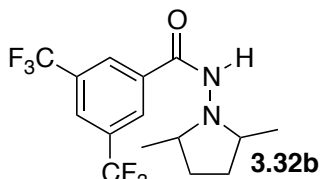
Table 3.6 Scan of hydrazide derivatives for the intramolecular Cope-type hydroamination^a

Entry	Substrate	R ¹	Temp/ °C	Product	Yield ^b (%)
1	 X = O (3.17a)	H	150	3.18a	50
2	 X = S (3.17b)	H	100	3.18b	86
3	 R = Et (3.19a)	H	120	3.20a	> 98 ^c
4	 R = Ph (3.19b)	H	110	3.20b	> 98 ^c
5	 R = <i>t</i> -Bu (3.21)	H	150	3.22	66
6	 R = 2-pyridyl (3.23)	H	170	3.24	64
7	 R = Ph (3.1a)	H	120	3.2a	93
8	 R = Ph (3.1a)	Me	120	3.2b	98 ^d
9	 R = H (3.25)	Me	90	3.26	90 ^d
10	 R = NO ₂ (3.27)	Me	70	3.28	88 ^d
11	 3.29	Me	90	3.30	91 ^d
12	 3.31b	H	95	3.32b	81

^a Conditions: heated in PhCF₃ (0.05 M), in sealed tubes (18–40 h) or in a microwave reactor (10–16 h). ^b Isolated yield. ^c ¹H NMR yield using 1,4-dimethoxybenzene as an internal standard. ^d Obtained as a mixture of diastereoisomers (see SI).

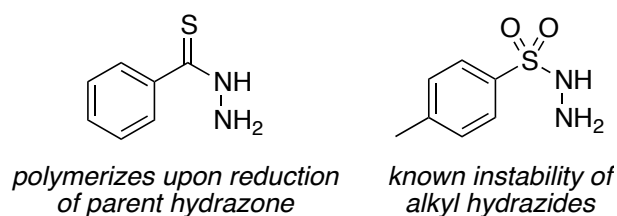
We were pleased to see increased reactivity for substrates possessing hydrogen-bond and electron-withdrawing substituents (Table 3.6, entries 9–12). Benzoic hydrazides possessing an ortho-hydroxyl group led to the desired reactivity occurring at 90 °C, as could para-nitro substituted compounds (entries 9, 11). The two effects could also be combined, with the substrate **3.27** allowing cyclization at a temperature of 70 °C. While this last result was interesting, the problematic low solubility of nitro-derivatives, for both substrates and reaction products in organic solvents, prompted us to explore the reactivity of 3,5-bis(trifluoromethyl)benzoic hydrazides (entry 12), a more soluble and easily accessed substrate, in more challenging intramolecular reactions. It should be noted that the temperatures in Table 3.7 are the optimal ones to achieve a reasonable yields in a reaction time kept under 24 h. Often times, as shown in Table 3.8, reactivity could be observed at lower temperatures, but gave lackluster yields over the desired shorter reaction times. Future runs for substrate **3.31b** were planned at 90 – 95 °C, but it showed potential even at lower temperatures.

Table 3.7 Temperature scans for the cyclization of two hydrazide derivatives.^a

Entry	Substrate	Temp (°C)	Product	NMR Yield ^b (%)
1	 <chem>CC(C)=CCNC(=O)c1ccc([N+](=O)[O-])cc1</chem> 3.29	70	 <chem>CC1CN(C)C(=O)c2ccc([N+](=O)[O-])cc2</chem> 3.30	48 ^c
2		80		76 ^c
3		90		95 ^c
4	 <chem>CC(C)=CCNC(=O)c1cc(C(F)(F)F)cc(C(F)(F)F)c1</chem> 3.31b	70	 <chem>CC1CN(C)C(=O)c2cc(C(F)(F)F)cc(C(F)(F)F)c2</chem> 3.32b	72 ^c
5		80		84 ^c
6		90		98 ^c

^a Conditions: heated in PhCF₃ (0.05 M), in a microwave reactor for 16 h. ^b ¹H NMR yield using 1,4-dimethoxybenzene as an internal standard. ^c All obtained as a mixture of diastereoisomers (3:1 d.r.).

Further expansion of the scope, to include thiobenzoic hydrazides and sulfonyl hydrazides as analogs, were problematic because of difficult access to the cyclization precursors. Thiobenzoic hydrazides, desired to combine the ultimately preferred aryl substitution with the thiocarbonyl effects observed in **3.17a**, proved to be unstable substrates, and rapidly led to polymerization adducts. Sulfonyl hydrazides, while possessing a very strong EWG attached to the hydrazine core, are known to decompose down to alkanes when they are alkylated.⁸¹ Attempts at synthesizing both precursors under mild conditions did not yield satisfying results.



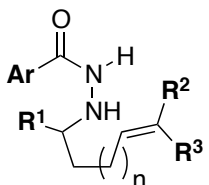
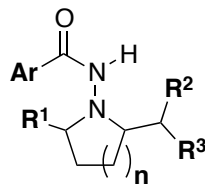
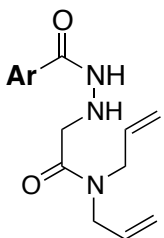
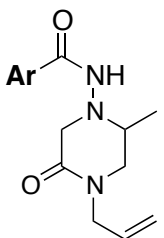
Scheme 3.7 *Hydrazide analogues not suitable for precursor synthesis*

Scope of Optimized Cyclization against Benzoic Hydrazide Substrates.

We next sought to investigate the cyclization of several substrates to access pyrrolidine and piperidine ring systems, using our optimal analog, 3,5-bis(trifluoromethyl)-benzoic hydrazides. The results are presented in Table 3.8, along with the reactivity of the simpler benzoic hydrazides (entries 2, 4, 6, 8, 10) to allow comparison. The efficiency of the cyclizations to simple 5- and 6-membered rings (**3.32a-e** & **3.34**) was comparable to that of the simple benzoic hydrazide derivatives, with all hydroaminations proceeding at lower temperatures (25 °C lower than the equivalent for benzoic hydrazides).

⁸¹ The reaction is useful in the sequence reduction of carbonyls to alkanes: Hutchins, R. O.; Maryanoff, B.; Milewski, C. *J. Am. Chem. Soc.* **1971**, *93*, 1793.

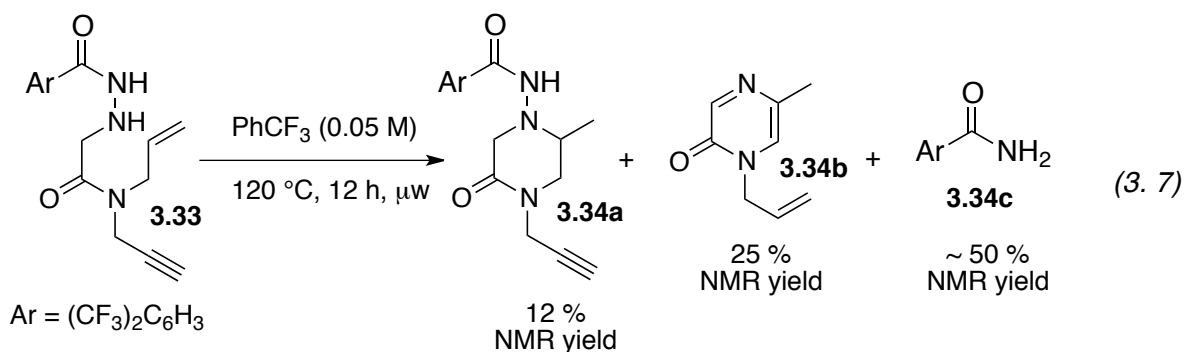
Table 3.8 Scope of 3,5-bis(trifluoromethyl)benzoic hydrazides cyclizations^a

Entry	Alkenyl Hydrazide	Temp (°C)	Product	Yield (%) ^b
				
	3.31a-e Ar = (CF ₃) ₂ C ₆ H ₃ 3.1a-f, 3.5a, 3.8b Ar = Ph			
1	3.31a R ¹ = R ² = R ³ = H, n = 1	95	3.32a	81
2	3.1a "	120	3.2a	93
3	3.31b R ¹ = Me, R ² = R ³ = H, n = 1	95	3.32b	85^c
4	3.1b "	120	3.2b	98 ^c
5	3.31c R ¹ = R ² = H, R ³ = Me, n = 1	150	3.32c	91
6	3.1f "	175	3.1f	75
7	3.31d R ¹ = R ² = R ³ = H, n = 2	175	3.32d	82
8	3.5a "	200	3.6b	90
9	3.31e R ¹ = R ³ = H, R ² = Me, n = 2	195	3.32e	53
10	3.8b "	220	3.9b	51 ^d
				
11	3.31f Ar = (CF ₃) ₂ C ₆ H ₃	150	3.32ff	92
12	3.9 Ar = Ph	175	3.10	76

^a Conditions: heated in microwave reactor in PhCF₃ (0.05M), for 10 - 24 h. ^b Isolated yield. ^c Obtained as a mixture of diastereoisomers. ^d ¹H NMR yield, calculated from 1,4-dimethoxybenzene internal standard.

While only a modest increase in reactivity was observed, the effect of the improvement was most noticeable with substrates possessing distal alkene substituents (entries 5–6 and 9–10). Such di-substituted alkenes typically afford lower yields of the cyclized products due to a more challenging hydroamination event and competing side reactions. For these systems, modified hydrazides resulted in a marked improvement in reactivity and in cleaner reactions.

Finally, substrate **3.33** was designed to compare the speed for the intramolecular reactivity of alkynes versus that of alkenes (more on alkynes in Section 3.5.2). The result of the reaction (Eq. 3.8), performed at 120 °C, was a mixture of products, which could be analyzed qualitatively as containing the expected hydroamination product from reaction on the alkene (**3.34a**), as well as degradation / redox products derived from the hydroamination product from a reaction on the alkyne.



3.4 Intermolecular Cope-type Hydroamination of Hydrazides

As highlighted and discussed in Chapter 2, intermolecular hydroaminations of alkenes are notoriously low yielding due to the overall thermoneutrality of the process. As such, early attempts to achieve intermolecular reactivity using benzoic hydrazides and norbornene proved unsuccessful.⁸² Following the expansion of the hydrazide scope to include various more reactive analogs, it was envisioned that they could provide an entry point into intermolecular reactivity.

3.4.1 High Throughput Screening For Reactivity

In partnership with the University of Ottawa's *Center for Catalysis Research and Innovation*, we set out to use their high throughput screening Symyx Technologies®

⁸² Jean-Grégoire Roveda & Francis Loiseau, unpublished results.

system.⁸³ The Symyx can run 96 reactions at the same time, allowing a rapid scan for intermolecular reactivity across a range of substrates and reaction conditions. The Symyx involves a metal plate in which all reactions can be inserted, and then covered by a PTFE film and a plate cover. It allows for some pressure build-up inside the reaction vials. The plate itself can be heated evenly to reaction temperatures reaching 200 °C, in a controlled, inert environment. The set-up allows for an automatic pipette system to distribute reagents and solvents from stock solutions into the reaction vials. All reactions can be analyzed for reaction completion or starting material consumption, by HPLC-MS or by large TLC plate.

Some of the most efficient hydrazide analogs were selected for screening against common double bonds, with norbornene and styrene, and triple bonds, with phenylacetylene, 1-octyne and 1-ethynylcyclohexanol, in a variety of solvents of different polarities (Figure 3.11). The hydrazides include the original benzoic hydrazide, as well as some of the best derivatives found to be effective in intramolecular reactions, salicylhydrazide and 3,5-bis(trifluoromethyl)benzoic hydrazide, capable of stabilization of the potential transition state for the reaction through H-bonding and inductive effects respectively. Thiosemicarbazide and bis-ethoxyphosphohydrazide were also selected for testing, for their high efficiency and stable products in intramolecular reactivity. Noticeably absent from the scope expansion in intermolecular hydrohydrazidation are the nitro-substituted hydrazides, which despite providing significant improvements to the reactivity, were deemed potentially problematic for reactions in pressurized conditions run at high temperatures (up to 200 °C), due to a high heteroatom content (5-nitrosalicylhydrazide has a N, O to C ratio of 1:1).

⁸³ Roxanne Clément, M.Sc. from the Catalysis Center was responsible for preparing and running all the reaction plates, and has worked at finding solutions to the problems with high-throughput screening that will be alluded to in the following section.

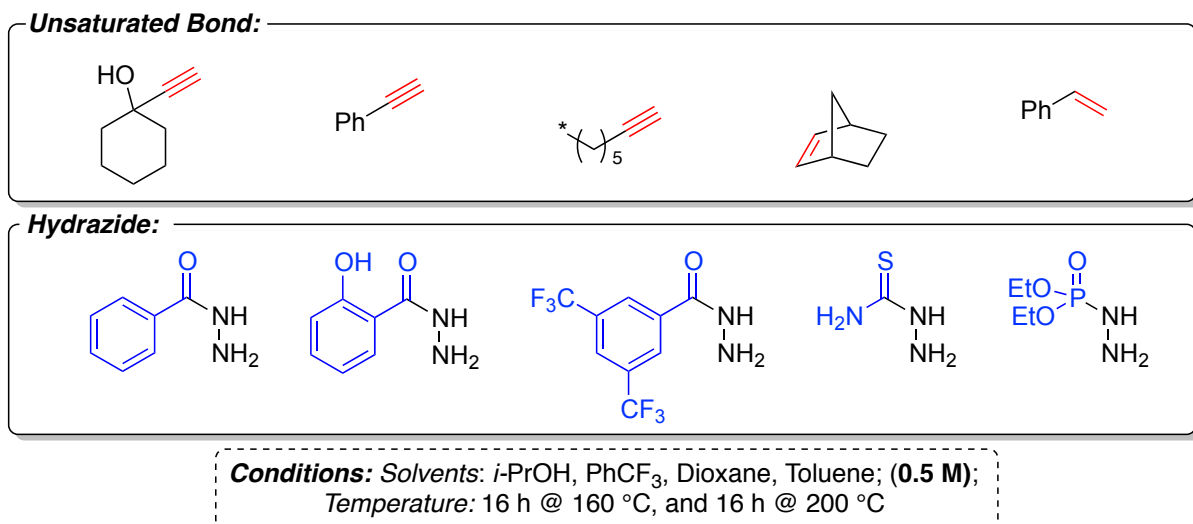


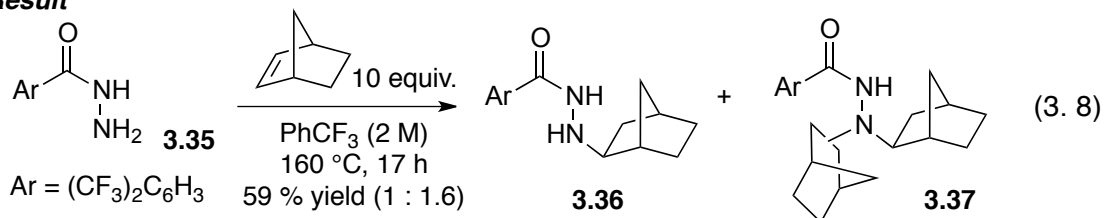
Figure 3.11 Hydrazides and unsaturated bonds used in SYMYX scan, with conditions.

Initial screening runs with the Symyx setup presented several challenges. The reaction were to be run at 160 °C and then rerun at 200 °C for a long 16 h at each temperature, with a sample of the each reaction taken between the two runs. Early solvents tested, methanol and dichloroethane, evaporated over the reaction time and left carbonized products in the reaction vials. All solvents would initially melt the PTFE films present in between the two plates and covering the reactions. Changes to the solvents used (to include *i*-PrOH and trifluorotoluene instead of MeOH and DCE) proved crucial, and a change to PFA films between the two plates proved more resistant to corrosion from boiling solvents.

Ultimately, the test reactions presented in Figure 3.11 were run, and all reactions were analyzed with TLC analyses, after reacting at both 160 and 200 °C, and compared to the starting materials. Major degradation could be observed in almost all reactions. NMR analyses on a variety of reactions proved useless, and HPLC-MS analyses did not help in deciphering any pattern of reactivity. Ultimately, long and difficult analyses of TLCs showed that the reaction of 3,5-bis-(trifluoromethyl)benzoic hydrazide with norbornene at 160 °C in PhCF₃, was one of the cleanest reactions (Eq. 3.9), showing conversions to a minimum

number of products. This substrate and the conditions used were selected to be repeated in the lab, with standard reaction scales.

Lead Result



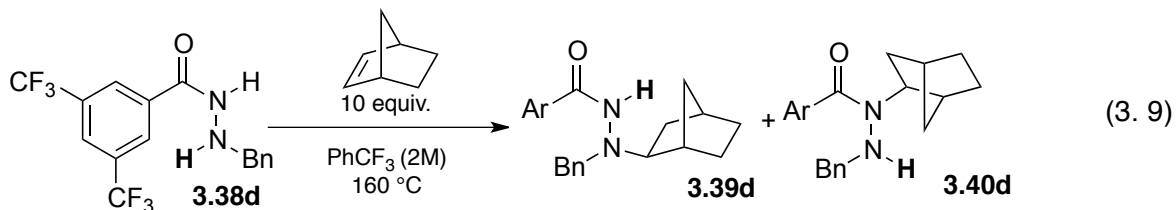
Reacting the 3,5-bis(trifluoromethyl)benzoic hydrazide with a large excess of norbornene (10 equiv.) in trifluorotoluene, and heating in a sealed tube in a simple wax bath showed interesting reactivity. Encouragingly, a mixture of mono- (3.36) and bis-hydroamination (3.37) products was formed, in a 1 : 1.6 ratio. The bis-hydroamination products were present in a seemingly non-separable mixture of diastereoisomers. Reasoning that the lack of control for mono-hydroamination observed could be avoided with the use of a substituted derivative, a benzylic substrate was synthesized for further development, hoping it would give rise to a mono-hydroamination product following proton transfer from the first dipole intermediate.

3.4.2 Reaction Optimization for *N*-Benzyl-3,5-bis(trifluoromethyl) benzoic Hydrazide

N'-Benzyl-3,5-bis(trifluoromethyl)benzoic hydrazide (**3.38d**) was synthesized, and tested once again for reactivity with norbornene.⁸⁴ The latter was kept as the alkene partner, because the high temperatures already required for intramolecular hydroamination were hinting at a guaranteed difficult intermolecular reactivity. Upon reacting the hydrazide with norbornene, two main products were visualized by TLC and were both isolated by column

⁸⁴ Ms. Alishya Burrell, as part of her B.Sc. honours thesis work, contributed to many of results in section 3.4.

chromatography. One of the major difficulties in determining the identity of both the major and minor products was the strong and constant presence of rotamers in the spectra of these molecules, due to the presence of various hindered rotational axes, between a) the aryl substituent and the carbonyl, b) the carbonyl and the N_α of the hydrazine (sp^2 hybridized) and c) between the two nitrogens.



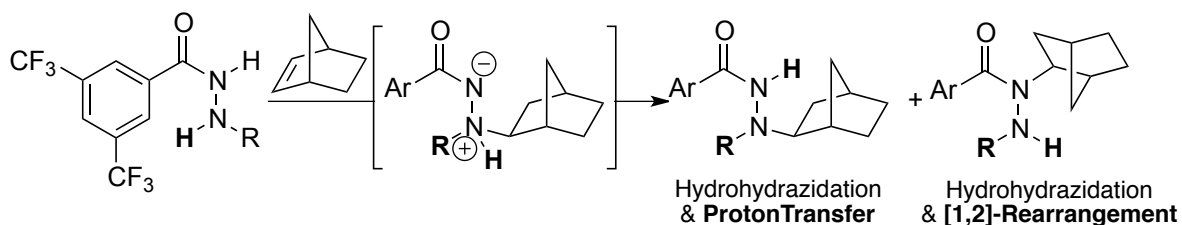
Identification of the Side Product

After unsuccessfully taking ^1H NMR spectra at room temperature, that proved too complex for analysis, subsequent spectra were collected at 80°C in benzene- d_6 , and at 120°C in DMSO- d_6 . The latter gave satisfactory spectra and allowed, with the help of other spectroscopic tools, to decipher the nature of the two products.⁸⁵ The major product proved to be the expected hydroamination product, arising from a proton transfer from the expected amine imide intermediate for the reaction (Eq. 3.10).

The second product, showing all the same basic components and chemical groups, was nonetheless different in a few key aspects. The most notable was the N-H proton shift, which was found to be much lower than in the standard hydroamination product, leading us to speculate that a shift had occurred for one of the other substituents of N_β . After initially deducing the benzyl was more likely to transfer, we established that it was instead the norbornyl group that had migrated in a [1,2]-shift to the adjacent nitrogen (proof to be shown

⁸⁵ Almost all spectra in this section, for similar heavy presence of rotamers, have also been analyzed for ^1H NMR in DMSO- d_6 , at 120°C .

later in section 3.4.3). Luckily, both products formed were easily separable, and more importantly both likely originated from the same dipolar intermediate (Scheme 3.8).



Scheme 3.8 Proton transfer and norbornyl transfer in intermolecular hydroamination of alkenes with hydrazides, shown to stem from the same amine imide intermediate.

Mechanism for the 1,2-Rearrangement

Such [1,2]-shifts are related to the Stevens rearrangement, which typically describes the [1,2] rearrangement of a benzyl from a positively charged nitrogen to a negatively-charged carbon.⁸⁶ A concerted transfer would require an antarafacial reaction,⁸⁷ however the rearrangement typically retains the initial configuration. A more likely pathway accepted involves a homolytic cleavage of the C-N bond to form a radical pair, present within a solvent cage, which can rearrange in the product.⁸⁸ 2-Norbornyl radicals are precededented and show some stability.⁸⁹

Solvent Scope for *N*'-Benzyl-3,5-bis(trifluoromethyl)-benzoic Hydrazide

The reaction of benzyl substituted hydrazide **3.38d** was also used in a scan of reactivity across solvents of different polarities and concentration. The results presented in

⁸⁶ (a) Stevens, T. S. *J. Chem. Soc.* **1930**, 2107. (b) Dunn, J. L.; Stevens, T. S. *J. Chem. Soc.* **1932**, 1926. (c) Thomson, T.; Stevens, T. S. *J. Chem. Soc.* **1932**, 55. (d) Millard, B. J.; Stevens, T. S. *J. Chem. Soc.* **1963**, 3397

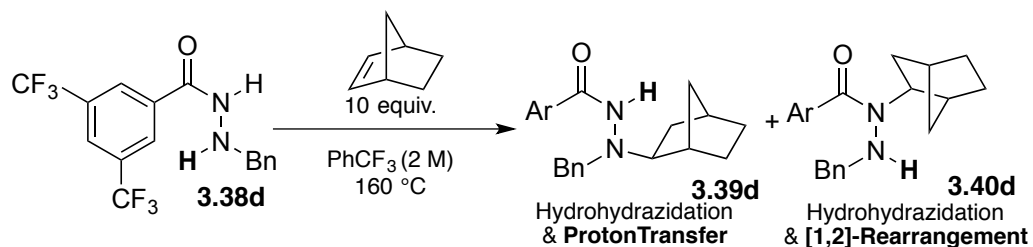
⁸⁷ (a) Kantor, S.W.; Hauser, C.R. *J. Am. Chem. Soc.* **1951**, 73, 4122. (b) Ollis, W. D.; Rey, M.; Sutherland, I. O. *J. Chem. Soc.* **1975**, 543.

⁸⁸ For a tutorial review, see: (a) Sweeney, J. B. *Chem. Soc. Rev.* **2009**, 38, 1027. For the rearrangement of hydrazinium ylides see: (b) Wawzonek, S.; Yeakey, E. *J. Am. Chem. Soc.* **1960**, 82, 5718. (c) Benecke, H. P.; Wikel, J. H. *Tetrahedron Lett.* **1971**, 12, 3479. (d) Chantrapromma, K.; Ollis, W. D.; Sutherland, I. O. *J. Chem. Soc., Perkin Trans. 1* **1983**, 1029.

⁸⁹ (a) Kropp, P. J.; Adkins, R. L. *J. Am. Chem. Soc.* **1991**, 113, 2709. (b) Kropp, P. J.; Jones, T. H.; Poindexter, G. S. *J. Am. Chem. Soc.* **1973**, 95, 5420.

Table 3.9 show that various solvents can be effective for the transformation, including fairly non-polar 1,4-dioxane and acetonitrile (entries 5, 6). The two best solvents were found to be trifluorotoluene and *tert*-butanol, performing equally well in giving overall good yields for the reaction. The reaction was therefore shown not to depend specifically on polar protic solvents, once again in agreement with hydrazides allowing easy proton transfers in varying reaction conditions. Additionally, higher concentrations of reactants proved beneficial for increased yields (entries 1,2).

Table 3.9 Scope of intermolecular hydroamination of *N'*-benzyl-3,5-bis(trifluoromethyl)-benzoic hydrazide with norbornene^a



Entry	Solvent	Concentration	NMR Yield ^b	Proton Transfer : [1,2] Ratio
1	PhCF ₃	1 M ^c	24 %	3 : 1
2	PhCF ₃	2 M ^d	60 %	2.8 : 1
3	PhCF ₃	2 M	54 %	2.6 : 1
4	DMSO	2 M	27 %	2.9 : 1
5	MeCN	2 M	38 %	2.8 : 1
6	Dioxane	2 M	42 %	2 : 1
7	<i>t</i> -BuOH	2 M	64 %	2.6 : 1

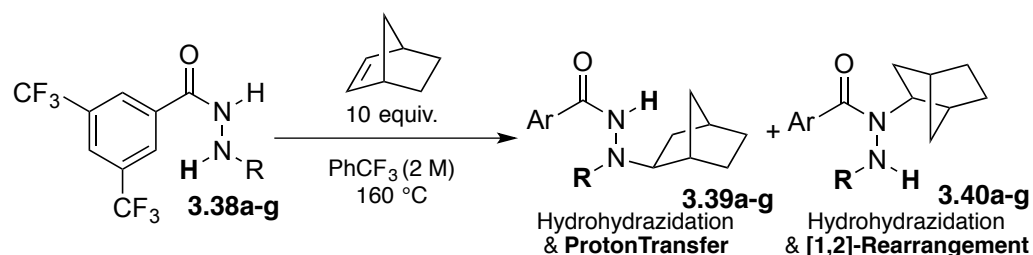
^a Conditions: performed by heating in the solvent (2 M) with 10 equiv. of norbornene, at 160 °C for 16 h in a sealed tube. ^b ¹H NMR yield, calculated from 1,4-dimethoxybenzene internal standard. ^c Done with 5 equivalents of norbornene. ^d Heated in a microwave reactor for 4 h.

From the solvent scan, it appears the product ratio is not severely affected by the choice of solvent. This ratio varied from 2:1 up to 3:1, with the only notable trend being that the least polar 1,4-dioxane appeared to promote the alkyl shift slightly more than its polar solvent counterparts.

3.4.3 Hydrazide Alkyl Scope for Intermolecular Reactivity

The scope of this intermolecular reactivity was explored with several hydrazides, as shown in Table 3.10. Though the first few substrates (**3.38b,d,e**) were tested in both *t*-BuOH and PhCF₃, the latter provided consistently higher yields (still in a similar range). The results shown therefore include only reactions performed in PhCF₃, as it was selected as the solvent of choice for the overall scan of hydrazides.

Table 3.10 Hydrazide alkyl scope of the intermolecular hydrohydrazidation on norbornene



Entry	R Group	Reaction time (h)	Products	Yield (%) ^b	Ratio PT : [1,2]
1	Me	17	3.39a , 3.40a	85	4.3 : 1
2	<i>i</i> -Pr	40	3.39b , 3.40b	74	1.7 : 1
3	<i>i</i> -Bu	17	3.39c , 3.40c	73	2.7 : 1
4	Bn	40	3.39d , 3.40d	81	3.1 : 1
5	C ₆ H ₁₁	40	3.39e , 3.40e	87	3.2 : 1
6	(CH ₂) ₂ CH=CH ₂	17	3.39f , 3.40f	87	3.7 : 1
7	(CH ₂) ₃ OBn	17	3.39g , 3.40g	86	3.3 : 1

^a Conditions: performed by heating in the PhCF₃ (2 M), with 10 equiv. of norbornene, at 160 °C for 16 h in a sealed tube. ^b isolated yield

Encouragingly, the hydroamination of norbornene proves efficient with several alkylhydrazides, providing the hydroamination products in combined yields ranging from 74% – 87% (entries 1–7). The presence of extra alkene and benzyl ether functionalities on the hydrazide is also well tolerated (entries 6 and 7). In all cases the expected hydroamination product **3.39** is favored over rearrangement product **3.40**, which consistently sees the norbornyl substituent transferring over the already present alkyl group. The ratios

of products show only a little dependence on the size of the hydrazide substituent (R), with larger groups favoring a faster alkyl shift. The results support a more facile proton transfer from the amine imide intermediate compared to the norbornyl group migration, with no rearrangement product derived from [1,2]-shift of the R substituent ever detected, highlighting the preference for the norbornyl substituent to migrate over several alkyl groups.

Proof of Structure for the [1,2]-Migration Side Product

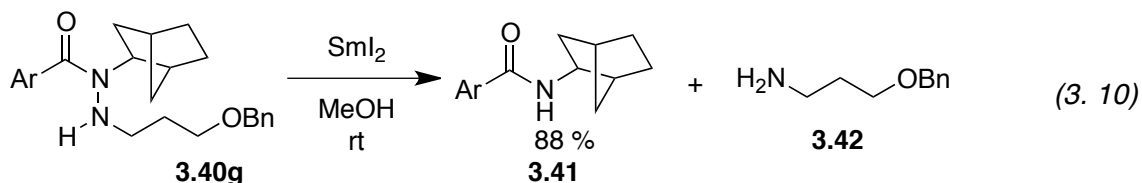
While the combined high yields of the hydroamination were encouraging, with both reaction products positively identified and characterized, an absolute proof of structure confirming the nature of the side product felt a necessary addition to our results. Previously, mass spectrometry fragment analysis was the most conclusive method in identifying which section of the molecule the various alkyl groups were attached to. With easy cleavage of the N-N bond in the mass spectrometer, fragments showing the norbornyl attached to the amide portion of the hydrazide were observed across all reaction side products (**3.40a-g**).

A chemical cleavage of the N-N bond and observation of both cleaved subsections remains the most desirable method to prove unequivocally the structure of our side product, and is a typical approach used for structure determination of many hydrazine derivatives.⁹⁰ Of note is the fact that most of the standard conditions are known to work best for cyclic hydrazides, hydrazides possessing significant steric encumbrance (tetra-substituted), or

⁹⁰ For N-N bond cleavage using Raney Nickel: (a) Selected examples for N-N bond cleavage in hydrazines: Hinman, R. L. *J. Org. Chem.* **1957**, *22*, 148–150; using diborane: (b) Feuer, H.; Brown, F., Jr. *J. Org. Chem.* **1970**, *35*, 1468–1471; using Li/NH₃: (c) Denmark, S. E.; Nicaise, O.; Edwards, J. P. *J. Org. Chem.* **1990**, *55*, 6219–6223; using NiCl₂: (d) Alonso, F.; Radivoy, G.; Yus, M. *Tetrahedron* **2000**, *56*, 8673–8678; using magnesium monoperoxy-phthalate (MMPP): (e) Fernandez, R.; Ferrete, A.; Lassaletta, J. M.; Llera, J. M.; Monge, A. *Angew. Chem., Int. Ed.* **2000**, *39*, 2893–2897. using Sml₂: (f) Ding, H.; Frestad, G. K. *Org. Lett.* **2004**, *6*, 637–640; using Zn/AcOH: (g) Sapountzis, I.; Knochel, P. *Angew. Chem., Int. Ed.* **2004**, *43*, 897–900. (h) Sinha, P.; Kofink, C. C.; Knochel, P. *Org. Lett.* **2006**, *8*, 3741–3744.

those substituted by multiple electron withdrawing groups. Our acyclic, tri-substituted and monoacyl products were therefore less conventional for most methods.

The 3-benzyloxy-propyl substituted hydrazide (side product **3.40g**) was selected for cleavage attempts, for the size of the substituent would make both cleaved fragments easily observable and isolable. Initial cleavage attempts using standard Birch reduction conditions proved unsuccessful.⁹¹ The use of samarium iodide for the cleavage resulted in an 88% isolation of the expected norbornyl substituted amide **3.41** (Eq. 3.11), and observation of the terminal amine **3.42** as well.⁹² This effectively proved the structure of the migration side product.



3.4.4 Extension of Intermolecular Hydroamination Beyond Norbornene

With the reaction now working in many solvents and amenable to various alkylated hydrazide, one drawback of the method was the apparent limitation of intermolecular reactivity to biased and strained alkenes. Efforts were made to expand this reactivity to other alkenes and to alkynes, with limited success. Reacting 3,5-bis(trifluoromethyl)benzoyl hydrazide with styrene based alkenes and allylic alcohols did not result in any reactivity.

⁹¹ Birch conditions N-N bond cleavage attempted: (a) Wasserman, H. H.; Robinson, R. P.; Matsuyama, H. *Tetrahedron Lett.* **1980**, *21*, 3494. (b) Jacobi, P.A.; Martinelli, M.J.; Polanc, S. *J. Am. Chem. Soc.* **1984**, *106*, 5595.

⁹² Samarium iodide N-N bond cleavage: Hashimoto, T.; Maeda, Y.; Omote, M.; Nakatsu, H.; Maruoka, K. *J. Am. Chem. Soc.* **2010**, *132*, 4076.

The reaction of hydrazide **3.35** with various alkynes was tested in various solvents and concentrations.⁹³ In our best results, presented in Table 3.11, Dr. Nicolas Das Neves showed that the reaction with phenyl acetylene results in low conversions to hydrazone **3.43**. At the high temperatures and long reaction times used, a notable decomposition of the hydrazide starting material started to occur, potentially competing with the desired process.

Table 3.11 Reactivity of Hydrazides in Intermolecular Hydroamination of Phenylacetylene

Entry	Equiv. Acetylene	Temp (°C)	NMR Yield ^a (%)
1	1	160	10
2	1	200	15
3	5	200	13

Conditions: heated in *t*-BuOH (1 M), sealed tube for 16 h. ^a NMR yield using TMB as an internal standard.

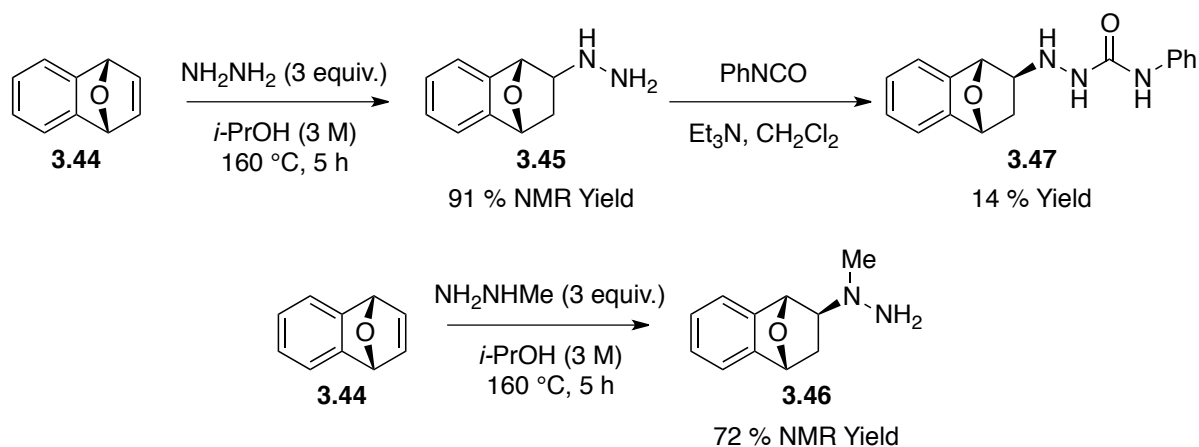
3.5 Other Developments in Cope-type Hydroamination of Hydrazines

While the Cope-type hydroamination reactivity of hydrazide in intramolecular systems (Section 3.3) proved very successful, results were more moderate for the intermolecular variants just discussed. In an effort to be extensive in our investigation of hydrazines and hydrazides as bifunctional reagents, a few approaches were missing, with hydrazines having shown no previous capabilities in intermolecular reactions with alkenes. These concerns will be addressed and be followed by a brief discussion of the intramolecular reactions of hydrazides with alkynes.

⁹³ Mr. Pierre Mouawad, as part of his honours thesis, and Dr. Nicolas Das Neves, took part in the attempted extension of the intermolecular reactivity of the Cope-type hydrohydrazination to alkynes.

3.5.1 Confirmation of Scope for the Reactivity of Hydrazines

Dr. Nicolas Das Neves attempted the intermolecular reactions of hydrazines onto alkenes. The results obtained from reactions with hydrazides were indicative that at best, the reaction could show some potential with biased alkenes. Due to the nature of the products expected, namely alkyl or aryl substituted hydrazines, which are notoriously difficult to isolate, large norbornene analog **3.44** was selected as a reaction partner.



Scheme 3.9 Reactivity of norbornene analog with hydrazine and methylhydrazine

Scheme 3.9 depicts the reactions of **3.44** with hydrazine and methylhydrazine, which gave at 160 °C interesting conversions to hydroamination products **3.45** and **3.46**. ^1H NMR yields of 91% and 72% were observed for the respective reactions, however isolation of both products proved unmanageable using standard purification methodologies.⁹⁴ Derivatization of **3.45** into the semicarbazide analog allowed for a 14% isolated yield of **3.47** for confirmation of structure through characterization.

⁹⁴ Of note is the fact that no reactivity could be observed with norbornene in similar conditions, although this is likely due to the increased volatility of the compound.

3.5.2 Concurrent Development of Intermolecular Hydroamination of Alkynes with hydrazides

The use of the 3,5-bis(trifluoromethyl)benzoyl substituted hydrazines proved key to the achieving better yields and smoother reaction conditions for the intramolecular reactions of alkenes, as well as opening the door to intermolecular reactivity with biased alkenes. The interest in the substitution was found to be high enough to warrant a closer look in terms of other projects concurrently developed in the Beauchemin group. Of note is the intramolecular reactivity of hydrazides with alkynes, which was developed in parallel to the hydroamination of alkenes. Ms. Ashley Hunt was responsible for most the ground work in this specific area of hydroamination.⁹⁵

In an interesting difference to the reactivity of alkenes with hydrazides, by design the reaction of alkynes has to give rise to a 1,3-dipolar azomethine imine products, which result from a tautomerization following the thermal hydroamination event. Such allyl anion dipoles are precedented in the literature and have known application as partners in dipolar cycloadditions and as electrophiles.⁹⁶ Their current use is limited due to the instability of most azomethine imines, and they therefore generally have to be generated in situ.

While work was underway with the alkenyl hydrazides, similar efforts were directed at reacting *N'*-alkynylbenzoic hydrazide in an intramolecular Cope-type hydroamination, performed by Ms. Ashley Hunt. Early efforts (Eq. 3.12) showed full consumption of the starting hydrazide, and a likely azomethine imine product observable through NMR

⁹⁵ The development of the intramolecular reactivity of alkynes was performed by Ms. Ashley Hunt and Ms Isabelle Dion as part of their Master's and Ph.D. programs respectively. Results are presented here for completeness and to better summarize the current limits of reactivity of hydrazine and hydrazide derivatives. All supporting information can be found in Ms. Hunt and Ms Dion's Master's and Ph.D. theses, and as part of publication currently in preparation.

⁹⁶ For examples: (a) Grigg, R.; Dowling, M.; Jordan, M. W.; Sridharan, V.; Thianpatanagul, S. *Tetrahedron*, **1987**, *43*, 5873. (b) Kanemasa, S.; Tomoshige, N.; Wada, E.; Tsuge, O. *Bull. Chem. Soc. Jpn.* **1989**, *62*, 3944.

spectroscopy. However, product isolation attempts resulted in its decomposition. It was speculated that the stability of the products could be improved through the use of the electron-withdrawing 3,5-bis(trifluoromethyl)benzoyl group to provide the necessary stabilization of the negative terminus of the dipole, allowing for complete characterization of the dipole products. This was attempted and a variety of cyclization precursors, once the process proved viable, were prepared and tested for hydroamination reactivity.

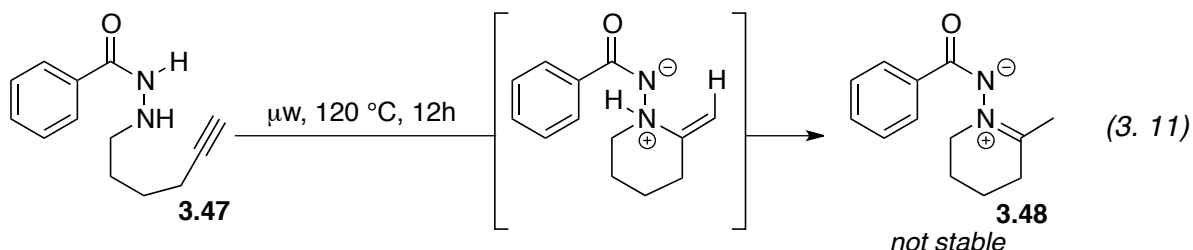


Table 3.12 shows that 3,5-bis(trifluoromethyl)-*N*'-alkynylbenzoic hydrazides are able to afford the hydroamination cyclized products in good yields (53 – 93%) for the formation of 6-membered cycles, with a lower reactivity observed in the formation of 5-membered cycles (entries 12, 13). Terminal and internal alkynes, possessing methyl or aryl groups, proved to be competent substrates. Substitution at the α position of the alkynyl chain also allowed good reactivity. Throughout the scope, the azomethine imine, embedded within the six-membered cycle product, proved to be robust and could be isolated through standard chromatographic techniques. By comparison, cyclization to form 5-membered cycles resulted in products of lower stability, which could be derived to the fully reduced hydrazide related compound for proper isolation.

Several later attempts at using other hydrazides (*ortho*-hydroxyl or mono- CF_3 substituted) resulted in a near complete shutdown of the reactivity, outlining the importance of 3,5-bis(trifluoromethyl)-benzoic hydrazides in stabilizing dipolar intermediates.

Table 3.12 Scope of hydroamination route to azomethine imines

Entry	Substitution	Temp (°C)	Product	Isolated Yield (%)
	 3.49a-k			
1	R ¹ = R ² = H	140	3.50a	68
2	R ¹ = H, R ² = Me	160	3.50b	67
3	R ¹ = H, R ² = Ph	140	3.50c	72
4	R ¹ = H, R ² = 3,5-(Me) ₂ C ₆ H ₃	140	3.50d	92
5	R ¹ = H, R ² = 4-BrC ₆ H ₄	140	3.50e	73
6	R ¹ = H, R ² = 4-MeOC ₆ H ₄	140	3.50f	86
7	R ¹ = H, R ² = 4-MeO ₂ CC ₆ H ₄	140	3.50g	53
8	R ¹ = H, R ² = thienyl	120	3.50h	53
9	R ¹ = Me, R ² = H	110	3.50i	91
10	R ¹ = <i>n</i> -Bu, R ² = H	120	3.50j	93
11	R ¹ = Ph, R ² = H	120	3.50k	91
	 3.51a-b			
12	R ¹ = R ² = H	140	3.52a	44 ^b
13	R ¹ = H, R ² = Ph	150	3.52b	62

^a Conditions: A solution of hydrazide in PhCF₃ (0.05 M) was heated for 14h (microwave reactor).

^b Isolated Yield after reduction with NaBH₄

3.6 Mechanistic Investigation: Results and Discussion

Despite having DFT calculations to support our claims that hydroamination with hydrazines and hydrazides is indeed operating under a Cope-type concerted, 5-membered hydroamination process, we wanted concrete proof of that fact, both for a complete understanding the mechanism, and to guide potential future changes to the system. Any plans to catalyze the reaction, or attempt asymmetric variations, would also greatly benefit from a thorough understanding of the process.

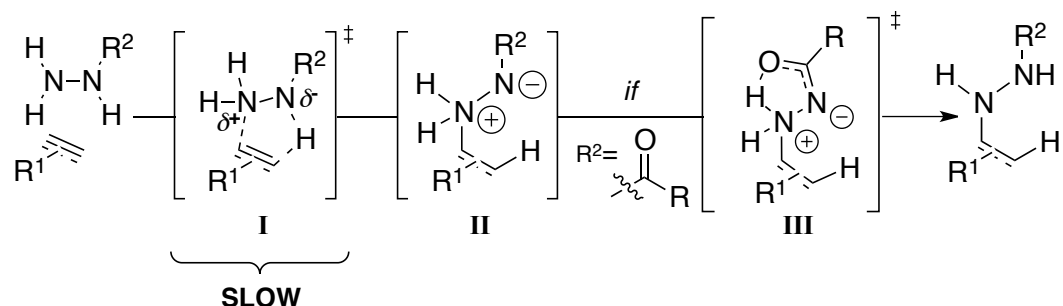


Figure 3.12 Identification of the slow step of the hydroamination of hydrazides based on DTF calculations ($\Delta G^\ddagger = 28.7$ kcal/mol)

The slow step for the hydroamination reaction of hydrazides is expected to be the hydroamination event (see Figure 3.12 I). Heavy support to the proposed concerted process for the reaction can come from a demonstration that two carbon atoms are involved in bond forming events in the transition state. For that reason kinetic isotope effect determinations seemed the best approach for a mechanistic investigation.

3.6.1 Kinetic Isotope Effects

Most elements are present in nature as mixture of different isotopes, notable examples being hydrogen (¹H) and its isotope deuterium (²H), as well as carbon (¹²C) and its ¹³C and ¹⁴C isotopes. Since isotopes vary only in their number of neutrons, they are fundamentally the same atoms and can be expected in almost all cases to participate in the same reactions.

However they have a different overall mass (^2H has a 100% increase in mass over ^1H , and ^{13}C has a 8% increase in mass over ^{12}C), which can affect the rate of reactions when the different isotopes are involved in bond forming/breaking events. For primary KIEs, in which the bond formed or broken involves directly the isotopic atom, rate changes can be of up to 6 – 10 times faster for ^1H vs. ^2H , while it can be up to only 1.04 times faster for ^{12}C vs. ^{13}C .⁹⁷

Secondary Deuterium KIEs (SDKIE), involving atoms not directly involved in a bond forming/breaking event during a transformation, are also possible. They arise because of variations in hybridization of adjacent atoms (involved in bond breaking or formation). For typical processes, both normal and inverse SDKIEs are possible, normally depending on the variation in the hybridization state that happens going into a transition state. For a reaction going from an sp^2 starting material into an sp^3 transition state, the higher energy (stiffer out of plane bending) distances vibrational states in the transition state, and gives rise to the inverse (< 1) SDKIE, with the heavy atom reacting faster. The opposite is normally true from reaction going from an sp^3 into an sp^2 transition state, which gives rise to a normal (> 1) SDKIE.

Singleton's Method for Natural Abundance KIE Determination

In trying to decipher reaction mechanisms, KIEs often play a key role, as they can give information primarily on the rate-determining step of the reaction. Atoms involved in bond forming events, or those adjacent to them, can exhibit KIEs or SDKIEs. Determining KIEs can cause many significant practical challenges. Standard KIE measurements must first be made using deuterium or ^{13}C enriched reagents. Both the original starting material and the isotope-enriched version must be allowed to react, and the relative speed of both reactions

⁹⁷ Anslyn, E. V.; Dougherty, D. A. (2006). *Modern Physical Organic Chemistry*. University Science Books. pp. 428–431.

must be accurately determined. Multiple different enrichments must be made for each required KIE value.

Singleton came up with a partial solution to the problem and developed in 1995 an approach by which KIE measurements can be made from multiple, high precision ^2H and ^{13}C experiments, directly with natural abundance (unlabeled) reactants.⁹⁸ The method, initially developed on a Diels-Alder reaction, can be summarized as follows: with all reactants possessing a random distribution across all atoms of naturally occurring heavier isotopes, reactions can be taken to near completion, having the lower isotopes involved in the bond forming/breaking steps reacting faster than their heavier counterparts. The residual starting materials are as such enriched in the heavier isotope (for a normal KIE) at positions involved in the transition state of the rate-determining step. Such an enrichment can be measured by comparing high purity, clean spectra of both the original starting material and the residual one from the reaction.

Attempts at Using Singleton's Method for Hydrazide Hydroamination

The simple cyclization to pyrrolidine rings, for example from **3.1a** to **3.2a**, seemed like the perfect reaction to use Singleton's method on. The starting materials were easily scalable, of a typically high purity, and could be recrystallized if needed. The reaction was very efficient, achieving yields approaching quantitative, and no side reaction was noticeably

⁹⁸ Original report from Singleton: (a) Singleton, D. A.; Thomas, A. A. *J. Am. Chem. Soc.* **1995**, *117*, 9357. Use in other reactions: (b) Singleton, D. A.; Merrigan, S. R.; Liu, J.; Houk, K. N. *J. Am. Chem. Soc.* **1997**, *119*, 3385. (c) Singleton, D. A.; Hang, C.; Szymanski, M. J.; Meyer, M. P.; Leach, A. G.; Kuwata, K. T.; Chen, J. S.; Greer, A.; Foote, C. S.; Houk, K. N. *J. Am. Chem. Soc.* **2003**, *125*, 1319. (d) Singleton, D. A.; Nowlan, D. T., III; Jahed, N.; Matyjaszewski, K. *Macromolecules* **2003**, *36*, 8609. (e) Singleton, D. A.; Hang, C.; Szymanski, M. J.; Greenwald, E. E. *J. Am. Chem. Soc.* **2003**, *125*, 1176. (f) Saettel, N. J.; Wiest, O.; Singleton, D. A.; Meyer, M. P. *J. Am. Chem. Soc.* **2002**, *124*, 11552. (g) Singleton, D. A.; Merrigan, S. R.; Kim, B. J.; Beak, P.; Phillips, L. M.; Lee, J. K. *J. Am. Chem. Soc.* **2000**, *122*, 3296. (h) Singleton, D. A.; Merrigan, S. R. *J. Am. Chem. Soc.* **2000**, *122*, 11035.

present, ensuring no competing pathway could affect the measured ratios of isotopes. Reactions were planned to use the HPLC in order to follow ongoing large-scale reactions, so they could be stopped at the desired time and get an optimal amount of residual starting material for NMR analyses using Singleton's method (Figure 3.14).

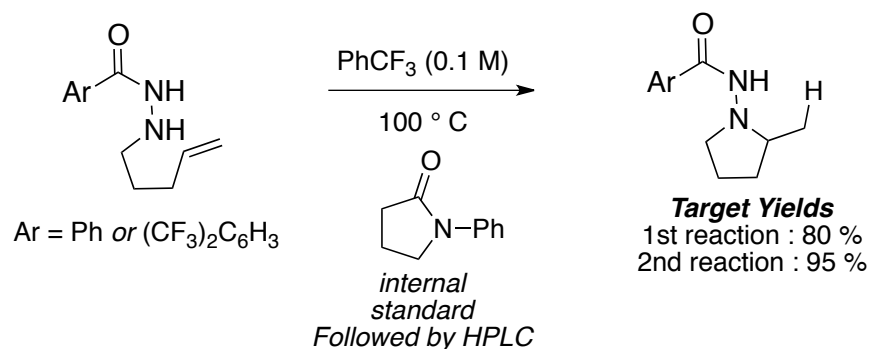


Figure 3.13 Attempted experiments using Singleton's method for KIE determination at natural abundance.

Most products for the intramolecular hydroaminations (**3.2**, **3.4**) had strong rotamer problems during characterization, as mentioned earlier, and required constant high temperature NMRs. The starting materials, important for the current method discussed, did not appear to have the same issues. However, as the analytical techniques for the upcoming Singleton runs were being finalized, and starting materials were batched up to multi-gram scales, problems started to appear. Both the alkenylated version of 3,5-bis-(trifluoromethyl)benzoic hydrazide and benzoic hydrazide proved, once purified and recrystallized attentively, to have minor amounts of rotamers present (< 2% by area).

Following the first completed runs of the developed analytical technique, residual starting materials were collected, purified, and compared to the original starting material. The minute amounts of rotamers observed in the starting material were found to add too much uncertainty to the integration values obtained from the best available NMRs, resulting in no clear trend or reliable data from which KIEs could be determined. It did seem, after

grueling efforts were invested in developing the system, that for this specific case, standard KIE determination, through chemical isotopic enrichment of selected atoms, would be the only way to determine our desired KIEs.

3.6.2 Standard KIE Measurements for The Hydrazide Hydroamination

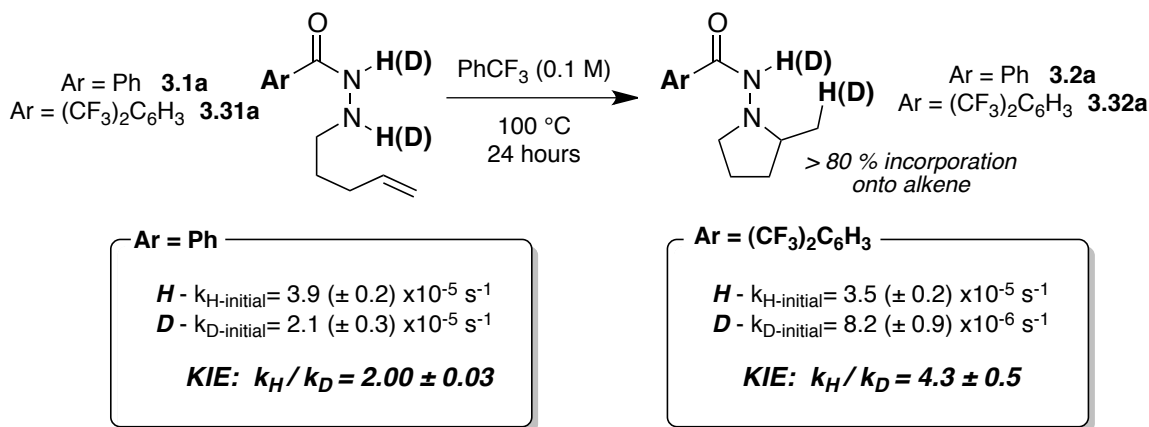
The hydroamination reaction presumably involves in its transition state the formation of both a C-N and a C-H bond, while the N-H bond breaks. These are the atoms we should expect to have a primary KIE. Because of the synthetic approach used to synthesize the precursors, ^{13}C enrichment was problematic on multiple levels, because of various functional group compatibility issues that could arise over the synthesis. Deuterations on the nitrogen atoms and on the alkene were the two fastest pathways to isotope-enriched products, and were both investigated.

Deuteration at the Hydrazide Nitrogens.

Deuteration at both nitrogens was achieved with benzoic and 3,5-bis-(trifluoromethyl)-benzoic hydrazides (**3.1a** and **3.31a**) using an inert atmosphere and sequential washes of the hydrazides with deuterated methanol (2 x CH_3OD & 1 x CD_3OD), followed by evacuation of the solvent under high vacuum. The resulting deuterated compounds were each reacted in parallel with their natural isotope analogues, with a known quantity of inert internal standard (*N*-phenyl-2-pyrrolidinone) in the sealed reaction flask (Scheme 3.10). Reactions initial rates were determined using HPLC,⁹⁹ and were calculated from starting material disappearance rates. All reactions were repeated twice, with both runs being averaged to the rate of the reaction, and further used in calculating the desired KIEs.

⁹⁹ Complete details can be found in the experimental section for both the Deuteration procedures and the analysis of the experimental data.

Gratifyingly, a KIE was observed for both substrates, with the cyclization of **3.1a** giving a k_H/k_D of 2.00 ± 0.03 , and the EWG-substituted **3.31a** having a large k_H/k_D of 4.3 ± 0.5 . What can be taken from those values is that in both cases, one of the two protons on the hydrazide nitrogens is kinetically relevant to the reaction, and involved in a bond breaking/forming event in or close to the rate-determining step of the reaction.

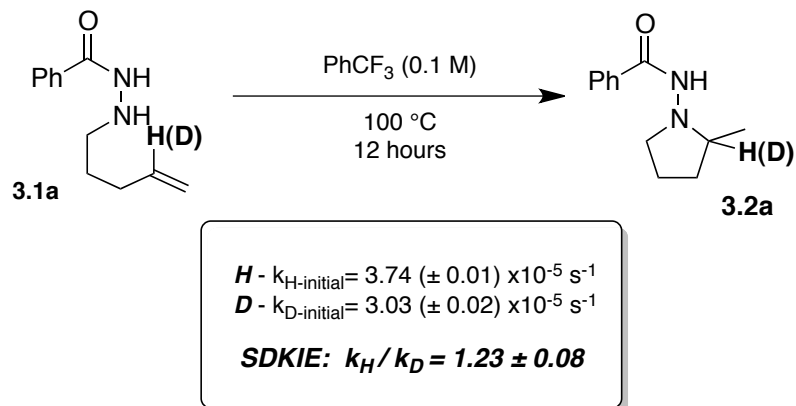


Scheme 3.10 Primary KIE on substrate **3.1a** and **3.31a**, observed following deuterium substitution on both hydrazide protons.

Working with the assumption that the proton transfer step is fast, as supported by the compatibility of the reaction with multiple solvents (which rules out the proton on N_β as the one responsible for the large KIEs), there remains only one proton that could be involved in the rate-determining step, the one on N_α. This hence supports the participation of this N_α-H bond in a concerted process, and also automatically involves the formation of a new bond with the terminal carbon of the alkene during the RDS. The size of the observed KIEs (>1) is consistent with a primary KIE, where the H/D is directly involved in a bond making/cleavage event. The larger KIE observed for **3.31a** would indicate a more ordered transition state. This could be consistent with a later TS for the reaction.

Deuteration on the Alkene.

A deuterium-enriched substrate *C(D)*-**3.1a** was also prepared, and tested in parallel to its ¹H analog **3.1a**. The initial rates of the reactions were measured by following the reaction by ¹H NMR at 100 °C. As seen in Scheme 3.11, a SDKIE of 1.23±0.08 was obtained for the reactions.

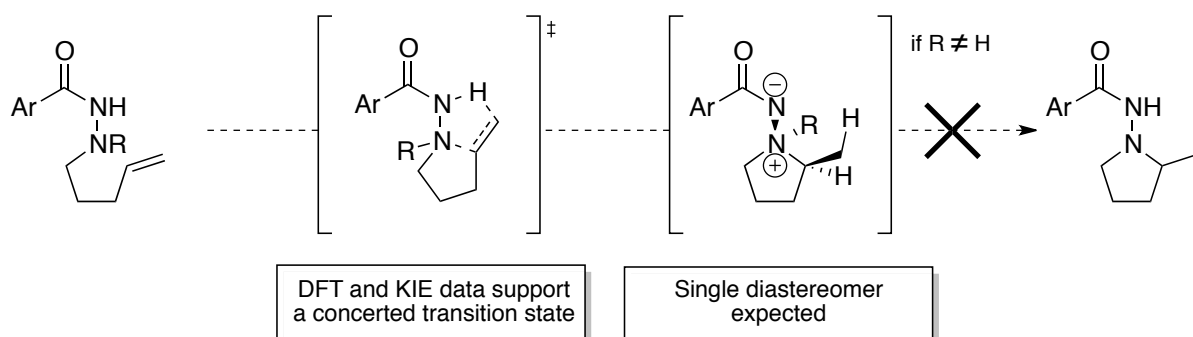


Scheme 3.11 Secondary normal KIE on substrate **3.1a**, observed following deuterium substitution at the internal alkene position.

This normal KIE is unexpected for a proton attached to a carbon undergoing a change in hybridization from sp^2 to sp^3 . With an access to a high energy cyclic amine imide intermediate from the starting material, it is reasonable to assume this would severely restrict the movements of bonds involved in the transition state, effectively increase their vibrational frequencies. With such an approach, an inverse KIE would be expected. Arguably, there are more factors at play, and with a concerted transition state, one theory could be that tunneling in a very ordered transition state favors a normal SDKIE for the internal carbon. The presence of the amine imide in close proximity to the studied proton could also influence observed KIEs. Still, the finding of a KIE for the internal carbon, effectively involving it in the transition state, now fully supports along with the previous KIEs, the reaction going through concerted 5-membered pathway.

3.6.3 Isolation of the Ammonium Ylide Intermediate

With experimental and theoretical support for the concerted mechanism in the hydroamination with hydrazides, we sought to identify and prove the structure of the amine imide intermediate.¹⁰⁰ The encouraging reactivity of 3,5-bis(trifluoromethyl)benzoic hydrazides in intra- and intermolecular systems, highlighted by a strong capacity to stabilize charges, made it a prime candidate to help in stabilizing the dipolar intermediates and allow their isolation. Scheme 3.12 depicts the approach to synthesize and isolate the intermediate, specifically through the use of cyclization precursors lacking the N_β-H bond necessary to allow proton transfer.

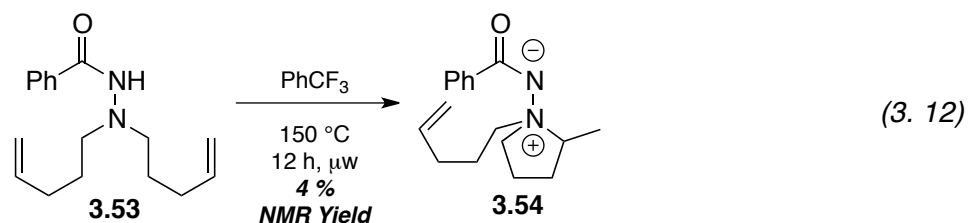


Scheme 3.12 Potential for isolation of the tetrahedral ammonium dipolar intermediate to help determine if the mechanism is concerted

With the reaction going through a planar, suprafacial and concerted 5-membered transition state, a single diastereoisomer would be expected to form. The N-N bond of the amine imide and the methyl group should both be on the same side of the pyrrolidine ring, in a geometry that would arise from the expected transition state. This is in agreement with the mechanistic support provided to the Cope-type hydroamination by Ciganek and Oppolzer.¹⁰¹

¹⁰⁰ Mr. Michaël Raymond, as part of his B.Sc. honours thesis work, contributed to some of the results of section 3.6.2. Dr. Nicolas Das Neves synthesized and isolated two of the key amine imide intermediates.

¹⁰¹ (a) Ciganek, E.; Read, J. M., Jr.; Calabrese, J. C. *J. Org. Chem.* **1995**, *60*, 5795. (b) Oppolzer, W.; Spivey, A. C.; Bochet, C. G. *J. Am. Chem. Soc.* **1994**, *116*, 3139.



Initial attempts at forming the amine imide intermediate (Eq. 3.13) using benzoic hydrazides initially appeared to have failed, with near complete recovery of starting materials. It was later determined that a 4% of the hydrazide had actually converted to a dipole, identified as the expected amine imide **3.54**. Changing the aryl group to add the bis(CF₃) substituents showed that cyclization to the ylide could be achieved in 34% NMR yield (Eq. 3.14). Though of a precarious stability, cyclization product **3.56b** could be partially characterized and more importantly analyzed through various spectroscopic techniques to prove that it was present only as one diastereoisomer.

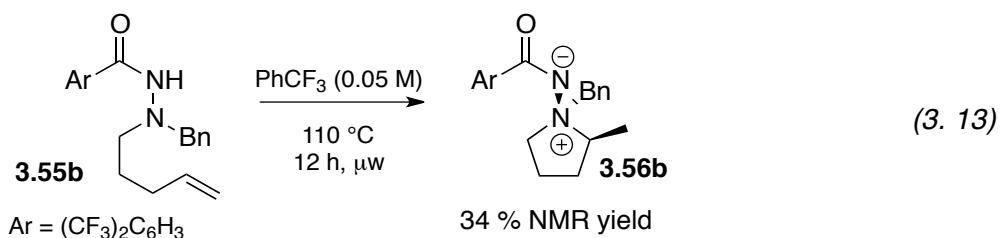
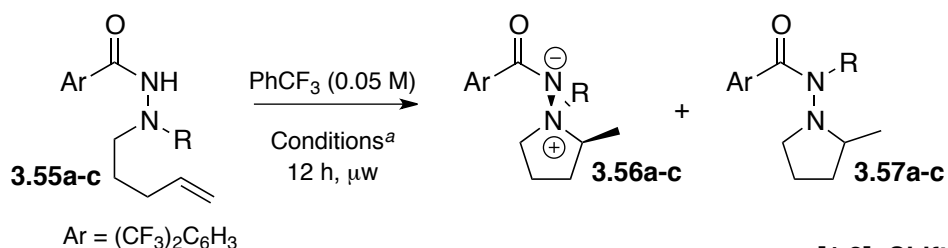


Table 3.14 presents the limited scope on the cyclization of di-substituted hydrazides to the amine imide intermediates. Low temperatures allow both the benzyl and the allyl-substituted hydrazides to cyclize to the dipolar intermediates, all observed and isolated as single diastereoisomers (entries 1, 2, 4). The methyl-substituted hydrazide **3.55a** (entry 1) can remarkably form the intermediate **3.56a** cleanly in quantitative yield, the latter found to be stable at room temperature over 24 hours.

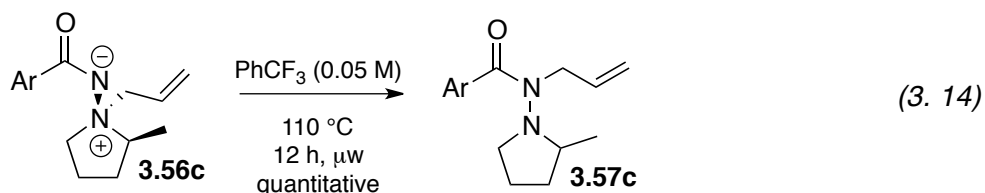
Table 3.13 Scope of the amine imide isolation and migration side reactivity



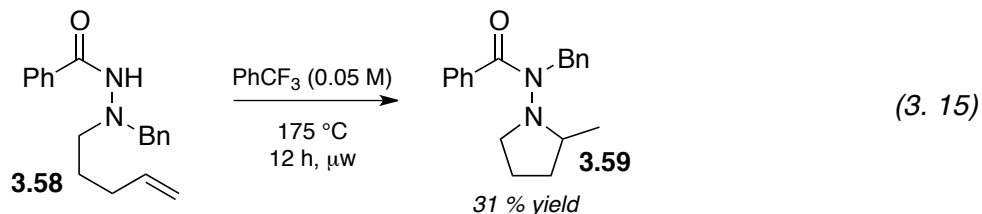
Entry	Substrate	Conditions	Products	Ylide Yield (%)	[1,2]- Shift Yield (%)
1	R = Me	110 °C	3.56a	> 98 ^b	--
2	R = Bn	110 °C	3.56b	34 ^c	--
3		150 °C	3.57b	--	66 ^b
4	R =	80 °C	3.56c + 3.57c	35 ^b	traces
5		110 °C	3.56c + 3.57c	12 ^b	59 ^b

^a Conditions: heated in PhCF₃ (0.05 M), in a microwave reactor for 12 h. ^b Isolated Yield. ^c ¹H NMR yield using 1,4-dimethoxybenzene as an internal standard.

The benzyl and allyl substituted substrates possess a second substituent that can migrate to the adjacent N_α from the dipole intermediate. These substrates can be used to form the amine imide (entries 2, 4), or pushed towards the available rearrangement through the use of higher reaction temperatures (entries 3, 5). In separate tests (Eq. 3.15), the dipole intermediate **3.56c** was shown, when exposed to the reaction conditions at higher temperatures, to undergo complete conversion to **3.57c**, establishing a direct link between the two species. Migration is thus confirmed to occur from the intermediates, presumably following Stevens-like and 2,3-Meisenheimer rearrangements.



These encouraging yields prompted a final look at standard di-substituted benzoic hydrazides, where we saw substrate **3.58** undergo a cyclization/benzyl shift sequence to form 31% of tetra-substituted hydrazine **3.59**. Overall, we have successfully shown the isolation of multiple dipole intermediates, and shown how they can be directly converted to neutral products when a transfer from the ylide is possible.



Proof of Structure for the Ammonium Ylide Intermediates

Cyclized intermediates **3.56a-c** were all analyzed using standard spectroscopy as well as COSY and NOESY, to help determine the proton assignments of each product, and get insight into the 3D structure of the dipoles. All three were very close in structure, allowing some main points to be summarized. In all intermediates, the benzoyl substituent was located syn to the methyl group, as expected for a concerted process. All ^1H NMR signals were assigned for each intermediate through the use of COSY and NOESY spectra. The molecule appeared to be locked in a specific conformation (judged by ^1H NMR), with slow rotation of the substituents on the hydrazide and diastereotopic benzylic and allylic protons. In particular, NOESY data showed these to be which were locked in place, and could only see a limited amount each of their potential neighbors.

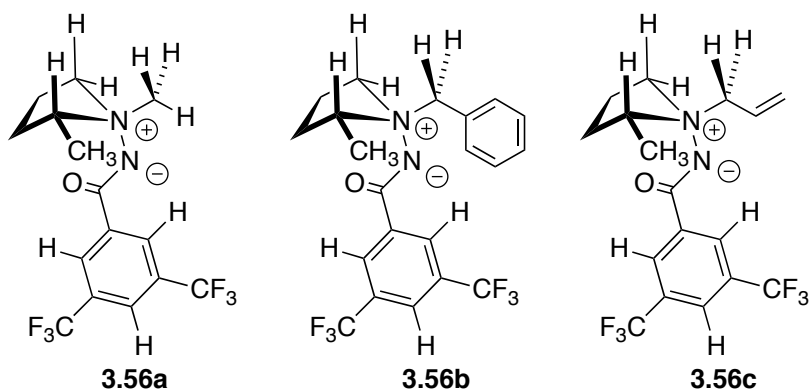


Figure 3.14 Tentative spatial arrangements of amine imide intermediates **3.56a-c** based on NOESY and COSY assignments.

Figure 3.14 shows the 3D spatial configuration determined for the three amine imides, while Figure 3.15 shows the complete assignment of resonances for **3.56c**, based on a cross-referenced NOESY spectrum. Figure 3.16 shows all the observed NOE interactions (with the key ones in bold), and the 3D representation of some the key interactions that helped most in the structural assignment.¹⁰²

¹⁰² A more complete analysis for all amine imides is provided in the Experimental section

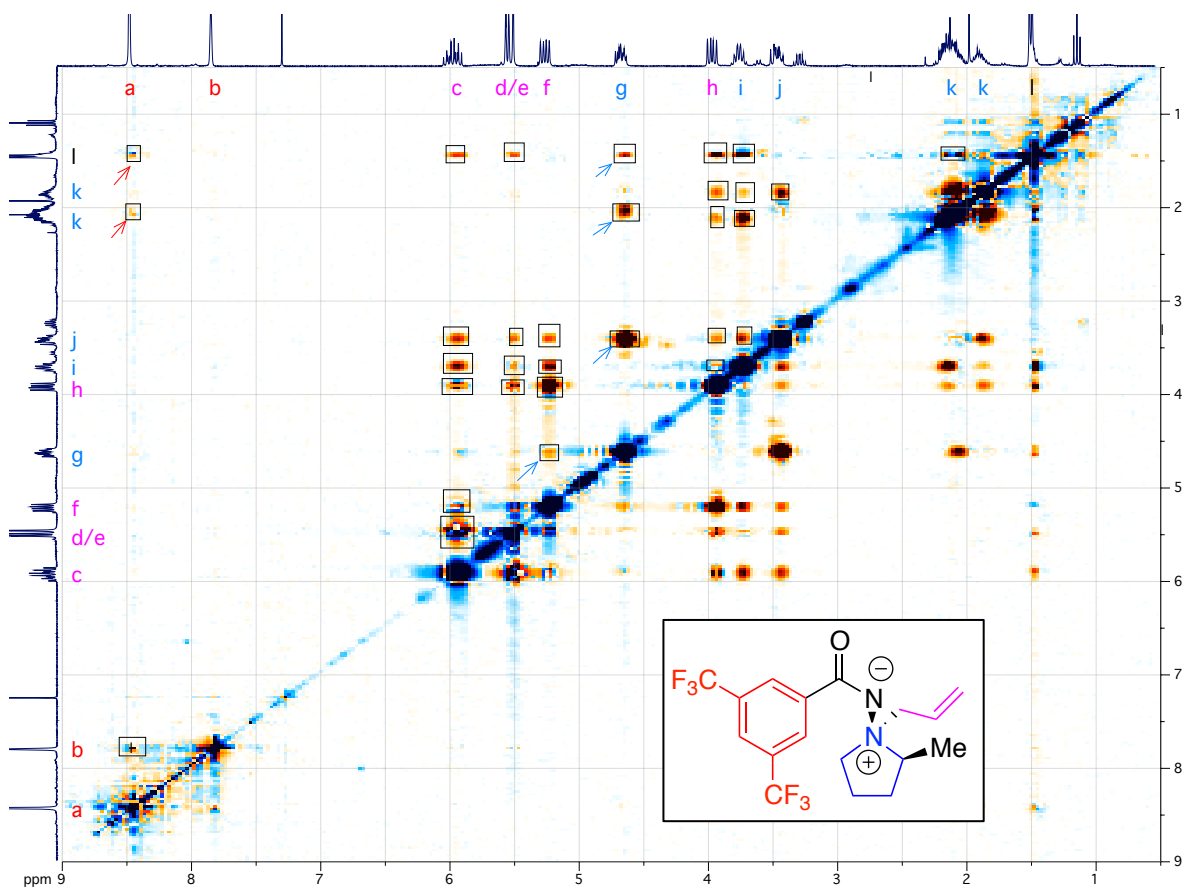
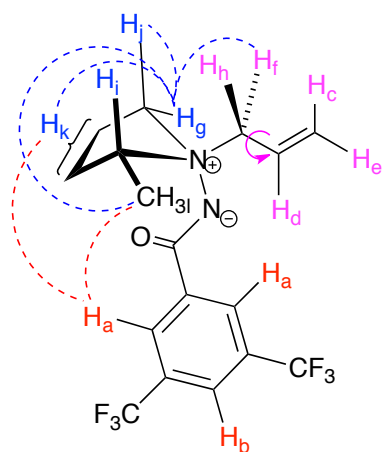


Figure 3.15 2D NOESY spectrum of isolated amine imide intermediate **3.56c**



Proton(s)	δ (ppm)	NOE Interactions
a	8.44	b, k, l
b	7.81	a
c	5.94	(d/e), f, h, i, j, l
d/e	5.52 & 5.57	c, f, h, i, j, l
f	5.23	c, d/e, g, h, i, j
g	4.64	f, j, k, l
h	3.93	c, d/e, f, i, j, k, l
i	3.72	c, d/e, f, h, j, k, l
j	3.43	c, d/e, f, g, i, k
k	(1.96 - 2.24) & (1.77 - 1.92)	a, g, h, i, j, k
l	1.47	a, c, d/e, g, h, i, k

in red: Benzoyl hydrazide protons. in purple: allyl substituent. in blue: pyrrolidine ring. in black: methyl substituent on the pyrrolidine ring.

Figure 3.16 Summary of NOE interactions observed in intermediate **3.56c** (right), and probable special orientation of functional groups explaining the observed NOEs (left)

3.7 Summary and Outlook

This chapter presented a complete picture of the Cope-type hydroamination using hydrazines, hydrazides and related hydrazine derivatives. Helped by a basic understanding of the mechanism, supported by DFT calculations, the initial scope of the intramolecular hydroamination was extended to use a wider range of hydrazide analogs. We have shown in a systematic approach the synthetic potential of the method to form 5 and 6-membered cycles, allowing for varied substitution of side chains, and incorporation of heteroatoms in the rings (25 examples: 40% – 98%). Benzoic hydrazides possessing EWGs helped in achieving otherwise difficult cyclizations, and also opened the door to the first Cope-type intermolecular alkene hydroamination of a hydrazine derivative. This reactivity was found to be applicable solely to biased strained alkenes, and required temperatures of 160°C (7 examples: 73% to 87% hydroamination yield), but is still noteworthy in the context of the hydroamination field, in which intermolecular alkene hydroamination is still rare. The formation of azomethine imines through intramolecular hydroamination on alkynes, along with limited results in the intermolecular hydroamination of alkenes and alkynes with hydrazine, complete the reactivity overview of hydrazines and its derivatives. Table 3.14 provides summary of successful, whether mild or interesting, for hydrazines and hydrazides with alkenes and alkynes, and indicate the section of this chapter where the reactivity is covered.

Table 3.14 Reactivity summary of hydrazines and derivatives with alkenes and alkynes.

	$\begin{array}{c} \text{H} \\ \\ \text{R}-\text{N} \\ \\ \text{N}-\text{H} \\ \\ \text{H} \end{array}$		$\begin{array}{c} \text{H} \\ \\ \text{R}-\text{N} \\ \\ \text{N}-\text{EWG} \\ \\ \text{H} \end{array}$	
$\text{R}-\text{CH}=\text{CH}_2$	Intramolecular Section 3.1.5	Intermolecular Section 3.5	Intramolecular Section 3.1.6 & Section 3.3	Intermolecular Section 3.4
$\text{R}-\text{C}\equiv\text{C}$	-----	Intermolecular Section 3.1.5	Intramolecular Section 3.5	Intermolecular Section 3.5

Kinetic experiments have determined primary and secondary KIEs for the hydrogens on N_α and on the internal carbon of the alkene, providing support for a concerted, suprafacial, 5-membered cyclization for the reaction. Isolation of the amine imide intermediates in good yields and complete diastereoselectivity provided evidence for the mechanism and transition state of the hydroamination with hydrazides as being a true Cope-type hydroamination process.

Subsequent work to achieve better reactivity in the Cope-type hydroamination using hydrazines and hydrazides could go in many directions. Activation of the hydrazides through Lewis acid activation, hydrogen-bond catalysis or other means could pave the way to improved reaction conditions as well as stereoselective variants.

4

Hydrogen Bonding Catalyzed Cope-type Hydroamination

This chapter revisits the hydroamination reaction of hydroxylamines, last discussed in Chapter 2, in order to address concerns with respect to the proton transfer step of the reaction, and then show the discovery of a new hydrogen-bond catalyzed approach to the intermolecular Cope-type hydroamination using hydroxylamines. The concepts behind general hydrogen-bond catalysis will be summarized in the introduction, before presenting the early results of the new reactivity. The potential for the strategy to be applicable to the field of Cope-type hydroamination amongst other avenues will be discussed.

4.1 Introduction

In order to address some of the key results that will be described later in this chapter, it is important to present the underlying principles behind hydrogen-bond catalysis, and consider a few of the current limitations of the field.

4.1.1 Enzymes Mimics & Oxyanion Holes

The field of hydrogen-bond catalysis stems from the use of molecules that can act as mimics of oxyanion holes. Oxyanion holes are at the active sites of many enzymes and

stabilize negatively charged oxygens in transition states or high-energy intermediates.¹⁰³ They do so through the use of two and sometimes three hydrogen bonds directed at the oxygen atom. Catalysis traditionally takes place through the stabilization of tetrahedral or enolate intermediates (Figure 4.1). The prevalence of enzymes in catalysis, over their surrounding aqueous cell media, also capable of H-bonding, can be explained by means of a predisposed and organized hydrogen bonding geometry in the active site of oxyanion holes. They hence require less reorganization and have a lower entropic cost for activation compared to water in the cellular matrix.¹⁰⁴ Replicating enzymatic functions is an incredibly attractive goal, and the development of small molecules that mimic oxyanion holes has thus been an active area of research in recent decades.

Figure 4.1 *Standard oxyanion hole showing transition state stabilization for a tetrahedral intermediate through multiple H-bond donors. Hydrolysis of acetylcholine with acetylcholinesterase*

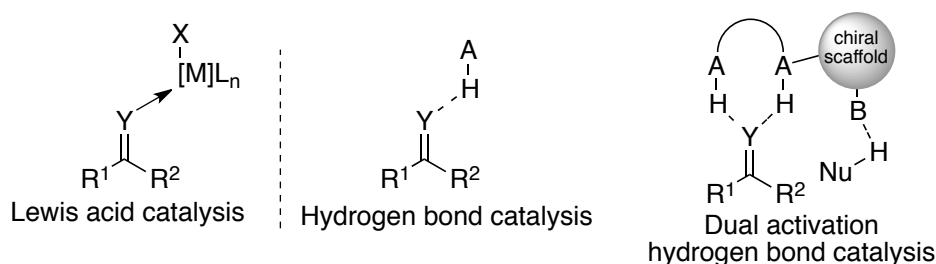
4.1.2 Hydrogen-bond Catalysis

The use of non-covalent interactions in catalysis, primarily hydrogen bonds and electrostatic attraction, has allowed hydrogen bonding and counteranion catalysis to emerge, with the former currently the best small molecule approach to mimic enzyme oxyanion holes.¹⁰³ A powerful alternative to other modes of activation, such as those in Lewis-acid and transition metal catalysis, H-bond catalysis uses stable small organic molecules tolerant of water/moisture, and usually existing in their active conformations. A wide variety of central cores have been used, all tunable to various extents, having one or two polar protic groups

¹⁰³ Pihko, P. M. *Hydrogen Bonding in Organic Synthesis*; Wiley-VCH: Weinheim, **2009**.

¹⁰⁴ Warshel, A.; Sharma, P. K.; Kato, M.; Ziang, Y.; Liu, H.; Olsson, M. H. M. *Chem. Rev.* **2006**, *106*, 3210.

capable of activation and initial substrate binding (Scheme 4.1).¹⁰⁵ These include diols, dipeptides and phosphoric acids amongst others.¹⁰⁶ An important part of the recent research focuses on urea-based (thioureas) and squaramide-based systems.¹⁰⁷ Recent developments also have a heavy focus on dual activation systems, in which typically well-established catalyst cores are used for substrate binding, and varying chiral side chains are used to facilitate a directed attack from a nucleophile through the interaction with a moiety in close proximity to the core.



Scheme 4.1 Standard Lewis acid activation compared with mono and dual hydrogen bonding activation.

Activation occurs through the polar protic groups, which can point hydrogen bonds at the substrates, most often α - β unsaturated carbonyls or analogs. Diels-Alder reactions, Claisen rearrangements or similar reactions, wherein only a small partial negative charge builds on the substrate oxygen, can be catalyzed. Conjugate additions, wherein an anion forms on the substrate and is still part of a conjugated system, are also common and serve

¹⁰⁵ Recent reviews on hydrogen bonding organocatalysis (section or entirely): (a) Connon, S. J. *Chem. Eur. J.* **2006**, *12*, 5418; (b) Taylor, M. S.; Jacobsen, E. N. *Angew. Chem. Int. Ed.* **2006**, *45*, 1520; (c) Doyle, A. G.; Jacobsen, E. N. *Chem. Rev.* **2007**, *107*, 5713; (d) Akiyama, T. *Chem. Rev.* **2007**, *107*, 5744; (e) Zhang, A.; Schreiner, P. R. *Chem. Soc. Rev.* **2009**, *38*, 1187; (f) Schreiner, P. R. *Chem. Soc. Rev.* **2003**, *32*, 289; (g) Giacalone, F.; Gruttadauria, M.; Agrigento, P.; Noto, R. *Chem. Soc. Rev.* **2012**, *41*, 2406.

¹⁰⁶ Examples with (a) dipeptides: Oku, J. I.; Inoue, S. *J. Chem. Soc., Chem Commun.* **1981**, 229. (b) diols: Huang, Y.; Unni, A. K.; Thadani, A. N.; Rawal, V. H. *Nature* **2003**, *424*, 146 and Thadani, A. N.; Stankovic, A. R.; Rawal, V. H. *Proc. Natl. Acad. Sci. U.S.A.* **2004**, *101*, 5846; (c) phosphoric acids: Akiyama, T.; Itoh, J.; Yokota, K.; Fuchibe, K. *Angew. Chem., Int. Ed.* **2004**, *43*, 1566 and Uruguchi, D.; Terada, M. *J. Am. Chem. Soc.* **2004**, *126*, 5356.

¹⁰⁷ (a) Knowles, R. R.; Jacobsen, E. N. *Proc. Natl. Acad. Sci. USA.* **2010**, *107*, 20678; Review on the use of squaramides: (b) Aleman, J.; Parra, A.; Jiang, H.; Jørgensen, K. A. *Chem. Eur. J.* **2011**, *17*, 6890.

as standard tests for newly developed catalyst families.¹⁰⁸ In one of the most apparent limitations, less attention is given to reactions that build a localized anionic character on oxygens in the reaction intermediates (ex. tetrahedral intermediates), since they often lead to increased reaction temperatures and longer reaction times, hinting at the increased complexity in stabilizing such charged monoatomic anionic intermediates.

4.1.3 Group Efforts for Catalytic Hydroamination

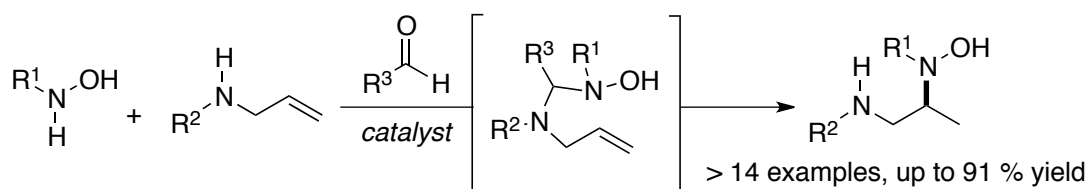
As a testament to the constant efforts that are spent in the Beauchemin group trying to surpass the problems associated with the intermolecular alkene hydroaminations, it is worth noting that we have in recent years developed two new strategies to catalyze or promote the process.

In a first development, led by Mr. Peter Ng and Ms. Melissa MacDonald, the tethering catalytic hydroamination of allylic amines was presented. The process allows a formally intermolecular hydroamination to be performed through an intramolecular pathway through the use of a temporary tether (Scheme 4.2).¹⁰⁹ Using an aldehyde as precatalyst, the reaction can promote the formation of an amination tethered complex, which can undergo easy intramolecular hydroamination, at ambient temperatures, before releasing the product and regenerating the catalyst. The method, so far applicable to allylic primary and secondary amines, can also be catalyzed using chiral aldehydes, providing access to enantiopure diamines in up to 97% ee.

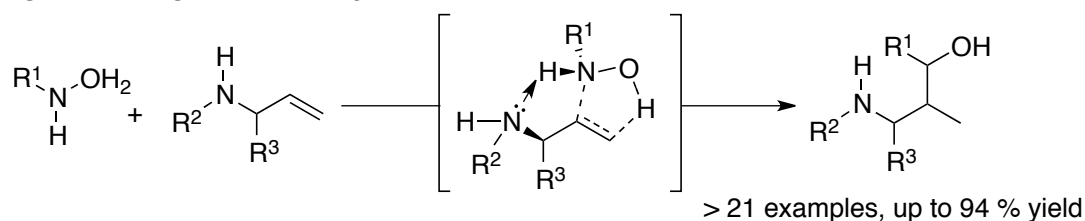
¹⁰⁸ Reactions on conjugated systems with squaramides: a) Xu, D.-Q.; Wang, Y.-F.; Zhang, W.; Luo, S.-P.; Zhong, A.-G.; Xia, A.-B.; Xu, Z.-Y. *Chem. Eur. J.* **2010**, *16*, 4177; b) Zhu, Y.; Malerich, J. P.; Rawal, V. H. *Angew. Chem., Int. Ed.* **2010**, *49*, 153.

¹⁰⁹ MacDonald, M. J.; Schipper, D. J.; Ng, P. J.; Moran, J.; Beauchemin, A. M. *J. Am. Chem. Soc.* **2011**, *133*, 20100.

Hydroamination Tethering Catalysis



Hydrogen-Bonding Facilitated Hydroamination



Scheme 4.2 Recent strategies to catalyze and promote the difficult intermolecular Cope-type hydroamination of alkenes.

More recently, Dr. Shu-Bin Zhao, Mr. Eric Bilodeau and Ms Valérie Lemieux have also shown that allylic amines could also, at higher temperatures (80 °C), undergo hydroamination in high yields.¹¹⁰ This approach is suggested to work by substituting the tether strategy previously used with weak hydrogen-bond interactions between the allylic amine and the N-H bond of the hydroxylamine, thereby facilitating the reaction and achieving synthesis of diamines with high regioselectivity. The two approaches are applicable with similar substrates, and could be extended to a variety of allylic amines, alcohols and thiols. Thus far, functionalization of the simplest unbiased alkenes (alkyl substituted) remains elusive with the Cope-type hydroaminations of hydroxylamines.

4.2 Results and Discussion

As new methodologies were developed to achieve efficient alkene hydroamination with hydroxylamines, a few questions remained on the original publications of the Beauchemin group, and the specific reasons behind the lack of good intermolecular

¹¹⁰ Zhao, S.-B.; Bilodeau, E.; Beauchemin, A. M. *manuscript in preparation*.

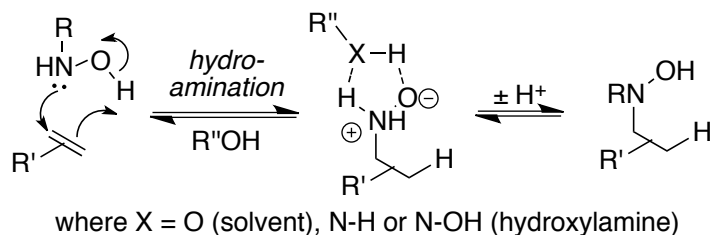
reactivity in simple systems with alkyl hydroxylamines. Though interesting in their approaches to the thermodynamic problem, none of the cascade reactions developed and presented in Chapter 2 had provided the desired easy access to Cope-type hydroamination products from unbiased alkene starting materials.^{14c}

4.2.1 The Proton Transfer Step & Kinetic Data

In previous publications, we have presented the hydroxylamine-based Cope-type hydroaminations of alkenes, allenes and alkynes.¹⁴ A recurring theme across all reactions was the use of alcoholic solvents, an early finding by the Beauchemin group that significantly improved the reaction efficiency, and allowed for an expanded intramolecular and intermolecular scope across a variety of substrates. It was believed that the reaction involved an initial cyclization through a 5-membered, suprafacial and planar concerted transition state, since the reaction is the microscopic reverse of the Cope elimination.¹¹¹

Our original conclusion was that the effect of protic solvents on the process was a facilitation of the proton transfer step through a bimolecular pathway in that the solvent served as a transfer agent. With a unimolecular proton transfer heavily disfavored, it was assumed that in the absence of a protic solvent, the bimolecular transfer would still be required, but slowed and hence kinetically dependent on the participation of extra hydroxylamines present in the reaction media.

¹¹¹ See Section 1.3.



Scheme 4.3 Proton transfer step, mediated by the solvent or existing hydroxylamines (starting material or product)

Such a perspective was strongly backed by experimental evidence, but also supported our analysis of numerous DFT calculations performed by Dr. Serge Gorelsky at the University of Ottawa.¹¹² Figure 4.2 shows the potential energy surfaces of the reaction of hydroxylamine with ethylene and norbornene, calculated in the gas phase at the B3LYP/TZVP level of theory (298K and 1 atm). Free energies calculated for the bimolecular process for proton transfer is heavily favored ($\Delta G^\ddagger = \sim 20.9$ kcal/mol) over the intramolecular transfer ($\Delta G^\ddagger = \sim 38.3$ kcal/mol). This indicates that the intramolecular proton transfer (which would have to occur through three-membered cyclic intermediate) is an unlikely pathway.

¹¹² (a) Beauchemin, A. M.; Moran, J.; Lebrun, M.-E.; Séguin, C.; Dimitrijevic, E.; Zhang, L.; Gorelsky, S. I. *Angew. Chem., Int. Ed.* **2008**, *47*, 1410. (b) Cebrowski, P. H.; Roveda, J.-G.; Moran, J.; Gorelsky, S. I.; Beauchemin, A. M. *Chem. Commun.* **2008**, 492. (c) Moran, J.; Dimitrijevic, E.; Lebrun, M.-E.; Bédard, A.-C.; Séguin, C.; Gorelsky, S. I.; Beauchemin, A. M. *J. Am. Chem. Soc.* **2008**, *130*, 17893.

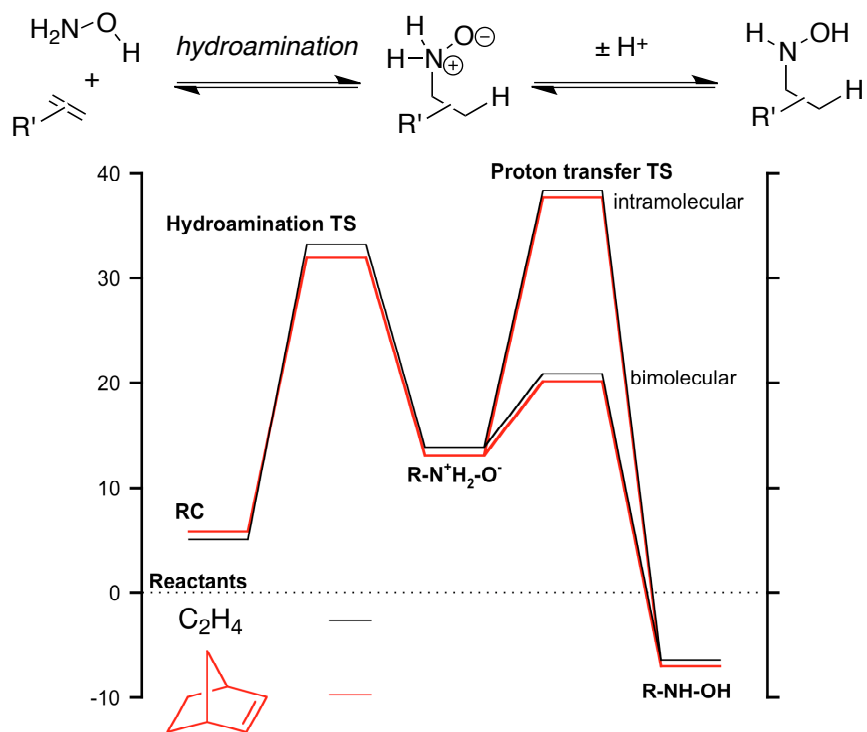


Figure 4.2 Free energies of reaction species and transition states for hydroamination of ethylene, C_2H_4 and norbornene at the B3LYP/TZVP level of theory.

4.2.2 Determination of the Reaction Order in Both Reactants

Since we knew there was a background reaction even in aprotic solvents, we decided to evaluate the order of the reaction in both reactants in the absence of an alcoholic solvent. If a protic solvent is indeed required for proton transfer, it follows that in its absence, with a presumed non-accessible unimolecular proton transfer, that the hydroxylamine present as reactant or product would have to mediate the transfer, therefore showing a second order in the reactant.

The reaction of norbornene with *N*-cyclohexylhydroxylamine was selected for these tests. *N*-Cyclohexylhydroxylamine shows only minimal thermal decomposition, which has historically made it one of the best substrates to use in exploratory work with in the Beauchemin group. Since the reactions were to be run in toluene at an arguably slow rate,

prevention of rapid decomposition of the starting materials was important. Great attention was given to have the reaction run without the presence of any water, which could have served as a proton transfer agent and biased our results.

Preliminary experiments were run, and a plot of the log of the rate of appearance of the product versus the log of the initial concentration in norbornene provided a straight line, supporting a first order in norbornene for the reaction (Figure 4.3- Top).¹¹³ This was expected and in agreement with norbornene being involved in either the rate-determining step or the steps leading to it. The reaction order in hydroxylamine was shown to also approximate to one (Figure 4.3- Bottom).¹¹³ This was inconsistent with a difficult proton transfer step that would result a second hydroxylamine required to help achieve a bimolecular pathway. A first order reaction in each reactant was indicative of a hydroamination rate-limiting event, which implies that the proton transfer step is facile.

¹¹³ During the reactions, due the necessity to keep all starting materials and solvents dry, no attempts were made to keep the overall volume constant. The values obtained from plotting $\log(\text{rate})$ vs. $\log(\text{conc})$ for the experiments therefore have a built-in inaccuracy. The tables and graphs presented in the supporting information clearly show a linear dependency between the rate of the reaction and both starting materials.

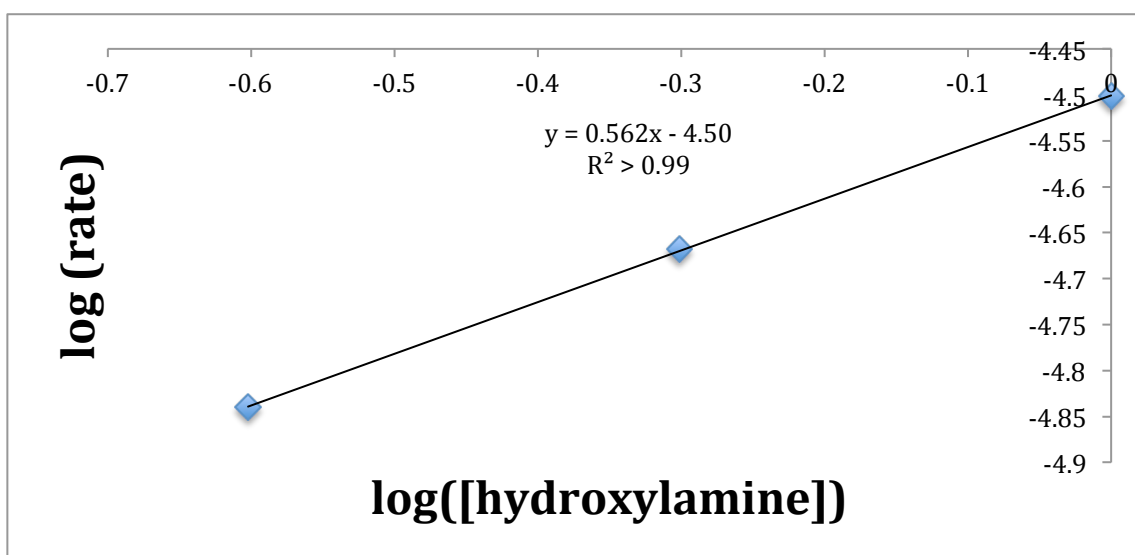
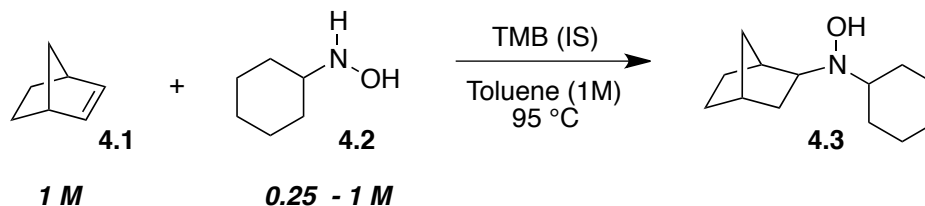
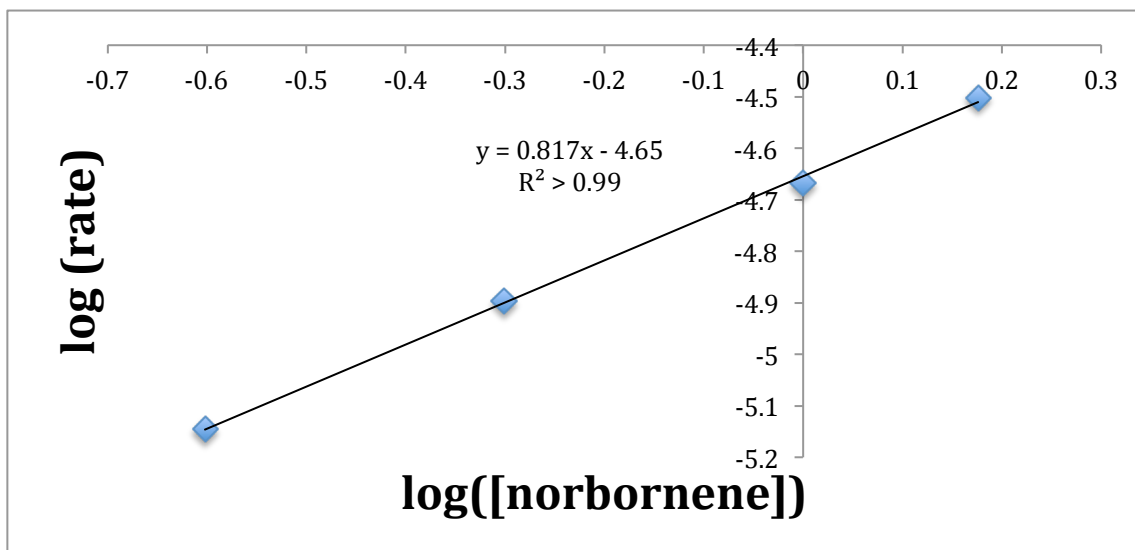
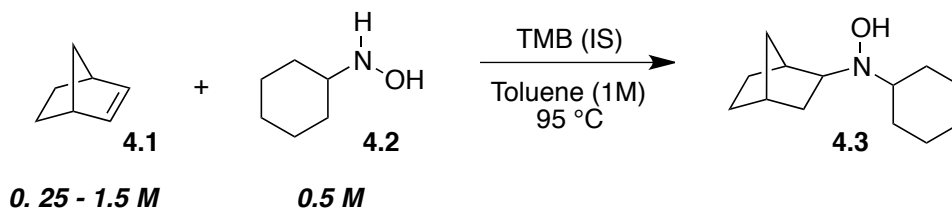


Figure 4.3 Reaction order in norbornene (top) and hydroxylamine, determined by following the reaction by NMR using trimethoxybenzene as an internal standard. ^aTMB = 1,3,5-trimethoxybenzene

Taking a step back to analyze our system, especially the DFT calculations, brought some perspective on the issues addressed. The assumption that the bimolecular proton transfer would be slow and demanding of the system in the absence of protic solvent, thereby forcing the reaction to be second order in hydroxylamine, had several flaws upon closer inspection. Primarily, a comparison in the gas phase calculations performed (Figure 4.2) revealed that the bimolecular proton transfer pathways remained significantly lower, at roughly 20.9 kcal/mol for ethylene or norbornene, than the hydroamination transition states, themselves at around 33.2 kcal/mol. Therefore, from the viewpoint of an intermediate dipole formed in the reaction, the intermolecular proton transfer was about 12.3 kcal/mol lower than the Cope elimination (intramolecular) process required to revert back the starting materials.

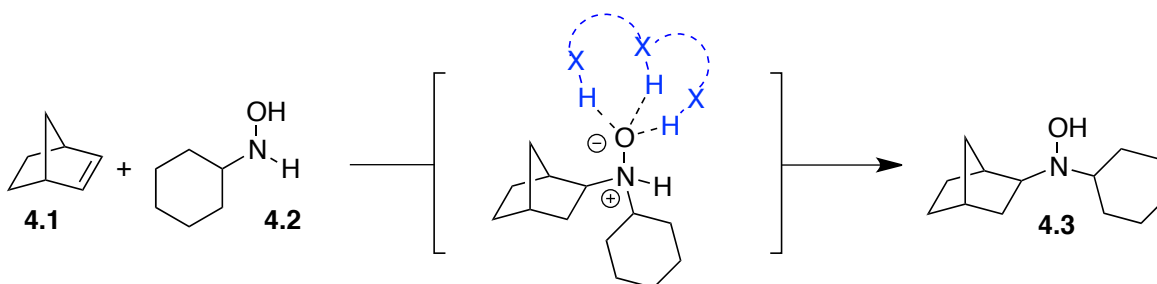
In retrospect, it seemed fairly inconceivable that in reactions performed in the highly concentrated conditions used in our hydroaminations (1-2 M) that the intermolecular proton transfer could be anything other than fast. This is supported by the fact that at all times in the reaction one equivalent of hydroxylamine is available to help mediate the proton transfer, (with both the starting material and the product of the reaction possessing N-H or O-H bonds).

From such an analysis, a more probable explanation for the vast difference of reactivity between the hydroamination done in protic vs. aprotic solvents, had to lay in the stabilization of the dipolar *N*-oxide intermediate, and hence in the transition states leading to it. The *N*-oxide dipole possesses two charges, yet with the positive nitrogen center being tetrahedral and fully substituted, only the oxyanion is accessible from the surrounding environment. Hypotheses were made that in such a case, the only way a protic solvent could achieve significant stabilization over other solvents, was through a number or network of hydrogen bonds.

4.2.3 Development of the Hydrogen Bonding Catalyzed Hydroamination

A clear path emerged to demonstrate such a new hypothesis; that the Cope-type hydroamination was more effective in polar protic solvents through the stabilization by hydrogen bond donors of the *N*-oxide intermediates and the transition states leading to it. If the reaction could be run in standard non-protic solvents, with additives capable of activating the substrate hydroxylamine and providing the necessary hydrogen bonds during the transition state for the hydroamination, net improvements in yields should be observable. This would qualify if successful as hydrogen-bond catalysis, performed on a species very different from standard carbonyl derivatives, more akin to epoxide openings, and would generate an intermediate with a localized oxyanionic charge, less frequent in the field of H-bonding catalysis.

In order to uncover such new reactivity, the reaction of norbornene and cyclohexylhydroxylamine was kept as a test system, for its simplified analysis, and for the biased nature of strained norbornene providing an edge to see even slight improvements in yield (Scheme 4.4). The starting materials, containing no polar groups other than the hydroxylamine, were thought to be key in favoring an interaction between this target functionality and the additives.

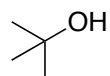


Scheme 4.4 Concept and desired interaction for the dipolar *N*-oxide intermediate.

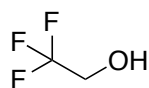
Selection of Catalysts / Additives

Interestingly, the oxyanion intermediate formed possesses three pairs of non-bonding electrons, allowing stabilization through potentially more than the two standard hydrogen bonds provided from standard hydrogen bonding catalysts. For that reason, the initial survey of catalysts and additives was developed to contain a variety of polyols, thought to be optimal in the stabilization of the intermediate through multiple hydrogen bonds (Figure 4.4). Alcohols, diols and polyols were included, to see if any trend in reactivity could validate a portion of the proposed methodology. A standard hydrogen bonding catalyst was also chosen for the initial test.

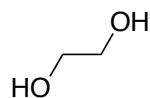
Alcohols & Diols



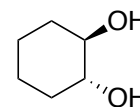
tert-butanol



2,2,2-trifluoroethanol

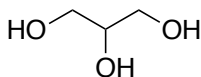


ethylene glycol

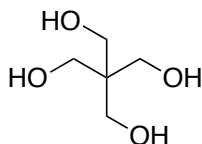


trans-cyclohexane diol

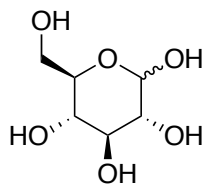
Polyols



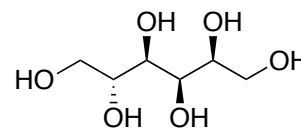
glycerol



pentaerythriol

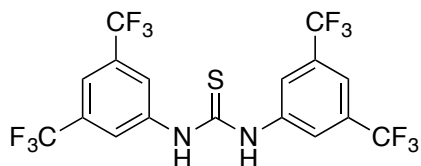


glucose



sorbitol

H-bonding Catalyst



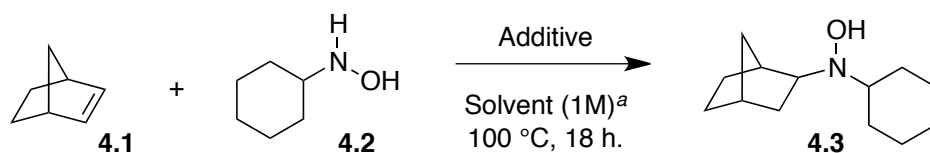
N,N'-bis[3,5-bis(trifluoromethyl)phenyl]thiourea

Figure 4.4 List of potential candidates to catalyze or promote the Cope-type hydroaminations in aprotic solvents

Benzene and chloroform were selected as solvents, to help bring some solubility to the hydroxylamine and to be as free as possible of interaction with the reactions tested. The

reactions were thus run at 100 °C, using an excess of norbornene (2 equivalents) compared to the hydroxylamine, in order to prevent low yields from excess evaporation / sublimation of norbornene. The additives were all added in a subs-stoichiometric ratio of 0.4 to the hydroxylamine, to give as fair a chance as possible to observe any hint of catalytic potential.

Table 4.1 Systematic investigation of alcohols and polyols to uncover hydrogen-bond potential.



Entry	Additive	Additive (equiv.)	Solvent	NMR Yield (%) ^c
Controls				
1	<i>none</i>	--	CDCl ₃	6
2	<i>none</i>	--	Benzene- <i>d</i> ₆	10
Alcohols & Diols				
3	<i>t</i> -BuOH	0.4	Benzene- <i>d</i> ₆	18
4	2,2,2-trifluoroethanol	0.4	CDCl ₃	14
5	2,2,2-trifluoroethanol	0.4	Benzene- <i>d</i> ₆	14
6	ethylene glycol	0.4	CDCl ₃	6
7	ethylene glycol	0.4	Benzene- <i>d</i> ₆	10
8	<i>trans</i> -cyclohexanediol	0.4	Benzene- <i>d</i> ₆	31
Polyols				
9	glycerol	0.4	CDCl₃	36
10	glycerol	0.4	Benzene-<i>d</i>₆	53
11	pentaerythriol	0.4	CDCl ₃	20
12	pentaerythriol	0.4	Benzene- <i>d</i> ₆	5
13	glucose	0.4	CDCl ₃	10 ^b
14	glucose	0.4	Benzene- <i>d</i> ₆	14 ^b
15	sorbitol	0.4	Benzene-<i>d</i>₆	79
H-bonding Catalyst				
16	(3,5-(CF ₃) ₂ C ₆ H ₃ N) ₂ C=S	0.05	Benzene- <i>d</i> ₆	39

^a Conditions: heated in a wax bath at 100 °C in a sealed vial for 18 h, with *N*-cyclohexylhydroxylamine (1 equiv.) and norbornene (2 equiv.). ^b Decomposition of the additive occurred. ^c NMR yield calculated from trimethoxybenzene internal standard.

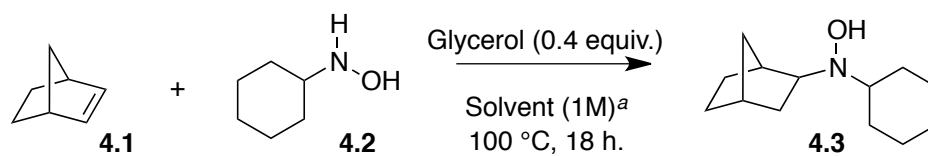
Table 4.1 summarizes the results of the first intensive scan. The controls performed in benzene- d_6 and chloroform- d showed that a background reaction was present in both solvents. *tert*-Butanol, trifluoroethanol and ethylene glycol, all showed very small effects on the NMR yield of the reaction (entries 3-7), effectively suggesting that alcohols need to be present in higher quantities to help significantly the reaction. *trans*-Cyclohexane diol however add a substantial effect on the yield, boosting it to 31% (vs. 10% for the control or ethylene glycol), for the reaction in benzene (entry 8). Such a 200% increase on the yield, going from one free diol to one with hydroxyl groups locked facing in the same direction, provided us with a first clue that dual activation of a hydroxylamine starting material could work.

The change to polyols saw glycerol, the simplest triol commercially available, providing increased yields in both solvents, with 36% for $CDCl_3$ and 53% for benzene (entries 9, 10). Pentaerythriol and glucose both provided low yields for the reaction, explained tentatively by the larger distance between hydroxyl groups on the former, and the heavy caramelization of the sugar on the latter (entries 11-14). The use of catalytic sorbitol, a reduced analog of glucose, provided the hydroaminated product in an astounding 79% yield (entry 15). The initial scan was finalized with the trial of *N,N'*-bis[3,5-bis(trifluoromethyl)phenyl]thiourea, which, added in a only 5% to the reaction, was able to yield 39% of the hydroamination product, suggesting that the reaction had successfully been catalyzed.

Across Table 4.1, we could see that the reaction performed in $CDCl_3$ typically provided lower yields than benzene. A preliminary solvent scan in Table 4.2 shows that these two solvents, along with acetonitrile, provide similar trends of background versus promoted/catalyzed reactivity. The use of *t*-BuOH, known to be an effective solvent in the reaction, is

characterized by a strong background reaction. The addition of the additive paired with such a protic solvent barely has an effect on the reaction yield.

Table 4.2 Solvent scan for the hydrogen bonding promoted/catalyzed hydroamination



Entry	Additive	Solvent	NMR Yield (%) ^b
1	<i>none</i>	CDCl ₃	6 %
2	glycerol	CDCl ₃	36 %
3	<i>none</i>	Benzene- <i>d</i> ₆	10 %
4	glycerol	Benzene- <i>d</i> ₆	53 %
5	<i>none</i>	<i>t</i> -BuOH	43 %
6	glycerol	<i>t</i> -BuOH	57 %
7	<i>none</i>	MeCN- <i>d</i> ₃	8 %
8	glycerol	MeCN- <i>d</i> ₃	33 %
9	<i>none</i>	DMSO- <i>d</i> ₆	44 %
10	glycerol	DMSO- <i>d</i> ₆	39 %

^a conditions: heated in a wax bath at 100 °C in a sealed vial for 18 h, with cyclohexylhydroxylamine (1 equiv.) and norbornene (2 equiv) and glycerol (0.4 equiv.). ^b NMR yield calculated from trimethoxybenzene internal standard.

DMSO and *t*-BuOH together show that in systems where a significant polar solvent is used, not only is the background reactivity more present, but also the effect of an H-bonding protic additive is expectedly diminished. Interestingly, the reaction performed in DMSO provided significant background reactivity, which is the first observation made by our group of efficient intermolecular hydroamination in an aprotic solvent. Such a result would have seriously undermined previous claims that the proton transfer step was kinetically relevant if discovered earlier.

Previous research mainly used DMSO in solvents where water was also present in the reactions, at a time when the proton transfer step was not a crucially important concern.¹¹⁴ While several results over the years hinted at sometimes moderate reactivity in aprotic solvents (mainly benzene), reduced yields that would result from the use of dried solvents supported our analysis that polar protic bonds were required for proton transfer. Constant problems, where even slightly higher temperatures, or failure to use sodium cyanoborohydride as an additive would result in several decomposition pathways for the hydroxylamines used. This prevented at the time the observation of any clear trend outside of the optimal protic systems.

4.3 Outlook and Perspectives

Overview of Methodology Developed

This chapter presented a critical investigation on the nature of the proton transfer step in the Cope-type hydroamination. After finding it to be first order in both reactants, the reaction was inferred to have a fast proton transfer step regardless of the choice of solvent. This led us to suggest that H-bonding stabilization of the *N*-oxide intermediate and of the transition state leading to it may be responsible for the previous success of protic solvents in enabling intermolecular reactions.

The use of equimolar quantities of different additives possessing the same amount of hydroxyl groups on their structures influenced the reaction in vastly different ways, further supporting that alcohols cannot merely help through mediation of the proton transfer. The use of polyols and H-bonding catalysts has suggested how the intermolecular hydroamination could be catalyzed by hydrogen bonding. The methodology, which is

¹¹⁴ DMSO has been used in preliminary reactions of aqueous hydroxylamines with alkynes. Moran, J. Lebrun, M.-È. Dimitrijevic, E. *unpublished results*

centered on an activation of the hydroxylamine partner for intermolecular reactions, has the potential to be applicable to the functionalization of a wide range of alkenes, biased or not.

It remains to be shown whether the observed reactions and trends are not due to some other factor, such as an increase in dipole moment that favors the reaction and the dipolar intermediate formation. Glycerol, cyclohexane diol amongst some of the solvents are ones with the highest dipole moments, and result in some of the better yields. As it stands, the encouraging results from even a small amount of the thiourea catalyst, which has limited potential on the overall polarity of the reaction media, seem to indicate hydrogen bonding as a viable option and pathway.

Catalyst Source and Design

Whether the polyols found to be competent in promoting the reaction were stabilizing the *N*-oxide through two hydrogen-bonds, stabilized themselves by a surrounding network of H-bonds, or three H-bonds were directly interacting with the oxyanion is an interesting question. Triactivation of an anionic oxygen would allow new catalyst design, aimed at promoting specifically such interactions, in a process analogous to the enzymatic oxyanion hole activation.

Naturally, the commercially readily available H-bonding organocatalysts (thioureas, squaramides, diols, phosphoramides) provide a simple platform for the extension of the chemistry. The availability or easy synthesis of variety of chiral catalysts for these families of compounds opens the prospect of intermolecular asymmetric catalysis of the Cope-type hydroamination, one of the early and still a current goal in the group.

Wider Application of the Methodology

The methodology could be extended to all Cope-type processes, since they all feature the presence of a similar dipolar intermediate. Hydroamination using hydroxylamines, hydrazines, hydrazides, and reacting on alkenes, alkynes or allenes, in intra- and intermolecular reactivity, could all benefit from optimized stabilization of the dipolar intermediates. Related newly developed methodologies of tethering catalysis and H-bonding promoted hydroamination (see section 4.1.3) could also benefit from the described chemistry. In providing a stabilization of localized oxyanion intermediate, any development of the reactivity could be extended to the catalysis of other reactions providing localized anionic intermediates.

Appendix I.

Collaboration with the Murugesu Group

Description of the Collaboration:

The Murugesu Group at the University of Ottawa has used oxime products, synthesized through intermolecular reactions of aqueous hydroxylamines with alkynes containing various polar groups, and prepared by the Beauchemin Group. Throughout the ongoing collaboration between the two groups, I have participated in the synthesis of a variety these oxime-based ligands, which have aided in the formation of metallic coordination complexes.

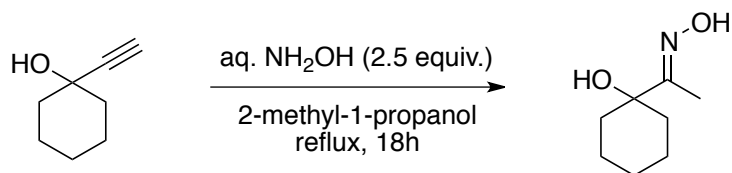
The following is an Organic Syntheses manuscript, submitted following an invitation by the journal to publish the Beauchemin gram-scale syntheses of oxime-based ligands. The procedure improves on previous laboratory methodologies that used sealed tube or microwave irradiation to instead achieve the ligand synthesis is achieved by a simple reflux system, much more amenable to gram scale synthesis.

Papers published using the discussed methodology:

- 1: "Combining Oximes with Azides to Create a Novel 1-D[NaCoIII2] System: Synthesis, Structure, and Solid-State NMR" Pathmalingam, T.; Habib, F.; Widdifield, C. M.; Loiseau, F.; Burchell, T. J.; Gorelsky, S. I.; Beauchemin, A. M.; Bryce, D. L.; Murugesu, M. *Dalton Trans.* **2010**, *39*, 1504.
- 2: "A Novel High-Spin Tridecanuclear Ni(II) Cluster with an Azido-Bridged Core Exhibiting Disk-Like Topology" Brunet, G.; Habib, F.; Cook, C.; Pathmalingam, T.; Loiseau, F.; Korobkov, I.; Burchell, T. J.; Beauchemin, A. M.; Murugesu, M. *Chem. Comm.* **2012**, *48*, 1287.
- 3: "Intermolecular retro-Cope Hydroxylamination of Alkynes with NH₂OH: (E-1-(1-Hydroxycyclohexyl)ethanone oxime)" Loiseau, F.; Beauchemin, A. M.; Murugesu, M. *Org. Synth.* **2013**, *90*, 87-95. (invited contribution). (**Attached to this current Appendix, see next page.**)
- 4: "Turning on Single-Molecule Magnet Behavior in a Linear {Mn₃} Complex" Habib, F.; Brunet, G.; Loiseau, F.; Pathmalingam, T.; Burchell, T. J.; Beauchemin, A. M.; Werndorfer, W.; Clérac, R.; Murugesu, M. *Manuscript accepted for publication*

Intermolecular Cope-Type Hydroamination of Alkynes with NH₂OH

(*E*-1-(1-Hydroxycyclohexyl)ethanone oxime)



Submitted by Francis Loiseau and André M. Beauchemin.¹

1. Procedure

A. *E*-1-(1-Hydroxycyclohexyl)ethanone oxime. A 100 mL round-bottom flask is charged with 1-ethynylcyclohexanol (5.00 g, 40.3 mmol, 1 equiv.) (Note 1), aqueous hydroxylamine (6.18 mL, 101 mmol, 2.5 equiv.) and 2-methyl-1-propanol (40 mL, Note 2). The flask is equipped with a magnetic stir bar, a reflux condenser, a rubber septum and an argon inlet, and is flushed with argon for 5 minutes (Note 3). The reaction mixture is then refluxed for 18 hours under an argon atmosphere (Note 4). The solution stays clear and colorless for the duration of the reaction. After cooling to room temperature, the reaction mixture is transferred to a 250 mL round-bottom flask and concentrated by rotary evaporation (45 °C, 25 mmHg). The resulting mixture is azeotroped twice by the adding hot toluene (2 x 50 mL) to the flask and concentrating by rotary evaporation (45 °C, 25 mmHg, Note 5). The crude solid (6.38 g) is transferred to a 50 mL Erlenmeyer and dissolved in 18 mL of near-boiling 1,2-dichloroethane (80 °C). The resulting solution is left to cool to ambient temperature over 2 hours, allowing crystallization to occur, and is further cooled at 0 °C for another 2 hours. The resulting crystals are collected by suction filtration on a Buchner funnel, and dried for 30 minutes. They are rinsed with 5 mL of ice-cold hexanes and dried again for 30 minutes, and then transferred to a 50 mL, round bottomed flask and dried for one hour at 0.1 mmHg to provide *E*-1-(1-hydroxycyclohexyl)ethanone oxime as white needle crystals (5.50 g, 87% yield) (Notes 6, 7).

2. Notes

1. 1-Ethynylcyclohexanol ($\geq 99\%$) and aqueous hydroxylamine (50 wt.%) were purchased from Aldrich Chemical Co., and used as received. 2-Methyl-1-propanol (reagent ACS grade, $\geq 99\%$) was purchased from GFS chemicals and used as received. Toluene (ACS grade, 99.9%), 1,2-dichloroethane (ACS grade, 99.9%) and hexanes (ACS grade, 99.9%) were purchased from Fisher Scientific and used as received.

2. 2-Methyl-1-propanol was chosen as a solvent for the reaction, because its boiling point was in the temperature range needed for the desired reactivity and reaction times. 1-Propanol can be alternatively used as a solvent, and the reaction performed using microwave heating (4 hours, 140 °C) or heating in a sealed tube placed in an oil bath (18 hours, 110 °C), yielding similar results.

3. The success of the reaction does not depend on having previously dried the glassware or on adding the reagents under an inert atmosphere.

4. Reflux is achieved by placing the reaction set-up in an oil bath kept at 115 °C. The progress of the reaction can be followed by TLC analysis on silica gel with 30% EtOAc-hexanes as eluent and visualized with potassium permanganate, ensuring proper evaporation of the reaction solvent by heating the plate pre-elution. The propargylic alcohol starting material has $R_f = 0.55$ and the α -hydroxyoxime product has $R_f = 0.37$.

5. The high affinity of the oxime product for H-bonding causes alcoholic solvents to adhere well to the compound. Toluene is used to azeotrope out the remaining 2-methyl-1-propanol. In cases when the oxime is obtained as a solid after the initial or second concentration, the mixture, after addition of hot toluene, can be heated and swirled until complete dissolution before concentrating again (The crude oxime melts below the boiling point of toluene, and is miscible with it once liquefied).

6. The product displayed the following physicochemical properties: mp 103-104 °C; ^1H NMR (300 MHz, CDCl_3) δ ppm: 8.40 (br s, 1H), 2.85 (br s), 1.90 (s, 3H), 1.44-1.79 (m, 9H), 1.12-1.32 (m, 1H); ^{13}C NMR (75 MHz, CDCl_3) δ ppm: 160.5, 71.9, 35.0, 25.5, 21.6, 9.1; IR (film) cm^{-1} : 3340, 2980, 2934, 2856, 1463, 1455, 1368, 1186, 1134, 1071, 1060, 1004, 952, 894, 745; HRMS (EI) m/z : $[\text{M}]^+$ calcd for $\text{C}_7\text{H}_{13}\text{NO}_2$: 157.11028. Not found; m/z : $[\text{M}-\text{OH}]^+$ for $\text{C}_7\text{H}_{12}\text{NO}$: 140.1080. Found: 140.1068; Anal. Calcd for $\text{C}_7\text{H}_{13}\text{NO}_2$: C, 61.12; H, 9.62; N, 8.91. Found: C, 61.02; H, 9.70; N, 8.86.

7. The product was found to be stable upon storage for 2 weeks at room temperature and ambient air.

Safety and Waste Disposal Information

Due to the high energy content of NH_2OH , appropriate care should be taken when conducting these experiments. The hydroxylamine concentration should not be increased beyond 5–10 wt% (i.e. the typical reaction conditions), and appropriate safety controls should be performed before scaling up this chemistry above the gram-scale, especially at very high temperatures. Note: NH_2OH has been used on the 2 mol scale under similar conditions (reflux in EtOH) in a previously reported procedure. (Steiger, R. E. *Org. Synth., Coll. Vol. III*, 1955, 91). All hazardous materials should be handled and disposed of in accordance with “Prudent Practices in the Laboratory”; National Academy Press; Washington, DC, 1995.

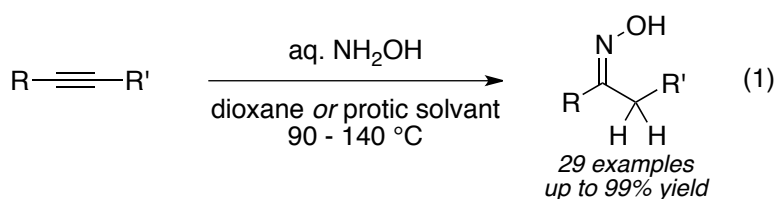
3. Discussion

Oximes are useful building blocks or key intermediates for a variety of organic transformations, including the Beckman rearrangement (yielding amides), the Neber reaction (yielding α -amino carbonyl moieties), and in diverse amination strategies with applications ranging from amination of organometallic reagents (electrophilic amination) to heterocyclic synthesis (via electrophilic, nucleophilic, radical-based or amino-Heck amination manifolds).² *O*-Protected oximes are also good electrophiles providing access to amine derivatives upon reaction with various nucleophiles, and stereoselective variants have been investigated.³ As such, oximes provide access to various nitrogen-containing functional groups, which are prevalent in medicinal chemistry and in natural products.

A variety of approaches are available to access oximes efficiently. The simple condensation of carbonyl compounds and NH_2OH (typically formed from its salt $\text{NH}_2\text{OH}\cdot\text{HCl}$ and a mild base such as NaOAc) is often simple, efficient and practical.⁴ However, several routes have been developed to complement this method, which are especially useful when the desired carbonyl compound is not readily available or when alternative starting materials are commercially or more readily available. Such routes include (1) the direct oxidation of primary amines to oximes;⁵ (2) the reduction of nitroalkanes or

nitroalkenes;⁶ (3) a 2-step Mitsunobu approach on primary and secondary alcohols;⁷ and (4) the nitrosation reactivity of alkenes.⁸

Recently, numerous important developments have extended the synthetic reach of alkene and alkyne hydroamination to a variety of nitrogen-containing molecules.⁹ In particular, metal-catalyzed alkyne hydroamination is emerging as a direct approach to a variety of imine derivatives, through intra- and intermolecular reactions.¹⁰ As part of efforts to enable oxime formation using alkyne hydroamination, and to develop the use of hydroxylamines and hydrazines in metal-free Cope-type hydroaminations,¹¹ we previously reported that oximes are formed directly upon heating alkynes and NH₂OH (eq 1).^{12,13}



After several rounds of reaction optimization, we developed several conditions that allow both terminal and internal alkynes to afford the Markovnikov hydroamination products effectively. The original conditions (Table 1, *conditions A*) involve conventional heating done in sealed tubes with 1,4-dioxane used as the solvent, and an excess of aqueous hydroxylamine (2.5 equiv). Optimized and preferred reaction conditions (*conditions B*) feature the use of a microwave reactor, which allows slightly increased yields and significantly shorter reaction times (<10 hours), and use alcoholic solvents.

The present procedure describes one representative example for the synthesis of oximes from alkynes and NH₂OH, and produces *E*-1-(1-hydroxycyclohexyl)ethanone oxime (5.50 g) in 87% yield. The procedure uses a simple reflux in 2-methyl-1-propanol (*conditions C*) and is complementary to our previously published conditions. Further modifications can be necessary in some cases when product degradation occurs under standard reflux conditions (notably when using the propargylamine-based substrates). These last reaction conditions (*conditions D*) are milder, involve conventional reflux for a longer reaction time at a lower temperature, and feature the use of a reduced excess of aqueous hydroxylamine (1.5 equiv rather than 2.5 equiv, as reaction optimization revealed that the reaction is higher yielding under those conditions).¹⁴

Table 1. Synthesis of Oximes from the Cope-type hydroamination of alkynes with NH₂OH

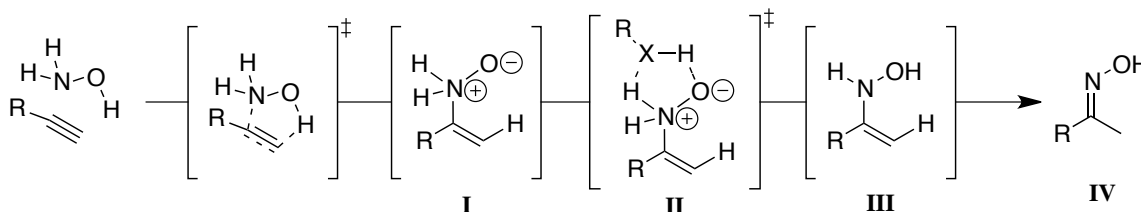
Entry	Substrate	Conditions ^a	Major Product	Yield (%) ^b	
1	R = Ph, R' = H	A		87(5)	
2	R = 4-OMeC ₆ H ₄ , R' = H	A		83(3)	
3	R = 4-FC ₆ H ₄ , R' = H	A ^c		71(8)	
4	R = 2-MeC ₆ H ₄ , R' = H	A		45(11)	
5		A ^c		73(15)	
6		B		72(3)	
7	R = <i>n</i> -C ₆ H ₁₃ , R' = H	B		86(2)	
8	R = <i>c</i> -C ₆ H ₁₂ , R' = H	B		72	
9	R'' = H	B		91	
10	R'' = TBS	B		86	
11	R'' = Bn	B		98	
12	R'' = Piv	B		90	
13	R'' = PMB	B		98	
14	R'' = THP	B		0 ^d	
15		R'' = H	B		89 (<1)
16		R'' = Me	B		89 (<1)
17		R'' = Ph	B		89
18		R'' = -(CH ₂) ₂ -	C		81
19		R'' = -(CH ₂) ₃ -	C		87
20		R'', R''' = Me	D		71
21		R'' = Bz, R''' = H	B		58
23	Ph—C≡C—Me	B		53(5)	
24	<i>n</i> -Pr—C≡C— <i>n</i> -Pr	B		12	

^a Reaction conditions: Alkyne (1 equiv.), aq. NH₂OH (2.5 equiv.) A: dioxane (1M), sealed tube (behind a blast shield), 113 °C, 16-18 h; B: *i*-PrOH, (1M), 140 °C (Biotage Initiator or CEM microwave), 5-10h; C: (*this work*) *i*-BuOH, reflux (107 °C), 18 h; D: Alkyne (1 equiv.), aq. NH₂OH (1.5 equiv.) *n*-PrOH, reflux (97 °C), 40 h. ^b Yield of isolated products. Yield of minor regioisomer shown in parentheses. ^c 2M in dioxane. ^d Led to isolation of unprotected oxime in 65 % yield.

As shown in Table 1, the reaction is compatible with a variety of alkynes (aromatic, aliphatic, enynes, sterically hindered), standard protecting groups, free hydroxyl groups, basic nitrogen atoms (sp^2 and sp^3), and amides. Internal alkynes can also be reacted, albeit resulting in reduced yields. In most cases, the unreacted starting alkynes can be recovered, and the products can be conveniently isolated by recrystallization or chromatography.

The reaction is most efficient when protic solvents (such as 1-propanol, 2-propanol or 2-methylpropan-1-ol) are used. The increased reactivity observed under these conditions is consistent with such alcohols both stabilizing the expected enamine *N*-oxide intermediate (**I**) and facilitating the proton transfer step required to access a neutral *N*-hydroxyenamine (**III**), that can subsequently tautomerize to the oxime product (**IV**). Computational results support a bimolecular proton transfer pathway in which the alcohol mediates the proton transfer through a five-membered, cyclic transition state (**II**), over an intramolecular proton transfer or stepwise alternatives.

Scheme 1



1. Centre for Catalysis Research and Innovation, Department of Chemistry, University of Ottawa, 10 Marie-Curie – D'Iorio Hall, Ottawa, Canada, K1N 6N5. andre.beauchemin@uottawa.ca.

2. For selected reviews, see: (a) Yamane, M.; Narasaka, K. In *Science of Synthesis*; Padwa, A., Ed.; Georg Thieme Verlag: Stuttgart, 2004; Vol. 27, pp. 605-647. (b) Narasaka, K.; Kitamura, M. *Eur. J. Org. Chem.* **2005**, 4505.

3. Moody, C. J. *Chem. Commun.* **2004**, 1341 (and references cited therein).

4. For an example: Bousquet, E.W. *Org. Synth., Coll. Vol. II*, **1943**, 313.

5. Suzuki, K.; Watanabe, T.; Murahashi, S.-I. *Angew. Chem., Int. Ed.* **2008**, *47*, 2079.

6. (a) Mourad, M. S.; Varma, R. S.; Kabalka, G. W. *J. Org. Chem.* **1985**, *50*, 133. (b) Kabalka, G. W.; Laila, G. M. H.; Varma, R. S. *Tetrahedron* **1990**, *46*, 7443. (c) Ghosh, A. K.; Gong, G. *Org. Lett.* **2007**, *9*, 1437.

7. Kitahara, K.; Toma, T.; Shimokawa, J.; Fukuyama, T. *Org. Lett.* **2008**, *10*, 2259.

8. Prateptongkum, S.; Jovel, I.; Jackstell, R.; Vogl, N.; Weckbecker, C.; Beller, M. *Chem. Commun.* **2009**, 1990.

9. For selected reviews, see : (a) Müller, T. E.; Hultsch, K. C.; Yus, M.; Foubelo, F.; Tada, M. *Chem. Rev.* **2008**, *108*, 3795 (and reviews cited therein). (b) Aillaud, I.; Collin, J.; Hannedouche, J.; Schulz, E. *Dalton Trans.* **2007**, 5105. (c) Hultsch, K. C. *Adv. Synth. Catal.* **2005**, *347*, 367. (d) Nobis, M.; Drießen-Hölscher, B. *Angew. Chem. Int. Ed.* **2001**, *40*, 3983. (e) Müller, T. E.; Beller, M. *Chem. Rev.* **1998**, *98*, 675.

10. (a) Severin, R.; Doye, S. *Chem. Soc. Rev.* **2007**, *32*, 1407. (b) Alonso, F.; Beletskaya, I. P.; Yus, M. *Chem. Rev.* **2004**, *104*, 3079. (c) Pohlki, F.; Doye, S. *Chem. Soc. Rev.* **2003**, *32*, 104.

11. Such reactions are also referred to as reverse Cope eliminations in the literature. For a review, see: Cooper, N. J.; Knight, D. W. *Tetrahedron* **2004**, *60*, 243.

12. (a) Beauchemin, A. M.; Moran, J.; Lebrun, M.-E.; Séguin, C.; Dimitrijevic, E.; Zhang, L.; Gorelsky, S. I. *Angew. Chem. Int. Ed.* **2008**, *47*, 1410. (b) Moran, J.; Gorelsky, S. I.; Dimitrijevic, E.; Lebrun, M.-E.; Bédard, A.-C.; Séguin, C.; Beauchemin, A. M. *J. Am. Chem. Soc.* **2008**, *130*, 17893. For related work, see : (c) Bourgeois, J.; Dion, I.; Cebrowski, P. H.; Loiseau, F.; Bédard, A.-C.; Beauchemin, A. M. *J. Am. Chem. Soc.* **2009**, *131*, 874. (d) Moran, J.; Pfeiffer, J. Y.; Gorelsky, S. I.; Beauchemin, A. M. *Org. Lett.* **2009**, *11*, 1895. (e) MacDonald, M. J.; Schipper, D. J.; Ng, P. J.; Moran, J.; Beauchemin, A.M. *J. Am. Chem. Soc.* **2011**, *133*, 20100.

13. For related reactivity of hydrazines and hydrazides, see: (a) Roveda, J.-G.; Clavette, C.; Hunt, A. D.; Gorelsky, S. I.; Whipp, C. J.; Beauchemin, A. M. *J. Am. Chem. Soc.* **2009**, *131*, 8740. (b) Cebrowski, P. H.; Roveda, J.-G.; Moran, J.; Gorelsky, S. I.; Beauchemin, A. M. *Chem. Commun.* **2008**, 492. (c) Loiseau, F.; Clavette, C.; Raymond, M.; Roveda, J.-G.; Burrell, A.; Beauchemin, A. M. *Chem. Commun.* **2011**, *47*, 562.

14. Conditions primarily used for the reaction of *N,N*-dimethylpropargylamine. The resulting oxime was used as a ligand in the synthesis of novel Ni(II) clusters : Brunet, G.; Habib, F.; Cook, C.; Pathmalingam, T.; Loiseau, F.; Korobkov, I.; Burchell, T. J.; Beauchemin, A. M.; Murugesu, M. *Chem. Commun.* **2012**, *48*, 1287.

Appendix II.

Claims to Original Research

Claims to Original Research

1. Development of a simple hydroxylamine methallylation strategy for the preparation of Cope-type intermolecular hydroaminations substrates.
2. Development of the Cope-type hydroamination / Meisenheimer & the Cope-type hydroamination / Cope elimination sequences to help overcome the thermoneutrality of intermolecular hydroaminations of alkenes.
3. Expansion of the scope of the intramolecular Cope-type hydroaminations of hydrazides through a systematic investigation of hydrazine analogs and development of the intermolecular Cope-type hydroamination of biased alkenes using hydrazides as bifunctional reagents.
4. Isolation of ammonium ylide dipolar intermediates for the Cope-type hydroaminations, and obtention of key primary and secondary KIEs, to help provide strong support for a concerted reaction mechanism.
5. Discovery and early development of a hydrogen-bond catalyzed methodology for the Cope-type hydroaminations, centered on the preferential stabilization of the dipolar intermediate.

Publications from This Work

1. Loiseau, F., Das Neves, N., Raymond, M., Hunt, A. D., Beauchemin, A.M. *Manuscript in preparation.*
2. "Turning on Single-Molecule Magnet Behavior in a Linear $\{Mn_3\}$ Complex" Habib, F., Brunet, G., Loiseau, F., Pathmalingam, T., Burchell, T. J., Beauchemin, A. M., Murugesu, M. *Manuscript accepted for publication.*
3. "Intermolecular retro-Cope Hydroxylamination of Alkynes with NH_2OH : (*E*-1-(1-Hydroxycyclohexyl)ethanone oxime)" Loiseau, F.; Beauchemin, A. M.; Murugesu, M. *Org. Synth.* **2013**, *90*, 87-95.

4. "A Novel High-Spin Tridecanuclear Ni(II) Cluster with an Azido-Bridged Core Exhibiting Disk-Like Topology" Brunet, G.; Habib, F.; Cook, C.; Pathmalingam, T.; Loiseau, F.; Korobkov, I.; Burchell, T. J.; Beauchemin, A. M.; Murugesu, M. *Chem. Comm.* **2012**, *48*, 1287-1289. (Collaboration with the Murugesu group)
5. "Improved Cope-Type Hydroamination Reactivity of Hydrazine Derivatives " Loiseau, F.; Clavette, C.; Raymond, M.; Roveda, J.-G.; Burrell, A.; Beauchemin, A. M. *Chem. Comm.* **2011**, *47*, 562-564. (Invited contribution)
6. "Combining Oximes with Azides to Create a Novel 1-D[NaCoIII2] System: Synthesis, Structure, and Solid-State NMR" Pathmalingam, T.; Habib, F.; Widdifield, C. M.; Loiseau, F.; Burchell, T. J.; Gorelsky, S. I.; Beauchemin, A. M.; Bryce, D. L.; Murugesu, M. *Dalton Trans.* **2010**, *39*, 1504-1510. (Collaboration with the Murugesu and Bryce research groups)
7. "The Tandem Cope-Type Hydroamination / [2,3]-Rearrangement Sequence: A Strategy to Favour the Formation of Intermolecular Hydroamination Products and Enable Difficult Cyclizations" Bourgeois, J.; Dion, I.; Cebrowski, P. H.; Loiseau, F.; Bédard, A.-C.; Beauchemin, A. M. *J. Am. Chem. Soc.* **2009**, *131*, 874-875.

Presentations from This Work

- * denotes an oral presentation
- 8. "*Probing the scope and mechanism of metal-free hydroamination reactions involving hydrazines and hydroxylamines.*" QOMSBOC 2011 (University of Concordia), **2011**. (*Best poster award*)
- 9. * "*Probing the scope and mechanism of metal-free hydroamination reactions involving hydrazines and hydroxylamines.*" ACS National meeting (Denver, CO), **2011**.
- 10. "*Novel Intra- and Intermolecular Hydroamination Reactivity Using Hydrazine Derivatives.*" QOMSBOC 2010 (Brock University), **2010**.
- 11. * "*Novel Intra- and Intermolecular Hydroamination Reactivity Using Hydrazine Derivatives.*" QOMSBOC 2009 (Université de Laval), **2009**.
- 12. "*Towards Increased Reactivity in Intermolecular Cope-Type Hydroamination of Alkenes.*" Pharmaqam 2009 (University of Qc in Montreal), **2009**.

13. *“Towards Increased Reactivity in Intermolecular Cope-Type Hydroamination of Alkenes.”* CSC National Conference 2009 (Hamilton), June **2009**.
14. *“Towards a solution to the hydroamination thermodynamic problem: design of new metal-free hydroamination tandem sequences.”* QOMSBOC 2008 (Toronto), November **2008**.
15. *“Towards a solution to the hydroamination thermodynamic problem: design of new metal-free hydroamination tandem sequences.”* Synthesis Day (Ottawa), June **2008**.

Appendix III.

Experimental Section

GENERAL EXPERIMENTAL

All reactions were performed under an atmosphere of argon in oven-dried glassware equipped with a magnetic stir bar and rubber septum unless otherwise stated. Microwave reactions were carried out in a Biotage Innovator microwave oven, using Biotage glassware specifically made for use with the instrument, and crimped rubber stoppers. Purification of reaction products was carried out by flash column chromatography using Silicycle silica gel (40-63 μm), unless otherwise noted. Analytical thin layer chromatography (TLC) was performed on aluminium or glass sheets pre-coated with silica gel 60 F254 (E. Merck), cut to size. Visualization was accomplished with UV light followed by dipping in a potassium permanganate, ceric ammonium molybdate or vanillin solution (unless otherwise indicated) and heating.

^1H NMR and ^{13}C NMR spectra were recorded on Bruker AVANCE 300 MHz, 400 MHz, 500 MHz and INOVA 500 MHz spectrometers at ambient temperature, unless otherwise indicated. Spectral data was reported in ppm using solvent as the reference (CDCl_3 at 7.26 ppm, C_6D_6 at 7.15 ppm or DMSO-d_6 at 2.50 ppm for ^1H NMR and CDCl_3 at 77.0 ppm, C_6D_6 at 128.02 ppm or DMSO-d_6 at 39.43 for ^{13}C NMR). ^1H NMR data was reported as: multiplicity (ap = apparent, br = broad, s = singlet, d = doublet, t = triplet, q = quartet, p = pentet, sext = sextuplet, sept = septuplet, m = multiplet), integration and coupling constant(s) in Hz.

Infrared (IR) spectra were obtained with neat thin films on a sodium chloride disk and were recorded on a Bomem Michelson 100 Fourier transform infrared spectrometer (FTIR). Melting points were determined with a Thomas-Hoover Unit or a Gallenkamp P1106G melting point apparatus and were uncorrected. High-resolution mass spectroscopy (HRMS) was performed on a Kratos Concept-11A mass spectrometer with an electron beam of 70eV at the Ottawa-Carleton Mass Spectrometry Centre.

MATERIALS

Dichloromethane, isopropanol, DME and toluene were dried by distillation over calcium hydride. Tetrahydrofuran and diethyl ether were dried by distillation over sodium/ benzophenone. Toluene, Benzene, DCE, PhCF₃, DMSO and DMF were dried over activated 3Å molecular sieves. Triethylamine was dried by distillation over calcium hydride. Unless otherwise noted, all commercial materials were used without further purification.

PROCEDURES AND CHARACTERIZATION FOR CHAPTER 2

◆ GENERAL COMMENTS

Procedures for the synthesis of compounds 2.14-2.19, 2.28-2.30, 2.31-2.33 can be found as part of our original publication.¹ Preparation of primary hydroxylamines: Based on a procedure by the House and Warner groups.²

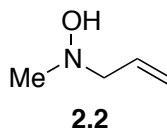
◆ CHARACTERIZATION OF THE OLIGOMER OBTAINED FROM THE SIDE REACTIONS

As mentioned in paragraph preceding Table 1 in the communication, reaction optimization was first performed using *N*-allyl-*N*-methyl-hydroxylamine. Encouraging but variable conversions were obtained. Supporting information is presented below, including preparations and characterization data for the hydroxylamine reagent and its norbornene adduct. These reactions typically led to the formation of multiple byproducts. In an attempt to isolate the byproducts formed, unpurified reaction mixtures (obtained upon heating *N*-allyl-*N*-methyl-hydroxylamine and norbornene) were combined and purified by silica gel chromatography. The spectral data of several isolated byproducts were consistent with a hydroamination side reaction on

¹ Bourgeois, J.; Dion, I.; Cebrowski, P. H.; Loiseau, F.; Bédard, A.-C.; Beauchemin, A. M. *J. Am. Chem. Soc.* **2009**, *131*, 874.

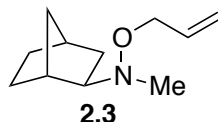
² (a) House, H. O.; Lee, L. F. *J. Org. Chem.* **1976**, *41*, 863. (b) Davison, E. C.; Forbes, I. T.; Holmes, A. B.; Warner, J. A. *Tetrahedron* **1996**, *52*, 11601.

the *O*-allyl side chain of the norbornene adduct. One of these byproducts could be isolated in sufficient quantities to allow characterization: this data is shown last, and was likely formed via an “anti-Markovnikov” hydroamination pathway. Related oligomers were also observed.



***N*-Allyl-*N*-methylhydroxylamine (2.2).**

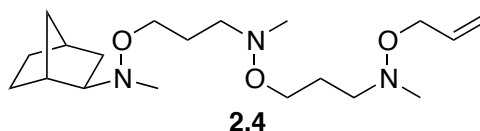
In a 100 mL round bottom flask charged with a magnetic stir bar was added potassium carbonate (19.9 g, 144 mmol) and *N*-Methylhydroxylamine hydrochloride (4.00 g, 47.9 mmol). The flask was purged with argon and dry ether (48 mL) was added via syringe. After vigorous stirring, allyl bromide (freshly distilled, 3.92 mL, 45.3 mmol) was added via syringe. The solution was stirred at room temperature for 20 h. After filtration of the potassium carbonate, the organic phase was extracted with a 10% hydrochloric acid solution. The aqueous phase was then neutralized with sodium hydroxide pellets, saturated with sodium chloride and extracted 5 times with ether. The resulting organic phase was dried over magnesium sulfate, filtered and concentrated over reduced pressure. Isolated 1.90 g (46%) of a clear colorless oil after purification by silica gel column chromatography. TLC R_f = 0.41 (100% ether) ^1H NMR (400 mhz, CDCl_3) δ ppm 7.20 (br, 1H), 5.98-5.87 (m, 1H), 5.27-5.16 (m, 2H), 3.32-3.30 (d, J = 8 Hz, 2H), 2.62 (s, 3H); ^{13}C NMR (100 mhz, CDCl_3) δ ppm 134, 119, 65, 48 cm^{-1} ; IR (film) 3337 (br), 2959, 2853, 1438, 923 cm^{-1} . Exact mass calcd for $\text{C}_4\text{H}_9\text{NO}$ $[\text{M}]^+$: 87.0684. Found: 87.07002.



***N*-(Allyloxy)-*N*-methylbicyclo[2.2.1]heptan-2-amine (2.3).**

An oven dried 15 mL sealed tube was charged with a stir bar, capped with a septum and purged with argon and an outlet for 5 minutes. *N*-Allyl-*N*-methylhydroxylamine

(277 mg, 3.18 mmol) and norbornene (200 mg, 2.12 mmol, 14.4 mmol, 5.0 equiv) and freshly distilled trifluorotoluene (2 mL) were added to the seal tube, while keeping it under an argon atmosphere. The septum was removed and the tube was then quickly sealed with a screw cap and Teflon tape and heated while stirring in a wax bath for 20 hours at 120°C. The tube was cooled to ambient temperature, concentrated under reduced pressure and analyzed by ¹H NMR using styrene as an internal standard, then again concentrated under reduced pressure. Yields obtained varied greatly (40% - 70%) following purification by silica gel chromatography. TLC *R_f* = 0.75 (20% EtOAc/80% Hexanes); ¹H NMR (400 mhz, CDCl₃) δ ppm 5.99-5.88 (m, 1H), 5.29-5.12 (m, 2H), 4.19 (d, *J* = 4 Hz, 2H), 2.47 (s, 3H), 2.41-2.39 (m, 1H), 2.23 (s, 1H), 1.59-1.54 (m, 1H), 1.60-1.39 (m, 3H), 1.38-1.29 (m, 1H), 1.16-1.03 (m, 4H); ¹³C NMR (100 mhz, DMSO-*d*₆) δ ppm 134.5, 115.9, 72.6, 71.8, 42.1, 38.6, 35.4, 35.3, 34.2, 27.7, 26.2; IR (film): 3079, 2955, 2870, 2783, 1038, 921 cm⁻¹. Exact mass calcd for C₁₁H₁₉NO [M]⁺: 181.1467. Found: 181.14523.



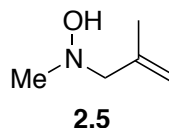
Oligomer formed by further reaction of *N*-(Allyloxy)-*N*-methylbicyclo[2.2.1]-heptan-2-amine (2.4).

¹H NMR (500 MHz, DMSO) δ 5.93-5.85 (m, 1 H), 5.23-5.18 (m, 1 H), 5.13-5.10 (m, 1 H), 4.11-4.07 (m, 2 H), 3.65-3.59 (m, 4 H), 2.62-2.54 (m, 4 H), 2.52-2.44 (m, 6 H), 2.37 (br, 3 H), 2.32-2.28 (m, 1 H), 2.18 (s, 1 H), 1.69-1.61 (m, 4 H), 1.51-1.36 (m, 4 H), 1.31-1.25 (m, 1 H), 1.09-0.95 (m, 4 H); ¹³C NMR (500 MHz, DMSO) δ 135.5, 116.7, 73.8, 73.2, 70.9, 70.5, 58.3, 45.9, 45.8, 36.9, 36.8, 35.4, 29.0, 27.4, 27.3. IR (film) 3079, 2955, 2869, 2793, 1440, 1034 cm⁻¹; HRMS (EI): Exact mass calcd for C₁₉H₃₇N₃O₃ [M]⁺: 355.2835. Not found. Exact mass calcd for C₁₆H₃₂N₃O₂ [M - C₃H₅O]⁺: 298.2500. Found: 298.2463.

◆ SYNTHESIS OF *N*-METHALLYL HYDROXYLAMINE PRECURSORS

General Procedure A for *N*-methallylation of hydroxylamines.

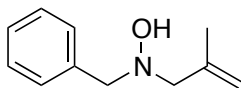
An oven dried round bottom flask and condenser were assembled and charged with a stir bar, capped with a septum and purged with argon and an outlet for 10 minutes. *N*-alkylhydroxylamine (4.06 mmol), 1,8-Diazabicyclo[5.4.0]undec-7-ene (680 mg, 4.47 mmol, 1.1 equiv) dissolved in a minimum of THF, 3-chloromethylpropene (1.20 mL, 12.3 mmol, 3 equiv) and 16 mL of THF:DMF (4:1), were added to the reaction flask, which was brought to reflux for 2.5 hours. The reaction mixture was dissolved in EtOAc and washed 4 times with water, then with brine. The organic layer was dried over sodium sulfate, filtered, evaporated under reduced pressure and concentrated to yield the corresponding *N*-alkyl-*N*-(methallyl)hydroxylamines, which may be further purified by silica gel chromatography.



***N*-Hydroxy-*N*,2-dimethylprop-2-en-1-amine (2.5)**

A flame-dried round bottom flask (100 mL) charged with a magnetic stir bar, potassium carbonate (19.9 g, 144 mmol) and the *N*-methylhydroxylamine (4.00 g, 47.9 mmol) was purged with argon for 10 minutes. Dry THF (48 mL) was added, the solution was strongly agitated and the 3-chloro-methylpropene (4.63 mL) was added via syringe. A condenser was added and the solution was heated to reflux for 20 h. Potassium carbonate was filtered under vacuum and the filtrate was extracted 3 times with 10% hydrochloric acid (~40 mL). The aqueous layer was neutralized with potassium hydroxide pellets and saturated with sodium chloride, and extracted with 5 times ether (300 mL total). The organic layer was dried over magnesium sulfate, filtered evaporated under reduced pressure. Further purification of the hydroxylamine was achieved by distillation at 65 mm Hg, to yield 2.3g (38%) as a colourless oil. TLC R_f 0.22 (20% EtOAc/hexanes); ^1H NMR (300 MHz, CDCl_3) δ 6.32-5.99 (s, 1 H),

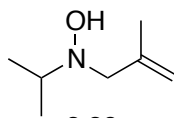
4.93 (s, 1 H), 4.91 (s, 1 H), 3.23 (s, 2 H), 2.62 (s, 3 H), 1.78 (s, 3 H); ^{13}C NMR (100 MHz, CDCl_3) δ 141.6, 114.4, 69.0, 47.7, 21.1; IR (film) 3259 (large), 3078, 2969, 2851, 2783, 1651, 1441, 1092, 901 cm^{-1} ; HRMS (EI): Exact mass calcd for $\text{C}_5\text{H}_{11}\text{NO}$ $[\text{M}]^+$: 101.0841 Found: 101.0846.



2.10

***N*-Benzyl-*N*-(2-methylallyl)hydroxylamine (2.10).**

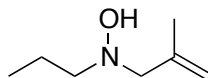
Synthesized according to General Procedure A. Isolated 670 mg (93%) as white crystals after concentration of the crude. mp: 60.0-61.0 $^{\circ}\text{C}$. TLC R_f 0.65 (20% EtOAc/hexanes); ^1H NMR (300 MHz, CDCl_3) δ 7.40-7.28 (m, 5H), 5.14 (br, 1H), 4.97 (s, 1H), 4.91 (s, 1H), 3.79 (s, 2H), 3.30 (s, 2H), 1.80 (s, 3H); ^{13}C NMR (100 MHz, CDCl_3) δ 142.1, 137.9, 129.4, 128.3, 127.3, 113.8, 66.7, 64.0, 21.1; IR (film): 3236, 3080, 3035, 2973, 2938, 2896, 2844, 1452, 909, 748, 699 cm^{-1} ; HRMS (EI): Exact mass calcd for $\text{C}_{11}\text{H}_{15}\text{NO}$ $[\text{M}]^+$: 177.1154 Found: 177.1156.



2.20

***N*-Isopropyl-*N*-(2-methylallyl)hydroxylamine (2.20).**

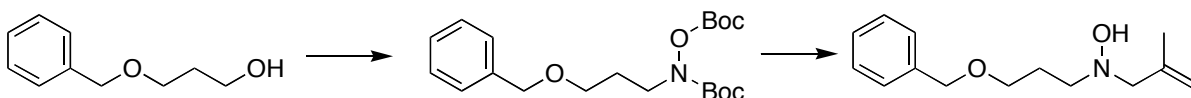
Synthesized according to General Procedure A, using 400 mg (5.33 mmol) of hydroxylamine. All reagents and solvents were scaled up accordingly. Isolated 440 mg (64%) as white crystals after concentration of the crude. ^1H NMR (500 MHz, CDCl_3) δ 5.20 (s, 1H), 4.94 (s, 1H), 4.88 (s, 1H), 3.24 (s, 2H), 2.93 (sept, $J = 6.4$ Hz, 1H), 1.78 (s, 3H), 1.11 (s, 3H), 1.10 (s, 3H); ^{13}C NMR (100 MHz, CDCl_3) δ 142.4, 113.6, 62.6, 56.3, 21.2, 18.0; IR (film): 3449, 3251 (br), 2972, 2916, 1650, 1447, 900 cm^{-1} ; HRMS (EI): Exact mass calcd for $\text{C}_7\text{H}_{15}\text{NO}$ $[\text{M}]^+$: 129.1154 Found: 129.1170.



2.22

***N*-(2-Methylallyl)-*N*-propylhydroxylamine (2.22)**

The General Procedure A, was inappropriately changed to using *n*-propylhydroxylamine (1.00 g, 13.3 mmol), 1,8-Diazabicyclo[5.4.0]undec-7-ene (1.62 g, 10.6 mmol), 3-chloro-methylpropene (2.85 mL, 29.1 mmol) and THF:DMF 4:1 (39 mL). The reaction was refluxed for 2.0 hours. The crude was purified by a short column chromatography (100% CHCl₃), and isolated as a colourless oil (420 mg, 42% yield). TLC *R*_f 0.72 (100% EtOAc); ¹H NMR (500 MHz, CDCl₃) δ ppm 6.17 (br, 1H), 4.91 (s, 1H), 4.88 (s, 1H), 3.26 (s, 2H), 2.61-2.56 (m, 2H), 1.78 (s, 3H), 1.67-1.57 (m, 2H), 0.92 (t, *J* = 7.45 Hz, 3H); ¹³C NMR (100 MHz, CDCl₃) δ ppm 141.8, 114.1, 67.6, 61.4, 21.3, 20.4, 11.8; IR (film): 3449, 3254 (br), 3079, 2964, 2880, 2844, 1451, 900 cm⁻¹; HRMS (EI): Exact mass calcd for C₉H₁₉NO [M]⁺: 129.1154 Found: 129.1152



***N*-(Benzyloxy)propyl-*N*,*O*-Di-*tert*-Butyloxycarbonylhydroxylamine**

(Based on: Parry *et al. Org. Lett.* **2003**, *5*, 1213) To a 0°C solution of *N*-*tert*-butyl carbamate-*O*-*tert*-butyl carbonate hydroxylamine (2.81 g, 12.0 mmol), 3-Benzyloxypropanol (2.00 g, 12.0 mmol) and triphenylphosphine (9.47 g, 36.1 mmol) in THF (120 mL) under argon was added freshly distilled diisopropylazodicarboxylate (7.00 mL, 39.1 mmol) dropwise. The solution was stirred at 0°C for 25 min. It was then concentrated *in vacuo*. Isolated 4.00 g (87%) as a white powder after column chromatography (5% EtOAc/hexanes). mp 45.5-46.0. TLC *R*_f 0.55 (20% EtOAc/hexanes); ¹H NMR (300 MHz, CDCl₃) δ ppm 7.37-7.23 (m, 5H), 4.50 (s, 2H), 3.72 (t, *J* = 6.21, 6.21 Hz, 2H), 3.55 (t, *J* = 6.18, 6.18 Hz, 2H), 1.91 (p, *J* = 6.53, 6.53, 6.51, 6.51 Hz, 2H), 1.52 (s, 9H), 1.47 (s, 9H); ¹³C NMR (75 MHz,

CDCl₃) δ ppm 154.9, 152.3, 138.4, 128.3, 127.6, 127.5, 84.7, 82.2, 73.0, 67.5, 47.5, 28.1, 27.6, 27.5; IR (film): 2987, 2941, 2877, 1790, 1729, 1447, 1375, 1265, 1162, 1079, 832 cm⁻¹.

***N*-(Benzyloxy)propyl-*N*-(2-methylallyl)hydroxylamine (2.24).**

To the previously formed diboc-protected hydroxylamine (4.00 g, 10.5 mmol) was added a 4:1 solution of dichloromethane and trifluoroacetic acid (105 mL). The reaction was left to stir at room temperature for 30 minutes. The reaction was concentrated under reduced pressure, and quenched with triethylamine (6.60 mL). The resulting solution was extracted with 3 times ether, the organic phases were combined, dried over magnesium sulfate, filtered and concentrated under reduced pressure. Crude free hydroxylamine (1.90 g, 100% yield.) was obtained and used directly in the next step.

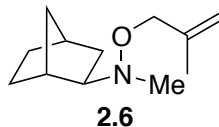
To a solution of the crude (3-benzyloxypropyl)hydroxylamine (1.90 g, 10.5 mmol) and 2-methylpropene (3.16 mL, 32.3 mmol) in THF:DMF 4:1 (43 mL) under an argon atmosphere was added 1,8-Diazabicyclo[5.4.0]undec-7-ene (1.93 mL, 12.9 mmol). The reaction was refluxed for 2.5 h. After cooling down the reaction contents to room temperature, the reaction was concentrated under reduced pressure. The resulting mixture was dissolved in EtOAc and washed 5 times with H₂O:Brine 1:1. The resulting organic phase was dried over sodium sulfate, filtered and concentrated under reduced pressure. Isolated 1.95 g (77%) of **2.24** as a clear liquid after column chromatography (17.5% EtOAc/hexanes). TLC *R*_f 0.29 (20% EtOAc/hexanes); ¹H NMR (300 MHz, CDCl₃) δ ppm 7.37-7.24 (m, 5H), 6.19 (br s, 1H), 4.92 (br s, 1H), 4.89 (s, 1H), 4.51 (s, 2H), 3.57 (t, *J* = 6.19, 6.19 Hz, 2H), 3.28 (s, 2H), 2.76 (t, *J* = 6.94, 6.94 Hz, 2H), 1.94 (p, *J* = 6.45, 6.66, 6.31, 6.85 Hz, 2H), 1.77 (s, 3H); ¹³C NMR (75 MHz, CDCl₃) δ ppm 141.8, 138.4, 128.3, 127.6, 127.5, 113.9, 72.9, 68.5, 67.4, 56.7, 27.6, 21.1; IR (film): 3409 (br), 3074 (w), 3028 (w), 2926, 2861, 1455, 1371, 1102, 1026, 904 cm⁻¹; HRMS (EI): Exact mass calcd for C₁₄H₂₁NO₂ [M]⁺: 235.1572 Found: 235.15407.

◆ SCOPE EXPANSION OF INTRAMOLECULAR HYDROAMINATION

General Procedure B for the reaction of alkenes with *N*-Alkyl-*N*-(2-methylallyl)-hydroxylamines.

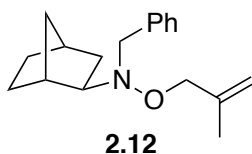
General Procedure B1: An oven dried 15 mL sealed tube was charged with a stir bar, capped with a septum and purged with argon and an outlet for 5 minutes. *N*-Alkyl-*N*-methallylhydroxylamine (2.97 mmol, 1.0 equiv), the alkene (14.4 mmol, 5.0 equiv) and benzene (2.97 mL) were added to the seal tube, while keeping it under an argon atmosphere. The septum was removed and the tube was then quickly sealed with a screw cap and Teflon tape and heated while stirring in a wax bath for 38 hours at 110°C. The tube was then cooled to ambient temperature, and the reaction mixture was concentrated under reduced pressure and analyzed by ¹H NMR using styrene as an internal standard, then again concentrated under reduced pressure and purified by silica gel chromatography to give the corresponding *O*-methallyl-*N,N*-dialkyhydroxylamine.

General Procedure B2: An oven dried 2 mL sealed tube was charged with a stir bar, capped with a septum and purged with argon and an outlet for 5 minutes. *N*-Alkyl-*N*-methallylhydroxylamine (1.0 mmol, 1.0 equiv), sodium cyanoborohydride (63 mg, 1.0 mmol, 1.0 equiv), norbornene (753 mg, 8.0 mmol, 8.0 equiv), *n*-propanol (1.0 mL) were added to the sealed tube, while keeping it under an argon atmosphere. The septum was removed and the tube was then quickly sealed with a screw cap and Teflon tape and heated while stirring in a wax bath for 96 hours at 120°C. The tube was cooled to ambient temperature, concentrated under reduced pressure and analyzed by ¹H NMR using dimethoxybenzene as an internal standard, then again concentrated under reduced pressure and purified by silica gel chromatography to give the corresponding *O*-methallyl-*N,N*-dialkyhydroxylamine.



***N*-(2-Methylallyloxy)-*N*-methylbicyclo[2.2.1]heptan-2-amine (2.6).**

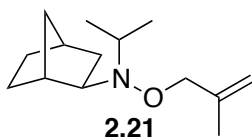
Synthesized according to General Procedure B1, using 300 mg (2.97 mmol) of the hydroxylamine and norbornene. Reaction was heated at 110 °C for 38 h. Isolated 414 mg (72%) of the title compound as a clear colorless oil after column chromatography (100% hexanes → 5% EtOAc/hexanes). TLC R_f 0.65 (20% EtOAc/hexanes); ^1H NMR (500 MHz, CDCl_3) δ ppm 4.97 (s, 1 H), 4.87 (s, 1 H), 4.15-4.07 (m, 2 H), 2.49 (br s, 3 H), 2.45-2.41 (m, 1 H), 2.24 (s, 1H), 1.77 (s, 3 H), 1.61-1.55 (m, 1 H), 1.54-1.41 (m, 3 H), 1.40-1.31 (m 1 H), 1.16-1.05 (m, 4 H); ^{13}C NMR (75 MHz, DMSO) δ ppm 142.9, 113.0, 77.3, 73.3, 43.1, 40.0, 36.9, 36.7, 35.7, 29.2, 27.7, 20.6; IR (film) 3077, 2955, 2870, 2782, 1655, 1452, 1356, 1022, 898 cm^{-1} . HRMS (EI): Exact mass calcd for $\text{C}_{12}\text{H}_{21}\text{NO}$ $[\text{M}]^+$: 195.1623. Found: 195.1594.



***N*-(2-Methylallyloxy)-*N*-benzylbicyclo[2.2.1]heptan-2-amine (2.12).**

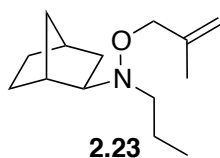
Synthesized according to General Procedure B2, using 400 mg (2.25 mmol) of hydroxylamine and norbornene. A larger 15 mL sealed tube was used. All reagents and solvents were scaled up accordingly. Isolated 269 mg (44%) of the title compound as a clear colorless oil after column chromatography using silver nitrate treated silica gel (30% toluene/hexanes → 100% toluene). TLC R_f 0.85 (20% EtOAc/hexanes); ^1H NMR (500 MHz, CDCl_3) δ ppm 7.37 (d, $J = 7.30$ Hz, 2H), 7.29 (t, $J = 7.19, 7.19$ Hz, 2H), 7.24 (t, $J = 7.16, 7.16$ Hz, 1H), 4.75 (ap d, $J = 5.26$ Hz, 2H), 3.88 (d, $J = 12.86$ Hz, 2H), 3.60 (br s, 2H), 2.64 (m, 1H), 2.47 (br s, 1H), 2.29 (br s, 1H), 1.73 (d, $J = 9.29$ Hz, 1H), 1.54 (s, 3H), 1.52-1.30 (m, 4H), 1.12 (t, $J = 8.99, 8.99$ Hz, 3H); ^{13}C NMR (75 MHz, CDCl_3) δ ppm 141.5, 138.3, 130.0, 127.9, 126.9, 113.1, 78.8, 71.2, 60.2, 39.3, 37.0, 36.7, 35.1, 28.7, 27.2, 20.2; IR (film) 3070, 3030, 2953,

2869, 1657, 1497, 1451, 1341, 1048, 900 cm^{-1} . HRMS (EI): Exact mass calcd for $\text{C}_{18}\text{H}_{25}\text{NO}$ $[\text{M}]^+$: 271.19361. Found: 271.19327.



***N*-(2-Methylallyloxy)-*N*-isopropylbicyclo[2.2.1]heptan-2-amine (2.21).**

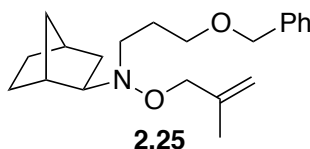
Synthesized according to General Procedure B1, using 60 mg (0.46 mmol) of the hydroxylamine and a modified ratio of norbornene (10 equiv). All reagents and solvents were scaled down accordingly. Reaction was heated at 130 °C for 45 h. Isolated 22 mg (21%) of the title compound as a clear colorless oil after column chromatography (100% hexanes \rightarrow 20% toluene/hexanes). TLC R_f 0.18 (20% toluene/hexanes); ^1H NMR (500 MHz, CDCl_3) δ ppm 4.96 (s, 1 H), 4.84 (s, 1H), 4.22-4.09 (m, 2H), 3.03-2.93 (m, 1H), 2.84-2.76 (m, 1H), 2.44-2.30 (s, 1H), 2.23 (s, 1H), 1.76 (s, 3H), 1.70-1.65 (m, 1H), 1.54-1.41 (m, 3H), 1.31-1.24 (m, 1H), 1.17-1.10 (m, 4H), 1.09-1.06 (m, 2H), 1.05-1.00 (m, 3H); ^{13}C NMR (75 MHz, C_6D_6 , 80 °C) δ ppm 142.4, 111.6, 80.5, 67.7, 53.0, 40.3, 37.2, 36.9, 35.3, 29.2, 28.0, 20.7, 20.1, 16.1; IR (film): 2954, 2871, 1655, 1451, 896 cm^{-1} ; HRMS (EI): Exact mass calcd for $\text{C}_{14}\text{H}_{25}\text{NO}$ $[\text{M}]^+$: 223.1936. Found: 223.1903



***N*-(2-Methylallyloxy)-*N*-propylbicyclo[2.2.1]heptan-2-amine (2.23).**

Synthesized according to General Procedure B1, using 100 mg (0.77 mmol) of the hydroxylamine, and a modified ratio of norbornene (8 equiv). All reagents and solvents were scaled down accordingly. Reaction was heated at 130 °C for 45 h. Isolated 83 mg (48%) of the title compound as a clear colorless oil after column chromatography (100% hexanes \rightarrow 10% EtOAc/hexanes) followed by column chromatography using silver nitrate treated silica gel (100% benzene). TLC R_f 0.65

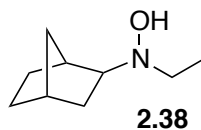
(5% EtOAc/hexanes); ^1H NMR (300 MHz, CDCl_3) δ ppm 4.96 (s, 1H), 4.86 (s, 1H), 4.23-4.09 (m, 2 H), 2.69-2.51 (m, 2H), 2.50-2.34 (m, 2H), 2.27-2.19 (s, 1H), 1.76 (s, 1H), 1.70-1.54 (m, 3H), 1.53-1.39 (m, 2 H), 1.38-1.19 (m, 2H), 1.18-1.01 (m, 3H), 0.91 (t, $J = 7.4$ Hz, 3H); ^{13}C NMR (300 MHz, C_6D_6) δ ppm 142.5, 111.9, 79.4, 71.8, 59.0, 40.2, 37.2, 37.1, 35.5, 29.3, 27.9, 20.8, 20.1, 12.2; IR (film): 3077, 2957, 2872, 1656, 1452, 1024, 897 cm^{-1} . HRMS (EI): Exact mass calcd for $\text{C}_{14}\text{H}_{25}\text{NO}$ $[\text{M}]^+$: 223.1936. Found: 223.1932



***N*-(2-Methylallyloxy)-*N*-(3-(benzyloxy)propyl)bicyclo[2.2.1]heptan-2-amine (2.25).**

Synthesized according to General Procedure B2, using 235 mg (1.0 mmol) of hydroxylamine and norbornene. Isolated 192 mg (52%) of the title compound as a clear colorless oil containing rotamers after column chromatography (1.5% EtOAc/hexanes). TLC R_f 0.80 (5% EtOAc/hexanes); ^1H NMR (300 MHz, $\text{DMSO}-d_6$, 120 $^\circ\text{C}$) δ ppm 7.40-7.22 (m, 5H), 4.95-4.80 (m, 2H), 4.48 (s, 2H), 4.19-4.06 (m, 2H), 3.60-3.52 (m, 2H), 2.84-2.55 (m, 3H), 2.37 (br s, 1H), 2.23 (br s, 1H), 1.90-1.74 (m, 3H), 1.71 (m, 3H), 1.66-1.55 (m, 1H), 1.55-1.38 (m, 2H), 1.36-1.24 (m, 2H), 1.19-1.01 (m, 2H); ^{13}C NMR (75 MHz, $\text{DMSO}-d_6$, 120 $^\circ\text{C}$) δ ppm 143.0, 142.8, 142.6, 139.8, 128.9, 128.1, 128.0, 114.0, 112.9, 112.5, 79.0, 77.5, 72.9, 71.4, 69.3, 69.2, 65.7, 55.7, 53.6, 40.0, 36.9, 36.8, 35.7, 29.2, 28.0, 27.9, 27.9, 21.6, 20.5, 20.4; IR (film) 3082, 3036, 2949, 2861, 1656, 1451, 1363, 1098, 892 cm^{-1} HRMS (EI): Exact mass calcd for $\text{C}_{21}\text{H}_{31}\text{NO}_2$ $[\text{M}]^+$: 329.23548. Found: 329.23335.

◆ TYPICAL PROCEDURE FOR THE HYDROAMINATION/COPE ELIMINATION CASCADE.



***N*-exo-(Bicyclo[2.2.1]heptan-2-yl)-*N*-ethylhydroxylamine (2.38).**

N,N-Diethylhydroxylamine (0.4 g, 4.5 mmol) and norbornene (2.1 g, 22 mmol) were added to a sealed tube containing a magnetic stirbar and dissolved in benzene (4.5 mmol). The tube was capped with a septum and purged with argon and an outlet for 5 minutes while stirring. The septum was removed and the tube was quickly sealed with a Teflon screwcap and immersed in an oil bath set at 100 °C for 24 h while stirring. The tube was cooled to ambient temperature, and the reaction was then monitored by thin layer chromatography (40% EtOAc/hexanes). The crude reaction mixture was concentrated under reduced pressure and purified by silica gel chromatography (10% EtOAc/hexanes) to give the titled compound (0.43 g, 62%) as a clear colourless oil. TLC R_f 0.32 (5% MeOH/ CH₂Cl₂). ¹H NMR (CDCl₃, 300 MHz) δ ppm 7.00 (br s, 1H), 2.76 (br s, 1H), 2.50 (s, 2H), 2.19 (br s, 2H), 1.60-1.26 (m, 4H), 1.15-0.99 (m, 6H); ¹³C NMR (CDCl₃, 75 MHz) δ ppm 70.7, 50.5, 39.5, 36.4, 36.2, 35.2, 28.3, 27.5, 11.2; IR (film): 3362, 2955, 2870, 2360, 2341, 1376, 1344, 1089, 944, 890, 611 cm⁻¹; HRMS (EI): Exact mass calculated for C₉H₁₇NO [M⁺]: 155.1310. Found: 155.1303.

PROCEDURES AND CHARACTERIZATION FOR CHAPTER 3

◆ GENERAL COMMENTS

Several compounds can be found in previous theses or communications in the Beauchemin group. Namely, the following compounds can be found in previous communications: **3.2a,b,d,e,f**; **3.6a,b,d**; **3.8a-b**; **3.14**; **3.18a**, **3.22**, **3.34** and their precursors can be found in a previous publication.³ Compounds **3.4** and **3.12** can be found in thesis of Mr. Jean-Grégoire Roveda, while compounds **3.50a-k** and **3.52a-b** can be found in Ms. Isabelle Dion and Ms. Ashley Hunt's Graduate Theses.⁴ The syntheses of 4-pentenal, 4-hexenal, 5-hexenal, 5-octenal and 3-benzyloxypropionaldehyde can also be found in a recent publication.⁵

◆ SYNTHESIS OF CYCLIZATION PRECURSORS

General Procedure C for reparation of the Alkylhydrazides

General Procedure C1: Hydrazone Formation: The corresponding aldehyde or ketone (1.25 equiv.) was dissolved in MeOH (0.2 M) at 25 °C. The corresponding hydrazide was added to the reaction flask. The reaction was stirred at room temperature and monitored by TLC until consumption of the hydrazide was completed. Depending on substrates, the conditions varied from 30 min to 5 hours either at room temperature or at reflux, with aldehydes typically reacting faster than ketones and electron-poor hydrazides requiring longer or more forcing conditions to reach completion. The unpurified hydrazone was then dried over sodium sulfate,

³ Roveda, J.-G.; Clavette, C.; Hunt, A. D.; Gorelsky, S. I.; Whipp, C. J.; Beauchemin, A. M. *J. Am. Chem. Soc.* **2009**, *131*, 8740.

⁴ Hunt, A. D.. "Intramolecular Cope-Type Hydroamination of Alkenes and Alkynes Using Hydrazides." M.Sc. Thesis, University of Ottawa, ON, 2010. & Dion, I. "Intramolecular Cope-Type Hydroamination of Alkenes in the Synthesis of Alkaloids: Total Synthesis of (+)-Coniine and (+)-Desbromoarborescidine A and Studies on a Novel Amination Strategy Towards Manzamine A." Ph.D. Thesis, University of Ottawa, ON, 2012.

⁵ Bourgeois, J.; Dion, I.; Cebrowski, P. H.; Loiseau, F.; Bédard, A.-C.; Beauchemin, A. M. *J. Am. Chem. Soc.* **2009**, *131*, 874.

filtered over cotton, and used directly in the reduction to the alkyl hydrazide. (alternatively, silica-gel chromatography can be performed on certain hydrazones. Use of the unpurified reaction mixture was preferred, due to the lability of some hydrazones used)

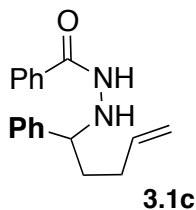
Reduction of the Hydrazone: Performed via a modification of Lane's procedure.⁶ The hydrazone was diluted further with MeOH (0.1 M) under argon and cooled to 30 °C. NaCNBH₃ (2.4 equiv.) and methyl orange is added to the solution. A mixture of 1:1 HCl/MeOH was added fast via syringe until the solution was dark red (pH < 3), while keeping vigorous stirring. The reaction was monitored visually, and extra HCl solution was added if the solution lost its dark color within the first 30 minutes, while following the reaction by TLC. Upon completion (typically 1-3 hours), the reaction was diluted with 50 mL of CH₂Cl₂ and transferred to a separatory funnel. After adding 10 mL of water was added to the solution, the pH was raised slowly to 6.5-7.0 with saturated aq. NaHCO₃. The solution was extracted three times with CH₂Cl₂, the combined organic layers were washed with brine, dried over Na₂SO₄, filtered and concentrated under reduced pressure. The crude product was then purified by column chromatography to give the corresponding alkyl or alkenyl hydrazide.

General Procedure C2: Hydrazone Formation: The corresponding aldehyde or ketone (1.25 equiv.) was dissolved in *t*-BuOH (0.2 M) at 40 °C. The corresponding hydrazide was added to the reaction flask. The reaction was monitored by TLC until consumption of the hydrazide was completed. The crude solution of hydrazone was then dried over sodium sulfate, filtered over cotton, and used directly in the reduction to the alkyl hydrazide. *Note: For supporting info on the synthesis of the aldehydes, see reference 6.

Reduction of the Hydrazone: Performed via a modification of Lane's procedure.⁶ The crude hydrazone solution was diluted further with *t*-BuOH (0.1 M) under argon and

⁶ Lane, C. F. *Synthesis* **1975**, 135.

cooled to 30 °C. NaCNBH₃ (2.4 equiv.) and a pinch of methyl orange was added to the solution. A mixture of 1:1 HCl/MeOH was added fast via syringe until the solution was dark red (pH < 3), while keeping vigorous stirring. The reaction was monitored visually, and extra HCl solution was added if the solution loses its dark color within the first 30 minutes, while following the reaction by TLC. Upon completion (typically 1-3 hours), the reaction was diluted with 50 mL of CH₂Cl₂ and transferred to a separatory funnel. After adding 10 mL of water was added to solution, the pH was raised slowly to 6.5-7.0 with saturated aq. NaHCO₃. The solution was extracted three times with CH₂Cl₂, the combined organic layers were washed with brine, dried over Na₂SO₄, filtered and concentrated under reduced pressure. The crude product was then purified by column chromatography to give the corresponding alkyl or alkenyl hydrazide.

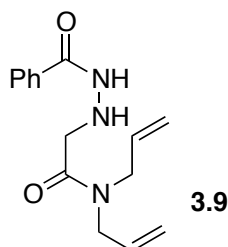


***N'*-(1-Phenylpent-4-enyl)benzohydrazide.**

Phenylpent-4-en-1-one (2.4 g, 15.0 mmol, 1 equiv), methanol (75 mL), benzohydrazide (2.47 g, 18.7 mmol, 1.25 equiv), acetic acid (0.43 mL, 0.5 equiv) and sodium sulfate were added together and the reaction mixture was refluxed at 80 °C for 4 hours. 40 mL of a saturated sodium bicarbonate solution was added to the reaction. Then, 15 mL H₂O/Brine (1 : 1) was added to the solution and the reaction mixture was extracted 3 times with 75 mL of dichloromethane. The combined organic layers were dried with sodium sulfate, filtered and concentrated under reduced pressure. The corresponding hydrazone was used as is.

The hydrazone (15.0 mmol, 1 equiv) and methanol (30 mL) were added to a 25 mL round balloon flask. Sodium cyanoborohydride (36 mmol, 2.4 equiv) was then added to the solution. A pinch of methyl orange was added and a solution of methanol and hydrochloric acid (1 : 1) was added generously until the solution turned red and kept

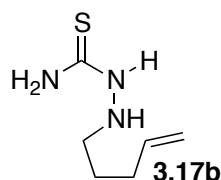
the colour for 5 min. The solution was stirred at room temperature for 1 hour. Sodium hydroxide 25% (w/w) was added dropwise to a pH of 8.5. 40 mL of H₂O was added and the resulting solution was extracted 3 times with 50 mL of dichloromethane. Combined organic layers were dried with sodium sulfate, filtered and concentrated under reduced pressure. The reaction mixture was concentrated under reduced pressure and isolated using flash chromatography (25% ethyl acetate in hexanes). The compound was obtained as a white solid (2.74 g, 65% yield). TLC R_f 0.50 in 60% EtOAc in hexanes; ¹H NMR (400 MHz, CDCl₃) δ ppm 7.87-7.14 (m, 10H), 5.87-5.70 (m, 1H), 5.06-4.90 (m, 2H), 4.76 (br s, 1H), 4.10 (dd, *J* = 8.27, 5.00 Hz, 1H), 2.11-1.88 (m, 3H), 1.87-1.72 (m, 1H); ¹³C NMR (100 MHz, CDCl₃) δ ppm 167.2 (C), 141.4 (C), 137.8 (CH), 132.8 (C), 131.7 (CH), 128.6 (CH), 128.5 (CH), 127.9 (CH), 127.7 (CH), 126.8 (CH), 115.0 (CH₂), 64.8 (CH), 34.2 (CH₂), 30.0 (CH₂); IR (film) 3282, 3063, 3027, 2934, 2856, 1639, 1580, 1530, 1452, 1312, 909, 694 cm⁻¹; HRMS (EI): Exact mass calcd for C₁₈H₂₀N₂O [M]⁺: 280.1576 Found : 280.1577.



2-[2-(phenylcarbonyl)hydrazinyl]-N,N-di(prop-2-en-1-yl)acetamide. (3.9)

N,N-diallyl-2-iodoacetamide (250 mg, 0.943 mmol, 1 equiv), 3,5-bis(trifluoromethyl)-benzohydrazide (0.623 g, 4.72 mmol, 5 equiv) and dimethylformamide (4.7 mL) were mixed together in a round balloon flask at room temperature for 4h30. 30 mL of ethyl acetate was added and the reaction mixture was washed five times with 8 mL of a (1 : 1) H₂O/Brine solution. The organic layer was then dried with sodium sulfate, filtered, concentrated under reduced pressure and isolated using flash chromatography (8% methanol in dichloromethane). The compound was obtained as a yellow oil (213 mg, 83% yield). TLC R_f 0.51 (8% methanol in dichloromethane); ¹H NMR (Benzene-*d*₆, 300 MHz) δ ppm 8.65-8.43 (m, 1H), 7.80-7.70 (m, 2H), 7.07-

6.92 (m, 3H), 5.66-5.46 (m, 1H), 5.44-5.29 (m, 1H), 5.21-5.04 (m, 1H), 4.95-4.62 (m, 4H), 3.83 (d, $J = 5.99$ Hz, 1H), 3.43 (s, 1H), 3.06 (d, $J = 4.88$ Hz, 1H) cm^{-1} . ^{13}C NMR (CDCl_3 , 300 MHz) δ ppm 170.3 (C), 166.6 (C), 133.0 (C), 132.6 (CH), 131.9 (CH), 131.8 (CH), 128.6 (CH), 127.0 (CH), 118.0 (CH_2), 117.4 (CH_2) 52.1 (CH_2), 48.4 (CH_2), 48.2 (CH_2) cm^{-1} ; IR (film) 3289, 3072, 2983, 2919, 1654, 1533, 1459, 1416, 1285, 1228, 993, 926, 691 cm^{-1} ; HRMS (EI): Exact mass calcd for $\text{C}_{15}\text{H}_{19}\text{N}_3\text{O}_2$ $[\text{M}]^+$: 273.1477 Not found. Exact mass calcd for $\text{C}_8\text{H}_{13}\text{N}_2\text{O}$ $[\text{M} - \text{C}_7\text{H}_6\text{NO}]$: 153.1028. Found: 153.1039.

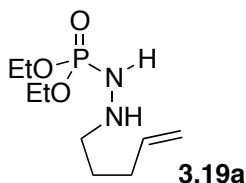


1-(Pent-4-enyl)thiosemicarbazide (3.17b).

Synthesized according to **General Procedure C1**. The hydrazone derived from the title compound was isolated as a white crystalline solid (0.997 g, 65% yield) using flash chromatography (40% EtOAc in toluene with 1% Et_3N). TLC R_f 0.29 in 10% MeOH in CH_2Cl_2 ; ^1H NMR (300 MHz, CDCl_3) * denotes minor isomer δ ppm 10.58 (s, 1H), *9.13 (s, 1H), 7.44 (t, $J = 4.8$ Hz, 1H), 7.08 (s, 1H), 6.90 (s, 1H), *6.56 (t, $J = 5.1$ Hz, 1H), 5.78 (tdd, $J = 16.4, 10.2, 6.2$ Hz, 1H), 5.09-4.95 (m, 2H), 2.42-2.20 (m, 4H); ^{13}C NMR (75 MHz, CDCl_3) δ ppm 177.4, 148.0, 136.5, 115.7, 31.3, 29.9; IR (film) 3417, 3390, 3268, 3211, 3166, 2987, 2919, 1596, 1538, 1535, 1471, 1364, 1284, 1239, 1098, 912, 828 cm^{-1} ; HRMS (EI): Exact mass calculated for $\text{C}_6\text{H}_{11}\text{N}_3\text{S}_1$ $[\text{M}]^+$: 157.0674. Found: 157.0690.

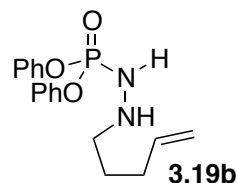
The title compound, obtained after reduction of the thiosemicarbazone, was isolated (0.700 g, 74%) as a white solid using flash chromatography (40-60% EtOAc in hexanes with 1% Et_3N). TLC R_f 0.49 in 10% MeOH in CH_2Cl_2 ; ^1H NMR (300 MHz, CDCl_3) δ ppm 7.80 (s, 1H), 7.10 (s, 1H), 6.36 (s, 1H), 5.77 (tdd, $J = 16.9, 10.1, 6.7$ Hz, 1H), 5.07-4.93 (m, 2H), 3.89 (t, $J = 5.3$ Hz, 1H), 2.91-2.82 (m, 2H), 2.15-2.05 (m, 2H), 1.58 (tt, $J = 7.3$ Hz, 2H); ^{13}C NMR (75 MHz, CDCl_3) δ ppm 182.1, 137.5, 115.4,

51.1, 31.1, 26.6; IR (film) 3412, 3287, 3204, 3169, 3101, 2991, 2934, 2892, 2846, 1637, 1595, 1561, 1459, 1265, 934, 889, 851, 801 cm^{-1} ; HRMS (EI): Exact mass calculated for $\text{C}_6\text{H}_{13}\text{N}_3\text{O}$ $[\text{M}]^+$: 159.0830. Found: 159.0859.



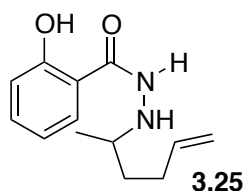
Bis-ethoxyphospho-*N*-(pent-4-enyl)-hydrazide (3.19a).

Synthesized according to **General Procedure C1**. Isolated 1.49 g (72% yield) of **1c** as a yellow oil. TLC R_f 0.69 in 10% MeOH/ CH_2Cl_2 . ^1H NMR (CDCl_3 , 300 MHz) δ ppm 5.78 (tdd, $J = 16.9, 10.2, 6.6\text{ Hz}$, 1H), 5.05-4.91 (m, 2H), 4.48 (d, $J = 30.2\text{ Hz}$, 1H), 4.17-4.02 (m, 4H), 3.24 (s, 1H), 2.83 (t, $J = 7.2\text{ Hz}$, 2H), 2.07 (dd, $J = 14.7, 6.9\text{ Hz}$, 2H), 1.63-1.51 (m, 2H), 1.32 (dt, $J = 7.07, 7.06, 0.60\text{ Hz}$, 6H); ^{13}C NMR (CDCl_3 , 100 MHz) δ ppm 138.0, 114.9, 62.8, 62.7, 53.0, 53.0, 31.1, 26.6, 16.2, 16.2; IR (film); 3473, 3272, 2983, 2914, 2858 cm^{-1} ; HRMS (EI): Exact mass calculated for $\text{C}_9\text{H}_{21}\text{N}_2\text{O}_3\text{P}$ $[\text{M}]^+$: 236.129; found: 236.129.



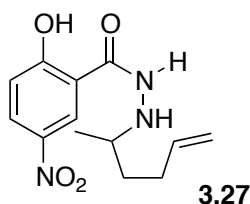
Bis-phenoxyphospho-*N*-(pent-4-enyl)-hydrazide (3.19b).

Synthesized according to **General Procedure C1**. Isolated 0.419 g (82% yield) of **1d** as a white solid. TLC R_f 0.34 in 20% EtOAc/hexanes). ^1H NMR (CDCl_3 , 300 MHz) δ ppm 7.39-7.24 (m, 8H), 7.17 (t, $J = 7.1\text{ Hz}$, 2H), 5.75 (tdd, $J = 16.9, 10.3, 6.7\text{ Hz}$, 1H), 5.03-4.91 (m, 2H), 4.72 (d, $J = 36.1\text{ Hz}$, 1H), 3.50-3.35 (m, 1H), 2.79 (dd, $J = 10.8, 6.6\text{ Hz}$, 2H), 2.06 (q, $J = 6.9, 6.7\text{ Hz}$, 2H), 1.60-1.49 (m, 2H); ^{13}C NMR (CDCl_3 , 100 MHz) δ ppm 138.1, 129.8, 125.1, 120.5, 120.5, 115.2, 53.1, 53.1, 31.1, 26.7; IR (film); 2918, 2850, 1580, 1542, 1470 cm^{-1} ; HRMS (EI): Exact mass calculated for $\text{C}_{11}\text{H}_{21}\text{N}_2\text{O}_3\text{P}$ $[\text{M}]^+$: 332.129; found: 332.126.



***N*-(Hex-5-en-2-yl)-2-hydroxybenzohydrazide (3.25).**

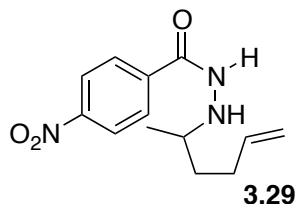
Synthesized according to **General Procedure C1**. The reaction mixture was concentrated under reduced pressure and isolated using flash chromatography (30% EtOAc in hexanes). The title compound was obtained as white solid (3.84 g, 88%). TLC R_f 0.7 in 100% EtOH; ^1H NMR (300 MHz, CDCl_3) δ ppm 7.48-7.31 (m, 2H), 6.99 (d, $J = 8.7$ Hz, 1H), 6.84 (t, $J = 7.6$ Hz, 1H), 5.80 (tdd, $J = 16.8, 10.2, 6.6$ Hz, 1H), 5.10-4.92 (m, 2H), 3.15-3.02 (m, 1H), 2.32-1.97 (m, 2H), 1.74-1.57 (m, 1H), 1.50-1.35 (m, 1H), 1.11 (d, $J = 6.3$ Hz, 3H); ^{13}C NMR (75 MHz, CDCl_3) δ ppm 169.5, 161.0, 138.0, 134.4, 125.2, 118.9, 118.5, 114.9, 113.1, 55.6, 34.0, 30.0, 18.4; IR (film) 3287, 3074, 2975, 2922, 2873, 1641, 1604, 1550, 1482, 1455, 1375, 1309, 1253, 1151, 1102, 1033, 991, 913, 824, 754 cm^{-1} ; HRMS (EI): Exact mass calculated for $\text{C}_{13}\text{H}_{18}\text{N}_2\text{O}_2$ $[\text{M}]^+$: 234.1368. Found: 234.1362.



***N*-(Hex-5-en-2-yl)-2-hydroxy-5-nitrobenzohydrazide (3.27).**

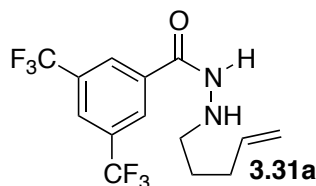
Synthesized according to **General Procedure C2** using 2-hydroxy-5-nitrobenzohydrazide (1.00 g, 4.69 mmol) and 4-penten-2-one (0.598 mL, 5.16 mmol). Isolated 0.595 g (45% yield) of the title compound following silica-gel chromatography (30% EtOAc / hexanes); TLC R_f 0.52 (30% EtOAc/hexanes). ^1H -NMR (300 MHz, CDCl_3): δ ppm 8.42 (d, $J = 2.5$ Hz, 1H), 8.29 (dd, $J = 9.2, 2.6$ Hz, 1H), 7.09 (d, $J = 9.2$ Hz, 1H), 5.83 (ddt, $J = 16.9, 10.2, 6.6$ Hz, 1H), 5.10-4.98 (m, 2H), 3.10 (sextet, $J = 6.4$ Hz, 1H), 2.17 (quintet, $J = 13.6, 6.8$ Hz, 2H), 1.73-1.61 (m, 1H), 1.48 (td, $J = 14.7, 7.0$ Hz, 1H), 1.15 (d, $J = 6.3$ Hz, 3H). ^{13}C NMR (CDCl_3 , 100

MHz): δ ppm 167.9, 166.6, 139.4, 138.0, 129.4, 121.9, 119.5, 115.1, 112.6, 55.8, 34.0, 30.0, 18.5. IR (film): 3290, 3077, 2986, 1649, 1607, 1543, 1485, 1341, 1299, 1275, 1261, 764, 750 cm^{-1} . HRMS (EI): Exact mass calculated for $\text{C}_{13}\text{H}_{17}\text{N}_3\text{O}_4$ $[\text{M}]^+$: 279.12191. Found: 279.11942.



***N*-(Hex-5-en-2-yl)-4-nitrobenzohydrazide (3.29).**

Synthesized according to **General Procedure C2** using 4-nitrobenzohydrazide (1.25 g, 6.90 mmol) and 4-penten-2-one (0.879 mL, 7.59 mmol). Isolated 1.62 g (90% yield) of the title compound following silica-gel chromatography (40% EtOAc / hexanes); TLC R_f 0.49 (50% EtOAc/hexanes). $^1\text{H-NMR}$ (400 MHz, $\text{DMSO-}d_6$): δ ppm 10.30 (s, 1H), 8.32-8.29 (m, 2H), 8.07-8.04 (m, 2H), 5.82 (ddt, $J = 17.0, 10.3, 6.6$ Hz, 1H), 5.08-4.92 (m, 3H), 2.96 (sextet, $J = 6.2$ Hz, 1H), 2.18-2.02 (m, 2H), 1.64-1.55 (m, 1H), 1.38-1.29 (m, 1H), 1.02 (d, $J = 6.3$ Hz, 3H). $^{13}\text{C NMR}$ (CDCl_3 , 100 MHz): δ ppm 163.9, 149.2, 138.9, 138.7, 128.6, 123.6, 114.7, 54.5, 33.7, 29.7, 18.5. IR (film): 3290, 3077, 2979, 2941, 2857, 1640, 1595, 1518, 1352, 1261, 764, 750 cm^{-1} . HRMS (EI): Exact mass calculated for $\text{C}_{13}\text{H}_{17}\text{N}_3\text{O}_3$ $[\text{M}]^+$: 263.12699. Found: 263.12899.

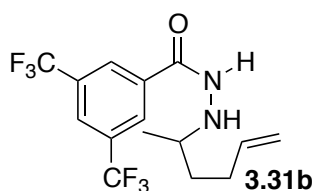


3,5-Bis(trifluoromethyl)-*N*-(pent-4-enyl)benzohydrazide (3.31a).

The hydrazide was synthesized according to **General Procedure C2** from 4-pentenal⁷ (2.76 mmol) and using 3,5-bistrifluoromethylbenzohydrazide (0.500 g, 1.84

⁷. The 4-pentanal used was synthesized in a previous step through a Swern or Parikh-Doering oxidation from the respective alcohol, and used as an unpurified reaction mixture. Some examples

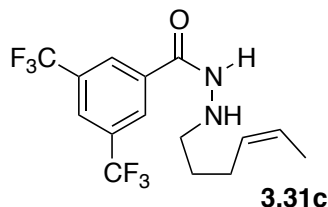
mmol). The compound was obtained as a white solid (0.225 g, 36% yield). TLC R_f 0.41 (20% EtOAc/Hexanes); ^1H NMR (300 MHz, CDCl_3) δ ppm 8.23 (s, 2H), 8.06-7.99 (m, 1H), 5.81 (tdd, $J = 16.9, 10.2, 6.7$ Hz, 1H), 5.11-4.94 (m, 2H), 3.00 (t, $J = 7.3$ Hz, 2H), 2.22-2.09 (m, 2H), 1.75-1.57 (m, 2H); ^{13}C NMR (100 MHz, CDCl_3) δ ppm 164.5, 137.8, 134.8, 132.4 (q, $J = 34.0$ Hz, 1), 127.3, 125.4, 122.8 (q, $J = 273.0$ Hz, 1), 115.2, 51.7, 31.1, 27.1; IR (film) 3245, 3085, 2941, 2861, 1641, 1545, 1449, 1382, 1279, 1129, 908, 699, 680 cm^{-1} ; HRMS (EI): Exact mass calculated for $\text{C}_{14}\text{H}_{14}\text{F}_6\text{N}_2\text{O}$ $[\text{M}]^+$: 354.1010. Found 354.0995



3,5-Bis(trifluoromethyl)-*N*-(hex-5-en-2-yl)benzohydrazide (3.31b).

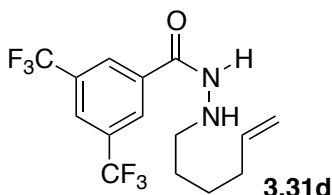
Synthesized according to General Procedure C2 using 3,5-bistrifluoromethylbenzohydrazide (2.00 g, 7.34 mmol) and 5-hexen-2-one (1.21 mL, 10.3 mmol). Isolated 2.08 g (80% yield); TLC R_f 0.79 (40% EtOAc/hexanes). ^1H -NMR (400 MHz; CDCl_3): δ ppm 8.21 (s, 2H), 8.00 (s, 1H), 5.79 (ddt, $J = 17.0, 10.3, 6.7$ Hz, 1H), 5.05-4.94 (m, 2H), 3.09 (sextet, $J = 6.4$ Hz, 1H), 2.22-2.04 (m, 2H), 1.69-1.60 (m, 1H), 1.43 (dddd, $J = 13.5, 9.2, 7.4, 6.2$ Hz, 1H), 1.11 (d, $J = 6.3$ Hz, 3H). ^{13}C NMR (CDCl_3 , 400 MHz): δ ppm 164.5, 138.0, 134.8, 132.3 (q, $J = 34.2$ Hz, CCF_3), 127.3, 125.4, 122.8 (q, $J = 273$ Hz, CF_3), 115.0, 55.7, 34.0, 30.0, 18.4. IR (film): 3271, 3089, 2982, 2937, 1641, 1546, 1443, 1275, 1261, 1135, 907, 764, 750 cm^{-1} . HRMS (EI): Exact mass calculated for $\text{C}_{15}\text{H}_{16}\text{F}_6\text{N}_2\text{O}$ $[\text{M}]^+$: 354.11668. Found: 354.11556.

of procedures can be found in previous publications, as outlined in the **starting materials** section of this supporting information. The quantity of aldehyde included in the condensation with hydrazides assumes a quantitative conversion.



3,5-Bis(trifluoromethyl)-*N*-((*Z*)-hex-4-enyl)benzohydrazide (3.31c).

The hydrazide was synthesized according to **General Procedure C2** from *cis*-hex-4-enal⁸ (4.13 mmol) and using 3,5-bistrifluoromethylbenzohydrazide (0.750 g, 2.76 mmol). The reaction mixture was concentrated under reduced pressure and isolated using flash chromatography (15% EtOAc/Hexanes). The compound was obtained as a white solid (0.931 g, 36% yield). TLC R_f 0.40 (30% EtOAc/Hexanes); ¹H NMR (400 MHz, CDCl₃): δ ppm 8.24 (s, 2H), 8.02 (s, 1H), 5.64-5.21 (m, 2H), 2.97 (t, $J = 7.3$ Hz, 2H), 2.25-2.01 (m, 2H), 1.66-1.55 (m, 5H); ¹³C NMR (100 MHz, CDCl₃) δ ppm 164.4, 134.8, 132.3 (q, $J = 34.0$ Hz, 129.4, 127.3, 125.3, 124.8, 122.8 (q, $J = 272.9$ Hz, 51.8, 27.8, 24.2, 12.7; IR (film) 3274, 3092, 3017, 2940, 2866, 1661, 1455, 1367, 1334, 1131, 928, 908, 848, 770, 696 cm⁻¹; HRMS (EI): Exact mass calculated for C₁₅H₁₆F₆N₂O [M]⁺: 354.1167. Found : 354.1187

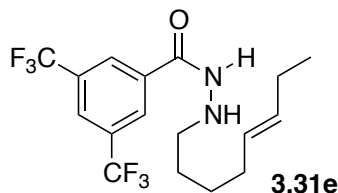


3,5-Bis(trifluoromethyl)-*N*-(hex-5-enyl)benzohydrazide (3.31d).

The hydrazide was synthesized according to **General Procedure C2** from hex-5-enal⁸ (2.40 mmol), using 3,5-bistrifluoromethylbenzohydrazide (0.384 g, 1.41 mmol). The reaction mixture was concentrated under reduced pressure and isolated using flash chromatography (20% EtOAc/Hexanes). The title compound was obtained as a

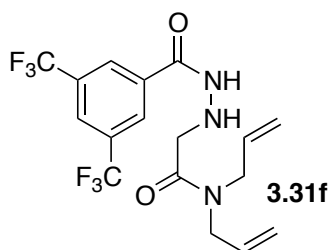
⁸. The *cis*-hex-4-enal, hex-5-enal and *trans*-oct-5-enal used were synthesized in previous steps through a Swern or Parikh-Doering oxidation of the respective alcohols, and used as unpurified reaction mixtures. Some examples of procedures can be found in previous publications,^{3,5} as outlined in the **starting materials** section of this supporting information. The amount of aldehyde included in the condensation with hydrazides assumes a quantitative conversion.

white solid (0.203 g, 57% yield). TLC R_f 0.38 in (30% EtOAc/Hexanes); ^1H NMR (400 MHz, CDCl_3) δ ppm 8.26 (d, $J = 12.0$ Hz, 2H), 8.03 (s, 1H), 5.80 (tdd, $J = 16.9, 10.1, 6.7$ Hz, 1H), 5.02 (ddd, $J = 17.1, 3.5, 1.6$ Hz, 1H), 4.96 (tdd, $J = 10.2, 2.1, 1.2, 1.2$ Hz, 1H), 3.03 (t, $J = 7.2$ Hz, 2H), 2.14-2.05 (m, 2H), 1.66-1.55 (m, 2H), 1.55-1.44 (m, 2H); ^{13}C NMR (100 MHz, CDCl_3) δ ppm 164.4, 138.3, 134.7, 132.4 (d, $J = 34.0$ Hz, CCF_3), 127.3, 125.5, 122.8 (d, $J = 272.98$ Hz, CF_3), 114.9, 52.1, 33.4, 27.1, 26.1; IR (film) 3265, 3083, 2936, 2862, 1827, 1646, 1616, 1544, 1452, 1379, 1334, 1283, 1141, 909, 847, 778, 703, 678 cm^{-1} ; HRMS (EI): Exact mass calculated for $\text{C}_{15}\text{H}_{16}\text{F}_6\text{N}_2\text{O}$ $[\text{M}]^+$: 354.1167 Found : 354.1167



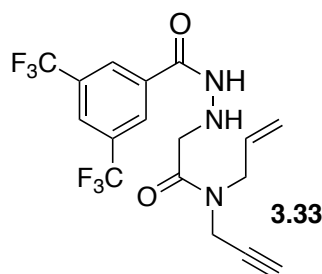
3,5-Bis(trifluoromethyl)-*N*-((*E*)-oct-5-enyl)benzohydrazide (3.31e).

Synthesized according to general procedure **General Procedure C1**, using 3,5-bistrifluoromethylbenzohydrazide (1.25 g, 4.63 mmol) and *trans*-oct-5-enal (7.84 mmol).⁸ The reaction mixture was concentrated under reduced pressure. The title compound was isolated as a white solid (1.27 g, 72% yield) following flash chromatography (15% EtOAc/Hexanes). The reaction mixture was concentrated under reduced pressure and isolated using flash chromatography (5% MeOH/DCM), TLC R_f 0.39 in 5% MeOH/ CH_2Cl_2 . ^1H NMR (CDCl_3 , 300 MHz) δ ppm ^1H NMR (300 MHz, CDCl_3) δ ppm 8.24 (s, 2H), 8.02 (s, 1H), 5.33 (ddt, $J = 17.8, 10.8, 7.0$ Hz, 2H), 2.97 (t, $J = 7.0$ Hz, 2H), 2.10-1.95 (m, 4H), 1.62-1.50 (m, 2H), 1.48-1.36 (m, 2H), 0.93 (t, $J = 7.5$ Hz, 3H); ^{13}C NMR (CDCl_3 , 100 MHz) δ ppm *denotes minor traces of isomers 164.4, 134.9, 132.3 (q, $J = 33.9$ Hz, 2C), 132.2, 128.4, 127.3, *124.6, 121.0, 52.1, 27.5, 27.1, 26.8, 20.5, 14.3; IR (film) 3443, 2097, 1653 cm^{-1} ; HRMS (EI): Exact mass calculated for $\text{C}_{17}\text{H}_{20}\text{F}_6\text{N}_2\text{O}$ $[\text{M}]^+$: 382.148; found: 382.1488.



2-(2-([3,5-bis(trifluoromethyl)phenyl]carbonyl)hydrazinyl)-N,N-di(prop-2-en-1-yl)acetamide. (3.31f)

N,N-diallyl-2-iodoacetamide (150 mg, 0.566 mmol, 1 equiv), 3,5-bis(trifluoromethyl)benzohydrazide (0.77 g, 2.03 mmol, 5 equiv) and dimethylformamide (2 mL) were mixed together in a round balloon flask at room temperature for 5h. 15 mL of ethyl acetate was added and the reaction mixture was washed five times with 4 mL of a (1 : 1) H₂O/Brine solution. The organic layer was then dried with sodium sulfate, filtered, concentrated under reduced pressure and isolated using flash chromatography (4% methanol in dichloromethane). The compound was obtained as a white solid (180 mg, 78% yield). TLC R_f 0.38 (4% methanol in dichloromethane); ¹H NMR (400 MHz, CDCl₃) δ ppm 8.22 (s, 2H), 8.01 (s, 1H), 5.81-5.68 (m, 2H), 5.27-5.12 (m, 4H), 4.06-4.00 (m, 2H), 3.86-3.78 (m, 4H). ¹³C NMR (CDCl₃, 400 MHz) δ ppm 170.2 (C), 163.9 (C), 135.1 (C), 132.3 (CH), 132.1 (q, *J* = 34 Hz, C), 131.8 (CH), 127.7 (CH), 125.2 (CH), 124.2 (q, *J* = 273 Hz, C), 118.1 (CH₂), 117.4 (CH₂), 51.9 (CH₂), 48.5 (CH₂), 48.3 (CH₂); IR (film) 3320, 3255, 3090, 2916, 1657, 1539, 1453, 1282, 989, 930, 907, 772, 700 cm⁻¹; HRMS (EI): Exact mass calcd for C₁₇H₁₇F₆N₃O₂ [M]⁺: 409.1225 Not found. Exact mass calcd for C₈H₁₃N₂O [M – C₉H₄F₆NO]: 153.1028. Found: 153.1025.

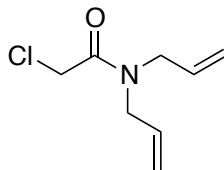


2-(2-([3,5-bis(trifluoromethyl)phenyl]carbonyl)hydrazinyl)-N-(prop-2-en-1-yl)-N-

(prop-2-yn-1-yl)acetamide (3.33)

2-iodo-*N*-(prop-2-en-1-yl)-*N*-(prop-2-yn-1-yl)acetamide (100 mg, 0.380 mmol, 1 equiv), 3,5-bis(trifluoromethyl)benzohydrazide (207 mg, 0.760 mmol, 2 equiv) and dimethylformamide (2.5 mL) were mixed together in a round balloon flask at room temperature for 5h. 25 mL of ethyl acetate was added and the reaction mixture was washed five times with 6 mL of a (1 : 1) H₂O/Brine solution. The organic layer was then dried with sodium sulfate, filtered, concentrated under reduced pressure and isolated using flash chromatography (3% methanol in dichloromethane). The compound was obtained as an orange solid (146 mg, 97% yield). TLC R_f 0.28 (3% methanol in dichloromethane); ¹H NMR (400 MHz, CDCl₃) δ ppm 9.26-9.08 (m, 1H), 8.49-8.19 (m, 2H), 8.00 (s, 1H), 5.87-5.62 (m, 1H), 5.30-5.16 (m, 2H), 5.16-4.99 (br s, 1H), 4.22 (d, *J* = 2.48 Hz, 1H), 4.09 (d, *J* = 6.13 Hz, 1H), 4.03- 3.90 (m, 2H), 3.85 (s, 1H), 2.25 (td, *J* = 30.49, 2.41, 2.41 Hz, 1H); ¹³C NMR (100 MHz, CDCl₃) δ ppm 168.8 (C), 162.2 (C), 135.2 (C), 133.1 (CH), 132.9 (C), 130.4 (q, *J* = 34 Hz, C), 128.1 (CH'), 127.9 (CH), 124.9 (CH), 123.0 (q, *J* = 273 Hz, C), 117.3 (CH₂'), 116.7 (CH₂), 79.6 (CH'), 79.3 (CH); IR (film) 3264, 3087, 2930, 1661, 1559, 1461, 1379, 1333, 1274, 1173, 1134, 937, 699, 679 cm⁻¹; HRMS (EI): Exact mass calcd for C₁₇H₁₅F₆N₃O₂ [M]⁺: 407.1068 Not found. Exact mass calcd for C₈H₁₁N₂O [M – C₉H₄F₆NO]: 151.0871. Found: 151.0872.

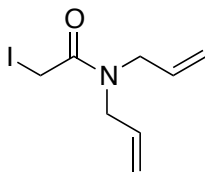
◆ SYNTHESIS OF PRECURSORS TO 3.31F AND 3.33



***N,N*-diallyl-2-chloroacetamide.**

Diallylamine (3.04 g, 31.3 mmol, 1 equiv), triethylamine (3.20 g, 31.6 mmol, 1.01 equiv) and dichloromethane (100 mL) were added together in a round balloon flask at 0 °C. A solution of chloroacetyl chloride (3.55 g, 31.3 mmol, 1 equiv) in

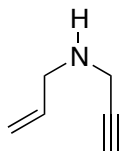
dichloromethane (100 mL) was added dropwise to the reaction mixture. The reaction was left to stir at 0 °C for 75 min. The reaction mixture was washed three times with 100 mL of a saturated solution of sodium bicarbonate. The organic layer was then dried with sodium sulfate, filtered, concentrated under reduced pressure and isolated using flash chromatography (20% ethyl acetate in hexanes). The compound was obtained as an orange oil (5.22 g, 96% yield). TLC R_f 0.66 (40% EtOAc in hexanes); ^1H NMR (CDCl_3 , 400 MHz) δ ppm 5.87-5.70 (m, 2H), 5.28-5.13 (m, 4H), 4.06 (s, 2H), 4.03-3.98 (m, 2H), 3.98-3.94 (m, 2H). ^{13}C NMR (CDCl_3 , 400 MHz) δ ppm 166.6 (C), 132.5 (CH), 132.2 (CH), 117.8 (CH_2), 117.3 (CH_2), 49.5 (CH_2), 48.3 (CH_2), 41.1 (CH_3); IR (film) 3084, 2989, 2915, 1658, 1455, 1415, 1221, 1128, 993, 925, 793, 663 cm^{-1} ; HRMS (EI): Exact mass calcd for $\text{C}_8\text{H}_{12}\text{ClNO}$ $[\text{M}]^+$: 173.0607 Not found. Exact mass calcd for $\text{C}_8\text{H}_{12}\text{NO}$ $[\text{M} - \text{Cl}]$: 138.0919. Found: 139.0915.



***N,N*-diallyl-2-iodoacetamide.**

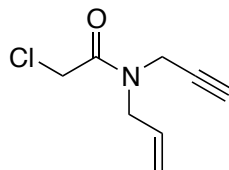
N,N-diallyl-2-chloroacetamide (2.5 g, 14.4 mmol, 1 equiv), sodium iodide (21.6 g, 144 mmol, 10 equiv) and acetone (144 mL) were mixed together in a round balloon flask at room temperature for 20h. 450 mL of ethyl acetate was added and the reaction mixture was washed three times with 100 mL of a (1 : 1) H_2O /Brine solution. The organic layer was then dried with sodium sulfate, filtered, concentrated under reduced pressure and isolated using flash chromatography (30% ethyl acetate in hexanes). The compound was obtained as a yellow oil (3.64 g, 95% yield). TLC R_f 0.29 (25% EtOAc in hexanes); ^1H NMR (CDCl_3 , 300 MHz) δ ppm 5.88-5.70 (m, 2H), 5.24-5.12 (m, 4H), 3.99-3.94 (m, 2H), 3.93-3.89 (m, 2H), 3.71-3.68 (m, 2H). ^{13}C NMR (CDCl_3 , 400 MHz) δ ppm 168.1 (C), 132.4 (CH), 132.1 (CH), 117.4 (CH_2), 116.9 (CH_2), 50.6 (CH_2), 48.2 (CH_2), -3.6 (CH_2); IR (film) 3081, 2983, 2919, 1638,

1450, 1251, 1184, 993, 920 cm^{-1} ; HRMS (EI): Exact mass calcd for $\text{C}_8\text{H}_{12}\text{INO}$ $[\text{M}]^+$: 264.9964 Found : 264.9961.



***N*-(prop-2-yn-1-yl)prop-2-en-1-amine.**

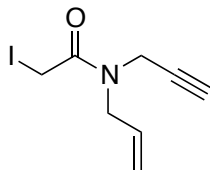
Allylamine (6.85 g, 120 mmol, 3 equiv) and H_2O (4.6 mL) were mixed together in a round balloon flask at $0\text{ }^\circ\text{C}$ for 5 min. Then, propargyl bromide (5.95 g, 40 mmol, 1 equiv) was added dropwise over 60 min. The reaction was then stirred at room temperature for 20h. 15 mL of a (1 : 1) H_2O /Brine solution. The reaction mixture was extracted three times with 12 mL of diethylether. The reaction was then purified by distillation of the impurities at $86\text{ }^\circ\text{C}$ under atmospheric pressure. The compound was obtained as a (1 : 1) mixture of *N*-(prop-2-yn-1-yl)prop-2-en-1-amine (0.797 g, 21% yield) and *N*-(prop-2-yn-1-yl)prop-2-en-1-amine (1.12 g, 21% yield) and was used as is for the next reaction.



2-chloro-*N*-(prop-2-en-1-yl)-*N*-(prop-2-yn-1-yl)acetamide.

N-(prop-2-yn-1-yl)prop-2-en-1-amine (0.797 g, 8.34 mmol, 1 equiv), triethylamine (0.854 g, 8.44 mmol, 1.02 equiv) and dichloromethane (25 mL) were added together in a round balloon flask at $0\text{ }^\circ\text{C}$. A solution of Chloroacetyl chloride (1.14 g, 10.1 mmol, 1.2 equiv) in dichloromethane (25 mL) was added dropwise to the reaction mixture. The reaction was left to stir at $0\text{ }^\circ\text{C}$ for 75 min. The reaction mixture was washed three times with 25 mL of a saturated solution of sodium bicarbonate. The organic layer was then dried with sodium sulfate, filtered, concentrated under reduced pressure and isolated using flash chromatography (20% ethyl acetate in

hexanes). The compound was obtained as an orange oil (1.36 g, 95% yield). TLC R_f 0.27 (20% EtOAc in hexanes); ^1H NMR (400 MHz, CDCl_3) δ ppm 5.91-5.69 (m, 1H), 5.33-5.19 (m, 2H), 4.26-4.16 (m, 2H), 4.14-4.07 (m, 4H), 2.38-2.19 (m, 1H). ^{13}C NMR (CDCl_3 , 400 MHz) δ ppm 166.3 (d, $J = 10$ Hz, C), 131.9 (d, $J = 14$ Hz, CH), 118.4 (d, $J = 48$ Hz, CH_2), (d, $J = 27$ Hz, C), 72.8 (d, $J = 89$ Hz, CH), 48.9 (d, $J = 116$ Hz, CH), 41.1 (d, $J = 17$ Hz, CH_2), 35.7 (d, $J = 181$ Hz, CH_2); IR (film) 3296, 3086, 2985, 2949, 1666, 1458, 1348, 1279, 1215, 1179, 1144, 995, 923, 797, 677, 560 cm^{-1} ; HRMS (EI): Exact mass calcd for $\text{C}_8\text{H}_{10}\text{ClNO}$ $[\text{M}]^+$: 171.0451 Found: 171.0422.



2-iodo-*N*-(prop-2-en-1-yl)-*N*-(prop-2-yn-1-yl)acetamide.

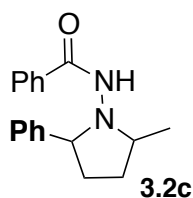
2-chloro-*N*-(prop-2-en-1-yl)-*N*-(prop-2-yn-1-yl)acetamide (1.38 g, 8.01 mmol, 1 equiv), sodium iodide (12 g, 80.1 mmol, 10 equiv) and acetone (80 mL) were mixed together in a round balloon flask at room temperature for 20h. 240 mL of ethyl acetate was added and the reaction mixture was washed three times with 100 mL of a (1 : 1) H_2O /Brine solution. The organic layer was then dried with sodium sulfate, filtered, concentrated under reduced pressure and isolated using flash chromatography (25% ethyl acetate in hexanes). The compound was obtained as a yellow oil (1.24 g, 59% yield). TLC R_f 0.40 (50% EtOAc in hexanes); ^1H NMR (CDCl_3 , 400 MHz) δ ppm 5.94-5.70 (m, 1H), 5.31-5.20 (m, 2H), 4.25-4.18 (m, 1H), 4.11-4.04 (m, 3H), 3.79 (d, $J = 42.02$ Hz, 1H), 2.28 (td, $J = 37.70, 2.48, 2.48$ Hz, 1H). ^{13}C NMR (CDCl_3 , 400 MHz) δ ppm 167.8 (d, $J = 4$ Hz, C), 131.8 (d, $J = 11$ Hz, CH), 118.1 (d, $J = 36$ Hz, CH_2), 77.9 (d, $J = 20$ Hz, C), 72.8 (d, $J = 87$ Hz, CH), 49.5 (d, $J = 233$ Hz, CH_2), 36.3 (d, $J = 256$ Hz, CH_2), -4.0 (d, $J = 21$ Hz, CH_2); IR (film) 3293, 3241, 2986, 1646, 1447, 1408, 1349, 1248, 1182, 1094, 1025, 927, 669 cm^{-1} ; HRMS (EI): Exact mass calcd for $\text{C}_8\text{H}_{10}\text{INO}$ $[\text{M}]^+$: 262.9807 Found: 262.9797.

◆ SCOPE EXPANSION OF INTRAMOLECULAR HYDROAMINATION – KEY STEPS

General Procedure D for Intramolecular Hydrohydrazidation

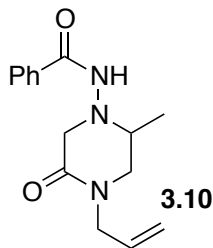
General Procedure D1: Microwave: The corresponding hydrazide and α,α,α -trifluorotoluene (such that the concentration of the hydrazide was 0.05 M) were added to a Biotage Initiator microwave vial (0.5, 2, 5 or 20 mL), while keeping it under an argon atmosphere. The septum was removed and the tube was then quickly sealed with a microwave cap and heated in a Biotage Initiator microwave for 10-16 hours at 70 °C to 195 °C. The tube was cooled to ambient temperature, concentrated under reduced pressure and analyzed by ^1H NMR using 1,4-dimethoxybenzene as an internal standard, then again concentrated under reduced pressure and purified by silica gel chromatography to give the corresponding hydrohydrazidation products.

General Procedure D2: Standard Heating: The corresponding hydrazide and α,α,α -trifluorotoluene (such that the concentration of the hydrazide was 0.05 M) were added to a Biotage Initiator microwave vial (0.5, 2, 5 or 20 mL), while keeping it under an argon atmosphere. The septum was removed and the tube was then quickly sealed with a microwave cap and heated in a wax bath with constant stirring for 18-40 hours at 70 °C to 195 °C. The tube was cooled to ambient temperature, concentrated under reduced pressure and analyzed by ^1H NMR using 1,4-dimethoxybenzene as an internal standard, then again concentrated under reduced pressure and purified by silica gel chromatography to give the corresponding hydrohydrazidation products.



***N*-(2-Methyl-5-phenylpyrrolidin-1-yl)benzamide. 3.2c**

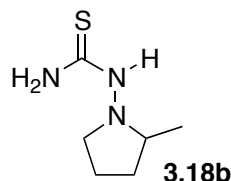
Synthesised according to general procedure A (120 °C, 10h) using *N'*-(1-phenylpent-4-enyl)benzohydrazide (77.1 mg, 0.275 mmol, 1 equiv). The reaction mixture was concentrated under reduced pressure and isolated using flash chromatography (25% ethyl acetate in hexanes). The compound was obtained as a brown solid (50.9 mg, 66% yield). TLC R_f 0.27 40% EtOAc in hexanes; ^1H NMR (400 MHz, CDCl_3) δ ppm 7.49-7.27 (m, 10H), 6.29 (br s, 1H), 4.56-4.45 (m, 1H), 3.48-3.31 (m, 1H), 2.52-2.39 (m, 1H), 2.34-2.20 (m, 1H), 2.08-1.95 (m, 1H), 1.83-1.69 (m, 1H) 1.19 (d, $J = 6.21$ Hz, 3H); ^{13}C NMR (100 MHz, CDCl_3) δ ppm 166.4 (C), 140.0 (C), 134.0 (C), 131.3 (CH), 128.6 (CH), 128.4 (CH), 128.3 (CH), 127.8 (CH), 126.8 (CH), 66.5 (CH), 58.3 (CH), 29.8 (CH_2), 29.2 (CH_2), 17.3 (CH_3); IR (film) 3243, 3063, 3032, 2965, 2873, 1645, 1579, 1546, 1492, 1291, 1149, 1028, 906, 801, 754, 699 cm^{-1} ; HRMS (EI): Exact mass calcd for $\text{C}_{18}\text{H}_{20}\text{N}_2\text{O}$ $[\text{M}]^+$: 280.1576 Found : 280.1593



2-[2-(phenylcarbonyl)hydrazinyl]-*N,N*-di(prop-2-en-1-yl)acetamide. (3.10)

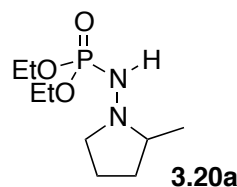
N,N-diallyl-2-iodoacetamide (250 mg, 0.943 mmol, 1 equiv), 3,5-bis(trifluoromethyl)benzohydrazide (0.623 g, 4.72 mmol, 5 equiv) and dimethylformamide (4.7 mL) were mixed together in a round balloon flask at room temperature for 4.5 h. 30 mL of ethyl acetate was added and the reaction mixture was washed five times with 8 mL of a (1 : 1) H_2O /Brine solution. The organic layer was then dried with sodium sulfate, filtered, concentrated under reduced pressure and isolated using flash chromatography (8% methanol in dichloromethane). The compound was obtained as a yellow oil (213 mg, 83% yield). TLC R_f 0.51 (8% methanol in dichloromethane); ^1H NMR (Benzene- d_6 , 300 MHz) δ ppm 8.65-8.43 (m, 1H), 7.80-7.70 (m, 2H), 7.07-6.92 (m, 3H), 5.66-5.46 (m, 1H), 5.44-5.29 (m, 1H), 5.21-5.04 (m, 1H), 4.95-4.62 (m, 4H), 3.83 (d, $J = 5.99$ Hz, 1H), 3.43 (s, 1H), 3.06 (d,

$J = 4.88$ Hz, 1H) cm^{-1} . ^{13}C NMR (CDCl_3 , 300 MHz) δ ppm 170.3 (C), 166.6 (C), 133.0 (C), 132.6 (CH), 131.9 (CH), 131.8 (CH), 128.6 (CH), 127.0 (CH), 118.0 (CH_2), 117.4 (CH_2) 52.1 (CH_2), 48.4 (CH_2), 48.2 (CH_2) cm^{-1} ; IR (film) 3289, 3072, 2983, 2919, 1654, 1533, 1459, 1416, 1285, 1228, 993, 926, 691 cm^{-1} ; HRMS (EI): Exact mass calcd for $\text{C}_{15}\text{H}_{19}\text{N}_3\text{O}_2$ $[\text{M}]^+$: 273.1477 Not found. Exact mass calcd for $\text{C}_8\text{H}_{13}\text{N}_2\text{O}$ $[\text{M} - \text{C}_7\text{H}_6\text{NO}]$: 153.1028. Found: 153.1039



1-(2-Methylpyrrolidin-1-yl)thiourea (3.18b).

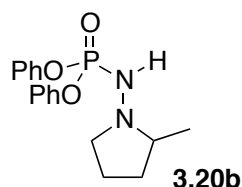
Synthesized according to **General Procedure D1** using 1-(pent-4-enyl)thiosemicarbazide (**3.17b**) (0.0580 g, 0.364 mmol) and heated at 150 °C for 16 h. Isolated 0.0477 g (82% yield) of the title compound as a white solid after column chromatography (40% EtOAc/hexanes). TLC R_f 0.35 (60% EtOAc/hexanes). ^1H -NMR (300 MHz; CDCl_3): δ ppm 7.80 (s, 1H), 7.09 (s, 1H), 6.36 (s, 1H), 5.84-5.70 (m, 1H), 5.05-4.96 (m, 2H), 3.89 (t, $J = 5.3$ Hz, 1H), 2.90-2.83 (m, 2H), 2.10 (q, $J = 7.2$ Hz, 2H), 1.60 (q, $J = 7.3$ Hz, 2H). ^{13}C NMR (CDCl_3 , 75 MHz): δ ppm 182.1, 137.5, 115.4, 51.1, 31.1, 26.6. IR (film): 3412, 3287, 3203, 3169, 3100, 2990, 2933, 2846, 1595, 1561, 1458, 1265, 934 cm^{-1} . HRMS (EI): Exact mass calculated for $\text{C}_6\text{H}_{13}\text{N}_3\text{S}$ $[\text{M}]^+$: 159.083. Found: 159.08591.



1-(2-Methylpyrrolidin-1-yl)-bis-ethoxyphospho hydrazide (3.20a).

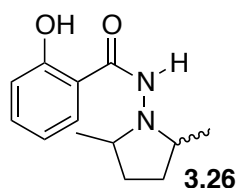
Synthesized according to **General Procedure D1** (120 °C, 24 h) on 0.252 mmol of bisethoxyphospho-*N'*-(pent-4-enyl)-hydrazide (**3.19a**). Isolated 0.0584 g (98% yield) as a yellow oil and purified over column chromatography (6% MeOH/ CH_2Cl_2). TLC

R_f 0.64 (7.5% MeOH/CH₂Cl₂). ¹H NMR (CDCl₃, 300 MHz) δ ppm 4.24-4.00 (m, 4H), 3.58 (d, J = 29.8 Hz, 1H), 3.39 (dt, J = 8.5, 3.0 Hz, 1H), 2.50-2.39 (m, 1H), 2.36 (dd, J = 18.1, 9.0 Hz, 1H), 1.97-1.82 (m, 1H), 1.82-1.59 (m, 2H), 1.50-1.35 (m, 1H), 1.33 (t, J = 7.1 Hz, 6H), 1.15 (d, J = 6.1 Hz, 3H); ¹³C NMR (CDCl₃, 100 MHz) δ ppm 63.8, 63.1, 63.0, 30.0, 19.9, 18.1, 16.4, 16.4, 16.4, 16.3; IR (film) 3488, 3184, 2976, 1645, 1444, 1394, 1231, 1036 cm⁻¹; HRMS (EI): Exact mass calculated for C₉H₂₁N₂O₃P[M]⁺: 236.1290; found: 236.1290.



1-(2-Methylpyrrolidin-1-yl)-bis-phenoxyphospho hydrazide (3.20b).

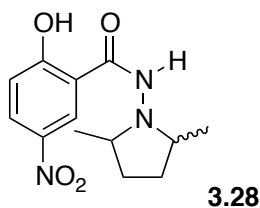
Synthesized according to **General Procedure D1** (110 °C, 18 h) on 0.250 mmol of bisphenoxyphospho-*N*-(pent-4-enyl)-hydrazide (**3.19b**). Isolated 0.0837 g (99% yield) as a white solid. TLC R_f 0.92 (10% MeOH/CH₂Cl₂). ¹H NMR (DMSO-*d*₆, 300 MHz, 120 °C) δ ppm 7.36-7.23 (m, 8H), 7.20-7.10 (m, 2H), 4.26 (br s, 1H), 3.44-3.21 (m, 1H), 2.90-2.22 (m, 2H), 2.02-1.59 (m, 3H), 1.56-1.37 (m, 1H), 1.10 (d, J = 6.0 Hz, 3H). ¹³C NMR (CDCl₃, 100 MHz) δ ppm 129.8, 129.7, 125.0, 124.9, 120.3, 64.1, 64.0, 58.5, 30.1, 20.0. Exact mass calculated for C₁₇H₂₁N₂O₃P [M]⁺: 332.1290. Found: 332.1297.



(±)-2-Hydroxy-*N*-((2*R*,5*S*)-2,5-dimethylpyrrolidin-1-yl)benzamide and (±)-2-hydroxy-*N*-((2*R*,5*R*)-2,5-dimethylpyrrolidin-1-yl)benzamide (3.26)

Synthesized according to **General Procedure D2** (90 °C, 16 h) using 2-hydroxybenzohydrazide (0.207 g, 0.883 mmol). The reaction mixture was concentrated under reduced pressure and isolated using flash chromatography (20

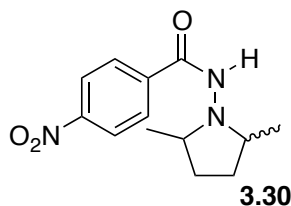
to 40% EtOAc/Hexanes). The title compounds were obtained as brown oils (0.036 g and 0.144 g, 87% yield, 1:4 syn:anti). **3.26-anti**: TLC R_f 0.4 in (40% EtOAc/Hexanes); ^1H NMR (300 MHz, CDCl_3)^{*} denotes minor rotomer δ ppm *12.56 (s, 1H), 12.15 (s, 1H), 7.48-7.31 (m, 2H), 7.01 (d, $J = 8.3$ Hz, 1H), 6.85 (t, $J = 7.7$ Hz, 2H), 6.57 (s, 1H), *3.54 (s, 1H), 2.83 (dd, $J = 11.3, 5.9$ Hz, 2H), *2.68-2.56 (m, 2H), 2.41-2.29 (m, 2H), 2.02-1.90 (m, 2H), 1.69-1.51 (m, 2H), *1.43-1.32 (m, 2H), 1.19 (d, $J = 6.1$ Hz, 6H); ^{13}C NMR (75 MHz, $\text{DMSO}-d_6$) δ ppm 168.6, 159.7, 133.4, 127.5, 118.4, 117.2, 115.0, 59.9, 28.4, 18.8; IR (film) 3295, 3067, 2968, 2930, 2873, 2705, 2588, 1637, 1603, 1550, 1493, 1455, 1371, 1311, 1238, 1151, 1098, 1037, 908, 752 cm^{-1} ; HRMS (EI): Exact mass calculated for $\text{C}_{13}\text{H}_{18}\text{N}_2\text{O}$ $[\text{M}]^+$: 234.1368. Found: 234.1377. **3.26-syn**: TLC R_f 0.11 in (40% EtOAc/Hexanes); ^1H NMR (300 MHz, $\text{DMSO}-d_6$)^{*} denotes minor rotomer δ ppm *12.40 (s, 1H), 12.10 (s, 1H), *7.94 (d, $J = 7.6$ Hz, 1H), 7.47-7.30 (m, 1H), 6.99 (d, $J = 8.5$ Hz, 1H), 6.94-6.77 (m, 2H), *4.04-3.79 (m, 1H), *3.71-3.49 (m, 1H), 3.44-3.26 (m, 2H), *2.44-2.21 (m, 2H), 2.20-2.04 (m, 2H), 1.62-1.44 (m, 2H), *1.44-1.27 (m, 1H), *1.26-1.21 (m, 6H), 1.10 (d, $J = 6.4$ Hz, 6H); ^{13}C NMR (75 MHz, $\text{DMSO}-d_6$) δ ppm 167.2, 159.2, 133.2, 127.9, 118.5, 117.1, 115.3, 55.7, 28.9, 17.1; IR (film) 3295, 3067, 2968, 2930, 2873, 2705, 2588, 1637, 1603, 1550, 1493, 1455, 1371, 1311, 1238, 1151, 1098, 1037, 908, 752 cm^{-1} ; HRMS (EI): Exact mass calculated for $\text{C}_{13}\text{H}_{18}\text{N}_2\text{O}_2$ $[\text{M}]^+$: 234.1368. Found: 234.1377.



(±)-2-Hydroxy-5-nitro-*N*-((2*R*,5*S*)-2,5-dimethylpyrrolidin-1-yl)benzamide and (±)-2-hydroxy-5-nitro-*N*-((2*R*,5*R*)-2,5-dimethylpyrrolidin-1-yl)benzamide (3.28).

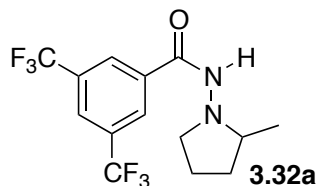
Synthesized according to **General Procedure D2** (90 °C, 18 h) using *N*-(hex-5-en-2-yl)-2-hydroxy-5-nitrobenzohydrazide (0.035 g, 0.13 mmol). The reaction mixture was concentrated under reduced pressure and isolated using flash chromatography (55-70% EtOAc/Hexanes). The compound was obtained as a white solid (0.030 g,

88% yield, obtained as a mixture of diastereoisomers, 3.2:1 anti:syn). **Major product:** TLC R_f 0.20 in (50% EtOAc/Hexanes); ^1H NMR (300 MHz, $\text{DMSO-}d_6$, 120 $^\circ\text{C}$): δ ppm 8.75 (s, 1H), 8.16 (d, $J = 8.7$, 1H), 7.00 (d, $J = 9.1$, 1H), 3.69-3.54 (m, 2H), 2.20-2.05 (m, 2H), 1.64-1.49 (m, 2H), 1.15 (d, $J = 6.3$, 7H). ^{13}C NMR (75 MHz, $\text{DMSO-}d_6$, 120 $^\circ\text{C}$): δ ppm 165.9, 139.4, 127.8, 125.3, 118.3, 60.2, 29.6, 16.7; IR (film) 2983, 2857, 1604, 1485, 1451, 1336, 1303, 1272, 1071, 824, 748 cm^{-1} ; HRMS (EI): Exact mass calculated for $\text{C}_{13}\text{H}_{17}\text{N}_3\text{O}_4$ $[\text{M}]^+$: 279.1219 Found : 279.1223.



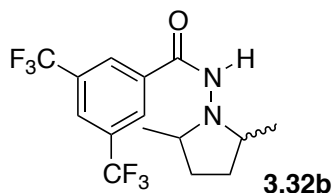
(±)-2-Hydroxy-4-nitro-*N*-((2*R*,5*S*)-2,5-dimethylpyrrolidin-1-yl)benzamide and (±)-2-hydroxy-4-nitro-*N*-((2*R*,5*R*)-2,5-dimethylpyrrolidin-1-yl)benzamide (3.30).

Synthesized according to **General Procedure D2** (90 $^\circ\text{C}$, 18 h) using *N*-(hex-5-en-2-yl)-4-nitrobenzohydrazide (0.070 g, 0.266 mmol). The reaction mixture was concentrated under reduced pressure and isolated using flash chromatography (40-65% EtOAc/Hexanes). The compound was obtained as a white solid (0.064 g, 91% yield, obtained as a mixture of diastereoisomers, 3:1 anti:syn). **Major product:** TLC R_f 0.36 in 50% EtOAc in hexanes; ^1H NMR (300 MHz; $\text{DMSO-}d_6$, 120 $^\circ\text{C}$): δ ppm 8.79 (br s, 1H), 8.23 (d, $J = 8.3$, 2H), 7.98 (d, $J = 7.9$, 2H), 3.48-3.37 (m, 2H), 2.05-1.94 (m, 2H), 1.45-1.26 (m, 3H), 1.04 (d, $J = 6.2$, 6H); ^{13}C NMR ($\text{DMSO-}d_6$, 100 MHz, 120 $^\circ\text{C}$): δ ppm 164.3, 149.5, 141.5, 129.2, 123.4, 47.3, 29.9, 17.5; IR (film) 3219, 2971, 2880, 1660, 1603, 1550, 1519, 1341, 1275, 1267, 764, 750 cm^{-1} ; HRMS (EI): Exact mass calculated for $\text{C}_{13}\text{H}_{17}\text{N}_3\text{O}_3$ $[\text{M}]^+$: 263.12699 Found : 263.12498.



***N*-(2-Methylpyrrolidin-1-yl)-3,5-bis(trifluoromethyl)benzamide (3.32a).**

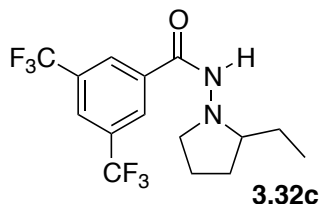
Synthesized according to **General Procedure D1** (95 °C, 16 h) using 3,5-bis(trifluoromethyl)-*N*-(pent-4-enyl)benzohydrazide (0.0770 g, 0.225 mmol). The reaction mixture was concentrated under reduced pressure and isolated using flash chromatography (32% EtOAc/Hexanes). The compound was obtained as a white solid (0.0621 g, 81% yield). TLC R_f 0.14 (25% EtOAc/Hexanes); ^1H NMR (300 MHz, DMSO- d_6 , 120 °C) δ ppm 9.34 (br s, 1H), 8.40 (s, 2H), 8.13 (s, 1H), 3.33-2.65 (m, 3H), 2.11-1.92 (m, 1H), 1.90-1.69 (m, 2H), 1.49-1.27 (m, 1H), 1.16-0.98 (m, 3H); ^{13}C NMR (75 MHz, DMSO- d_6 , 120 °C) δ ppm 162.6, 136.5, 129.9 (q, $J = 33.5$ Hz, 127.3, 123.0, 122.4 (q, $J = 272.9$ Hz, 58.8, 53.1, 29.9, 19.8, 17.5; IR (film) 3186, 3054, 2971, 2922, 2849, 2304, 1663, 1558, 1376, 1274, 1142, 908, 846, 747 cm^{-1} ; HRMS (EI): Exact mass calculated for $\text{C}_{14}\text{H}_{14}\text{F}_6\text{N}_2\text{O}$ $[\text{M}]^+$: 340.1010 Found : 340.1000



3,5-Bis(trifluoromethyl)-*N*-(2,5-dimethylpyrrolidin-1-yl)benzamide (3.32b).

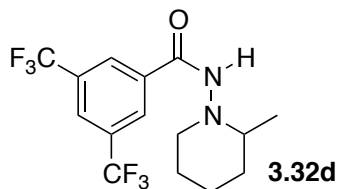
Synthesized according to **General Procedure D1** (90 °C, 10 h) using 3,5-bis(trifluoromethyl)-*N*-(hex-5-enyl)benzohydrazide (0.100 g, 0.282 mmol, 1 equiv.). The reaction mixture was concentrated under reduced pressure and isolated using flash chromatography (30% EtOAc/Hexanes). The compound was obtained as a white solid (0.098 g, 98% yield, obtained as a mixture of diastereoisomers, 3:1 anti:syn). **Major product:** TLC R_f 0.38 in (30% EtOAc/Hexanes); ^1H NMR (300 MHz, DMSO- d_6): δ ppm 9.06 (s, 1H), 8.39 (s, 2H), 8.10 (s, 1H), 3.45 (dq, $J = 1.9, 0.6$, 2H), 2.03-2.00 (m, 2H), 1.51-1.21 (m, 2H), 1.05 (d, $J = 6.0$, 6H) ^{13}C NMR (CDCl_3 , 100

MHz): δ ppm 162.5, 136.7, 129.9 (q, $J = 33.8$ Hz, CCF_3), 127.5, 123.0, 122.5 (q, $J = 273.1$ Hz, CF_3), 55.9, 28.8, 16.4; IR (film) 3427, 3252, 3070, 2975, 2967, 1653, 1550, 1380, 1279, 1175, 1134, 907 cm^{-1} ; HRMS (EI): Exact mass calculated for $\text{C}_{15}\text{H}_{16}\text{F}_6\text{N}_2\text{O}$ $[\text{M}]^+$: 354.1167. Found : 354.1149.



***N*-(2-Ethylpyrrolidin-1-yl)-3,5-bis(trifluoromethyl)benzamide (3.32c).**

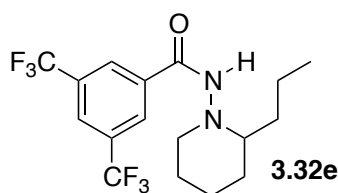
Synthesized according to **General Procedure D1** (150 °C, 16 h) using 3,5-bis(trifluoromethyl)-*N*'-((*Z*)-hex-4-enyl)benzohydrazide (0.197 g, 0.565 mmol, 1 equiv.). The reaction mixture was concentrated under reduced pressure and isolated using flash chromatography (25% EtOAc/Hexanes). The compound was obtained as a white solid (0.182 g, 91% yield). TLC R_f 0.27 in (30% EtOAc/Hexanes); ^1H NMR (300 MHz, $\text{DMSO-}d_6$, 120 °C) δ ppm 9.45 (br s, 1H), 8.40 (s, 2H), 8.13 (s, 1H), 3.39-2.68 (m, 3H), 2.12-1.16 (m, 6H), 0.86 (s, 3H); ^{13}C NMR (75 MHz, $\text{DMSO-}d_6$, 120 °C) δ ppm 161.9, 136.4, 129.9 (q, $J = 32.9$ Hz,., 127.4, 123.2, 122.5 (q, $J = 273$ Hz,., 64.7, 53.6, 27.2, 25.1, 20.2, 9.0; IR (film) 3220, 3072, 2972, 2877, 1659, 1556, 1462, 1377, 1279, 1138, 905, 697, 682 cm^{-1} ; HRMS (EI): Exact mass calculated for $\text{C}_{15}\text{H}_{16}\text{F}_6\text{N}_2\text{O}$ $[\text{M}]^+$: 354.1167. Found : 354.1166.



3,5-Bis(trifluoromethyl)-*N*-(2-methylpiperidin-1-yl)benzamide (3.32d).

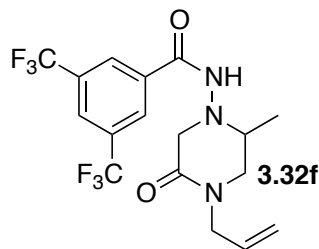
Synthesized according to **General Procedure D1** (175 °C, 16 h) using 3,5-bis(trifluoromethyl)-*N*'-(hex-5-enyl)benzohydrazide (0.0950 g, 0.268 mmol, 1 equiv.). The reaction mixture was concentrated under reduced pressure and isolated using

flash chromatography (26% EtOAc/Hexanes). The compound was obtained as a white solid (0.0816 g, 86% yield). TLC R_f 0.43 in 40% EtOAc in hexanes; ^1H NMR (300 MHz, $\text{DMSO-}d_6$, 120 °C) δ ppm 9.26 (br s, 1H), 8.40 (s, 2H), 8.09 (s, 1H), 3.18-2.63 (m, 3H), 1.79-1.47 (m, 4H), 1.40-1.15 (m, 2H), 1.12-0.93 (m, 3H); ^{13}C NMR (75 MHz, $\text{DMSO-}d_6$, 120 °C) δ ppm 161.6, 136.6, 129.9 (q, $J = 33.3$ Hz, 2), 127.4, 123.1, 122.4 (q, $J = 272.9$, 57.6, 54.9, 33.1, 24.8, 22.8, 18.4; IR (film) 3222, 3069, 2943, 2861, 1655, 1553, 1455, 1380, 1281, 1134, 906, 848, 702, 682 cm^{-1} ; HRMS (EI): Exact mass calculated for $\text{C}_{15}\text{H}_{16}\text{F}_6\text{N}_2\text{O}$ $[\text{M}]^+$: 354.1167 Found : 354.1157



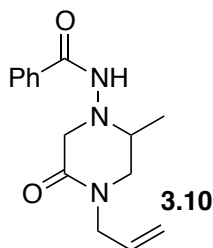
3,5-Bis(trifluoromethyl)-N-(2-propylpiperidin-1-yl)benzamide (3.32e).

Synthesized according to **General Procedure D1** (195 °C, 24 h) using 3,5-bis(trifluoromethyl)-*N*-((*Z*)-oct-5-enyl)benzohydrazide (0.0968 g, 0.253 mmol). The reaction mixture was concentrated under reduced pressure and isolated using flash chromatography (20% EtOAc in hexanes). The title compound was obtained as a brown crystal (0.0511 g, 53% yield). TLC R_f 0.63 (50% EtOAc/hexanes). ^1H NMR (CDCl_3 , 300 MHz) δ ppm 9.28 (s, 1H), 8.38 (s, 2H), 8.12 (s, 1H), 3.10 (d, $J = 10.3$ Hz, 1H), 2.87 (m, 4H), 1.82-1.49 (m, 5H), 1.28 (m, 2H), 0.83 (t, $J = 6.6$ Hz, 3H), ^{13}C NMR (CDCl_3 , 100 MHz) δ ppm * denotes traces of minor isomers 161.5, 136.5, 129.85 (q, $J = 33.6$ Hz, 2 CCF_3), *127.8, 122.50 (q, $J = 273$ Hz, 2 CF_3) 127.4, 123.1, 62.0, 55.1, 34.2, 29.9, 24.5, 22.8, 17.2, 13.2. HRMS (EI): Exact mass calculated for $\text{C}_{17}\text{H}_{20}\text{F}_6\text{N}_2\text{O}$ $[\text{M}]^+$: 382.148; found: 382.146.



***N*-[2-methyl-5-oxo-4-(prop-2-en-1-yl)piperazin-1-yl]-3,5-bis(trifluoromethyl)benzamide (3.32f).**

Synthesised according to General Procedure B1 (150 °C, 12h) using 2-(2-{{[3,5-bis(trifluoromethyl)phenyl]carbonyl}hydrazinyl})-*N,N*-di(prop-2-en-1-yl)acetamide (90 mg, 0.22 mmol, 1 equiv). The reaction mixture was concentrated under reduced pressure and isolated using flash chromatography (5% methanol in dichloromethane). The compound was obtained as a brown oil (82.7 mg, 92% yield). TLC R_f 0.23 (4% methanol in dichloromethane); ^1H NMR (DMSO-*d*₆, 400 MHz) δ ppm 10.10-10.00 (m, 1H), 8.54-8.41 (m, 2H), 8.38-8.24 (m, 1H), 5.82-5.70 (m, 1H), 5.23-5.15 (m, 2H), 4.03-3.87 (m, 2H), 3.76-3.57 (m, 2H), 3.44-3.35 (m, 1H), 3.28-3.18 (m, 1H), 3.13-3.03 (m, 1H), 1.13-1.04 (m, 3H). ^{13}C NMR (DMSO-*d*₆, 400 MHz) δ ppm 164.9 (C), 162.4 (C), 135.7 (CH), 132.6 (CH), 130.4 (q, $J = 33\text{Hz}$, C), 128.1 (d, $J = 3.7\text{ Hz}$, CH), 125.0 (CH), 123.0 (q, $J = 273\text{Hz}$, C), 117.4 (CH₂), 59.9 (CH₂), 54.3 (CH), 51.1 (CH₂), 47.3 (CH₂), 15.2 (CH₃); IR (film) 3233, 3066, 2918, 2850, 1659, 1450, 1276, 1132, 906, 845, 681 cm^{-1} ; HRMS (EI): Exact mass calcd for C₁₇H₁₇F₆N₃O₂ [M]⁺ : 409.1225 Found : 409.1233.

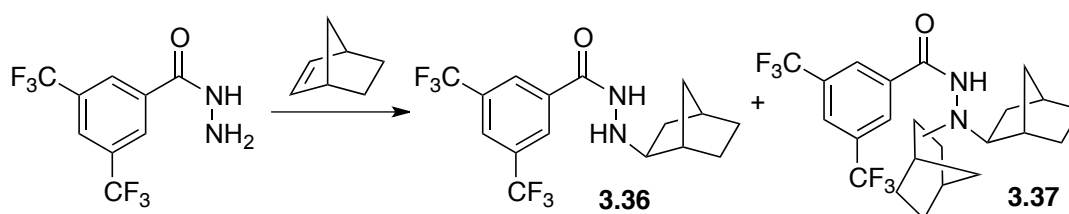


***N*-[2-methyl-5-oxo-4-(prop-2-en-1-yl)piperazin-1-yl]benzamide.**

Synthesised according to General Procedure D2 (175 °C, 12h) using 2-[2-(phenylcarbonyl)hydrazinyl]-*N,N*-di(prop-2-en-1-yl)acetamide (77.8 mg, 0.30 mmol, 1

equiv). The reaction mixture was concentrated under reduced pressure and isolated using flash chromatography (5% MeOH in CH₂Cl₂). The compound was obtained as a yellow oil (59.2 mg, 76% yield). TLC R_f 0.30 (5% methanol in dichloromethane); ¹H NMR (DMSO-*d*₆, 400 MHz) δ ppm 9.60 (s, 1H), 7.82-7.76 (m, 2H), 7.57-7.52 (m, 1H), 7.50-7.44 (m, 2H), 5.82-5.69 (m, 1H), 5.23-5.14 (m, 2H), 3.99-3.88 (m, 2H), 3.77-3.69 (m, 1H), 3.53 (d, *J* = 15.95 Hz, 1H), 3.44-3.37 (m, 1H), 3.21 (dd, *J* = 11.85, 3.74 Hz, 1H), 3.10-3.02 (m, 1H), 1.06 (d, *J* = 6.18 Hz, 3H) cm⁻¹. ¹³C NMR (DMSO-*d*₆, 400 MHz) δ ppm 165.4 (C), 165.1 (C), 133.5 (C), 132.6 (CH), 131.4 (CH), 128.3 (CH), 127.2 (CH), 117.3 (CH₂), 57.0 (CH₂), 54.1 (CH), 51.3 (CH₂), 47.3 (CH₂), 15.2 (CH₃) cm⁻¹; IR (film)

◆ **LEAD RESULT IN INTERMOLECULAR REACTIVITY OF HYDRAZIDES**



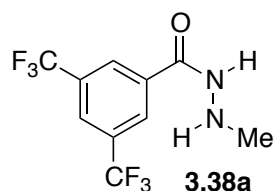
***N*-(Bicyclo[2.2.1]heptan-2-yl)-3,5-bis(trifluoromethyl)benzohydrazide (3.36) and *N,N*-di(bicyclo[2.2.1]heptan-2-yl)-3,5-bis(trifluoromethyl)benzohydrazide (3.37)**

In a 2 mL Biotage sealed tube were transferred 3,5-bis(trifluoromethyl)benzohydrazide (0.356 g, 1.31 mmol) and norbornene (13.1 mmol), which following an argon purge for 5 min., were diluted with trifluorotoluene (0.65 mL). After heating for 10 hours at 160 °C in the microwave, the solvent was evaporated and a NMR yield was taken (using dimethoxybenzene internal standard). The mono- and bis-hydroamination products (**3.36** and **3.37** respectively)⁹ were obtained in a 59% NMR yield (1:1.56 ratio). Some left over material (34%) and a condensation product (diacylhydrazine) derived from the starting material (7%) were also present. Column chromatography

⁹. Product **3.37**, resulting from 2 hydroamination events, is likely present as a mixture of diastereoisomers of the same R_f. The high temperature NMRs in DMSO-*d*₆ do not allow for differentiation between two diastereoisomers or residual rotamers being present.

(8-12% EtOAc / hexanes) afforded the products for characterization purposes. **3.36**: TLC R_f 0.43 (20% EtOAc/hexanes). $^1\text{H-NMR}$ (300 MHz; $\text{DMSO-}d_6$, 120 °C): δ ppm 8.13 (s, 2H), 8.00 (s, 1H), 4.12-4.05 (m, 1H), 2.46-2.29 (m, 3H), 1.84 (t, $J = 9.3$, 2H), 1.66-1.29 (m, 4H), 1.22-1.07 (m, 3H). $^{13}\text{C NMR}$ ($\text{DMSO-}d_6$, 100 MHz, 120 °C): δ ppm 166.8, 139.8, 129.3 (q, $J = 33.0$ Hz, CCF_3), 127.9, 122.5 (q, $J = 273$ Hz, CF_3), 59.3, 40.7, 35.8, 35.6, 34.7, 27.4, 26.9. IR (film): 3351, 3241, 2958, 2875, 1635, 1340, 1279, 1170, 1134, 905, 763, 750. HRMS (EI): Exact mass calculated for $\text{C}_{16}\text{H}_{16}\text{F}_6\text{N}_2\text{O}$ $[\text{M}]^+$: 366.11668. Found: 366.11836. **3.37**: TLC R_f 0.38 (20% EtOAc/hexanes). $^1\text{H NMR}$ (300 MHz; DMSO , 120 °C): δ ppm 9.01 (s, 1H), 8.40 (s, 2H), 8.13 (s, 1H), 3.10-2.92 (m, 2H), 2.36 (s, 2H), 2.20 (s, 2H), 1.71-1.25 (m, 10H), 1.21-0.91 (m, 6H); $^{13}\text{C NMR}$ ($\text{DMSO-}d_6$, 100 MHz, 120 °C): δ ppm 162.6, 136.4, 130.1 (q, $J = 34.1$ Hz, CCF_3), 127.3, 123.4, 122.5 (q, $J = 273$ Hz, CF_3), 65.6, 65.2, 38.5, 38.4, 36.2, 35.8, 34.9, 34.8, 34.7, 34.6, 27.5, 27.5, 27.0, 26.9. IR (film): 3309, 3252, 2960, 2876, 1656, 1276, 1176, 1134, 764, 750 cm^{-1} . HRMS (EI): Exact mass calculated for $\text{C}_{23}\text{H}_{26}\text{F}_6\text{N}_2\text{O}$ $[\text{M}]^+$: 460.19493. Found: 460.19104.

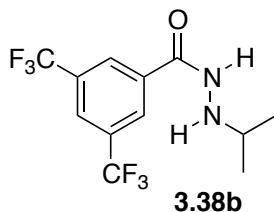
◆ SYNTHESIS OF INTERMOLECULAR SUBSTRATES



3,5-Bis(trifluoromethyl)-*N'*-methylbenzohydrazide (3.38a)

To *N'*-benzyl-3,5-bis(trifluoromethyl)benzohydrazide (0.400 g, 1.10 mmol) was dissolved in THF:DMF 4:1 (11 mL) and cooled to 0 °C. While keeping constant stirring, sodium hydride 95% (0.029 g, 1.2 mmol) was added to the reaction. Methyl iodide (0.34 mL, 5.5 mmol) was added and within 5 minutes, a solid crashed out of solution, and the solution became clear and colorless. Following a quench with water, the THF was evaporated over 20 minutes. The resulting slurry was taken in EtOAc, washed with brine:H₂O 1:1 (5 x 4 mL). The organic phase was dried over Na₂SO₄,

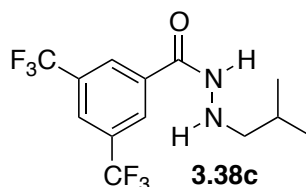
filtered and concentrated under reduced pressure to yield the crude *N*'-benzyl-*N*'-methyl-3,5-bis(trifluoromethyl)benzohydrazide. *Benzyl Cleavage*: The unpurified hydrazide (1.00 g, 266 mmol) was added to a flame dried round-bottom flask and diluted with EtOAc (133 mL). Palladium on Carbon (10 wt%, 0.330 g) was added in 2 portions, followed by 5 subsequent purges with high vacuum and refilling with hydrogen atmosphere. The reaction was left to stir overnight under a hydrogen atmosphere and then showed complete conversion by TLC. Filtration over celite, followed by concentration under reduced pressure and silica-gel column chromatography (50% EtOAc/Hexanes) gave the title compound (0.501 g, 65%), TLC R_f 0.24 (50% EtOAc/hexanes). ^1H NMR (DMSO- d_6 , 400 MHz): δ ppm 10.51 (br s, 1H), 8.47 (s, 2H), 8.32 (s, 1H), 5.28 (br s, 1H), 2.57 (s, 1H). ^{13}C NMR (DMSO- d_6 , 100 MHz): δ ppm 161.9, 135.5, 130.5 (q, $J = 33.4$ Hz, CCF_3), 127.8, 124.8, 123.1 (q, $J = 273$ Hz, CF_3), 38.3. IR (film): 3306, 3279, 3058, 2994, 2306, 1652, 1447, 1276, 1135, 915, 888, 748 cm^{-1} . HRMS (EI): Exact mass calculated for $\text{C}_{10}\text{H}_8\text{F}_6\text{N}_2\text{O}$ $[\text{M}]^+$: 286.05408. Found: 286.05267.



3,5-Bis(trifluoromethyl)-*N*'-isopropylbenzohydrazide. (3.38b)

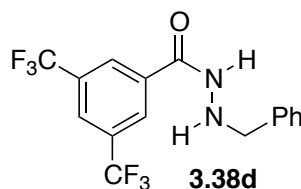
Synthesized according to General Procedure C2 on 3,5-bistrifluoromethylbenzohydrazide (1.30 g, 4.77 mmol) and acetone (0.346 g, 5.96 mmol). Isolated 1.12 g (75% yield) of the title compound as a white solid after column chromatography (20% EtOAc/hexanes). TLC R_f 0.58 (50% EtOAc/hexanes). ^1H NMR (CDCl_3 , 400 MHz): δ ppm 8.28 (s, 2H), 7.99 (s, 1H), 3.29-3.16 (m, 1H), 1.09 (dd, $J = 6.2, 1.7$ Hz, 6H). ^{13}C NMR (CDCl_3 , 100 MHz): δ ppm 164.7, 134.9, 132.3 (q, $J = 34.0$ Hz, CCF_3), 127.4, 125.3, 122.8 (q, $J = 272.9$ Hz, CF_3), 51.6, 20.7. IR (film): 3747, 3283, 3093, 2975, 2937, 2873, 1649, 1546, 1451, 1379, 1341, 1284,

1136 cm^{-1} . HRMS (EI): Exact mass calculated for $\text{C}_{12}\text{H}_{12}\text{F}_6\text{N}_2\text{O}$ $[\text{M}]^+$: 314.0854. Found: 314.0856.



3,5-Bis(trifluoromethyl)-*N*-isobutylbenzohydrazide. (3.38c)

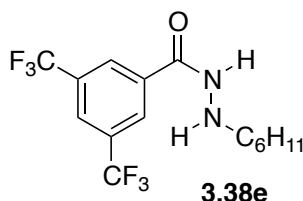
Synthesized according to General Procedure C2 on 3,5-bistrifluoromethylbenzohydrazide (1.87 g, 6.87 mmol) and isobutyraldehyde (0.597 mL, 6.54 mmol). Isolated 1.17 g (54% yield) of the title compound as a white solid after column chromatography (15% EtOAc/hexanes). R_f : 0.37 (20% EtOAc/hexanes). $^1\text{H-NMR}$ (300 MHz; $\text{DMSO-}d_6$): δ ppm 8.44 (s, 2H), 8.13 (s, 1H), 2.72 (d, $J = 6.6$ Hz, 2H), 1.84-1.77 (m, 1H), 0.97 (d, $J = 6.7$ Hz, 6H). $^{13}\text{C NMR}$ (75 MHz, $\text{DMSO-}d_6$): δ ppm 162.1, 135.4, 130.5 (q, $J = 33.0$ Hz, CCF_3), 127.8, 124.8, 123.1 (q, $J = 273$ Hz, CF_3), 58.9, 26.4, 20.5. IR ($\nu_{\text{max}}/\text{cm}^{-1}$): 3273, 3097, 2963, 2875, 1645, 1615, 1455, 1380, 1276, 1183, 1140, 937, 909, 846, 764, 750. HRMS (EI): Exact mass calculated for $\text{C}_{13}\text{H}_{14}\text{F}_6\text{N}_2\text{O}$ $[\text{M}]^+$: 328.10103. Found: 328.09771.



***N*-Benzyl-3,5-bis(trifluoromethyl)benzohydrazide. (3.38d)**

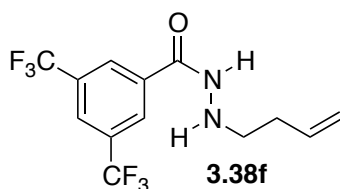
Synthesized according to General Procedure C2 on 3,5-bistrifluoromethylbenzohydrazide (4.30 g, 15.2 mmol) and benzaldehyde (2.02 g, 19.0 mmol). Isolated 3.18 g (56% yield) of the titled compound as a white solid after column chromatography (20% EtOAc/hexanes). TLC R_f 0.77 (50% EtOAc/hexanes). $^1\text{H NMR}$ (CDCl_3 , 400 MHz): δ ppm 8.13 (s, 2H), 8.00 (s, 1H), 7.41-7.27 (m, 5H), 4.11 (s, 2H). $^{13}\text{C NMR}$ (CDCl_3 , 100 MHz): δ ppm 164.4, 136.8, 134.7, 132.2 (q, $J = 34.0$ Hz, CCF_3), 129.0, 128.6, 127.9, 127.4, 125.4, 122.8 (q, $J = 273.0$ Hz, CF_3), 55.7. IR

(film): 3268, 3097, 3070, 3032, 2930, 2861, 1645, 1542, 1447, 1375, 1333, 1140 cm^{-1} . HRMS (EI): Exact mass calculated for $\text{C}_{16}\text{H}_{12}\text{F}_6\text{N}_2\text{O}$ $[\text{M}]^+$: 362.0854. Not Found. HRMS (EI): Exact mass calculated for $\text{C}_7\text{H}_8\text{N}$ $[\text{M}-3,5\text{-bis(trifluoromethyl)benzoamide}]^+$: 106.0657. Found: 106.0652.



***N*-Cyclohexyl-3,5-bis(trifluoromethyl)benzohydrazide. (3.38e)**

Synthesized according to General Procedure C2 on 3,5-bistrifluoromethylbenzohydrazide (1.17 g, 4.30 mmol) and cyclohexanone (0.527 g, 5.38 mmol). Isolated 0.820 g (54% yield) of the title compound as a white solid after column chromatography (12% EtOAc/hexanes). TLC R_f 0.81 (50% EtOAc/hexanes). ^1H NMR (CDCl_3 , 300 MHz): δ ppm 8.20 (s, 2H), 8.01 (s, 1H), 2.98-2.87 (m, 1H), 1.97-1.87 (m, 2H), 1.82-1.72 (m, 2H), 1.67-1.59 (m, 1H), 1.36-1.09 (m, 5H). ^{13}C NMR (CDCl_3 , 75 MHz): δ ppm 164.4, 134.8, 132.1 (q, $J = 33.99$ Hz, CCF_3), 127.2, 125.2, 122.7 (q, $J = 273.03$ Hz, CF_3), 59.2, 31.2, 25.7, 24.3. IR (film): 3747, 3276, 3089, 2934, 2854, 1641, 1539, 1451, 1371, 1276, 1136 cm^{-1} . HRMS (EI): Exact mass calculated for $\text{C}_{15}\text{H}_{16}\text{F}_6\text{N}_2\text{O}$ $[\text{M}]^+$: 354.1167. Found: 354.1149.

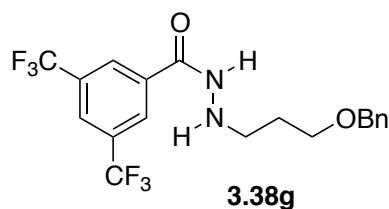


***N*-(But-3-enyl)-3,5-bis(trifluoromethyl)benzohydrazide. (3.38f)**

Prepared according to a modified procedure by Hansen.¹⁰ 1-Bromobut-3-ene (0.600 mL, 5.92 mmol) and 3,5-bistrifluoromethyl-benzohydrazide (8.00 g, 29.6 mmol) were stirred in DMF (30 mL) at 100 °C for 15 hours. Ethyl acetate was added to the

¹⁰. Hansen, T. K. *Tetrahedron Lett.* **1999**, *40*, 9119.

reaction mixture, and the resulting solution was washed with brine:H₂O 1:1 (5 x 60 mL). The organic phase was dried over Na₂SO₄, filtered and concentrated under reduced pressure. Purification by silica gel chromatography (20 – 70% EtOAc / Hexanes) gave the titled compound in 1.02 g (53% yield). TLC R_f 0.68 (50% EtOAc/hexanes). ¹H NMR (DMSO-*d*₆, 300 MHz, 120 °C): δ ppm 8.23 (s, 2H), 8.03 (s, 1H), 5.86 (ddt, *J* = 17.1, 10.2, 6.8 Hz, 1H), 5.19-5.08 (m, 2H), 3.08 (t, *J* = 6.9 Hz, 2H), 2.35 (q, *J* = 6.8 Hz, 2H). ¹³C NMR (DMSO-*d*₆, 75 MHz, 120 °C): δ ppm 164.3, 135.4, 134.6, 132.4 (q, *J* = 33.9 Hz, CCF₃). 127.3, 125.4, 122.8 (q, *J* = 272.8 Hz, CF₃), 116.9, 51.1, 32.3. IR (film): 3233, 3085, 2929, 2868, 1648, 1561, 1386, 1277, 1169, 1140, 907 cm⁻¹. HRMS (EI): Exact mass calculated for C₁₃H₁₂F₆N₂O [M]⁺: 326.08538. Found: 326.08849.



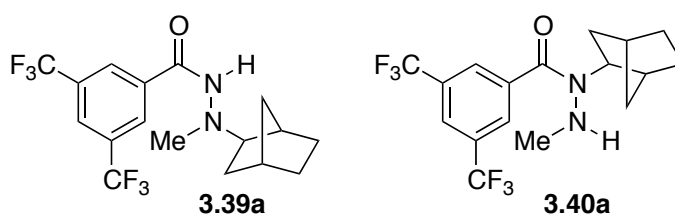
***N*-(3-(Benzyloxy)propyl)-3,5-bis(trifluoromethyl)benzohydrazide. (3.38g)**

Synthesized according to General Procedure C2 on 3,5-bistrifluoromethylbenzohydrazide (2.56 g, 9.41 mmol) and 3-benzyloxypropionaldehyde (1.70 g, 10.4 mmol). Isolated 2.04 g (52% yield) of the titled compound as a white solid after column chromatography (30% EtOAc/hexanes). TLC R_f 0.18 (25% EtOAc/hexanes). ¹H NMR (DMSO-*d*₆, 300 MHz): δ ppm 8.45 (s, 2H), 8.12 (s, 1H), 7.33-7.25 (m, 5H), 4.50 (s, 2H), 3.60 (t, *J* = 6.3 Hz, 2H), 2.99 (t, *J* = 6.9 Hz, 2H), 1.82 (quintet, *J* = 6.6 Hz, 2H). ¹³C NMR (DMSO-*d*₆, 75 MHz): δ ppm 161.2, 138.3, 135.6, 130.3 (q, *J* = 33.1 Hz, CCF₃), 127.1, 126.6, 126.4, 125.8, 123.4, 123.4, 123.3, 122.5 (q, *J* = 272.7 Hz, CF₃), 71.5, 67.6, 48.0, 27.6. IR (film): 3280, 3096, 3039, 2937, 2861, 1652, 1616, 1450, 1379, 1275, 1267, 1137, 908, 845, 763, 749 cm⁻¹. HRMS (EI): Exact mass calculated for C₁₉H₁₈F₆N₂O₂ [M]⁺: 420.12725. Found: 420.12952.

◆ INTERMOLECULAR COPE-TYPE HYDROAMINATION - KEY STEPS

General Procedure E for Intermolecular Hydrohydrazidation.

To a Biotage sealed tube equipped with a magnetic stir bar was added the hydrazide, norbornene (10 equiv.), and trifluorotoluene (2 M).¹¹ The tube was sealed and heated in a wax bath at 160 °C for 18-40 h. After cooling to room temperature, the reaction was transferred to a round bottom flask through chloroform rinses. The reaction was concentrated in vacuo to give the crude products, which were then purified by flash chromatography to afford both hydroamination products.

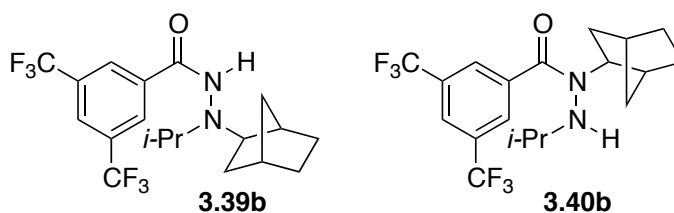


***N*-(Bicyclo-[2.2.1]heptan-2-yl)-3,5-bis(trifluoromethyl)-*N*-methylbenzohydrazide (3.39a) and *N*-(bicyclo[2.2.1]heptan-2-yl)-3,5-bis(trifluoromethyl)-*N*-methylbenzohydrazide (3.40a) - (Table 3, entry 2).**

Synthesized according to General Procedure E the parent alkyl hydrazide (0.139 g, 0.487 mmol) and norbornene, reacted for 18 hours at 160 °C. Isolated 0.128 g of **3.39a** as a white solid and 0.030 g of **3.40a** (85% yield, 4.28:1) after column chromatography (10–20% EtOAc/hexanes). **3.39a**: TLC R_f 0.48 (25% EtOAc/hexanes). ¹H NMR (DMSO-*d*₆, 300 MHz, 120 °C): δ ppm 9.45 (br s, 1H), 8.40 (s, 2H), 8.13 (s, 1H), 2.94 (s, 1H), 2.61 (s, 3H), 2.27-2.21 (m, 2H), 1.64 (br s, 1H), 1.50-1.27 (m, 3H), 1.10-1.02 (m, 4H). ¹³C NMR (DMSO-*d*₆, 75 MHz, 120 °C): δ ppm 161.5, 136.5, 130.0 (q, $J = 33.0$ Hz, CCF₃), 127.4, 123.4, 122.0 (q, $J = 272.9$ Hz, CF₃), 69.0, 41.8, 38.8, 35.9, 35.2, 34.1, 27.7, 25.9. IR (film): 3418, 3104, 2963, 1870, 1652, 1557, 1284, 1131 cm⁻¹. HRMS (EI): Exact mass calculated for C₁₇H₁₈F₆N₂O [M]⁺: 380.13233. Found: 380.13307. **3.40a**: TLC R_f 0.87 (25% EtOAc/hexanes). ¹H

¹¹. The size of the sealed tube is selected between 0.2, 2.0, 5.0 and 20 mL in order to minimize head space. Excess headspace in the reaction can lower the yield due to the volatility of norbornene.

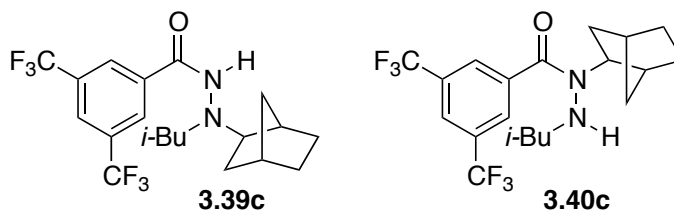
NMR (300 MHz; DMSO- d_6 , 120 °C): δ ppm 8.09 (s, 2H), 8.04 (s, 1H), 4.97 (q, $J = 5.0$ Hz, 1H), 3.72 (dd, $J = 8.0, 5.5$ Hz, 1H), 2.85 (s, 1H), 2.47 (d, $J = 5.5$ Hz, 4H), 2.29 (s, 1H), 1.89 (t, $J = 8.3$ Hz, 2H), 1.57 (t, $J = 11.3$ Hz, 1H), 1.47 (t, $J = 4.6$ Hz, 2H), 1.16 (d, $J = 9.7$ Hz, 1H), 1.09-1.05 (m, 2H). ^{13}C NMR (DMSO- d_6 , 300 MHz, 120 °C): δ ppm 168.6, 140.9, 130.8 (q, $J = 33.3$ Hz, CCF_3), 128.3, 123.6 (q, $J = 273.1$ Hz, CF_3), 122.8, 62.0, 41.5, 38.0, 37.0, 36.4, 36.0, 28.2. IR (film): 3351, 3298, 2957, 2875, 1642, 1415, 1385, 1327, 1280, 1165, 1137, 906 cm^{-1} . HRMS (EI): Exact mass calculated for $\text{C}_{17}\text{H}_{18}\text{F}_6\text{N}_2\text{O}$ $[\text{M}]^+$: 380.13233. Found: 380.13184.



***N*-(Bicyclo-[2.2.1]heptan-2-yl)-3,5-bis(trifluoromethyl)-*N*-isopropylbenzohydrazide (3.39b) and *N*-(bicyclo[2.2.1]heptan-2-yl)-3,5-bis(trifluoromethyl)-*N*-isopropylbenzohydrazide (3.40b).**

Synthesized according to General Procedure E (160 °C, 17 h) on *N*-(but-3-enyl)-3,5-bis(trifluoromethyl)-benzohydrazide. (0.636 mmol). Isolated 0.123 g (47% yield) of **3.39b** as a white solid and 0.070 g (27% yield) of **3.40b** after column chromatography (12% EtOAc/hexanes). **3.39b**: TLC R_f 0.34 (20% EtOAc/hexanes). ^1H NMR (DMSO- d_6 , 300 MHz, 120 °C): δ ppm 8.82 (s, 1H), 8.41 (s, 2H), 8.08 (s, 1H), 3.45-3.20 (m, 1H), 2.24 (d, $J = 19.9$ Hz, 2H), 1.72 (d, $J = 7.8$ Hz, 1H), 1.57-1.20 (m, 5H), 1.16-0.94 (m, 9H). ^{13}C NMR (DMSO- d_6 , 75 MHz, 120 °C): δ ppm 163.1, 136.7, 130.1 (q, $J = 32.8$ Hz, CCF_3), 127.3, 123.1, 122.5 (q, $J = 273$ Hz, CF_3), 64.4, 50.5, 38.8, 36.1, 35.1, 34.2, 27.7, 26.2, 17.7, 17.1. IR (film): 3264, 3074, 2960, 2873, 1653, 1550, 1466, 1447, 1387, 1341, 1280, 1174, 1132 cm^{-1} . HRMS (EI): Exact mass calculated for $\text{C}_{19}\text{H}_{22}\text{F}_6\text{N}_2\text{O}$ $[\text{M}]^+$: 408.1636. Found: 408.1632. **3.40b**: TLC R_f 0.66 (20% EtOAc/hexanes). ^1H NMR (DMSO- d_6 , 300 MHz, 120 °C): δ ppm 8.14 (s, 2H), 8.00 (s, 1H), 4.93 (s, 1H), 3.77-3.66 (m, 1H), 3.19-3.06 (m, 1H), 2.28 (s, 1H), 1.87 (t, $J = 13.2$ Hz, 2H), 1.60 (dd, $J = 11.2, 9.6$ Hz, 1H), 1.49 (d, $J = 7.9$ Hz, 2H), 1.13 (t, $J =$

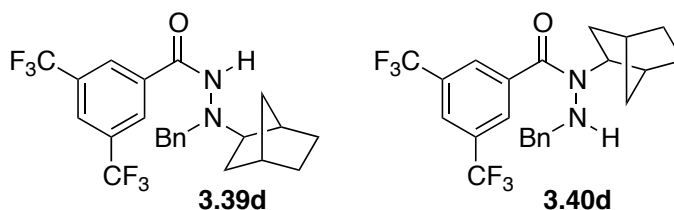
10.4 Hz, 3H), 0.83 (t, $J = 7.1$ Hz, 6H). ^{13}C NMR (DMSO- d_6 , 75 MHz, 120 °C): δ ppm 168.5, 139.8, 129.4 (q, $J = 33.2$ Hz, CCF_3), 128.1, 122.4 (q, $J = 273$ Hz, CF_3), 121.6, 61.7, 48.5, 39.8, 36.0, 35.2, 34.8, 27.0, 27.0, 19.6, 19.5. IR (film): 3325, 3276, 2964, 2876, 1641, 1447, 1325, 1280, 1177, 1135 cm^{-1} . HRMS (EI): Exact mass calculated for $\text{C}_{19}\text{H}_{22}\text{F}_6\text{N}_2\text{O}$ [M] $^+$: 408.1636. Found: 408.1643.



***N*-(Bicyclo-[2.2.1]heptan-2-yl)-3,5-bis(trifluoromethyl)-*N*-isobutylbenzohydrazide (3.39c) and *N*-(Bicyclo[2.2.1]heptan-2-yl)-3,5-bis(trifluoromethyl)-*N*-isobutylbenzohydrazide (3.40c).**

Synthesized according to General Procedure E (160 °C, 17 h) on 3,5-bis(trifluoromethyl)-*N*-isobutylbenzohydrazide (160 mg, 0.487 mmol). Isolated 0.115 g (53% yield) of **3.39c** as a white solid and 0.042 g (20% yield) of **3.40c** after column chromatography (5% EtOAc/hexanes). **3.39c**: TLC R_f 0.39 (10% EtOAc/hexanes). ^1H NMR (DMSO- d_6 , 300 MHz, 120 °C): δ ppm 9.19 (br s, 1H), 8.40 (s, 2H), 8.13 (s, 1H), 2.95-2.90 (m, 1H), 2.64-2.60 (m, 2H), 2.26-2.23 (m, 2H), 1.80-1.65 (m, 2H), 1.60-1.36 (m, 4H), 1.11-1.02 (m, 3H), 0.93-0.91 (m, 6H). ^{13}C NMR (DMSO- d_6 , 75 MHz, 120 °C): δ ppm 162.0, 136.4, 130.1 (1, $J = 33.3$ Hz, CCF_3), 127.2, 123.4, 122.5 (q, $J = 273$ Hz, CF_3), 68.1, 61.4, 39.5, 39.1, 36.1, 35.2, 34.1, 27.8, 25.9, 25.6, 19.9. IR (film): 3454, 3218, 3006, 2094, 1672, 1637, 1275, 1261, 764, 750 cm^{-1} . HRMS (EI): Exact mass calculated for $\text{C}_{20}\text{H}_{24}\text{F}_6\text{N}_2\text{O}$ [M] $^+$: 422.17928. Not Found. Exact mass calculated for $\text{C}_{17}\text{H}_{17}\text{F}_6\text{N}_2\text{O}$ [M-isopropyl] $^+$: 379.1250. Found: 379.1183. **3.40c**: TLC R_f 0.55 (10% EtOAc/hexanes). ^1H NMR (DMSO- d_6 , 300 MHz, 120 °C): δ ppm 8.40 (br s, 1H), 8.10 (s, 2H), 8.02 (s, 1H), 4.84 (t, $J = 5.9$ Hz, 1H), 3.75 (dd, $J = 7.8, 5.6$ Hz, 1H), 2.59-2.55 (m, 2H), 2.29 (s, 1H), 1.91-1.87 (m, 2H), 1.63-1.60 (m, 1H), 1.53-1.47 (m, 3H), 1.18-1.09 (m, 3H), 0.71 (dd, $J = 6.6, 2.6$ Hz, 6H). ^{13}C NMR (DMSO- d_6 , 75 MHz, 120 °C): δ ppm 167.8, 139.9, 129.6 (q, $J = 33.3$ Hz, CCF_3),

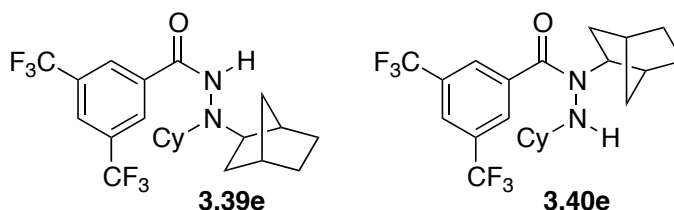
127.5, 122.5 (q, $J = 273$ Hz, CF_3), 121.5, 61.0, 57.9, 40.1, 36.0, 35.3, 34.9, 27.1, 27.1, 25.9, 19.3. IR (film): 2963, 2880, 1641, 1329, 1277, 1261, 1170, 1132, 764, 750 cm^{-1} . HRMS (EI): Exact mass calculated for $\text{C}_{20}\text{H}_{24}\text{F}_6\text{N}_2\text{O}$ $[\text{M}]^+$: 422.17928. Found: 422.1797.



***N*-Benzyl-*N*-(bicyclo[2.2.1]heptan-2-yl)-3,5-bis(trifluoromethyl)benzohydrazide (3.39d) and *N*-benzyl-*N*-(bicyclo[2.2.1]heptan-2-yl)-3,5-bis(trifluoromethyl)benzohydrazide (3.40d).**

Synthesized according to General Procedure E (160 °C, 40 h) on 0.636 mmol of the parent alkyl hydrazide. Isolated 0.153 g (61% yield) of **3.39d** as a white solid and 0.049 g (20% yield) of **3.40d** after column chromatography (12% EtOAc/hexanes). **3.39d**: TLC R_f 0.54 (20% EtOAc/hexanes). ^1H NMR (DMSO- d_6 , 300 MHz, 120 °C): δ ppm 9.30 (s, 1H), 8.17 (s, 2H), 8.04 (s, 1H), 7.38 (s, 2H), 7.30-7.12 (m, 3H), 4.08 (s, 2H), 3.17 (s, 1H), 2.88 (s, water), 2.38 (s, 1H), 2.27 (s, 1H), 1.80 (s, 1H), 1.64-1.37 (m, 4H), 1.20-1.02 (m, 3H). ^{13}C NMR (DMSO- d_6 , 300 MHz, 120 °C): δ ppm 162.2, 137.8, 136.4, 129.9, 128.1, 127.1, 127.0, 125.9, 123.1, 122.4 (CF_3), 67.8, 56.9, 39.0, 36.1, 35.2, 34.2, 27.7, 26.0. IR (film): 3238, 3070, 2953, 2867, 1652, 1550, 1447, 1379, 1349, 1276, 1185, 1128 cm^{-1} . HRMS (EI): Exact mass calculated for $\text{C}_{23}\text{H}_{22}\text{F}_6\text{N}_2\text{O}$ $[\text{M}]^+$: 456.1636. Not found. HRMS (EI): Exact mass calculated for $\text{C}_9\text{H}_5\text{F}_6\text{N}_2\text{O}$ $[\text{M-benzyl}]^+$: 365.1089. Found: 365.1074. **3.40d**: TLC R_f 0.71 (20% EtOAc/hexanes). ^1H NMR (DMSO- d_6 , 300 MHz, 120 °C): δ ppm 7.95 (s, 3H), 7.18-7.12 (m, 3H), 7.03-6.98 (m, 2H), 5.29 (t, $J = 5.3$ Hz, 1H), 3.85 (d, $J = 5.3$ Hz, 2H), 3.77 (dd, $J = 7.7, 5.3$ Hz, 1H), 2.79 (s, water), 2.28 (s, 1H), 1.95-1.81 (m, 2H), 1.61 (ddd, $J = 12.4, 8.2, 1.9$ Hz, 1H), 1.51-1.44 (m, 2H), 1.27- 1.04 (m, 3H). ^{13}C NMR (DMSO- d_6 , 75 MHz, 120 °C): δ ppm 167.8, 139.5, 136.5, 129.4 (q, $J = 33.2$ Hz), 128.0, 127.5, 127.5, 127.2, 126.4, 122.4 (q, $J = 273$ Hz, CF_3), 121.5 (td, $J = 7.6, 3.8$

Hz), 61.1, 53.7, 40.0, 36.1, 35.3, 34.9, 27.1, 26.9. IR (film): 2956, 2926, 2877, 1637, 1326, 1276, 1166, 1136, 1086 cm^{-1} . HRMS (EI): Exact mass calculated for $\text{C}_{23}\text{H}_{22}\text{F}_6\text{N}_2\text{O}$ $[\text{M}]^+$: 456.1636. Found: 456.1653.

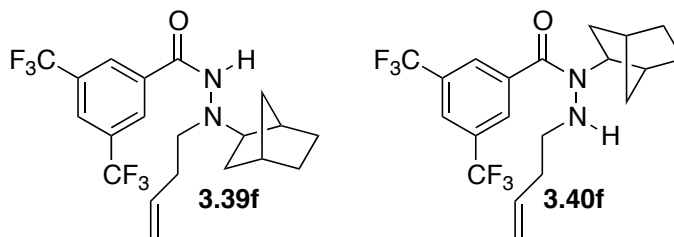


***N*-Bicyclo[2.2.1]heptan-2-yl)-3,5-bis(trifluoromethyl)-*N*-cyclohexylbenzohydrazide (3.39e) and (*N*-(bicyclo[2.2.1]heptan-2-yl)-3,5-bis(trifluoromethyl)-*N*-cyclohexylbenzohydrazide (3.40e).**

Synthesized according to General Procedure E (160 °C, 40 h) on 0.565 mmol of the parent alkyl hydrazide. Isolated 0.169 g (67% yield) of **3.39e** as a white solid and 0.053 g (21% yield) of **3.40e** after column chromatography (10% EtOAc/hexanes).

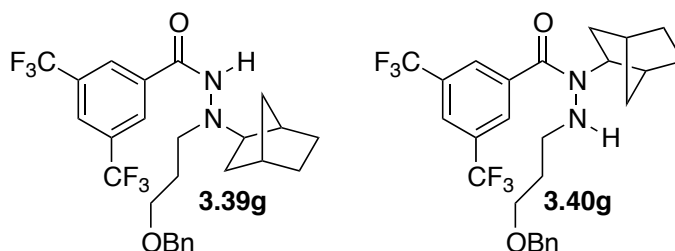
3.39e: TLC R_f 0.56 (20% EtOAc/hexanes). ^1H NMR (DMSO- d_6 , 300 MHz, 120 °C): δ ppm 8.91 (s, 1H), 8.41 (s, 2H), 8.10 (s, 1H), 3.10 (s, 1H), 2.24 (d, $J = 22.9$ Hz, 2H), 1.89 (s, 2H), 1.82-1.63 (m, 3H), 1.64-0.96 (m, 14H). ^{13}C NMR (DMSO- d_6 , 75 MHz, 120 °C): δ ppm 163.0, 136.5, 130.1, 127.4, 123.5, 122.6 (q, $J = 273$ Hz, CF_3), 63.7, 59.6, 38.7, 36.2, 35.2, 34.4, 28.5, 28.2, 27.8, 26.4, 25.2, 24.7. IR (film): 3241, 3067, 2941, 2861, 1656, 1561, 1550, 1451, 1379, 1345, 1280, 1159, 1132 cm^{-1} . HRMS (EI): Exact mass calculated for $\text{C}_{22}\text{H}_{26}\text{F}_6\text{N}_2\text{O}$ $[\text{M}]^+$: 448.1949. Found: 448.1949.

3.40e: TLC R_f 0.85 (20% EtOAc/hexanes). ^1H NMR (DMSO- d_6 , 300 MHz, 120 °C): δ ppm 8.15 (s, 2H), 8.00 (s, 1H), 4.90 (s, 1H), 3.70 (dd, $J = 7.0, 5.9$ Hz, 1H), 2.28 (s, 1H), 1.87 (t, $J = 11.5$ Hz, 2H), 1.64 (ap t, $J = 9.3$ Hz, 3H), 1.58-1.40 (m, 6H), 1.20-1.07 (m, 6H), 0.97-0.78 (m, 3H). ^{13}C NMR (DMSO- d_6 , 75 MHz, 120 °C): δ ppm 168.5, 139.8, 129.4 (q, $J = 33.2$ Hz, CCF_3), 128.2, 122.5 (q, $J = 273$ Hz, CF_3), 121.6, 61.7, 56.2, 39.8, 36.1, 35.2, 34.9, 29.9, 29.9, 27.1, 27.0, 24.8, 23.0, 22.9. IR (film): 3317, 3272, 2934, 2858, 1645, 1451, 1314, 1276, 1178, 1140 cm^{-1} . HRMS (EI): Exact mass calculated for $\text{C}_{22}\text{H}_{26}\text{F}_6\text{N}_2\text{O}$ $[\text{M}]^+$: 448.1949. Found: 448.1917.



***N*-(Bicyclo[2.2.1]heptan-2-yl)-3,5-bis(trifluoromethyl)-*N*-(but-3-enyl)benzohydrazide (3.39f) and *N*-(bicyclo[2.2.1]heptan-2-yl)-3,5-bis(trifluoromethyl)-*N*-(but-3-enyl)benzohydrazide (3.40f).**

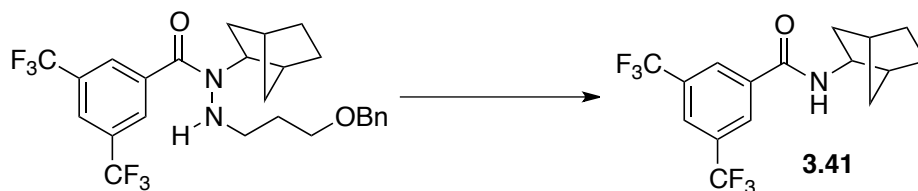
Synthesized according to General Procedure E on 0.487 mmol of the parent alkylated hydrazide and norbornene, reacted for 18 hours at 160 °C. Isolated 0.140 g of **3.39f** as a white solid and 0.038 g of **3.40f** (87% yield, 3.68:1) after column chromatography (8% EtOAc/hexanes). **3.39f**: TLC R_f 0.31 (10% EtOAc/hexanes). ^1H NMR (300 MHz; DMSO- d_6 , 120 °C): δ ppm 9.22 (br s, 1H), 8.42 (s, 2H), 8.12 (s, 1H), 5.93-5.84 (m, 1H), 4.99 (dd, $J = 26.2, 13.7$ Hz, 2H), 2.93 (dd, $J = 12.9, 6.2$ Hz, 3H), 2.27-2.22 (m, 4H), 1.69 (s, 1H), 1.50-1.34 (m, 4H), 1.07 (dd, $J = 17.9, 8.8$ Hz, 3H). ^{13}C NMR (DMSO- d_6 , 75 MHz, 120 °C): δ ppm 162.2, 136.3, 130.1 (q, $J = 33.9$ Hz, CCF_3), 127.3, 123.4, 122.5 (q, $J = 272.9$ Hz, CF_3), 114.3, 67.7, 52.7, 38.9, 36.0, 35.2, 34.1, 30.8, 27.7, 26.0. IR (film): 3248, 2960, 2868, 1645, 1275, 1261, 1120, 763, 749 cm^{-1} . HRMS (EI): Exact mass calculated for $\text{C}_{20}\text{H}_{22}\text{F}_6\text{N}_2\text{O}$ $[\text{M}]^+$: 420.16363. Not found. Exact mass calculated for $\text{C}_{17}\text{H}_{17}\text{F}_6\text{N}_2\text{O}$ $[\text{M-allyl}]^+$: 379.125. Found: 379.1259. **3.40f**: TLC R_f 0.51 (8% EtOAc/hexanes). ^1H NMR (500 MHz; benzene- d_6): δ ppm 7.93 (s, 2H), 7.73 (s, 1H), 5.65 (m, 1H), 5.01 (d, $J = 17.1$ Hz, 1H), 4.96 (d, $J = 10.2$ Hz, 1H), 4.35 (s, 1H), 3.45 (s, 1H), 2.81 (s, 1H), 2.71 (s, 1H), 2.03 (m, 4H), 1.85 (ap d, $J = 6.6$ Hz, 1H), 1.76 (ap d, $J = 11.9$ Hz, 1H), 1.24 (m, 3H), 0.95 (d, $J = 9.1$ Hz, 1H), 0.76 (d, $J = 7.7$ Hz, 2H). ^{13}C NMR (benzene- d_6 , 125 MHz): δ ppm 168.5, 139.8, 135.7, 132.1 (q, $J = 33.2$ Hz, CCF_3), 128.5, 123.7 (q, $J = 273$ Hz, CF_3), 123.4, 116.5, 63.2, 50.8, 42.5, 37.2, 36.5, 36.4, 32.6, 28.5, 28.3. IR (film): 3336, 3279, 3086, 2957, 2875, 1643, 1414, 1327, 1280, 1169, 1138, 900, 840, 716, 705, 681 cm^{-1} . HRMS (EI): Exact mass calculated for $\text{C}_{20}\text{H}_{22}\text{F}_6\text{N}_2\text{O}$ $[\text{M}]^+$: 420.16363. Found: 420.16452.



***N*-(3-(Benzyloxy)propyl)-*N*-(bicyclo[2.2.1]heptan-2-yl)-3,5-bis(trifluoromethyl)benzohydrazide (3.39g) and *N*-(3-(benzyloxy)propyl)-*N*-(bicyclo[2.2.1]heptan-2-yl)-3,5-bis(trifluoromethyl)benzohydrazide (3.40g).**

Synthesized according to General Procedure E on 0.487 mmol of the parent alkylated hydrazide and norbornene, reacted for 18 hours at 160 °C. Isolated 0.166 g of **3.39g** as a white solid and 0.051 g of **3.40g** (86% yield, 3.31:1) after column chromatography (15% EtOAc/hexanes). **3.39g**: TLC R_f 0.50 (25% EtOAc/hexanes). ^1H NMR (DMSO- d_6 , 300 MHz, 120 °C): δ ppm 9.31 (s, 1H), 8.43 (s, 2H), 8.17 (s, 1H), 7.37-7.20 (m, 5H), 4.45 (s, 2H), 3.59 (s, 2H), 2.93 (m, 3H), 2.30-2.17 (m, 2H), 1.78-1.65 (m, 3H), 1.45-1.37 (m, 4H), 1.09-1.03 (m, 3H). ^{13}C NMR (DMSO- d_6 , 75 MHz, 120 °C): δ ppm 162.2, 138.4, 136.2, 130.2 (q, $J = 33.6$ Hz, CCF_3), 127.5, 126.7, 126.5, 123.7, 122.6 (q, $J = 273.0$ Hz, CF_3), 71.5, 67.9, 67.4, 49.9, 39.1, 36.2, 35.3, 34.2, 27.9, 27.0, 26.0. IR (film): 3253, 3082, 2948, 2868, 2853, 1652, 1550, 1279, 1143, 1128 cm^{-1} . HRMS (EI): Exact mass calculated for $\text{C}_{26}\text{H}_{28}\text{F}_6\text{N}_2\text{O}_2$ $[\text{M}]^+$: 514.20550. Found: 514.19754. **3.40g**: TLC R_f 0.81 (25% EtOAc/hexanes). ^1H NMR (300 MHz; DMSO- d_6 , 120 °C): δ ppm 8.10 (s, 2H), 8.03 (s, 1H), 7.34-7.24 (m, 5H), 4.94 (t, $J = 5.9$ Hz, 1H), 4.36 (s, 2H), 3.72 (dd, $J = 7.4, 5.6$ Hz, 1H), 3.33 (t, $J = 6.3$ Hz, 2H), 2.45 (s, 2H), 2.28 (s, 1H), 1.90-1.84 (m, 2H), 1.62-1.46 (m, 6H), 1.11 (dd, $J = 19.5, 10.7$ Hz, 3H). ^{13}C NMR (DMSO- d_6 , 75 MHz, 120 °C): δ ppm 167.7, 139.7, 138.1, 129.6 (q, $J = 33.1$ Hz, CCF_3), 127.5, 127.3, 126.5, 126.4, 122.5 (q, $J = 273.1$ Hz, CF_3), 121.6, 71.4, 67.3, 61.1, 47.4, 40.2, 36.0, 35.3, 34.9, 27.2, 27.1. IR (film): 3282, 2955, 2873, 1641, 1326, 1279, 1268, 1169, 1137, 1101, 905, 848, 763, 749 cm^{-1} . HRMS (EI): Exact mass calculated for $\text{C}_{26}\text{H}_{28}\text{F}_6\text{N}_2\text{O}_2$ $[\text{M}]^+$: 514.20550. Found: 514.19897.

◆ CLEAVAGE OF THE *N-N* BOND FOR PROOF OF STRUCTURE:



***N*-(Bicyclo[2.2.1]heptan-2-yl)-3,5-bis(trifluoromethyl)benzamide (3.41)**

Sml₂ preparation: In a flame-dried round-bottom flask was added Sm powder (0.189 g, 1.28 mmol), which was stirred neat under high vacuum for 30 min. After purging with argon for 5 min, diiodoethane (freshly recrystallized, 0.282 g, 1.00 mmol) was added the resulting solid mixture was further purged for 15 min under high vacuum, and filled with argon. To the reaction flask was added freshly distilled THF (10 mL), to give a 0.1M solution of Sml₂. *Cleavage: Procedure adapted from the Maruoka group.*¹² To a stirred solution of the hydrazide (0.051 g, 0.10 mmol) in MeOH (0.5 mL) was added the Sml₂ in THF (0.1M) prepared above (4 mL) via syringe over 1 min. After 15 minutes of stirring at room temperature, the solution was shown to be complete by TLC analysis. The mixture was poured into sat. aq. NaHCO₃ and extracted 3 times with EtOAc. The combined organic layers were washed with brine, dried over Na₂SO₄, filtered and concentrated under reduced pressure. Silica-gel chromatography (20% EtOAc/hexanes) afforded the cleaved amide (0.031 g, 88%) as a colorless oil. TLC R_f 0.68 (25% EtOAc/hexanes). ¹H NMR (CDCl₃, 400 MHz): δ ppm 8.16 (s, 2H), 7.99 (s, 1H), 5.95 (br s, 1H), 3.94 (t, *J* = 7.4, 3.7, 1H), 2.37-2.36 (m, 1H), 1.94 (ddd, *J* = 13.1, 8.0, 2.4, 2H), 1.62-1.51 (m, 2H), 1.44-1.19 (m, 5H). ¹³C NMR (CDCl₃, 100 MHz): δ ppm 163.9, 137.0, 132.1 (q, *J* = 33.3 Hz, CCF₃), 127.2, 124.8, 122.9 (q, *J* = 273 Hz, CF₃), 77.2, 53.9, 42.3, 40.3, 35.7, 28.0, 26.5. IR (film): 3295, 3074, 2959, 2880, 1641, 1616, 1549, 1279, 1176, 1134, 908, 702, 681 cm⁻¹. HRMS (EI): Exact mass calculated for C₁₆H₁₅F₆NO [M]⁺: 351.10578. Found: 315.10766.

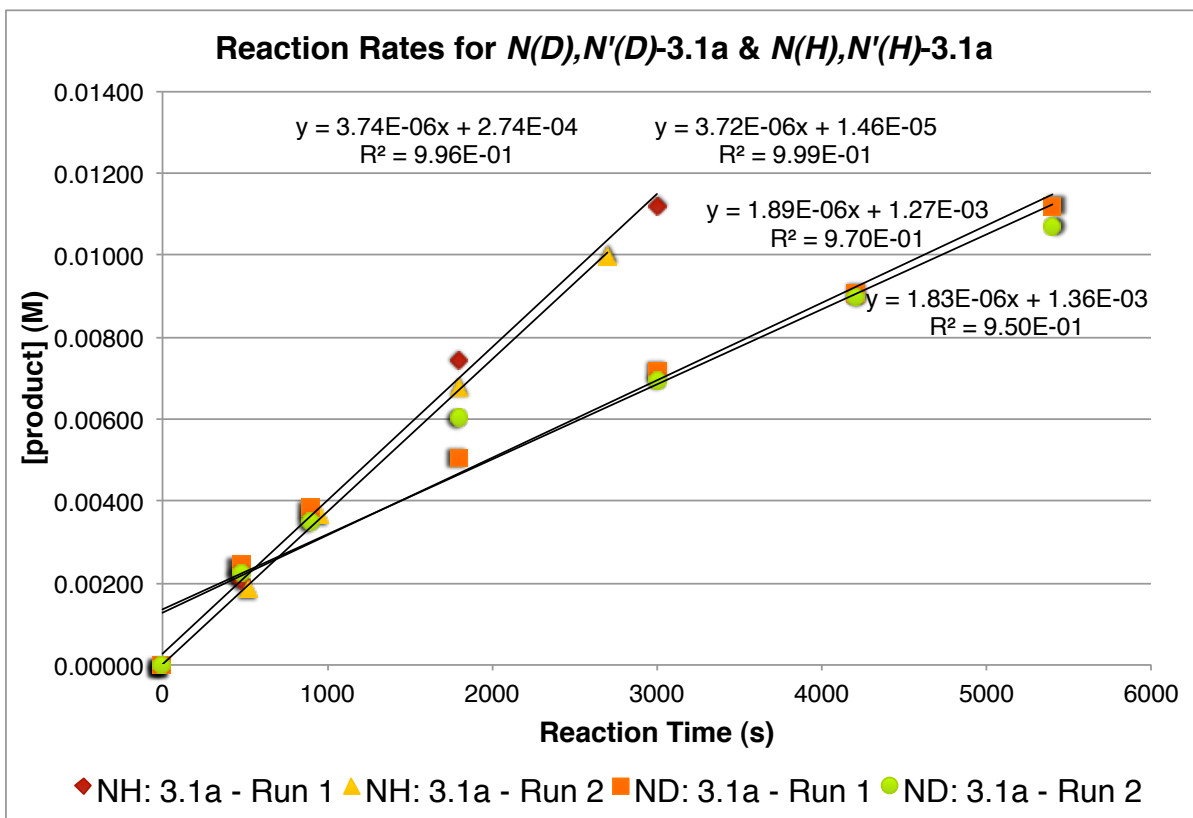
¹². Hashimoto, T.; Maeda, Y.; Omote, M.; Nakatsu, H.; Maruoka, K. *J. Am. Chem. Soc.* **2010**, *132*, 4076

◆ PRIMARY KIE BY DEUTERATION AT NITROGENS

N-deuteration procedure: **3.31a** was transferred into a flame dried and cooled Biotage microwave vial (0.5 – 2mL) and kept under an atmosphere of argon. N-phenylpyrrolidinone (internal standard found unreactive in the reaction conditions, and perfect for HPLC-UV tracing, 1028 mg) was added, followed by deuterated methanol (MeOD, 0.5 mL). The mixture was allowed to stir for 20 min at room temperature under argon. Then, the tube was placed under high vacuum to evaporate MeOD. Care was taken to minimize bumping of the reaction at this step. Once most of the MeOD was removed, the tube was refilled with argon and another portion of 0.5 mL MeOD was added. It was stirred for 20 min and then removed under high vacuum. This cycle was repeated until the mixture was allowed to stir 2 x 20 min in MeOD, and one final time with CD₃OD. After removal of the last portion of deuterated methanol, PhCF₃ was added (2.8 mL, 0.1 M) and the reaction vial was further purged for 2 minutes with argon.

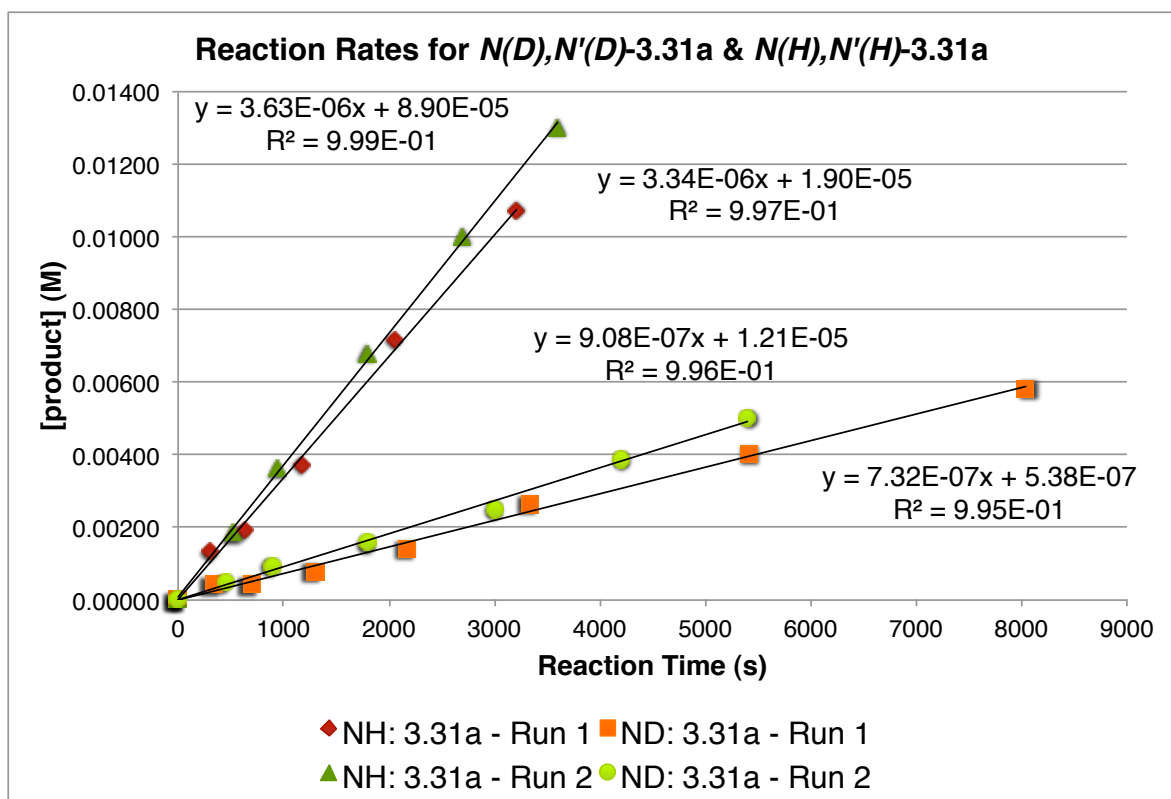
Kinetic Run: An initial aliquot was taken from the reaction through the use of a glass-tight syringe. The reaction vial was placed in a 90 °C oil bath, which was high enough to submerge the flask below the solvent level. At increasing time intervals (from 5 minutes early on to 30 minutes later in the reaction), aliquots were taken from the reaction with a glass-tight syringe and quickly transferred and diluted into a hexanes solution. The diluted samples were then run on the standard phase HPLC, and compared to the initial concentration of starting material to measure the rate of the reaction from the disappearance of starting material.

Additional Runs: The same procedure was used to deuterate substrate **3.1a** at the nitrogen positions, and all reactions, with standard and deuterated **3.1a** and **3.31a** were run twice to get a better estimate of the results. Again, averages were calculated and errors propagated from the combination of the two runs, each giving a slightly different value for the rate.



$N(H),N'(H)$ -3.1a			
Run 1		Run 2	
time (sec)	[product] (M)	time (sec)	[product] (M)
0	0.00000	0	0.00000
480	0.00209	525	0.00187
900	0.00377	950	0.00366
1800	0.00742	1800	0.00679
3000	0.01120	2700	0.00999
$k(H) = 3.74 \times 10^{-5} \text{ s}^{-1}$		$k(H) = 3.72 \times 10^{-5} \text{ s}^{-1}$	
$k(H)_{\text{avg}} = 3.73 (\pm 0.01) \times 10^{-5} \text{ s}^{-1}$			

$N(D),N'(D)$ -3.1a			
Run 1		Run 2	
time (sec)	[product] (M)	time (sec)	[product] (M)
0	0.00000	0	0.00000
480	0.00245	480	0.00222
900	0.00382	900	0.00350
1800	0.00507	1800	0.00603
3000	0.00717	3000	0.00696
4200	0.00904	4200	0.00897
5400	0.01118	5400	0.01068
$k(D) = 1.89 \times 10^{-5} \text{ s}^{-1}$		$k(D) = 1.83 \times 10^{-5} \text{ s}^{-1}$	
$k(D)_{\text{avg}} = 1.86 (\pm 0.03) \times 10^{-5} \text{ s}^{-1}$			



$N(H), N'(H)$-3.31a			
Run 1		Run 2	
time (sec)	[product] (M)	time (sec)	[product] (M)
0	0.00000	0	0.00000
310	0.00133	525	0.00187
630	0.00191	950	0.00366
1180	0.00375	1800	0.00679
2060	0.00713	2700	0.00999
3210	0.01071	3600	0.01298
$k(H) = 3.34 \times 10^{-5} \text{ s}^{-1}$		$k(H) = 3.63 \times 10^{-5} \text{ s}^{-1}$	
$k(H)_{\text{avg}} = 3.5 (\pm 0.2) \times 10^{-5} \text{ s}^{-1}$			

$N(D), N'(D)$-3.31a			
Run 1		Run 2	
time (sec)	[product] (M)	time (sec)	[product] (M)
0	0.00000	0	0.00000
340	0.00044	450	0.00047
700	0.00043	900	0.00094
1300	0.00081	1800	0.00159
2180	0.00142	3000	0.00251
3330	0.00266	4200	0.00387
5420	0.00402	5400	0.00501
8040	0.00583	6900	0.00594
$k(D) = 7.32 \times 10^{-6} \text{ s}^{-1}$		$k(D) = 9.08 \times 10^{-6} \text{ s}^{-1}$	
$k(D)_{\text{avg}} = 8.2 (\pm 0.9) \times 10^{-6} \text{ s}^{-1}$			

◆ SECONDARY KIE BY DEUTERATION ON ALKENE

Preparation of deuterated SM.

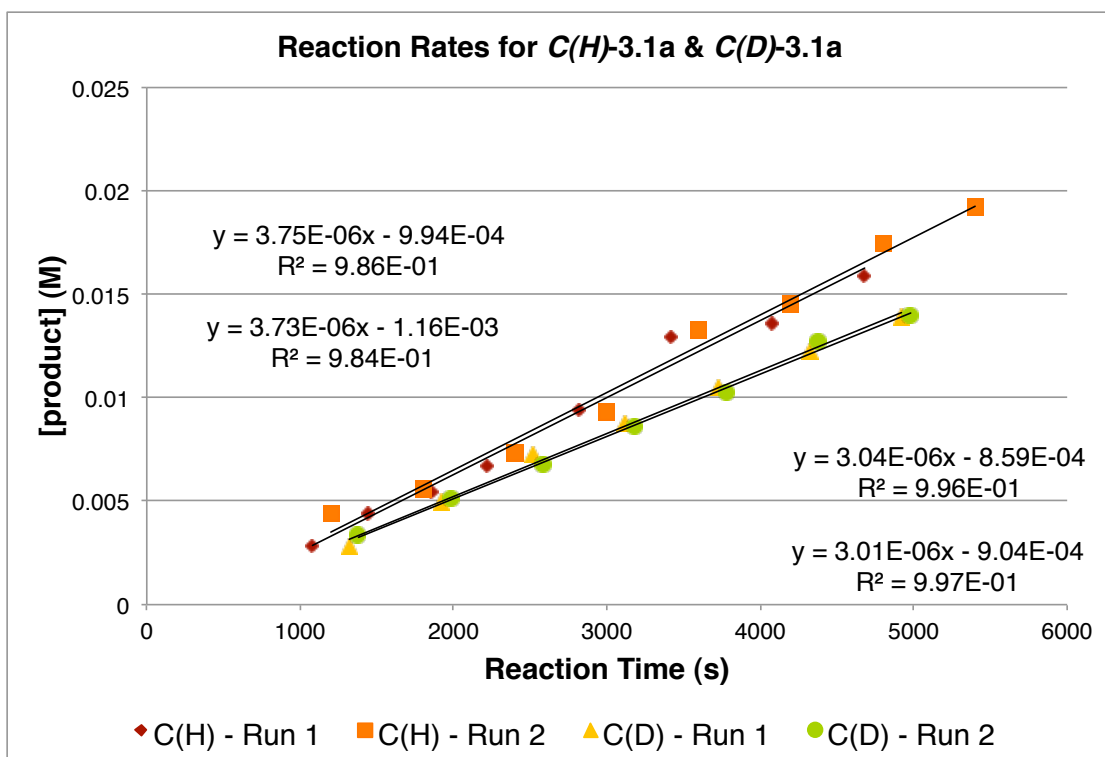
4-deutero-4-penten-1-ol was prepared from 4-pentyn-ol following a procedure from Gao & Hoveyda.¹³ Synthesis of the deuterated **3.1a** and followed standard procedures for the oxidation of the alcohol, condensation of benzoic hydrazide and reduction with sodium cyanoborohydride. All spectra looked identical to the non-deuterated version of the compound, albeit with a missing alkene proton signal.

Kinetic Runs.

In a 13x100 mm nmr test tube was added 1,3,5-trimethoxybenzene (the internal standard, 3.36 mg, 0.020 mmol, 0.333 equiv.) and the deuterated **3.1a** (12.3 mg, 0.06 mmol). The test tube was sealed with a rubber septum and flushed with argon after which deuterated DMSO (0.6 mL) was added. The reaction was analyzed a first time by NMR at room temperature to evaluate the exact quantity of internal standard present. The reaction was progressively heated to reach a temperature of 100°C, ensuring a constant heating process across trials. For the first scans at 10 and 15 minutes, the instrument was always re-tuned and shimmed, as temperature fluctuations affected the integration values and general look of the spectra. NMR analyses were then programmed for 2 hours at 10-minute time intervals. In the analysis of the data, correction for the internal standard value based on the initial run at room temperature was consistently better in interpreting the appearance of product. The concentration of product formed was determined by integrating the product's peak ($\delta = 1.05$ ppm (d, 3H)) relative to the internal standard peak ($\delta = 6.08$ ppm).

The exact same protocol was employed for the determination of the rate of the reaction with non-deuterated starting material. Each reaction was run twice and the average of the slopes were used to determine k_H and k_D respectively.

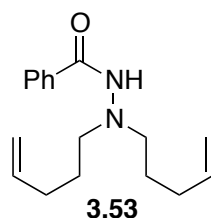
¹³ Gao, F.; Hoveyda, A. H. *J. Am. Chem. Soc.* **2010**, 132, 10961.



C(H)-3.1a			
Run 1		Run 2	
time (sec)	[product] (M)	time (sec)	[product] (M)
1080	0.00280	1200	0.00438
1440	0.00439	1800	0.00557
1860	0.00541	2400	0.00732
2220	0.00669	3000	0.00928
2820	0.00942	3600	0.01327
3420	0.01295	4200	0.01454
4080	0.01359	4800	0.01746
4680	0.01591	5400	0.01924
$k(H) = 3.75 \times 10^{-5} \text{ s}^{-1}$		$k(H) = 3.73 \times 10^{-5} \text{ s}^{-1}$	
$k(H)_{\text{avg}} = 3.74 (\pm 0.1) \times 10^{-5} \text{ s}^{-1}$			

C(D)3.1a			
Run 1		Run 2	
time (sec)	[product] (M)	time (sec)	[product] (M)
1320	0.00279	1380	0.00334
1920	0.00499	1980	0.00512
2520	0.00727	2580	0.00675
3120	0.00876	3180	0.00858
3720	0.01048	3780	0.01027
4320	0.01227	4380	0.01270
4920	0.01392	4980	0.01398
$k(D) = 3.04 \times 10^{-5} \text{ s}^{-1}$		$k(D) = 3.01 \times 10^{-5} \text{ s}^{-1}$	
$k(D)_{\text{avg}} = 3.03 (\pm 0.02) \times 10^{-5} \text{ s}^{-1}$			

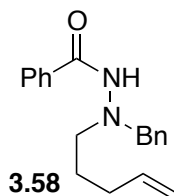
◆ SYNTHESIS OF TRI-SUBSTITUTED HYDRAZINE SUBSTRATES



***N',N'*-di(pent-4-en-1-yl)benzohydrazide.**

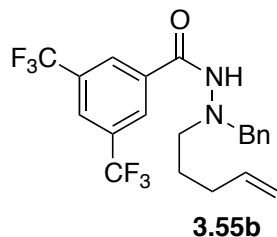
The corresponding aldehyde was synthesised according to general procedure B using pent-4-en-1-ol (0.834 g, 9.68 mmol, 1 equiv). The aldehyde (0.814 g, 9.68 mmol, 1.2 equiv), benzohydrazide (1.07 g, 8.07 mmol, 1 equiv) and methanol (48 mL) were then stirred together at room temperature for 100 min under argon atmosphere. 40 mL of a (1 : 1) solution of H₂O/Brine was added and the reaction mixture was extracted three times with 40 mL of dichloromethane. The combined organic layers were then dried with sodium sulfate, filtered and concentrated under reduced pressure. The resulting mixture was added to methanol (90 mL) and sodium cyanoborohydride (1.33 g, 19.4 mmol, 2.4 equiv) was then added. Glacial acetic acid (45 mL) was added at once and the reaction mixture was stirred at room temperature for 2h. Most of the glacial acetic acid was evaporated under reduced pressure and a saturated sodium bicarbonate solution was added dropwise to have a pH of 8.0. The reaction mixture was then extracted three times with 100 mL of dichloromethane. The combined organic layers were then dried with sodium sulfate, filtered, concentrated under reduced pressure and isolated using flash chromatography (40% ethyl acetate in hexanes). The compound was obtained as a yellow solid (106 mg, 5% yield from the alcohol). TLC R_f 0.50 (40% EtOAc in hexanes); ¹H NMR (benzene-*d*₆, 300 MHz, CDCl₃) δ ppm 7.63-7.46 (m, 2H), 7.11-6.94 (m, 3H), 6.34 (s, 1H), 5.77 (tdd, *J* = 16.91, 10.15, 6.72, 6.72 Hz, 2H), 5.13-4.92 (m, 4H), 2.82 (t, *J* = 7.00, 7.00 Hz, 4H), 2.12 (q, *J* = 7.12, 7.12, 7.11 Hz, 4H), 1.61-1.47 (m, 4H); ¹³C NMR (benzene-*d*₆, 75 MHz) δ ppm 166.1 (C), 138.9 (CH), 134.9 (C), 131.2 (CH), 128.6 (CH), 127.4 (CH), 114.9 (CH₂), 56.6 (CH₂), 31.6 (CH₂), 27.3

(CH₂); IR (film) 3237, 3064, 2949, 2838, 1646, 1541, 1462, 1306, 994, 912, 695, 667 cm⁻¹; HRMS (EI): Exact mass calcd for C₁₇H₂₄N₂O [M]⁺: 272.1889. Found: 272.1892.



***N*'-benzyl-*N*'-(pent-4-en-1-yl)benzohydrazide (3.58).**

N'-(pent-4-en-1-yl)benzohydrazide (500 mg, 2.44 mmol, 1 equiv), methanol (12 mL) and powder sieves (150 mg) are mixed together in a round balloon flask at room temperature. Benzaldehyde (387 mg, 3.66 mmol, 1.5 equiv) was added dropwise. Sodium cyanoborohydride (336 mg, 4.87 mmol, 2 equiv) was added and then, glacial acetic acid (745 mg, 12.2 mmol, 5 equiv) was added all at once. The reaction mixture was stirred at room temperature for 3h. 30 mL of a saturated solution of sodium bicarbonate was added. The reaction mixture was extracted three times with 30 mL of ethyl acetate. The organic layer was then dried with sodium sulfate, filtered, concentrated under reduced pressure and isolated using flash chromatography on silver nitrate treated silica gel (6% *i*-PrOH in dichloromethane). The compound was obtained as an orange oil (472 mg, 66% yield). TLC R_f 0.56 (6% *i*-PrOH in dichloromethane); ¹H NMR (CDCl₃, 400 MHz) δ ppm 7.64-7.51 (m, 2H), 7.50-7.42 (m, 1H), 7.41-7.26 (m, 7H), 6.79 (s, 1H), 5.80 (tdd, J = 16.90, 10.18, 6.66, 6.66 Hz, 1H), 5.06-4.89 (m, 2H), 4.18 (s, 2H), 3.07-2.95 (m, 2H), 2.20-2.09 (m, 2H), 1.75-1.64 (m, 2H). ¹³C NMR (CDCl₃, 400 MHz) δ ppm 166.9 (C), 138.2 (CH), 136.4 (C), 133.9 (C), 131.5 (CH), 129.5 (CH), 128.6 (CH), 128.4 (CH), 127.6 (CH), 126.8 (CH), 114.7 (CH₂), 61.0 (CH₂), 55.7 (CH₂), 31.2 (CH₂), 26.8 (CH₂); HRMS (EI): Exact mass calcd for C₁₉H₂₂N₂O [M]⁺: 294.1732 Not found. Exact mass calcd for C₁₂H₁₆N [M - C₇H₆NO]: 174.1283. Found: 174.1295.



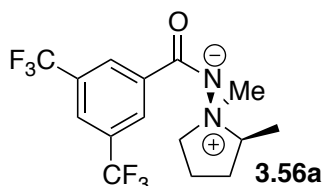
***N*-benzyl-*N*-(pent-4-en-1-yl)-3,5-bis(trifluoromethyl)benzohydrazide (3.55b).**

N-(pent-4-en-1-yl)-3,5-bis(trifluoromethyl)benzohydrazide (500 mg, 1.46 mmol, 1 equiv), methanol (7.3mL) and powder sieves (160 mg) are mixed together in a round balloon flask at room temperature. Benzaldehyde (223 mg, 2.19 mmol, 1.5 equiv) was added dropwise. Sodium cyanoborohydride (201 mg, 2.92 mmol, 2 equiv) was added and then, glacial acetic acid (451 mg, 7.3 mmol, 5 equiv) was added all at once. The reaction mixture was stirred at room temperature for 3h. 30 mL of a saturated solution of sodium bicarbonate was added. The reaction mixture was extracted three times with 30 mL of ethyl acetate. The organic layer was then dried with sodium sulfate, filtered, concentrated under reduced pressure and isolated using flash chromatography (1% isopropanol in dichloromethane). The compound was obtained as a white solid (245 mg, 39% yield). TLC R_f 0.40 (2% isopropanol in dichloromethane); (mix of isomers) ^1H NMR (DMSO-*d*₆, 300 MHz, 120 °C) δ ppm 9.65-9.24 (m, 1H), 8.31-8.00 (m, 3H), 7.53-7.09 (m, 5H), 5.97-5.63 (m, 1H), 5.04-4.85 (m, 2H), 4.23-3.92 (m, 2H), 3.06-2.91 (m, 2H), 2.31-1.94 (m, 2H), 1.69-1.51 (m, 2H). ^{13}C NMR (DMSO-*d*₆, 400 MHz) δ ppm 168.1 (C'), 162.2 (C), 138.5 (CH), 137.9 (CH'), 137.8 (C), 137.4 (C'), 136.1 (C'), 136.1 (C), 130.3 (q, $J = 33$ Hz, C), 129.1 (q, $J = 33$ Hz, C'), 128.7 (CH), 128.4 (CH'), 127.9 (CH), 127.9 (CH'), 127.2 (CH'), 126.9 (CH), 124.7 (C), 124.6 (C), 124.6 (C), 122.9 (q, $J = 273$, C'), 122.9 (q, $J = 273$, C'), 122.9 (CH'), 114.6 (CH₂), 114.6 (CH₂'), 61.6 (CH₂'), 60.5 (CH₂), 57.4 (CH₂'), 54.9 (CH₂), 30.6 (CH₂), 30.5 (CH₂'), 26.1 (CH₂), 25.4 (CH₂'); IR (film) 3231, 3068, 2938, 2843, 1662, 1553, 1455, 1381, 1287, 1132, 908, 699 cm^{-1} ; HRMS (EI): Exact mass calcd for C₂₁H₂₀F₆N₂O [M]⁺: 430.1480 Not found. Exact mass calcd for C₁₄H₁₃F₆N₂O [M – C₇H₇]: 339.0932. Found: 339.0907.

◆ ISOLATION OF DIPOLAR AMINE IMIDE INTERMEDIATES

General Procedure F for synthesis of dipolar amine imide intermediates (Table 3.14)

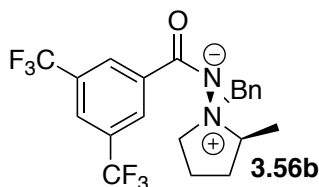
An oven dried sealed tube was charged with a stir bar, capped with a septum and purged with argon and an outlet for 5 minutes. The corresponding hydrazide (1.00 equiv) is added to the vial, and diluted with α,α,α -trifluorotoluene (such that the concentration of the hydrazide is 0.05 M), while keeping an argon atmosphere. The septum was removed and the tube was then quickly sealed with a microwave cap and heated for 12 h at 80 °C to 110 °C. The tube was cooled to ambient temperature, concentrated under reduced pressure and analyzed by ^1H NMR using 1,4-dimethoxybenzene or 1,3,5-trimethoxybenzene as an internal standard, then again concentrated under reduced pressure and purified by silica gel chromatography to give the amine imide intermediates.



***cis*-N-(3,5-bis(trifluoromethyl)benzoyl)-1,2-dimethylpyrrolid-1-ium 1-amidine (3.56a)**

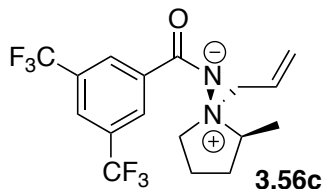
Synthesised according to General Procedure F (110 °C, 12h) using *N'*-methyl-*N'*-(pent-4-en-1-yl)-3,5-bis(trifluoromethyl)benzohydrazide (**3.55a**) 156 mg, 0.44 mmol, 1 equiv). The reaction mixture was concentrated under reduced pressure. The amine imide was obtained as oil (> 98% ^1H NMR) and characterized without further purification. TLC R_f 0.33 (2% MeOH in CH_2Cl_2). ^1H NMR (300 MHz, CDCl_3) δ ppm 8.42 (s, 2 H), 7.79 (s, 1 H), 4.86 - 5.08 (m, 1 H), 3.49 (s, 3 H), 3.33 - 3.48 (m, 1 H), 3.14 - 3.31 (m, 1 H), 1.85 - 2.25 (m, 4 H), 1.50 (d, $J=6.40$ Hz, 3 H); ^{13}C NMR (75 MHz, CDCl_3) δ ppm 166.5 (C), 141.3 (C), 131.2 (q, $J=33.2$ Hz, 2 C), 127.7 (d, $J=2.7$ Hz, 2 CH), 125.3 (C), 122.6 (quint. $J=3.84$ Hz, CH), 121.7 (C), 74.9 (CH_3), 62.72

(CH₂), 47.8 (CH), 29.30 (CH₂), 19.1 (CH₂), 13.4 (CH₃); COSY & NOESY spectrum are provided and analyzed within the next subsection. IR (film) 3746, 3629, 2364, 2341, 2323, 1698, 1653, 1563, 1504, 1454, 1081 cm⁻¹; HRMS (EI): Exact mass calcd for C₁₅H₁₆F₆N₂O [M]⁺ = 355.1167 found 354.1151



***cis*-1-Benzyl-*N*-(3,5-bis(trifluoromethyl)benzoyl)-2-methyl pyrrolid-1-ium 1-amidine (3.56b)**

Synthesised according to General Procedure F (110 °C, 12h) using *N'*-benzyl-*N'*-(pent-4-en-1-yl)-3,5-bis(trifluoromethyl)benzohydrazide (**3.55b**) 103 mg, 0.239 mmol, 1 equiv). The reaction mixture was concentrated under reduced pressure and isolated using flash chromatography (4% isopropanol in dichloromethane). The compound was kept under an argon atmosphere post purification. The amine imide was obtained as a yellow oil (34% ¹H NMR conv), with impurities still present. Complete characterization is unavailable., with all. TLC R_f 0.40 (4% MeOH in CH₂Cl₂). ¹H NMR (DMSO-d₆, 300 MHz) δ ppm 8.49-8.32 (m, 3H), 7.46-7.31 (m, 5H), 5.43 (d, *J* = 12.82 Hz, 1H), 4.62 (d, *J* = 12.82 Hz, 1H), 4.41-4.22 (m, 1H), 3.85-3.67 (m, 1H), 3.28-3.23 (m, 1H), 2.08-1.60 (m, 4H), 1.36-1.25 (m, 3H) cm⁻¹; COSY & NOESY spectrum are provided and analyzed within the next subsection.



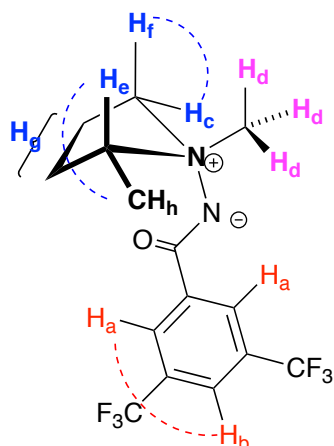
***cis*-1-Allyl-*N*-(3,5-bis(trifluoromethyl)benzoyl)-2-methyl pyrrolid-1-ium 1-amidine (3.56c)**

Synthesised according to General Procedure F (80 °C, 12h) using *N'*-allyl-*N'*-(pent-4-en-1-yl)-3,5-bis(trifluoromethyl)benzohydrazide (**3.55c**) 167 mg, 0.44 mmol, 1

equiv). The reaction mixture was concentrated under reduced pressure. The amine imide was obtained as oil (35% yield) after flash chromatography (1% MeOH in CH₂Cl₂). TLC R_f 0.42 (2% MeOH in CH₂Cl₂). ¹H NMR (300 MHz, CDCl₃) δ ppm 8.45 (s, 2 H), 7.82 (s, 1 H), 5.82 - 6.11 (m, 1 H), 5.39 - 5.64 (m, 2 H), 5.24 (dd, *J*=13.50, 7.10 Hz, 1 H), 4.50 - 4.75 (m, 1 H), 3.94 (dd, *J*=13.50, 7.65 Hz, 1 H), 3.73 (d, *J*=7.10 Hz, 1 H), 3.35 - 3.52 (m, 1 H), 1.98 - 2.21 (m, 2 H), 1.77 - 1.99 (m, 2H), 1.48 (d, *J*=6.40 Hz, 3 H); ¹³C NMR (75 MHz, CDCl₃) δ ppm 166.3 (C), 141.4 (C), 131.3 (C), 130.8 (C), 130.4 (C), 127.7 (2 CH), 127.2 (CH), 125.3 (CH₂), 122.5 (CH), 121.8 (C), 69.7 (CH), 60.2 (CH₂), 58.5 (CH₂), 29.0 (CH₂), 18.9 (CH₂), 13.8 (CH₃); COSY & NOESY spectrum are provided and analyzed within the next subsection. IR (film) 3747, 2361, 2323, 1703, 1652, 1638, 1548, 1089 cm⁻¹; HRMS (EI): Exact mass calcd for C₁₅H₁₆F₆N₂O [M]⁺ = 380.1323. Not found. Exact mass calcd for [M - CH₂CH=CH₂]⁺ = 339.0932. Found. 339.0964.

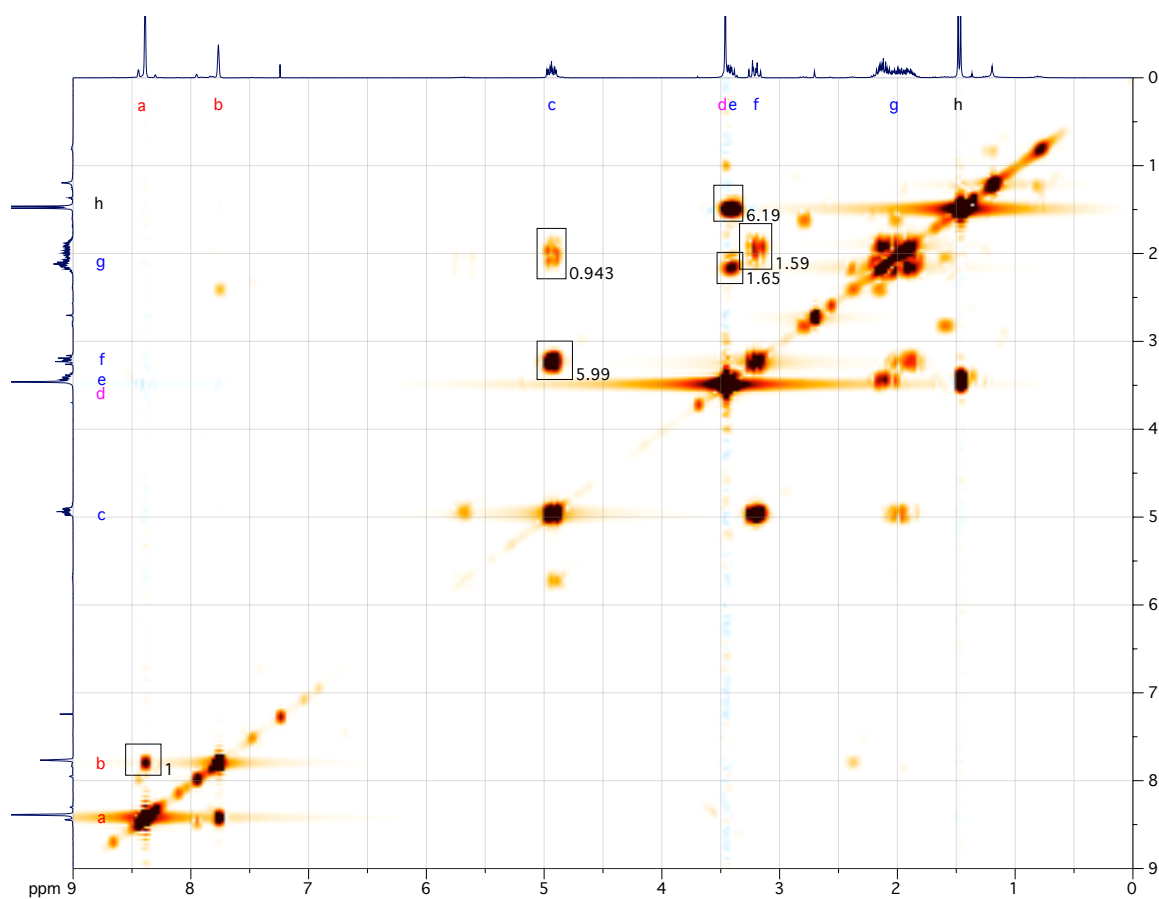
◆ STRUCTURAL ASSIGNMENT OF DIPOLAR AMINE IMIDE INTERMEDIATES

cis-*N*-(3,5-bis(trifluoromethyl)benzoyl)-1,2-dimethylpyrrolid-1-ium 1-amidine (3.56a) – COSY Spectra

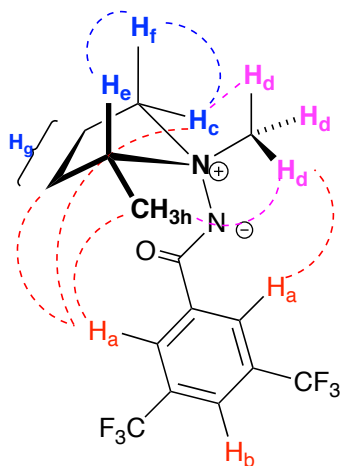


Proton(s)	δ (ppm)	COSY Interactions
<i>a</i>	8.42	<i>b</i> (strong)
<i>b</i>	7.79	<i>a</i> (strong)
<i>c</i>	4.86 - 5.08	<i>f</i> (strong), <i>g</i>
<i>d</i>	3.49	--
<i>e</i>	3.33 - 3.48	<i>g</i> , <i>h</i> (strong)
<i>f</i>	3.14 - 3.31	<i>c</i> (strong), <i>g</i>
<i>g</i>	1.85 - 2.25	<i>c</i> , <i>e</i> , <i>f</i>
<i>h</i>	1.50	<i>e</i> (strong)

in red: Benzoyl hydrazide protons. in purple: methyl substituent. in blue: pyrrolidine ring. in black: methyl substituent on the pyrrolidine ring.

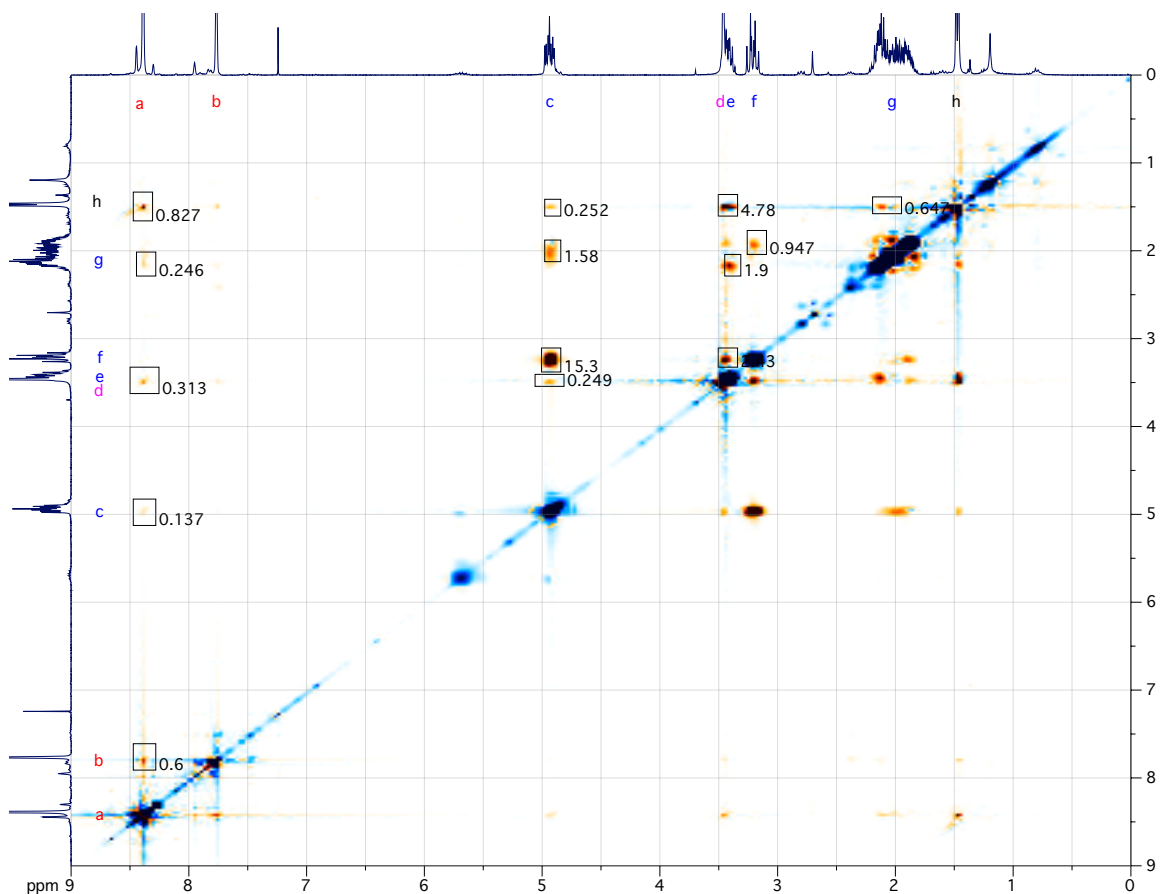


***cis*-N-(3,5-bis(trifluoromethyl)benzoyl)-1,2-dimethylpyrrolid-1-ium 1-amidine (3.56a) – NOESY Spectra**

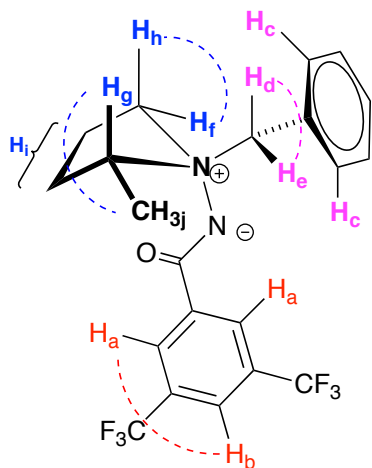


Proton(s)	δ (ppm)	NOESY Interactions
a	8.42	b, c, d, g, h
b	7.79	a
c	4.86 - 5.08	a, d, f, g, h
d	3.49	a, c, h
e	3.33 - 3.48	f, g, h
f	3.14 - 3.31	c, e, g
g	1.85 - 2.25	a, c, e, f, h
h	1.50	a, c, d, e, g

in red: Benzoyl hydrazide protons. in purple: methyl substituent. in blue: pyrrolidine ring. in black: methyl substituent on the pyrrolidine ring.

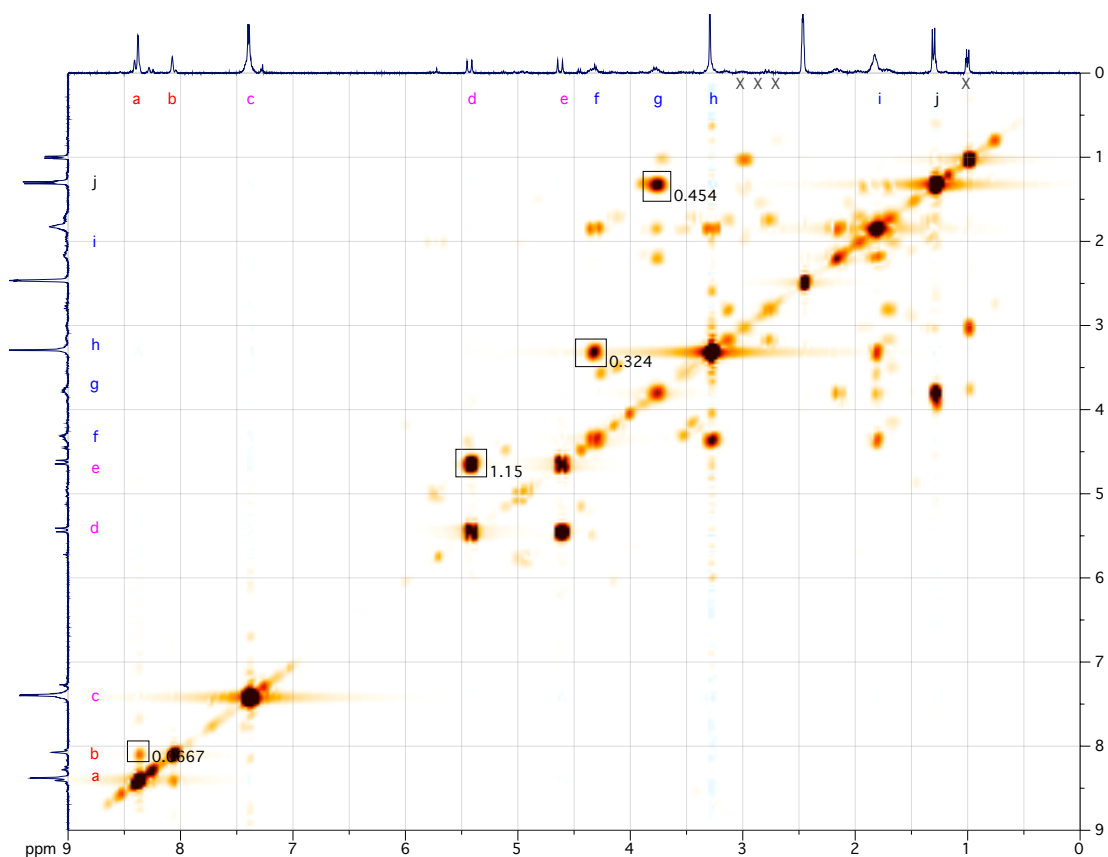


***cis*-1-Benzyl-*N*-(3,5-bis(trifluoromethyl)benzoyl)-2-methyl pyrrolid-1-ium 1-amidinium (3.56B) – COSY Spectra**

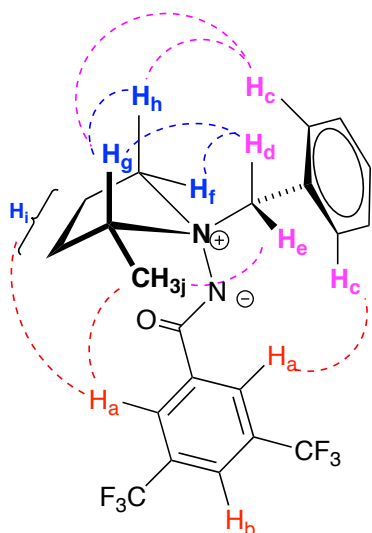


Proton(s)	δ (ppm)	COSY Interactions
a	8.37	b
b	8.07	a
c	7.31 - 7.46	-
d	5.42	e
e	4.62	d
f	4.25 - 4.39	h, i
g	3.77	i, j
h	3.21 - 3.34	f, i
i	1.61 - 2.27	f, g, h
j	1.29	g

in red: Benzoyl hydrazide protons. in purple: benzyl substituent. in blue: pyrrolidine ring. in black: methyl substituent on the pyrrolidine ring.

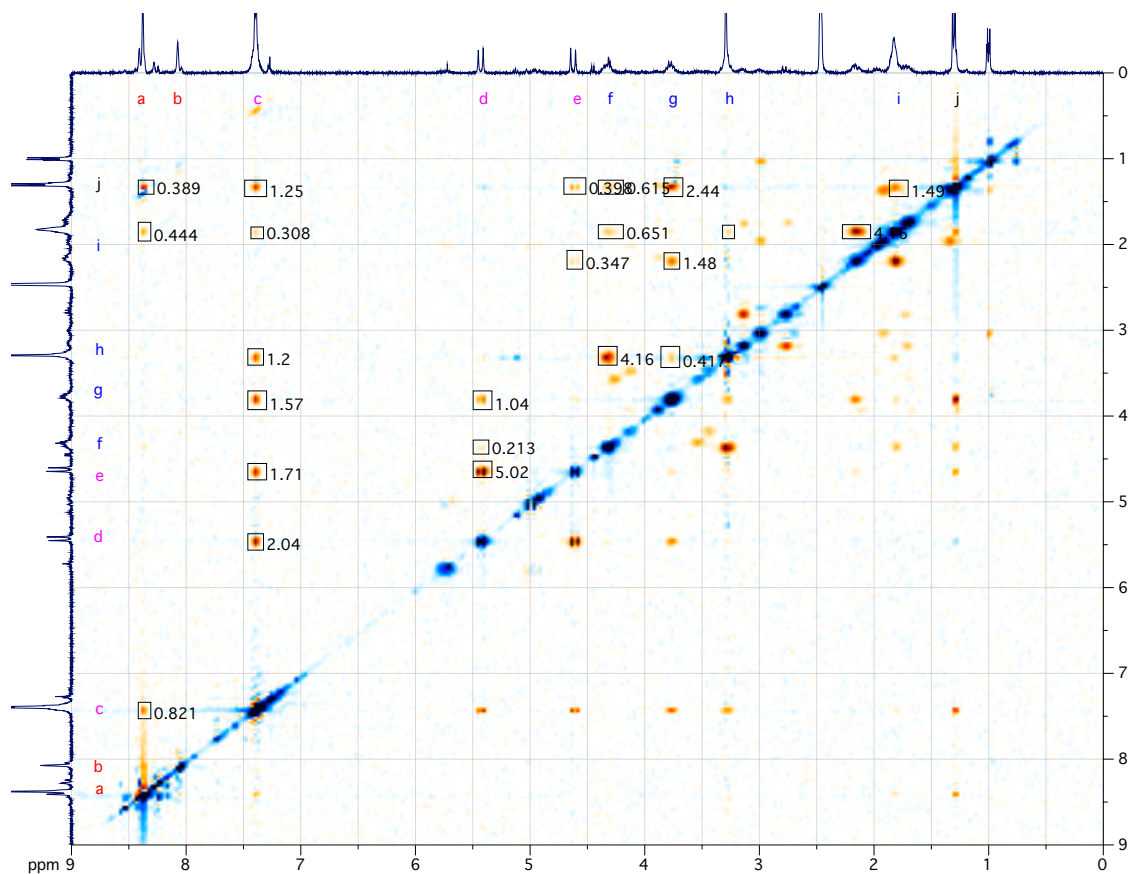


***cis*-1-Benzyl-*N*-(3,5-bis(trifluoromethyl)benzoyl)-2-methyl pyrrolid-1-ium 1-amidinium (3.56B) – NOESY Spectra**



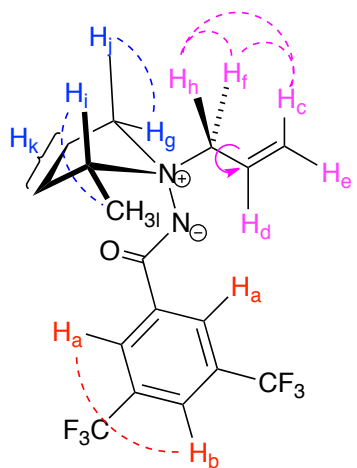
Proton(s)	δ (ppm)	NOESY Interactions
a	8.37	c, i, j
b	8.07	-
c	7.31 - 7.46	a, d, e, g, h, i, j
d	5.42	c, e, f, g
e	4.62	c, d, i, j
f	4.25 - 4.39	d, h, i, j
g	3.77	c, d, h, i, j
h	3.21 - 3.34	c, f, g, i, j
i	1.61 - 2.27	a, c, f, g, h, j
j	1.29	a, c, f, i

in red: Benzoyl hydrazone protons. in purple: benzyl substituent. in blue: pyrrolidine ring. in black: methyl substituent on the pyrrolidine ring.



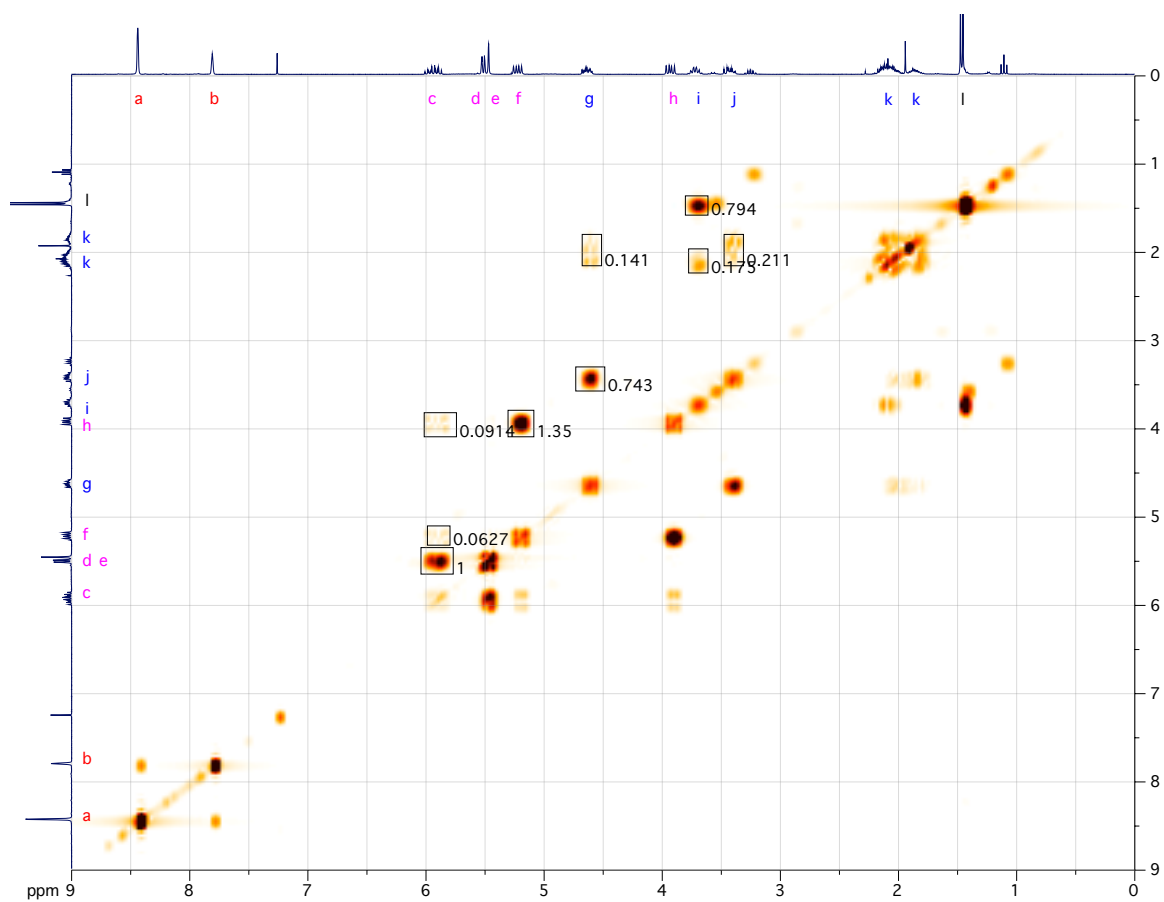
***cis*-1-Allyl-*N*-(3,5-bis(trifluoromethyl)benzoyl) -2-methyl pyrrolid-1-ium 1-**

amidine (3.56c) – COSY Spectra



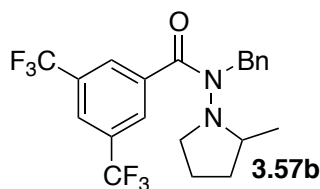
Proton(s)	δ (ppm)	COSY Interactions
<i>a</i>	8.44	<i>b</i>
<i>b</i>	7.81	<i>a</i>
<i>c</i>	5.94	<i>d/e</i> (strong), <i>f</i> , <i>h</i>
<i>d/e</i>	5.52 & 5.57	<i>c</i> (strong)
<i>f</i>	5.23	<i>c</i> , <i>h</i> (strong)
<i>g</i>	4.64	<i>j</i> (strong), <i>k</i>
<i>h</i>	3.93	<i>c</i> , <i>f</i> (strong)
<i>i</i>	3.72	<i>l</i> (strong), <i>k</i>
<i>j</i>	3.43	<i>g</i> (strong), <i>k</i>
<i>k</i>	(1.96 - 2.24) & (1.77 - 1.92)	<i>g</i> , <i>i</i> , <i>j</i>
<i>l</i>	1.47	<i>i</i> (strong)

in red: Benzoyl hydrazide protons. in purple: allyl substituent. in blue: pyrrolidine ring. in black: methyl substituent on the pyrrolidine ring.



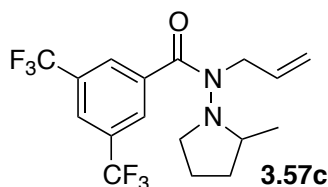
***cis*-1-Allyl-*N*-(3,5-bis(trifluoromethyl)benzoyl) -2-methyl pyrrolid-1-ium 1-**

◆ [1,2] & [1,3]-SHIFT OF TRISUBSTITUTED HYDRAZINE SUBSTRATES



***N*-benzyl-*N*-(2-methylpyrrolidin-1-yl)-3,5-bis(trifluoromethyl)benzamide (3.57b).**

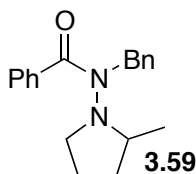
Synthesised according to General Procedure D (150 °C, 12h) using *N*-benzyl-*N*-(pent-4-en-1-yl)-3,5-bis(trifluoromethyl)benzohydrazide (50 mg, 0.12 mmol, 1 equiv). The reaction mixture was concentrated under reduced pressure and isolated using flash chromatography (2% isopropanol in dichloromethane). The compound was obtained as a yellow oil (32.8 mg, 66% yield). TLC R_f 0.72 (2% isopropanol in dichloromethane); ^1H NMR (DMSO- d_6 , 300 MHz, 120 °C) δ ppm 8.17-7.96 (m, 3H), 7.48-7.17 (m, 5H), 4.77 (q, J = 15.64, 15.42, 15.42 Hz, 2H), 3.16-2.99 (m, 1H), 2.98-2.89 (m, 2H), 1.97-0.80 (m, 4H), 0.69 (d, J = 6.12 Hz, 3H). ^{13}C NMR (DMSO, 400 MHz) δ ppm 169.3 (C), 139.3 (C), 138.4 (C), 129.4 (q, J = 33 Hz, C), 128.3 (CH), 127.2 (CH), 126.8 (CH), 123 (q, J = 273 Hz, C), 55.2 (CH), 50.2 (CH₂), 42.8 (CH₂), 29.5 (CH₂), 19.4 (CH₂), 17.3 (CH₃); IR (film) 2966, 2933, 2869, 1648, 1454, 1434, 1364, 1281, 1177, 897, 844, 700, 680 cm^{-1} ; HRMS (EI): Exact mass calcd for C₂₁H₂₀F₆N₂O [M]⁺: 430.1480 Not found. Exact mass calcd for C₁₄H₁₃F₆N₂O [M – C₇H₇]: 339.0932. Found: 339.0932.



***N*-allyl-*N*-(2-methylpyrrolidin-1-yl)-3,5-bis(trifluoromethyl)benzamide (3.57c).**

Synthesised according to General Procedure D (110 °C, 12h) using *N*-allyl-*N*-(pent-4-en-1-yl)-3,5-bis(trifluoromethyl)benzohydrazide (167 mg, 0.44 mmol, 1 equiv). The reaction mixture was concentrated under reduced pressure and isolated using flash chromatography (2% isopropanol in dichloromethane). The compound was obtained

as a yellow oil (32.8 mg, 66% yield). TLC R_f 0.58 (2% methanol in dichloromethane); ^1H NMR (300 MHz, CDCl_3) δ ppm 8.07 (s, 2 H), 7.88 (s, 1 H), 5.92 - 6.21 (m, 1 H), 5.10 - 5.42 (m, 2 H), 3.81 - 4.36 (m, 2 H), 2.86 - 3.17 (m, 3 H), 1.78 - 1.98 (m, 1 H), 1.59 - 1.76 (m, 2 H), 1.10 - 1.31 (m, 1 H), 0.77 (d, $J=6.05$ Hz, 3 H). ^{13}C NMR (75 MHz, CDCl_3) δ ppm NMR 169.5 (C), 138.5 (C), 133.6 (2 CH), 131.3 (q, $J=33$ Hz, 2 CF_3), 128.5 (CH), 125.0 (C), 122.9 (CH), 121.4 (C), 117.5 (CH_2), 56.0 (CH), 50.8 (CH_2), 42.7 (CH_2), 29.9 (CH_2), 19.8 (CH_2), 17.5 (CH_3); IR (film) 2357, 2322, 1757, 1703, 1695, 1652, 1471, 1461, 1403, 1363, 899 cm^{-1} ; HRMS (EI): Exact mass calcd for $\text{C}_{17}\text{H}_{18}\text{F}_6\text{N}_2\text{O}$ $[\text{M}]^+ = 380.1323$. Found 380.1334.



***N*-benzyl-*N*-(2-methylpyrrolidin-1-yl)benzamide (3.59).**

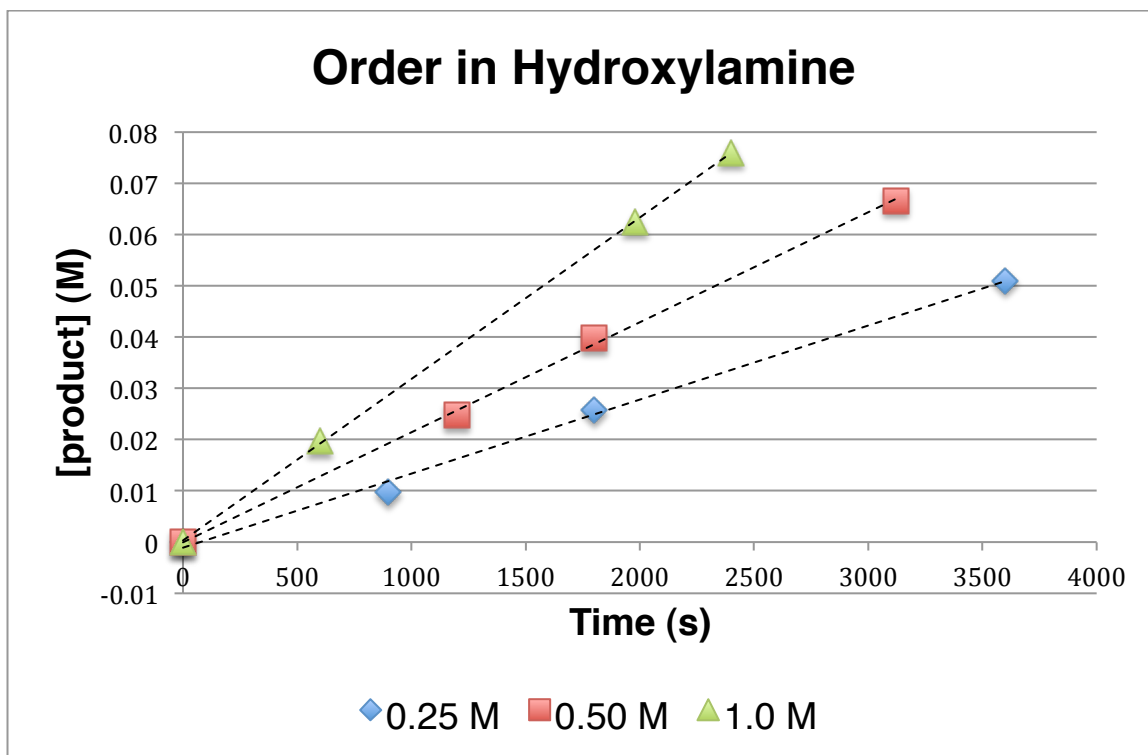
Synthesised according to General Procedure D (150 °C, 12h) using *N'*-benzyl-*N'*-(pent-4-en-1-yl)benzohydrazide (**3.58**, 69 mg, 0.235 mmol, 1 equiv). The reaction mixture was concentrated under reduced pressure and isolated using flash chromatography (15% EtOAc in hexanes). The compound was obtained as orange oil (21mg, 31% yield). TLC R_f 0.35 (15% EtOAc in hexanes); ^1H NMR (CDCl_3 , 400 MHz) δ ppm 7.67-7.50 (m, 2H), 7.50-7.20 (m, 8H), 4.99 (d, $J = 15.54$ Hz, 1H), 4.52 (d, $J = 15.31$ Hz, 1H), 3.11-2.73 (m, 3H), 1.87-1.70 (m, 1H), 1.69-1.52 (m, 2H), 1.32-1.03 (m, 1H), 0.74 (d, $J = 5.92$ Hz, 3H); ^{13}C NMR (100 MHz, CDCl_3) δ ppm 173.8 (C), 138.9 (C), 137.0 (C), 129.2 (CH), 128.5 (CH), 127.8 (CH), 127.4 (CH), 127.2 (CH), 126.9 (CH), 55.9 (CH), 50.9 (CH_2), 42.9 (CH_2), 30.1 (CH_2), 20.0 (CH_2), 17.7 (CH_3); IR (film) 3065, 3031, 2967, 2928, 2870, 1639, 1493, 1447, 1429, 1401, 1292, 1176, 1143, 1076, 1027, 975, 786, 725, 695, 625 cm^{-1} ; HRMS (EI): Exact mass calcd for $\text{C}_{19}\text{H}_{22}\text{N}_2\text{O}$ $[\text{M}]^+ : 294.1732$ Not found. Exact mass calcd for $\text{C}_{12}\text{H}_{15}\text{N}_2\text{O}$ $[\text{M} - \text{C}_7\text{H}_7]$: 203.1184. Found: 203.1195.

PROCEDURES AND CHARACTERIZATION FOR CHAPTER 4

◆ KINETIC EXPERIMENTS FOR CHAPTER 4

Order in Norbornene After drying reaction vials overnight in a oven, and taking precautions while cooling to not expose the vial to air or moisture, *N*-cyclohexylhydroxylamine (72.0 mg, 143 mg and 288 mg; 0.625 mmol, 1.25 mmol and 2.5 mmol) was added in each in a separate vial, along with 1,3,5-trimethoxybenzene (the internal standard, 70 mg, 0.416 mmol). After purging the flasks for 5 minutes, norbornene (412 mg, 2.5 mmol) was added in each flask quickly followed by toluene (2.5 mL, dried over activated molecular sieves) via syringe. No attempts to correct the total volume were made. After 1 minute of flushing with argon, the vials were capped and transferred to a 95 °C bath. Aliquots were taken from the reaction at approximately but accurately 15 minutes interval over 2 hours, for the reaction to be followed, post-evaporation of the solvent, by ¹H NMR. The concentration of product formed was determined by integrating the product's peak ($\delta = 2.11$ ppm (br s, 1H)) relative to the internal standard peak ($\delta = 6.08$ ppm).

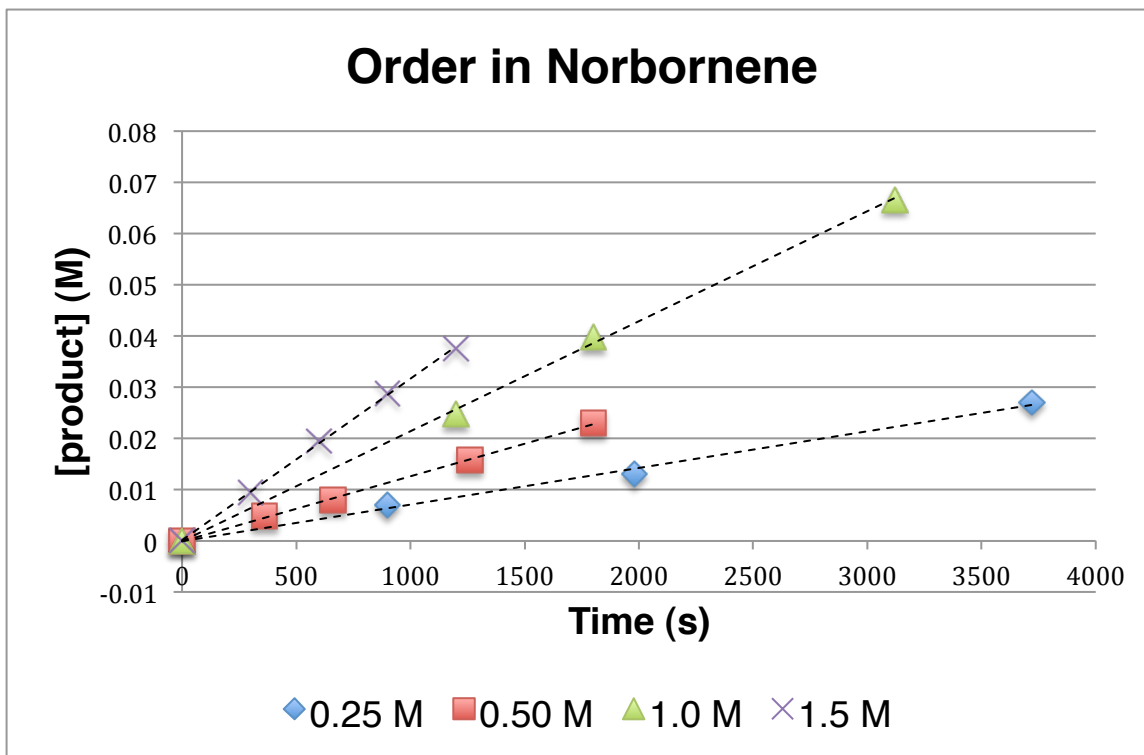
Order in Hydroxylamine After drying reaction vials overnight in a oven, and taking precautions while cooling to not expose the vial to air or moisture, *N*-cyclohexylhydroxylamine (143 mg; 1.25 mmol) was added in each in a separate vial, along with 1,3,5-trimethoxybenzene (the internal standard, 70 mg, 0.416 mmol). After purging the flasks for 5 minutes, norbornene (103, 206, 412 and 618 mg, 0.625, 1.25, 2.50 and 3.75 mmol) was added in each flask quickly followed by toluene (2.5 mL, dried over activated molecular sieves) via syringe. No attempts to correct the total volume were made. After 1 minute of flushing with argon, the vials were capped and transferred to a 95 °C bath. Aliquots were taken from the reaction at approximately but accurately 15 minutes interval over 2 hours, for the reaction to be followed, post-evaporation of the solvent, by ¹H NMR. The concentration of product formed was determined by integrating the product's peak ($\delta = 2.11$ ppm (br s, 1H)) relative to the internal standard peak ($\delta = 6.08$ ppm).



[hydroxylamine]	time (s)	Conc (M)	rate (M/s)
0.25 M	0	0	
	900	0.00987	0.0000145
	1800	0.0258	
	3600	0.051	

[hydroxylamine]	time (s)	Conc (M)	rate (M/s)
0.5 M	0	0	
	1200	0.0248	0.0000215
	1800	0.03982	
	3120	0.0666	

[hydroxylamine]	time (s)	Conc (M)	rate (M/s)
0.5 M	0	0	
	600	0.0197	0.0000315
	1980	0.0625	
	2400	0.076	



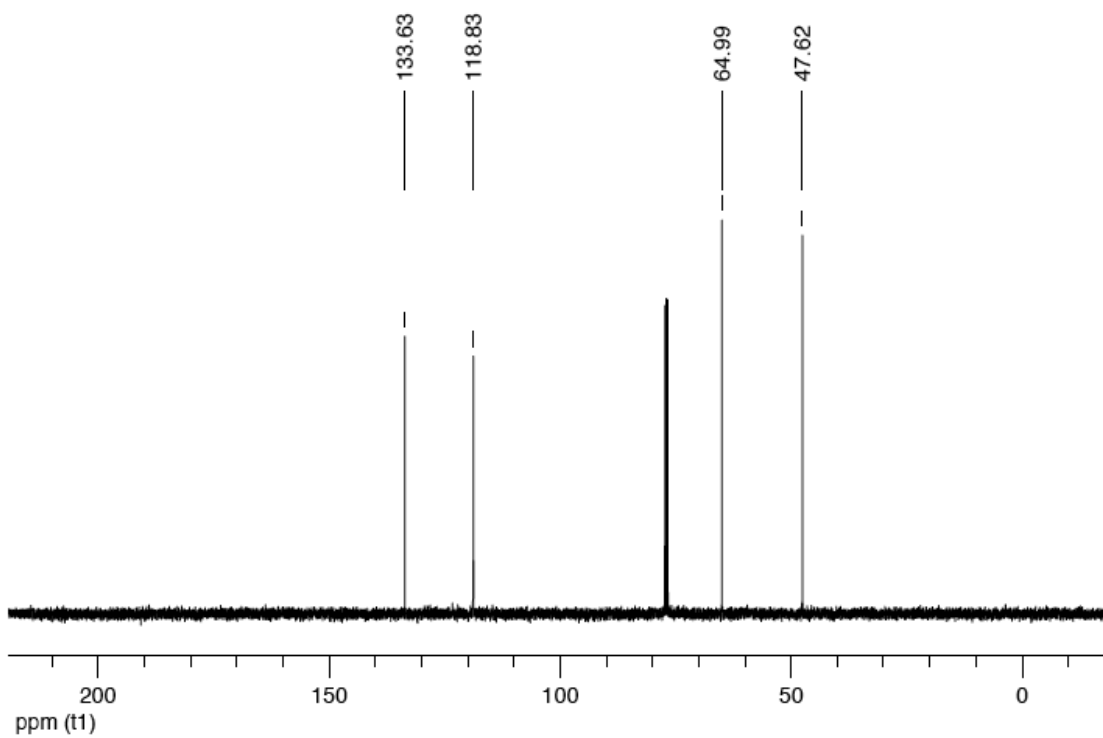
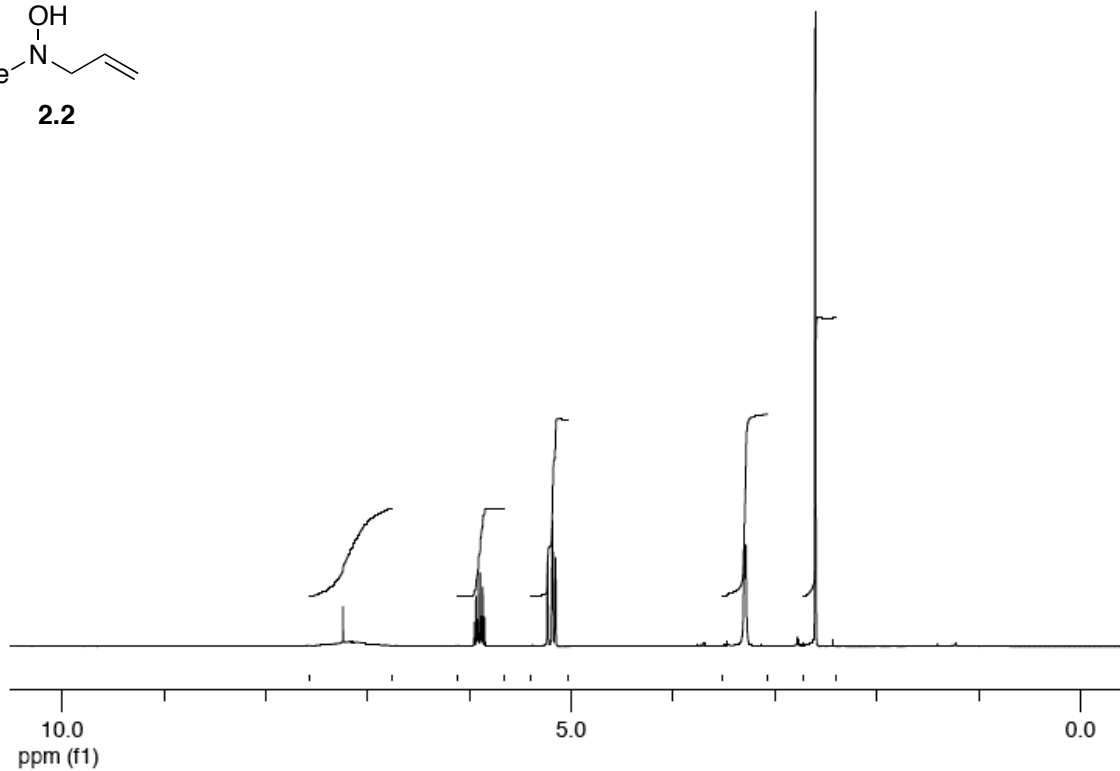
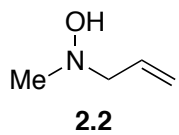
[hydroxylamine]	time (s)	Conc (M)	rate (M/s)
0.25 M	0	0	
	900	0.007	0.0000072
	1980	0.013	
	3720	0.027	

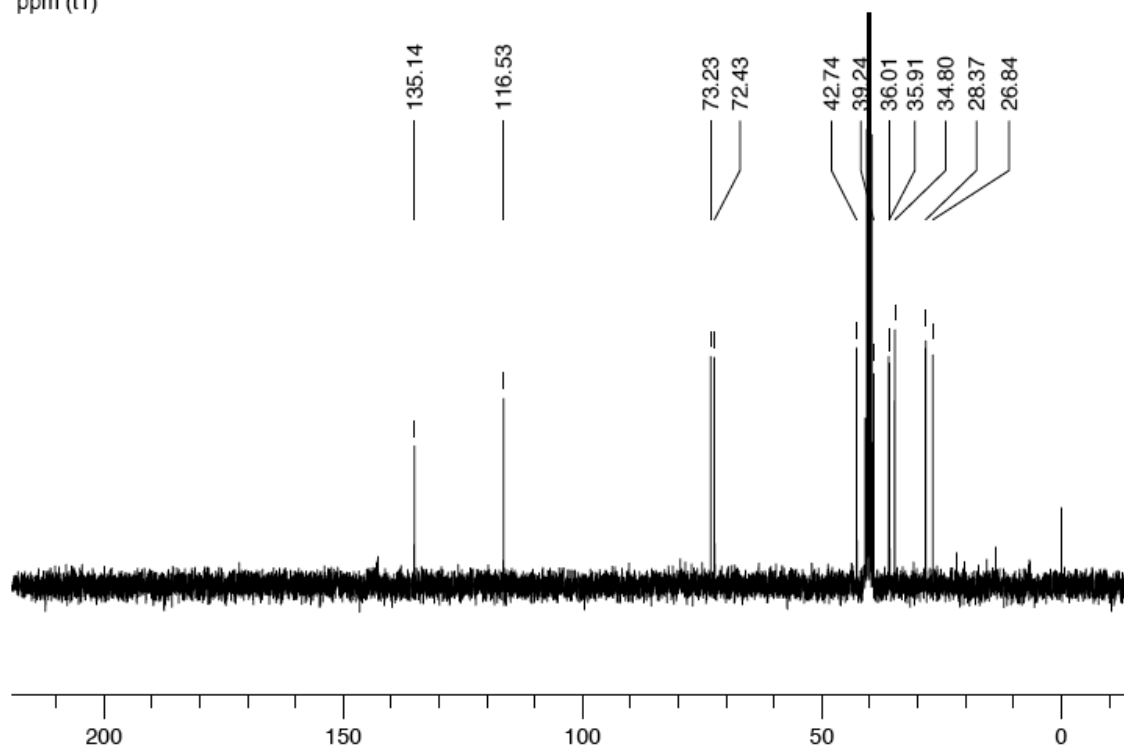
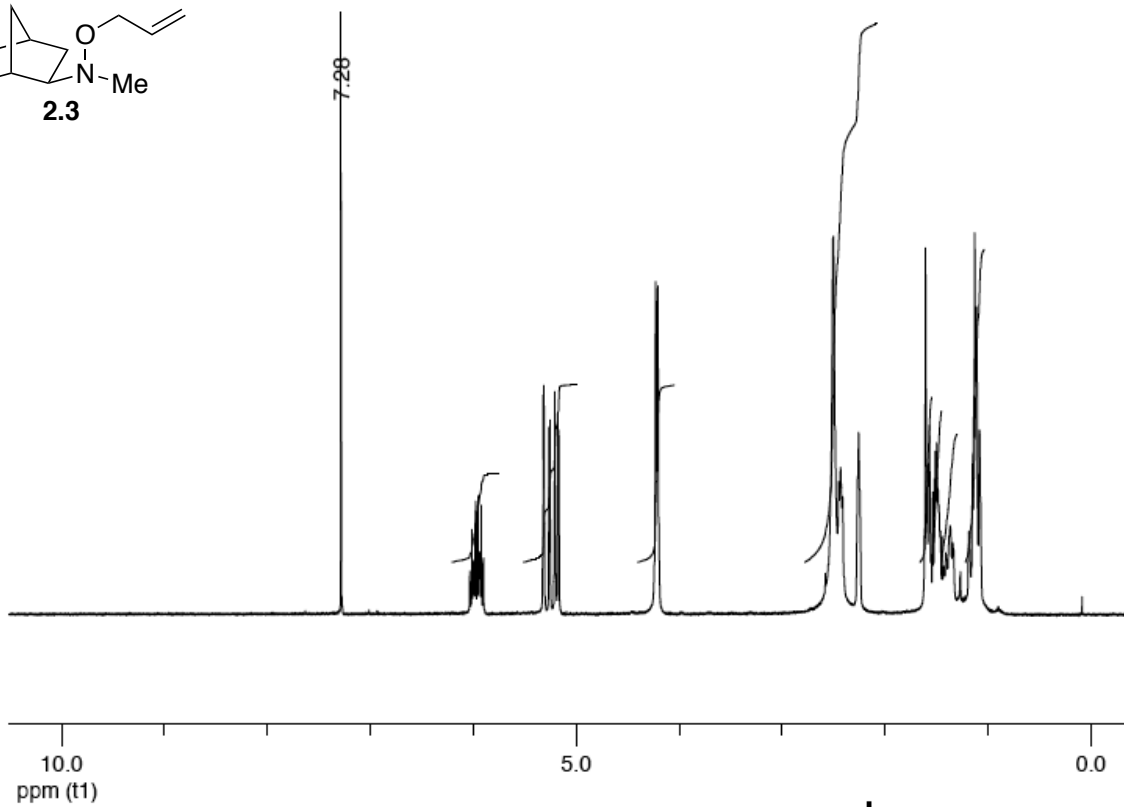
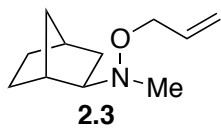
[hydroxylamine]	time (s)	Conc (M)	rate (M/s)
0.5 M	0	0	
	360	0.0048	0.0000127
	660	0.0079	
	1260	0.01576	
	1800	0.023	

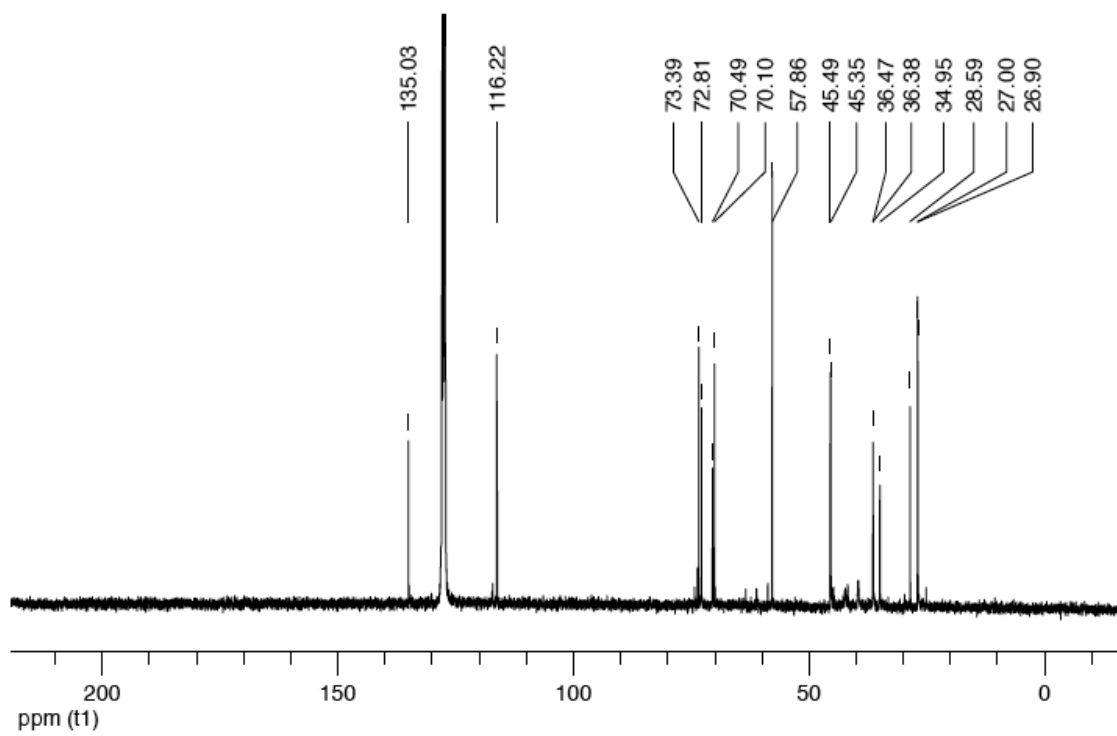
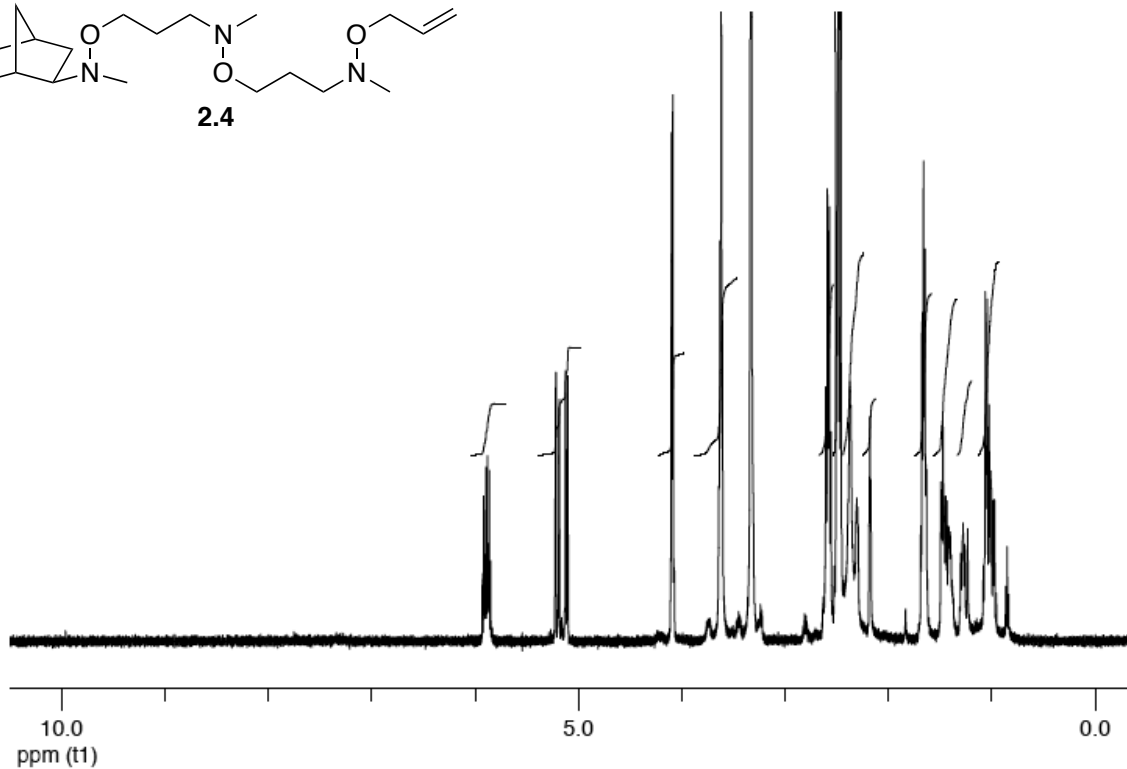
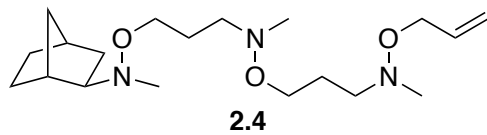
[hydroxylamine]	time (s)	Conc (M)	rate (M/s)
1 M	0	0	
	1200	0.0248	0.0000215
	1800	0.03982	
	3120	0.0666	

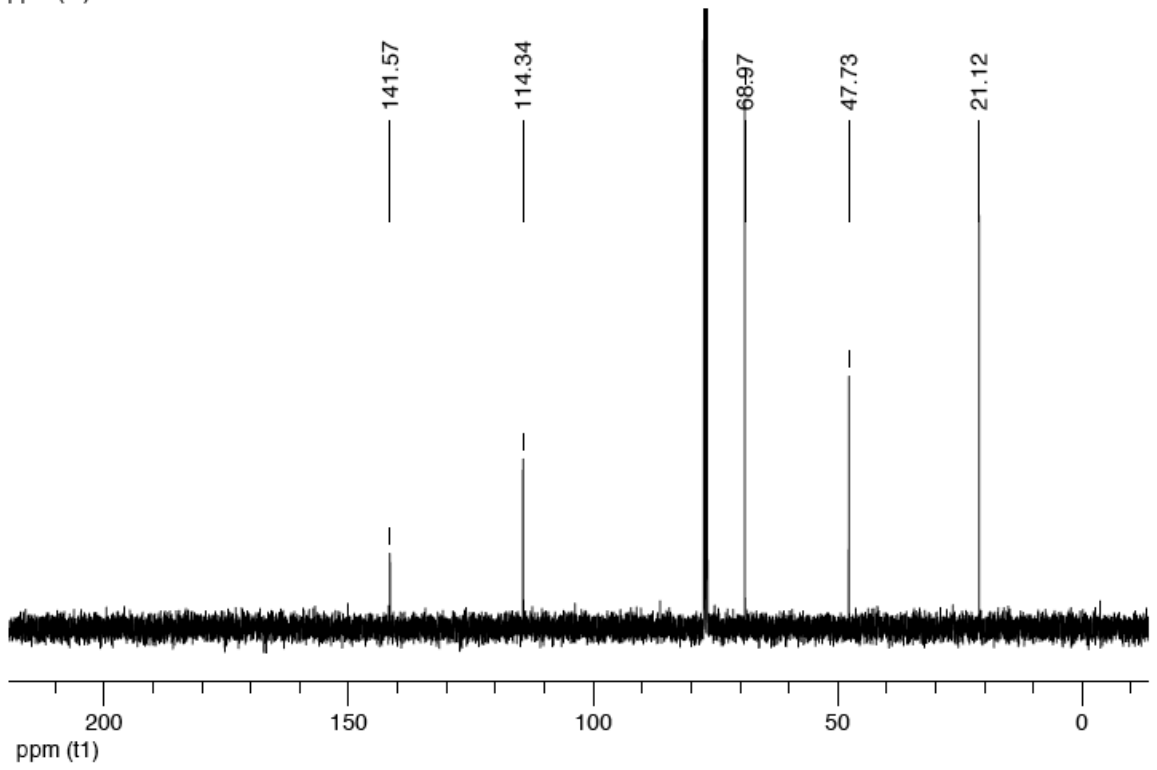
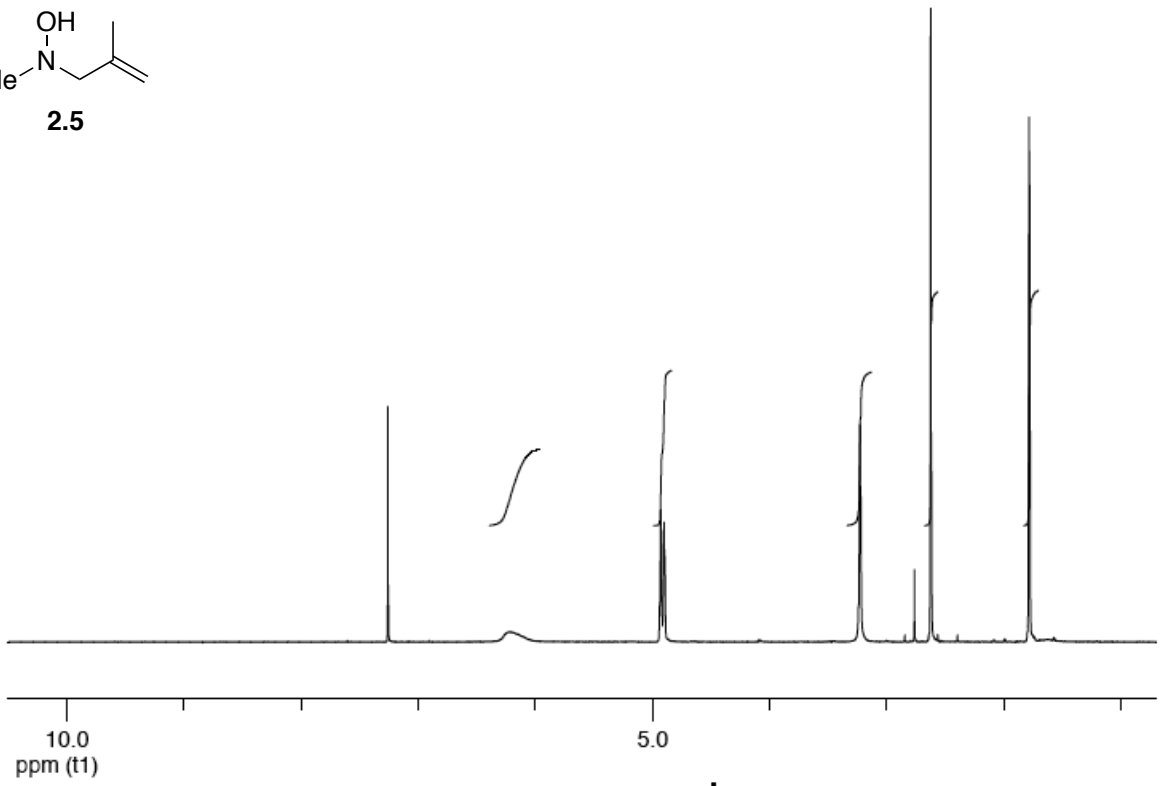
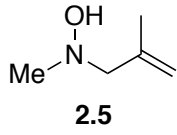
[hydroxylamine]	time (s)	Conc (M)	rate (M/s)
1.5 M	0	0	
	300	0.00938	0.0000315
	600	0.01958	
	900	0.02883	
	1200	0.03757	

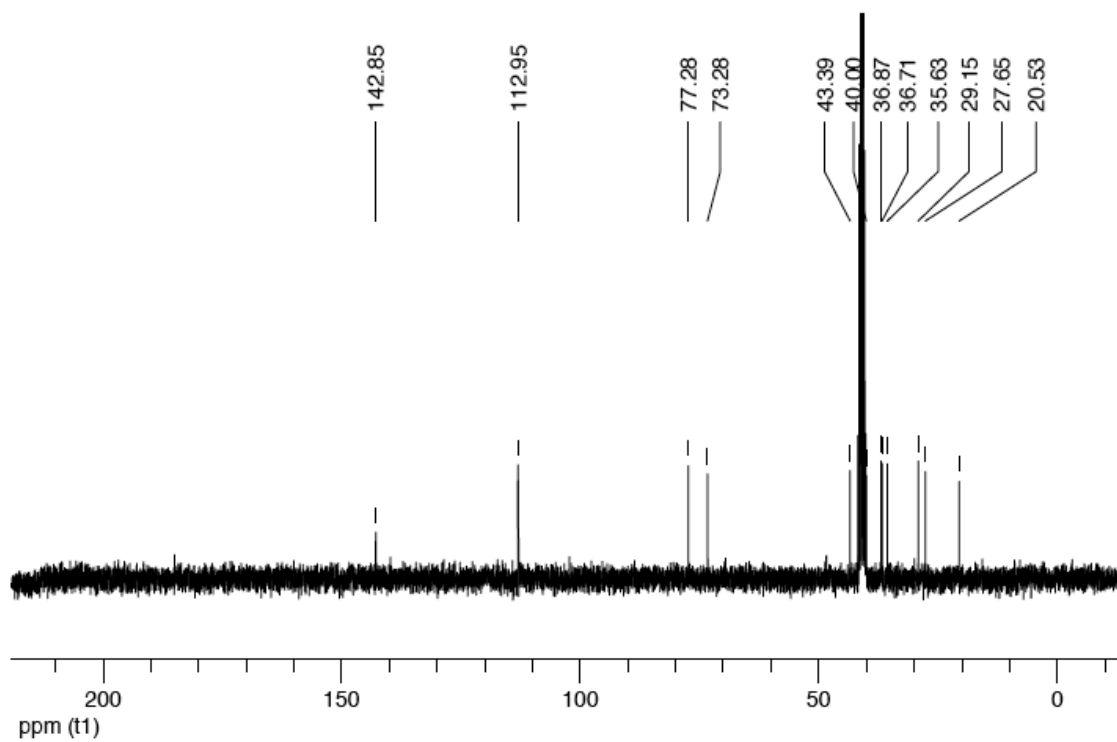
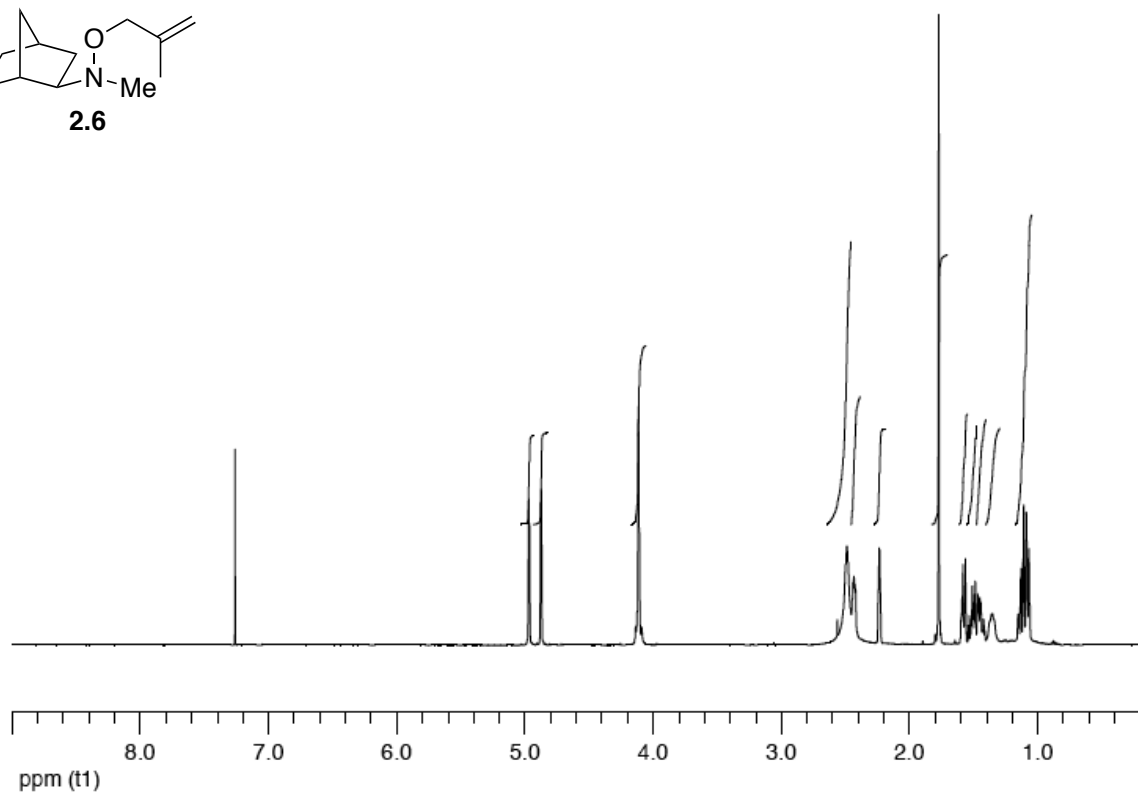
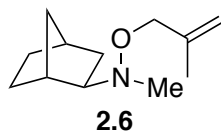
Appendix IV. NMR Spectra

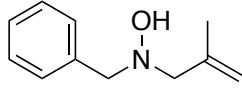




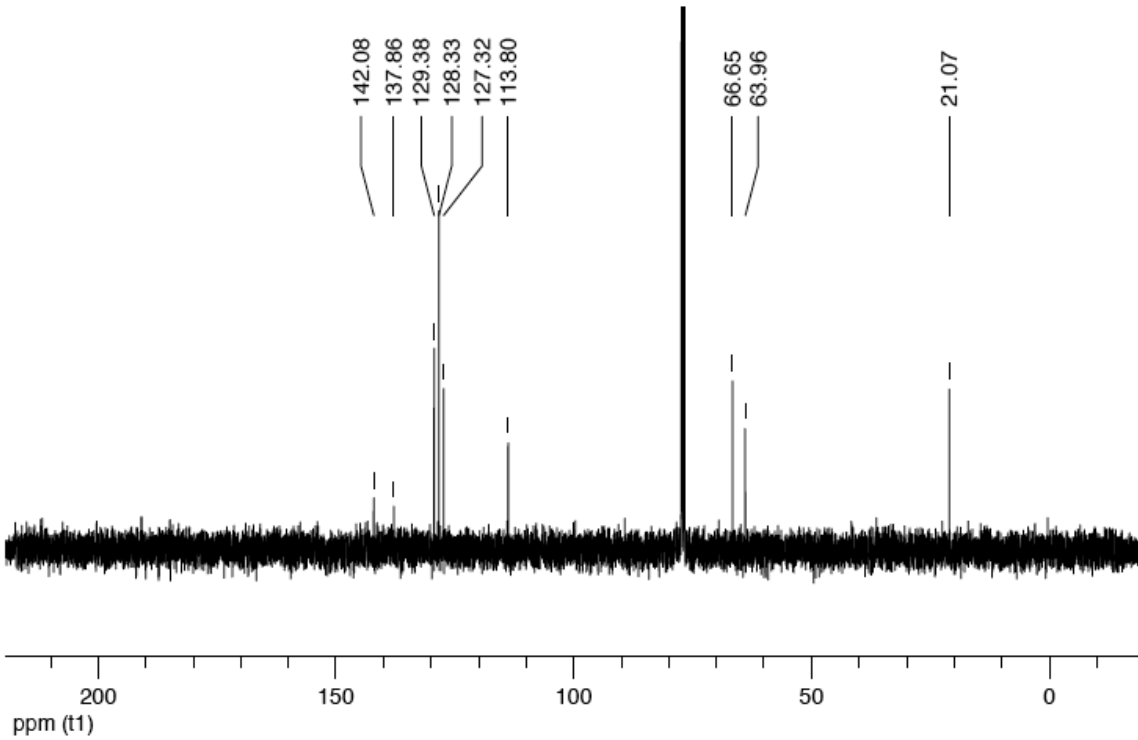
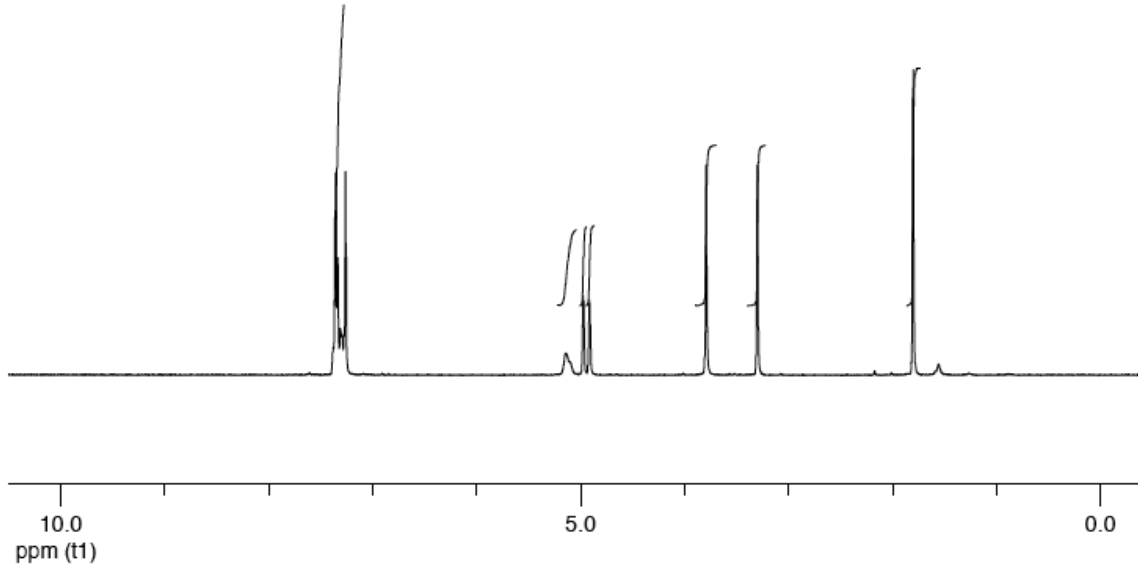


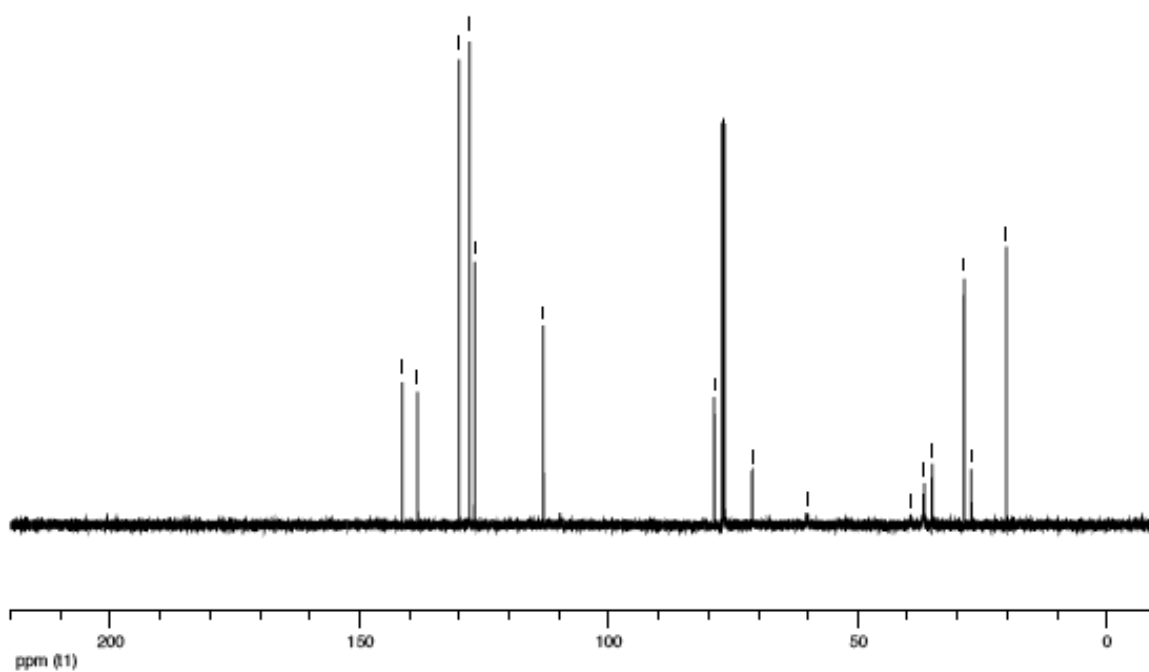
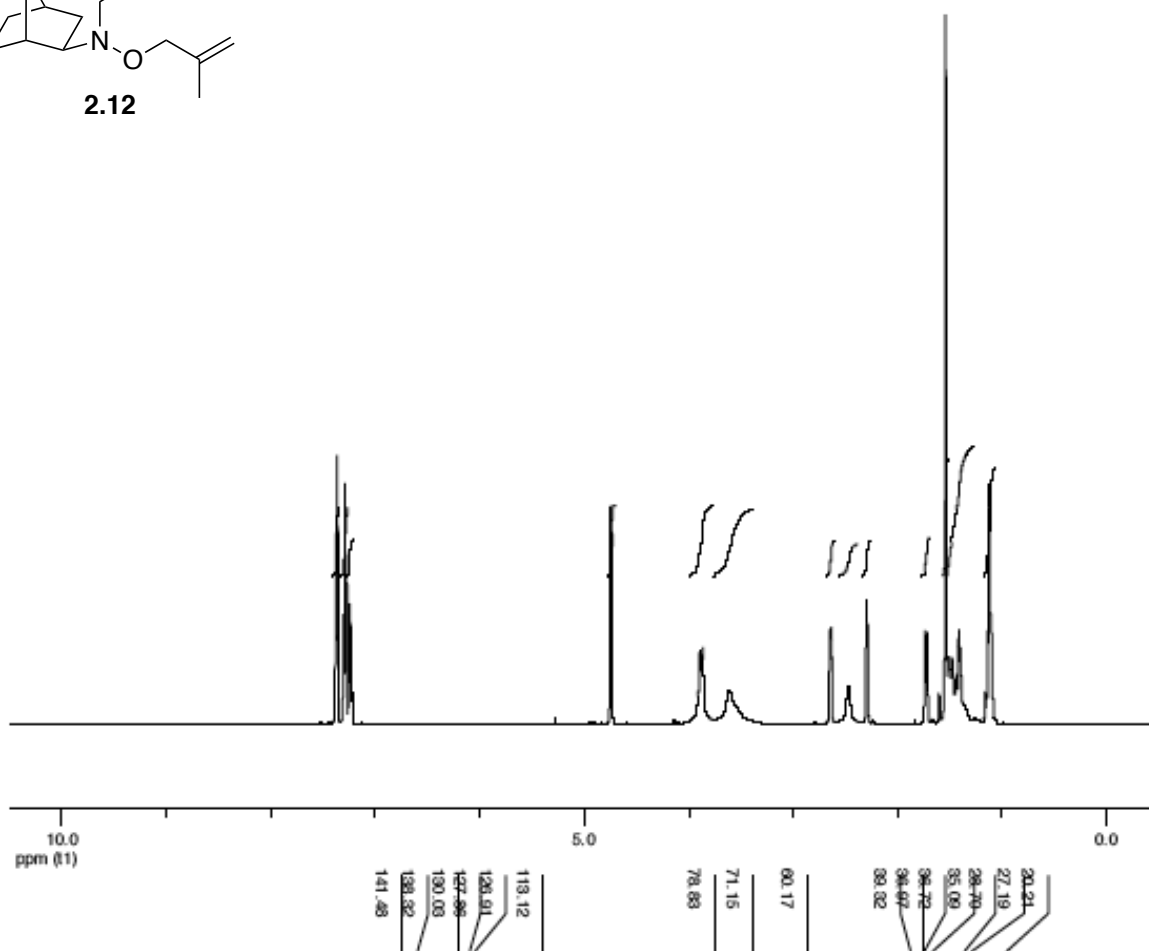
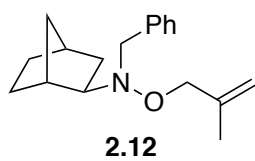


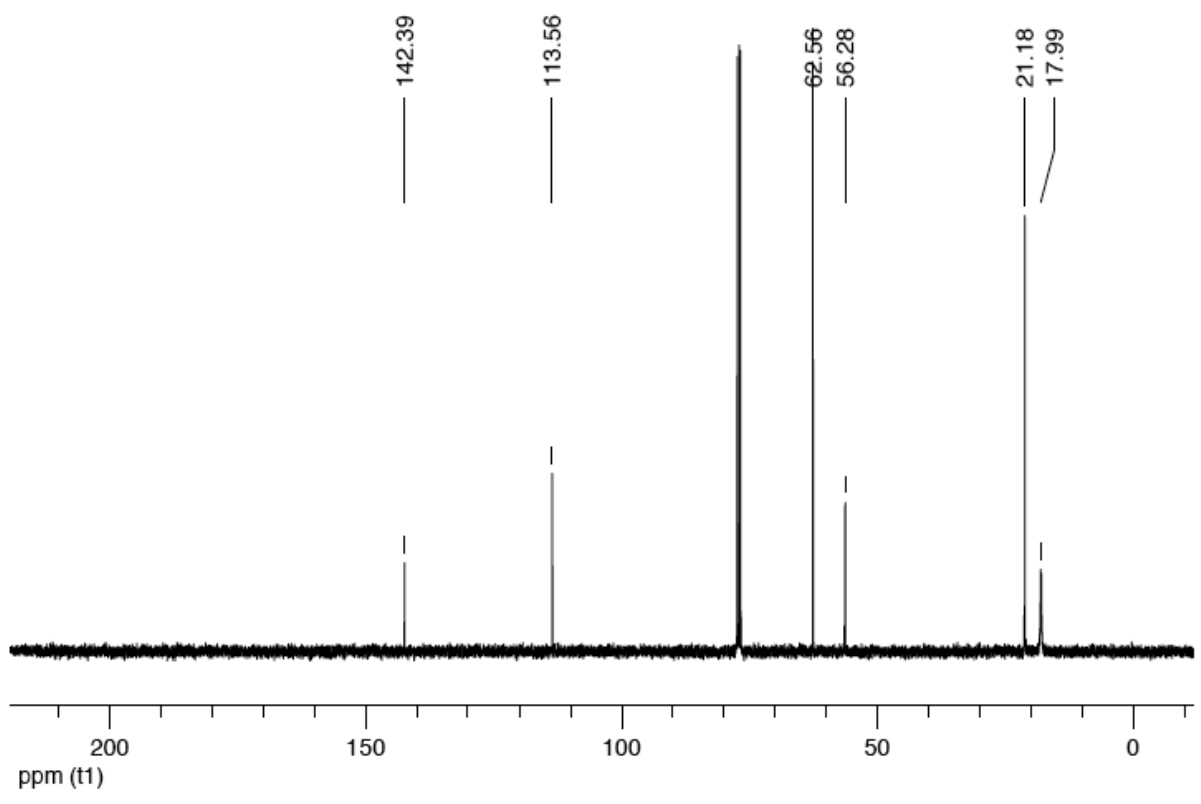
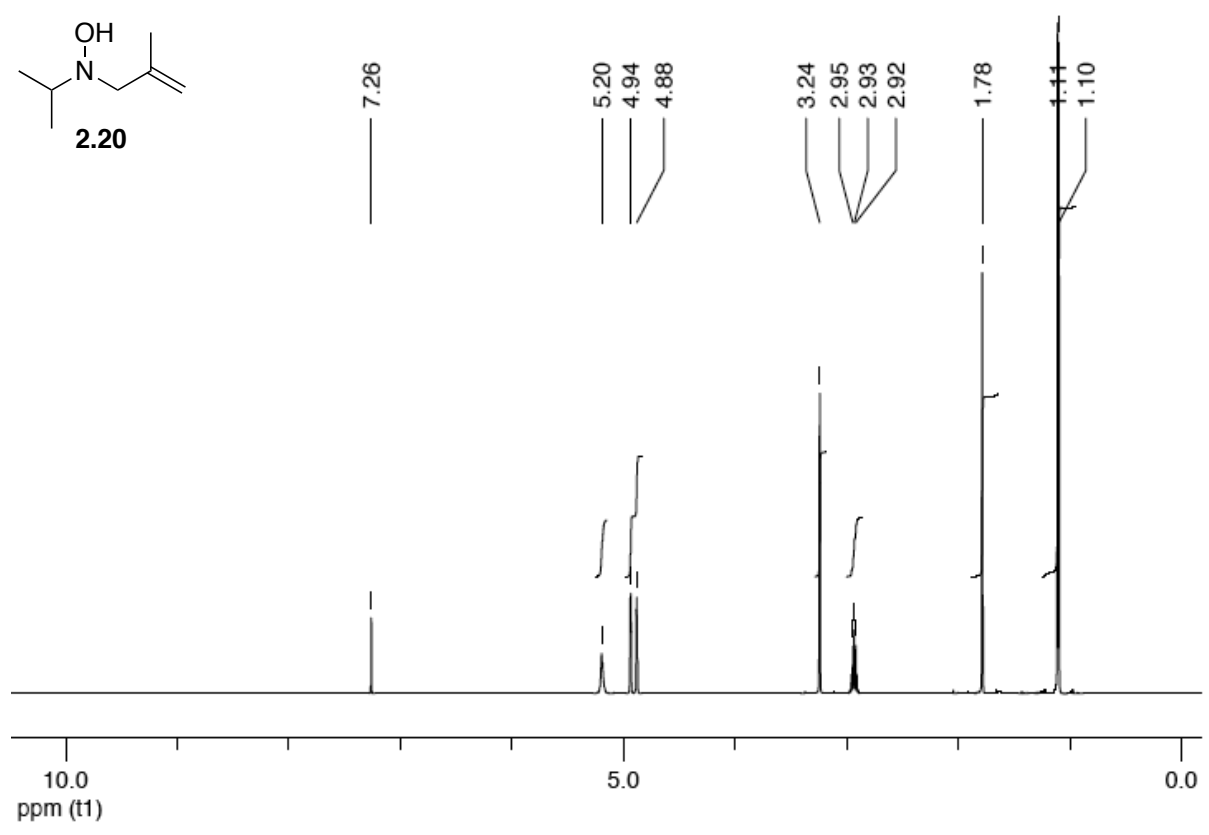
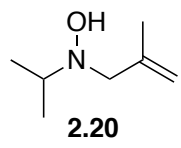


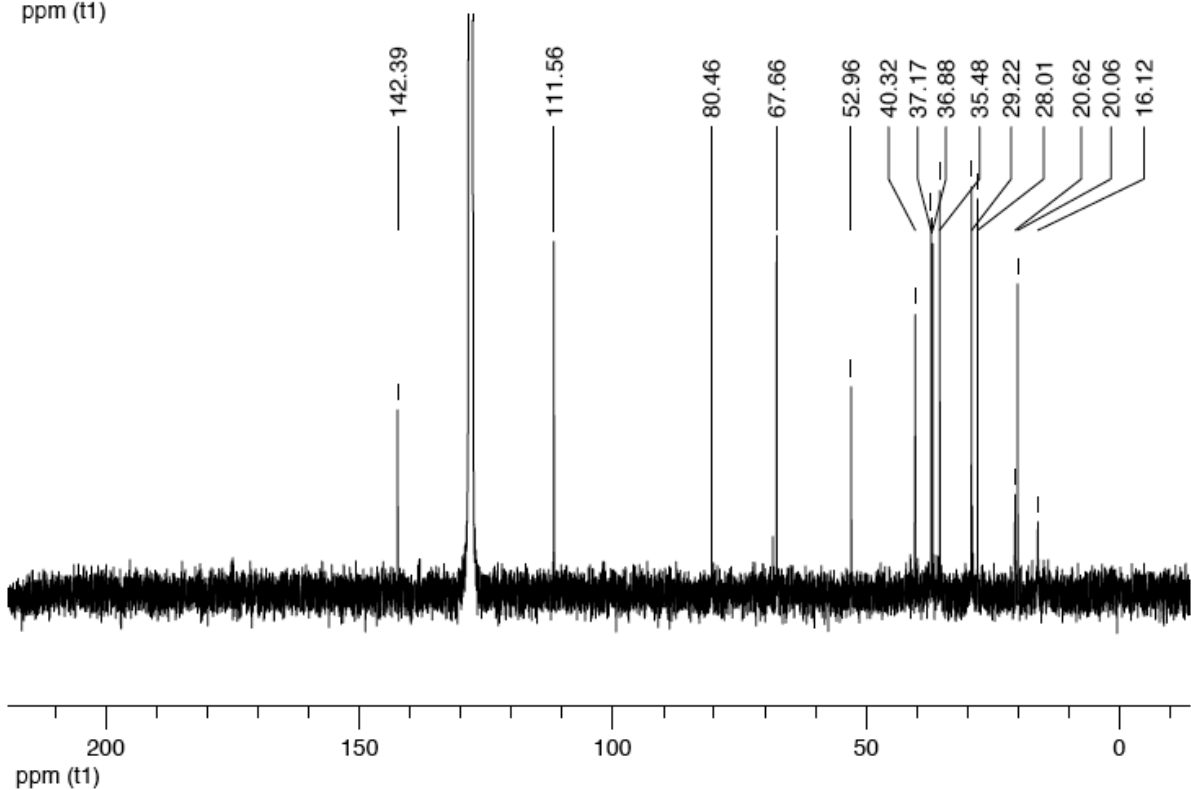
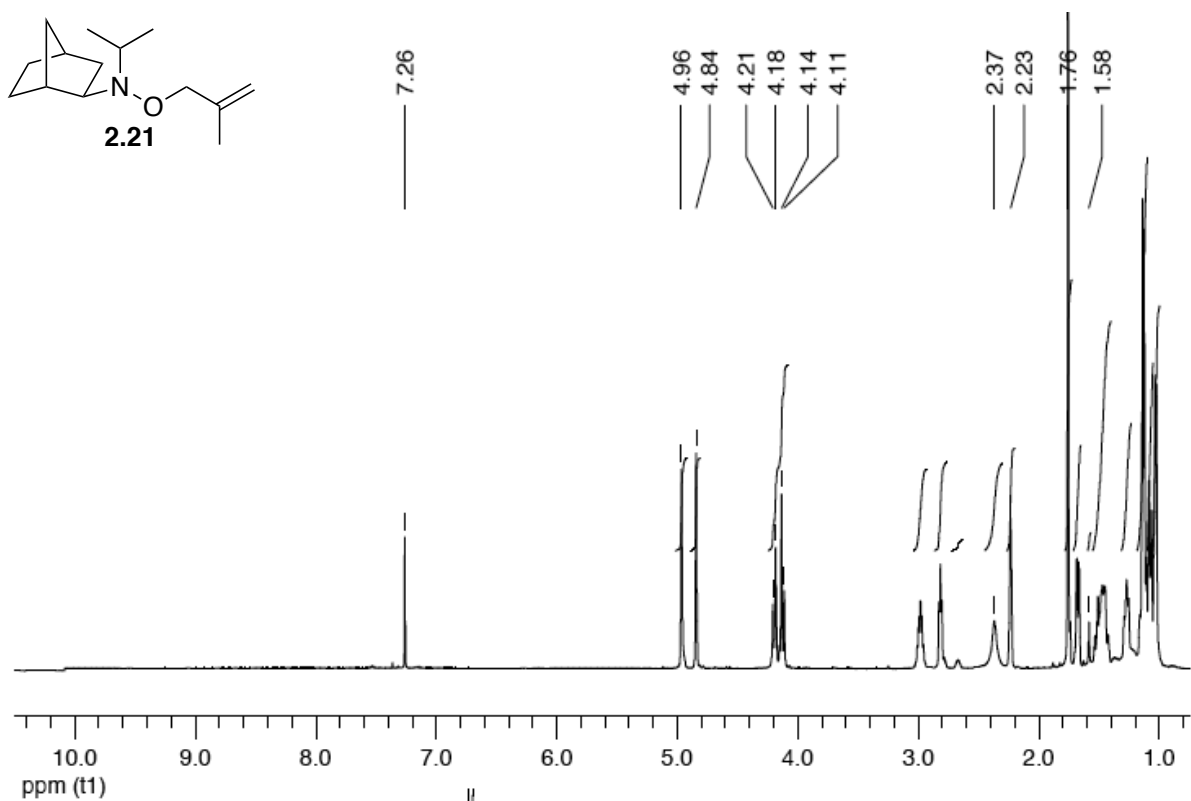
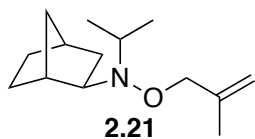


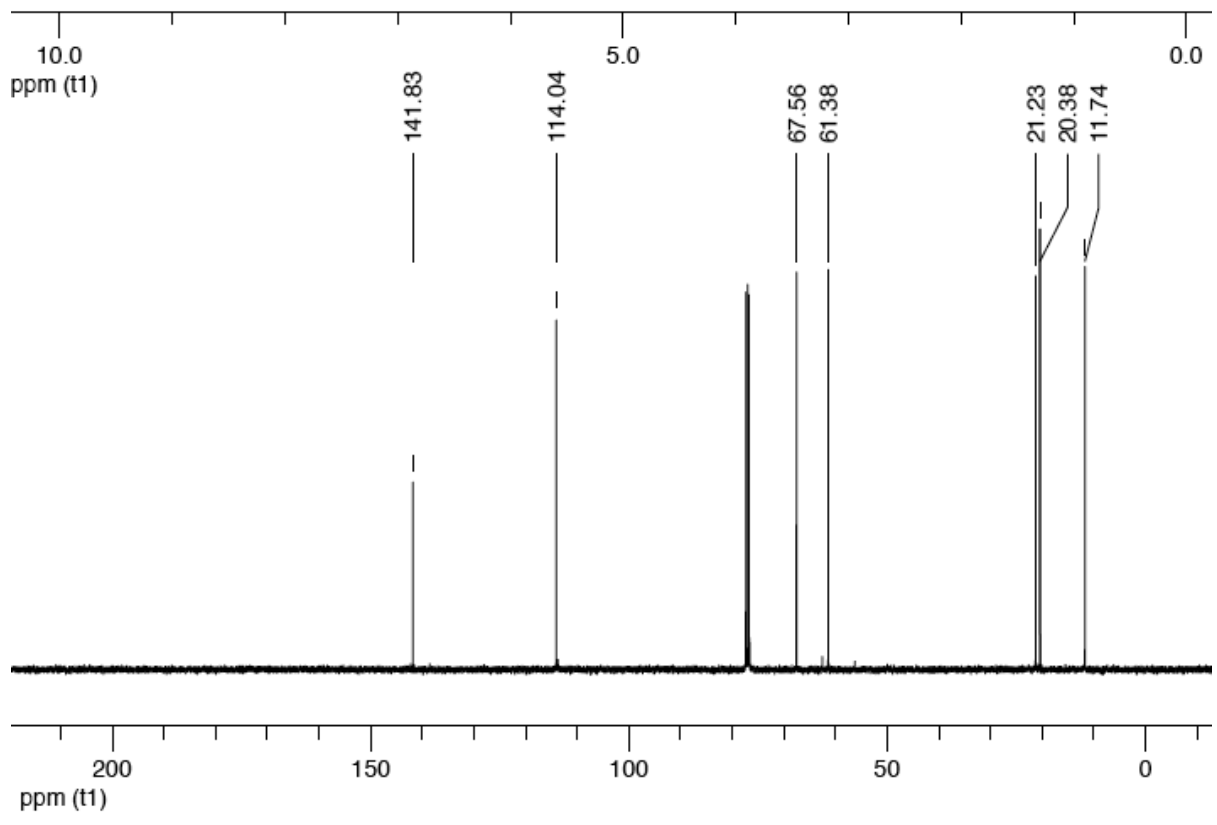
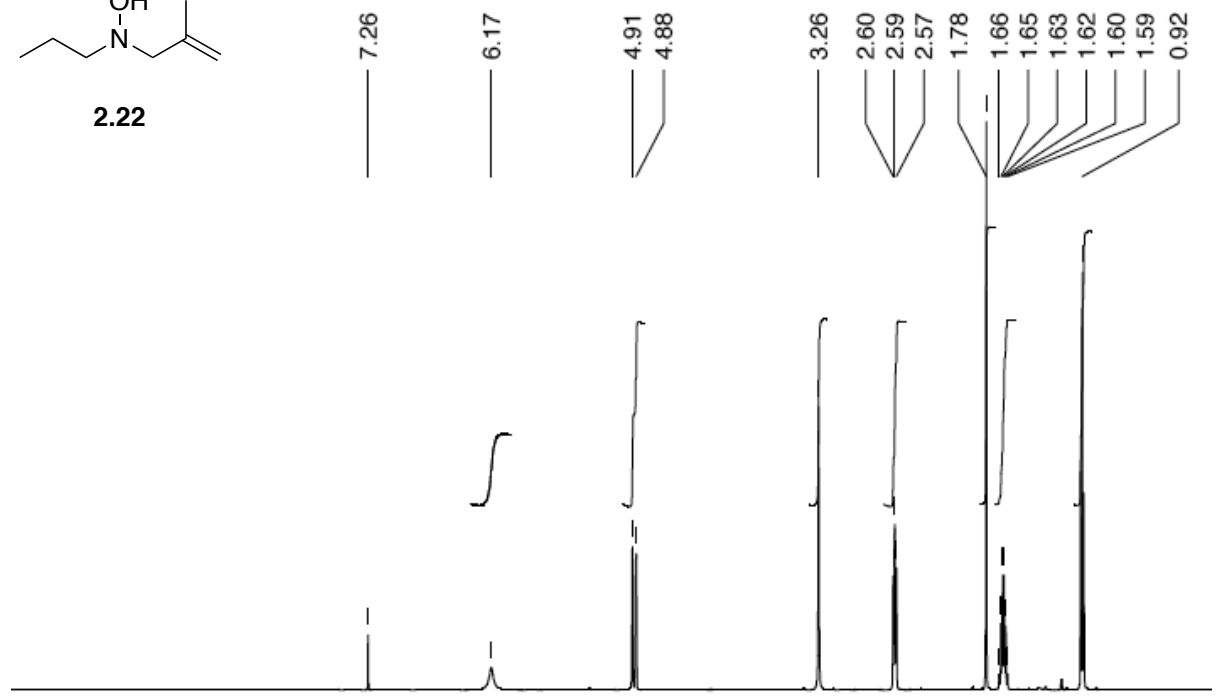
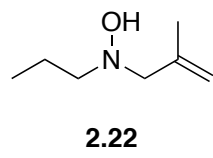
2.10

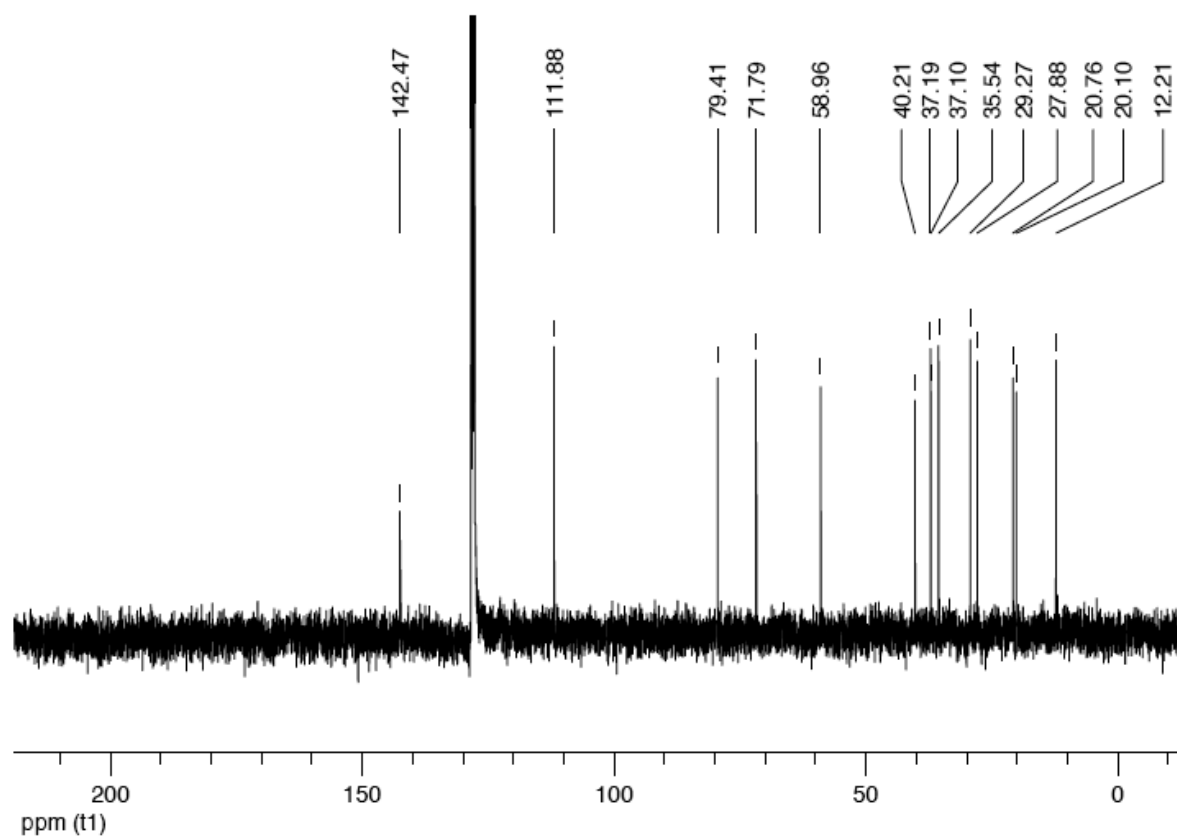
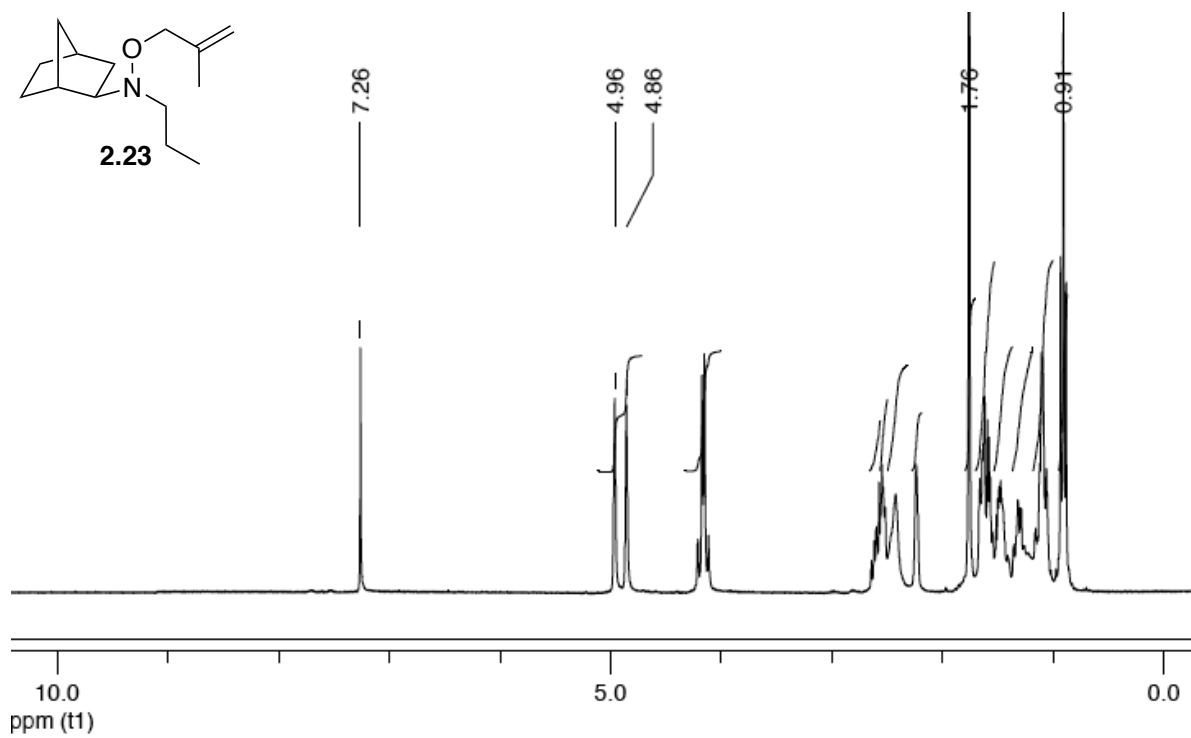
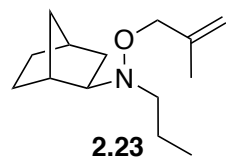


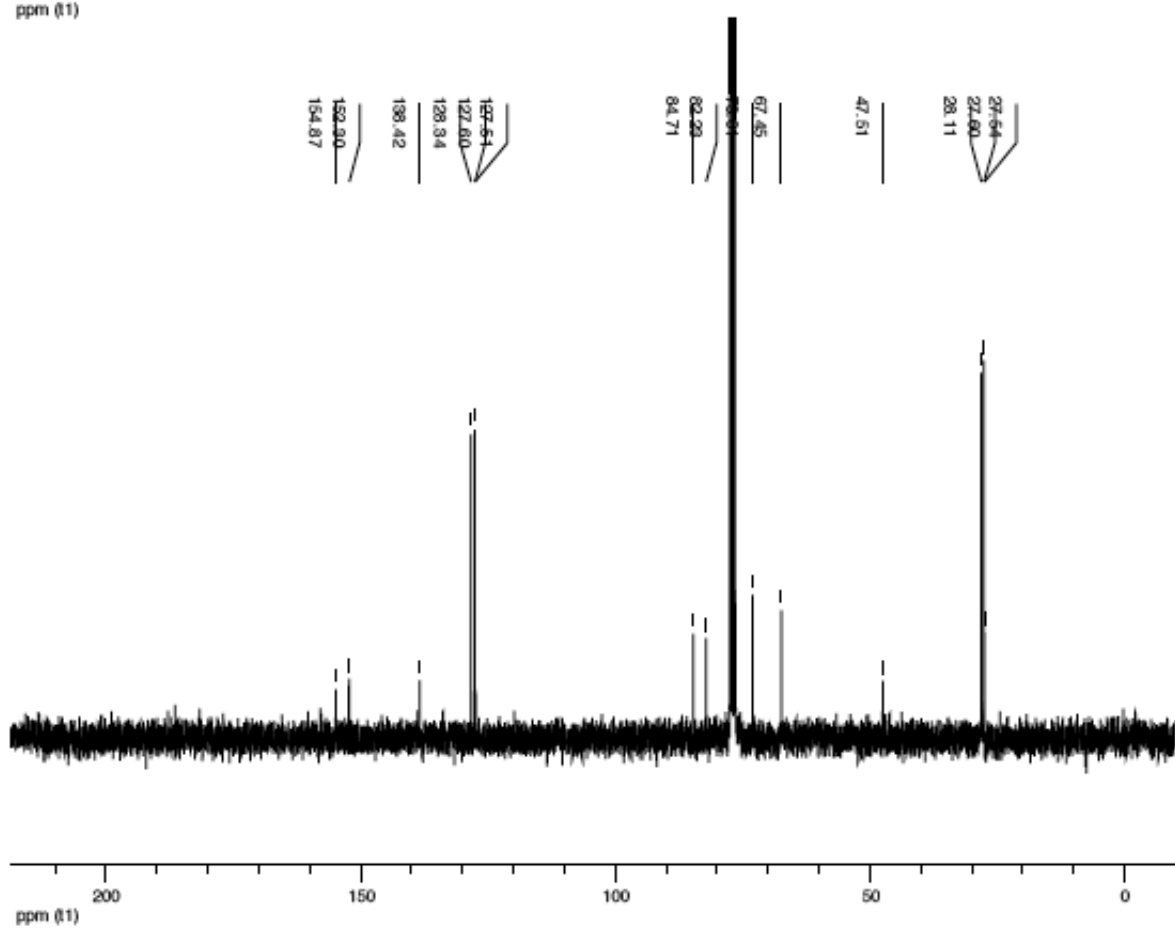
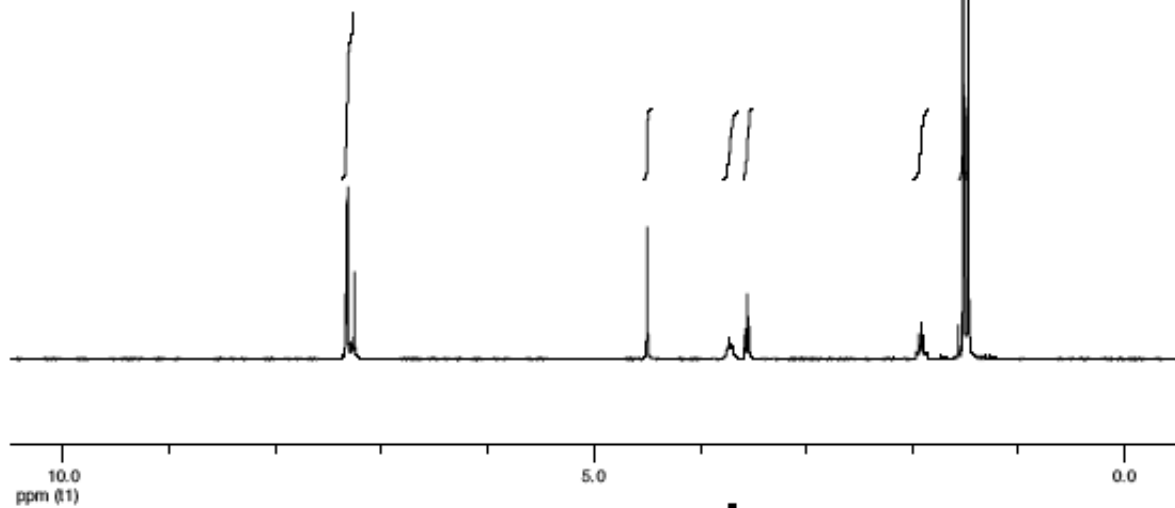
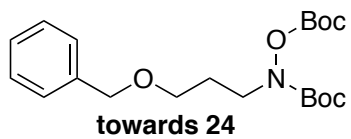


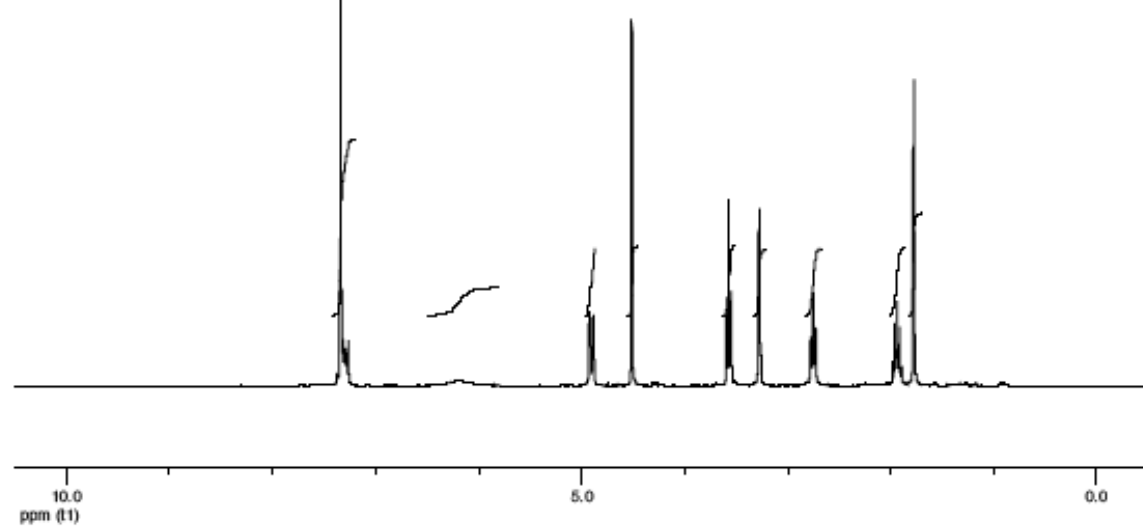
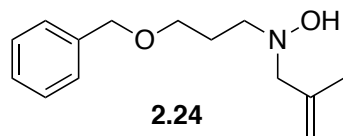




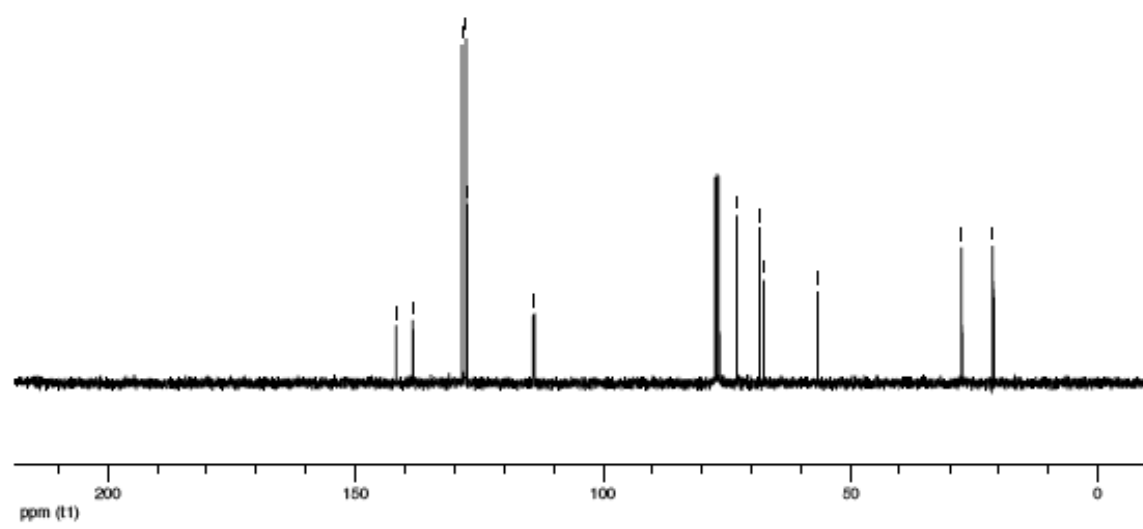


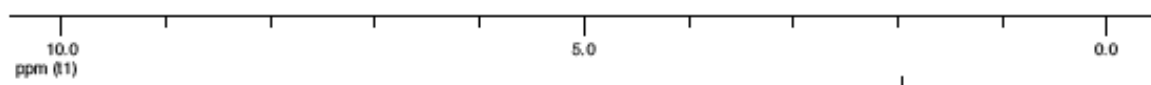
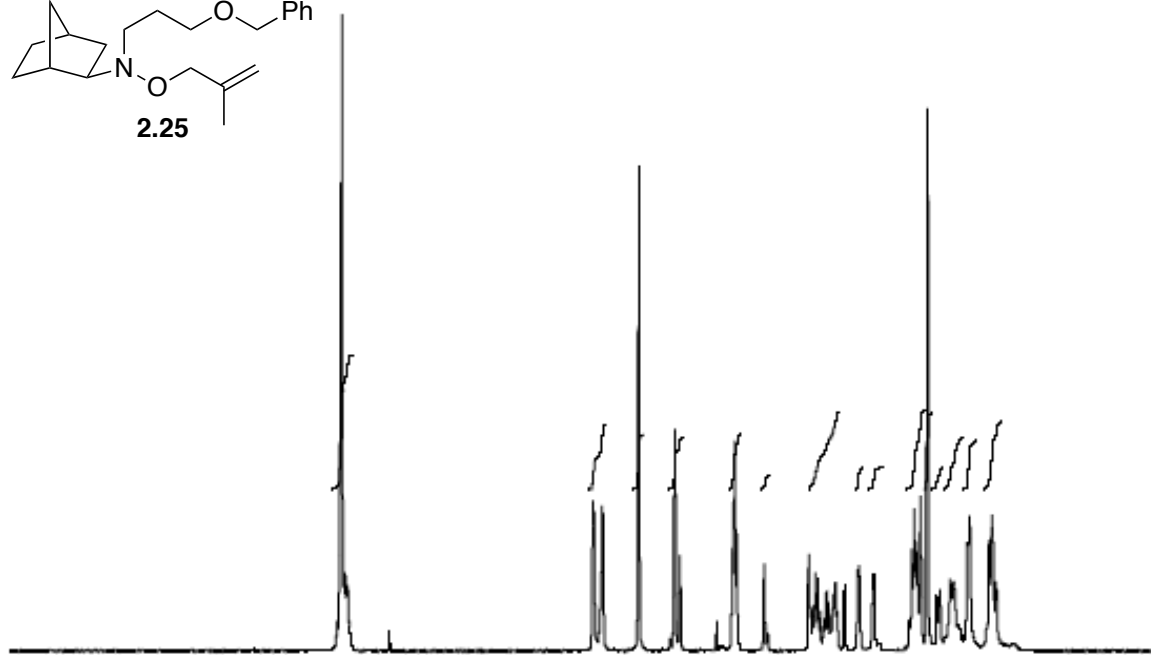
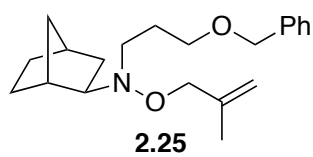




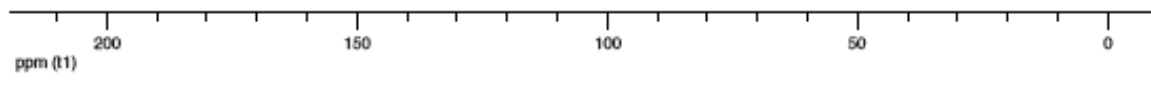


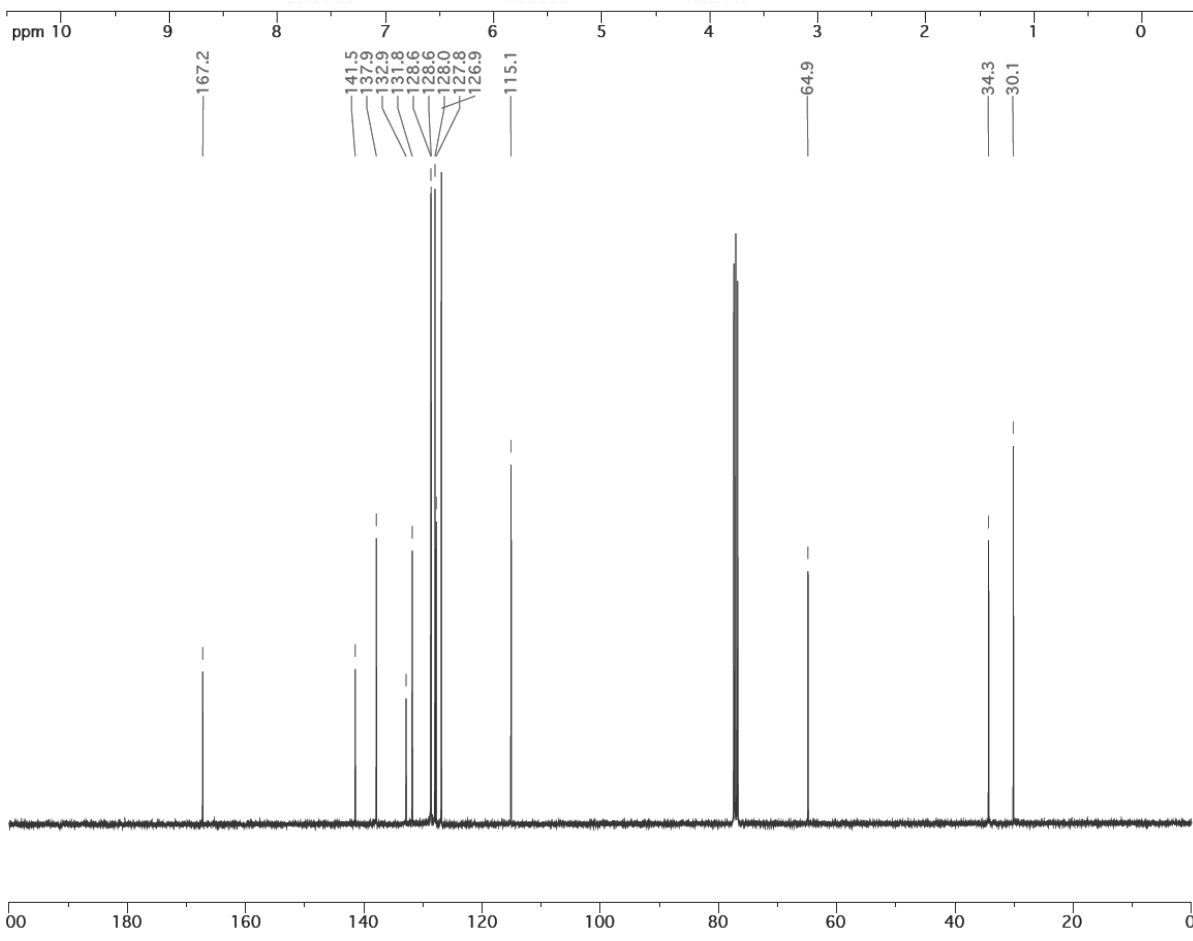
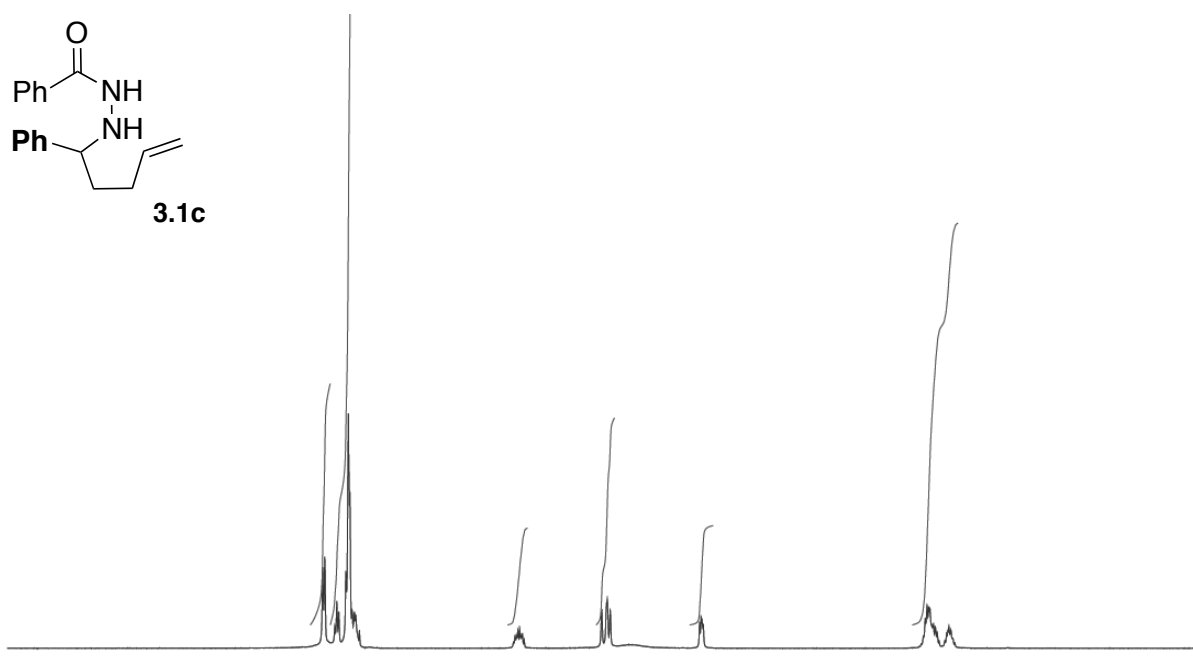
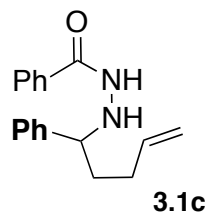
- 141.79
- 138.30
- 128.31
- 127.59
- 127.46
- 113.90
- 72.88
- 68.47
- 67.48
- 66.06
- 27.56
- 21.13

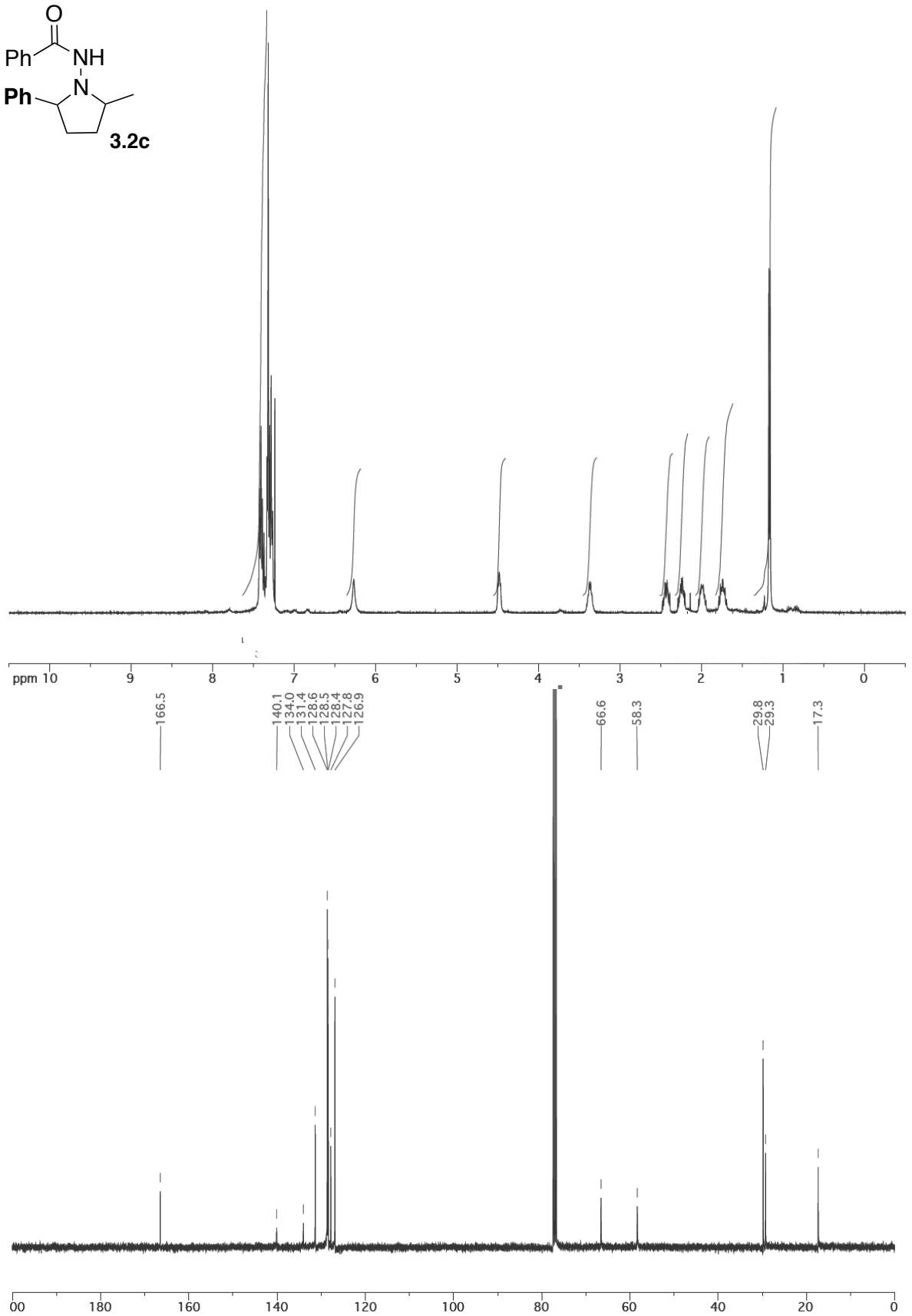
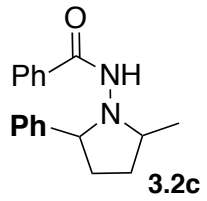


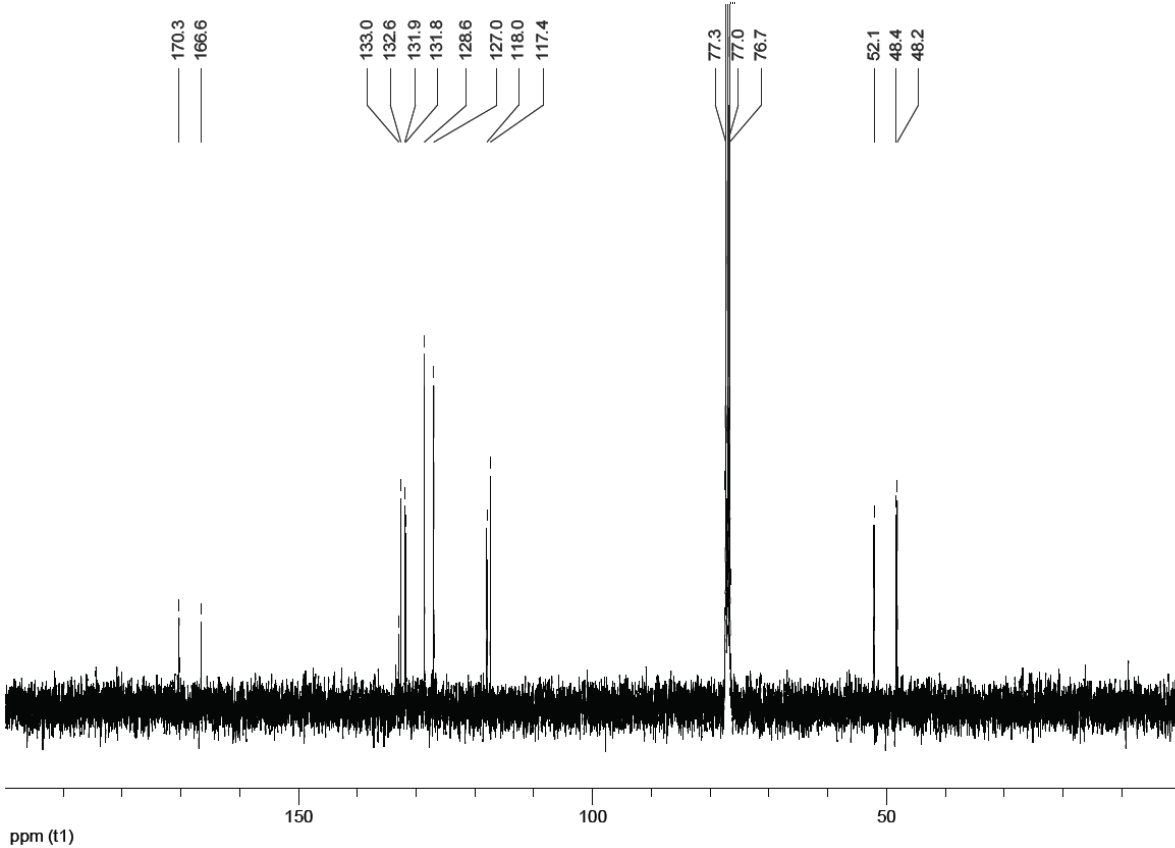
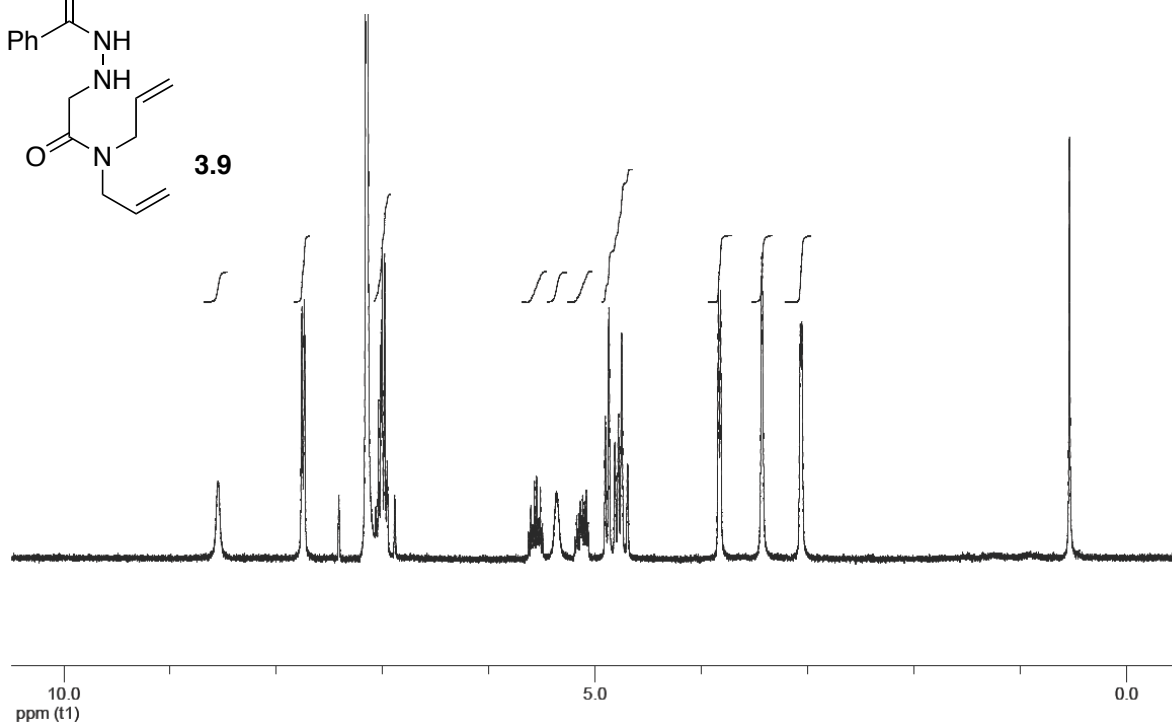
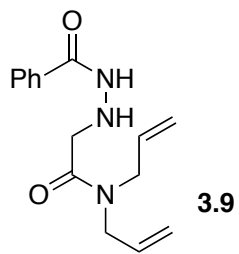


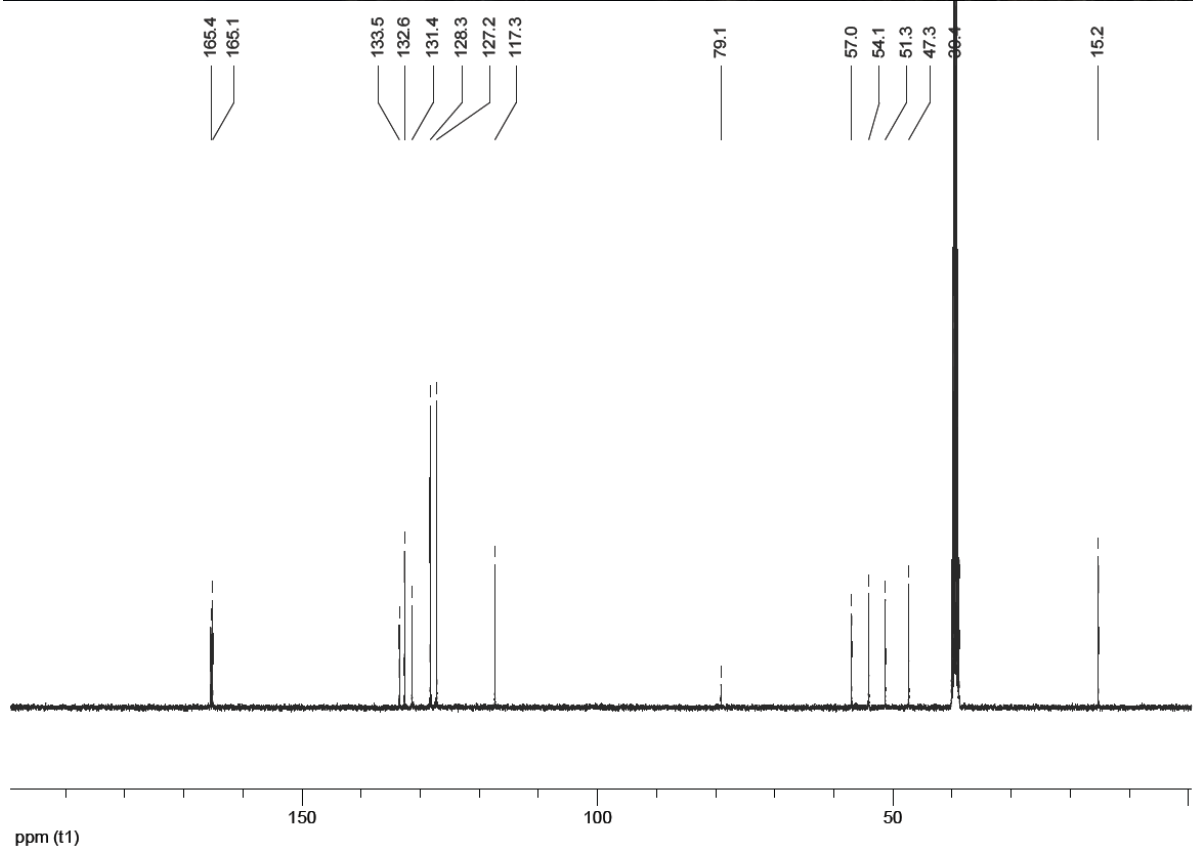
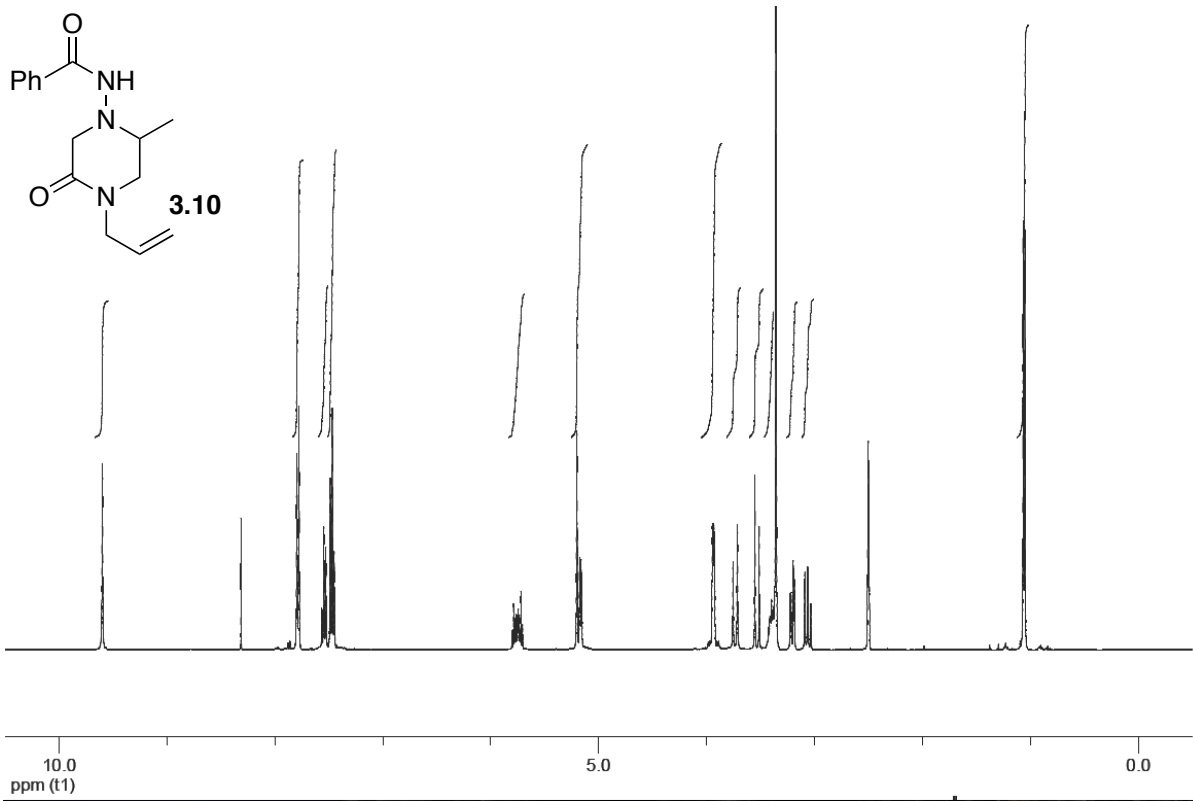
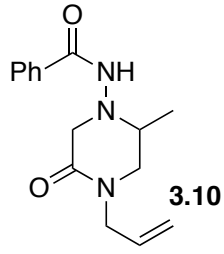
- | | |
|--------|-------|
| 142.97 | 78.99 |
| 142.76 | 77.48 |
| 142.59 | 72.94 |
| 139.84 | 71.36 |
| 128.88 | 68.27 |
| 128.10 | 66.15 |
| 127.95 | 65.67 |
| 114.01 | 55.69 |
| 112.91 | 53.58 |
| 112.53 | 40.03 |
| | 36.89 |
| | 36.84 |
| | 35.67 |
| | 28.21 |
| | 28.02 |
| | 27.90 |
| | 27.86 |
| | 21.64 |
| | 20.45 |
| | 20.40 |

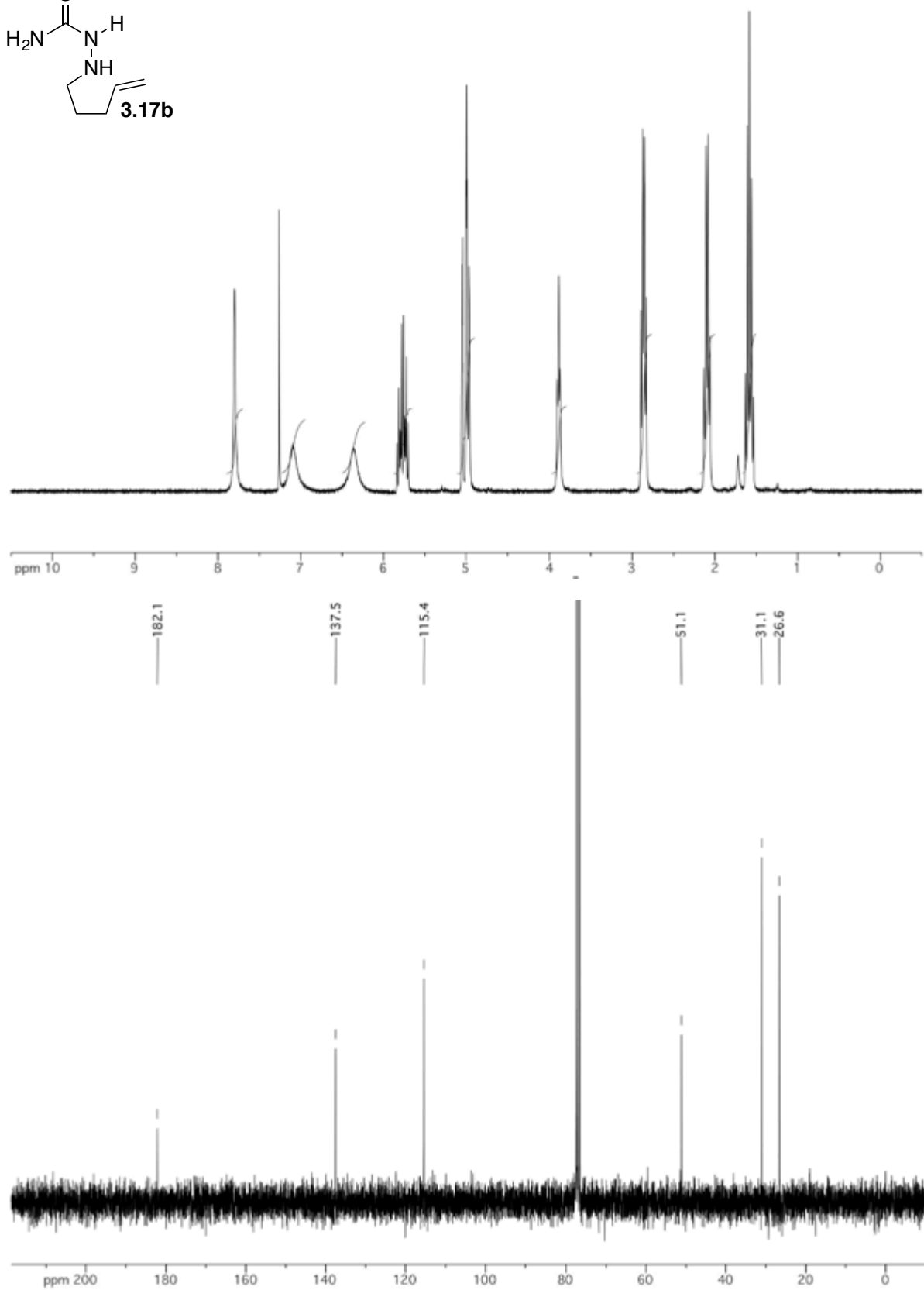
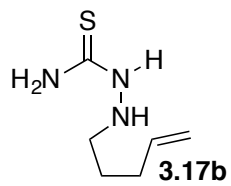


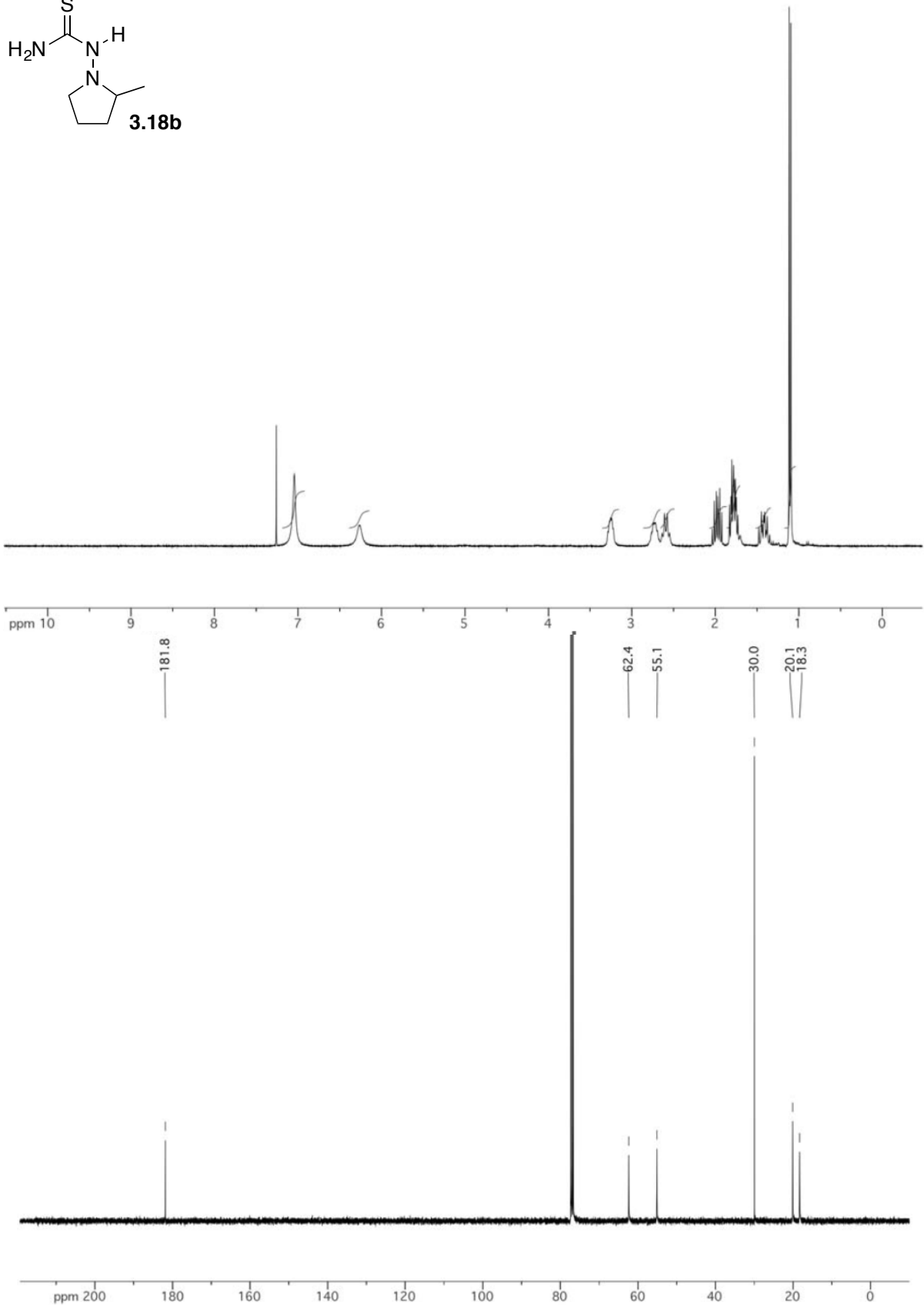
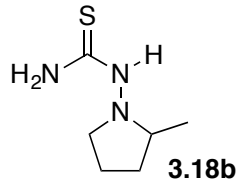


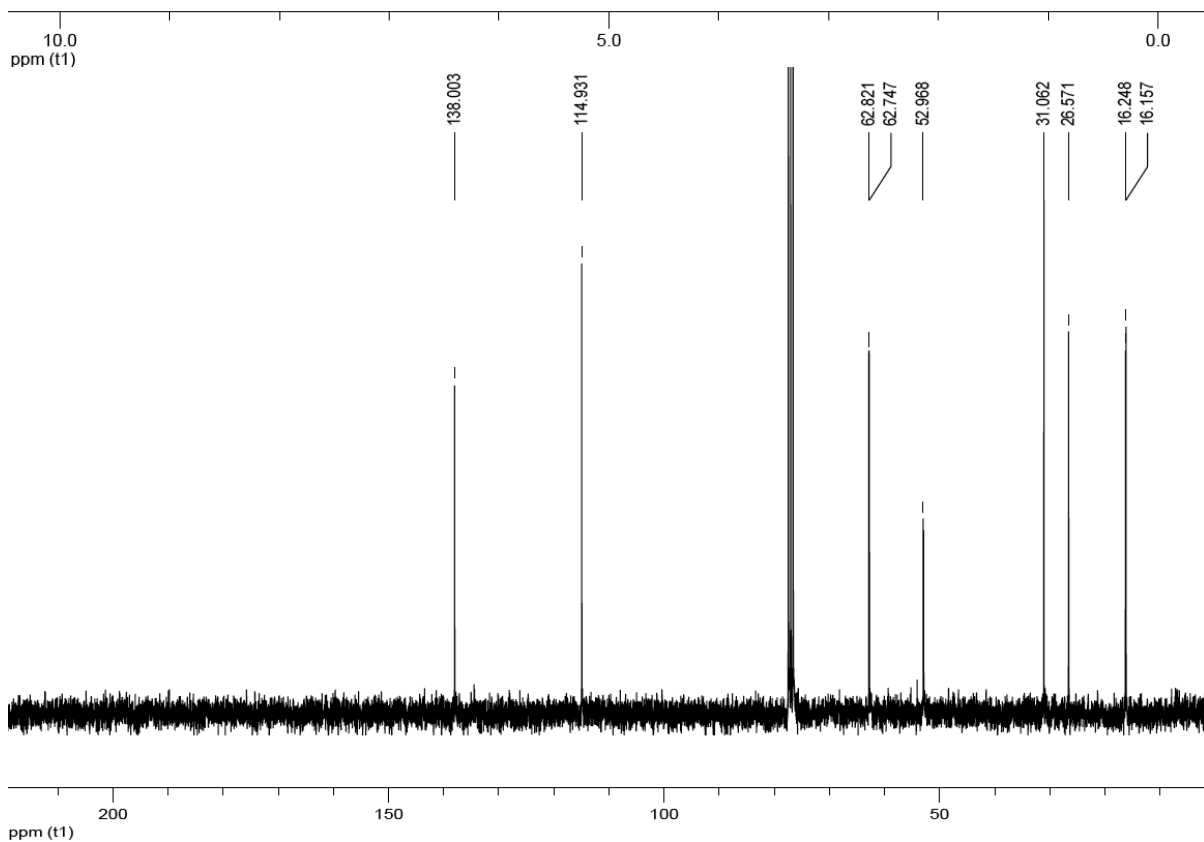
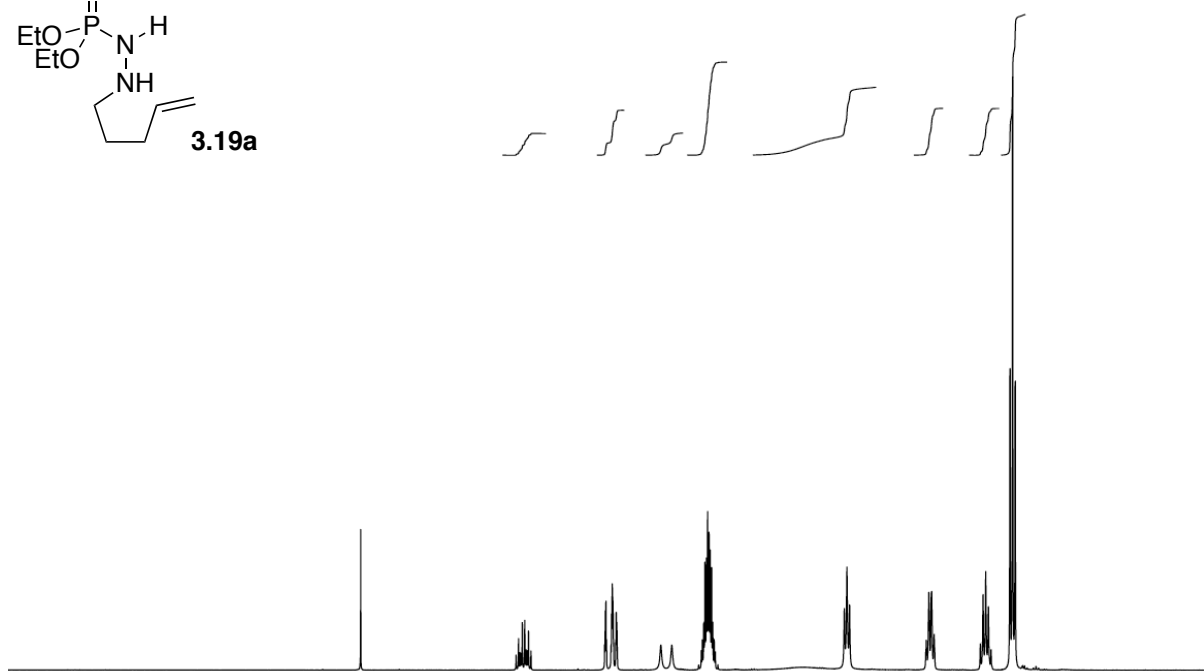
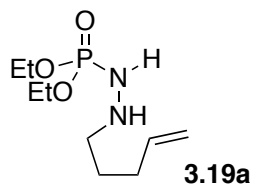


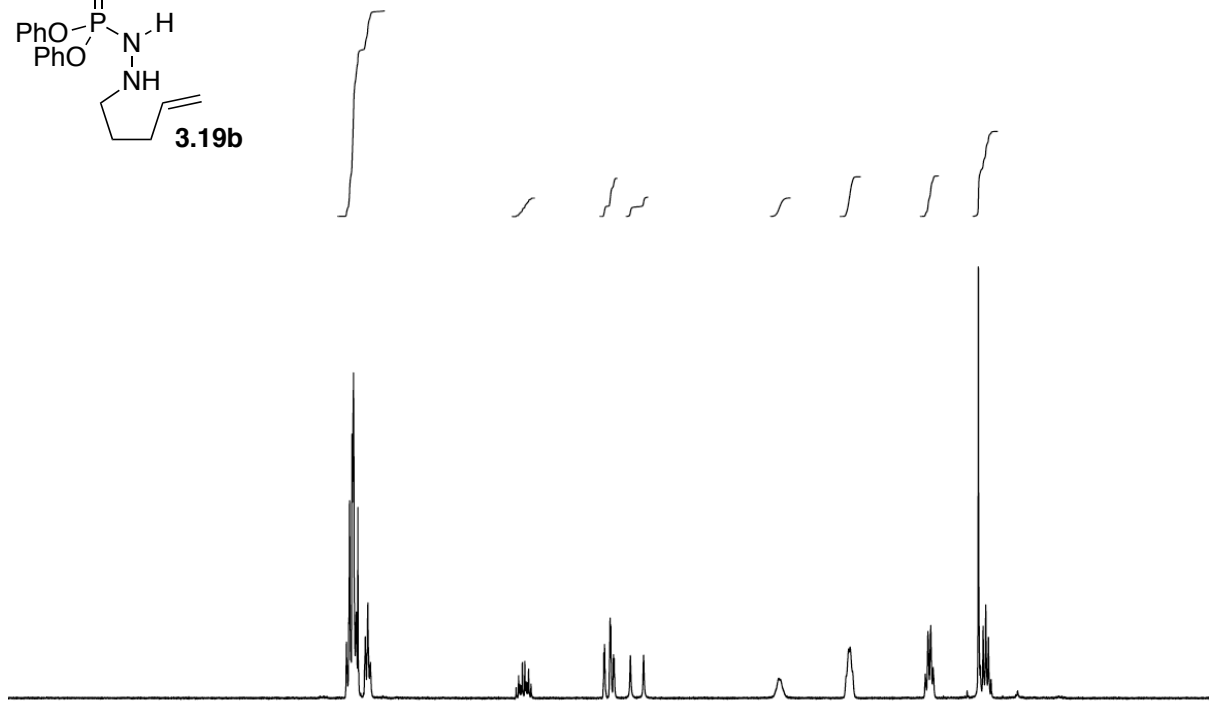
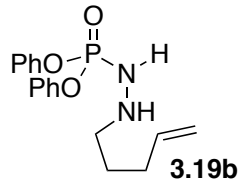




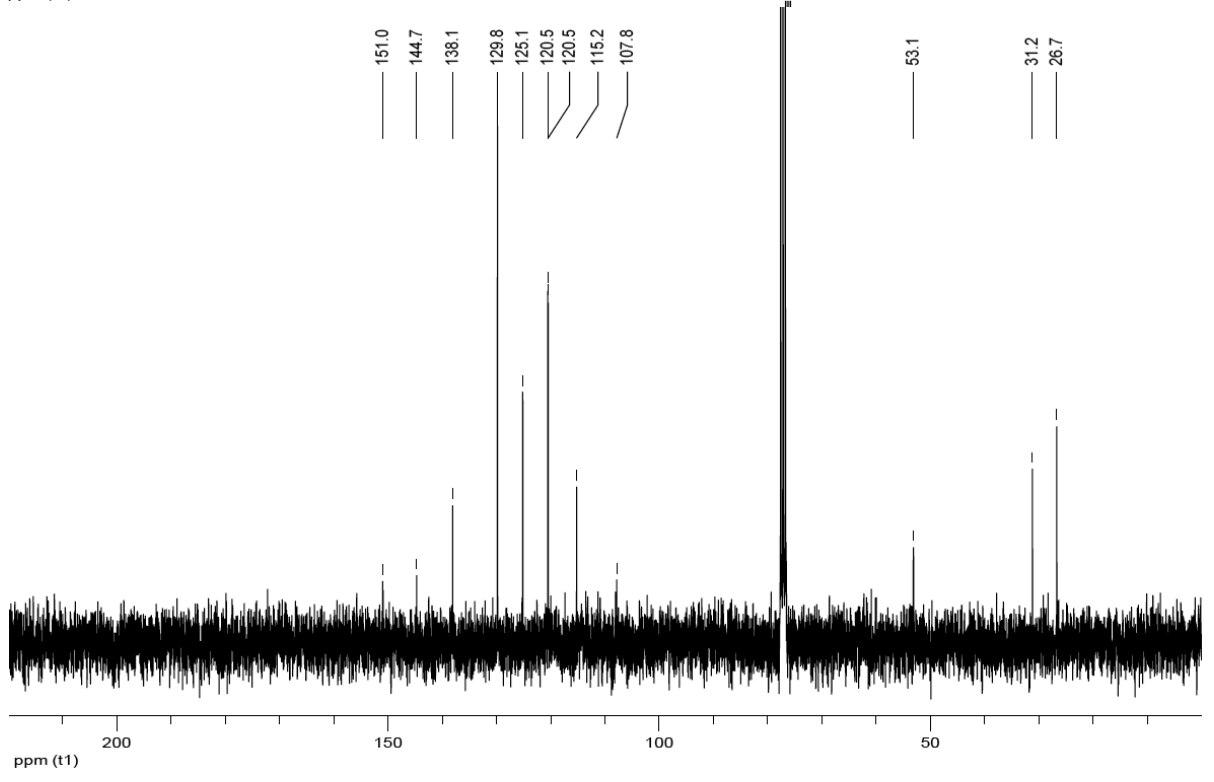




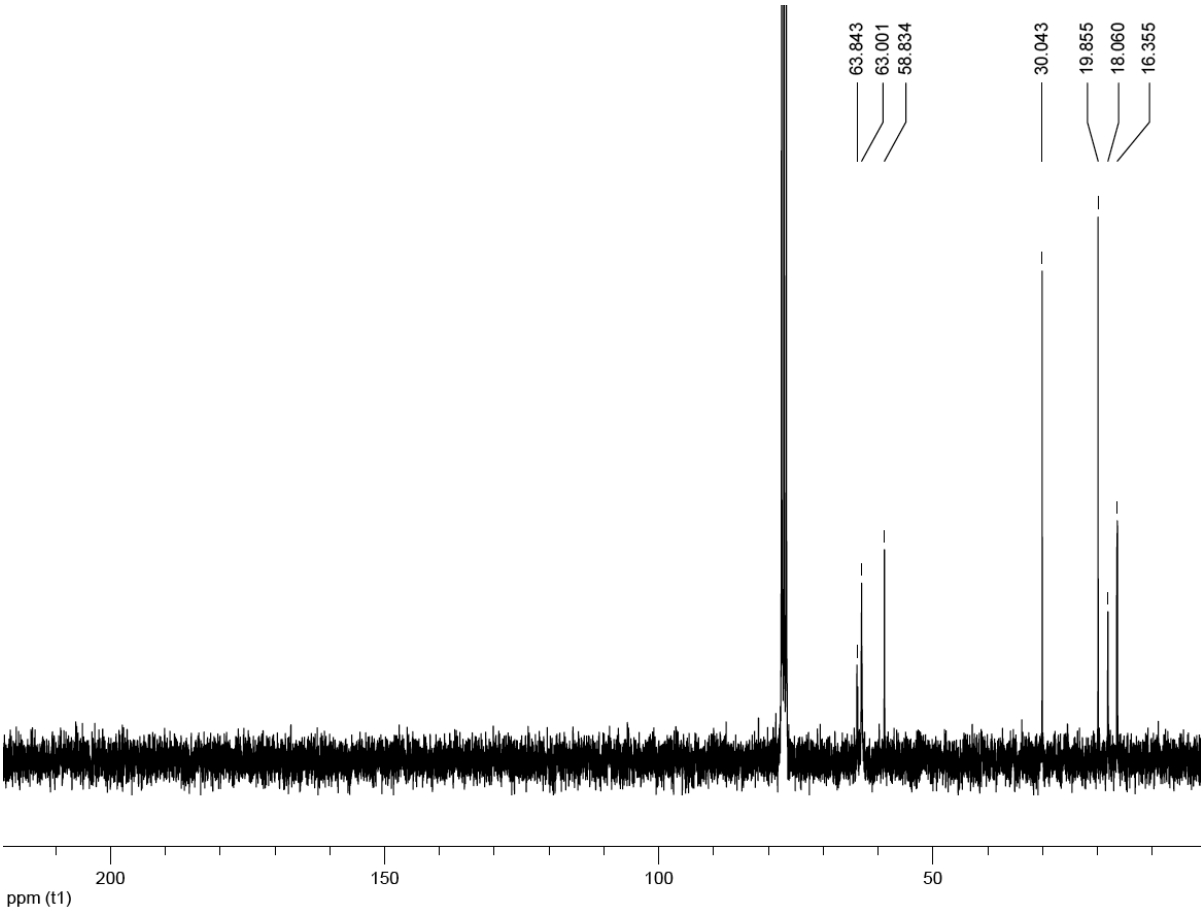
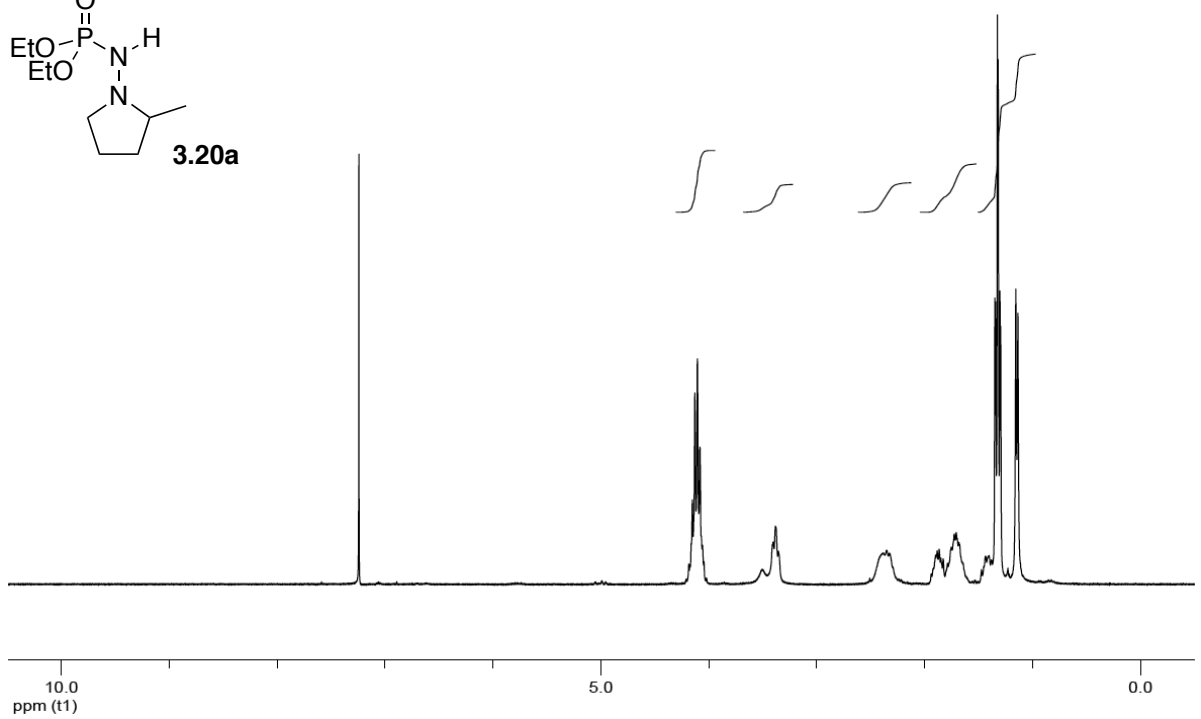
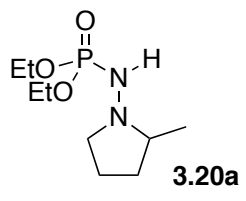


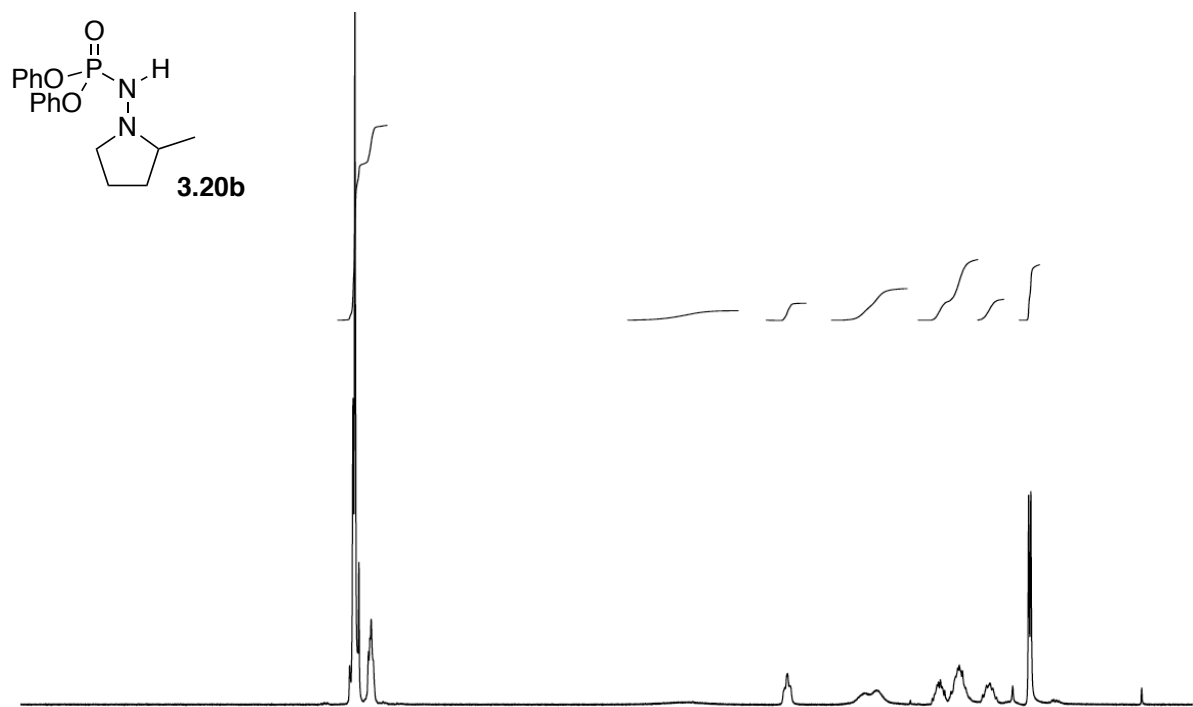
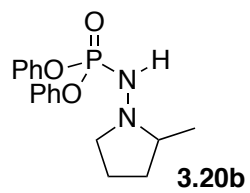


10.0 ppm (t1) 5.0 0.0



ppm (t1) 200 150 100 50

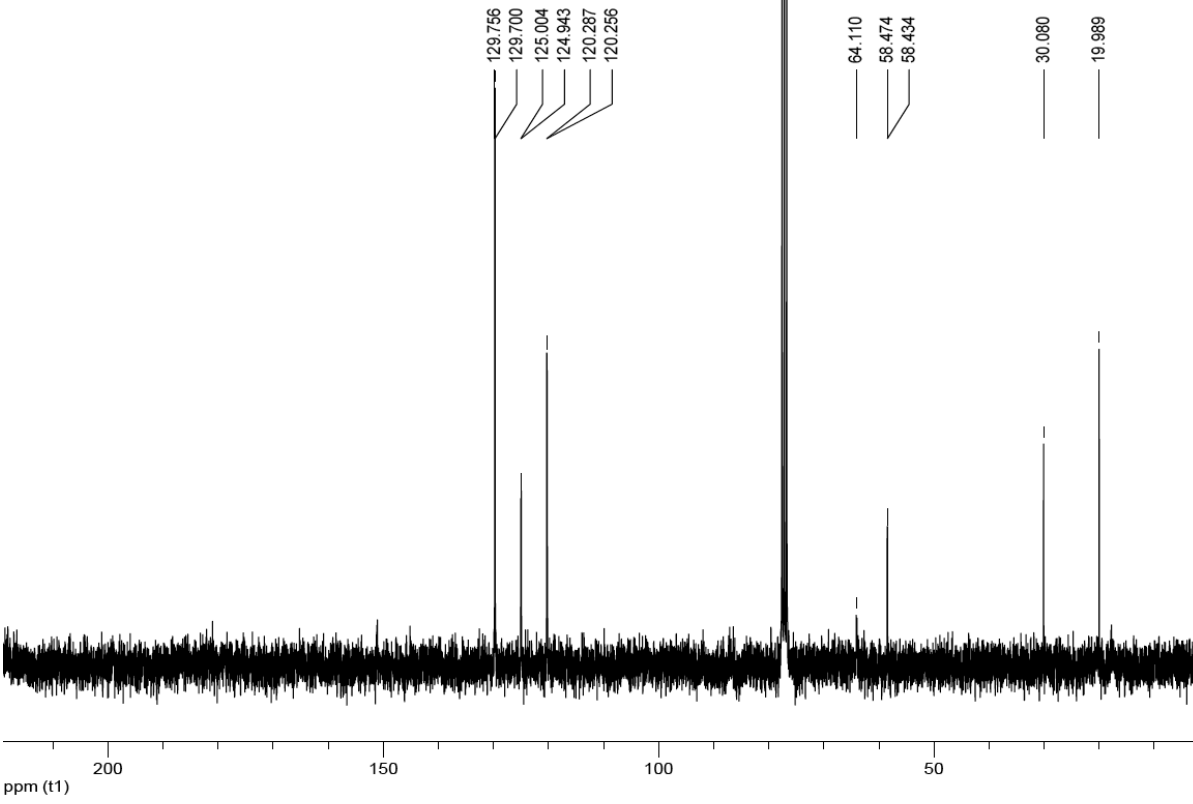


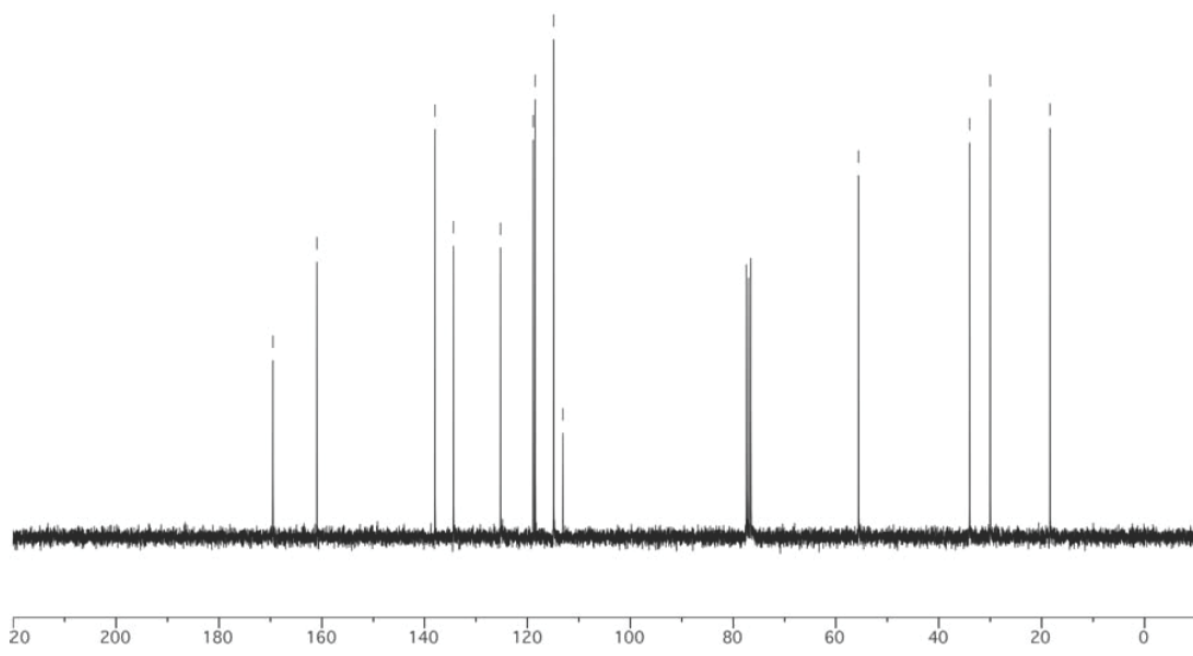
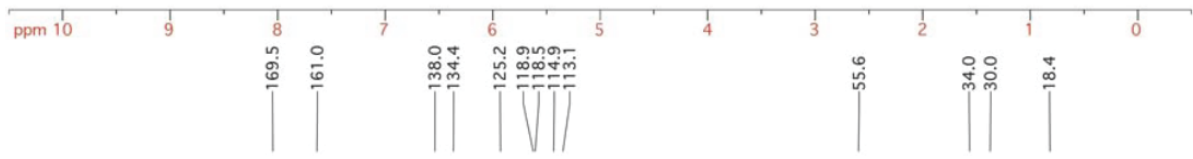
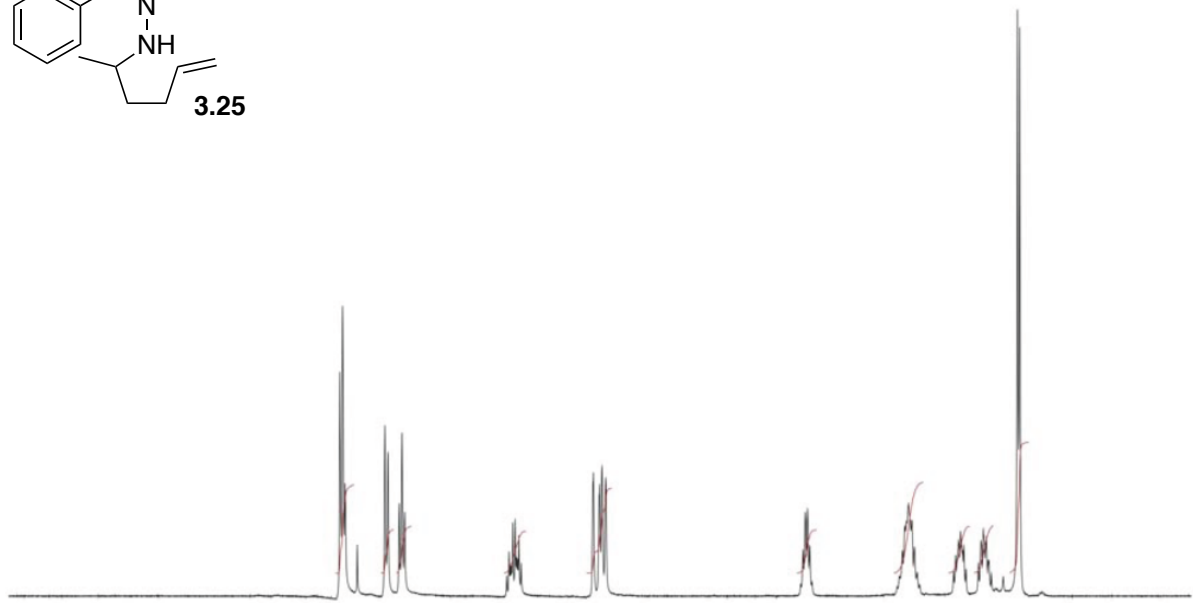
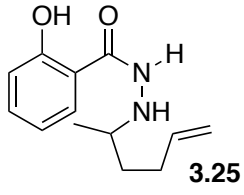


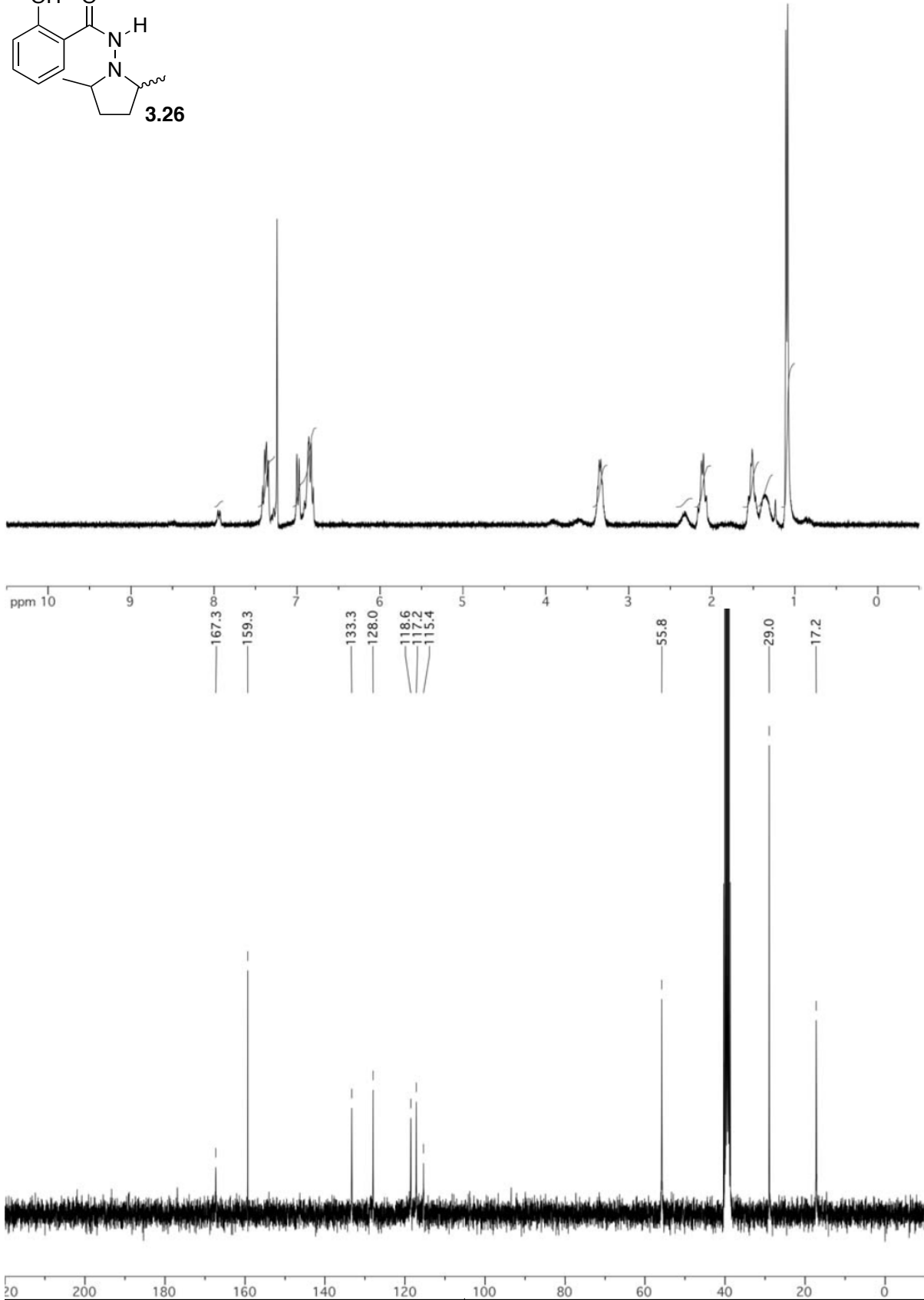
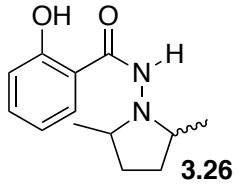
10.0
ppm (t1)

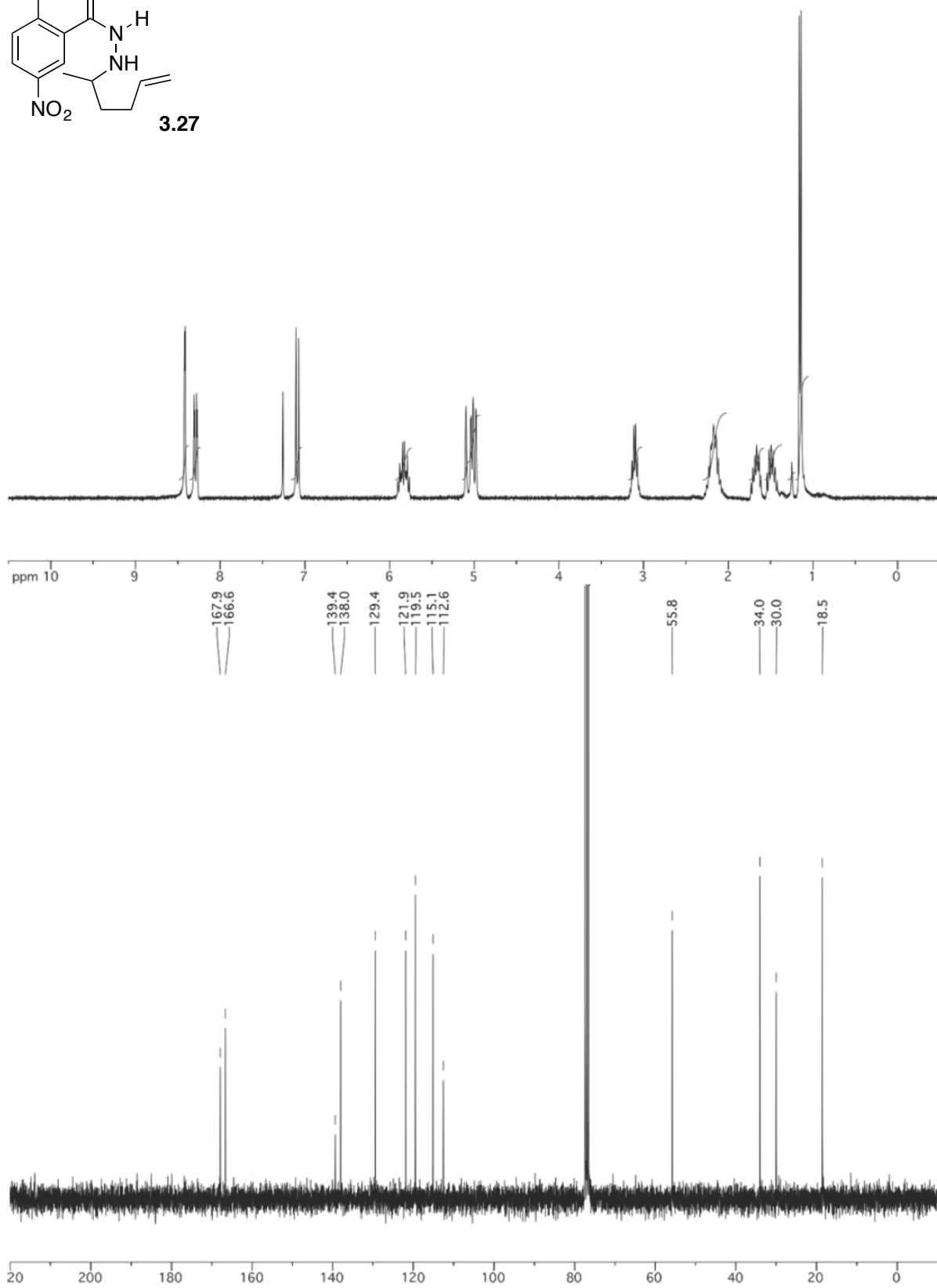
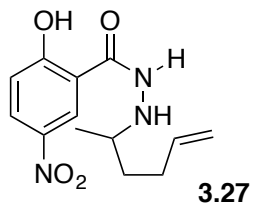
5.0

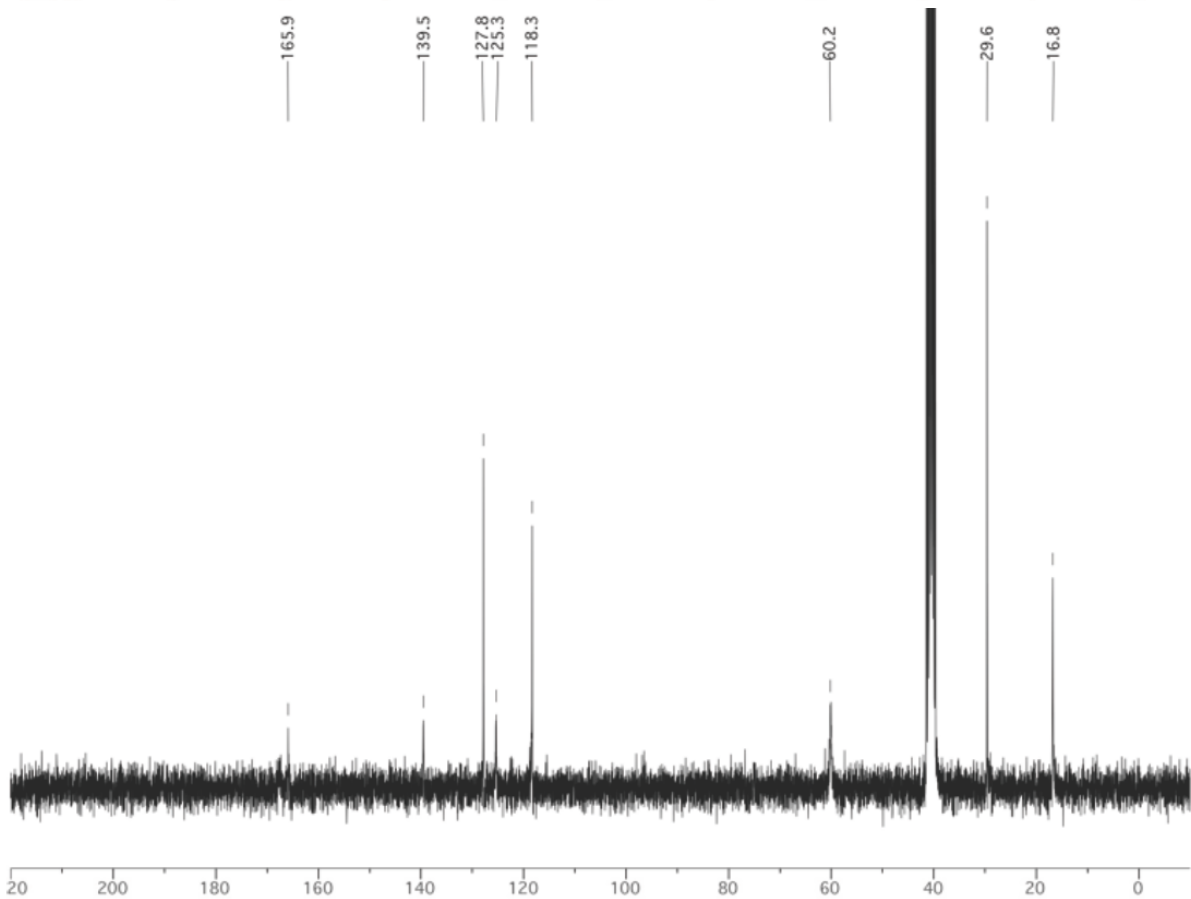
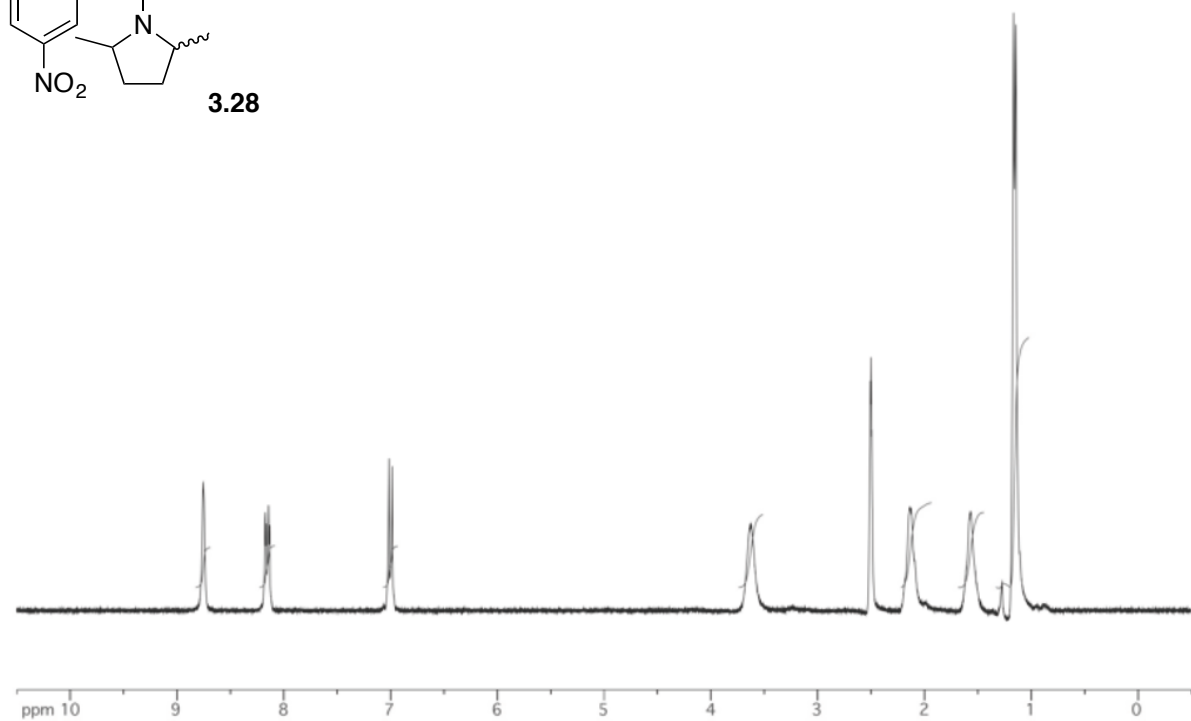
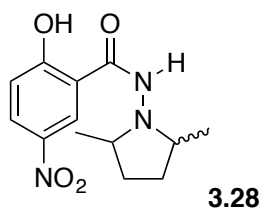
0.0

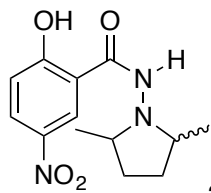




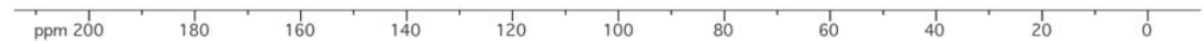
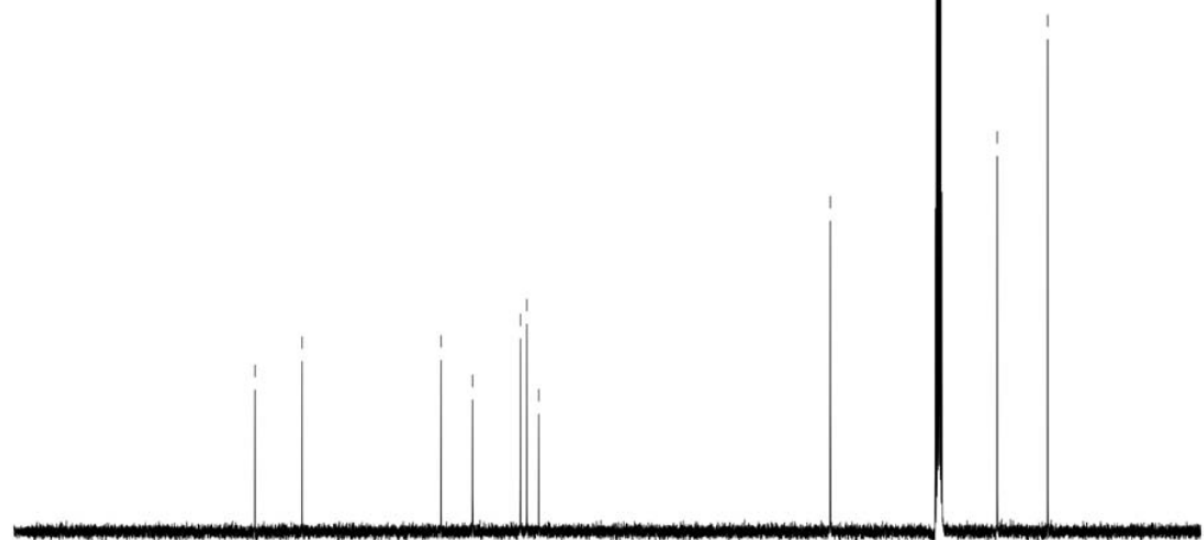
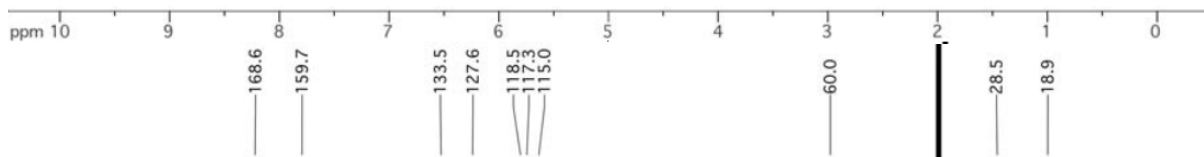
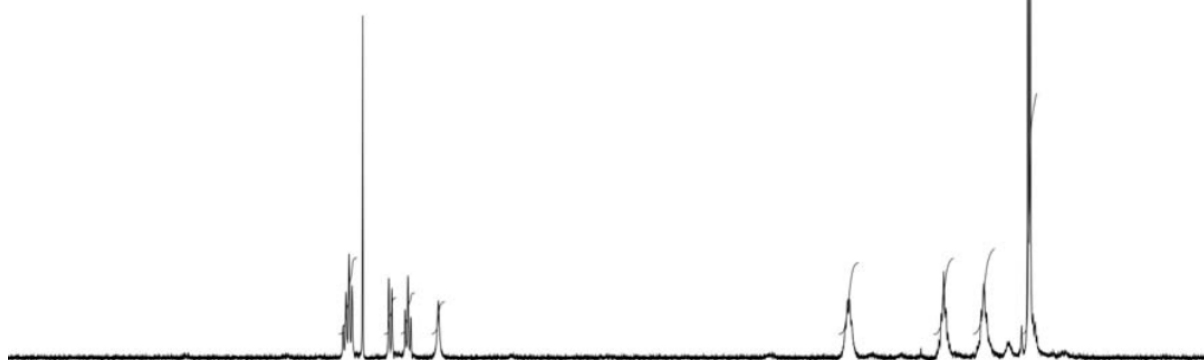


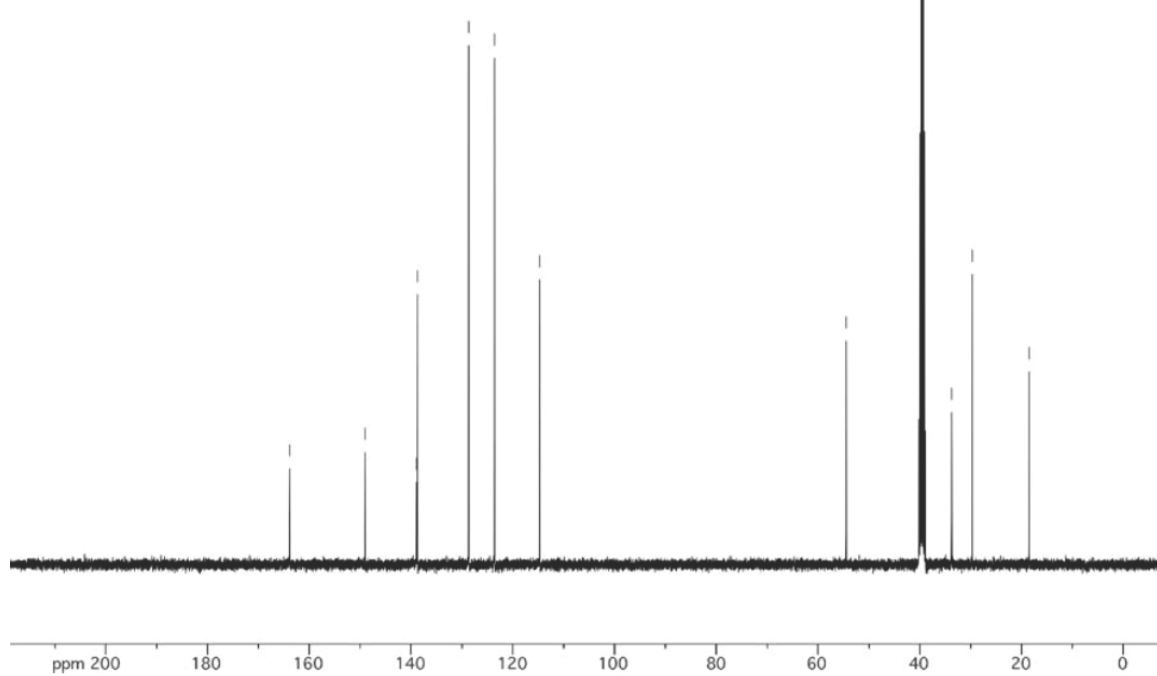
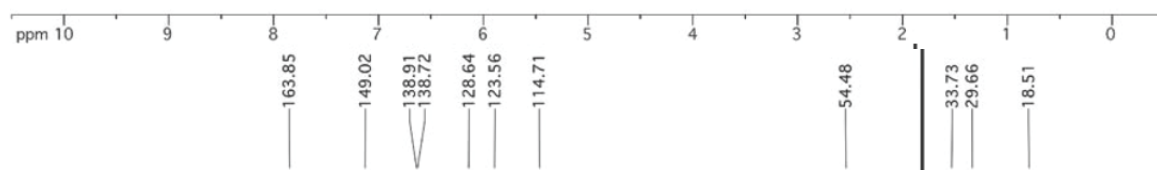
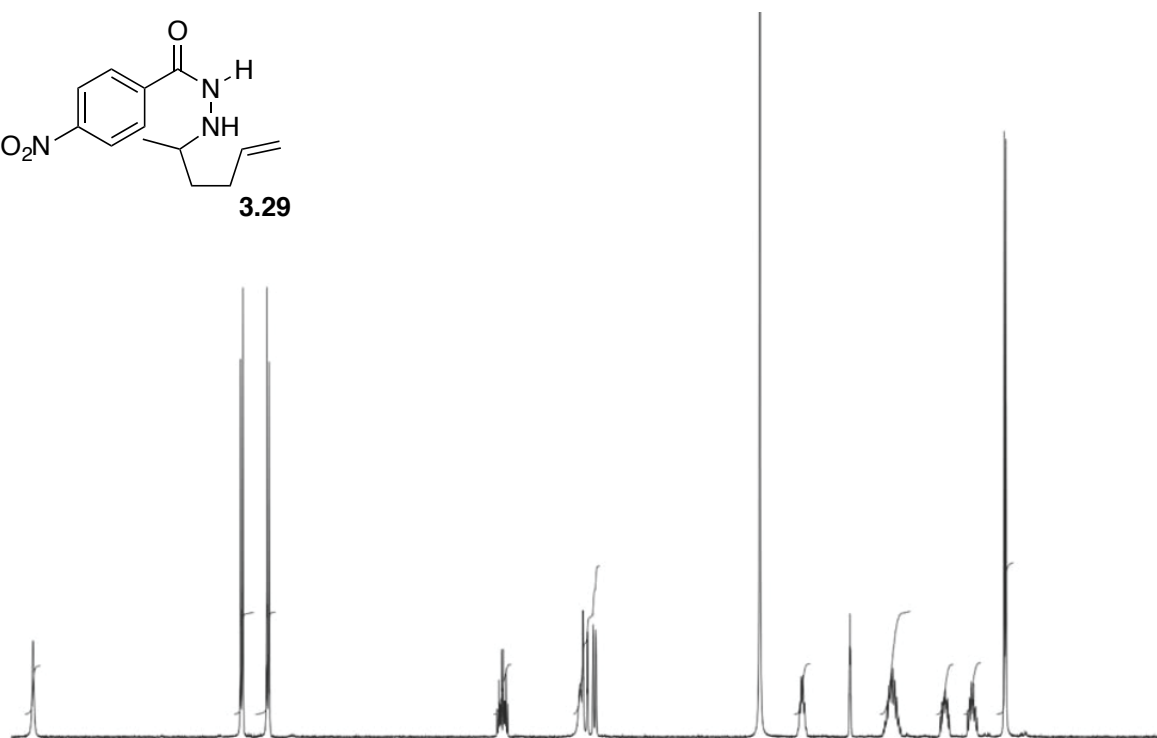
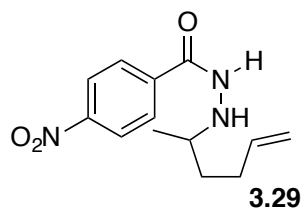


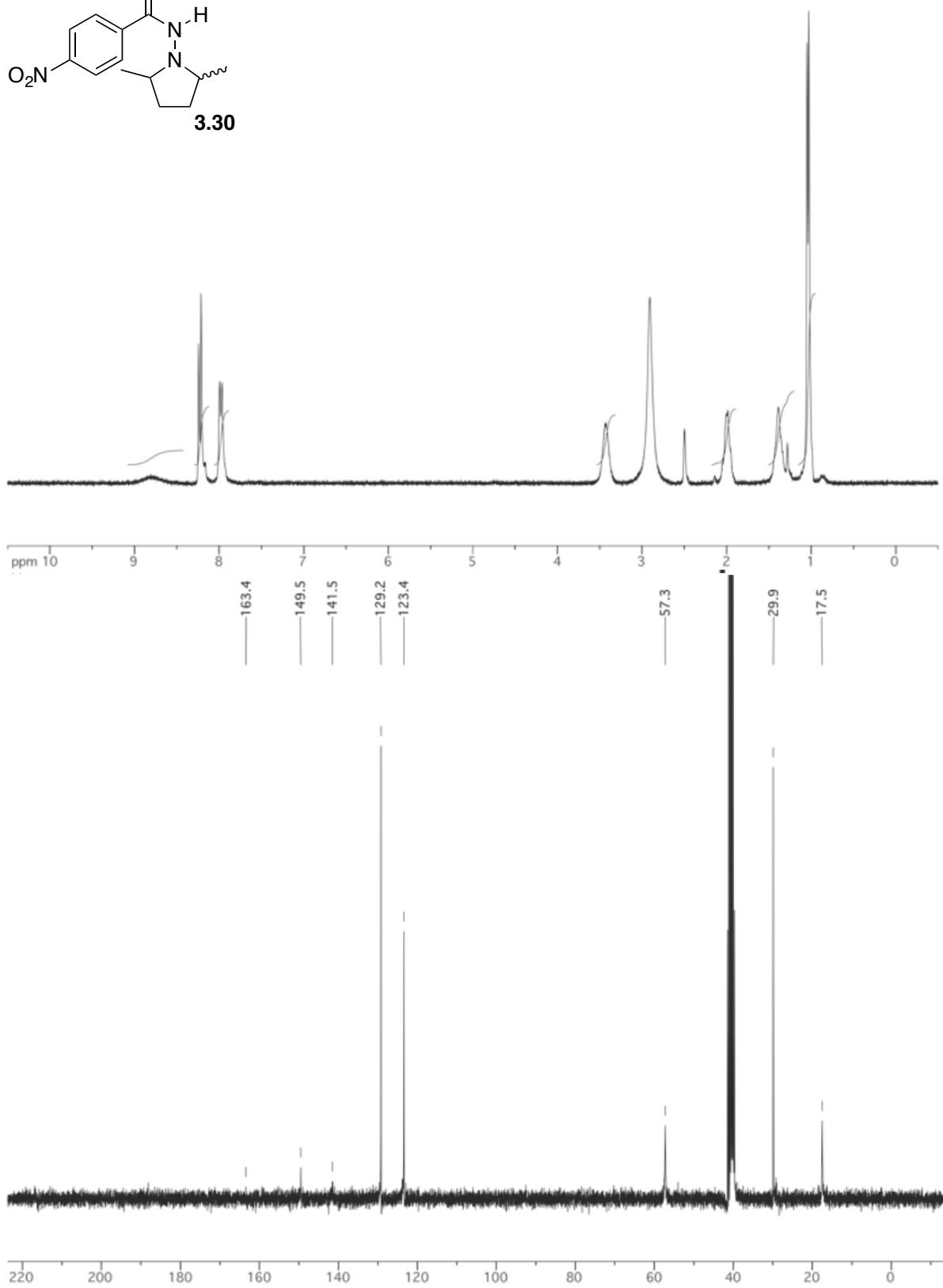
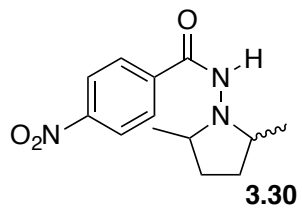


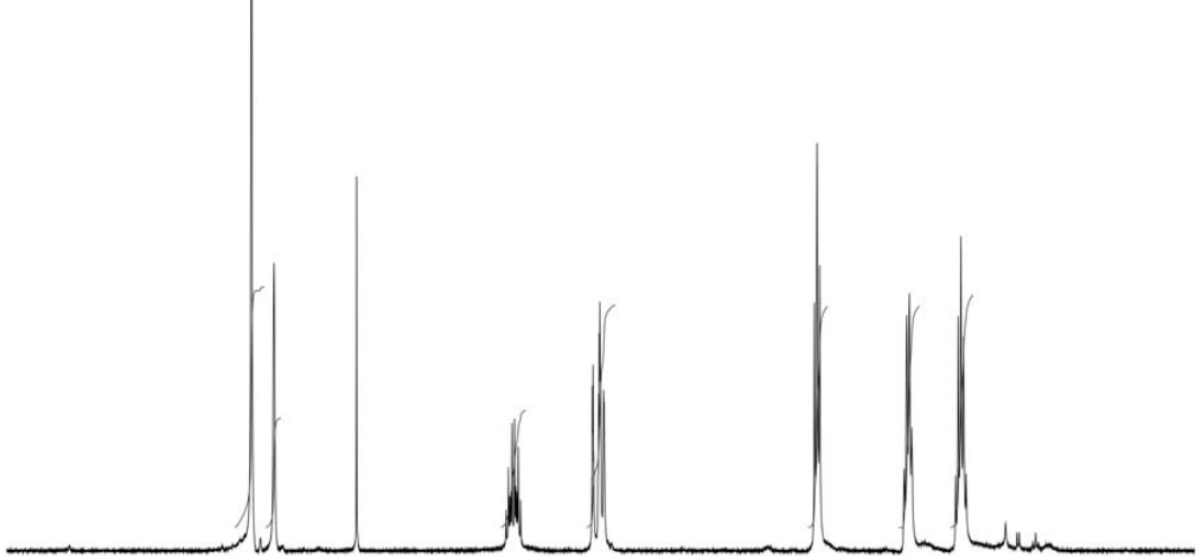
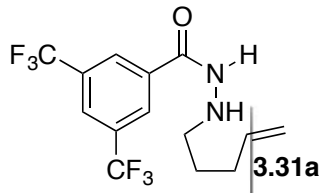


3.28 minor

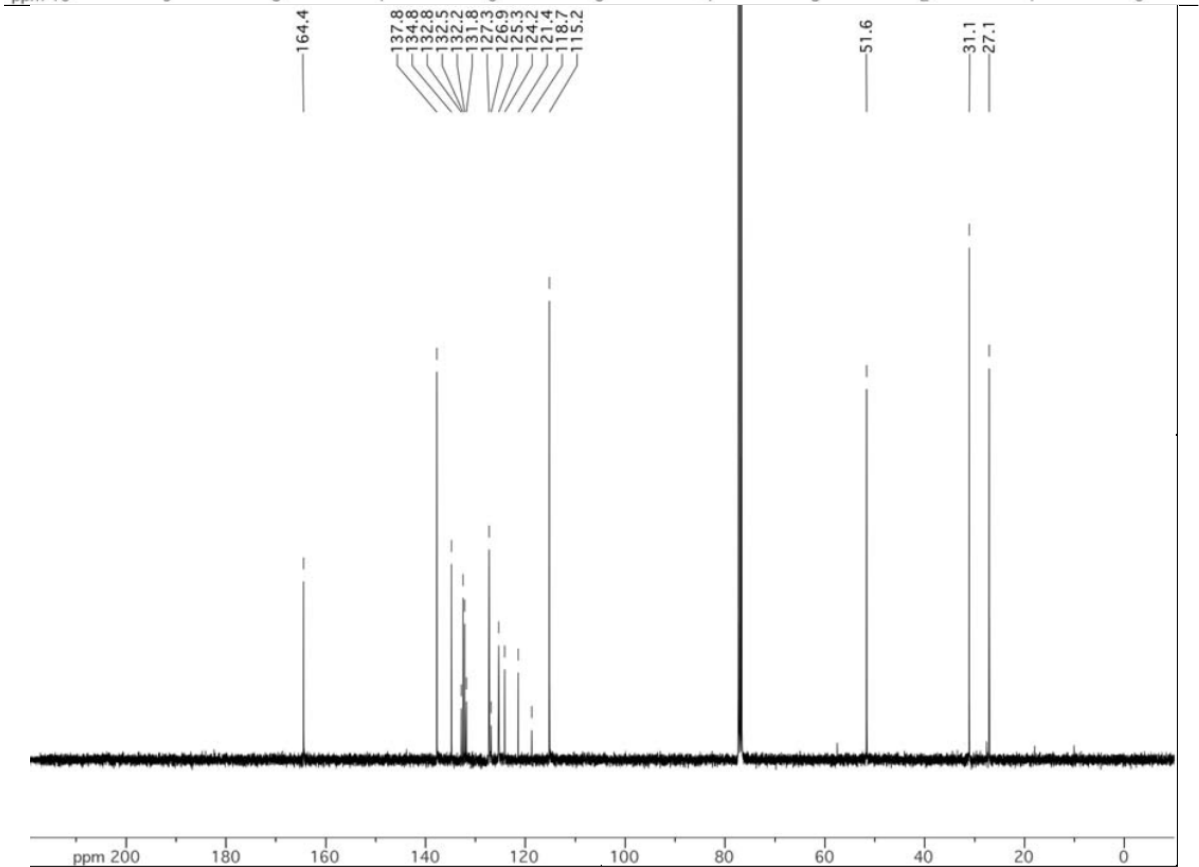


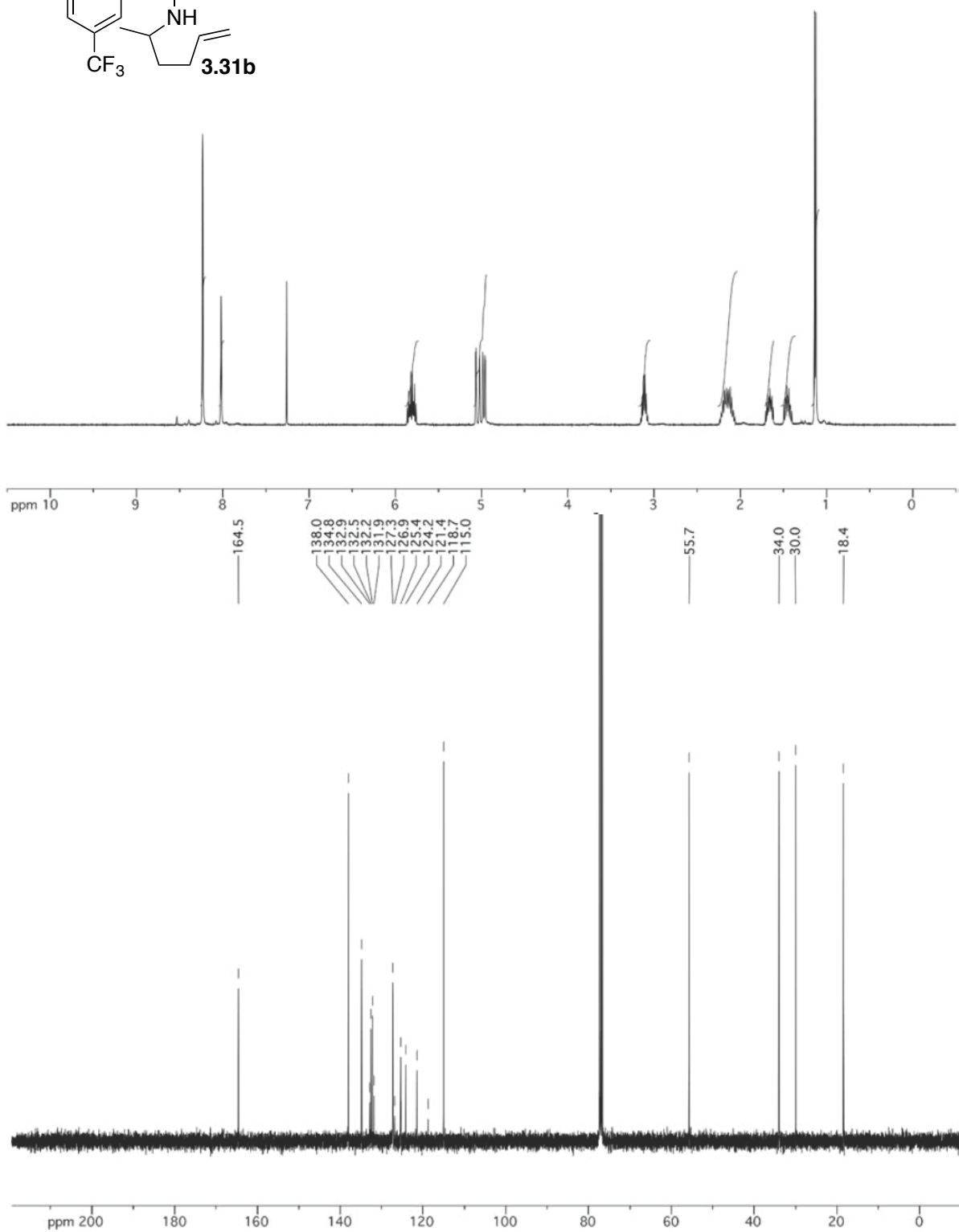
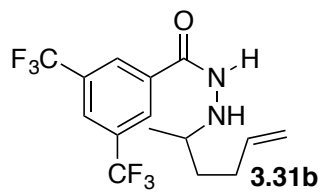


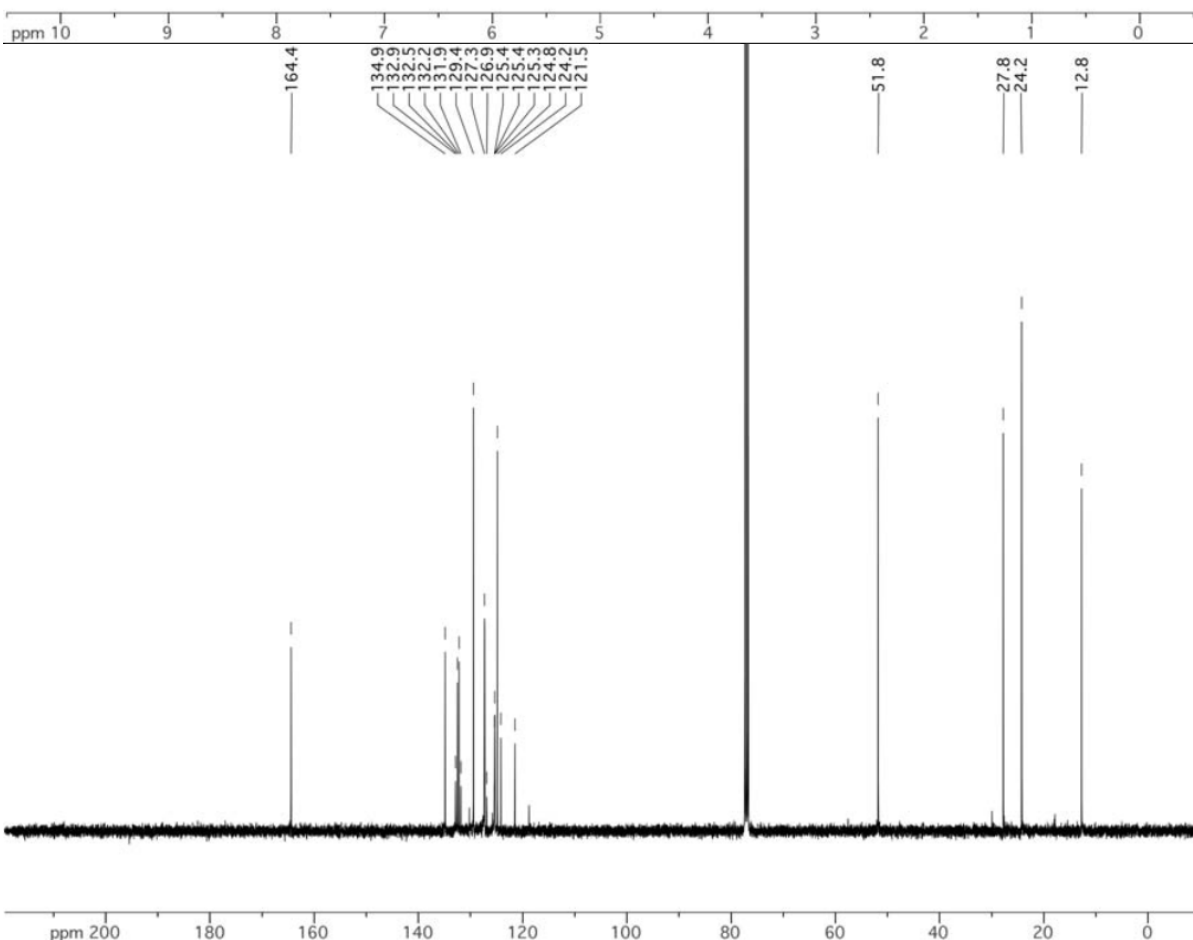
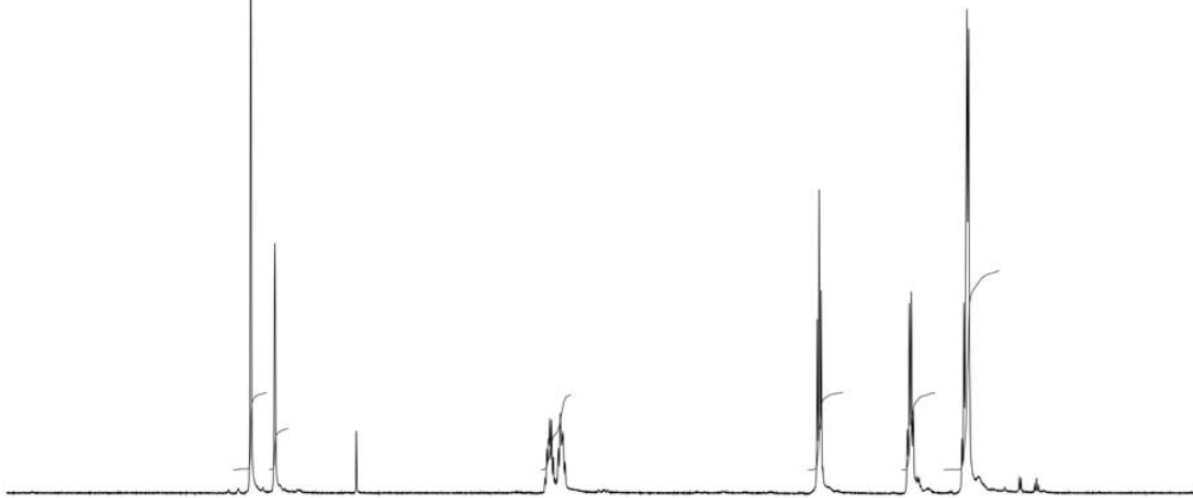
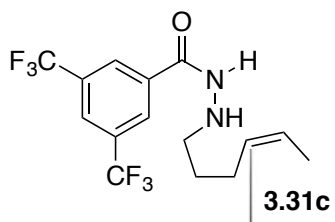


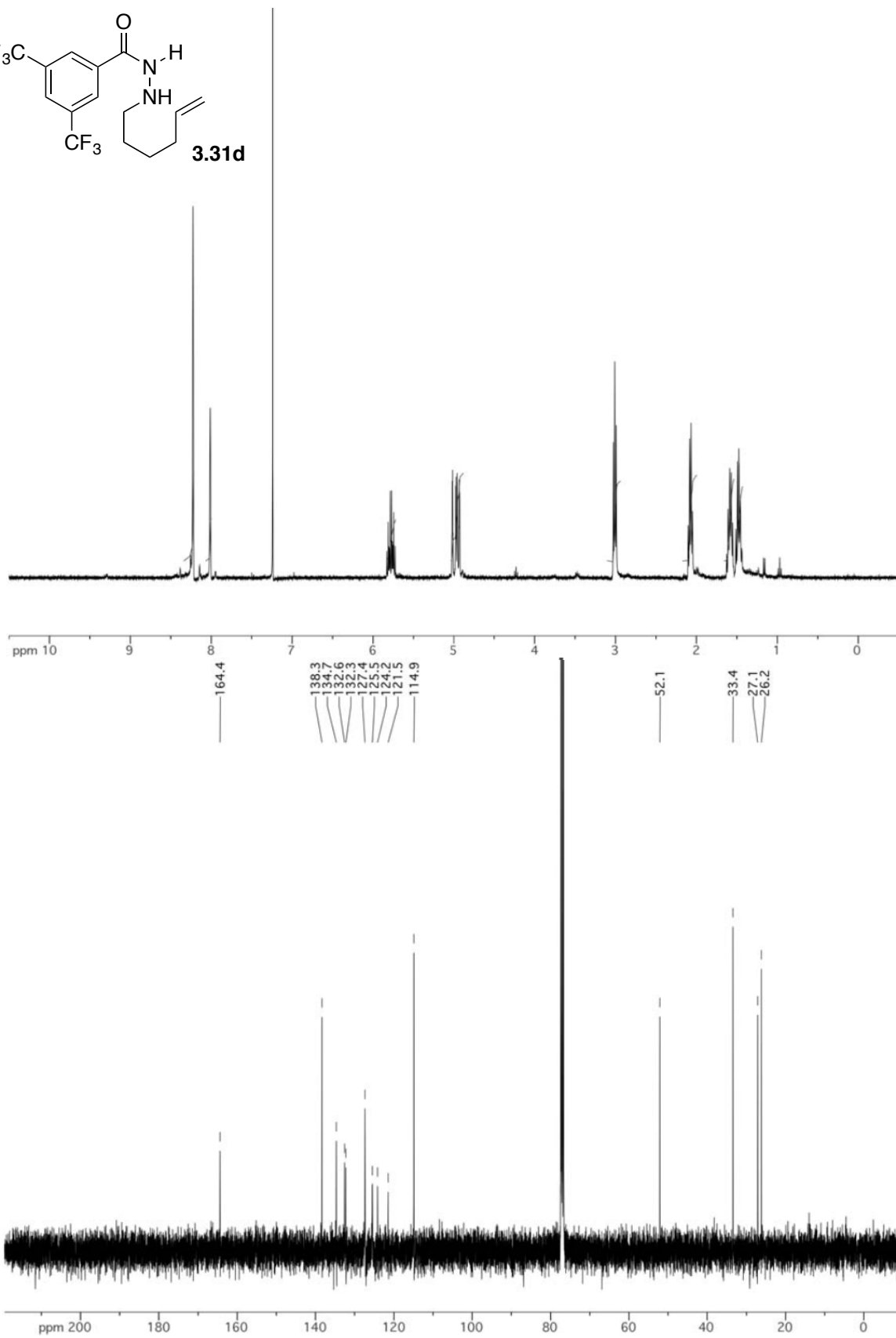
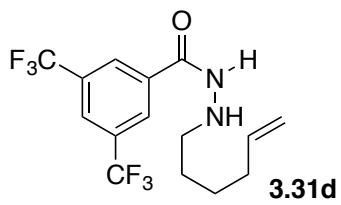


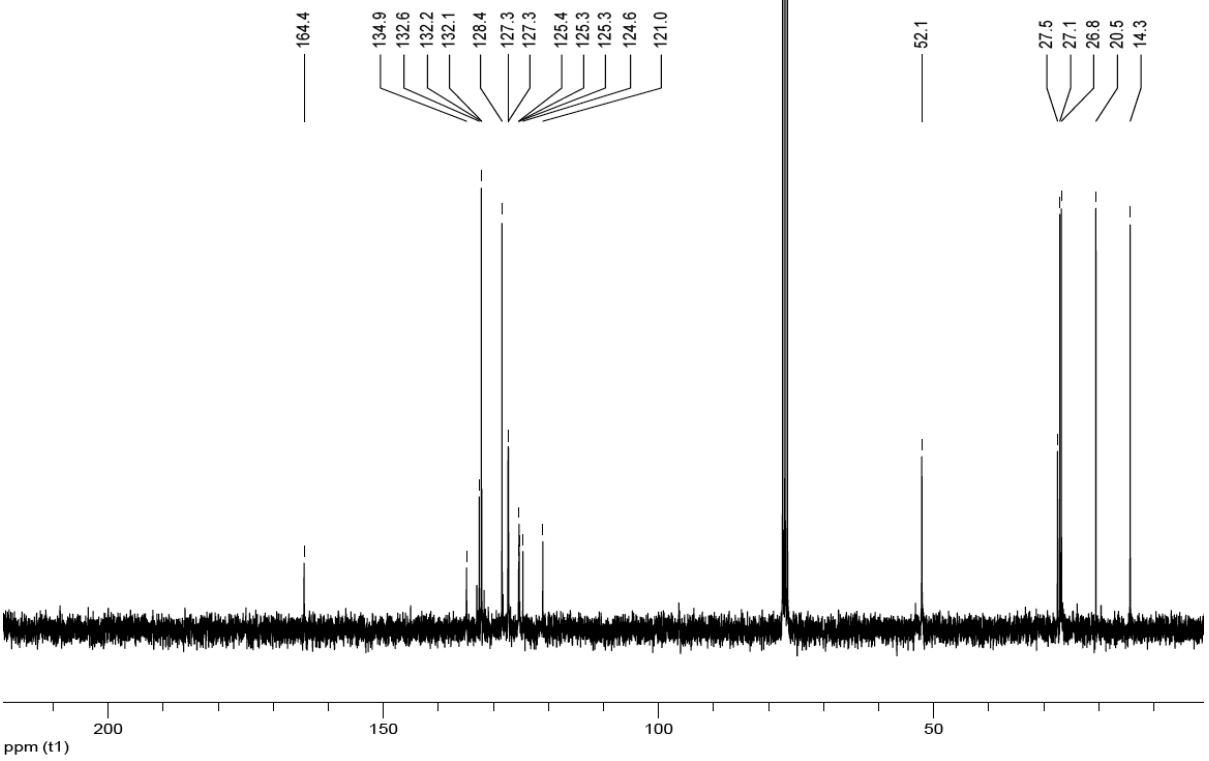
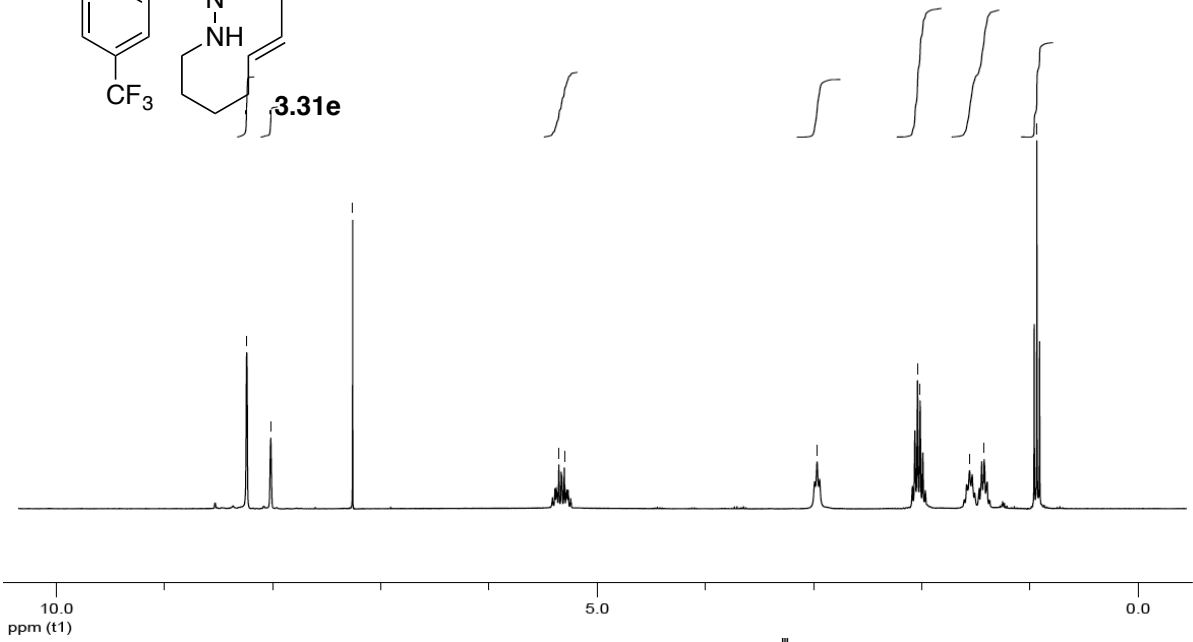
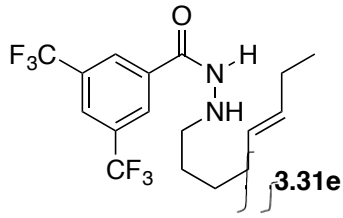
ppm 10 9 8 7 6 5 4 3 2 1 0

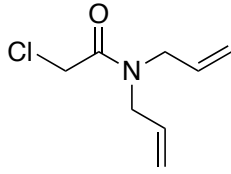




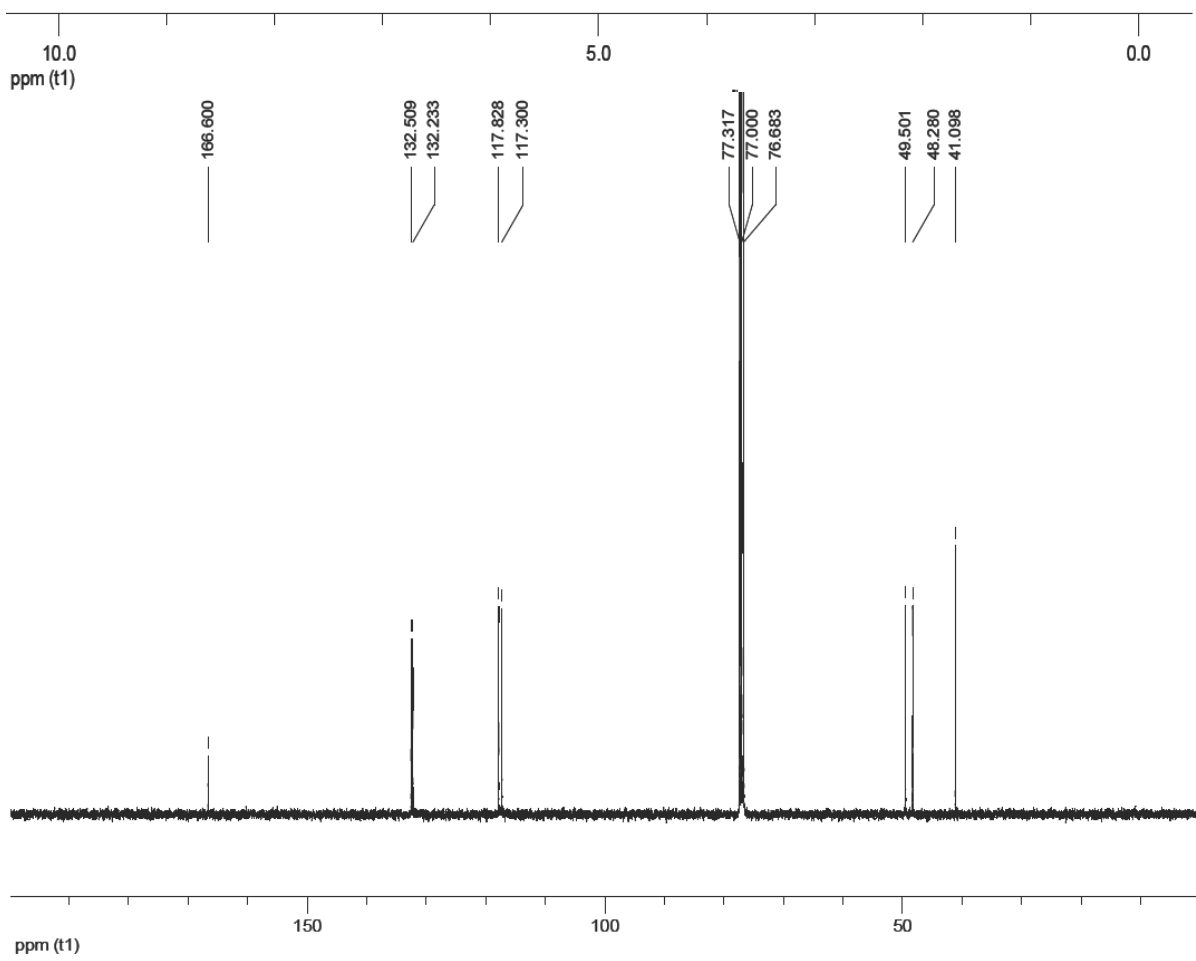
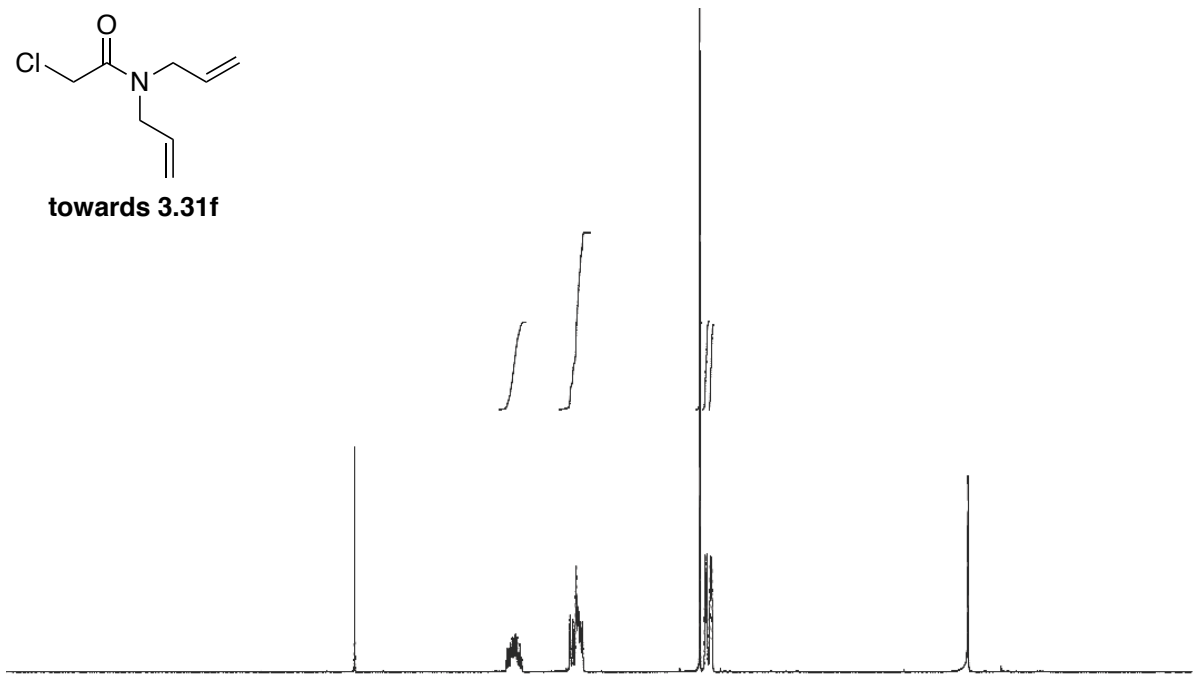


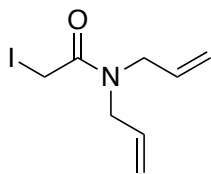




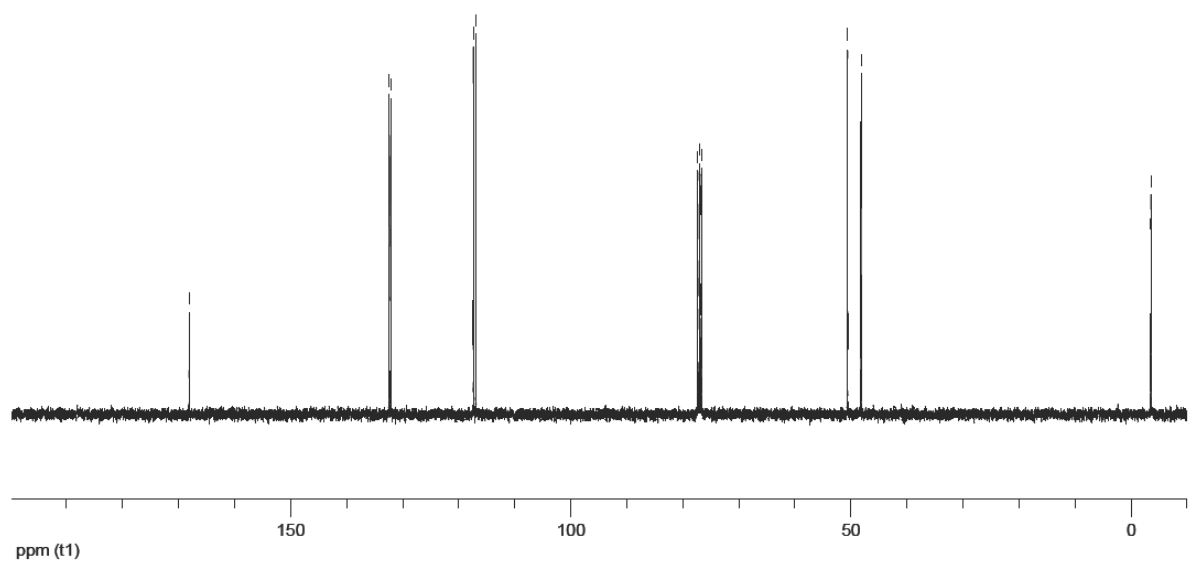
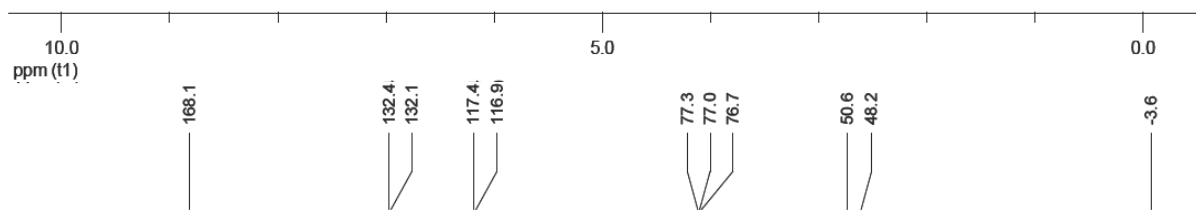
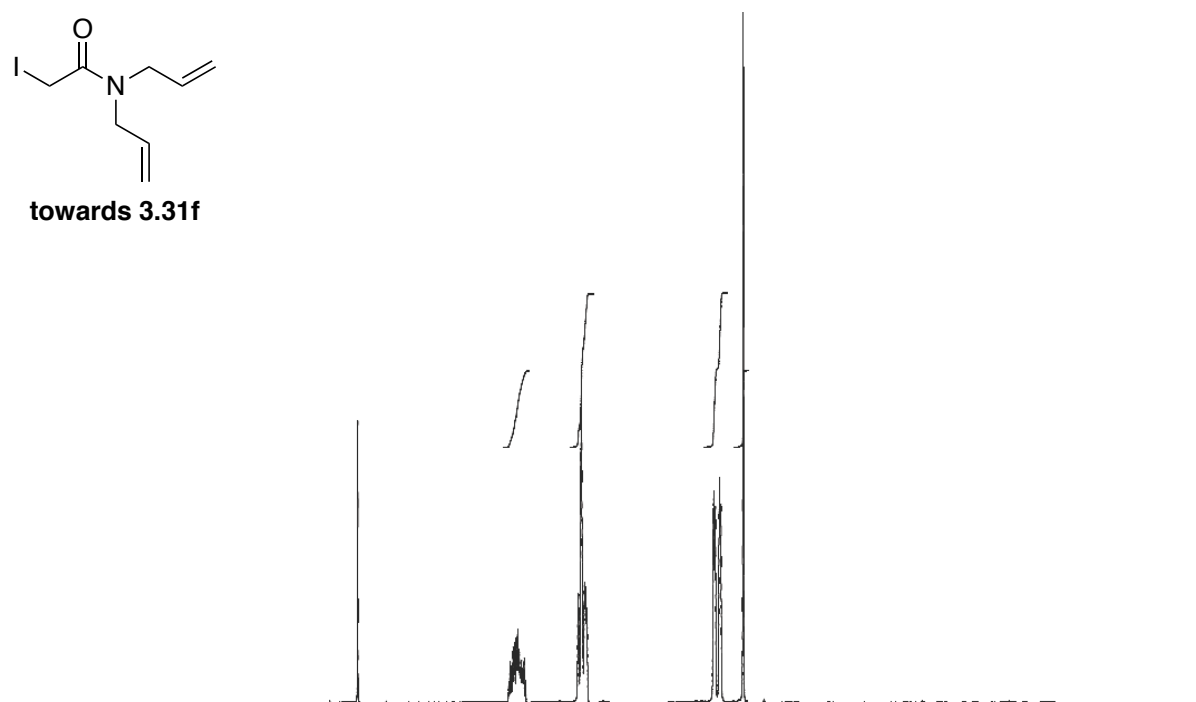


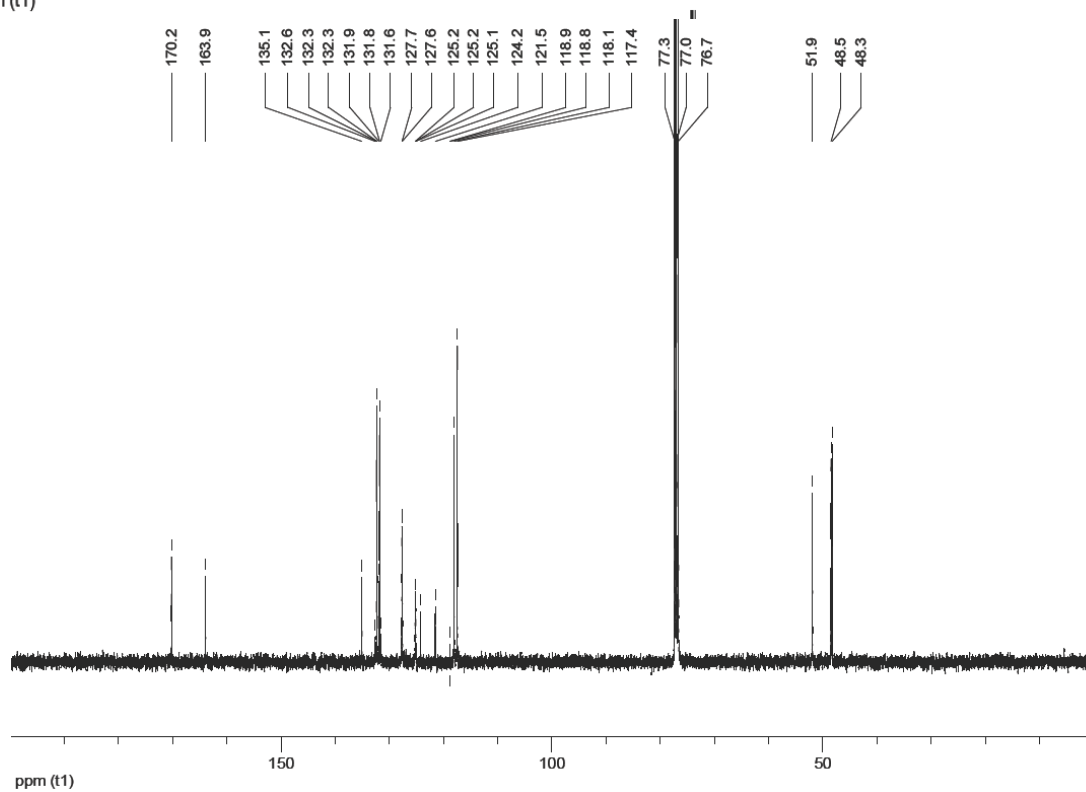
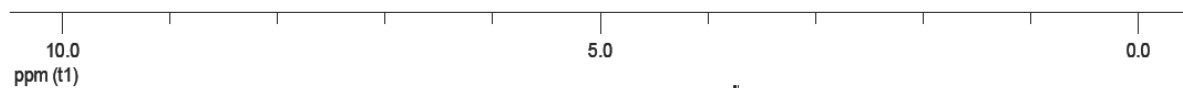
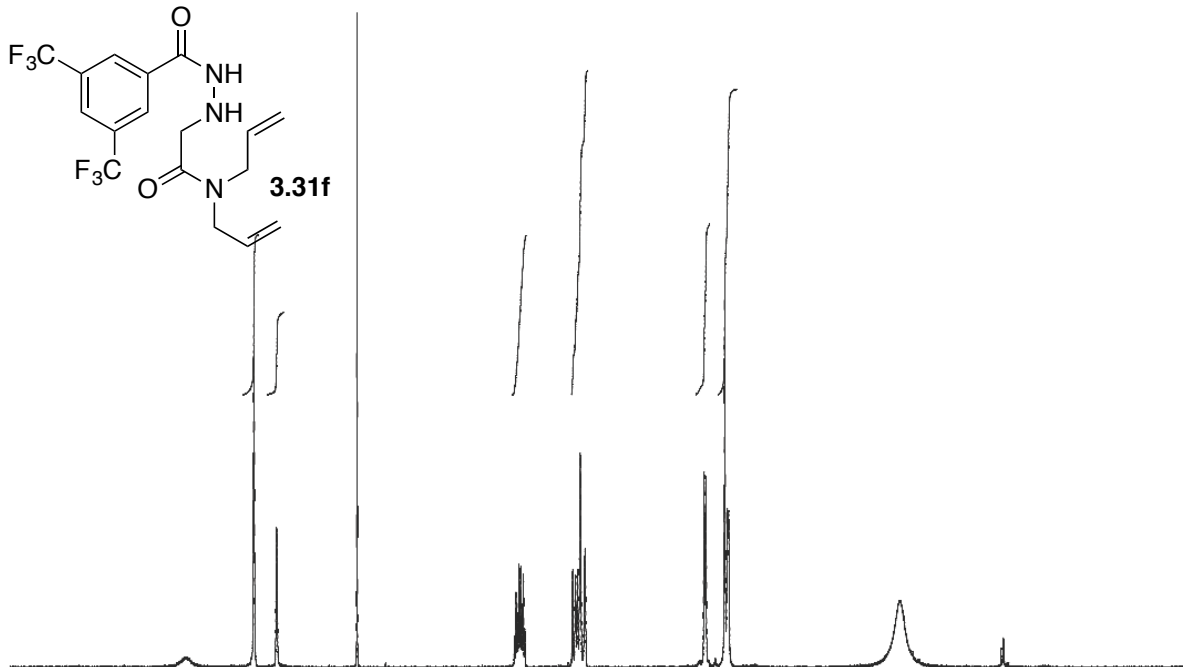
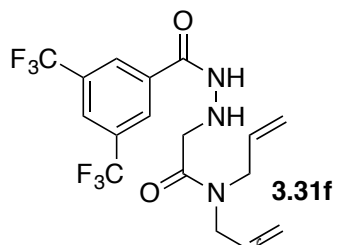
towards 3.31f

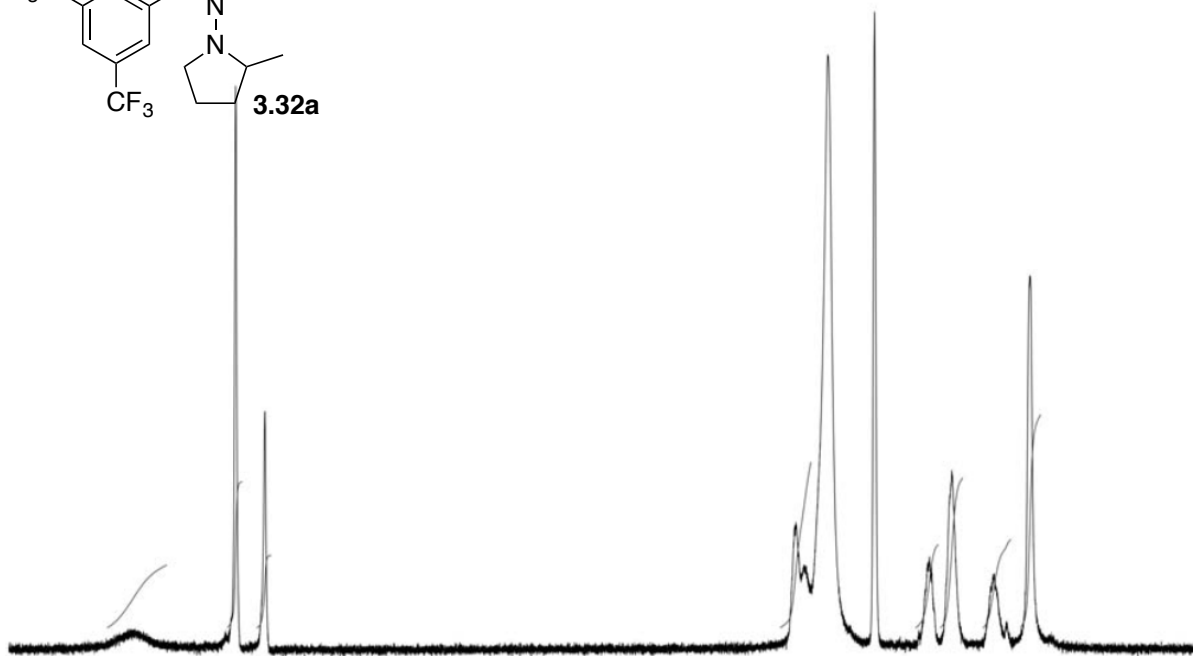
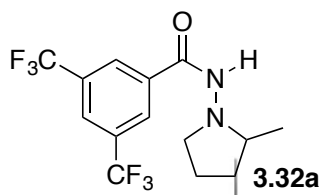




towards 3.31f

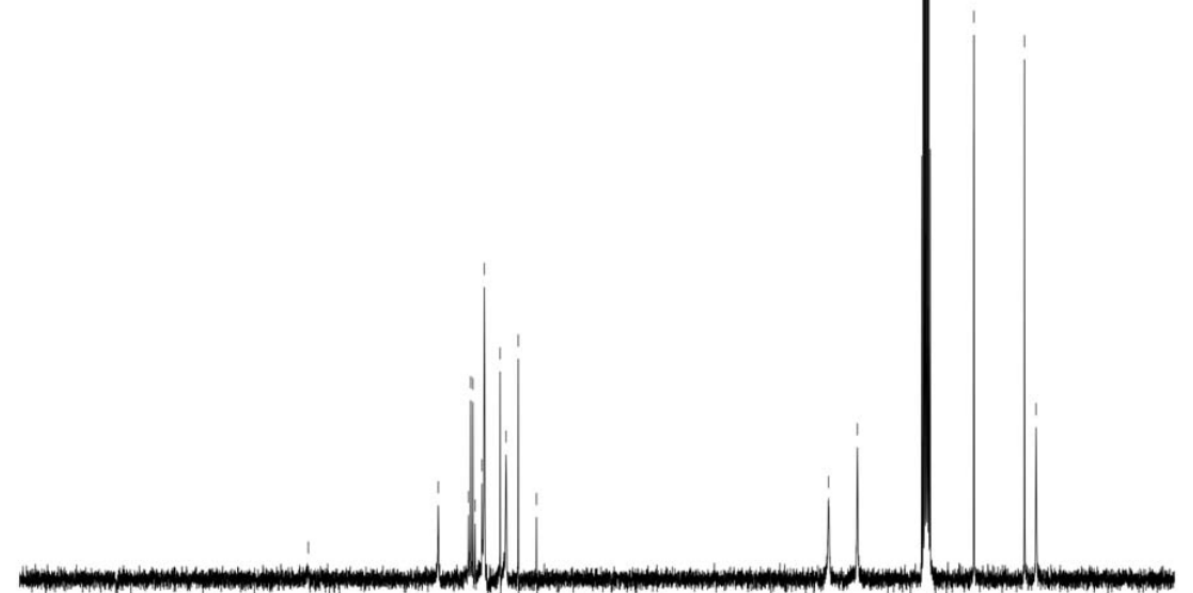




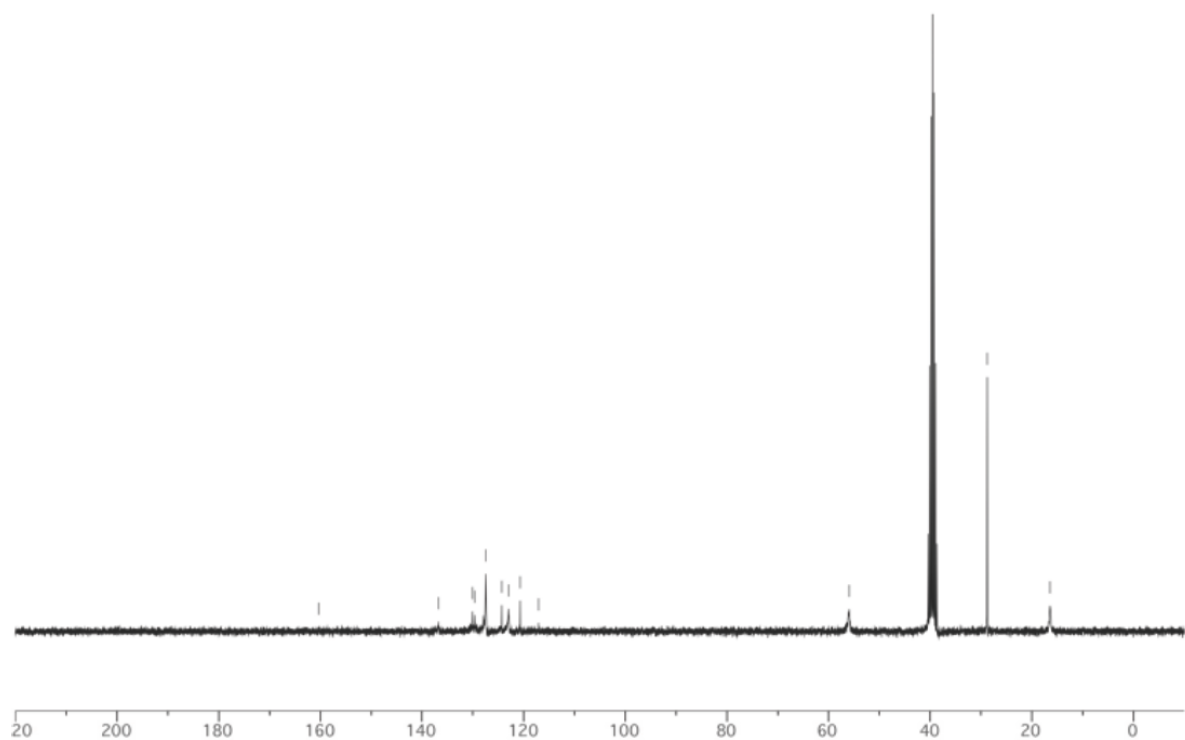
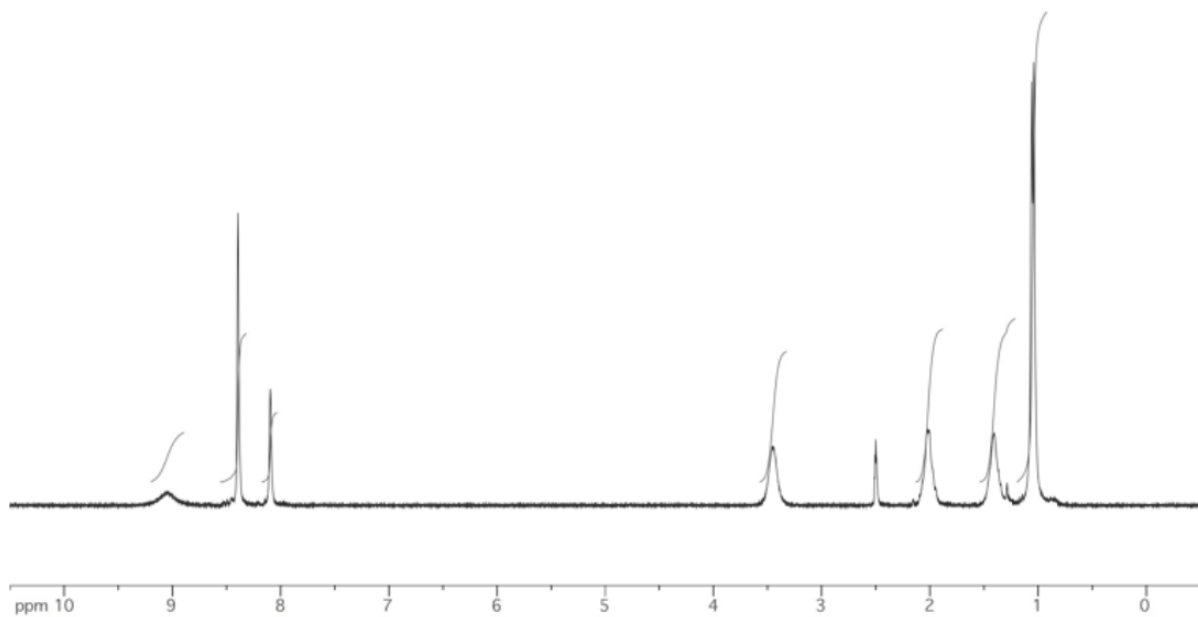
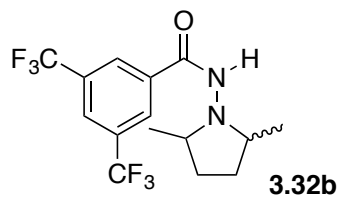


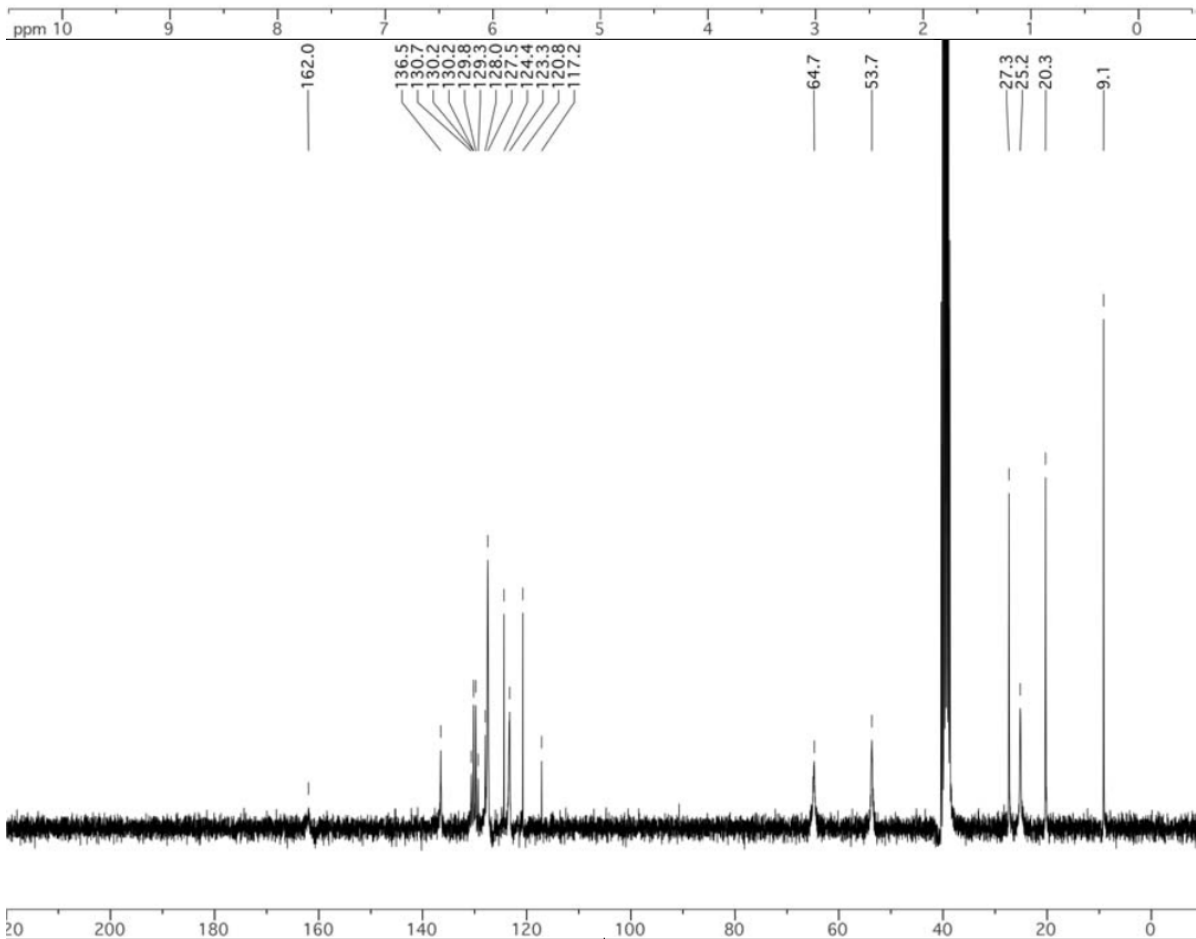
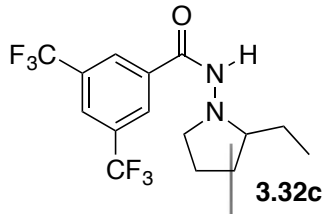
ppm 10 9 8 7 6 5 4 3 2 1 0

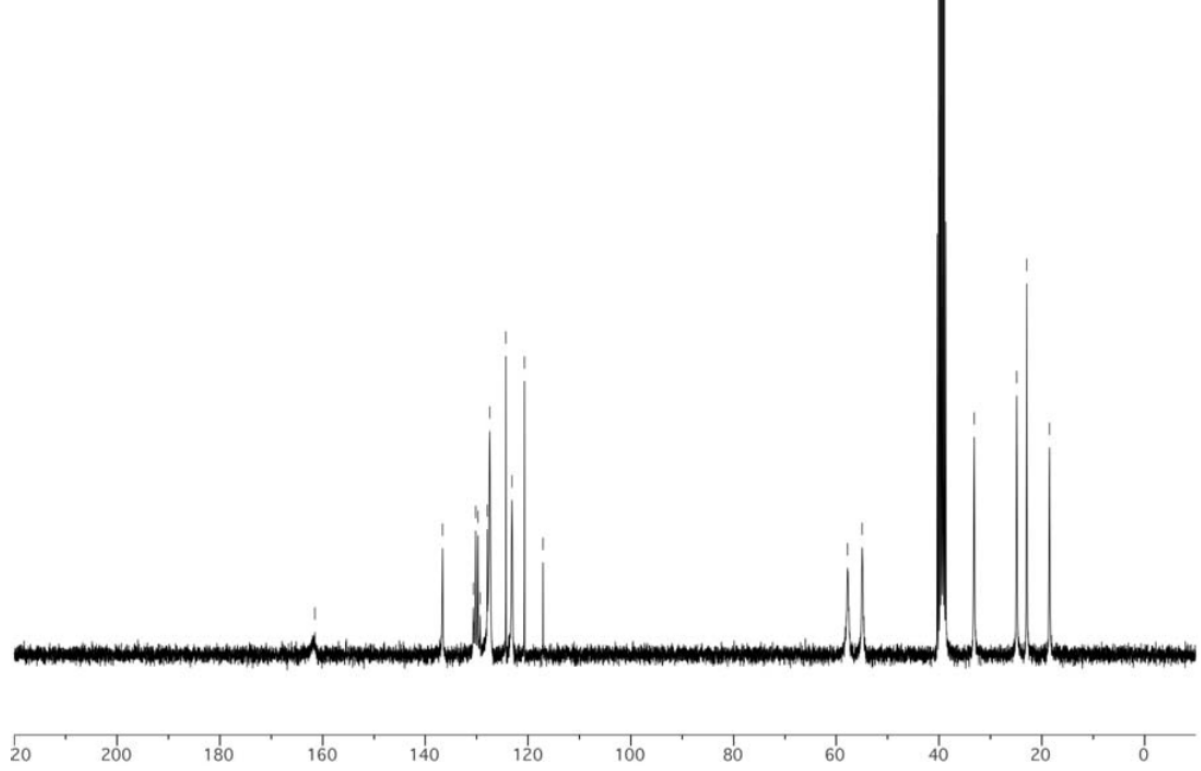
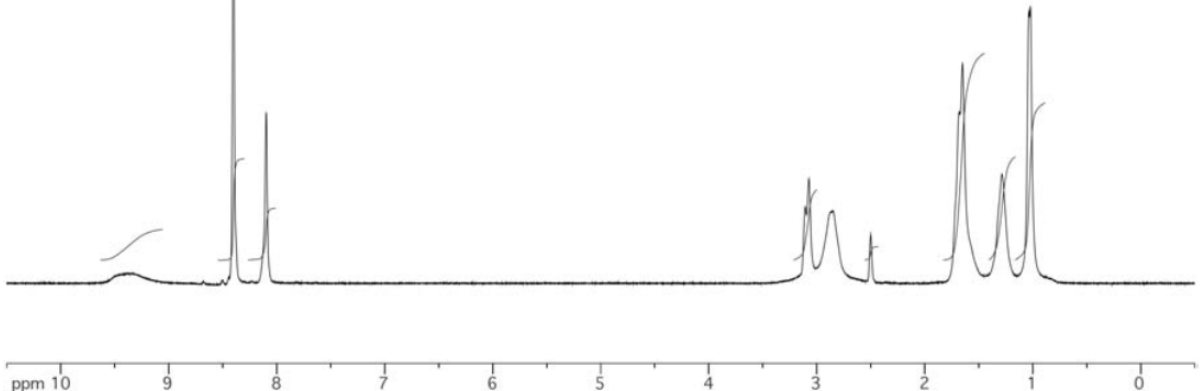
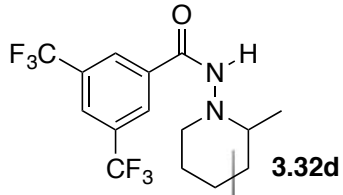
162.5
36.6
30.9
30.2
29.7
29.3
27.9
27.4
27.1
20.7
17.1
58.9
53.2
30.0
19.9
17.6

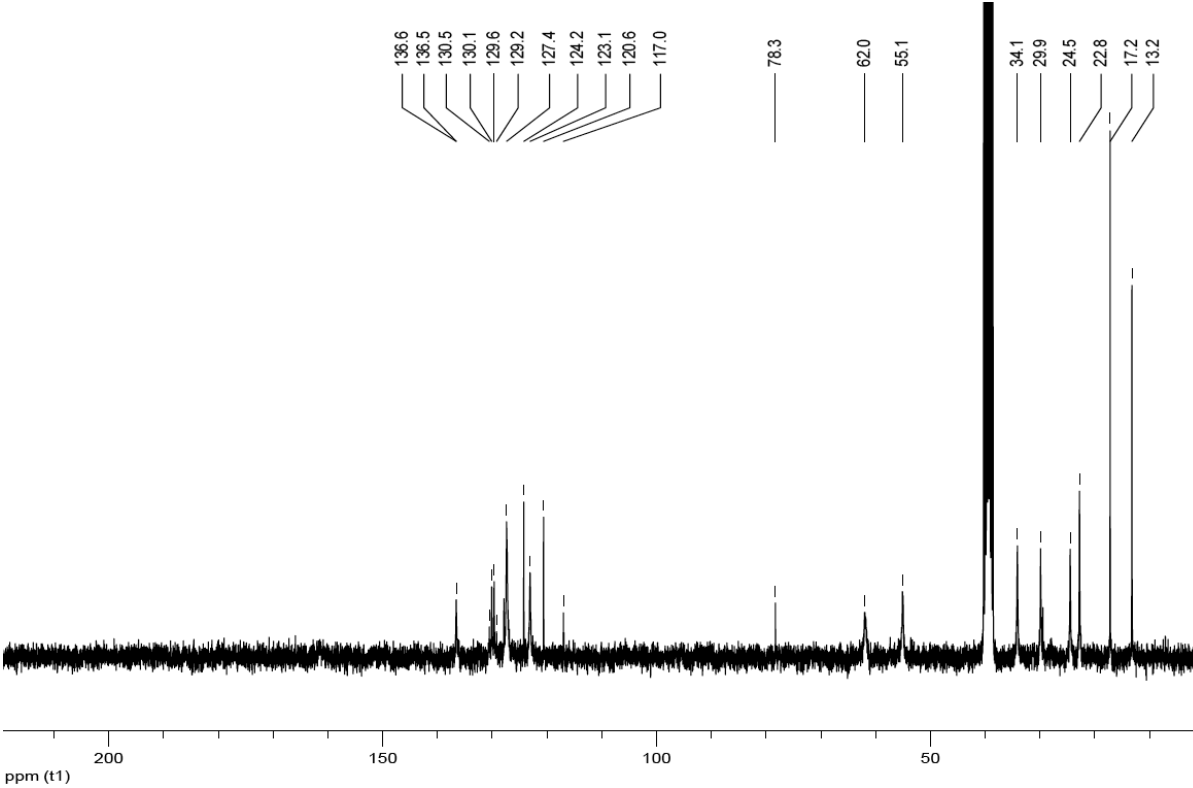
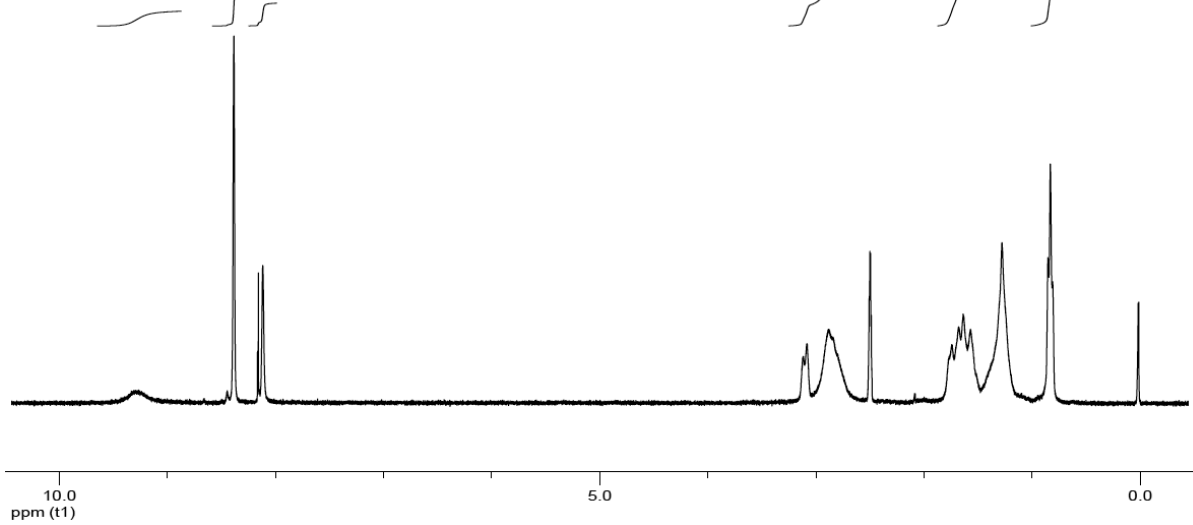
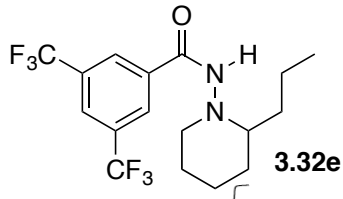


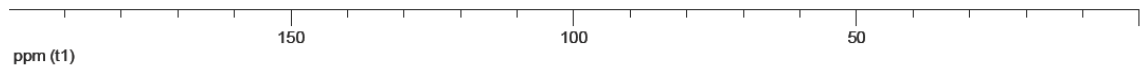
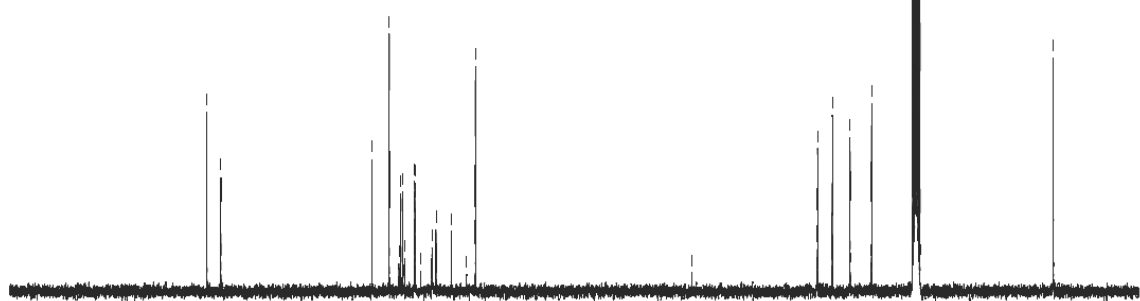
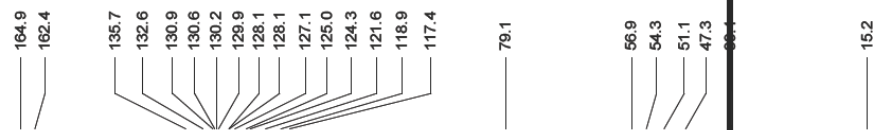
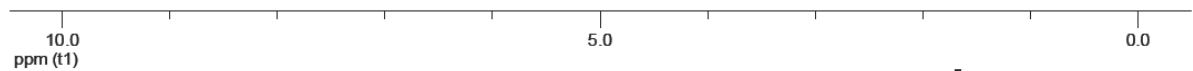
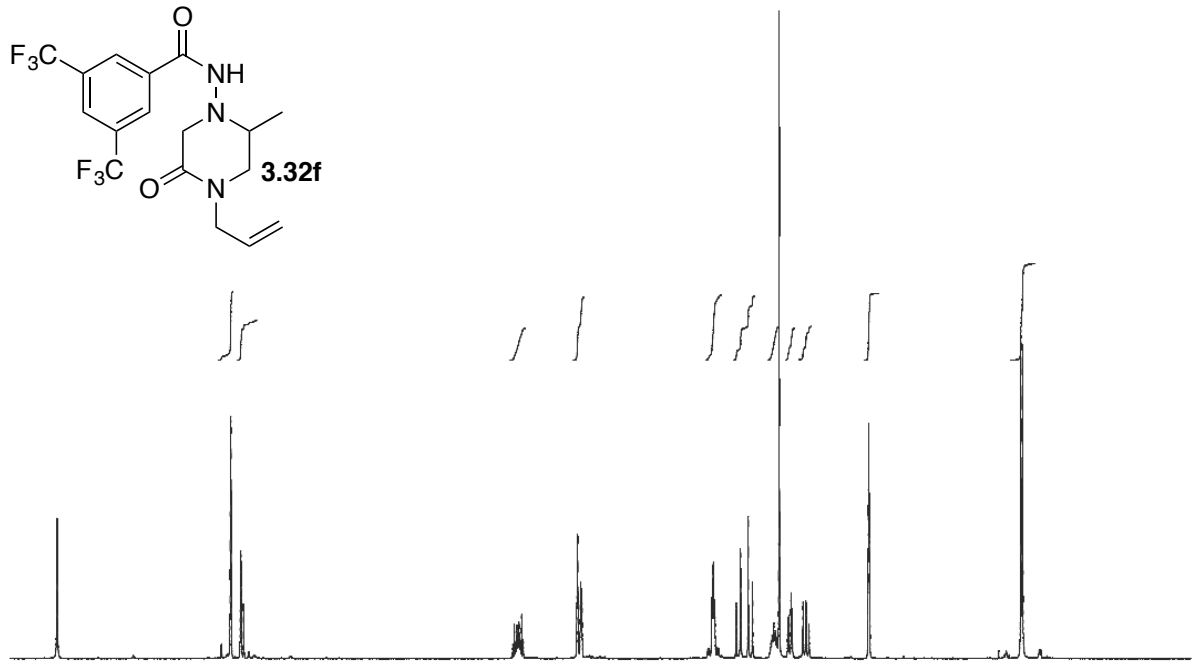
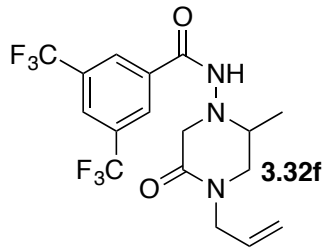
20 200 180 160 140 120 100 80 60 40 20 0

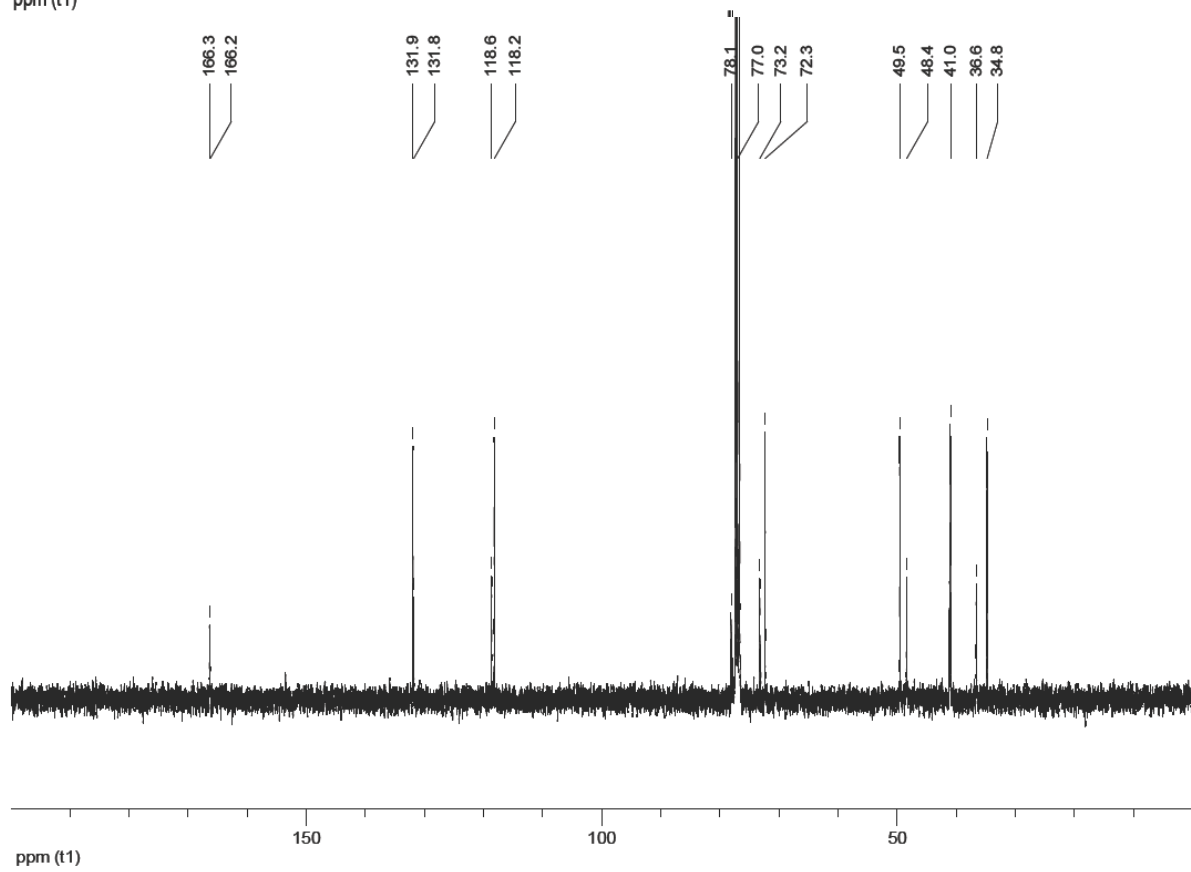
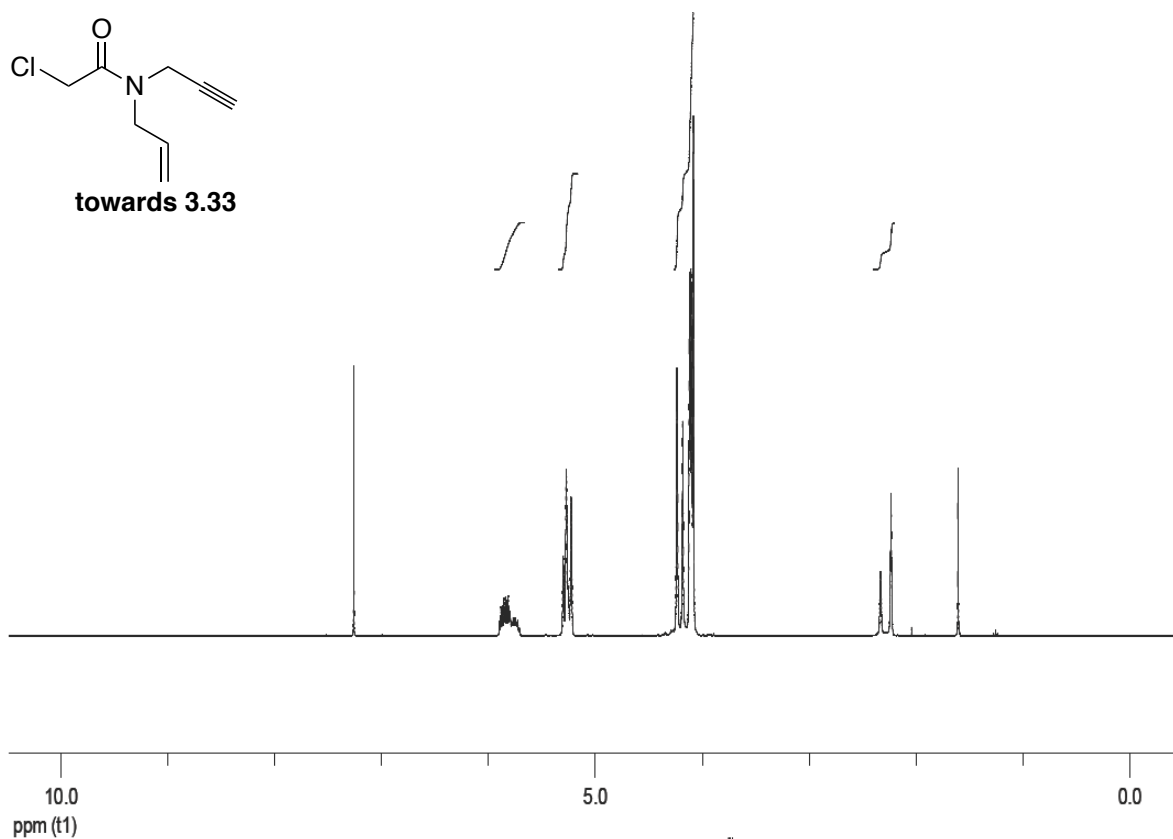
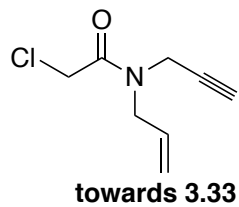


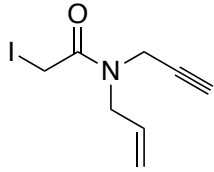




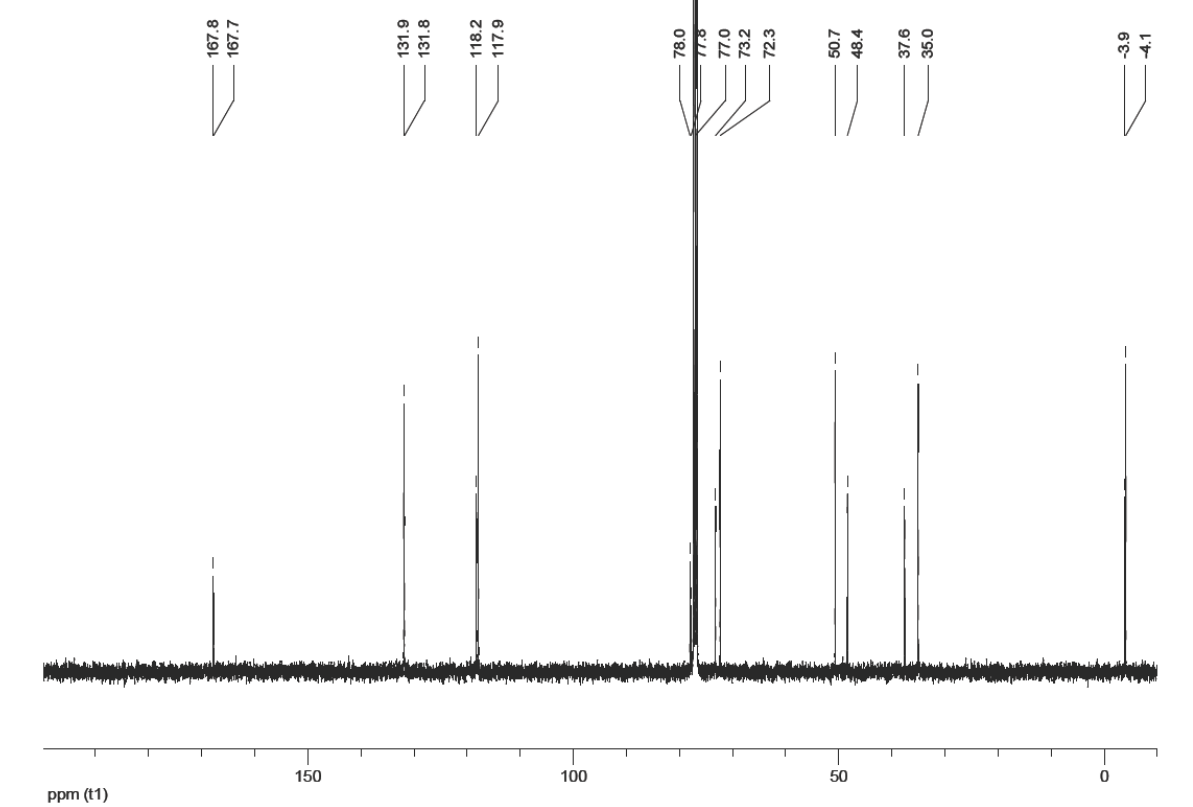
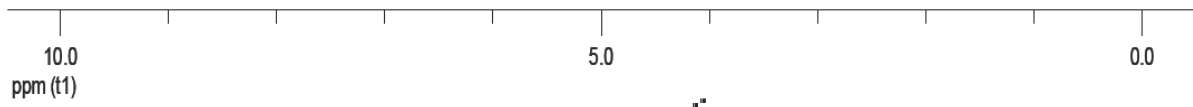
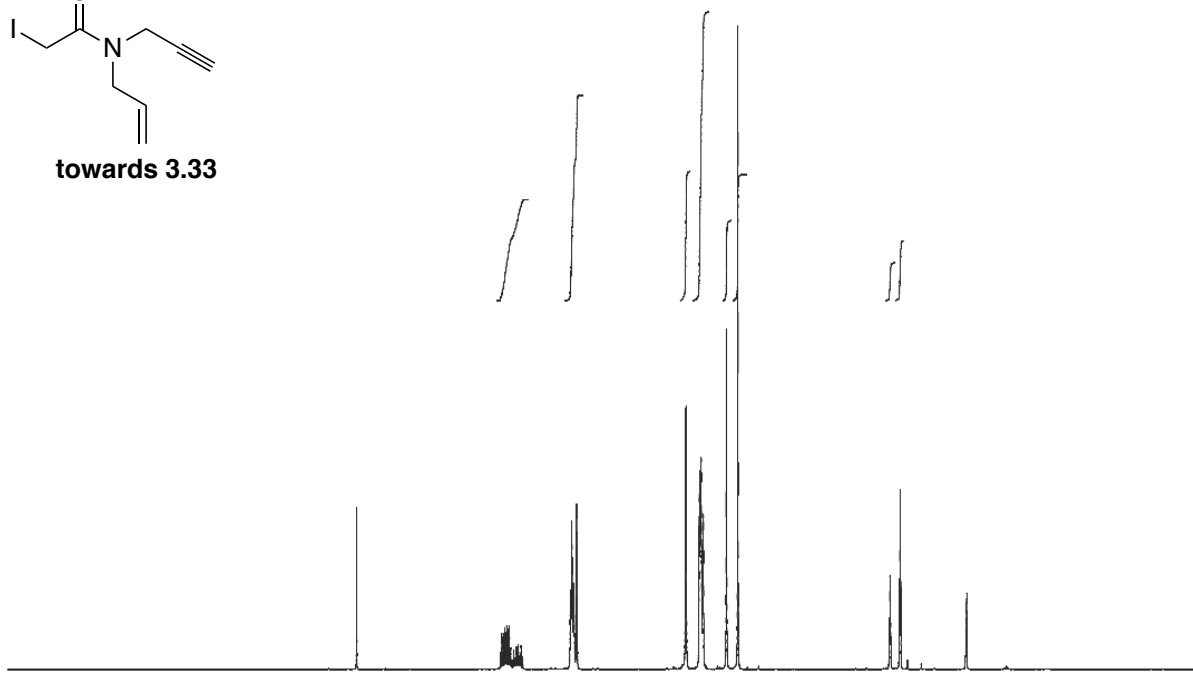


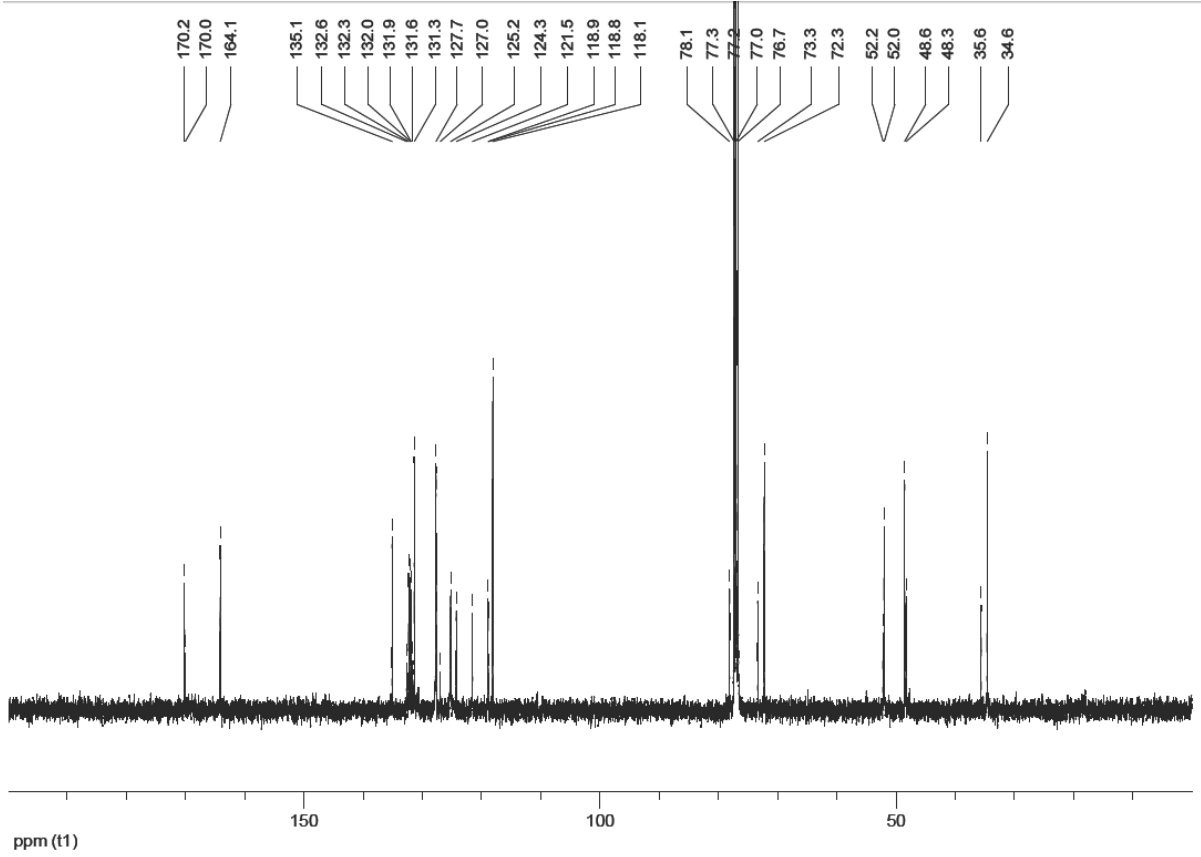
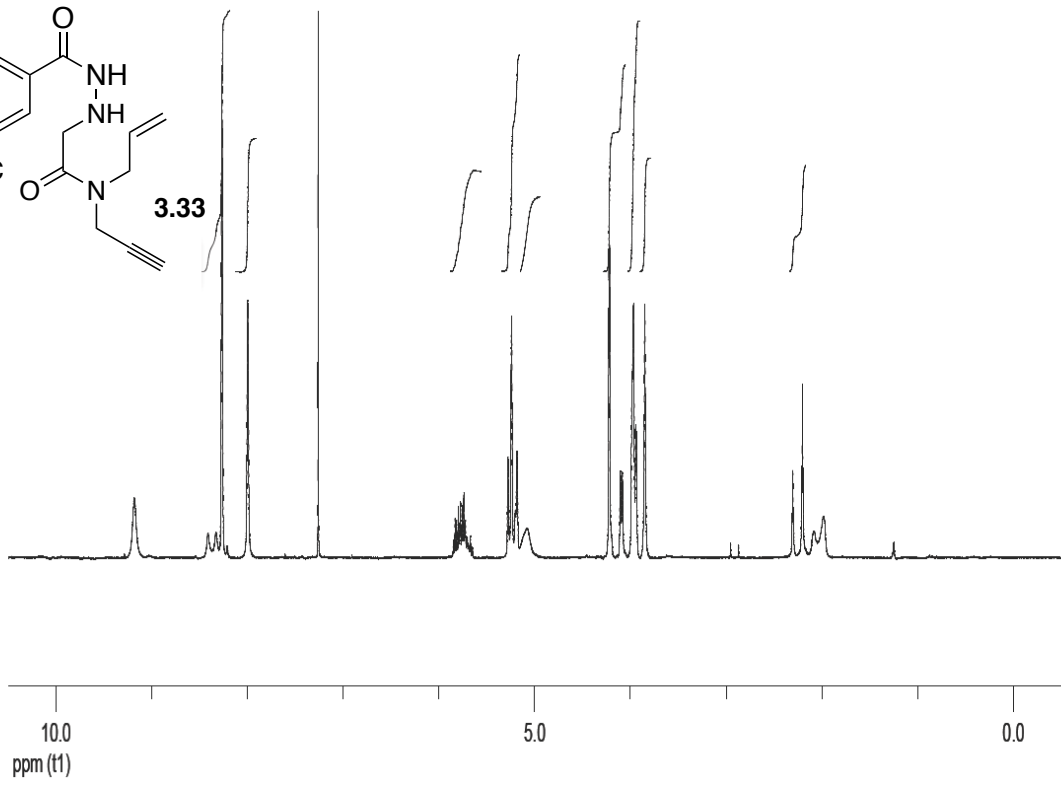
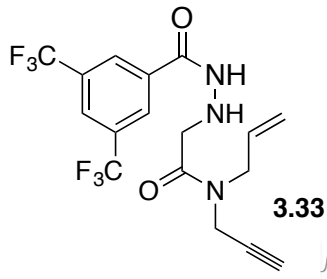


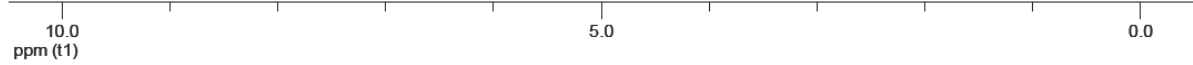
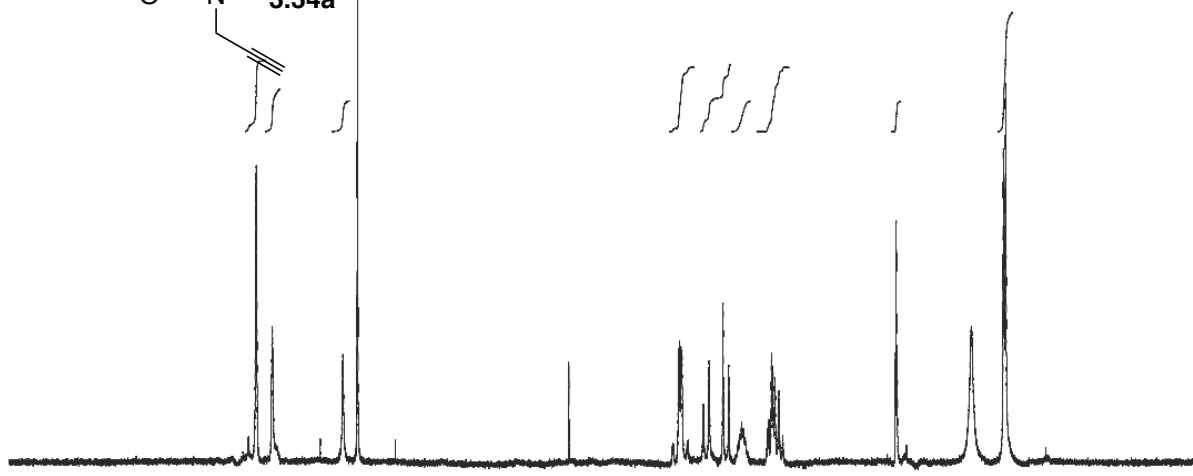
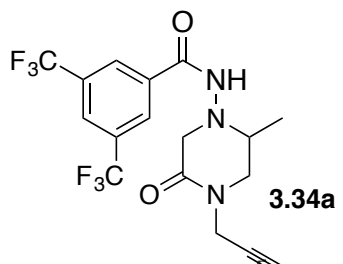


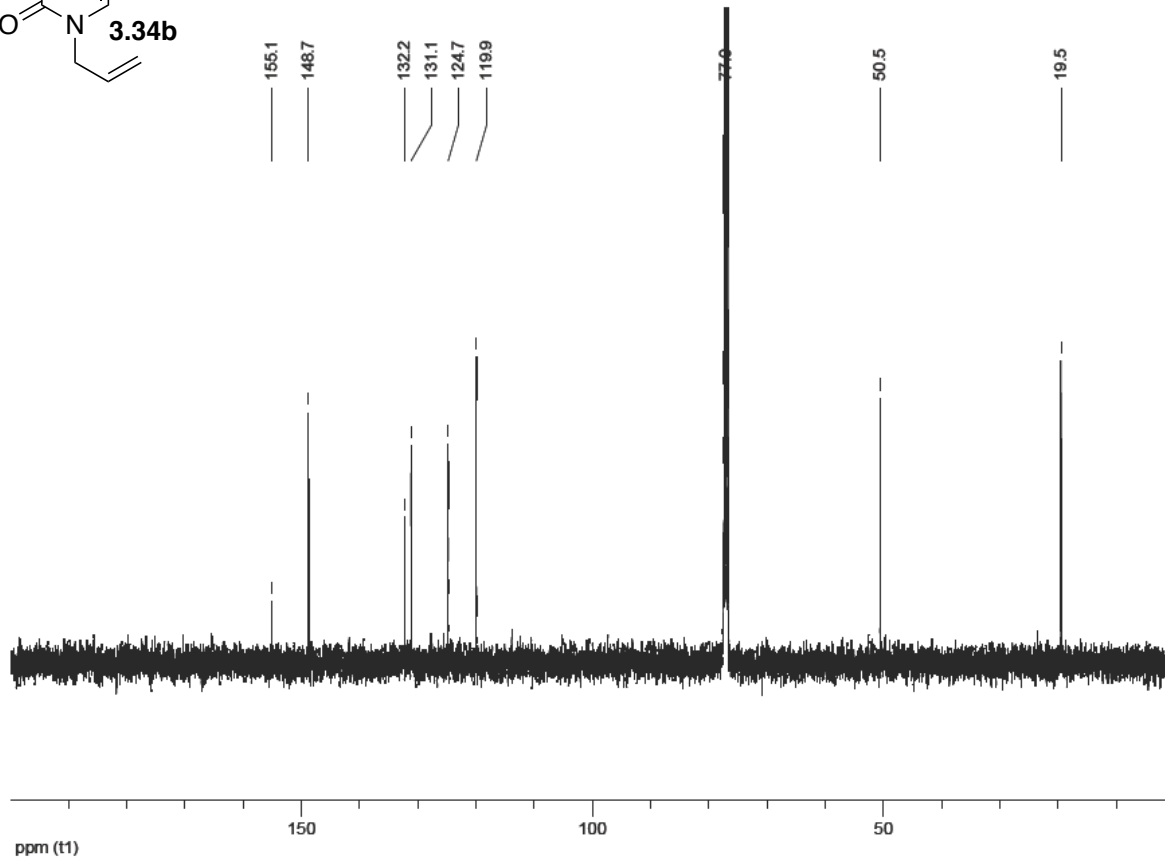
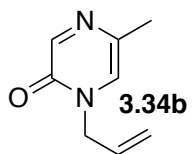


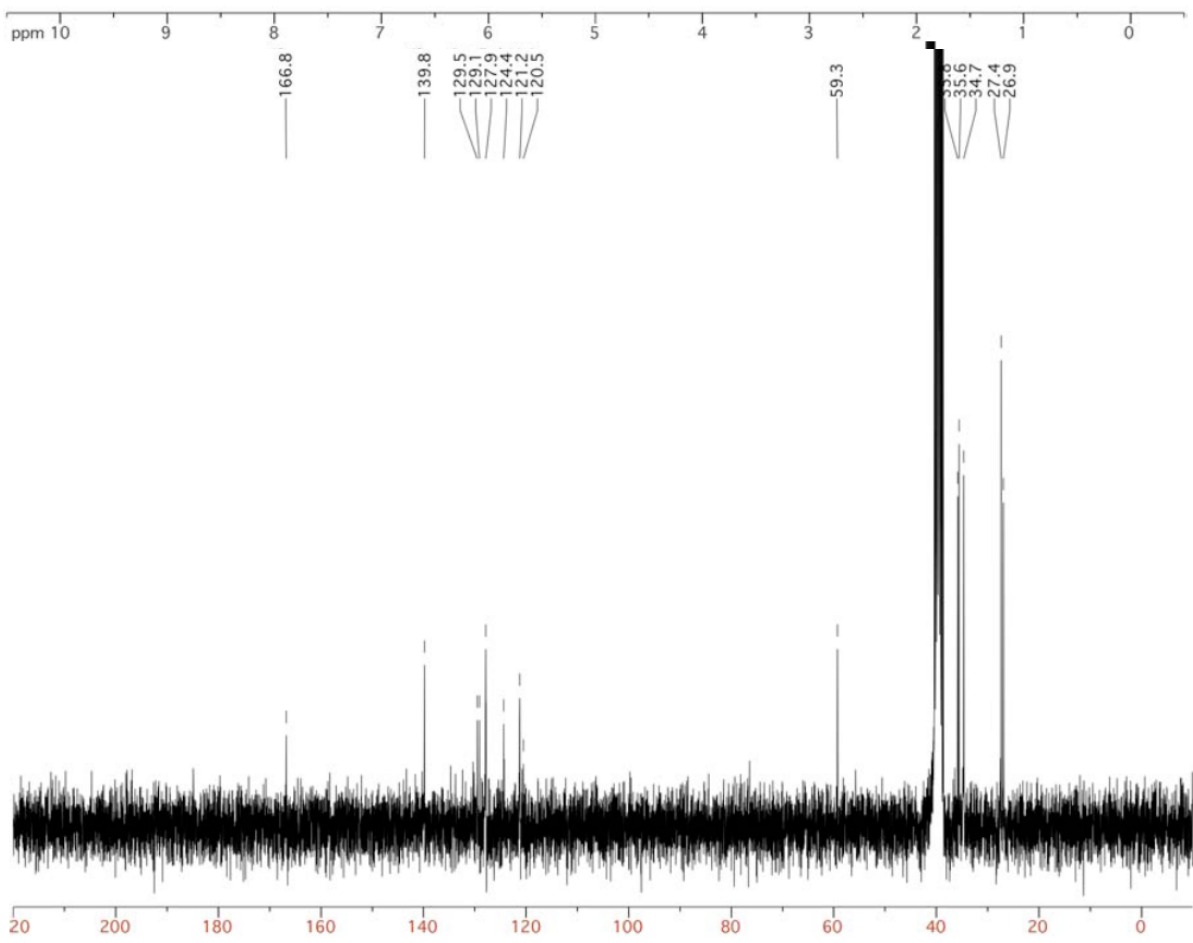
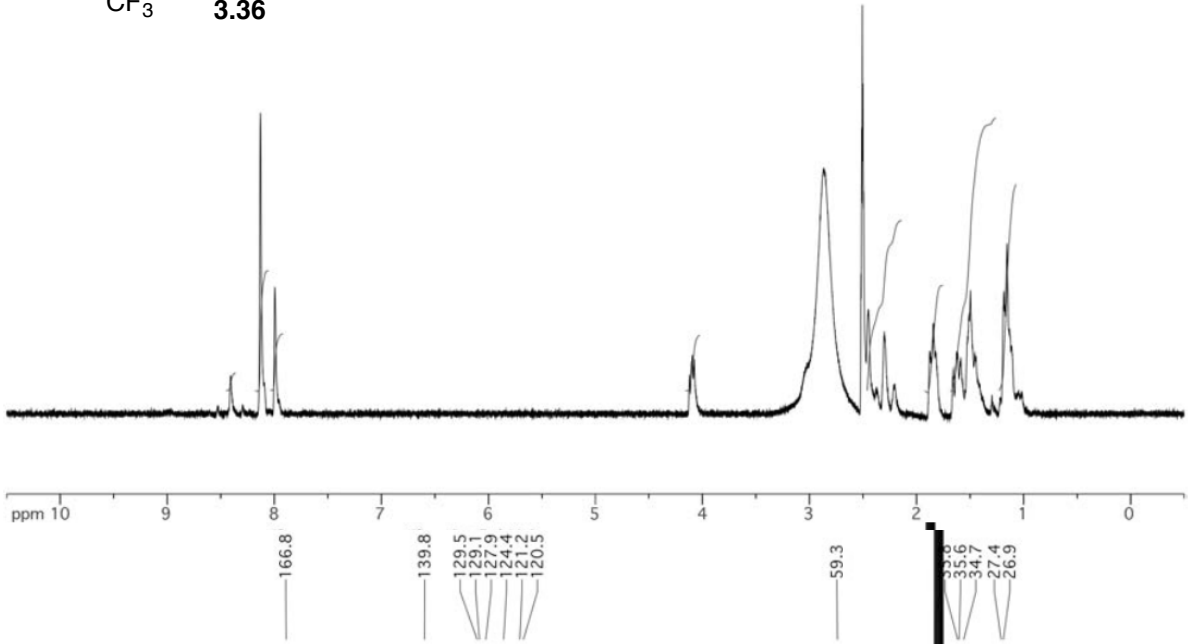
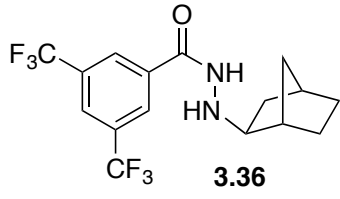
towards 3.33

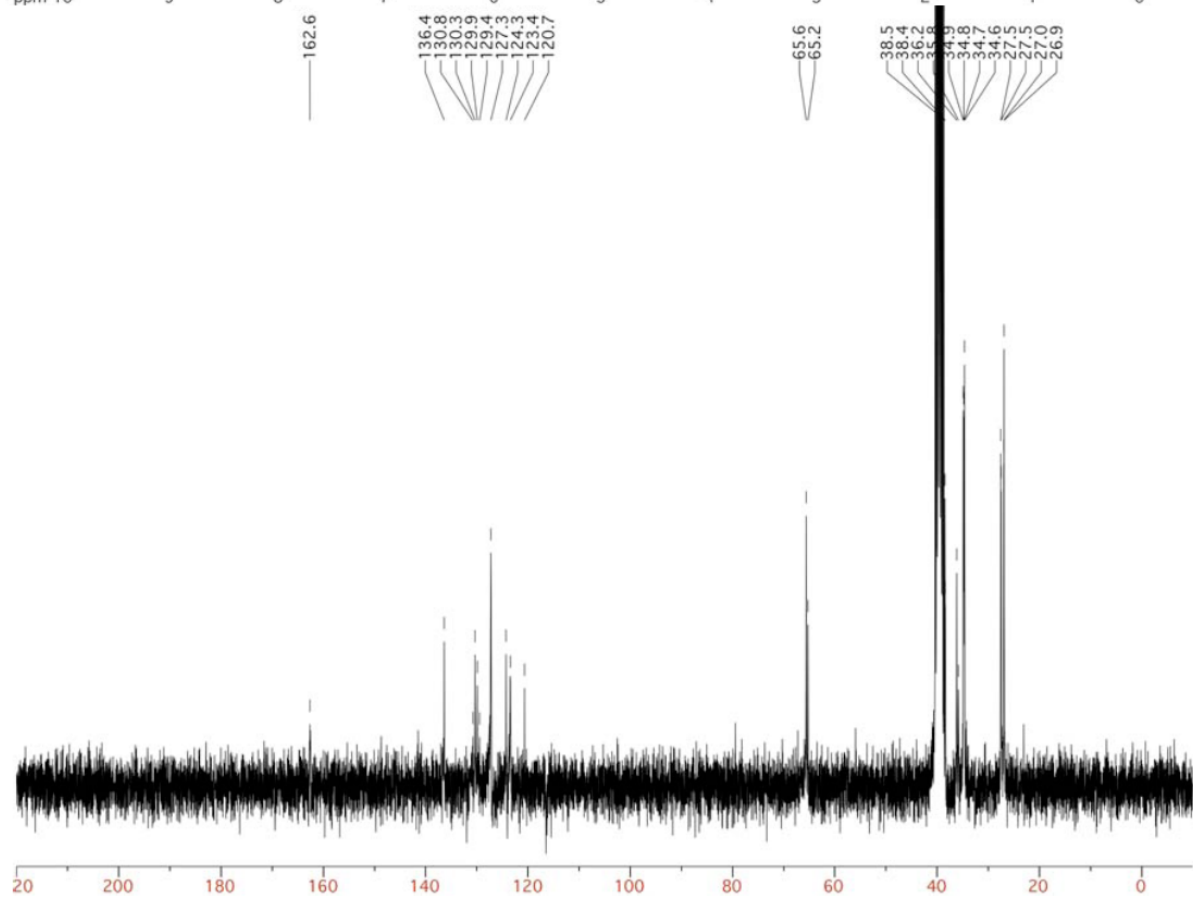
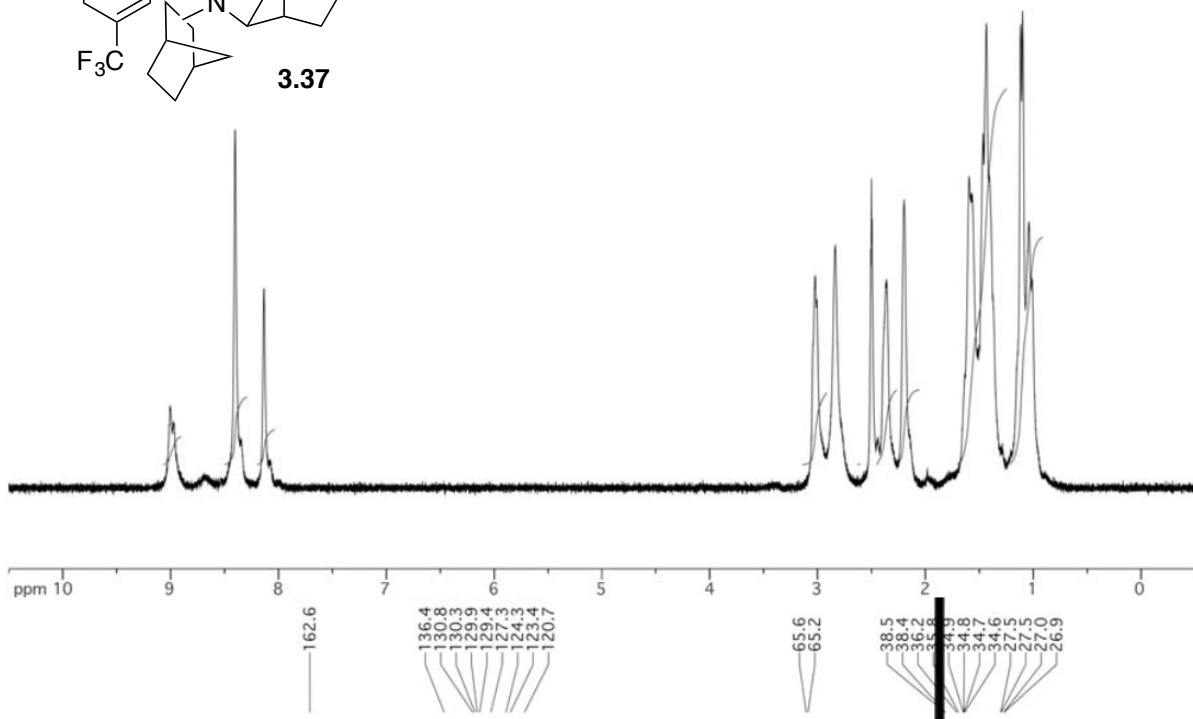
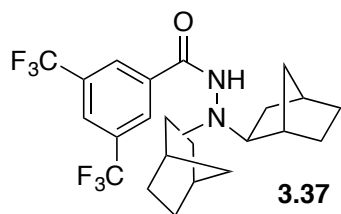


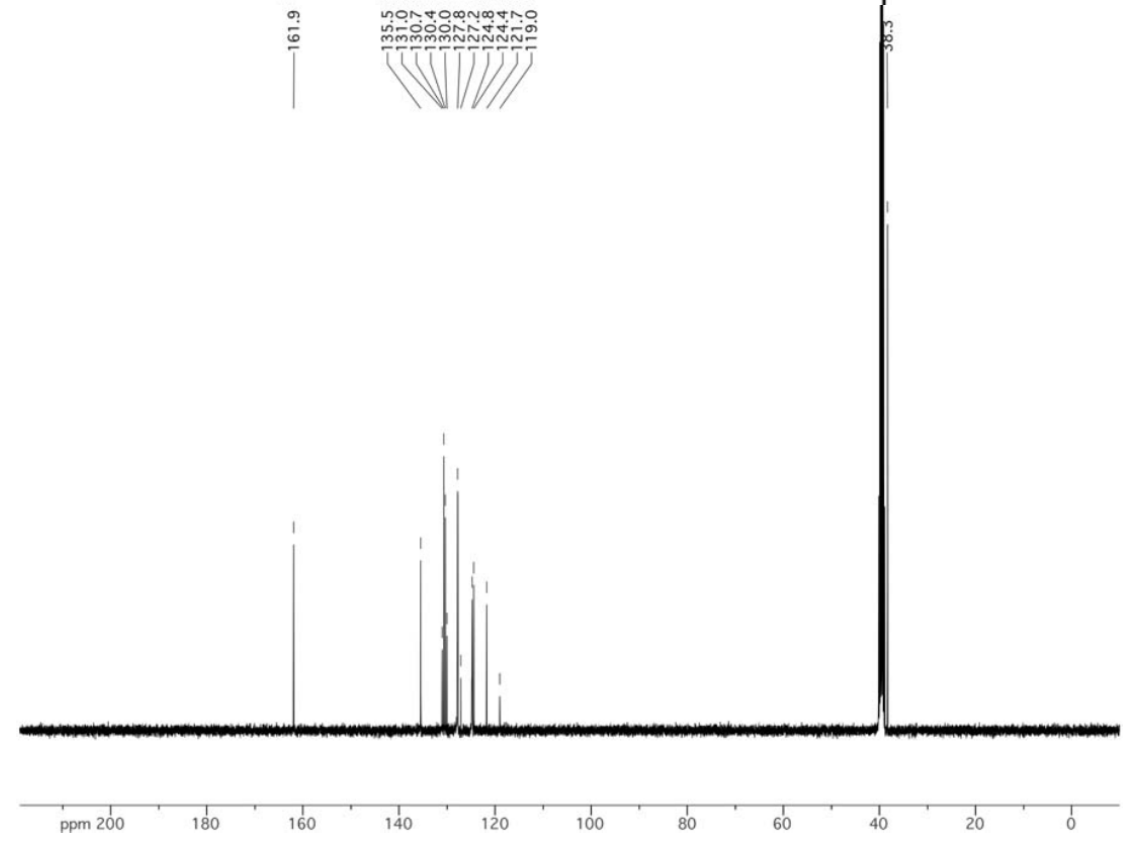
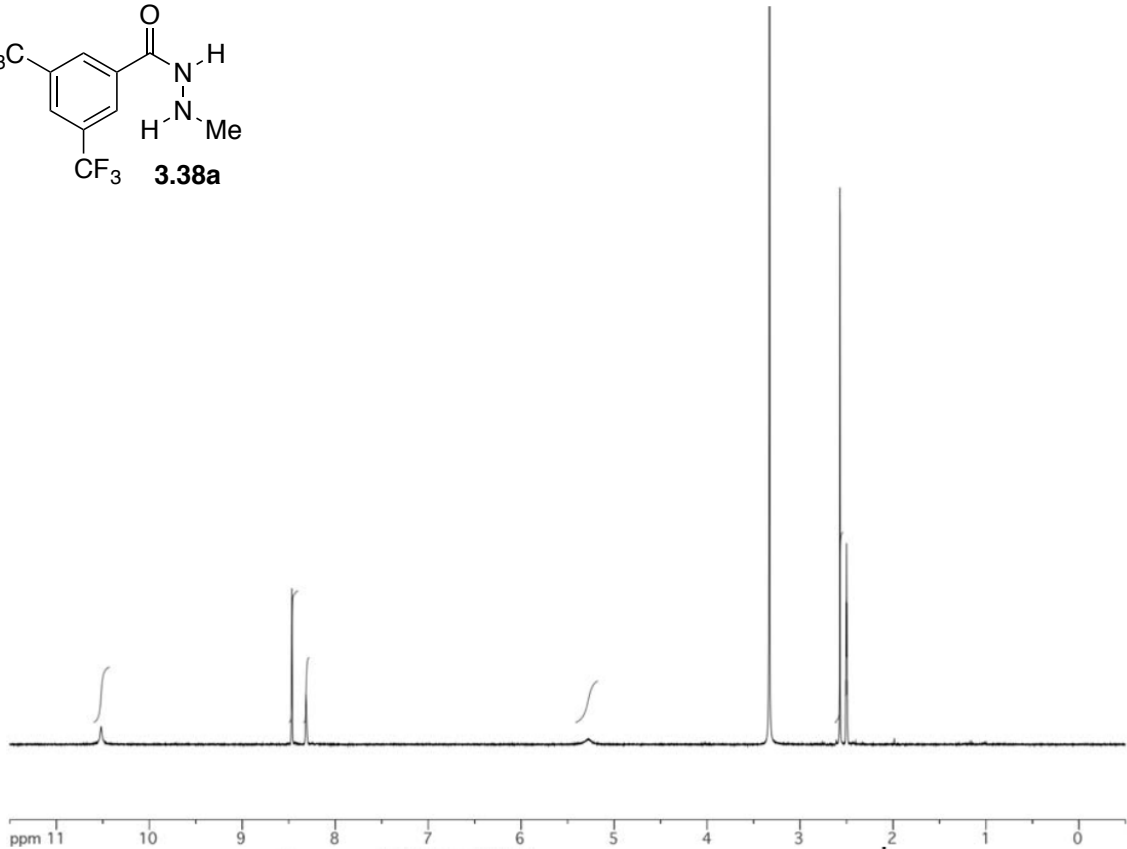
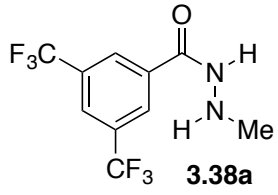


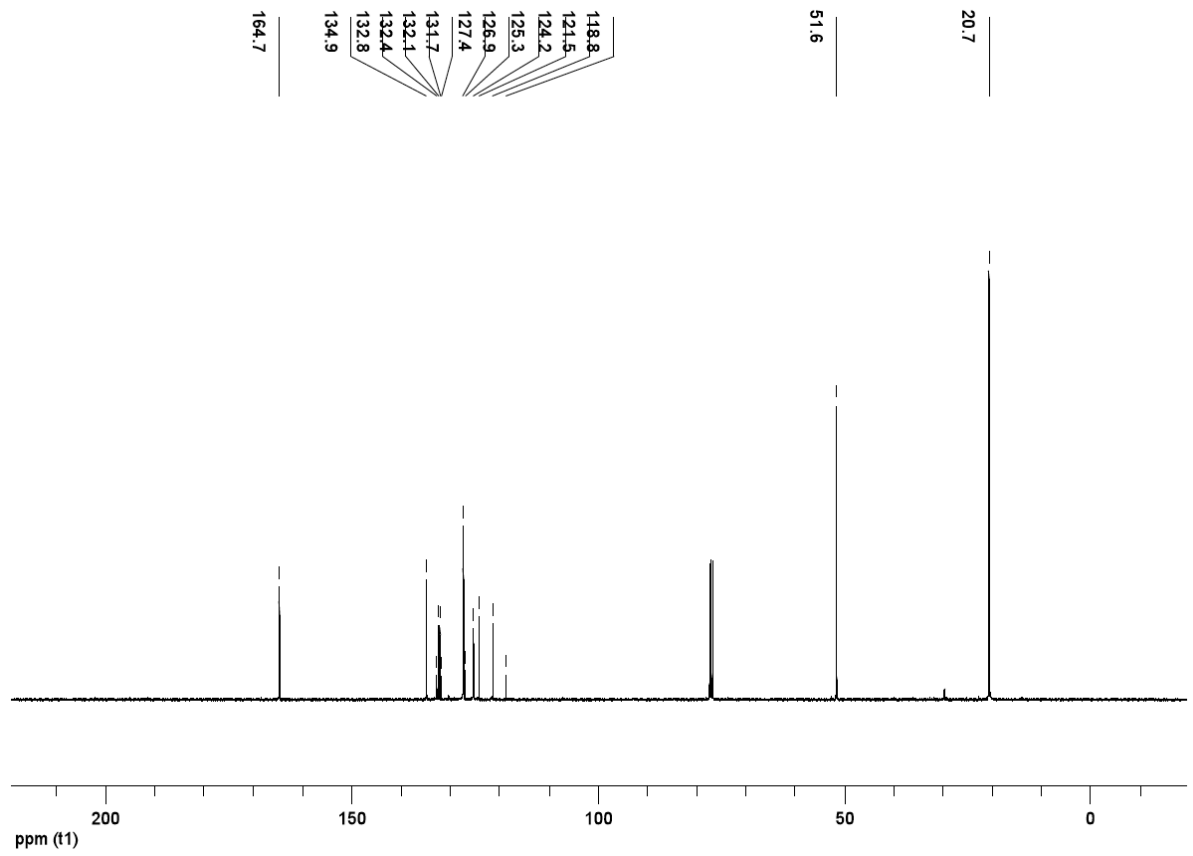
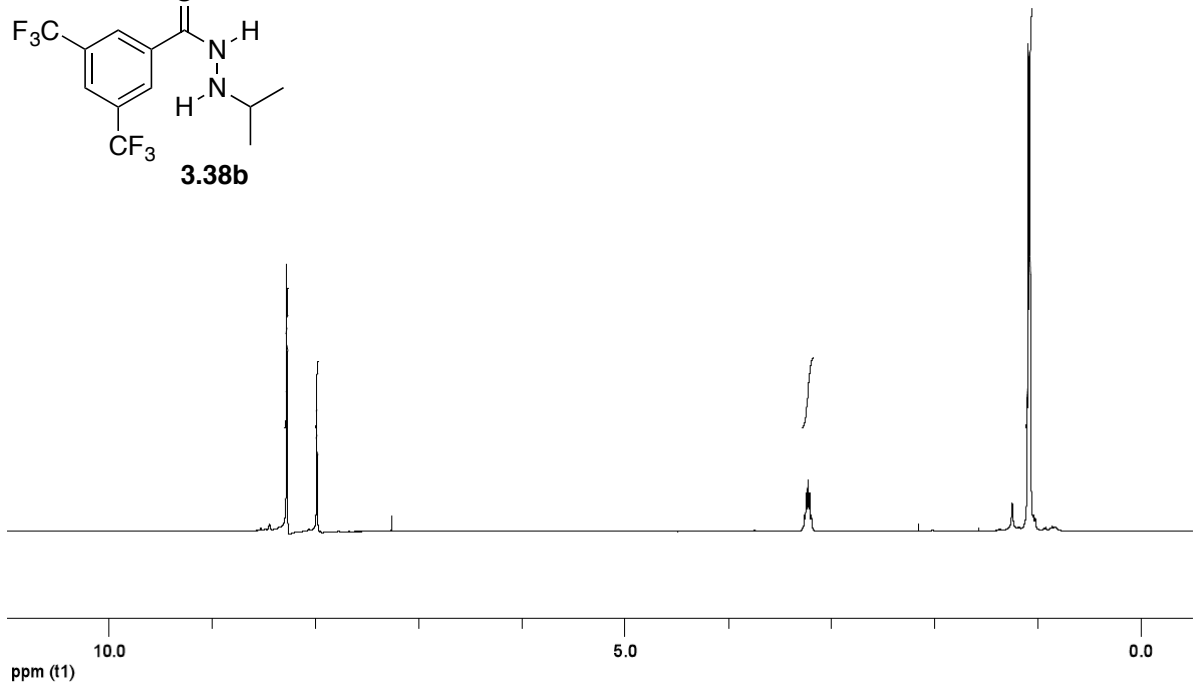
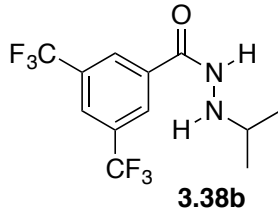


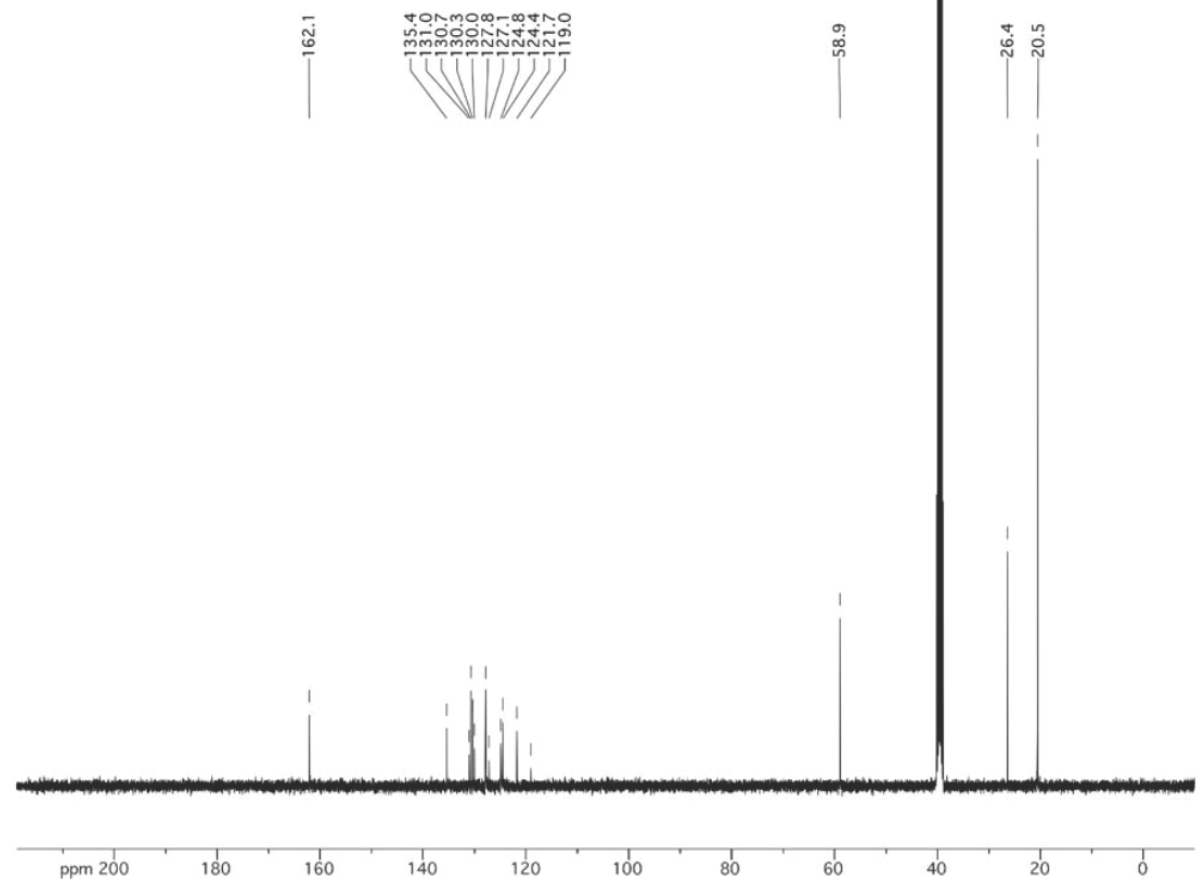
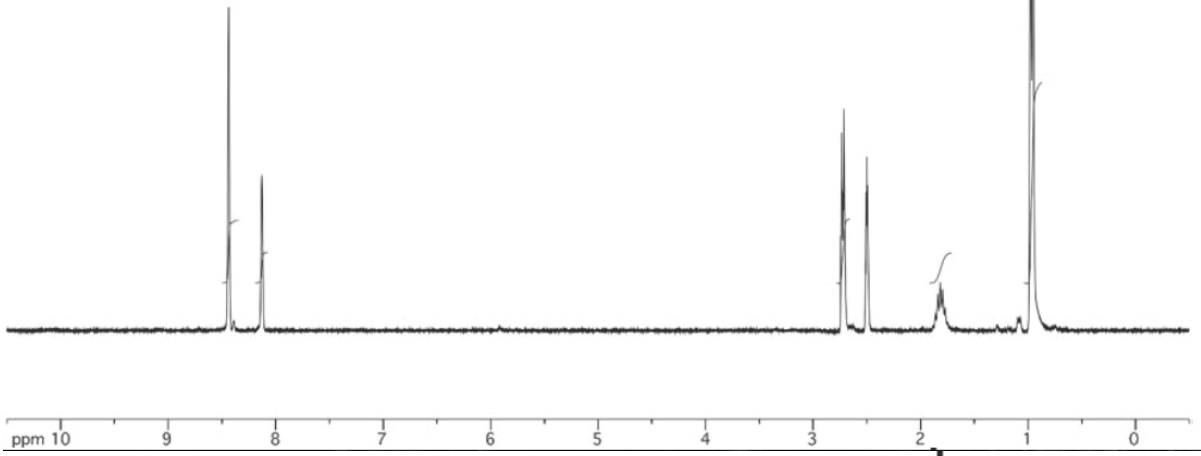
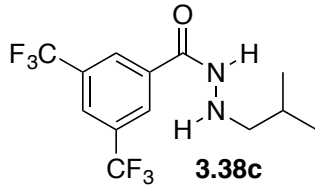


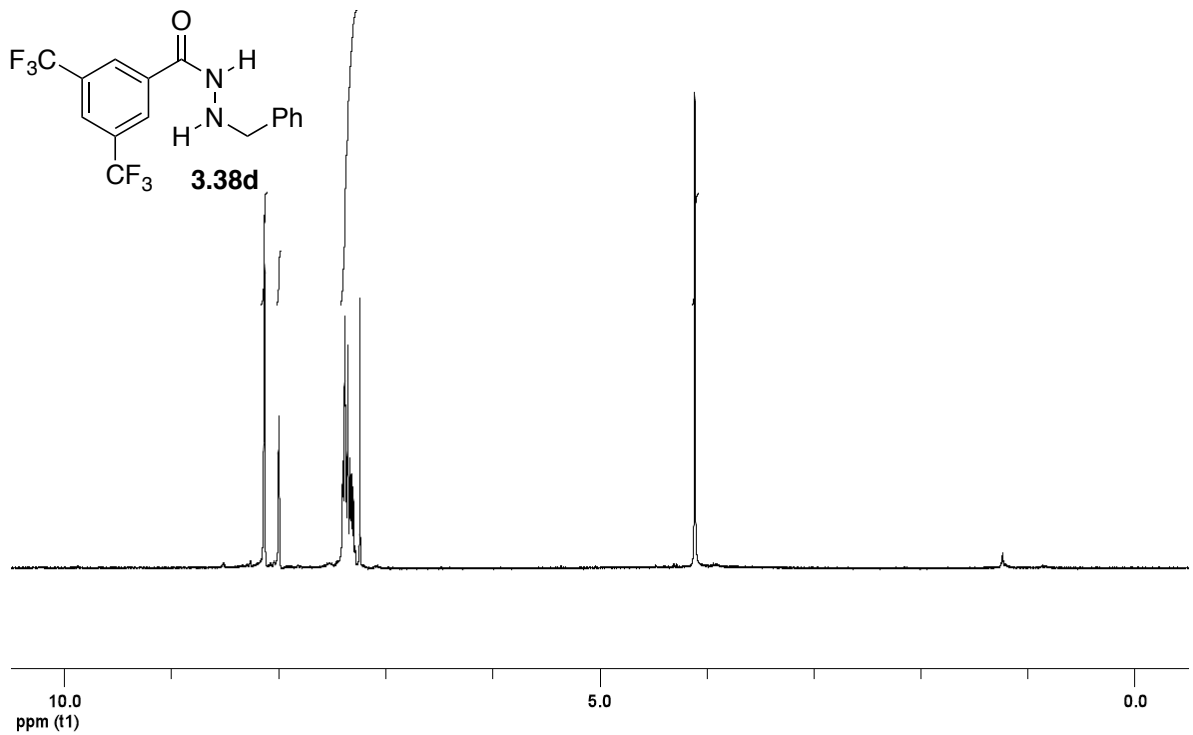
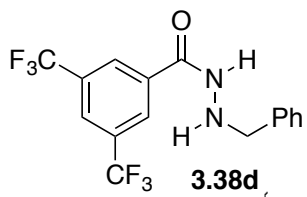




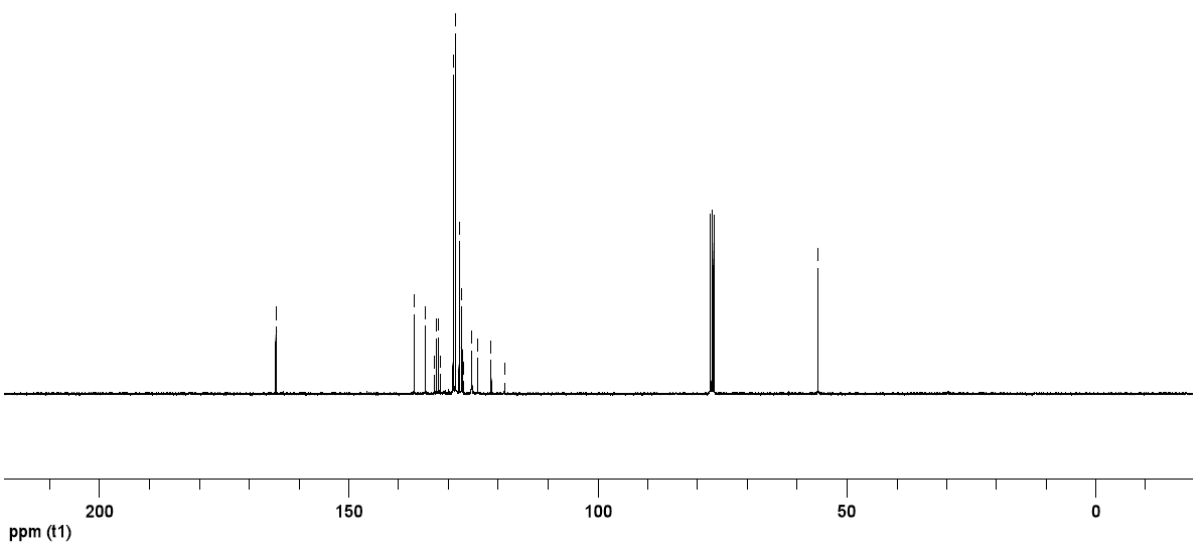


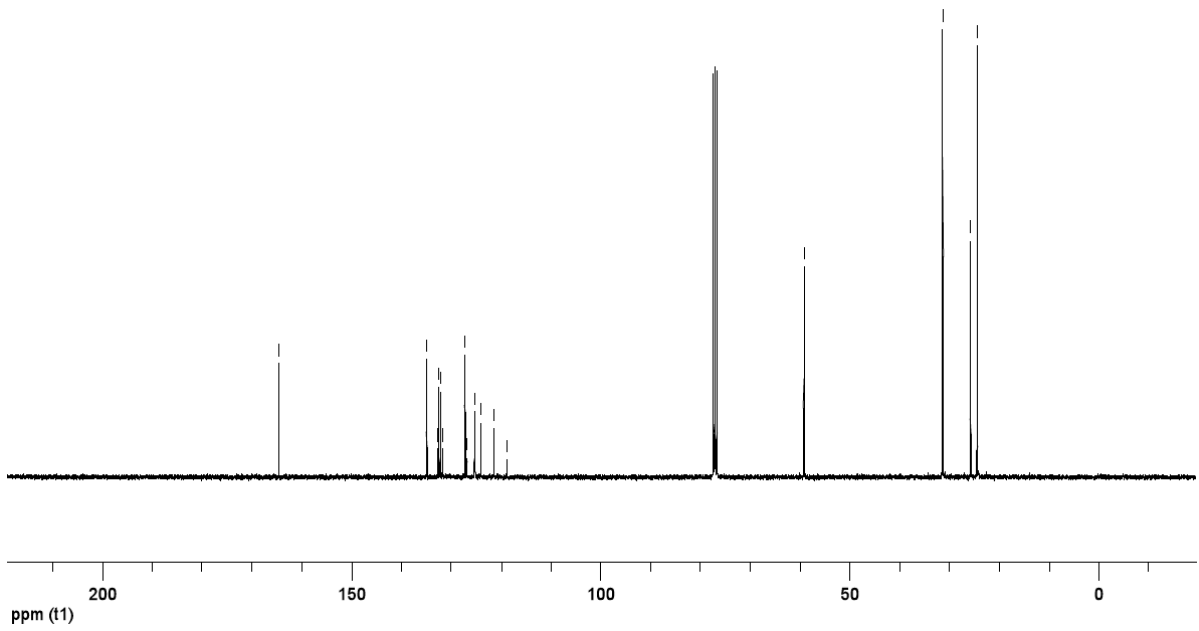
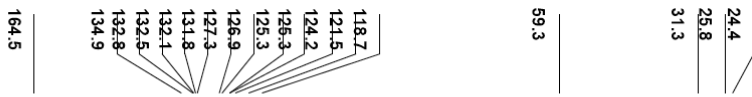
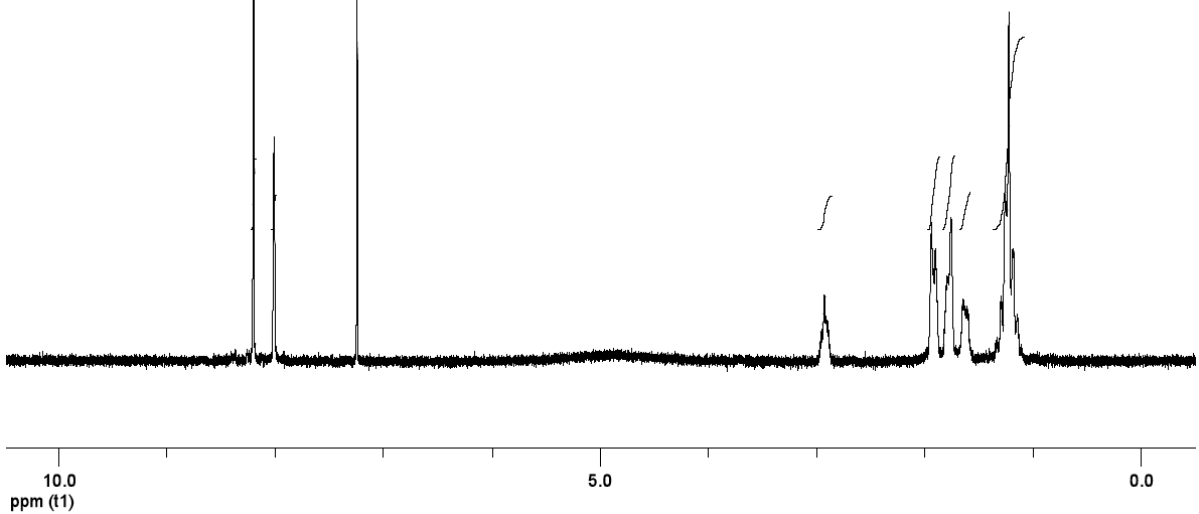
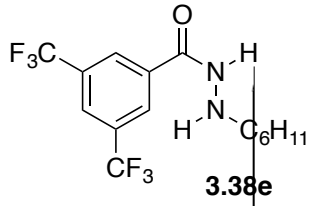


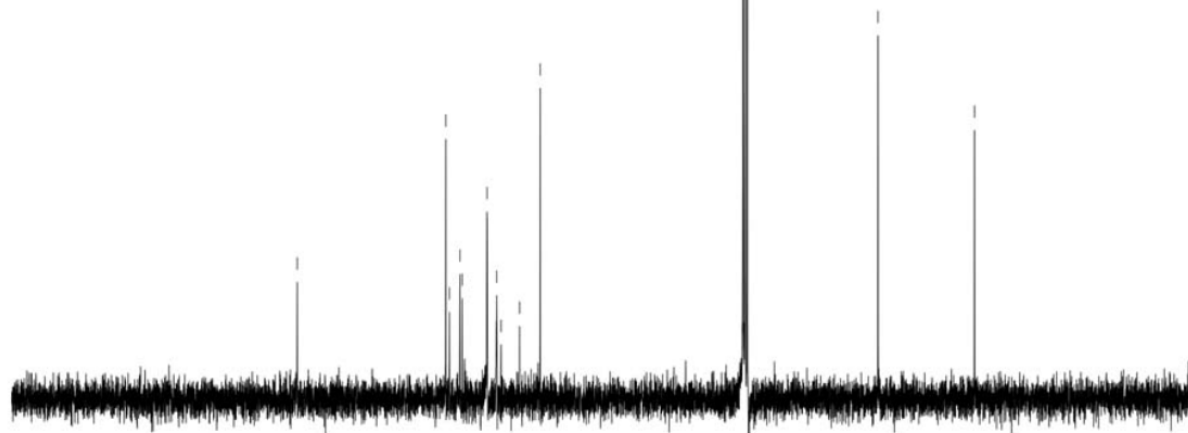
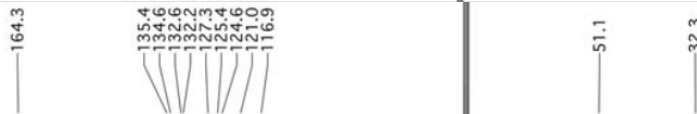
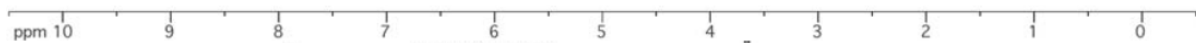
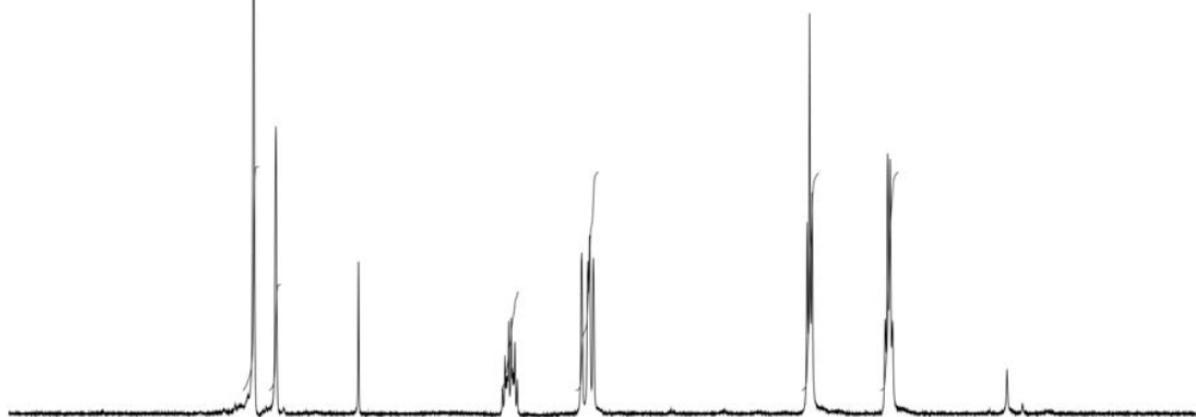
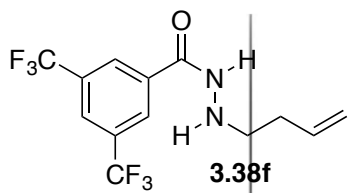


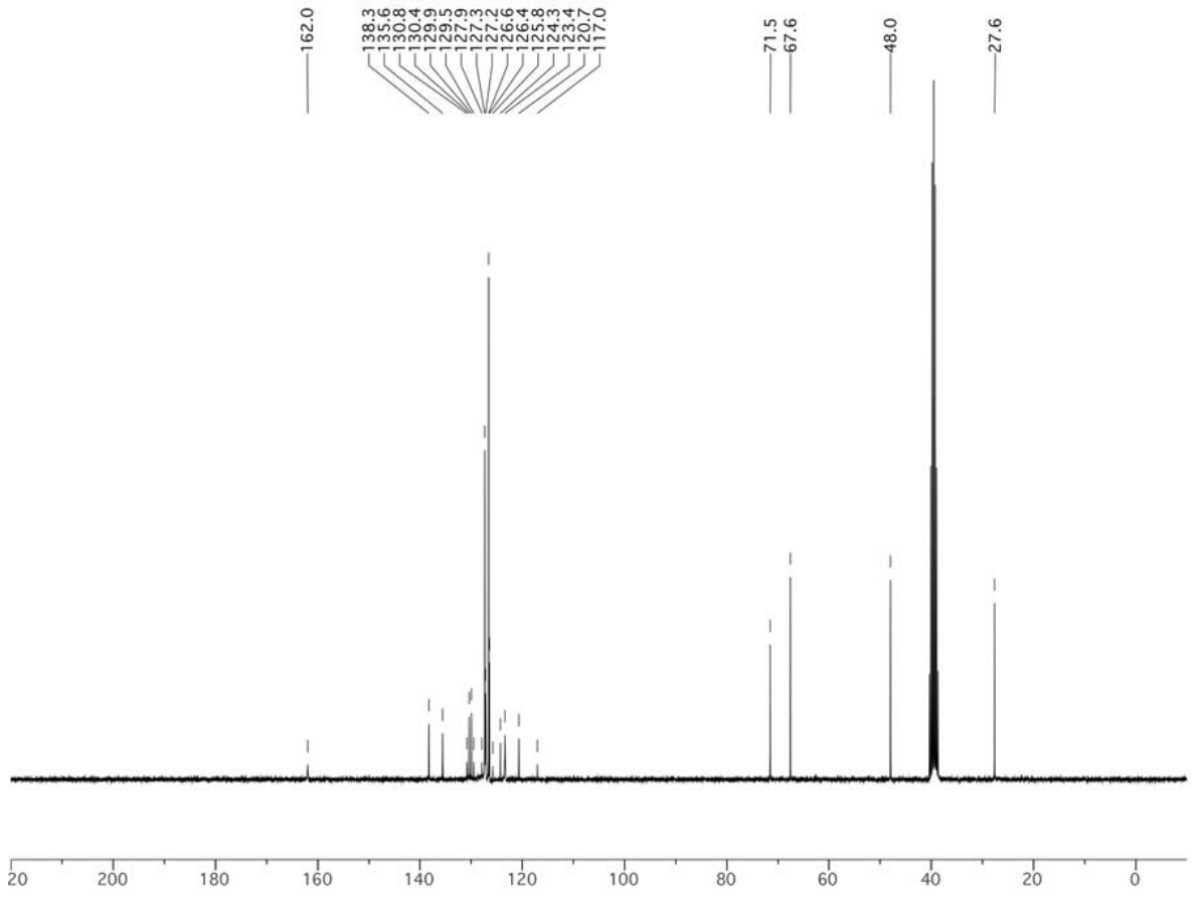
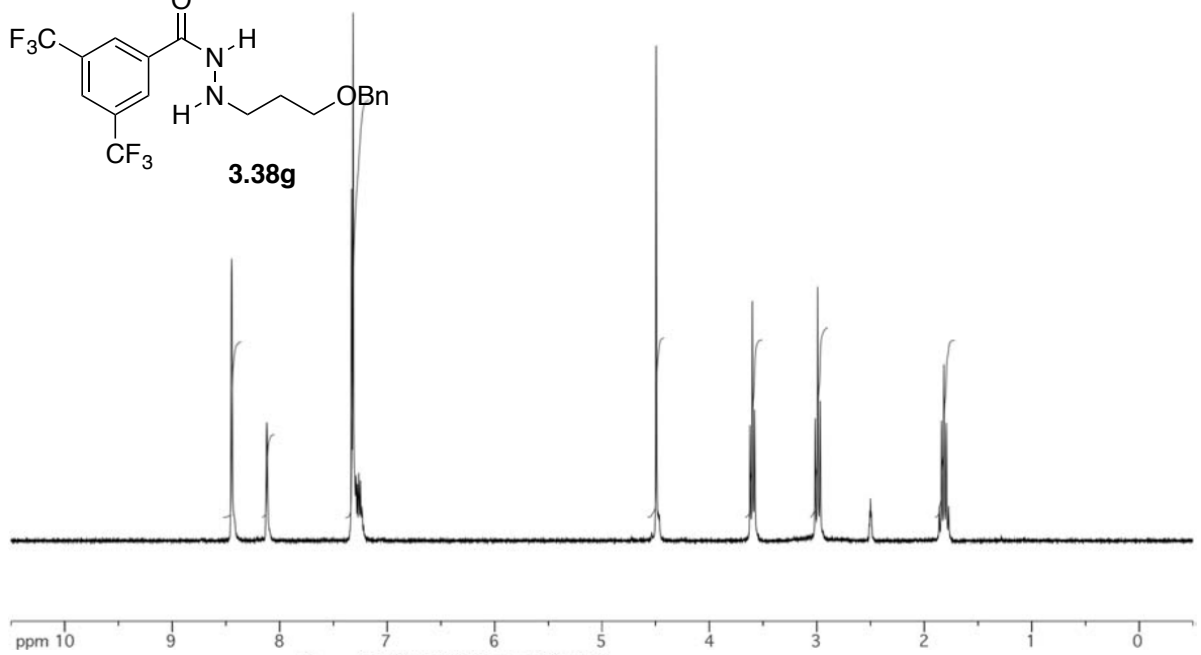
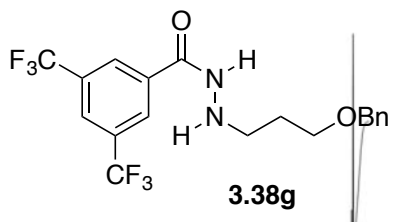


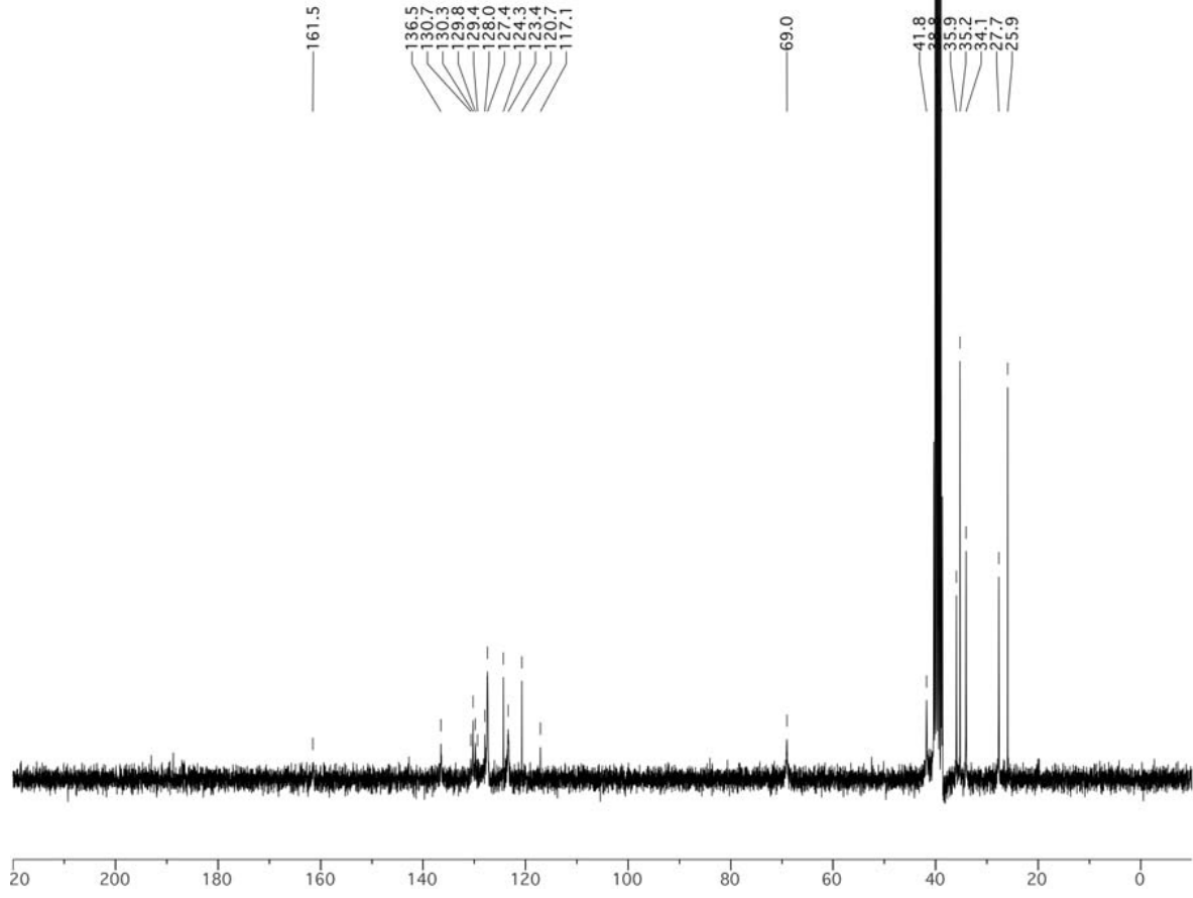
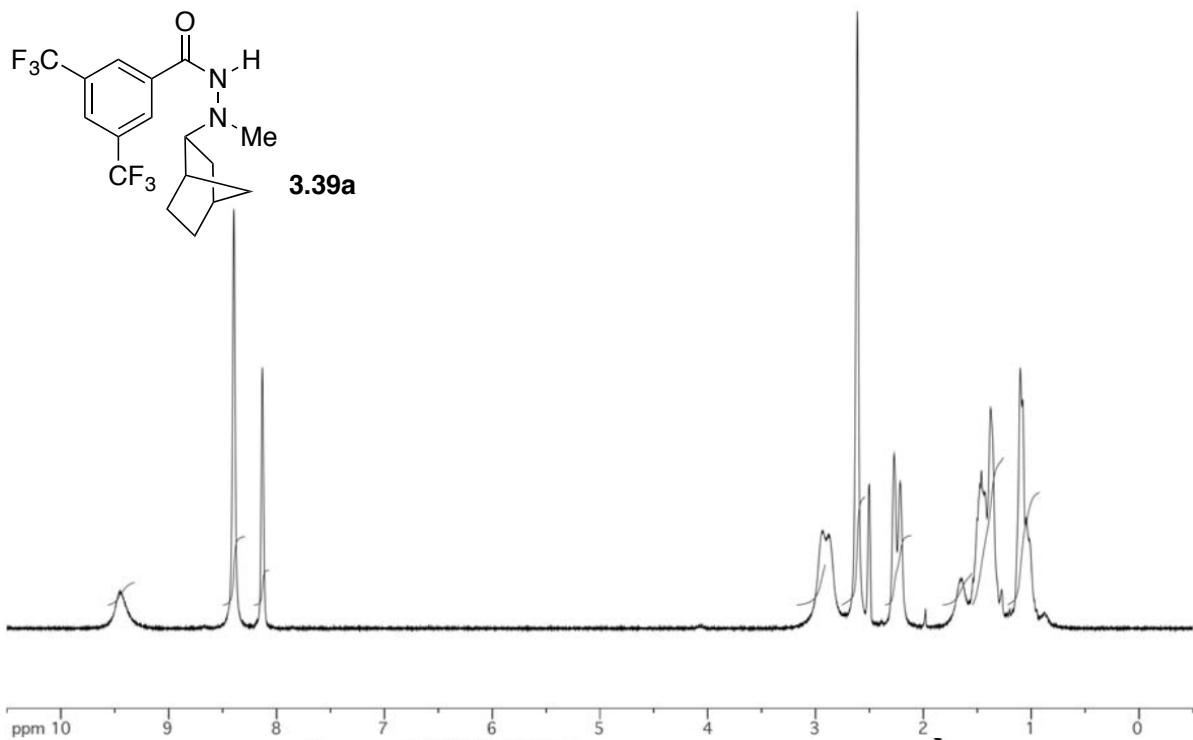
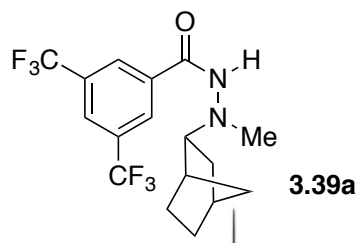
- 118.7
- 121.4
- 124.1
- 125.3
- 126.9
- 127.4
- 127.9
- 128.6
- 129.0
- 131.7
- 131.7
- 132.4
- 132.4
- 132.7
- 134.7
- 136.8
- 164.6
- 55.7

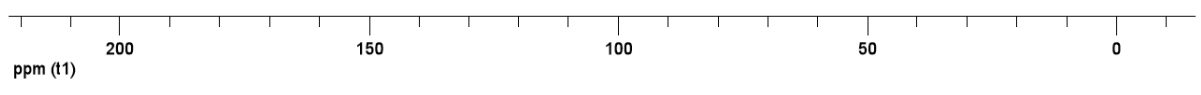
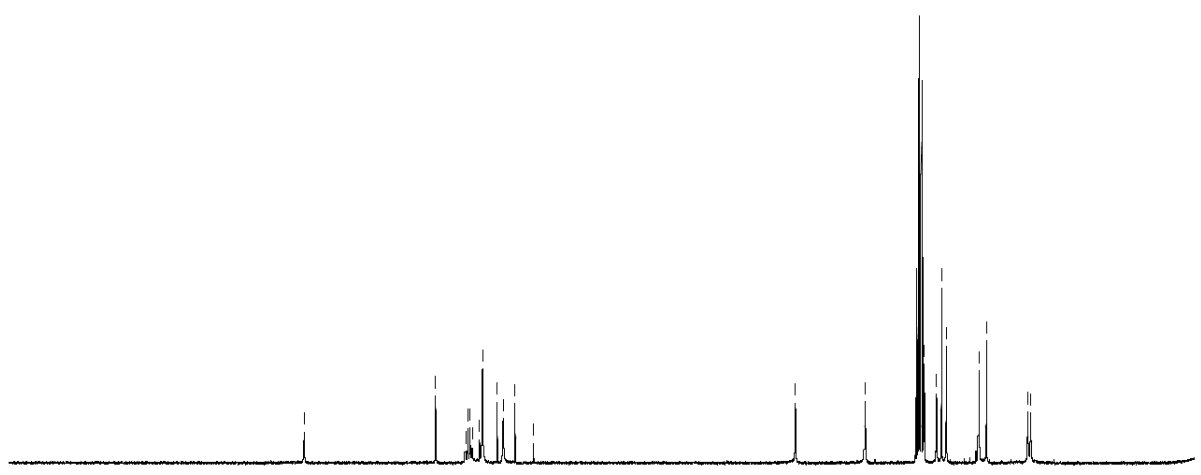
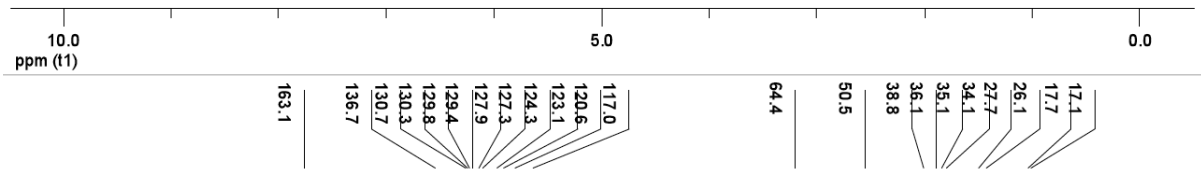
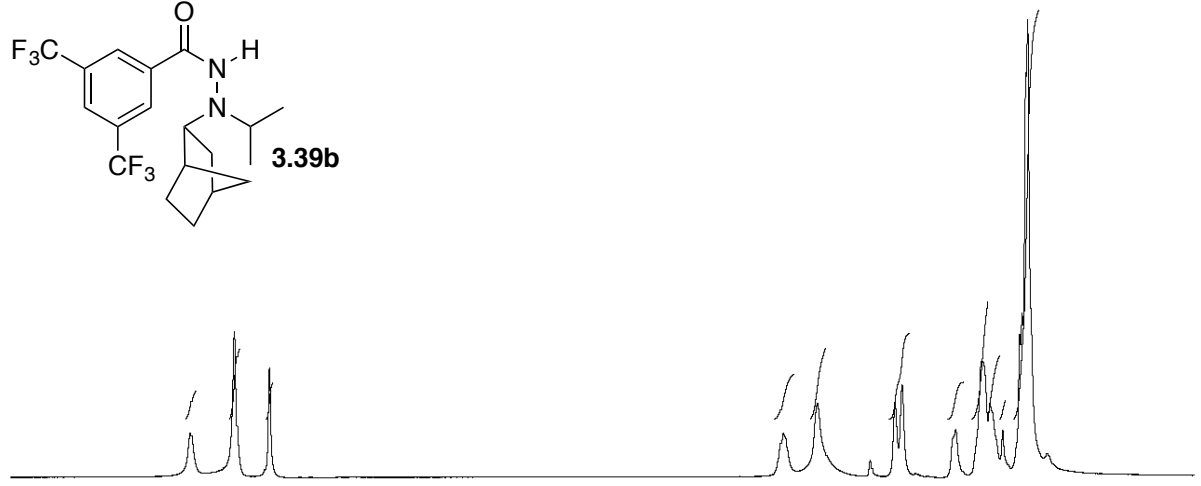
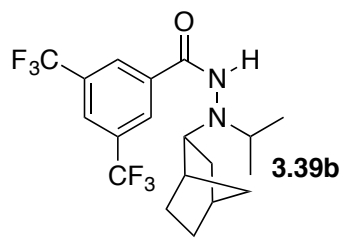


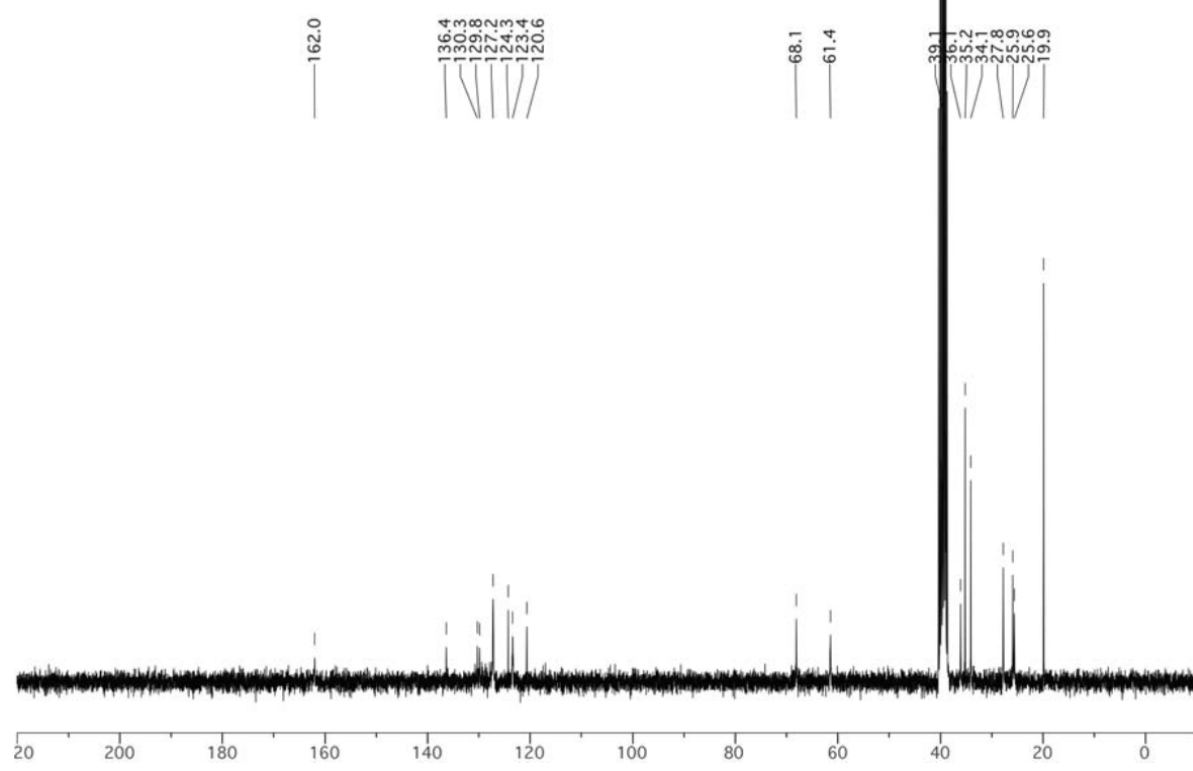
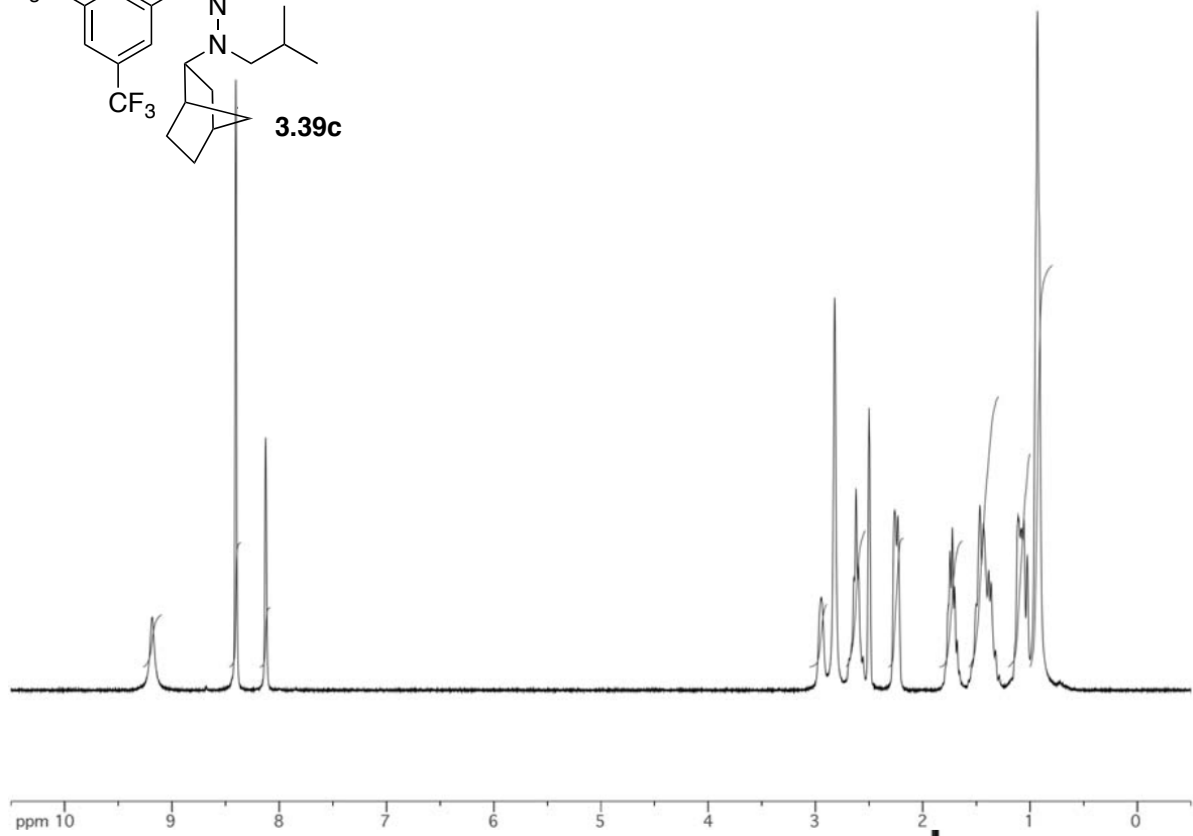
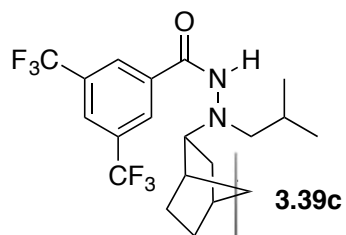


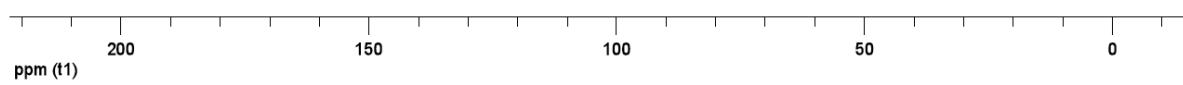
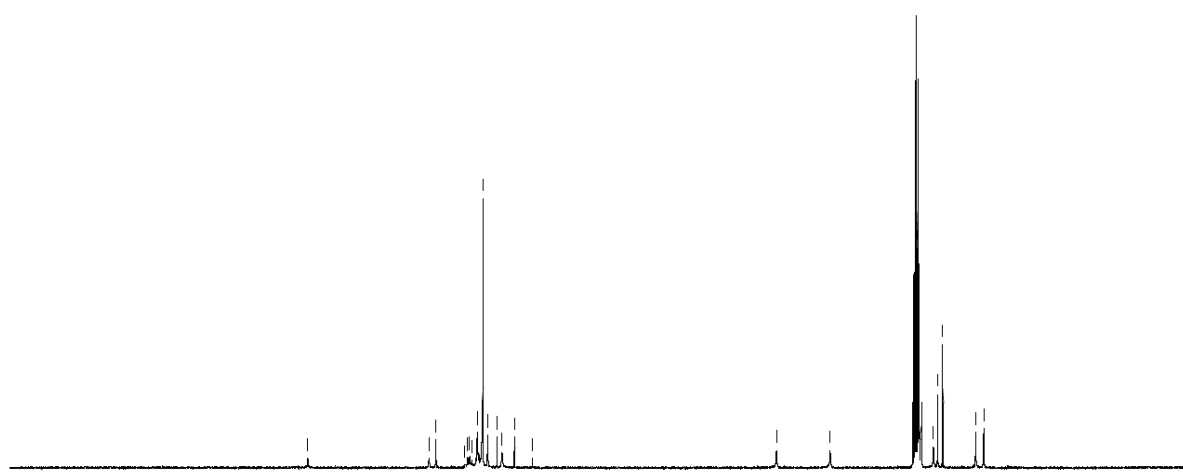
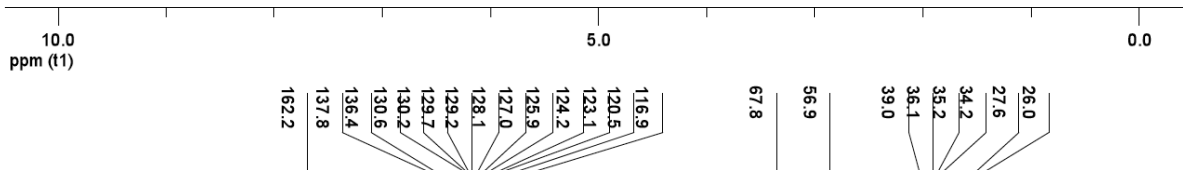
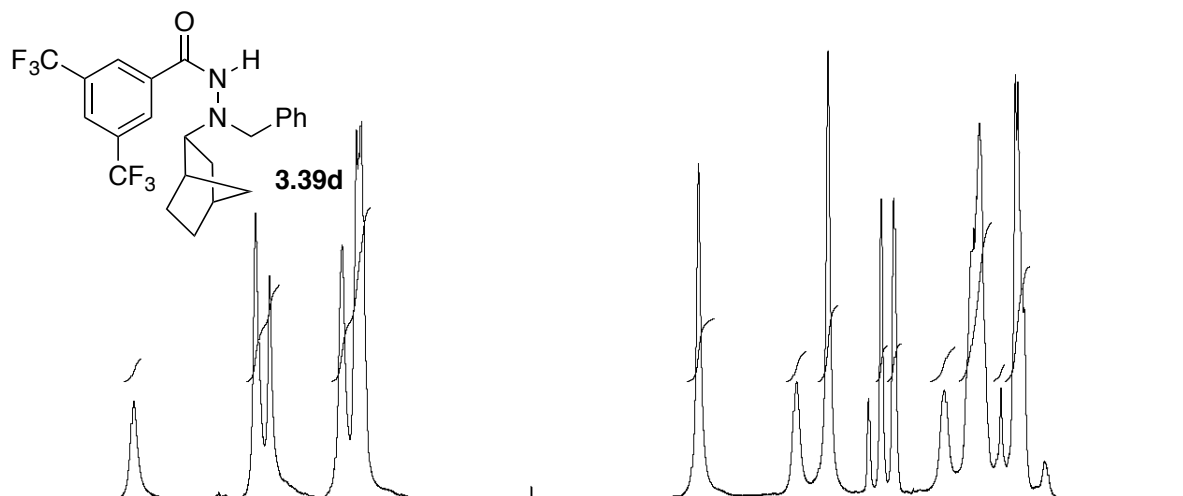


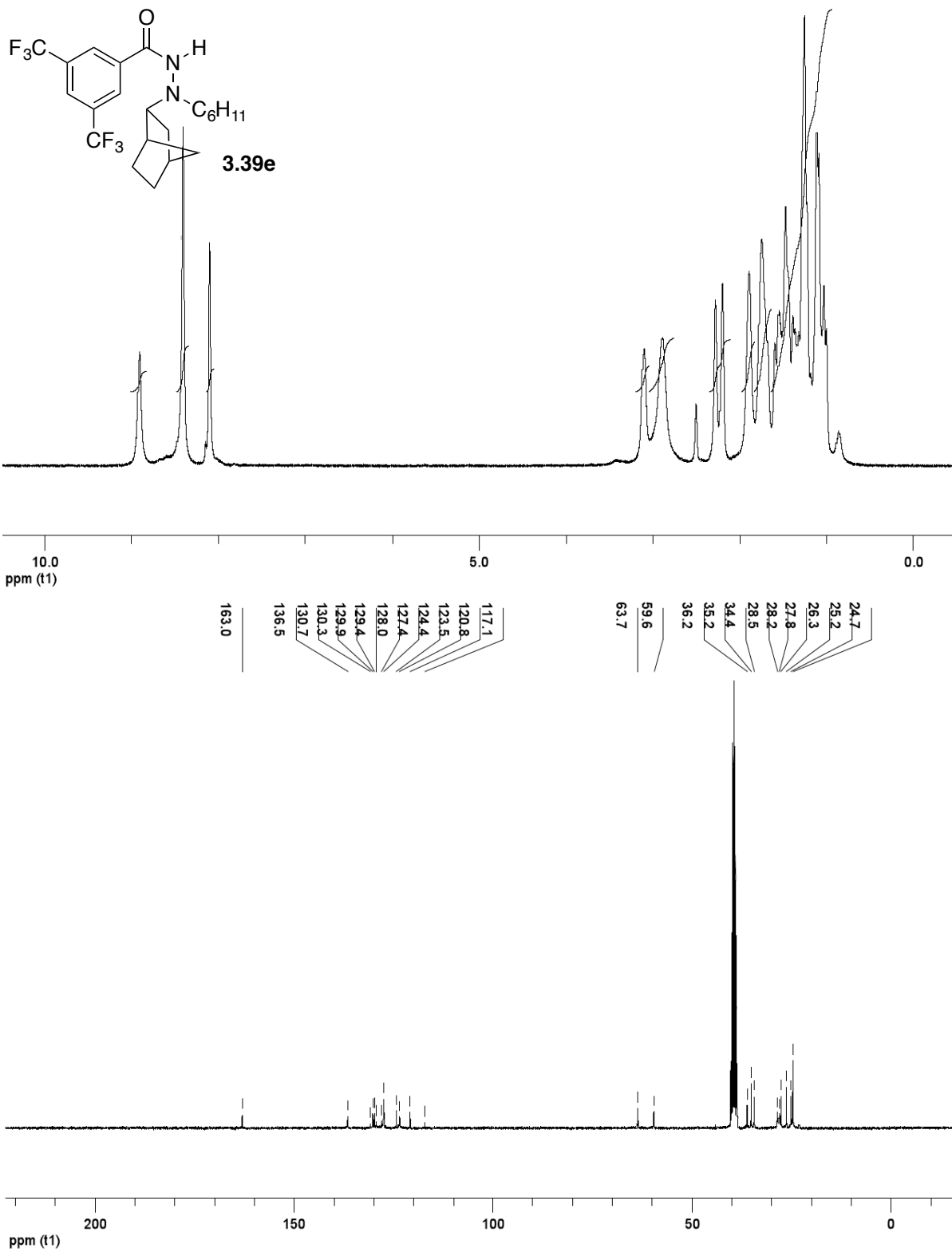


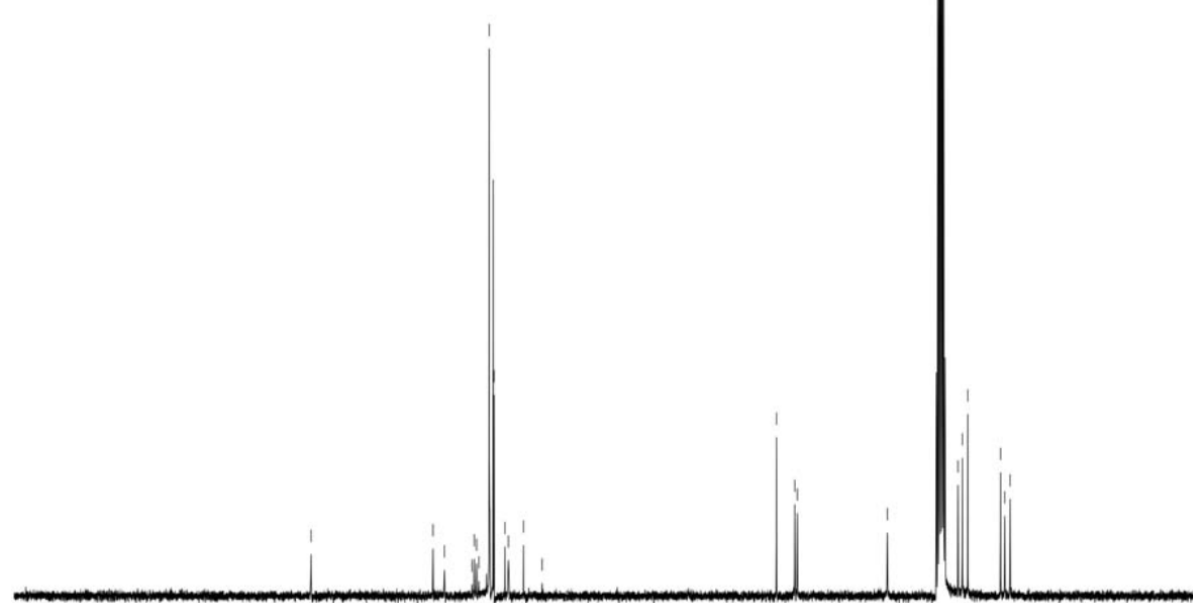
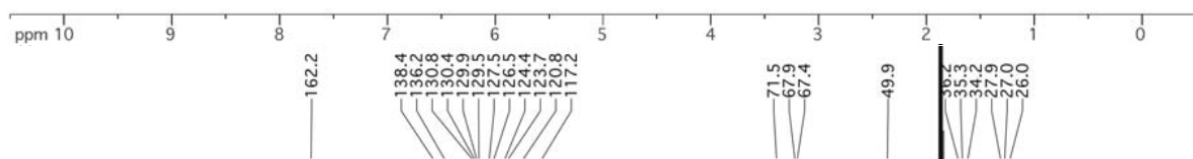
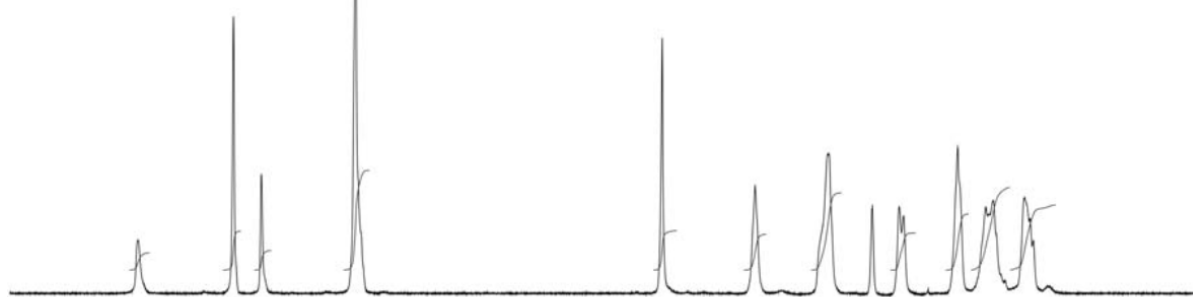
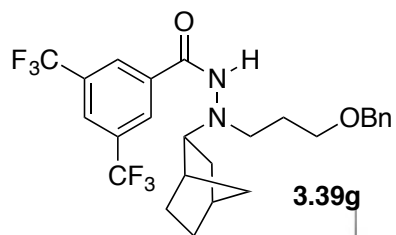


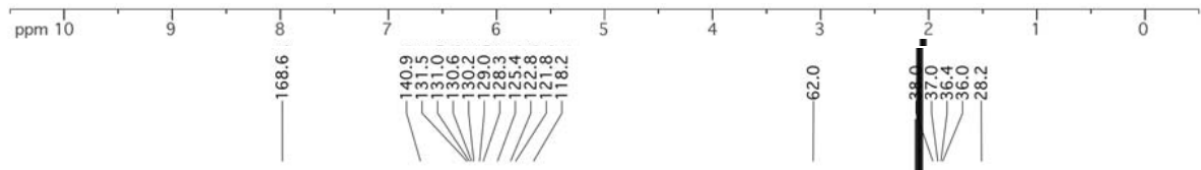
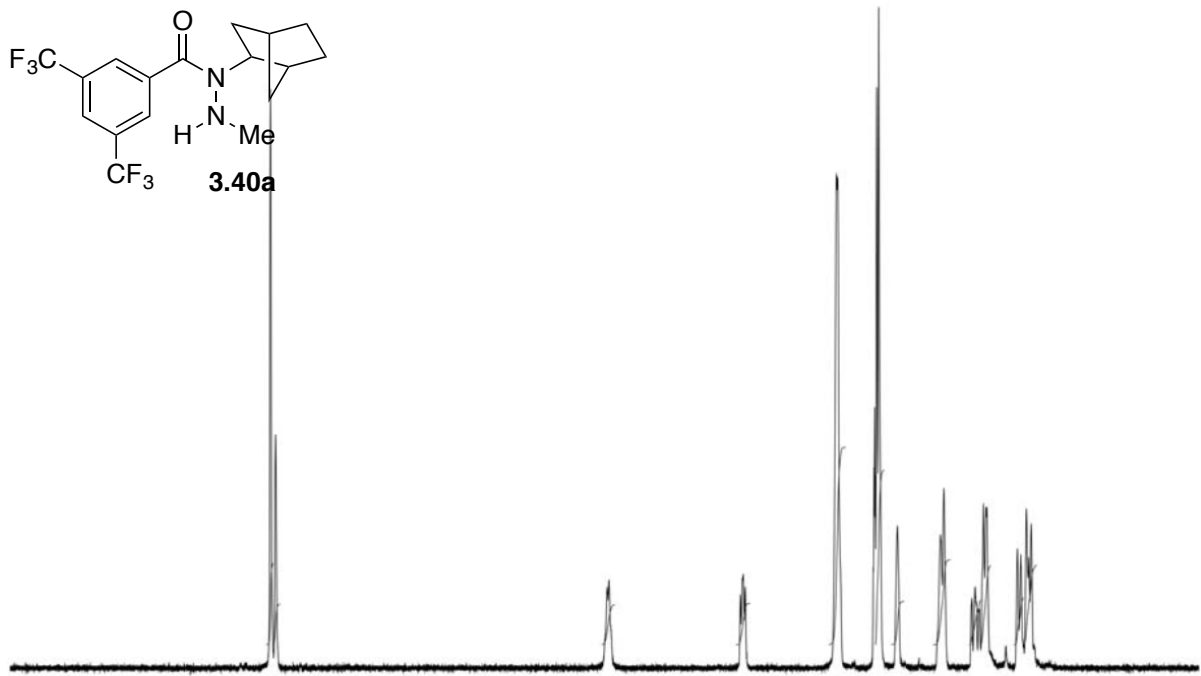
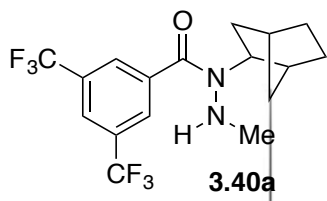


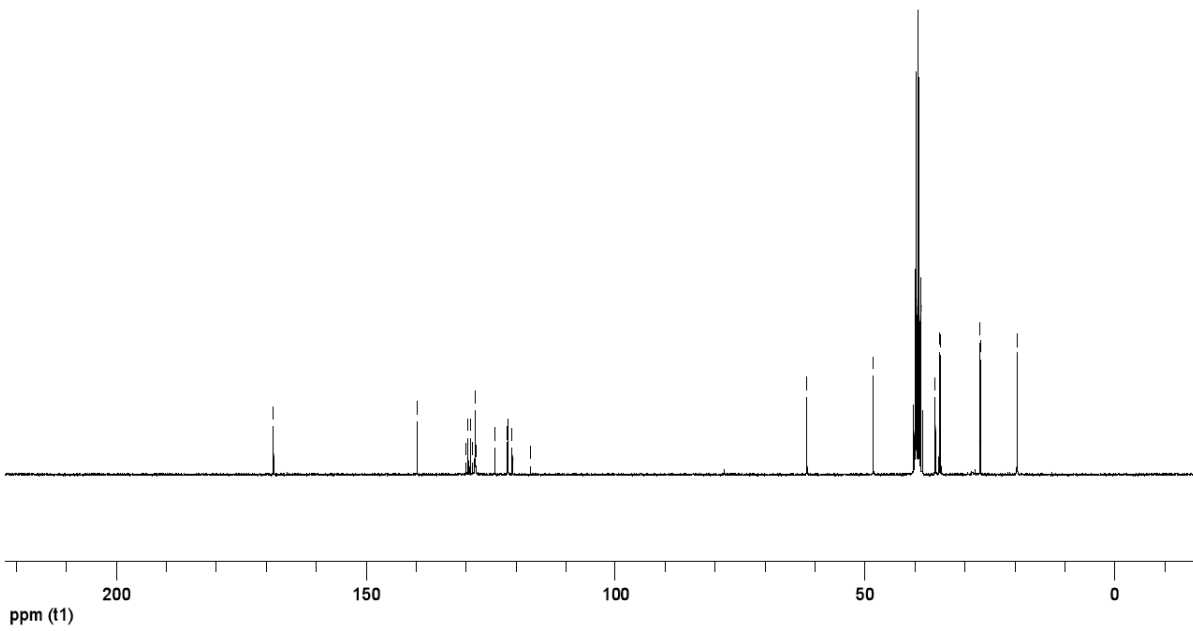
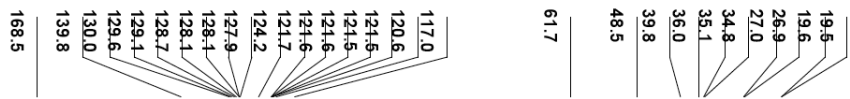
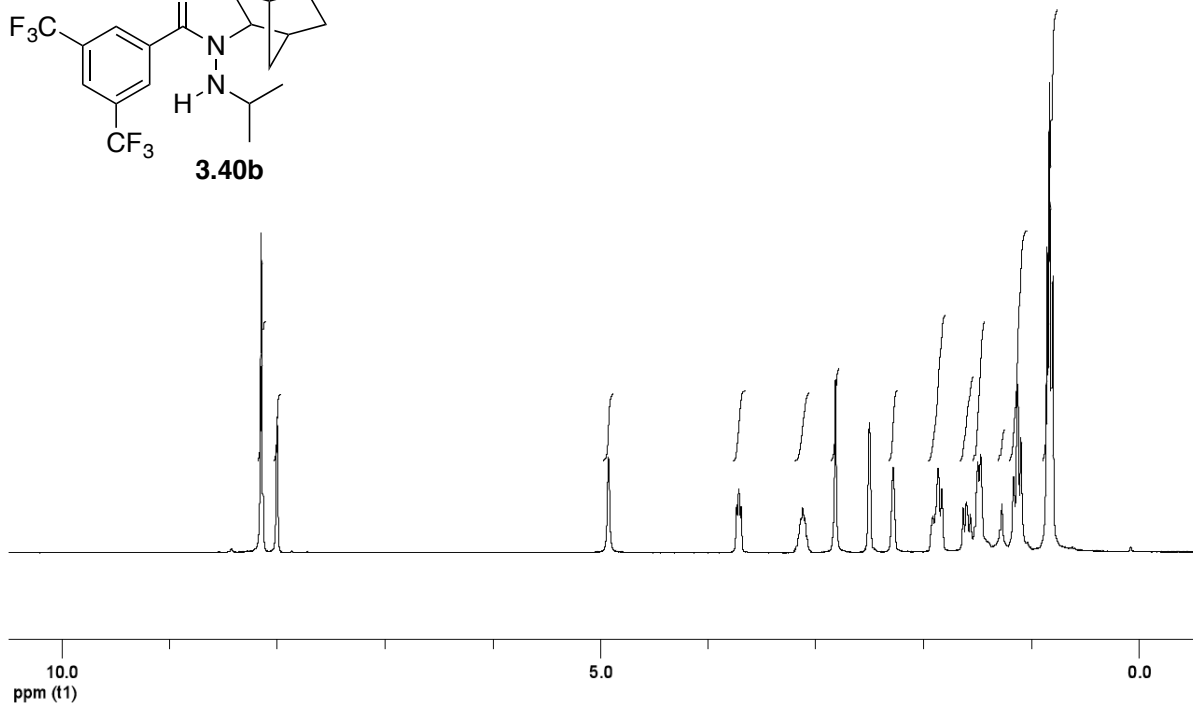
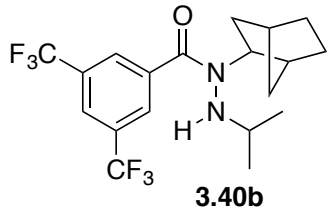


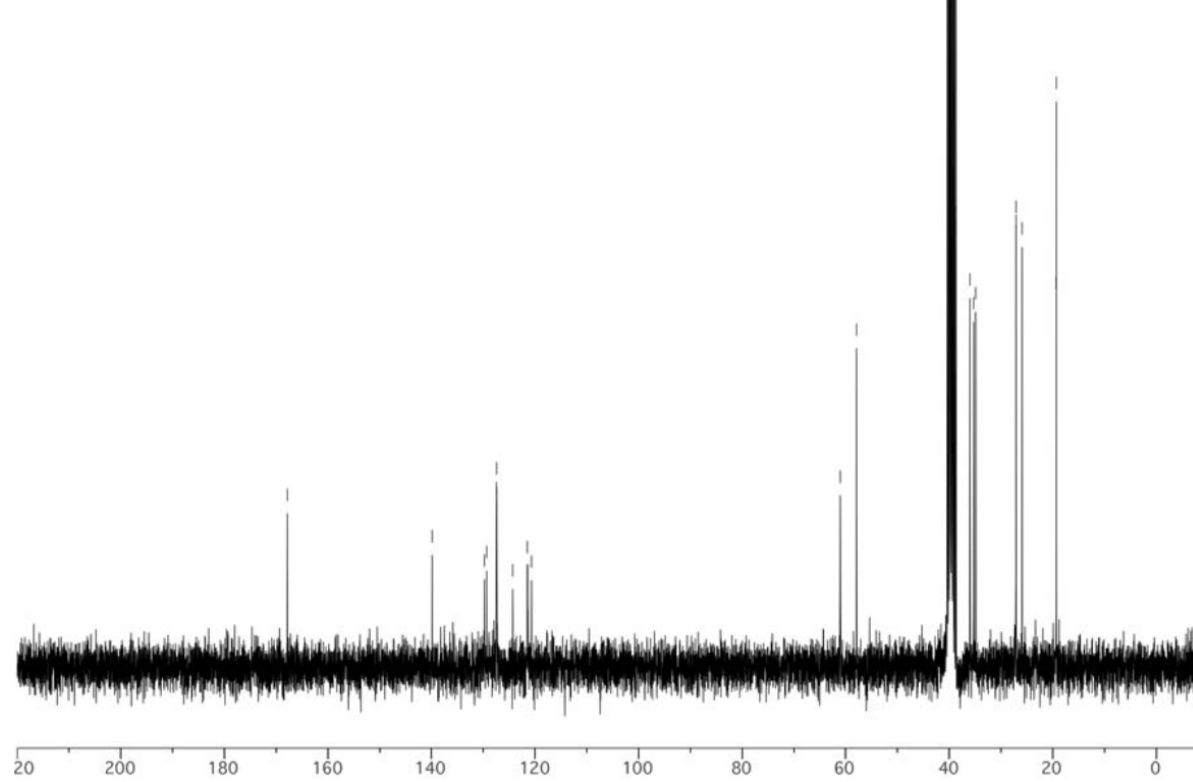
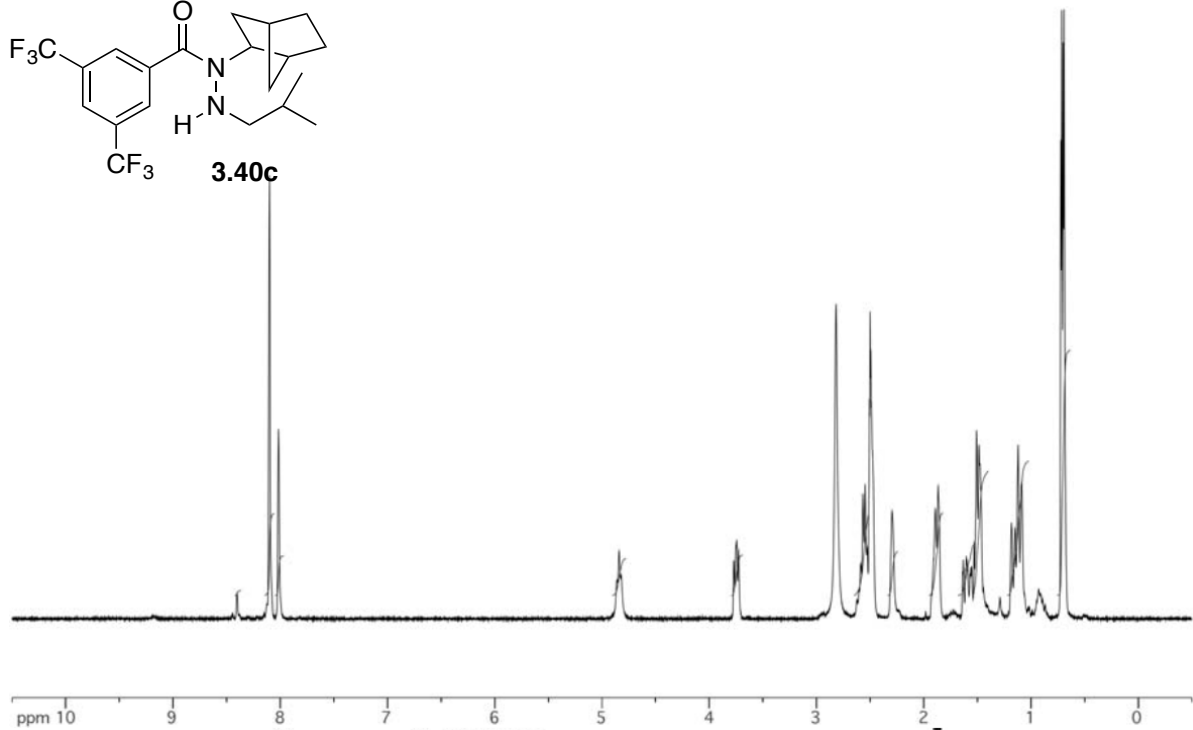
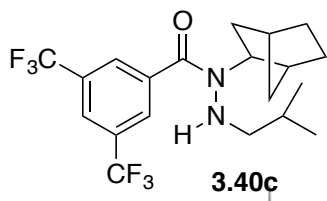


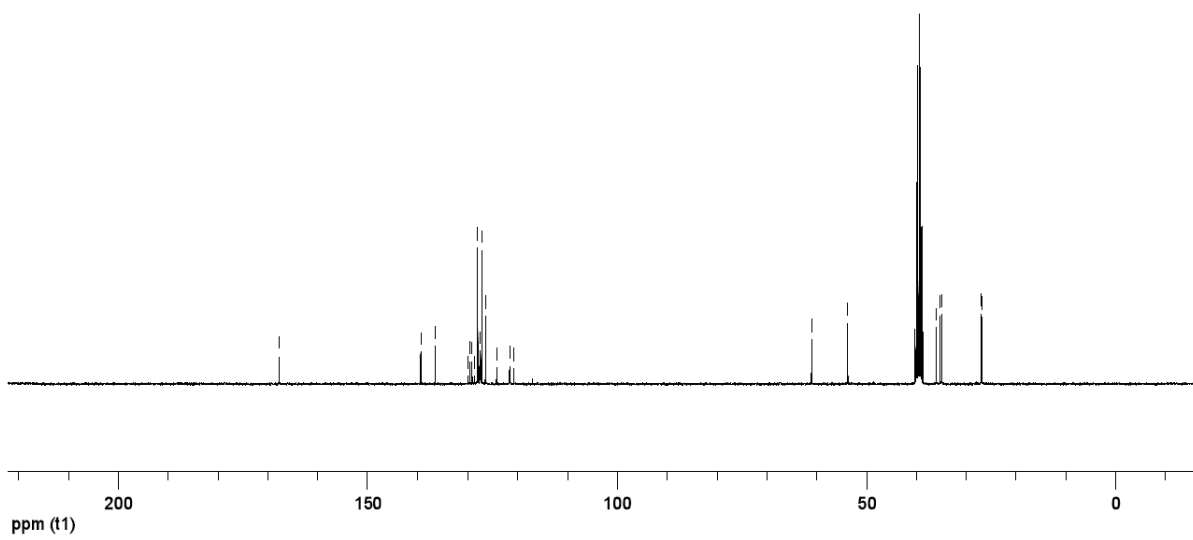
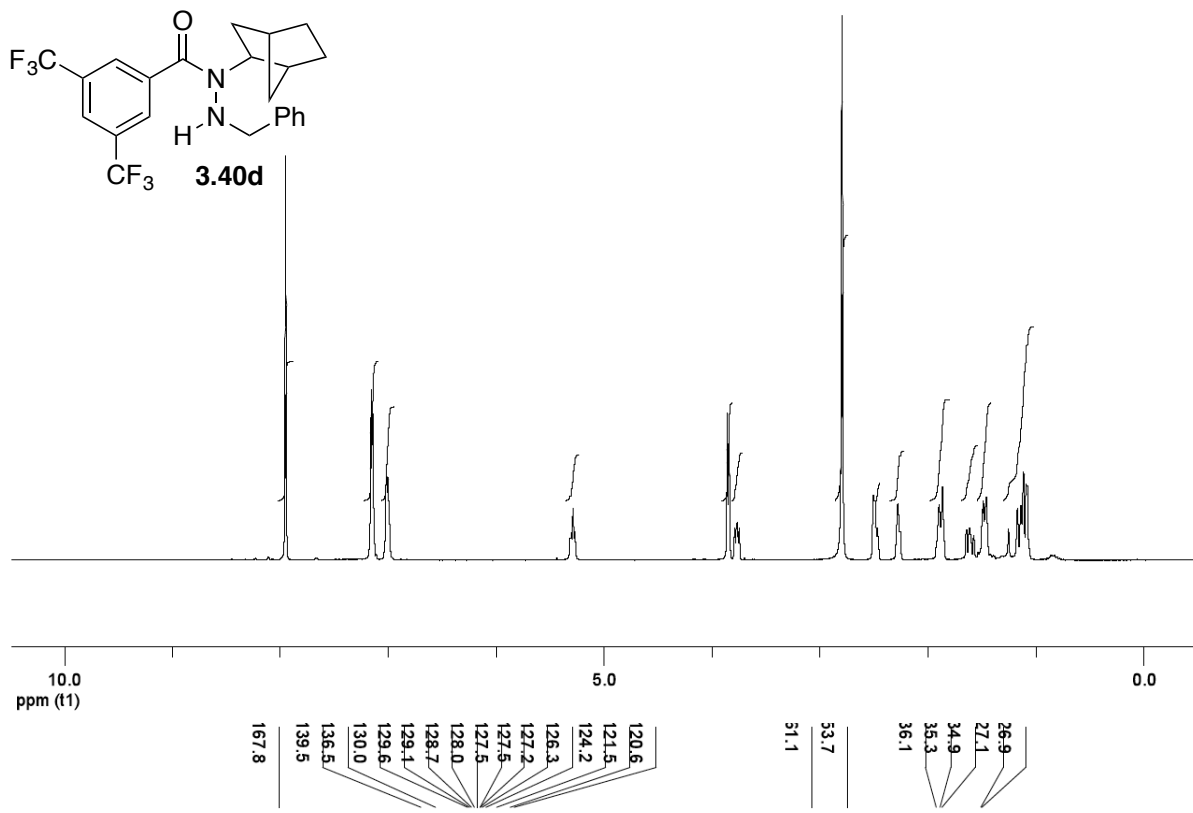
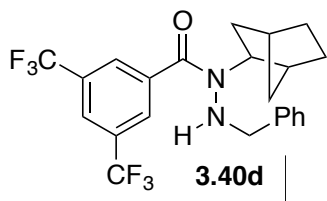


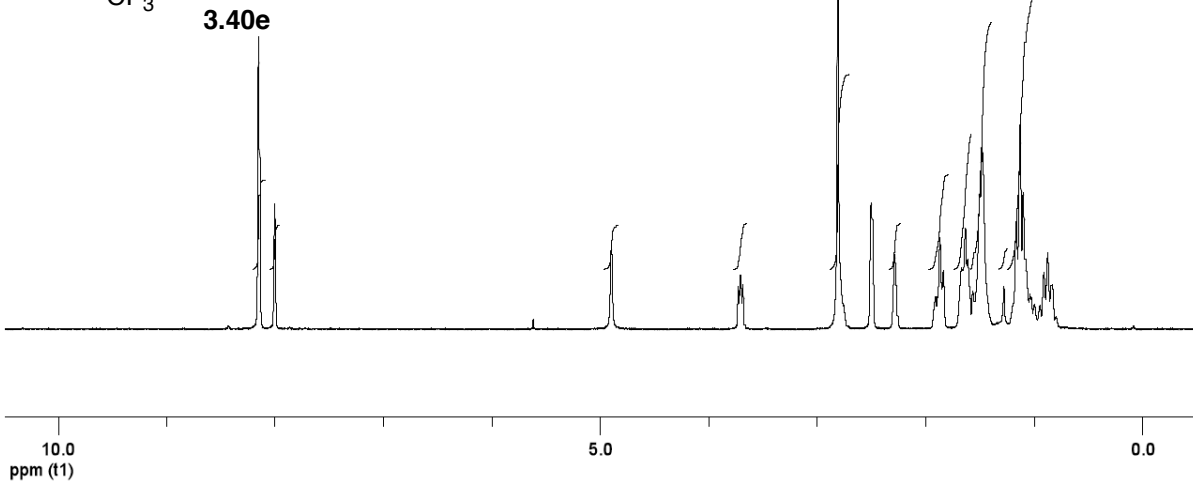
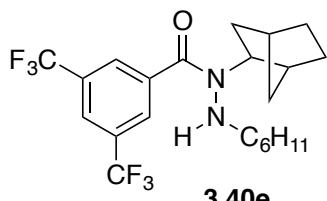




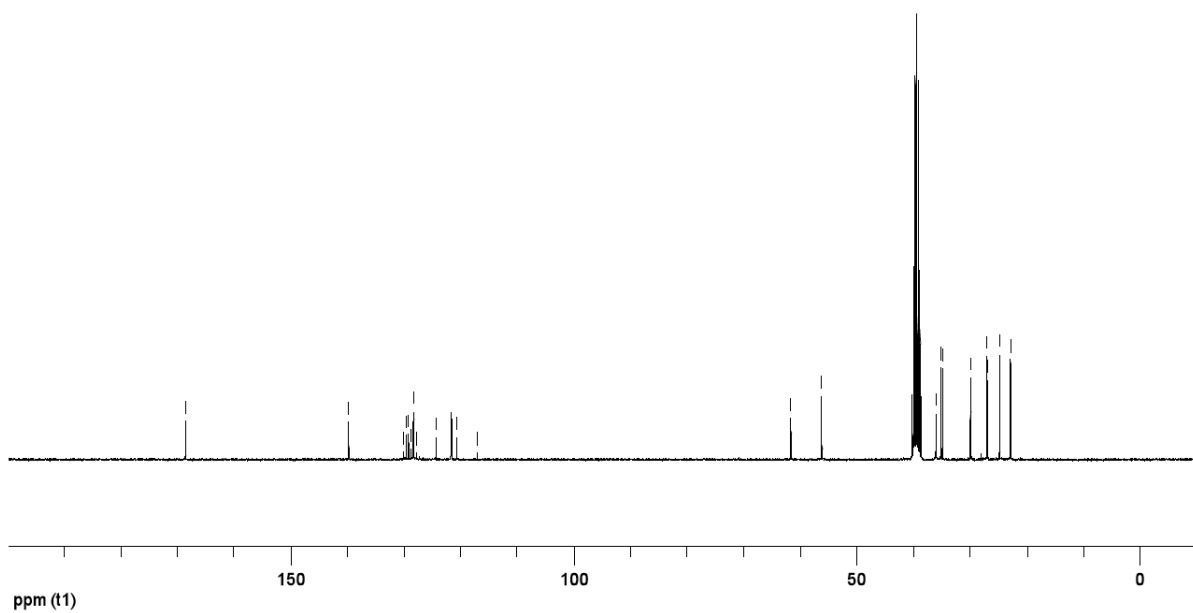


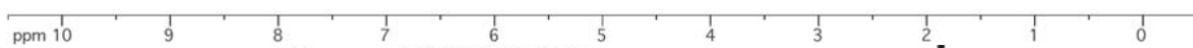
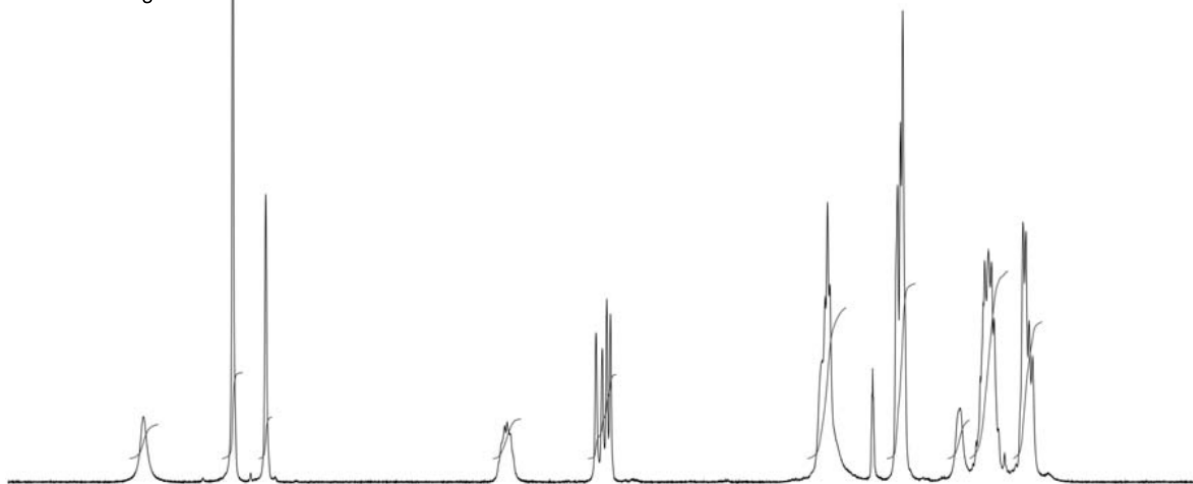
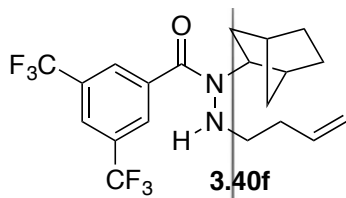






- 168.5
- 139.8
- 130.0
- 129.6
- 129.1
- 128.7
- 128.2
- 127.9
- 124.3
- 121.7
- 121.7
- 121.6
- 121.6
- 121.5
- 120.7
- 117.1
- 61.7
- 56.2
- 39.8
- 36.1
- 35.2
- 34.9
- 29.9
- 27.1
- 27.0
- 24.8
- 22.9





- 162.2
- 136.3
- 130.7
- 130.3
- 129.9
- 129.4
- 127.9
- 127.3
- 126.3
- 127.1
- 114.3
- 67.7
- 52.7
- 38.9
- 36.0
- 35.2
- 34.1
- 30.8
- 27.7
- 26.0

